

Dissertation zur Erlangung des Doktorgrades
der Fakultät für Chemie und Pharmazie
der Ludwig-Maximilians-Universität München

**Construction and Application of Reference Scales
for the Characterization of Cationic Electrophiles
and Neutral Nucleophiles**

Dipl.-Chem. Bernhard Kempf

aus
Buchloe

München, 2003

Erklärung

Diese Dissertation wurde im Sinne von § 13 Abs. 3 bzw. 4 der Promotionsordnung vom 29. Januar 1998 von Prof. Dr. H. Mayr betreut.

Ehrenwörtliche Versicherung

Diese Dissertation wurde selbständig, ohne unerlaubte Hilfe erarbeitet.

München, am 30.05.2003

Bernhard Kempf

Bernhard Kempf

Dissertation eingereicht am	30.05.2003
1. Gutachter	Prof. Dr. H. Mayr
2. Gutachter	Prof. Dr. H. Zipse
Mündliche Prüfung am	26.06.2003

Für Claudia

Danksagung

Für die Möglichkeit, diese Arbeit durchzuführen, gilt mein besonderer Dank Herrn Prof. Dr. H. Mayr, der mich in allen Belangen maßgeblich unterstützte und somit zum Gelingen dieser Arbeit beigetragen hat.

Bei allen ehemaligen und derzeitigen Arbeitskreismitgliedern möchte ich mich für die unzähligen Anregungen und Hilfestellungen bedanken. Besonders erwähnt sei hier Dr. Armin Ofial, der bei der Lösung von wissenschaftlichen Problemen stets eine Hilfe war. Für das Korrekturlesen dieser Arbeit möchte ich mich bei Thorsten Bug, Robert Loos und Dr. Armin Ofial bedanken.

Besonderer Dank gilt auch Nathalie Hampel, die mich maßgeblich bei den experimentellen Arbeiten unterstützte.

Im Rahmen des Literaturpraktikums leisteten die Studenten Ulrike Ritter, Anna Pfeifer, Julia Spatz, Helen Müller und Anna Gehrig wichtige Beiträge.

Für die Durchführung von zahlreichen NMR-Messungen danke ich Frau C. Dubler und Herrn Dr. D. Stephenson. Herrn H. Schulz und Frau M. Schwarz danke ich für die sorgfältige Bestimmung der Elementaranalysen sowie Herrn Dr. W. Spahl für die Aufnahme der Massenspektren.

Nicht zuletzt danke ich meinen Eltern für die Unterstützung während meines Studiums.

Teile dieser Dissertation sind publiziert in:

Reference Scales for the Characterization of Cationic Electrophiles and Neutral Nucleophiles. H. Mayr, T. Bug, M. F. Gotta, N. Hering, B. Irrgang, B. Janker, B. Kempf, R. Loos, A. R. Ofial, G. Remennikov, H. Schimmel, *J. Am. Chem. Soc.* **2001**, *123*, 9500-9512.

p-Nucleophilicity in Carbon-Carbon Bond-Forming Reactions. H. Mayr, B. Kempf, A. R. Ofial, *Acc. Chem. Res.* **2003**, *36*, 66-77.

5-Methoxyfuroxano[3,4-d]pyrimidine - a highly reactive neutral electrophile. G. Ya. Remennikov, B. Kempf, A. R. Ofial, K. Polborn, H. Mayr, *J. Phys. Org. Chem.* **2003**, in print.

Structure-Nucleophilicity Relationships for Enamines. B. Kempf, N. Hampel, A. R. Ofial, B. Kempf, N. Hampel, A. R. Ofial, H. Mayr, *Chem. Eur. J.* **2003**, *9*, 2209-2218.

Table of contents

0. Summary.....	1
1. Introduction and objectives.....	12
2. Kinetic methods and calculation of rate constants.....	16
2.1 Introduction.....	16
2.2 Irreversible reactions.....	16
2.3 Reversible reactions.....	18
2.4 Temperature dependence of the rate constants.....	19
2.5 Kinetic instruments.....	20
3. Reference scales for the characterization of cationic electrophiles and neutral nucleophiles.....	24
3.1 Introduction.....	24
3.2 Definition of reference compounds.....	25
3.3 Starting situation.....	26
3.4 Seeking for new reference compounds.....	27
3.5 Reactions of reference electrophiles with reference nucleophiles.....	30
3.6 Correlation analysis of the basis-set compounds.....	33
3.7 Three dimensional presentations of the reactivities of the basis-set compounds.....	37
3.8 New Hammett parameters.....	42
3.9 Does a certain reaction take place.....	44
3.10 Characterization of new compounds.....	45
4. Structure-nucleophilicity relationships for enamines.....	47
4.1 Introduction.....	47
4.2 Electrophiles.....	47
4.3 Nucleophiles.....	48
4.4 Reaction products.....	49
4.5 Kinetic measurements.....	50
4.6 Enamines as ambident nucleophiles.....	54
4.7 Nucleophilicities of enamines.....	57
4.8 Intrinsic barriers for the reactions of benzydrylium ions with enamines.....	58
4.9 Structure-reactivity relationships for enamines.....	59
4.10 Conclusion.....	66
5. 5-Methoxyfuroxano[3,4- <i>d</i>]pyrimidine - a highly reactive neutral electrophile.....	68
5.1 Introduction.....	68

Table of contents

5.2 Synthesis and reaction products.....	69
5.3 Kinetic measurements.....	69
5.4 Discussion.....	70
5.5 Conclusion.....	71
6. Rates and equilibria for the reactions of tertiary phosphanes and phosphites with carbocations.....	73
6.1 Introduction.....	73
6.2 Nucleophiles.....	74
6.3 Reaction products.....	74
6.4 Equilibrium constants.....	75
6.5 Kinetics.....	79
6.6 Solvent dependence of the rate constants.....	83
6.7 Determination of the nucleophilicities of phosphorous compounds.....	84
6.8 Intrinsic barriers.....	87
6.9 Quantitative analysis of ligand effects.....	90
6.10 Reactions of phosphanes and phosphites with other electrophiles.....	94
6.11 Conclusion.....	97
7. Electrophilicity parameters for metal- π -complexes.....	98
7.1 Introduction.....	98
7.2 Adaption of rate constants to standard conditions.....	99
7.3 Determination of the E parameters of metal- π -complexes.....	106
7.4 Checking the reliability of the metal- π -complexes E parameters.....	108
8. Nucleophilic reactivities of pyridine and its derivatives.....	113
8.1 Introduction.....	113
8.2 New pyridine derivatives.....	114
8.3 Determination of the nucleophilicities of pyridine derivatives.....	116
8.4 Rate-equilibrium relationships.....	120
8.5 Comparison of the nucleophilicities of pyridine derivatives with other properties..	122
8.6 Reactions of pyridines with other electrophiles.....	123
8.7 Catalytic activities of pyridine derivatives in acylation reactions.....	125
8.8 Determination of the catalytic activities.....	125
8.9 Comparison of the catalytic activities of pyridine derivatives.....	130
9. Conclusion and outlook.....	132

10. Experimental part.....	133
10.1 General conditions.....	133
10.2 Reference scales for the characterization of cationic electrophiles and neutral nucleophiles.....	135
10.2.1 Synthesis of benzhydryl cations.....	135
10.2.2 Synthesis of silyl ketene acetals.....	138
10.2.3 Reactions of nucleophiles with benzhydryl salts.....	139
10.2.4 Concentrations and rate constants of the individual kinetic runs.....	152
10.3 Structure-nucleophilicity relationships for enamines.....	166
10.3.1 Enamine synthesis by condensation of ketones or aldehydes with amines.....	166
10.3.2 Enamine synthesis by base-catalyzed isomerization of allylamines.....	171
10.3.3 Enamine synthesis by addition of amine to alkyne.....	172
10.3.4 Reactions of enamines, pyrroles, or indoles with benzhydrylium salts.....	173
10.3.5 Concentrations and rate constants of the individual kinetic runs.....	183
10.4 5-Methoxyfuroxano[3,4- <i>d</i>]pyrimidine - a highly reactive neutral electrophile.....	206
10.4.1 Concentrations and rate constants of the individual kinetic runs.....	206
10.5 Rates and equilibria for the reactions of tertiary phosphanes and phosphites with carbocations.....	207
10.5.1 Synthesis of triaryl phosphanes.....	207
10.5.2 Reactions of phosphanes and phosphites with benzhydryl salts.....	208
10.5.3 Concentrations and rate constants of the individual kinetic runs.....	216
10.5.4 Concentrations and equilibrium constants.....	249
10.6 Nucleophilic reactivities of pyridine and its derivatives.....	260
10.6.1 Reactions of pyridine derivatives with benzhydryl salts.....	260
10.6.2 Synthesis of acetic acid cyclohexyl ester.....	262
10.6.3 Concentrations and rate constants for the reactions of pyridine derivatives with benzhydryl salts.....	262
10.6.4 Concentrations and equilibrium constants for the reactions of pyridine derivatives with benzhydryl salts.....	274
10.6.5 Concentrations and rates for the base-catalyzed acetylations of cyclohexanol.....	276
11. References.....	279

0. Summary

1. Reactions of diarylcarbenium ions (benzhydryl cations) Ar_2CH^+ with various σ^- , π^- , and n^- nucleophiles (e. g. aliphatic and aromatic π -systems, metal- π -complexes, hydride donors, phosphanes and phosphites, carbanions) follow the linear relationship eq. 1.3, where electrophiles are characterized by the parameter E , whereas the nucleophiles are characterized by the two parameters N and s . The reactivities of Ar_2CH^+ can be modified widely by variation of para-substituents, while the steric situation at the reaction centers is kept constant.

$$\log k (20^\circ\text{C}) = s(E + N) \quad (1.3)$$

In collaboration with other members of this group, a basis-set of reference electrophiles (benzhydrylium ions) and reference nucleophiles (π -systems) has been constructed on the basis of eq. 1.3 (Figure 0.1).

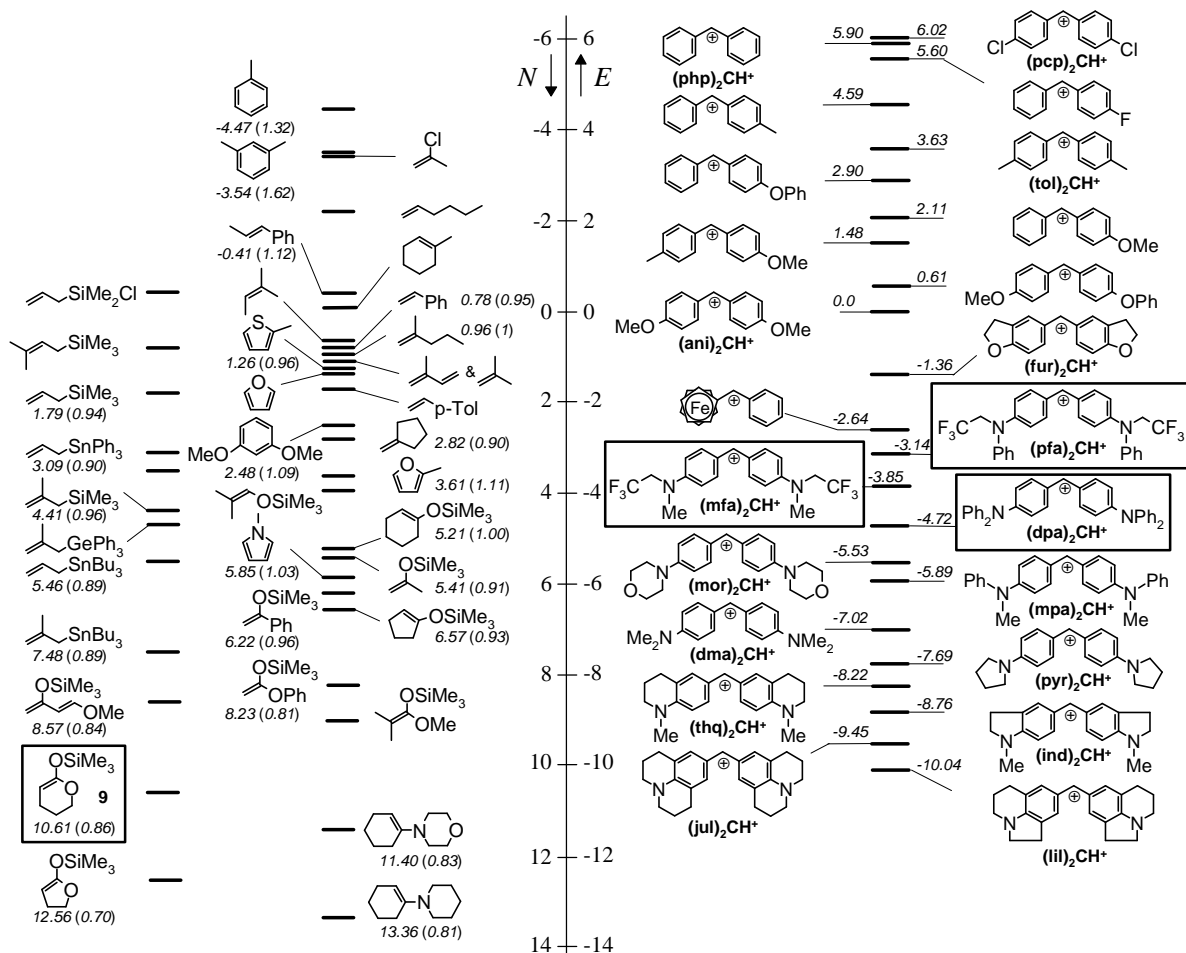


Figure 0.1: Compilation of all basis-set compounds used for the determination of E , N , and s . Compounds in frames were added to the basis-set by this work.

This basis set contains 23 reference electrophiles and 38 reference nucleophiles. The reference electrophiles and nucleophiles of the basis-set cover reactivity ranges of several orders of magnitude, and can be used for characterizing the reactivities of a large variety of new compounds by kinetic measurements.

2. A semi-quantitative test for nucleophilicity was developed (Chapter 3.9). A series of reference electrophiles was combined with reaction partners of different nucleophilicity. The photograph (taken after 1 min) reveals the reactivity order of the checked nucleophiles (Figure 0.2).

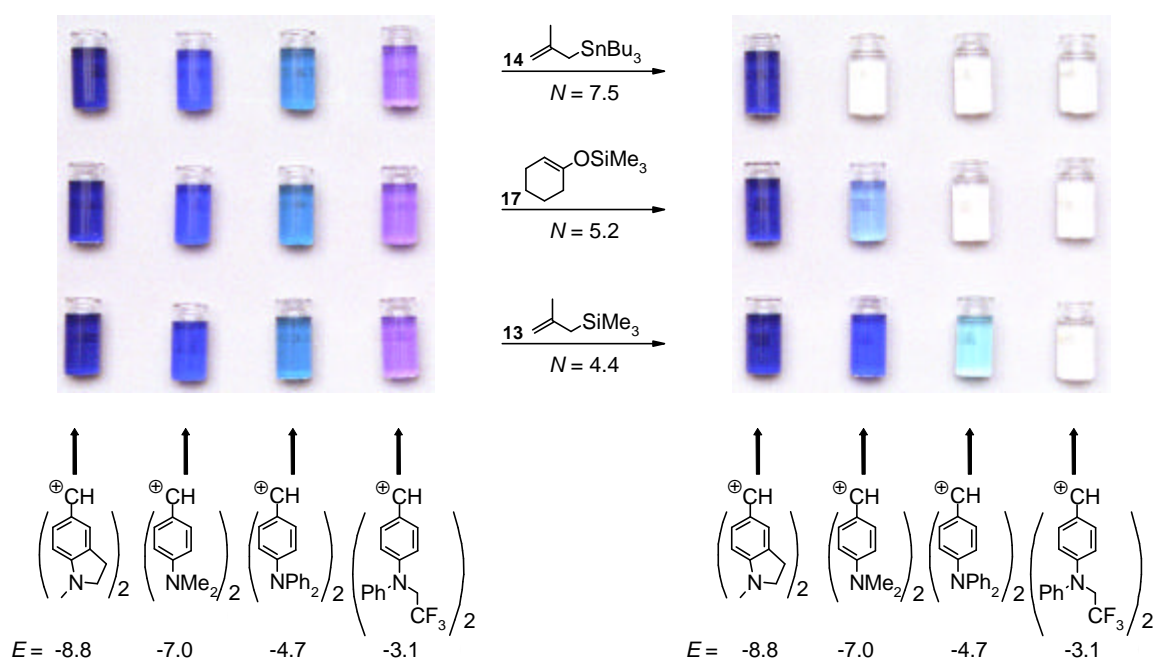
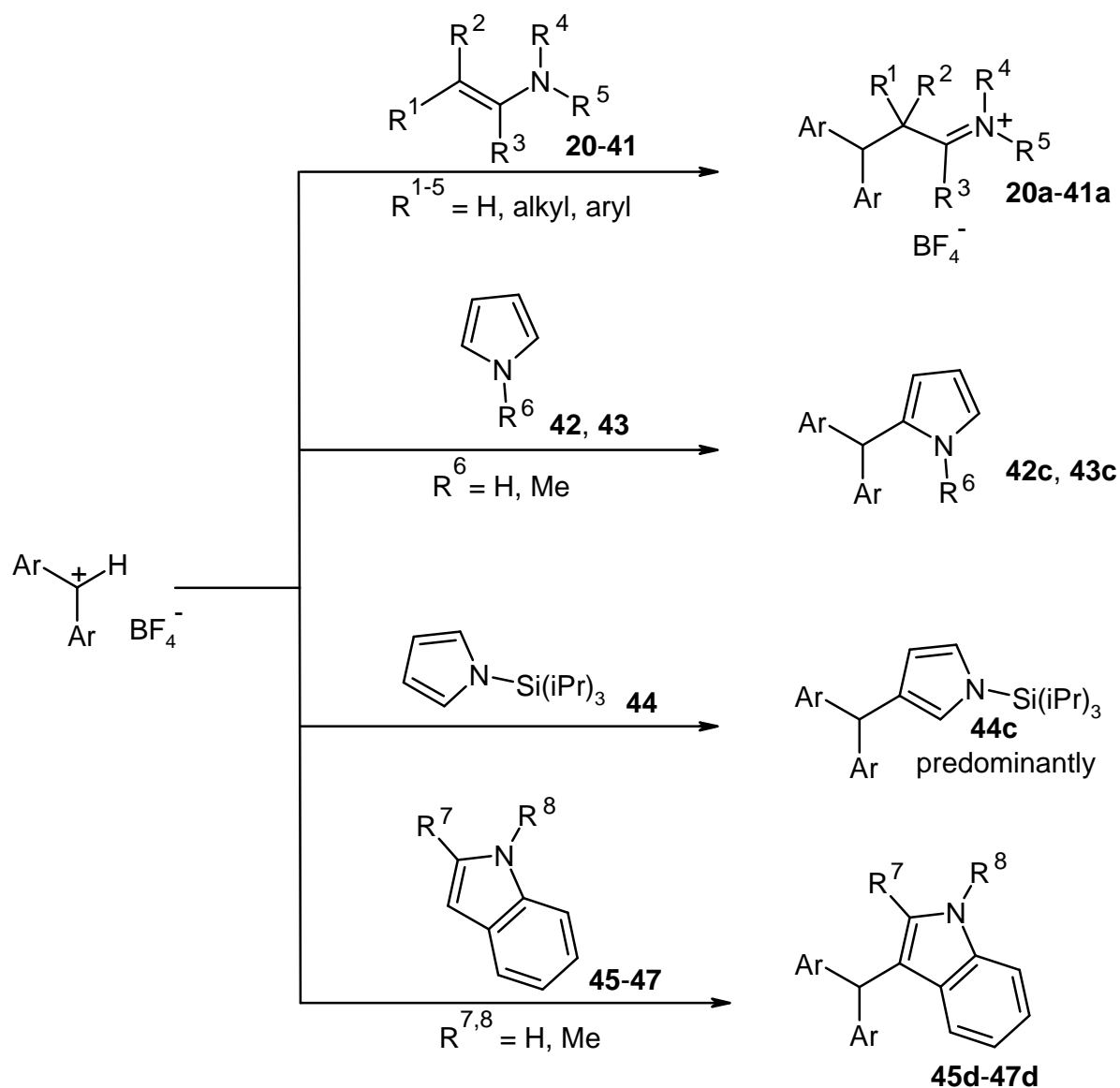


Figure 0.2: Quick-test of nucleophilicity.

In this way, nucleophiles of unknown reactivity can efficiently be characterized with a precision that suffices for many purposes.

3. The nucleophilicity parameters (N , s) of 22 enamines, three pyrroles, and three indoles were investigated by performing kinetic measurements of their reactions with reference electrophiles in methylene chloride (Scheme 0.1).



Scheme 0.1: Reactions of benzhydrylium ions with enamines, pyrroles, and indoles.

Product analysis indicated that benzhydryl cations attack indoles at position 3, and that pyrrole and its N-methyl derivative react at position 2. In contrast, N-triisopropylsilylpyrrole is mainly attacked at the 3-position (see Chapter 4.4).

When the rate constants ($\log k$) for the reactions of enamines with Ar_2CH^+ were plotted against the E parameters of the benzhydrylium ions, linear correlations are obtained, from which s and N according to eq. 1.3 can be determined (Figure 0.3).

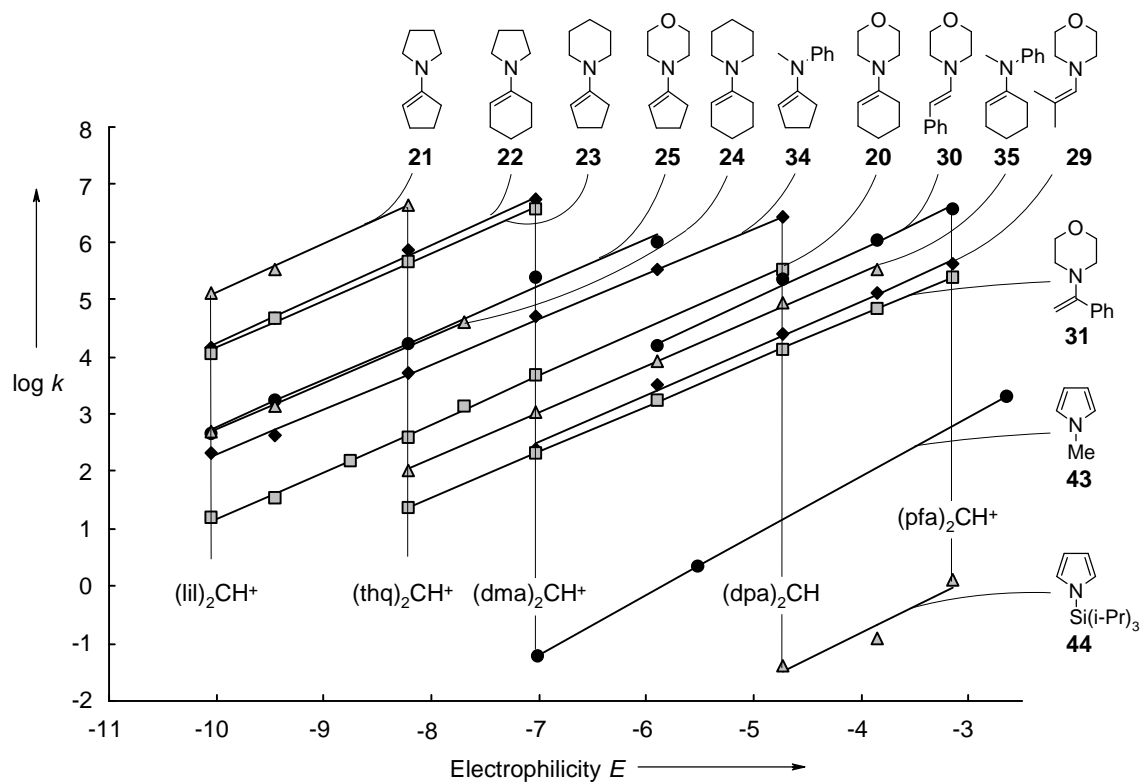


Figure 0.3: Correlations of the rate constants ($\log k$, 20 °C, CH_2Cl_2) for reactions of enamines and pyrroles with benzhydryl cations Ar_2CH^+ versus their E parameters.

Eneammonium ions are produced by attack of benzhydrylium ions at the nitrogen of enamines. It was shown that the products are thermodynamically unstable. The observed rate constants refer to the formation of carbon-carbon bonds.

The nucleophilic reactivities of enamines cover more than ten orders of magnitude ($4 < N < 16$), comparable to enol ethers on the low reactivity end and to carbanions on the high reactivity end (Figure 0.4).

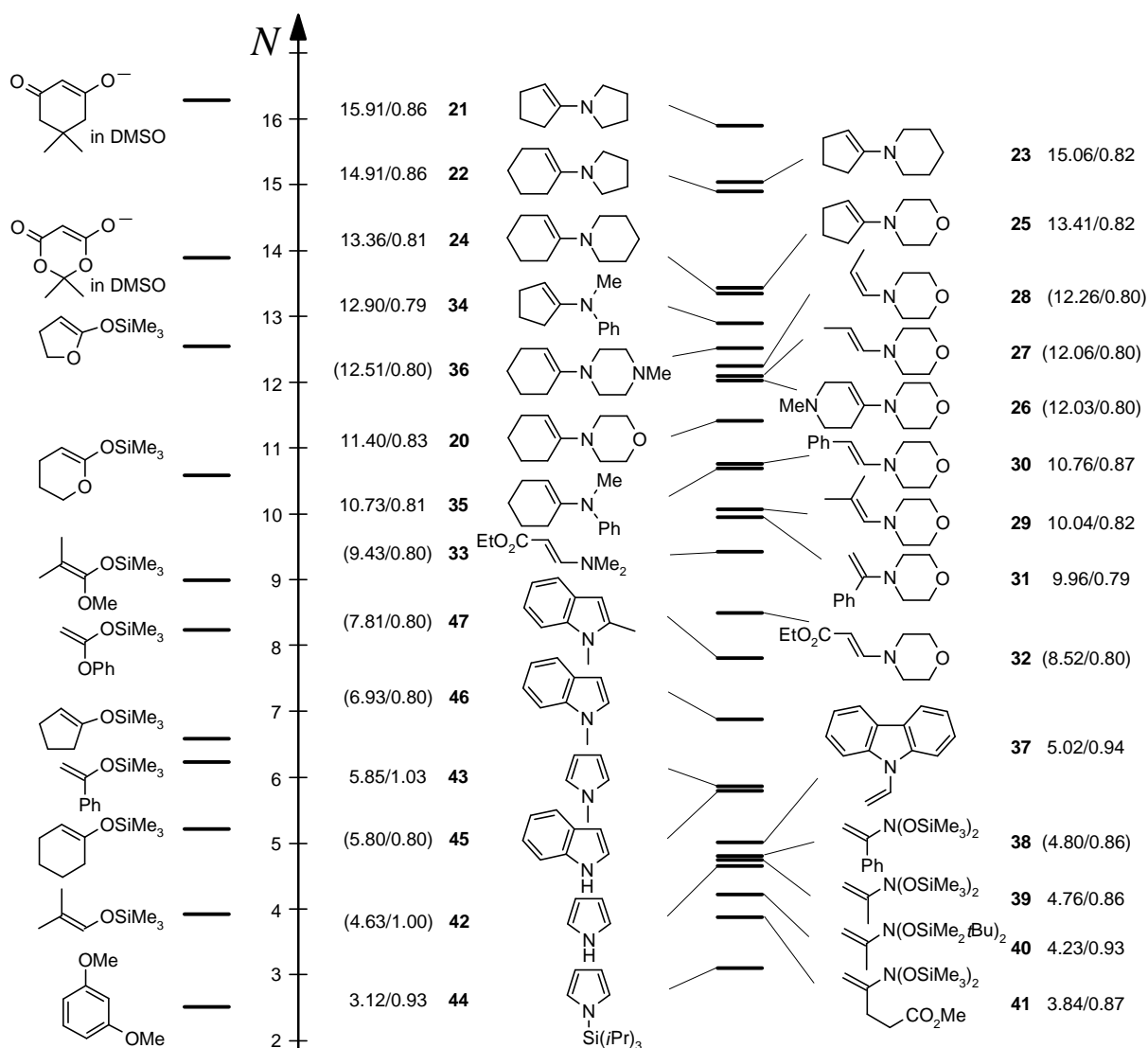
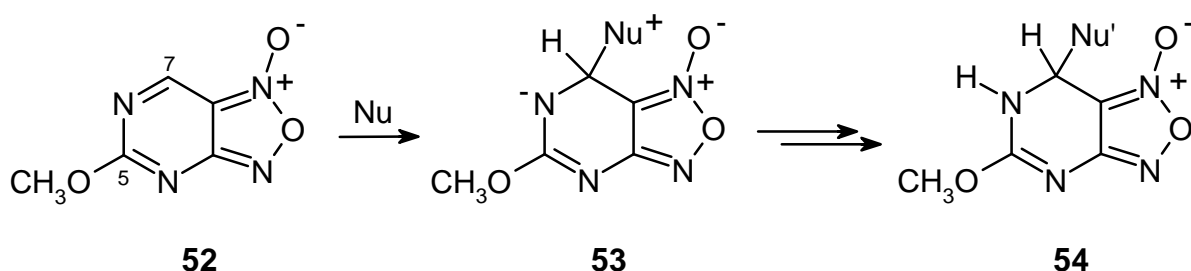


Figure 0.4: Nucleophilicity and slope parameters N/s of enamines, pyrroles and indoles compared with other π -systems and carbanions.

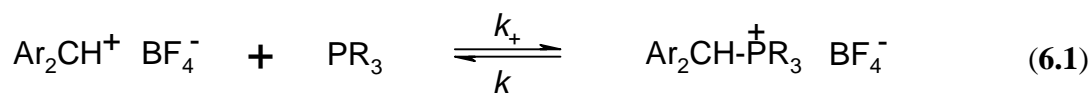
In some cases, equilibrium constants for the formation of iminium ions were measured, which allowed us to determine the intrinsic rate constants (k_2 (20 °C) $\approx 16.7 \text{ M}^{-1} \text{ s}^{-1}$) and the intrinsic barriers ($\Delta G_0^\ddagger \approx 65 \text{ kJ mol}^{-1}$) for the reactions of benzhydrylium ions with enamines (Chapter 4.8).

4. The electrophilicity parameter E of the neutral electrophile 5-methoxyfuroxano[3,4-*d*]pyrimidine (**52**) (Scheme 0.2) was determined by performing kinetic measurements with reference nucleophiles. With an electrophilicity parameter of $E = -8.37$, **52** ranks among the strongest noncharged electrophiles, comparable to the electrophilicity of stabilized carbocations and cationic metal- π -complexes.



Scheme 0.2: Reaction of 5-methoxyfuroxano[3,4-*d*]pyrimidine (**52**) with nucleophiles.

5. The rate and equilibrium constants for many combinations of tertiary phosphanes and phosphites with benzhydrylium ions and quinone methides were determined photometrically (eq. 6.1).



6. The influence of structure and substituents of tertiary phosphorous compounds on their carbon basicity (see Chapter 6.4) and nucleophilicity (see Chapter 6.5) was investigated. The nucleophilicities N and slopes s of tertiary phosphanes and phosphites were derived from the plots of $\log k_2$ versus E of the benzhydrylium ions and quinone methides (Figure 0.5).

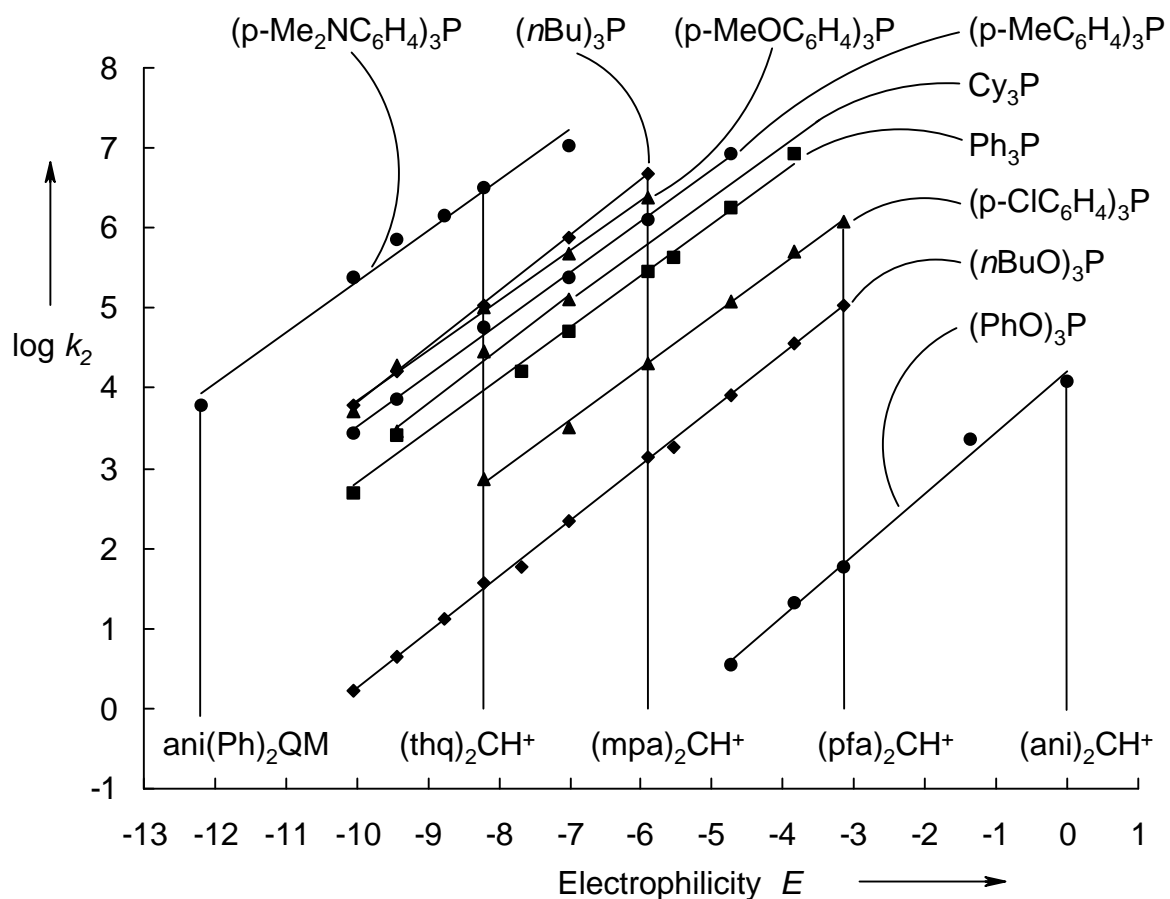


Figure 0.5: Correlations of the rate constants ($\log k$, 20 °C, CH_2Cl_2) for the reactions of R_3P with the benzhydryl cations Ar_2CH^+ (and quinone methides) versus their E parameters.

The range of the nucleophilicities of phosphanes and phosphites covers 13 orders of magnitude ($5.51 < N < 18.39$) and overlaps with that of carbanions, amines, enamines, silyl ketene acetals, silyl enol ethers, and allyl stannanes (Figure 0.6).

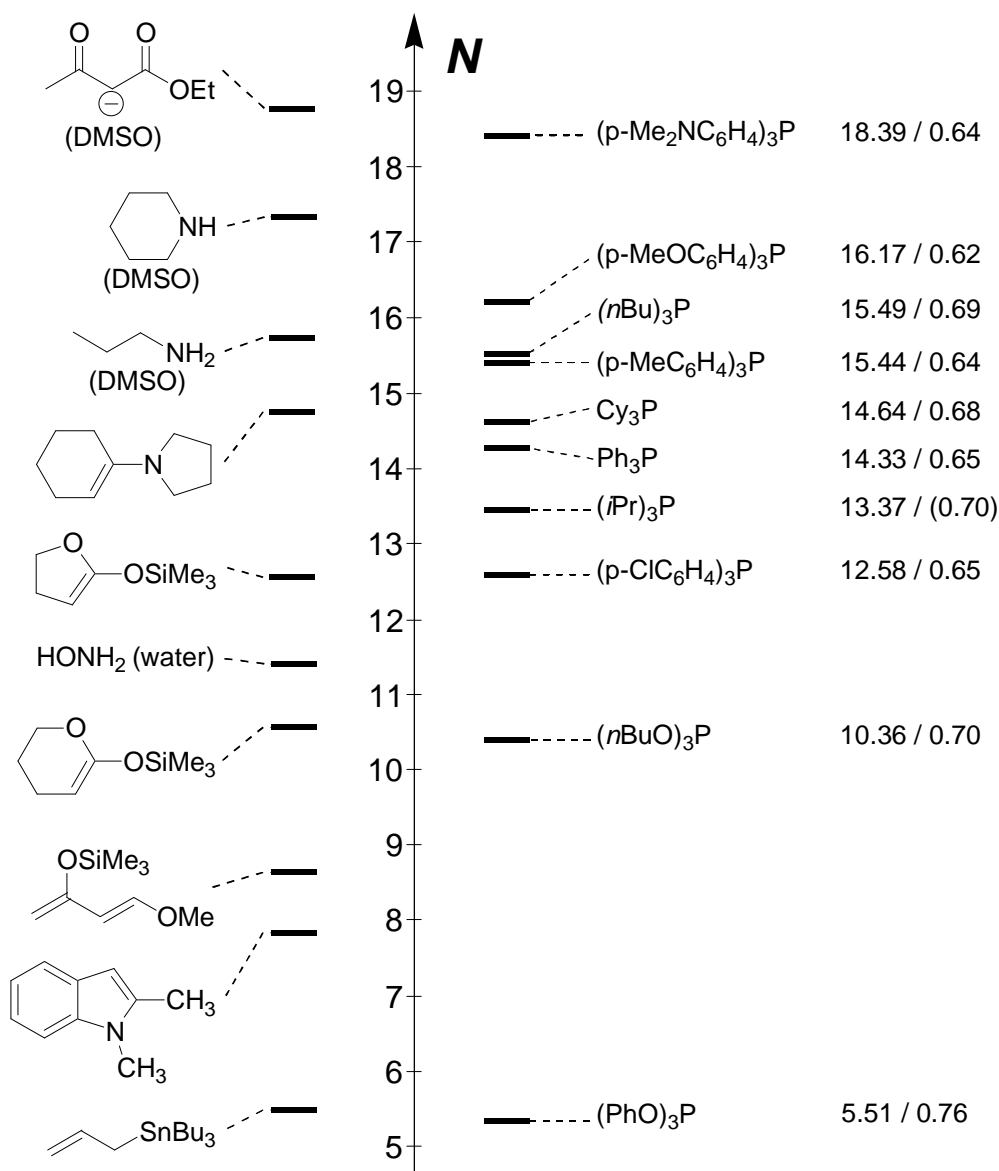


Figure 0.6: Comparison of the nucleophilic reactivities (N/s) of phosphanes and phosphites with other types of nucleophiles (solvent dichloromethane, if not mentioned otherwise).

For some combinations of benzhydrylium ions with phosphanes, rate and equilibrium constants could be determined (Chapter 6.8). Analysis of these data by Marcus theory shows that the intrinsic barriers for these reactions are almost constant (57-59 kJ mol⁻¹).

7. Correlation of the rate constants for the nucleophilic additions of various phosphanes and phosphites to metal- π -complexes determined by Kane-Maguire and Sweigart with the reactivity parameters for P-nucleophiles determined in this work (Chapter 6) yielded approximate E parameters for metal- π -complexes (Figure 0.7).

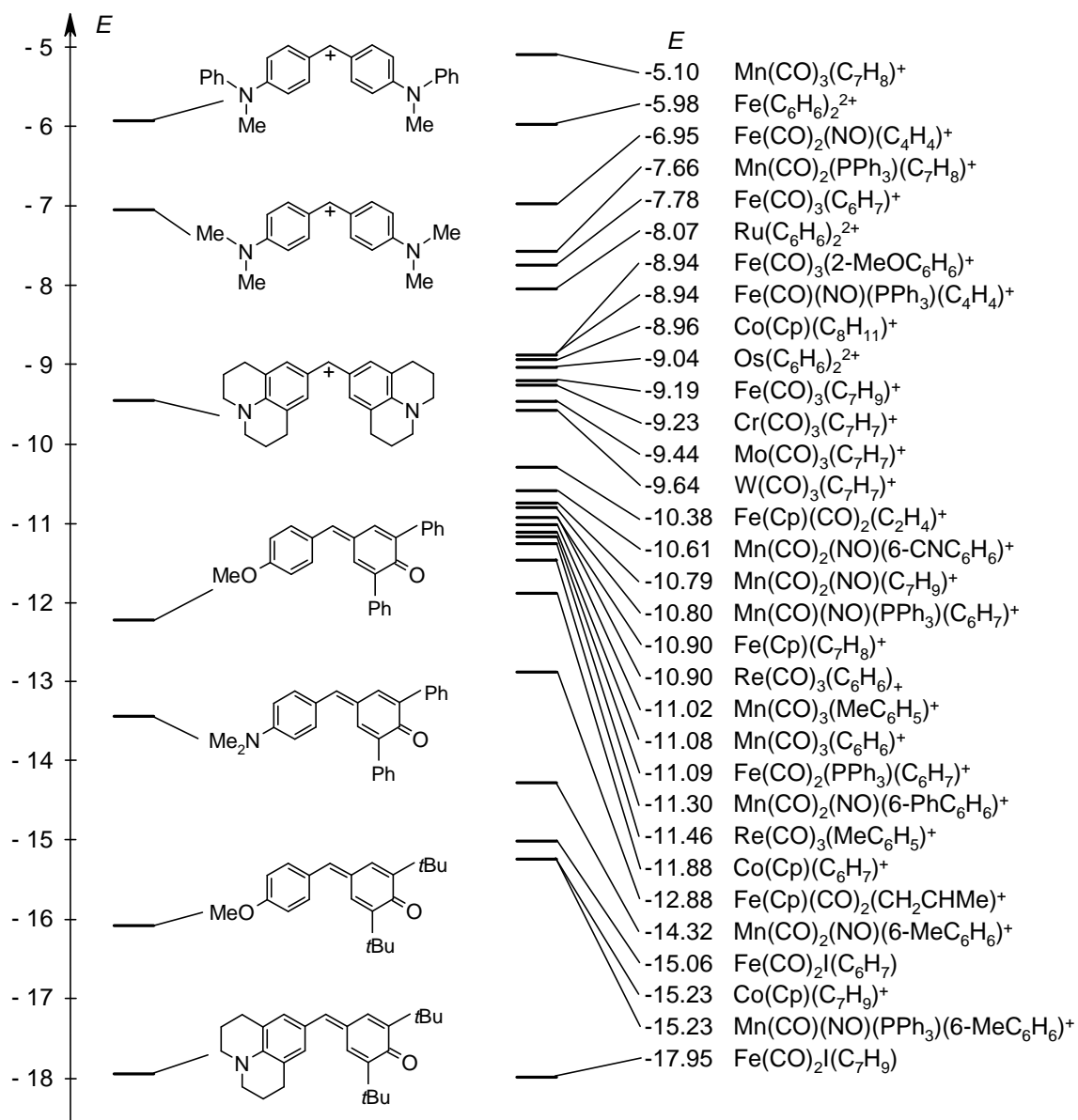
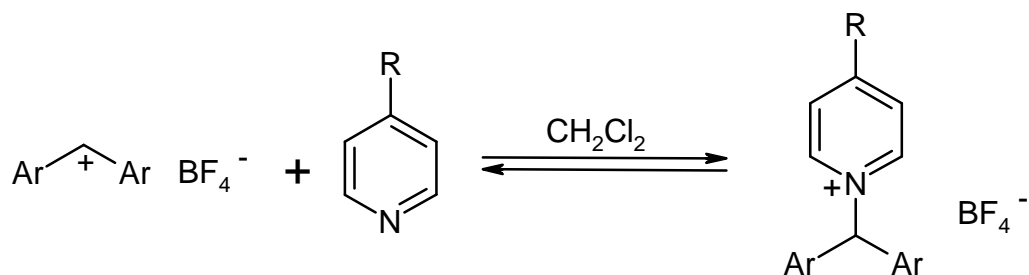


Figure 0.7: Comparison of the electrophilicities E of metal- π -complexes, quinone methides and benzhydryl cations.

8. The nucleophilicities N of several para-substituted pyridines have been determined, by performing kinetic measurements of their reactions with benzhydryl cations (Scheme 0.3).



Scheme 0.3: Addition of benzhydryl salts to para-substituted pyridine derivatives.

Their nucleophilicities range from $N \approx 12$ to $N \approx 17$ (Figure 0.8).

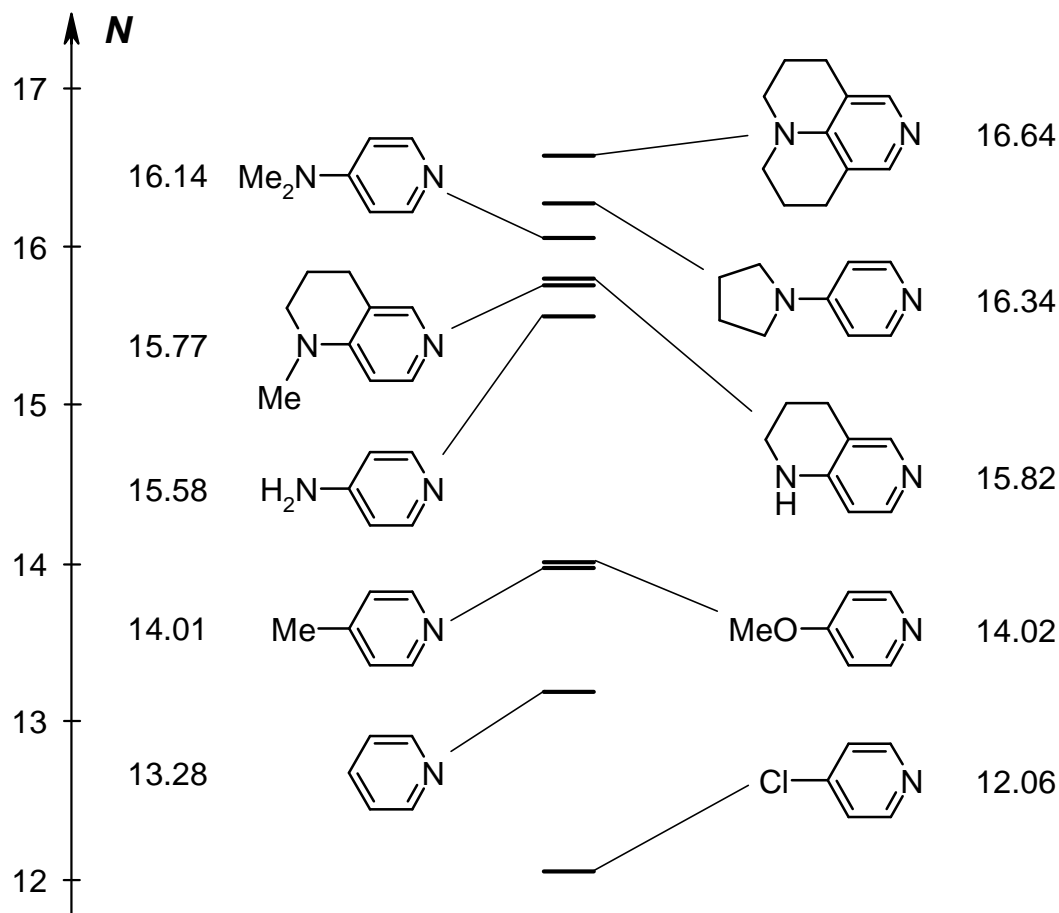
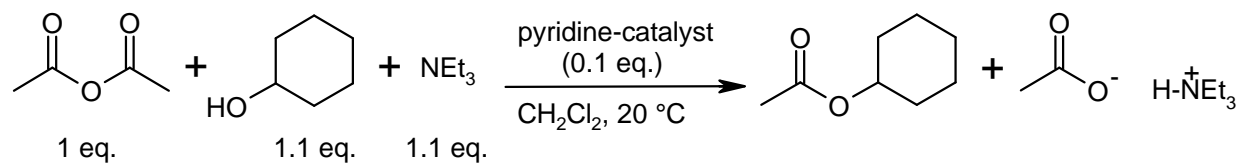


Figure 0.8: Nucleophilicity scale for para-substituted pyridine derivatives with $s = 0.64$.

The occurrence of reversible reactions allowed the determination of rate and equilibrium constants (Chapter 8.4) for some electrophile-nucleophile combinations. The intrinsic barriers calculated by Marcus equation, which were found to range from 50-60 kJ mol^{-1} .

The catalytic activities of para-substituted pyridines were investigated for the acetylation of cyclohexanol with acetic anhydride in methylene chloride (Scheme 0.4).



Scheme 0.4: Base catalyzed acetylation of cyclohexanol with acetic anhydride.

The reaction rates were found to increase linearly with the catalyst concentration, but there is no simple relationship between the nucleophilicity N and the catalytic efficiencies of substituted pyridines.

1. Introduction and objectives

Lapworth was the first who recognized that the reagents of polar organic reactions fall into two categories which he termed "cationoid" and "anionoid" (1925).^[1] Ingold suggested the alternative designations "electrophilic", signifying electron-seeking, and "nucleophilic", signifying nucleus-seeking, for these both classes of compounds.^[2] These two terms are now in general use for discussing organic reactivity.

The first systematic attempt to quantify the kinetic term "nucleophilicity" was reported by Swain and Scott, who investigated the rates of S_N2 reactions in 1953.^[3] They characterized nucleophiles by one parameter (*n*) and electrophiles by two parameters (*s*, log *k*_{water}) according to equation 1.1.^[4]

$$\log (k/k_{\text{water}}) = s n \quad (1.1)$$

The S_N2 reactions of nucleophiles with CH₃Br in water were used as reference reactions (*s* = 1). One year later, Edwards proposed a four-parameter equation in which the basicity and polarizability of the nucleophile were weighted differently according to the electrophile,^[5] but this equation also did not find wide application.

Succeeding investigations added more and more parameters,^[4,5] and finally Bunnett listed 17 factors that have to be considered in a quantitative description of nucleophilicity.^[6] Because the reactivities of nucleophiles towards *trans*-[Pt(py)₂Cl₂] did not correlate with nucleophilicity parameters known at the time, Pearson et al. concluded that "at present (in 1968) it was not possible to predict quantitatively the rates of nucleophilic displacement reactions if a number of substrates of widely varying properties are considered."^[7]

Ritchie's "constant selectivity relationship" attracted much attention because it calculates the rates of the reactions of carbocations or diazonium ions with nucleophiles from only a single parameter for electrophiles (log *k*₀) and a single parameter for nucleophiles (*N*₊) (eq. 1.2).^[8]

$$\log (k/k_0) = N_+ \quad (1.2)$$

This relationship is also referred to as the "constant selectivity relationship", because the relative reaction rates of two nucleophiles (= selectivity) do not depend on the reactivities of the electrophiles. Conversely, the relative reactivity of two electrophiles (= selectivity) is independent of the strength of the nucleophile. It was later shown that equation 1.2 is not strictly valid, and that better correlations are obtained when different families of electrophiles are treated separately.^[9] However, in view of the range of the nucleophilicity scale (approximately 13 orders of magnitude), these discrepancies are negligible to a first approximation. Furthermore, since the behaviour of uncharged electrophiles such as esters,^[10] acceptor-substituted ketones,^[8] and 2,4-dinitrohalobenzenes^[11] also appeared to be consistent with equation 1.2, its impact increases significantly.

Kane-Maguire, Sweigart et al. observed similar correlations in nucleophilic additions of phosphanes, amines, and arenes to metal-coordinated π -electron systems.^[12] The relative reactivities of the metal complexes are independent of the absolute reaction rates of the reference nucleophiles. Since the relative reactivities of phosphorous and nitrogen nucleophiles towards free carbocations and metal-coordinated π -electron systems are equal,^[13] the Kane-Maguire and Sweigart N_{Fe} scale can be considered to be representative for both classes of electrophiles. These results indicated that electrophile-nucleophile combinations that do not involve the cleavage of a C-X bond in the rate determining step follow a much simpler reactivity pattern than the S_N2 type reactions that were investigated earlier.

Constant selectivity relationships are also observed in the addition of diarylcarbenium ions to terminal double bonds, where the new CC bond is formed in the rate-determining step.^[14] The relative reactivities of π -nucleophiles are independent of the electrophilicity of the carbenium ions, even when the absolute reaction rates vary by several orders of magnitude. To satisfactorily describe the reactivities of a larger variety of nucleophiles, the introduction of a second parameter for nucleophiles^[15-17] was found to be necessary. In 1994, Patz and Mayr subjected the rate constants of 327 reactions of carbocations, metal- π -complexes, and diazonium ions with π -, σ -, and n-nucleophiles (Figure 1.1) to a correlation analysis on the basis of Equation 1.3,^[15]

$$\log k_{(20^\circ\text{C})} = s(N + E) \quad (1.3)$$

where E is the electrophilicity parameter, N is the nucleophilicity parameter, and s is the nucleophile-dependent slope parameter.

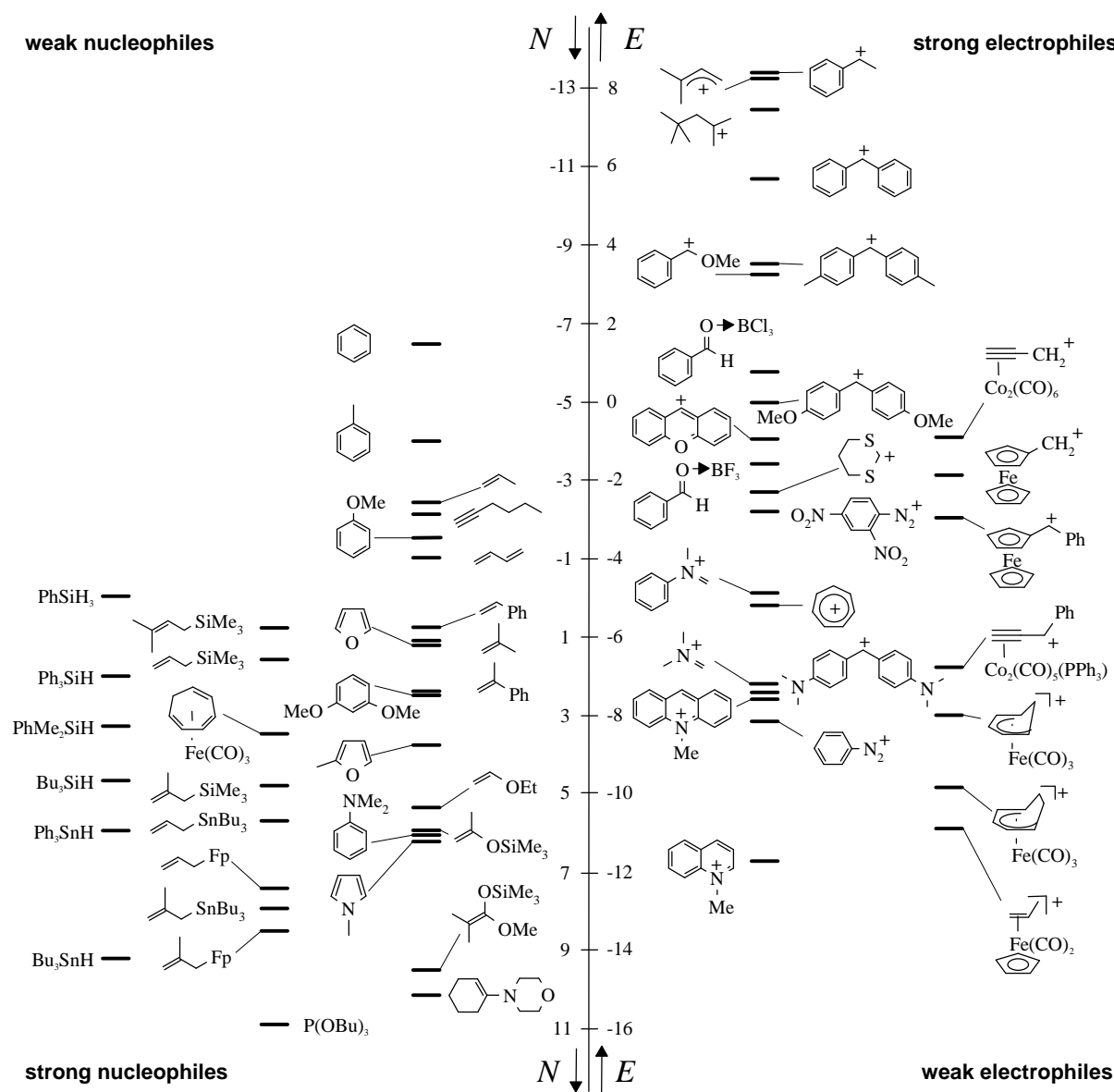


Figure 1.1: Reactivity scales of carbocations, metal- π -complexes, diazonium ions, and π -, σ -, n -nucleophiles developed by Patz and Mayr in 1994.^[15]

Despite the large structural variety of substrates and reactions considered, the rate constants k calculated by the three-parameter eq. 1.3 were usually found to be accurate within a factor of 10-100, when reagents of obvious steric bulk (e.g. tritylium ions) were excluded. This precision is quite remarkable in view of the fact that each of the scales covered more than 18 orders of magnitude, resulting in an overall reactivity range of approximately 36 orders of magnitude (Figure 1.1).

Since 1994 numerous other types of reactions have been found to follow eq. 1.3. N and s parameters of further classes of nucleophiles, e. g. amine boranes,^[18] metal- π -complexes,^[19,20] heteroarenes,^[21] silyl enol ethers,^[22] and silyl ketene acetals,^[22] have been determined, as well as E parameters of several new electrophiles.

In order to cope with the steadily increasing amount of data, a systematic way of parametrization became necessary. When I joined the group for my diploma thesis in September 1999 a concerted effort by five diploma and doctoral students started to develop a list of reference electrophiles and nucleophiles of widely varying reactivity that can be used for characterizing any further nucleophiles and electrophiles. My contribution to this program is documented in my diploma thesis^[23] and in Chapter 3 of this PhD thesis.

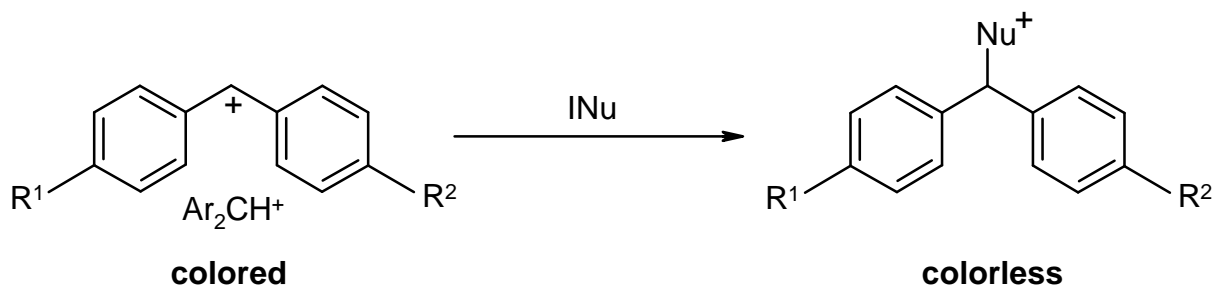
In the second part of this work, the reference compounds should be employed for characterizing the reactivities of various new n - and π -nucleophiles, as well as of new electrophiles. The data shall then be used for discussing structure-reactivity relationships, the validity of eq. 1.3 for new classes of compounds, as well as for the analysis of mechanistic aspects.

Since some of the reactions of electrophiles with nucleophiles were expected not to proceed quantitatively, equilibrium constants should also be determined. By the combination of rate and equilibrium constants intrinsic barriers should be determined, which are a key to the understanding of organic reactivity.

2. Kinetic methods and calculation of rate constants

2.1 Introduction

Diarylcarbenium ions Ar_2CH^+ absorb light in the visible region of the electromagnetic spectrum. The p-amino substituted representatives have absorption maxima at $\lambda_{\text{max}} = 590 - 680 \text{ nm}$. The attack of nucleophiles at the diarylcarbenium ions converts the sp^2 -carbenium center into an sp^3 center which is associated with the disappearance of the color (Scheme 2.1).



Scheme 2.1: Reaction of a colored diarylcarbenium ion Ar_2CH^+ with a nucleophile to form a colorless product.

Reactions of diaryl carbenium ions Ar_2CH^+ with nucleophiles can easily be studied by UV-Vis spectroscopy, by observing the decay of absorption with time. At low concentrations a linear relationship between absorption and concentration exists, which is described by the Lambert-Beer law (eq. 2.1).

$$A = \epsilon cd \quad (2.1)$$

with: A = absorbance, ϵ = molar absorption coefficient, c = concentration, d = thickness of the cell.

According to eq. 2.1, the concentrations of diaryl carbenium ions during a chemical reaction can be derived from the absorbance as a function of time.

2.2 Irreversible reactions

For the evaluation of rate constants, a second-order rate law, according to the mechanism shown in Scheme 2.1, was assumed. This reaction is first order in the concentration of the electrophile El (Ar_2CH^+) and first order in the concentration of the nucleophile Nu (equation

2.2). Equation 2.2 is only fulfilled for irreversible reactions with complete conversion of the electrophile.

$$\frac{d[El]}{dt} = -k_2[El][Nu] \quad (2.2)$$

Experiments with nucleophile concentrations at least 10 times higher than the electrophile concentrations give rise to pseudo-first-order kinetics with an exponential decay of the electrophile concentration with time. Under such conditions, the nucleophile concentration remains almost constant during the reaction, which simplifies equation 2.2 to 2.3.

$$\frac{d[El]}{dt} = -k_{1\psi}[El] \quad \text{with } k_{1\psi} = k_2[Nu] \quad (2.3)$$

Integration of the differential equation 2.3 leads to equation 2.4.

$$\ln[El] = -k_{1\psi}t + \ln[El]_0 \quad (2.4)$$

Since the absorbances correlate linearly with the concentrations of the diarylcarbenium ions (eq. 2.1), concentrations can be substituted by absorbances, which converts eq. 2.4 into eq. 2.5.

$$\ln A = -k_{1\psi}t + \ln A_0 \quad (2.5)$$

The plot of $\ln A$ versus t is a straight line with the slope corresponding to the pseudo-first-order rate constant $k_{1\psi}$. For all kinetic experiments performed in this work, a linear correlation between $\ln A$ and t was observed, which proves first-order with respect to the electrophile.

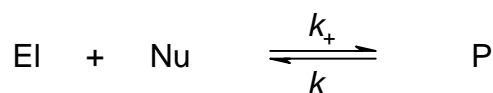
The second-order rate constant k_2 is obtained by division of the pseudo-first order rate constant $k_{1\psi}$ by the concentration of the nucleophile $[Nu]$ (eq. 2.6).

$$k_2 = \frac{k_{1\psi}}{[Nu]} \quad (2.6)$$

In all kinetic experiments, which were performed at variable concentrations of the nucleophile, the same values of the second-order rate constants k_2 were obtained. This proves a first-order dependence on the concentration of the nucleophile.

2.3 Reversible reactions

In the case of reversible chemical reactions, the consumption of the benzhydrylium ions and the decay of their absorbances is incomplete (Scheme 2.2).



Scheme 2.2: Reversible reaction of an electrophile El with a nucleophile Nu.

The determination of rate constants for reversible reactions is only possible, when the concentrations stay constant after reaching the equilibrium, i. e., when eventual consecutive reactions of the products are very slow (in the case of very fast consecutive reactions, the initial electrophile-nucleophile combination becomes irreversible).

Reversible reactions with nucleophile concentrations much higher than the electrophile concentrations, yield pseudo-first-order kinetics for the forward reaction (k_+), with $k_{1\psi+} = k_+[\text{Nu}]$. The reverse reaction (k_-) is first-order with respect to the concentration of the product P (eq. 2.7).

$$-\frac{d[\text{El}]}{dt} = \frac{d[\text{P}]}{dt} = k_{1\psi+}[\text{El}] - k_-[\text{P}] \quad (2.7)$$

Substitution of the concentrations by the absorbances and integration of the differential equation 2.7 yields equation 2.8.

$$\ln \frac{A_0 - A_\infty}{A - A_\infty} = (k_{1\psi+} + k_-)t = k_{\text{eff}}t \quad (2.8)$$

Therefore, a graph of $\ln (A - A_\infty)$ versus t gives a straight line of slope $(k_{1\psi+} + k_-) = k_{\text{eff}}$ as reported in ref. [24]. When varying the concentration of the nucleophile ($[\text{Nu}] \gg [\text{El}]$), a linear plot of k_{eff} versus $[\text{Nu}]$ is obtained, the slope of which equals k_+ (second-order rate constant of the forward reaction). The intercept on the ordinate yields k_- (first-order rate

constant of the backward reaction). In the case of simple second-order kinetics with negligible opposing reaction, and in absence of parallel reaction, the rate of which does not depend on [Nu], the straight line will pass through the origin.

The division of the rate constant for the forward reaction k_+ by the rate constant for the backward reaction k_- yields the equilibrium constant K (eq. 2.9).

$$K = \frac{k_+}{k_-} \quad (2.9)$$

For reversible reactions with fast forward reactions, and slow backward reactions (large equilibrium constants), the calculation of K by eq. 2.9 is not very accurate.

A more precise method for the determination of equilibrium constants for reversible reactions derives K directly from the UV-Vis absorbances of the diarylcarbenium ions in the presence of variable concentrations of the nucleophiles (eq. 2.10).

$$K = \frac{[EI]_0 - [EI]}{[EI]([Nu]_0 - [EI]_0 + [EI])} \quad (2.10)$$

2.4 Temperature dependence of the rate constants

It is well known that the rates of chemical reactions usually increase with temperature. The temperature dependence of the rate constants can be described by the Arrhenius equation 2.11.

$$\ln k = \ln A - \frac{E_a}{RT} \quad (2.11)$$

with: k = rate constant at temperature T , A = pre-exponential factor, E_a = Arrhenius activation energy, R = universal gas constant.

The plot of $\ln k$ versus $1/T$ gives a straight line, which allows one to calculate E_a from the slope and A from the intercept on the ordinate.

Alternatively the temperature dependence of the rate constants can be described by the Eyring equation 2.12.

$$\ln \frac{k}{T} = \ln \frac{k_b}{h} - \frac{\Delta H^\ddagger}{RT} + \frac{\Delta S^\ddagger}{R} \quad (2.12)$$

with: k = rate constant at temperature T , k_b = Boltzmann constant, h = Planck's constant, ΔH^\ddagger = Eyring activation enthalpy, ΔS^\ddagger = Eyring activation entropie, R = universal gas constant.

When plotting $\ln(k/T)$ versus $1/T$, a straight line is obtained; its slope provides ΔH^\ddagger and its intercept yields ΔS^\ddagger .

When kinetic experiments with diarylcarbenium ions and nucleophiles were performed at variable temperatures (-70 – 0 °C), the reported values of k (20 °C) have been derived from the Eyring parameters.

2.5 Kinetic instruments

The rates of slow reactions ($\tau_{1/2} > 10$ s) were determined by using a J&M TIDAS diode array spectrophotometer, which was controlled by Labcontrol Spectacle software and connected to a Hellma 661.502-QX quartz Suprasil immersion probe (5 mm light path) via fiber optic cables and standard SMA connectors (Figure 2.1). The combination of a tungsten lamp (10 W) with a deuterium lamp (35 W) as light sources provided a detectable range of wavelengths from 200 to 1000 nm.

Kinetic measurements were made in Schlenk glassware with exclusion of moisture. The temperature of solutions during all kinetic studies was kept constant (usually 20 ± 0.2 °C) by using a circulating bath thermostat and monitored with a thermocouple probe that was inserted into the reaction mixture (Figure 2.1).

The TIDAS diode array spectrophotometer provided multiwavelength measurements by taking complete absorption spectra in constant time intervals (example in Figure 2.2). These data were saved as 3d-files on an IBM-compatible PC.



Figure 2.1: J&M TIDAS diode array spectrometer connected to Hellma 661.502-QX quartz Suprasil immersion probe via fiber optic cables.

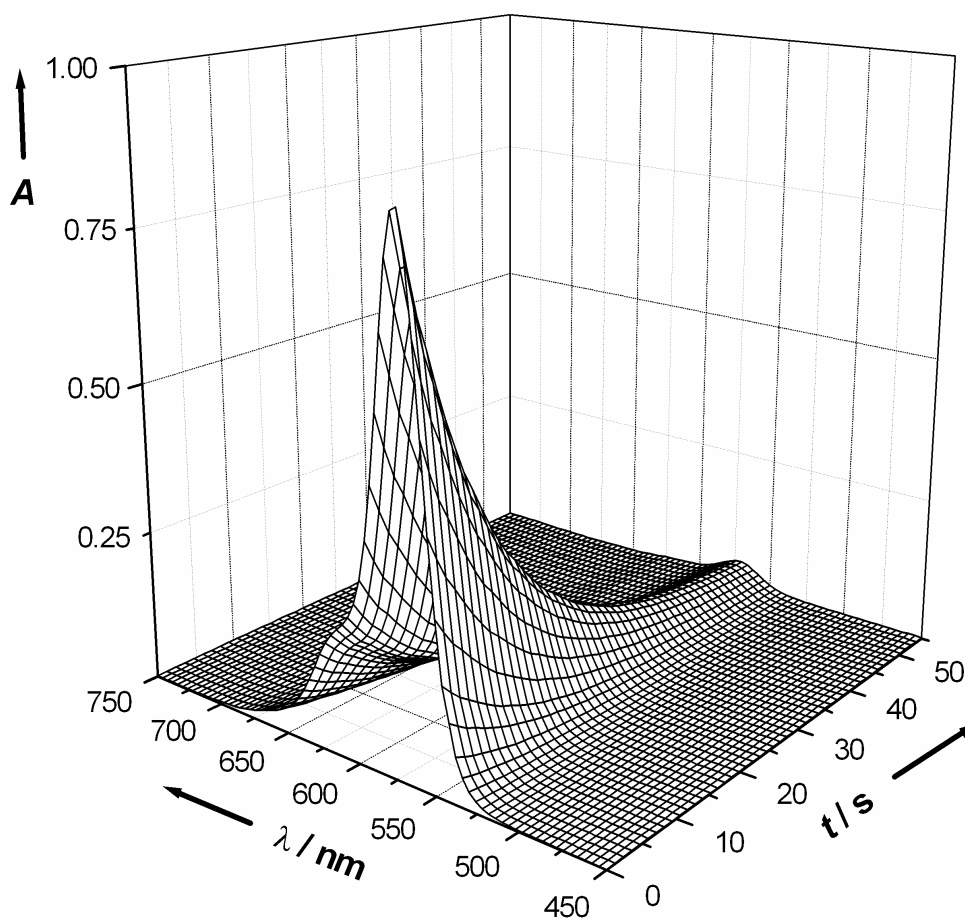


Figure 2.2: Example of multiwavelength kinetic measurements.

For the evaluation of rate constants, absorption-time curves at the absorption maxima of the employed diarylcarbenium ions Ar_2CH^+ were extracted. These curves were evaluated as described at the beginning of this chapter.

UV-Vis kinetic measurements of rapid reactions ($\tau_{1/2} < 10$ s) were performed on a Hi-Tech SF-61DX2 stopped flow spectrophotometer system (Figure 2.3) and controlled by using Hi-Tech KinetAsyst 2 software running on an IBM-compatible PC. The kinetic experiments were initiated by rapidly mixing equal volumes of the nucleophile and the diarylcarbenium salt solution, using syringes with pneumatically driven pistons (Figure 2.3, left side).

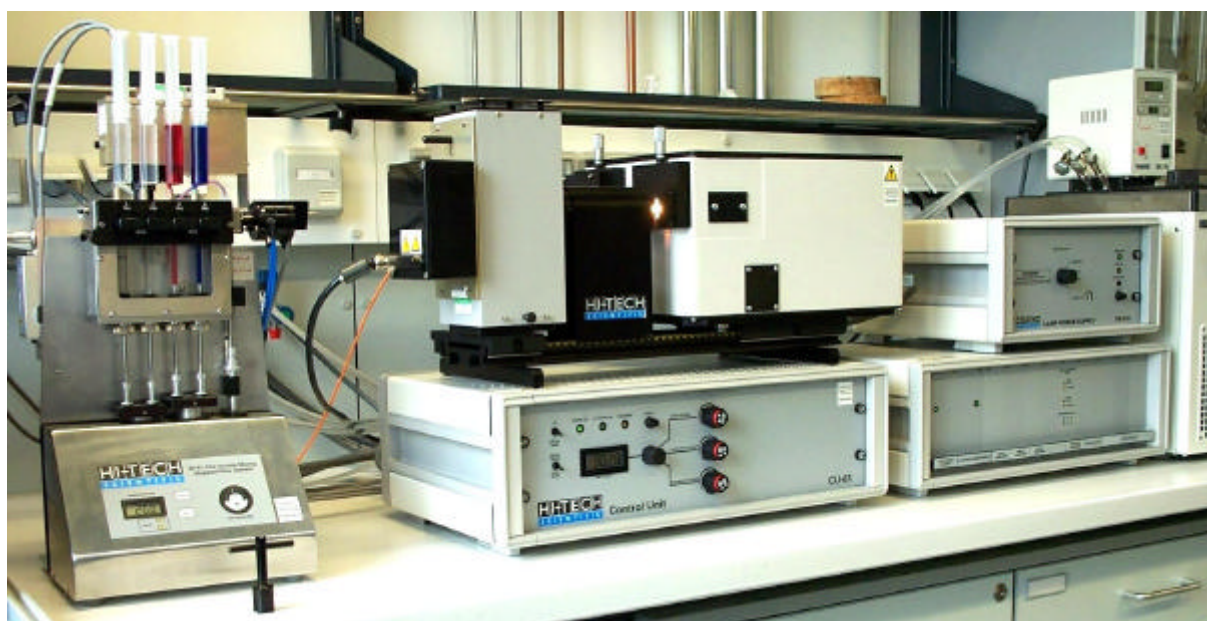


Figure 2.3: Hi-Tech SF-61DX2 stopped-flow spectrophotometer.

The temperature of the solutions was controlled within ± 0.1 °C by using a circulating water bath monitored with the Pt resistance thermometer of the SF-61DX2 mixing unit. The pseudo-first-order rate constants k_{obs} for the reactions of diarylcarbenium ions with nucleophiles were obtained from at least five runs at each nucleophile concentration by least-squares fitting of the absorbance data to the single exponential $A = A_0 \exp(-k_{\text{obs}}t) + C$ (example in Figure 2.4).

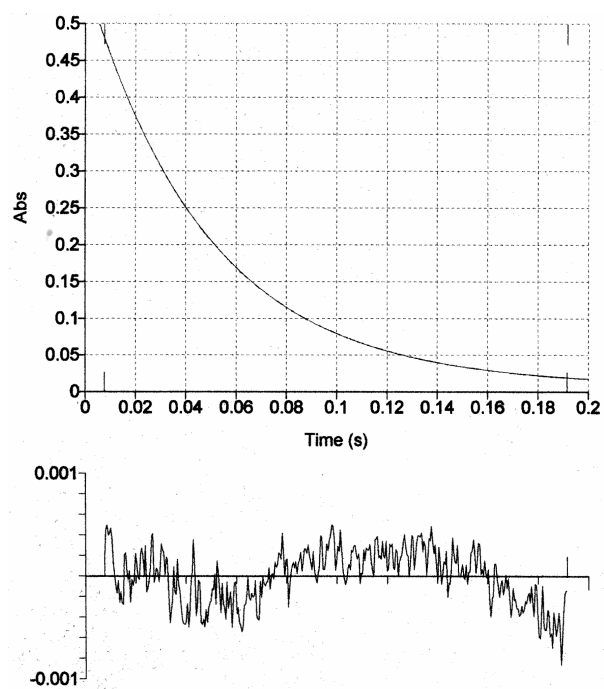


Figure 2.4: Exponential decay of the absorbance in the reaction of Ar_2CH^+ with nucleophiles (upper plot). The plot of $A_{\text{exp}} - A_{\text{calc}}$ vs t (lower plot) shows the quality of the fit.

3. Reference scales for the characterization of cationic electrophiles and neutral nucleophiles

3.1 Introduction

In 1994, Patz and Mayr introduced eq. 1.3 which describes the rates of a large variety of electrophile-nucleophile combinations by three reactivity parameters (see Chapter 1).^[15] The rates of 327 reactions of carbocations, metal- π -complexes, and diazonium ions with π -, σ -, and n-nucleophiles were subjected to a correlation analysis on the basis of eq. 1.3 to calculate the reactivity parameters of the employed electrophiles and nucleophiles. Since then many other types of reactions have been found to follow eq. 1.3. The reactivity parameters of these new compounds were calculated on the basis of the reactivity parameters, determined in 1994.

In order to cope with the steadily increasing amount of data a systematic way of parametrization was necessary. We discussed different models how to do this parametrization:

- One possibility would be to determine the electrophilicities or nucleophilicities of new compounds by using the E , N , and s parameters, which were published in 1994. In this case the originally published parameters^[15] are kept unchanged. But as a consequence, rate constants that had entered the data collection at an early stage (before 1994) received higher weight than data that were introduced later.
- An alternative and more consequent way of handling the kinetic data would be a complete correlation analysis of all available rate constants after the addition of each new entry. This procedure is not practicable, however, because it would continuously alter all reactivity parameters and thus cause confusion.
- The third way would be to define a basis set of well-behaved reference electrophiles and nucleophiles. The reactivity range in both scales must cover several orders of magnitude to achieve a wide applicability. After deriving the E , N , and s parameters, of the reference systems, these values should be kept constant in the future.

After comparing the advantages and disadvantages of these three possibilities, the third method was chosen to be the best.

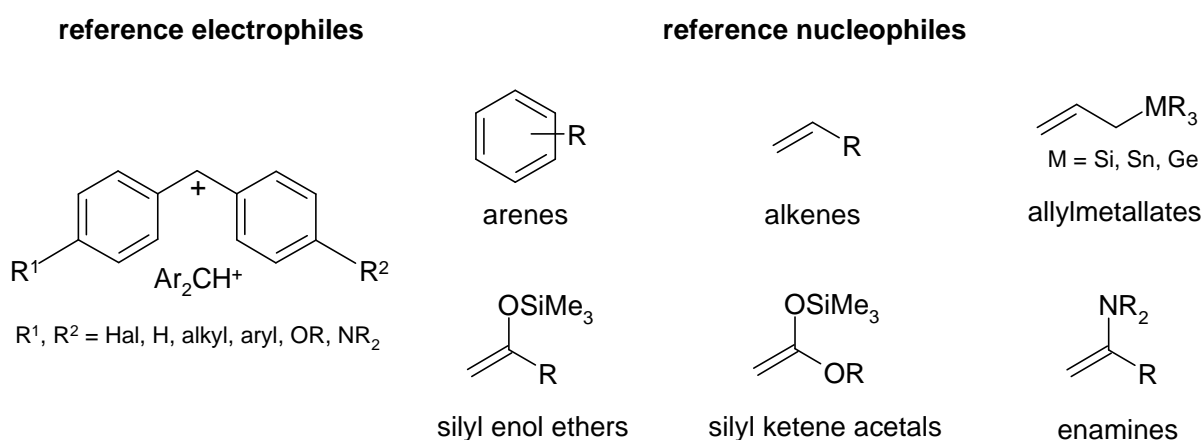
3.2 Definition of reference compounds

When looking back at the experiences, which were made in this working group in the 1990s, one can see that rate constants referring to certain classes of electrophiles and nucleophiles follow eq. 1.3 better than rate constants referring to compounds from other classes. Therefore, it seems to be reasonable to choose compounds, which fit best, as reference compounds.

Previous work has shown perfect linear reactivity-reactivity correlations for reactions of benzhydryl cations Ar_2CH^+ (Scheme 3.1) with numerous classes of nucleophiles,^[15,25] probably because the steric situation at the reaction centers is kept constant while the reactivities of the benzhydrylium ions are modified by variation of the para substituents in a wide range.

The reactions of benzhydrylium ions with many types of nucleophiles, including aliphatic and aromatic π -systems, metal π -complexes, hydride donors, and n-nucleophiles, follow linear reactivity-reactivity correlations of comparable quality.^[15] For that reason, representatives of all of these classes of compounds may be considered as potential reference nucleophiles.

Since carbon-carbon double-bonded systems, including substituted benzenes, heteroarenes, alkenes, allylsilanes, silyl enol ethers, and enamines, represent the largest group of structurally related nucleophiles,^[26] because all these compounds share an sp^2 -hybridized carbon atom as the center of nucleophilicity, representatives of these classes of compounds were selected as reference nucleophiles (Scheme 3.1).



Scheme 3.1: Reference electrophiles and reference nucleophiles for defining the basis-set.

3.3 Starting situation

Numerous benzhydrylium ions with $6 > E > 0$ had been characterized before this work. The 4,4'-bis(dimethylamino)benzhydrylium ion had been the only diarylcarbenium ion with $E < -3$ studied in 1999. For the construction of benzhydryl cation based reactivity scales, the characterization of more benzhydryl cations with $E < -3$ was, therefore, necessary (Figure 3.1).

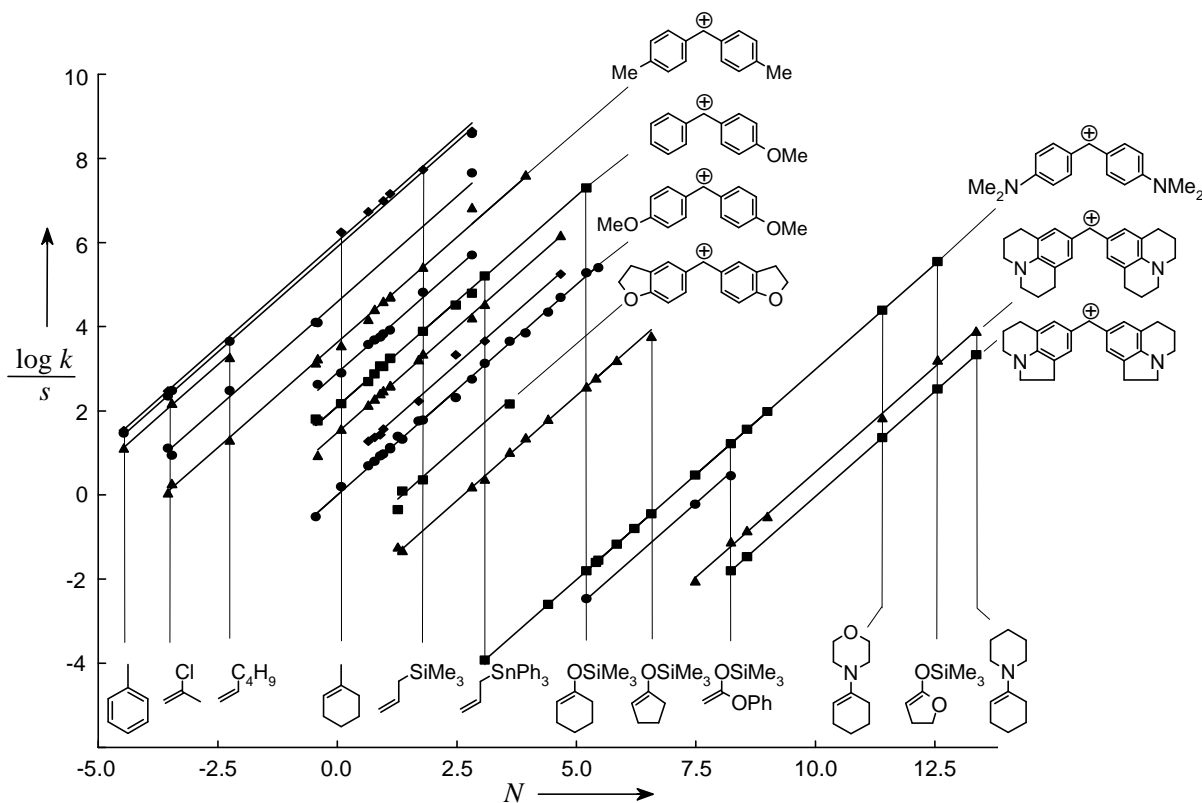


Figure 3.1: Plot of $(\log k)/s$ versus N for the reactions of benzhydryl cations Ar_2CH^+ with π -nucleophiles (situation in spring 2000).

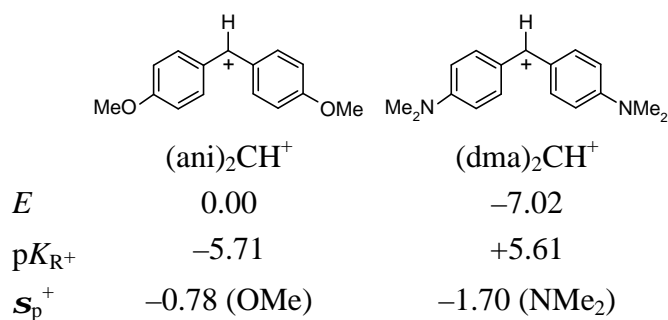
In my diploma work, I had synthesized two polycyclic para-amino substituted benzhydryl cations (Figure 3.1, two correlation lines on the far right side).^[23] The characterization of their electrophilicities E indicated that these new compounds are less reactive than the 4,4'-bis(dimethylamino)benzhydrylium ion by several orders of magnitude. Up to now (2003), these two compounds are the least electrophilic benzhydrylium ions so far characterized.

Figure 3.1 shows the situation in spring 2000. There are large gaps around the correlation line for the 4,4'-bis(dimethylamino)-benzhydrylium ion ($E \approx -7$). Some of the correlation lines are not very long, which means that the E parameters for these compounds are not well

corroborated. It was obvious, that the gaps in Figure 3.1 had to be closed, in order to obtain multiple overlap of the correlation lines and reference compounds with statistically corroborated reactivity parameters.

3.4 Seeking for new reference compounds

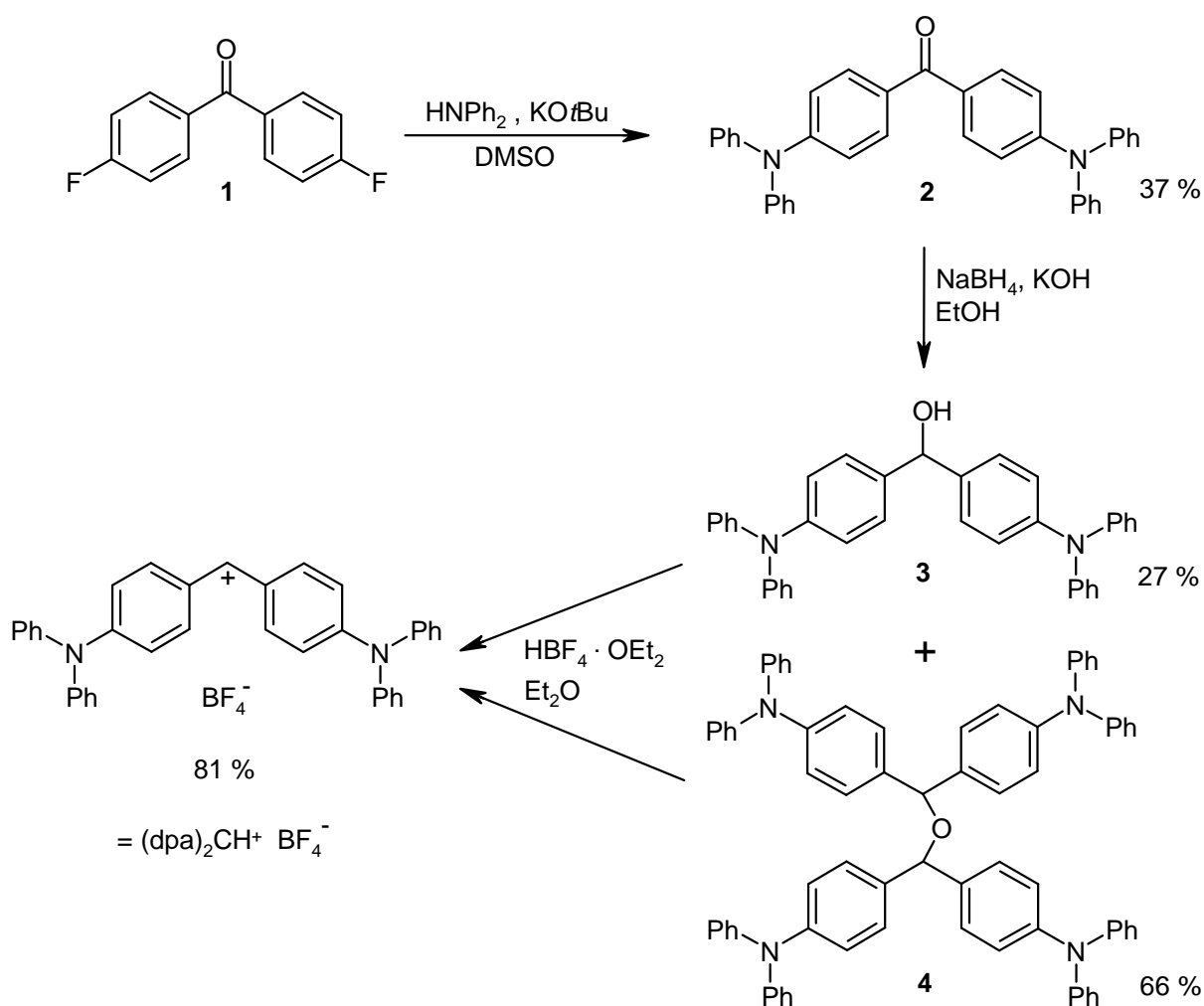
Since previous work showed a correlation between pK_{R^+} values and the electrophilicity parameters E of carbocations,^[17,27] the search for benzhydrylium ions with $pK_{R^+} > -5.71$ (for $(\text{ani})_2\text{CH}^+$) was necessary. However, while dozens of benzhydrylium ions with $pK_{R^+} < -5.71$ had been reported in literature,^[28,29] the 4,4'-bis(dimethylamino)-substituted benzhydryl cation $(\text{dma})_2\text{CH}^+$ was the only one with a higher pK_{R^+} value so far characterized. The surprising lack of compounds in this range mirrors the shortage of substituents with Hammett σ_p^+ parameters more negative than -0.78 .^[30,31]



In collaboration with other members of this group (T. Bug, B. Janker, R. Loos, G. Remennikov) new benzhydrylium cations were synthesized to fill in the gaps in the less reactive part of the electrophilicity scale. It was my task in this collaborative effort to identify benzhydrylium ions which are less electrophilic than the 4,4'-bis-methoxybenzhydrylium ion $(\text{ani})_2\text{CH}^+$ and more electrophilic than the 4,4'-bis(dimethylamino)benzhydrylium ion $(\text{dma})_2\text{CH}^+$ (see Figure 3.1), i. e. benzhydrylium ions with substituents in para-position which have electron donating effects between that of the methoxy- and that of the dimethylamino group. 4,4'-Diaminobenzhydrylium ions with electron acceptors or weaker electron donors than methyl at nitrogen should fulfill this criterion.

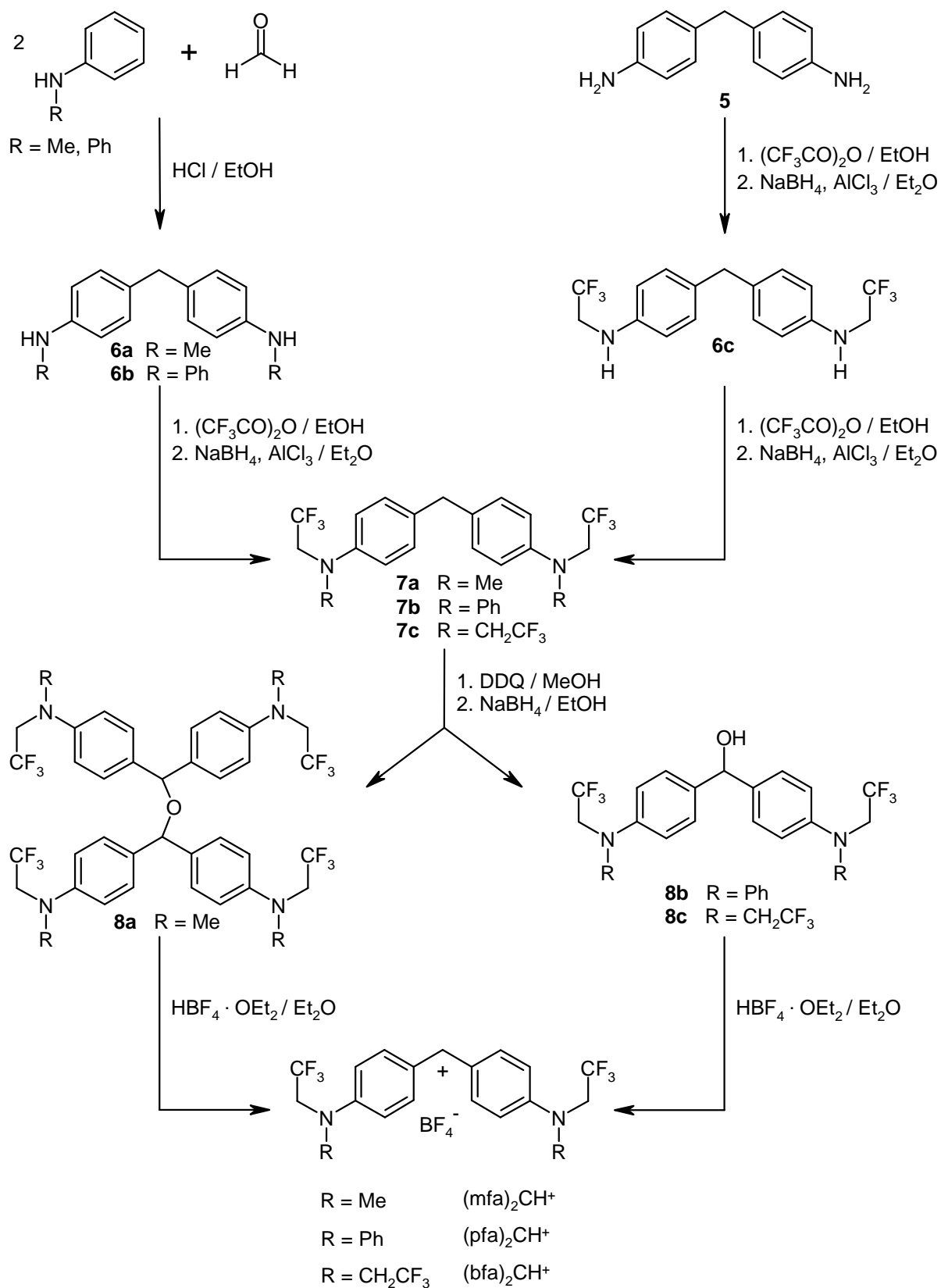
Preliminary results of H. Schimmel^[32] had indicated that phenyl groups instead of methyl groups at the nitrogen atoms of the 4,4'-diaminobenzhydrylium ion reduce its reactivity remarkably. Therefore, the 4,4'-bis(diphenylamino)benzhydrylium ion $(\text{dpa})_2\text{CH}^+$ was synthesized according to literature procedures (Scheme 3.2).

The 4,4'-bis(diphenylamino)-substituted benzophenone **2** was obtained in 37 % yield by heating dimethyl sulfoxide solutions of 4,4'-difluorobenzophenone **1** and excess of diphenylamine in the presence of potassium *tert*-butoxide, as described by Hepworth et al.^[33] (Scheme 3.2). Reduction of **2** with sodium borohydride^[33] gave a mixture of 4,4'-bis(diphenylamino)benzhydrol (**3**) and the bis(diarylmethyl) ether **4** in 27 % and 66 %. Treatment of the benzhydrol **3** or the ether **4** with tetrafluoroboric acid in ether generated the corresponding tetrafluoroborate $(\text{dpa})_2\text{CH}^+ \text{BF}_4^-$ with 81 % yield.



Scheme 3.2: Synthetic route for preparing the benzhydyl tetrafluoroborate $(\text{dpa})_2\text{CH}^+ \text{BF}_4^-$.

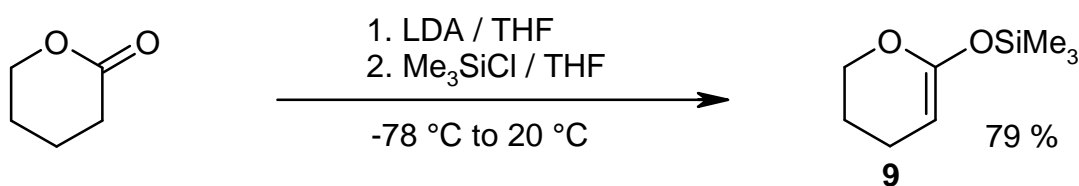
Another group member (Dr. G. Remennikov) developed syntheses of the tetrafluoroborates of $(\text{mfa})_2\text{CH}^+$, $(\text{pfa})_2\text{CH}^+$, and $(\text{bfa})_2\text{CH}^+$, which contain trifluoroethyl groups at the nitrogen atoms (Scheme 3.3).



Scheme 3.3: Synthesis of the tetrafluoroborates of (mfa)₂CH⁺, (pfa)₂CH⁺, and (bfa)₂CH⁺ by Dr. G. Remennikov.

The diarylmethanes **6a,b** were synthesized by acid promoted condensation of two equivalents of *N*-methylaniline ($R = \text{Me}$) or diphenylamine ($R = \text{Ph}$) with formaldehyde according to ref. [34]. Trifluoroacetylation of **6a,b** with trifluoroacetic acid anhydride and reduction with sodium borohydride leads to **7a,b**. Bis(4-bis(trifluoroethyl)aminophenyl)-methane **7c** was obtained by repeated trifluoroacetylation of bis(4-aminophenyl)methane **5** and reduction of the resulting trifluoroacetyl amides with sodium borohydride. Oxidation of the diarylmethanes **7a-c** with DDQ^[35] and reduction of the resulting benzophenones with sodium borohydride gave the bis(diarylmethyl) ether **8a** ($R = \text{Me}$) and the benzhydrols **8b** and **8c** ($R = \text{Phe}$, CH_2CF_3), respectively (Scheme 3.3). Treatment of these compounds with tetrafluoroboric acid in diethylether yielded the corresponding benzhydrylium salts $(\text{mfa})_2\text{CH}^+ \text{BF}_4^-$, $(\text{pfa})_2\text{CH}^+ \text{BF}_4^-$, and $(\text{bfa})_2\text{CH}^+ \text{BF}_4^-$.

Because of the shortage of reference nucleophiles with $N \approx 10$ (Figure 3.1), the characterization of π -nucleophiles in this range appeared to be desirable. Since trimethylsilyloxycyclohexene was found to be 20 times less nucleophilic than trimethylsilyloxycyclopentene (**16**), and 2-trimethylsiloxy-4,5-dihydrofuran (**55**), the lower homologue of **9**, was known to have $N \approx 12$, compound **9** was expected to possess a suitable reactivity. Therefore, **9** was synthesized according to procedures described in literature (Scheme 3.4). Deprotonation of tetrahydro-pyran-2-one with LDA in THF and silylation with chlorotrimethylsilane yielded **9** in 79 %.^[36]

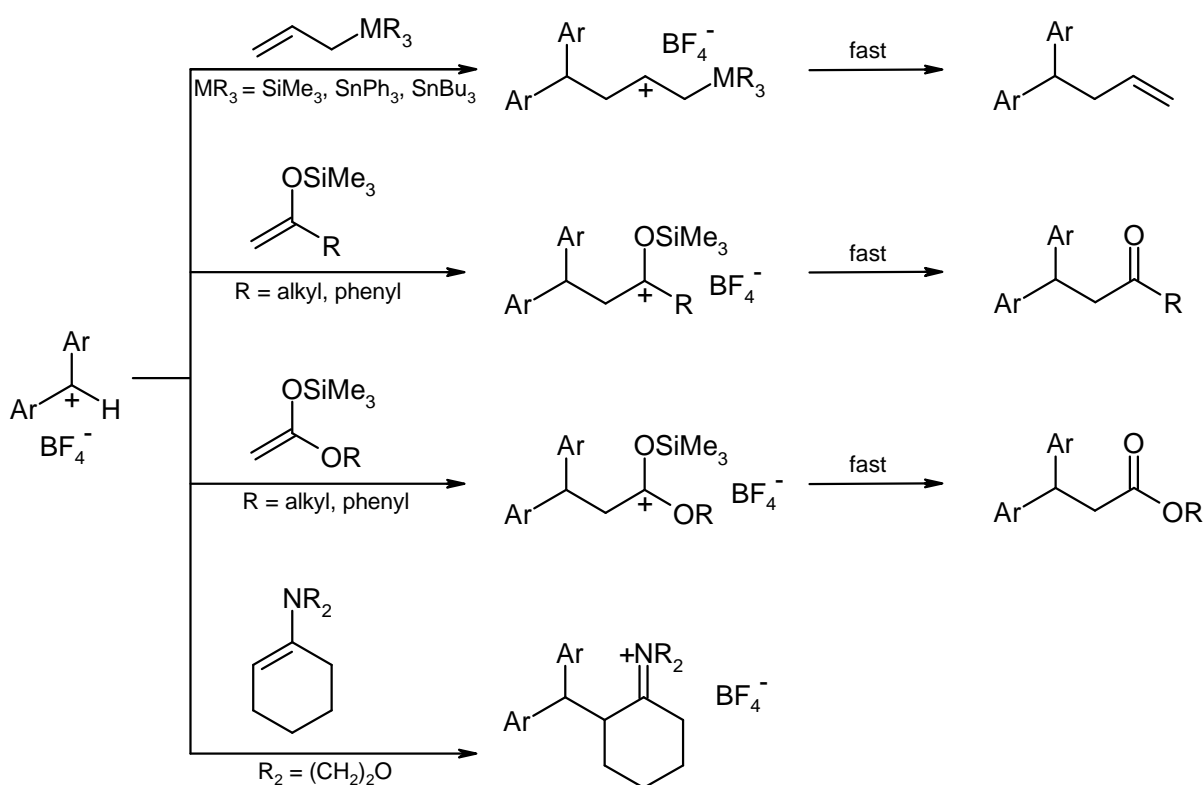


Scheme 3.4: Synthesis of 2-(trimethylsiloxy)-5,6-dihydro-4*H*-pyran (**9**).

3.5 Reactions of reference electrophiles with reference nucleophiles

For the extension and completion of the basis-set (see Chapter 3.3 and 3.4), many rates of the combinations of reference electrophiles and reference nucleophiles were determined by UV-Vis spectroscopy. The procedure of determination and evaluation of rate constants is described in detail in Chapter 2. Parallel to the kinetic investigations, reaction products of some of these combinations were isolated and characterized, to prove the course of the kinetically investigated reactions.

In Scheme 3.5, the reactions of diarylcarbenium ions with different types of π -nucleophiles (allyl silanes and stannanes, silyl enol ethers, silyl ketene acetals, and enamines) are shown. Electrophilic attack at the π -bond yields cationic adducts, which usually undergo fast consecutive reactions (Scheme 3.5), as proven by the independence of the reaction rates of the nature and concentration of the counterion.^[22,37,38] The reaction products characterized during this work are listed in the right column of Table 3.1, and are generally analogous to those identified in previous investigations.^[21,22,38,39]



Scheme 3.5: Reactions of benzhydryl cations with π -systems (allylsilanes and allylstannanes, silyl enol ethers and silyl ketene acetals, enamines).

For characterizing the reactivities of the four new benzhydryl cations $(\text{dpa})_2\text{CH}^+$, $(\text{mfa})_2\text{CH}^+$, $(\text{pfa})_2\text{CH}^+$, and $(\text{bfa})_2\text{CH}^+$ and the new silyl ketene acetal **9**, many kinetic experiments were performed. Table 3.1 lists the second-order rate constants k_2 of the combinations of reference electrophiles and reference nucleophiles, as well as the Eyring activation parameters of these reactions (where available). Yields of isolated products **9a-f-20a-f** are shown in the last column of Table 3.1.

Table 3.1: Rate constants, Eyring activation-parameters, and yields of identified products for reactions of reference electrophiles with reference nucleophiles.

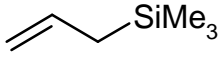
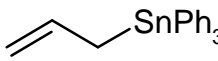
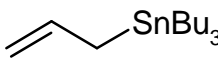
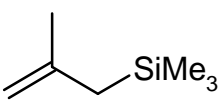
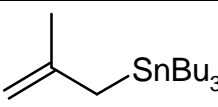
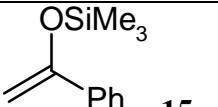
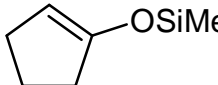
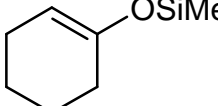
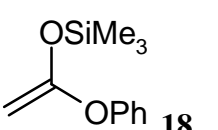
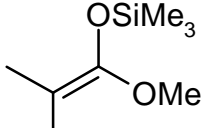
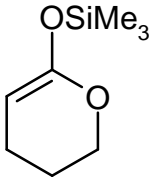
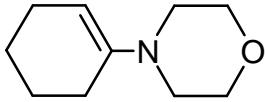
Nucleophile	Ar ₂ CH ⁺	<i>k</i> (20 °C) / L mol ⁻¹ s ⁻¹	ΔH^\ddagger / kJ mol ⁻¹	ΔS^\ddagger / J mol ⁻¹ s ⁻¹	Products ^[a]
 10	(bfa) ₂ CH ⁺	1.77	---	---	[b]
 11	(mfa) ₂ CH ⁺	2.24 × 10 ⁻¹	---	---	[b]
	(pfa) ₂ CH ⁺	1.07	---	---	[b]
 12	(dpa) ₂ CH ⁺	6.40	---	---	12a (56 %)
	(mfa) ₂ CH ⁺	2.84 × 10 ¹	---	---	12b (80 %)
	(pfa) ₂ CH ⁺	1.13 × 10 ²	---	---	12c (76 %)
 13	(dpa) ₂ CH ⁺	6.13 × 10 ⁻¹	---	---	13a (75 %)
	(mfa) ₂ CH ⁺	2.97	---	---	13b (76 %)
	(pfa) ₂ CH ⁺	1.35 × 10 ¹	---	---	13c (72 %)
 14	(mfa) ₂ CH ⁺	1.80 × 10 ³	---	---	[b]
	(pfa) ₂ CH ⁺	6.93 × 10 ³	---	---	[b]
 15	(pfa) ₂ CH ⁺	8.42 × 10 ²	24.28	-105.95	15a (55 %)
 16	(dpa) ₂ CH ⁺	5.80 × 10 ¹	24.34	-128.00	16a (81 %)
	(mfa) ₂ CH ⁺	3.19 × 10 ²	24.92	-111.83	16b (70 %)
 17	(mfa) ₂ CH ⁺	2.17 × 10 ¹	---	---	17a (70 %)
 18	(dpa) ₂ CH ⁺	5.42 × 10 ²	22.52	-115.63	18a (46 %)
	(mfa) ₂ CH ⁺	4.16 × 10 ³	---	---	18b (64 %)
	(pfa) ₂ CH ⁺	1.72 × 10 ⁴	---	---	18c (66 %)
 19	(dpa) ₂ CH ⁺	1.66 × 10 ⁴	---	---	19a (71 %)
	(pfa) ₂ CH ⁺	4.80 × 10 ⁵	---	---	19b (71 %)

Table 3.1: Continued

Nucleophile	Ar ₂ CH ⁺	<i>k</i> (20 °C) / L mol ⁻¹ s ⁻¹	Δ <i>H</i> [‡] / kJ mol ⁻¹	Δ <i>S</i> [‡] / J mol ⁻¹ s ⁻¹	Products ^[a]
 9	(lil) ₂ CH ⁺	2.84	---	---	9a (75 %)
	(jul) ₂ CH ⁺	1.11 × 10 ¹	---	---	9b (86 %)
	(thq) ₂ CH ⁺	1.13 × 10 ²	29.18	-105.94	9c (65 %)
	(dma) ₂ CH ⁺	1.31 × 10 ³	---	---	9d (71 %)
	(dpa) ₂ CH ⁺	1.12 × 10 ⁵	---	---	9e (48 %)
	(mfa) ₂ CH ⁺	6.40 × 10 ⁵	---	---	9f (51 %)
 20	(dpa) ₂ CH ⁺	3.38 × 10 ⁵	---	---	[b]

^[a] For structures see Scheme 3.5. ^[b] Isolation of product not attempted, because reactions with other benzhydrylium ions have previously been described in ref. [26].

3.6 Correlation analysis of the basis-set compounds

After the collaborative extension and completion of the basis-set by new compounds (see 3.4 and 3.5), the basis-set contains now twenty-three diarylcarbenium ions and 38 π -systems. The rate constants of 209 combinations of basis-set electrophiles and basis-set nucleophiles were available, and have been subjected to a correlation analysis according to equation 1.3 for determining the electrophilicity parameters *E* and the nucleophilicity parameters *N* and *s* of these compounds.

Following the previous treatment,^[15] the electrophilicity parameter of the dianisylcarbenium ion (ani)₂CH⁺ and the slope parameter of 2-methyl-1-pentene were selected as standard, i. e., *E* [(ani)₂CH⁺] = 0 and *s* [2-methyl-1-pentene] = 1. All other reactivity parameters *E*, *N*, and *s* as defined by eq. 1.3, were then calculated by minimizing Δ^2 specified by eq. 3.1 using the program "What'sBest! 4.0 Commercial" by Lindo Systems Inc.^[40]

$$\Delta^2 = \sum[\log k_{\text{exp}} - \log k_{\text{calc}}]^2 = \sum[\log k_{\text{exp}} - s(E + N)]^2 \quad (3.1)$$

Graphical representations of this correlation analysis are given in Figures 3.2 and 3.3. The plots $\log k$ versus the E parameters of the electrophiles show correlation lines with slightly different slopes for different nucleophiles (Figure 3.2). Deviations from the linear correlations occur as the diffusion limit ($5 \times 10^9 \text{ M}^{-1} \text{ s}^{-1}$) is approached,^[16,41] and for that reason, rate constants $k_{\text{exp}} > 10^8 \text{ M}^{-1} \text{ s}^{-1}$ have not been considered for the correlations. For the sake of clarity, only 20 out of 38 correlation lines are shown in Figure 3.2.

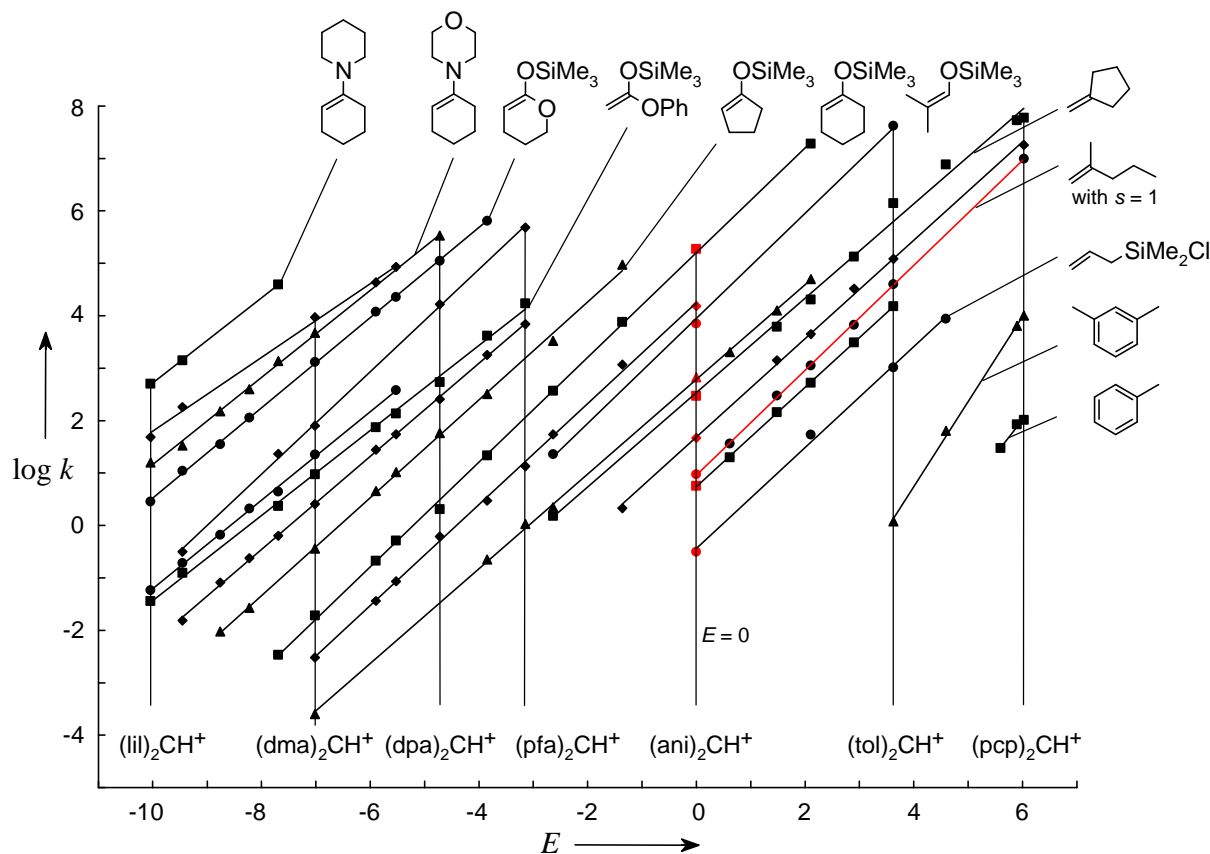


Figure 3.2: Plot of $\log k$ (20 °C) versus E for the reactions of benzhydryl cations with π -nucleophiles.

An important message can be taken from Figure 3.2. The similarities of the slopes and the narrow range accessible by second-order kinetics ($-6 < \log k < 9$) implies that crossing can only occur for correlation lines of nucleophiles with closely similar N parameters. In other words, nucleophiles with sufficiently different N values will not invert relative reactivities in the experimentally relevant range.

Since crossing above $\log k > 9$ (diffusion control) or below $\log k < -6$ (no reaction at room temperature) does not have any practical consequences, the definition of N as the intercepts of the correlation lines with the abscissa ($\log k = 0$) provides a useful measure for nucleophilic reactivity. Thus, N is generally defined within the experimentally accessible range, and its use avoids long-range extrapolations.

Figure 3.3 shows the plots of $(\log k)/s$ versus the N -parameters of the reference nucleophiles. Each correlation line refers to a reference electrophile. All lines are parallel because the effect of the slightly different s values is eliminated by division of the logarithms of the rate constants by s .

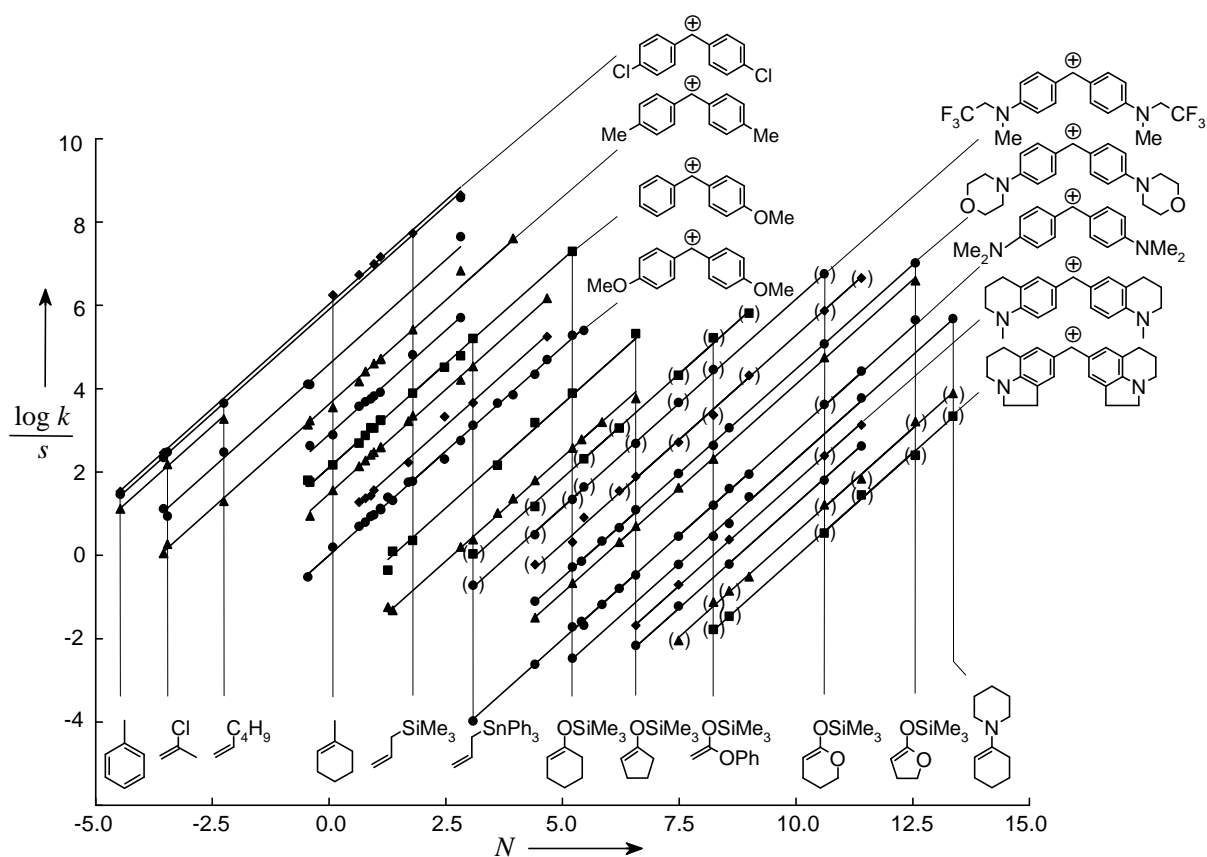


Figure 3.3: Plot of $(\log k)/s$ versus N for the reactions of benzhydryl cations with π -nucleophiles.

Data points which have been determined during this work and during my diploma thesis^[23] are identified by parentheses.

Comparison of Figure 3.1 with Figure 3.3 illustrates the progress made during this investigation. By achieving multiple overlap of the correlation lines, the derived reactivity parameters are statistically corroborated and can be used as a basis for further determinations of electrophilicity and nucleophilicity.

Comparison of the N and E parameters, derived from the correlation analysis of the basis set, with those given 1994^[15] shows that the parameters remained almost identical for systems with $E \geq 0$ or $N \leq 2$, because the data basis in these region has only slightly been altered. More remarkable, however, though $(dma)_2CH^+$ is the only electrophile with $E < -3$ which has been used in this and in the 1994 correlation, its E parameter and the N parameters of the nucleophiles linked to it ($3 < N < 13$) also have not changed by more than 0.5 units. Since the previous correlation^[15] rested predominantly on reactions with electrophilic metal- π -complexes and heteroaromatic cations in this range, this agreement implies that the reactivity parameters presented in this work are transferable to other types of compounds.

All 209 reactions of the combinations of basis set electrophiles and nucleophiles are included in Figure 3.4. One can see that the benzhydryl cations characterized so far, continuously cover the range $-10 < E < 6$ and thus allow the straightforward quantification of nucleophiles with $-8 < N < 16$. Vice versa, the nucleophiles in Figure 3.4 may be used to characterize electrophiles with $-15 < E < 7$. All compounds used for the determination of E , N , and s in Figure 3.2 and 3.3 are depicted in Figure 3.4.

In Figure 3.4, the three benzhydryl cations $(dpa)_2CH^+$, $(mfa)CH^+$, $(pfa)_2CH^+$, and the silyl ketene acetal **9**, which were characterized during this work, are marked by frames. The electrophilicity of $(bfa)_2CH^+$ was not characterized precisely, since the kinetics of its reaction with allyltrimethylsilane (see Table 3.1) indicated an electrophilicity parameter of $E [(bfa)_2CH^+] \approx -1.53$ similar to that of $E [(fur)_2CH^+] = -1.36$. Since $(fur)_2CH^+$ is more easily synthesized, $(bfa)_2CH^+$ was not selected as a reference electrophile.

In Figure 3.4 the structures and abbreviations of benzhydryl cations are summarized. These carbocations will be used in further parts of this work.

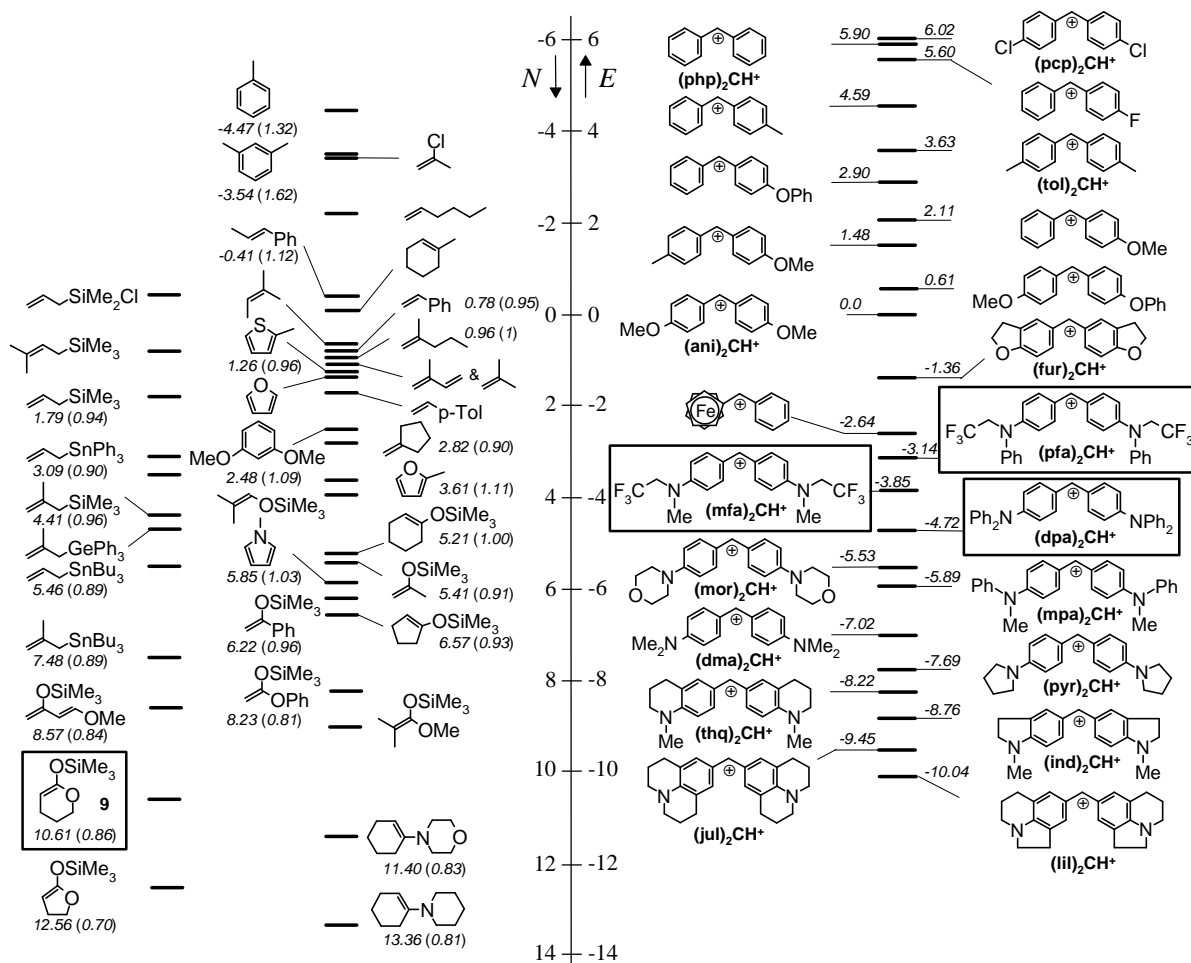


Figure 3.4: Compilation of all basis-set compounds used for the determination of E , N , and s . Compounds in frames were added to the basis set by this work.

3.7 Three dimensional presentations of the reactivities of the basis-set compounds

When plotting $(\log k)/s$ (Figure 3.5) or $\log k$ (Figure 3.6) versus E and N for the 209 reactions of basis-set electrophiles and nucleophiles, all data-points of the basis-set are presented in three-dimensional diagrams.

In these diagrams, the base is defined by the E and N values of the electrophiles and nucleophiles, respectively and the rate constants $(\log k)/s$ or $\log k$ for the corresponding combinations are plotted on axis perpendicular to this plane.

In Figures 3.5 and 3.6, the diagrams are shown from different points of view, by clockwise rotations (left column) and counterclockwise rotations (right columns).

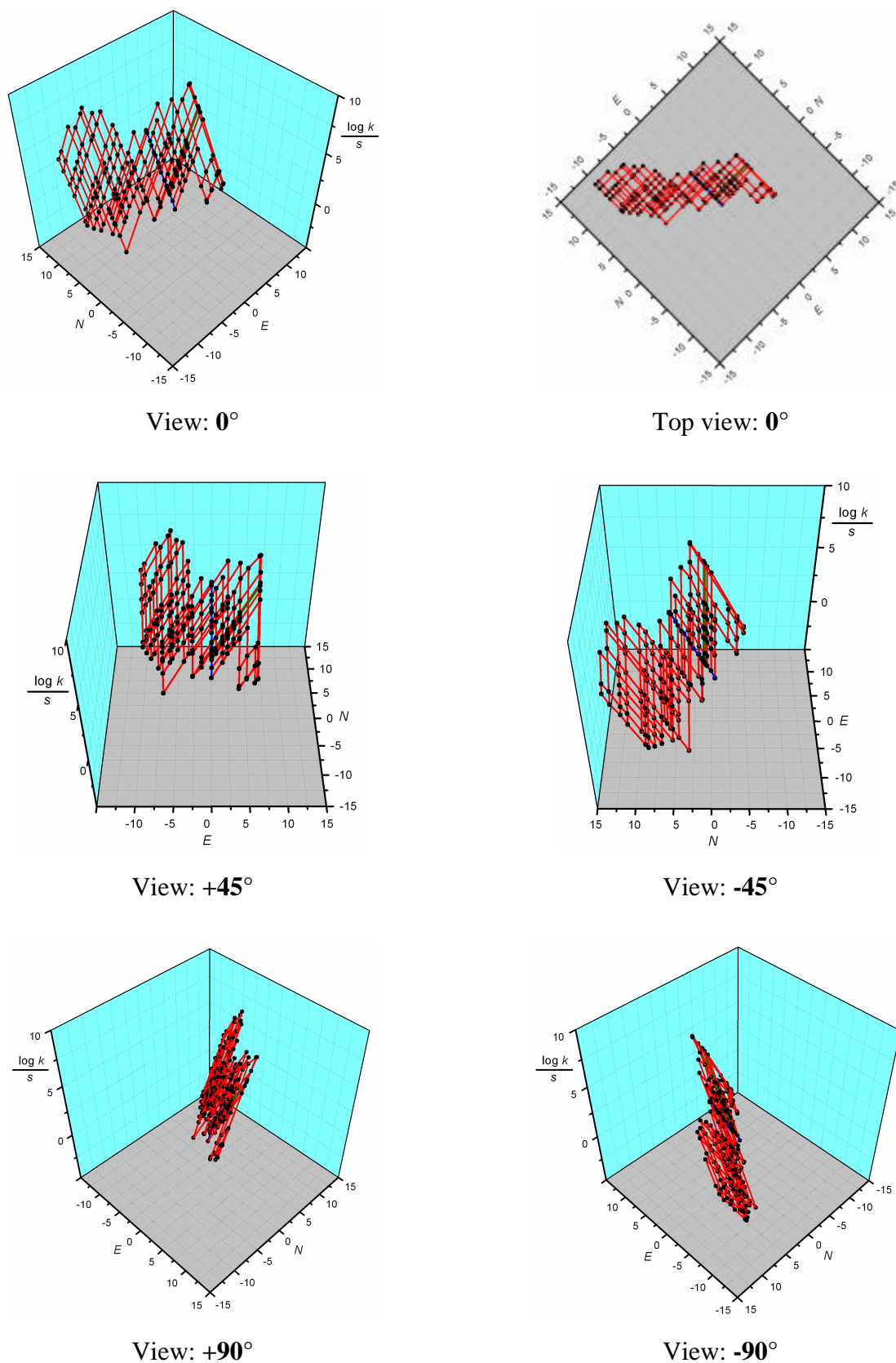
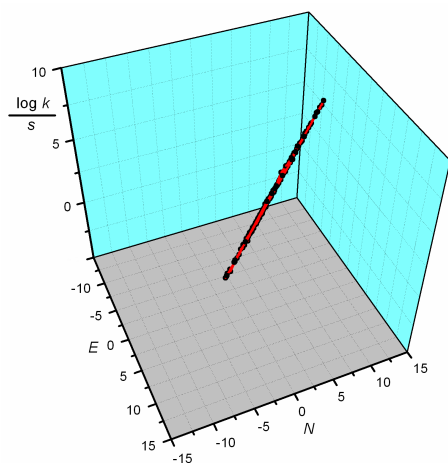
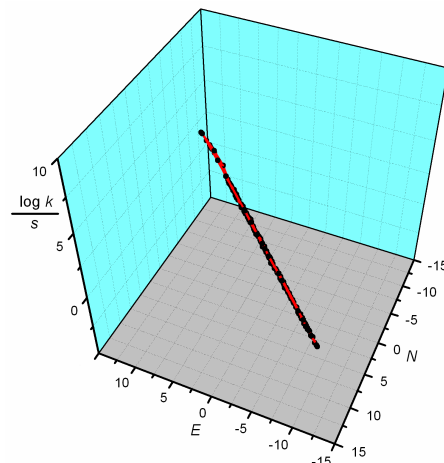


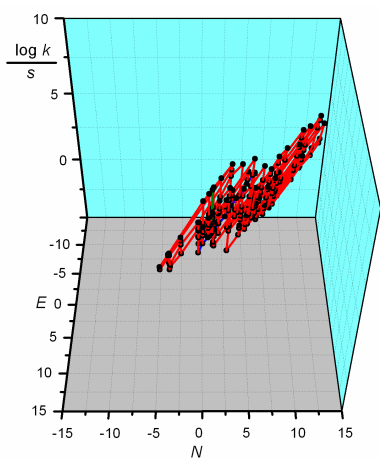
Figure 3.5: Plots of $(\log k)/s$ versus E and N for the 209 reactions of reference electrophiles with reference nucleophiles from different points of view.



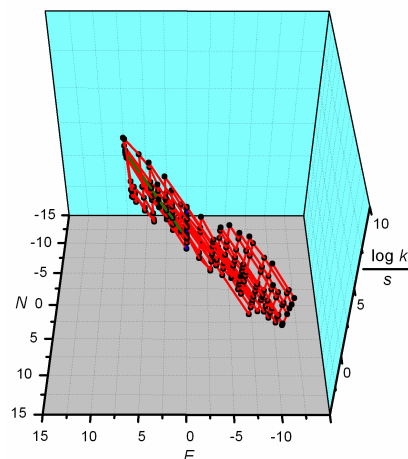
View: $+100^\circ$



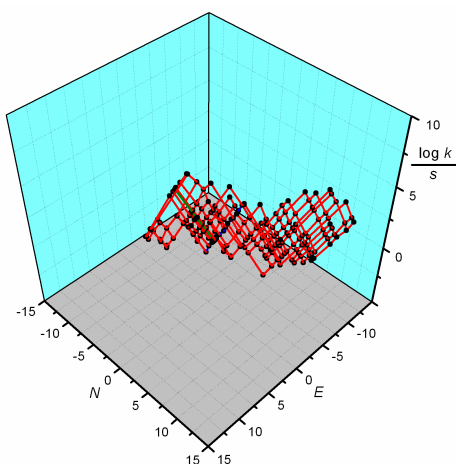
View: -100°



View: $+135^\circ$



View: -135°



View: $\pm 180^\circ$

Figure 3.5: Plots of $(\log k)/s$ versus E and N for the 209 reactions of reference electrophiles with reference nucleophiles from different points of view.

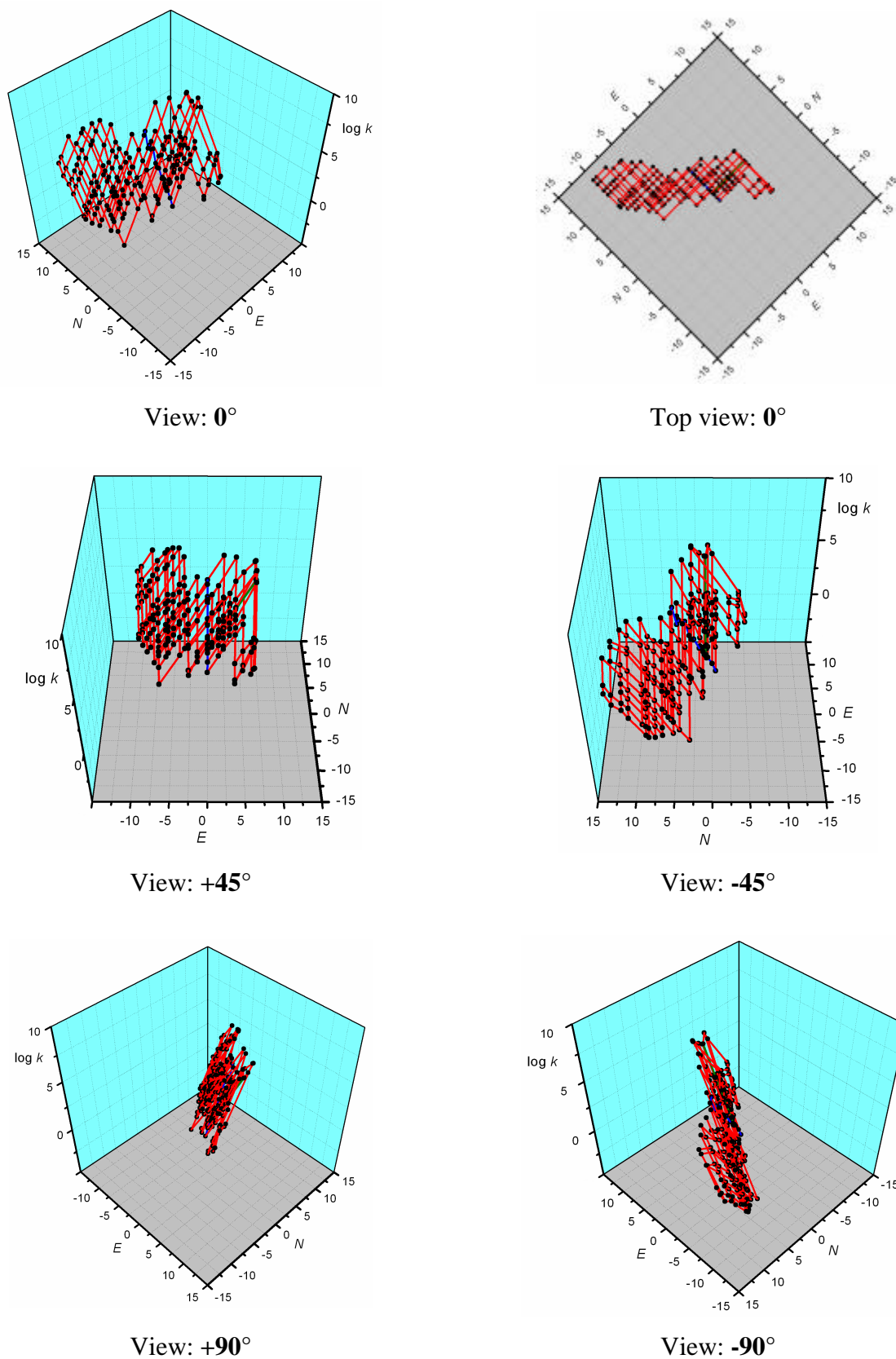


Figure 3.6: Plots of $\log k$ versus E and N for the 209 reactions of reference electrophiles with reference nucleophiles from different points of view.

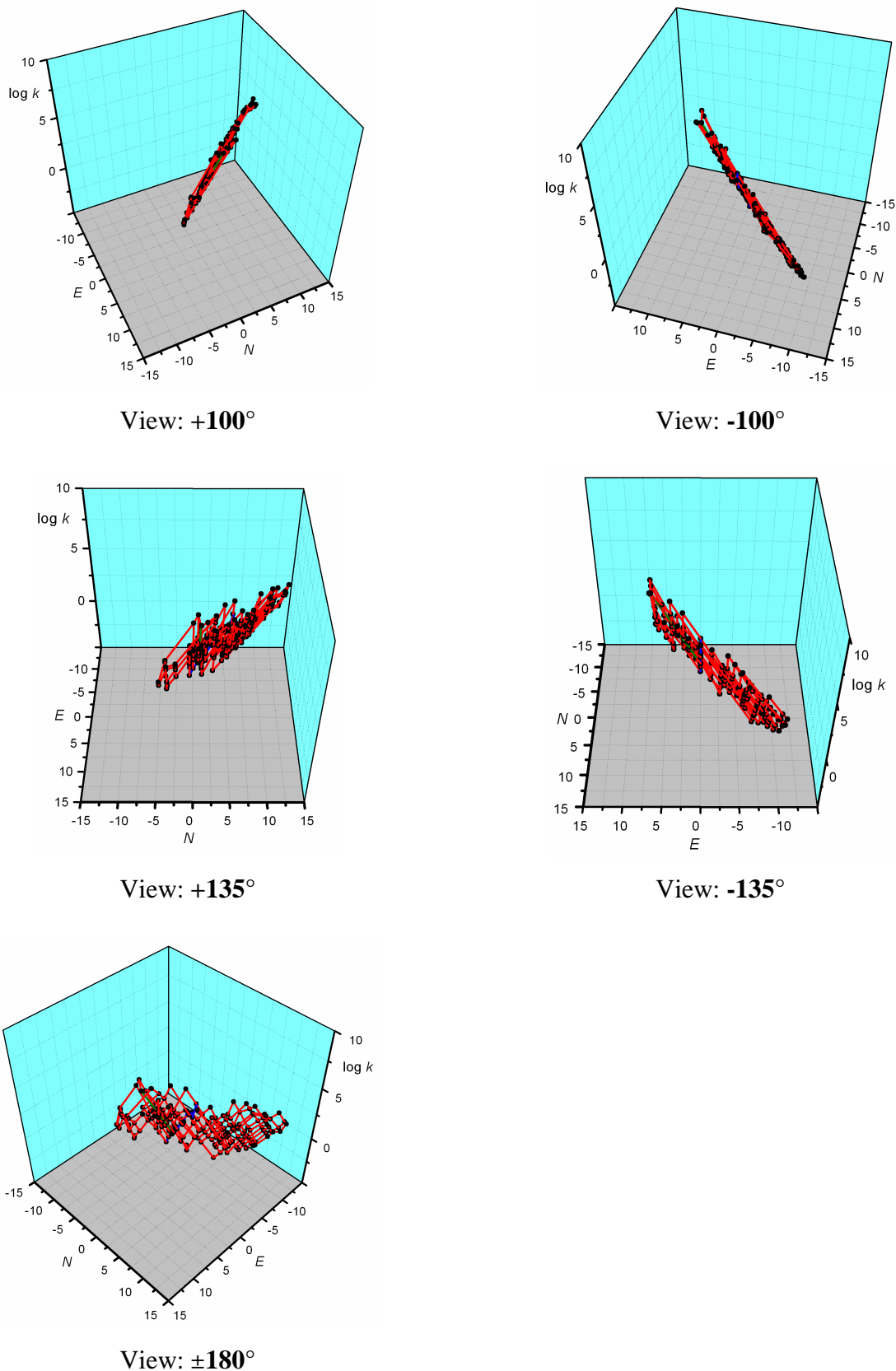


Figure 3.6: Plots of $\log k$ versus E and N for the 209 reactions of reference electrophiles with reference nucleophiles from different points of view.

One can see that the data points form a surface, which spans across the E/N -base, and is nearly plain. The surface is based on the data-points, provided from the 209 combinations of reference electrophiles and nucleophiles, which build up a net. Size and position of holes in the net can be seen. In most cases the holes are small, indicating that the crosslinking within the basis-set is very high, resulting in very consistent and persistent reactivity parameters for the basis-set compounds.

The surface rise from the corner of reactions with lowest rates ($E = -15$, $N = -15$, front of 0° view) to the corner of reactions with highest rates ($E = 15$, $N = 15$, rear of 0° view). For all data points on the line from $E = -15$, $N = 15$ to $E = 15$, $N = -15$ the condition $E + N = 0$ is fulfilled, which means that the rates are $k = 1$ in these cases. The surface forms a narrow band along this line. No data points are found far away from this line, which reflects the range accessible by kinetic experiments.

Three domains can be differentiated. Around the corner with $E = -15$, $N = -15$ there are no data points. Combinations of electrophiles and nucleophiles are too slow to be conveniently followed at room temperature. For example, the hypothetical combination of reaction partners with the reactivity parameters $E = -10$ ($\approx (\text{lil})_2\text{CH}^+$), $N = -5$ (\approx toluene), and $s = 1$ is expected to occur with a second-order rate constant $k_2 = 1 \times 10^{-15} \text{ M}^{-1} \text{ s}^{-1}$ (from eq. 1.3). This reaction would not be observable (half life 3×10^7 years for 1 M solutions). The part of the surface, covered by data points, represents the accessible range of kinetic experiments ($1 \times 10^{-3} < k_2 < 1 \times 10^7 \text{ M}^{-1} \text{ s}^{-1}$). In the rear of the 0° view there are no data points, because these reactions are very fast and mostly diffusion controlled ($1 \times 10^9 - 1 \times 10^{10} \text{ M}^{-1} \text{ s}^{-1}$).

Analogous plots of $\log k$ versus the E/N -plane (Figure 3.6) give rise to a rough surface with grooves in the $(\log k) / N$ -plains indicating that the reaction cannot be described precisely by using only one parameter for characterizing nucleophilicities.

3.8 New Hammett parameters

The Hammett equation is one of the oldest and the most widely used empirical relationship which has been employed for correlating kinetic and thermodynamic as well as spectroscopic properties.^[30,42-44] Most quantitative informations about substituent effects have been derived from Hammett's σ constants and modifications thereof. However, as indicated above, the

wealth of substituent constants for electron-withdrawing and weakly electron-donating groups is contrasted by a remarkable shortage of substituent constants for groups that are better electron donors than alkoxy.^[45] In agreement with earlier studies,^[46] there is only a moderate correlation ($r = 0.9955$) between the electrophilicity parameters E of benzhydrylium ions with $\Sigma\sigma^+$, because in the case of unsymmetrically substituted systems, the twisting angle of the two aryl rings is different.^[43,47] If only symmetrically substituted benzhydryl cations are considered, the linear correlation (Figure 3.7) is of higher quality, however, and can be used to determine the σ^+ parameters of a series of new donor substituents. For the three benzhydryl cations $(\text{dpa})_2\text{CH}^+$, $(\text{mfa})_2\text{CH}^+$, and $(\text{pfa})_2\text{CH}^+$ the σ^+ parameters, which were derived from the σ^+/E correlation are given numerically in parentheses in Figure 3.7.

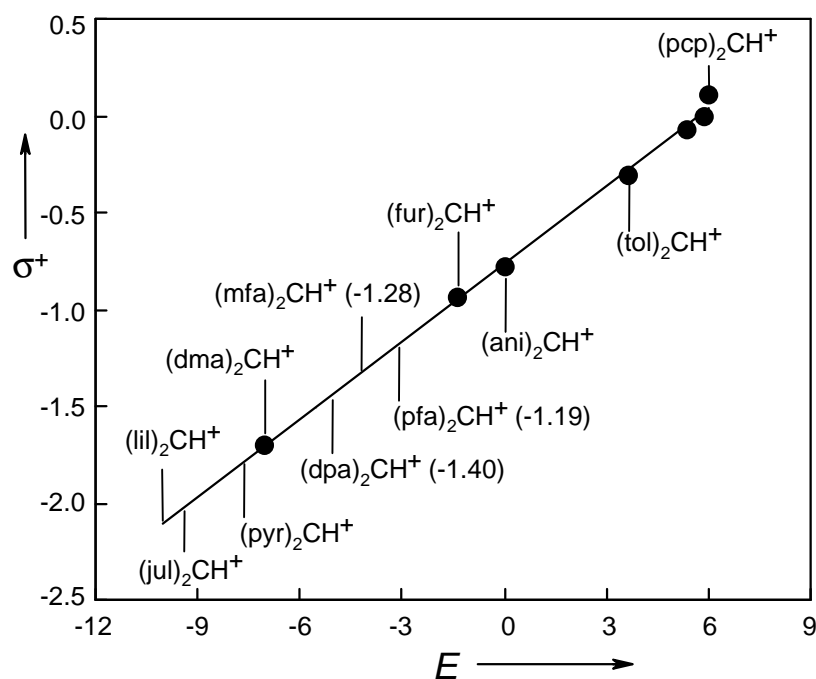


Figure 3.7: Correlation of Hammett's σ^+ constants^[30] with the E -parameters of benzhydryl cations ($n = 7$, $\sigma^+ = 0.134E - 0.767$, $r^2 = 0.9972$). Values of σ^+ in parentheses refer to substituent constants which are derived from this correlation for the compounds investigated in this doctoral thesis.

3.9 Does a certain reaction take place

Countless combinations of electrophiles with nucleophiles can be imagined, and the key question when considering a certain synthetic transformation is whether it will take place at all. This question is closely related to the expected reaction rates. The half-life of a bimolecular reaction with equal initial concentrations of the reactants (c_0) is $\tau_{1/2} = 1/(kc_0)$. A mixture that is 1 M in both reactants, therefore, requires a second-order rate constant of $k > 10^{-4} \text{ s}^{-1}$ to give 50 % conversion in less than 3 h. For a slope parameter of $0.7 < s < 1.2$, this condition is fulfilled when $E + N > -5.7$ to -3.3 . Considerations of that type have previously led to the rule of thumb that electrophiles can be expected to react with nucleophiles at room temperature when $E + N > -5$.^[15-17]

A semiquantitative nucleophilicity test is illustrated in Figure 3.8. A series of four reference electrophiles with $E = -8.8, -7.0, -4.7$, and -3.1 (Figure 3.8, left) are combined with an excess ($[\text{Nuc}] / [\text{EI}] \approx 100$) of reaction partners of different nucleophilicities ($N = 4.4, 5.2, 7.5$). The photograph was taken 1 minute after addition of the nucleophiles. Decolorations of the electrophile solutions (Figure 3.8, right) indicate roughly the reaction times for the individual electrophile-nucleophile combinations.

Half-lives of $\tau_{1/2} = 30 \text{ s}$ correspond to pseudo-first order rate constants of $k_{1\psi} \approx 0.02 \text{ s}^{-1}$ according to equation $\tau_{1/2} = (\ln 2) / k_{1\psi}$. For nucleophile concentrations of $[\text{Nuc}] \approx 0.1 \text{ M}$, this value is obtained with a second-order rate constant of $k_2 \approx 0.2 \text{ M}^{-1} \text{ s}^{-1}$ (from equation $k_{1\psi} = k_2 [\text{Nuc}]$). Since values of $0.7 < s < 1.2$ have been determined for most nucleophiles, the test in Figure 3.8 should be positive for $E + N > -1.0$ to -0.6 . All electrophile-nucleophile combinations with the benzhydryl cation of lowest electrophilicity ($E = -8.8$) give $E + N < -1.3$; therefore no reactions can be observed. On the other hand for the combinations with the benzhydryl cation of highest electrophilicity ($E = -3.1$) $E + N > 1.3$, resulting in decoloration of all solutions. For the reactions of Michler's hydrol blue $(\text{dma})_2\text{CH}^+$ ($E = -7.0$), $E + N$ ranges from -2.6 (with methallyltrimethylsilane **13**) to 0.5 (with methallyltributylstannane **14**). While the strong nucleophile **14** ($N = 7.5$) causes decoloration, no reaction takes place with **13** ($N = 4.4$). While the reaction of the bis(p-diphenylamino)benzhydrylium ion $(\text{dpa})_2\text{CH}^+$ ($E = -4.7$) with **13** ($N = 4.4$) is a borderline case (slow reaction indicated by partial decoloration), this electrophile reacts fast with the nucleophiles **17** and **14** ($E + N > 0.5$).

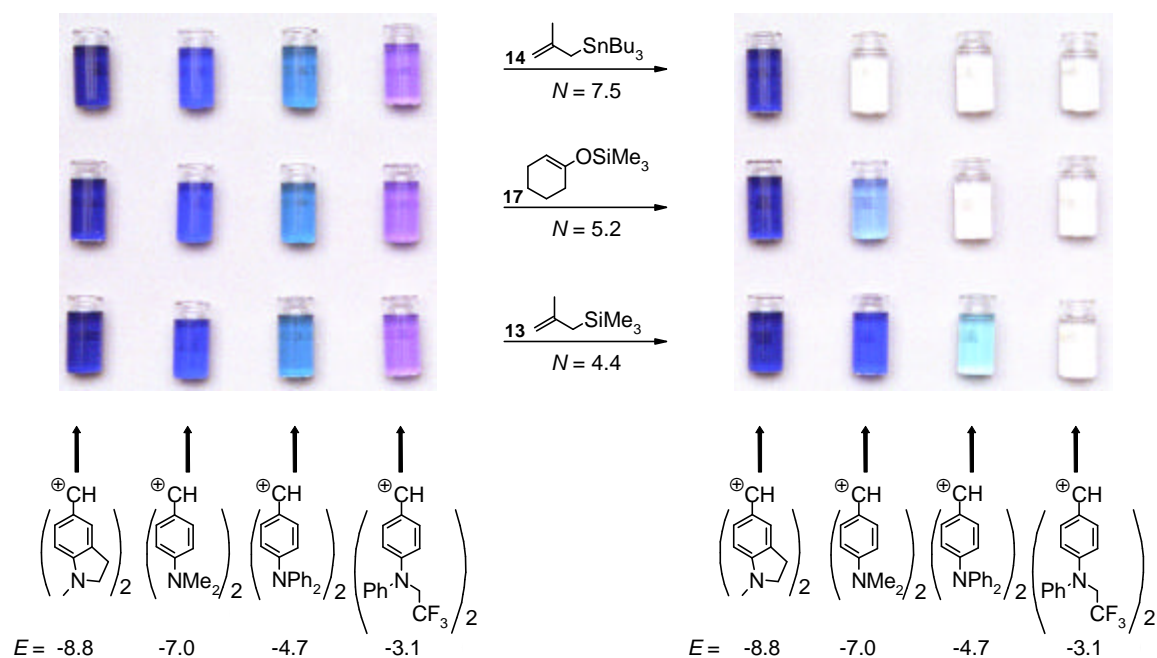


Figure 3.8: Quick-test of nucleophilicity.

Figure 3.8 reveals the reactivity order allylsilane < silyl enol ether < allylstannane without the need of any quantitative measurements. In this way, nucleophiles of unknown reactivity can efficiently be characterized with a precision that suffices for many purposes. This simple test then allows one to predict potential synthetic transformations of the corresponding nucleophile.

3.10 Characterization of new compounds

The basis-set provides reactivity parameters of reference electrophiles and nucleophiles in wide reactivity ranges. This allows the continuous addition of new compounds without the need for unending reparametrization of previously calculated E , N , and s values. From the reactivity parameters, which are delivered from the basis-set, one can characterize N and s for further nucleophiles, and E for further electrophiles.

The reactivity domains covered by the reference compounds in Figure 3.4 limit the procedures described so far for the characterization of further compounds in the ranges of approximately $-4 < N < 16$ and $-12 < E < 6$. To characterize more reactive as well as less reactive nucleophiles and electrophiles, an extension of the list of reference compounds is needed. Kinetic investigations of the reactions of stabilized carbanions with reference

benzhydrylium ions ($E < -8$) and quinone methides have already shown that the downward extension of Figure 3.4 is unproblematic and can be done without changing the parameters given in Figure 3.4.^[48] The extension beyond the upper border of Figure 3.4 appears to be more problematic, however, since reactivity parameters were usually derived from kinetic experiments with persistent carbocations. Since superacid solutions are not suitable for such types of experiments, the kinetic methods used so far will permit only minor extensions into the domain of stronger electrophiles and weaker nucleophiles.

The stepwise extension of the basis-set compounds opens another possibility. There are abundant data on electrophile nucleophile combinations in the literature.^[49] Most of them report structure-reactivity relationships of a group of nucleophiles toward a standard electrophile or of a group of electrophiles toward a standard nucleophile. In such cases, one can determine the reactivity parameter E of the standard electrophile or N and s of the standard nucleophile by kinetic experiments with reference compounds and thus link a large variety of isolated kinetic data to the common scale, which has been elaborated during this work (Figure 3.9).

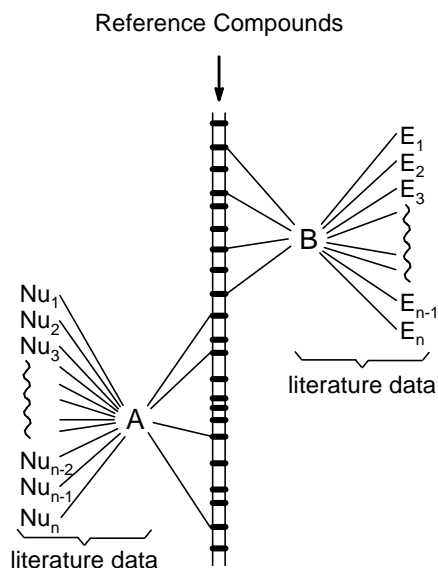


Figure 3.9: Method for linking reactivity data from literature to the reference scales.

4. Structure-nucleophilicity relationships for enamines

4.1 Introduction

Nine years before Mannich published the first general synthesis of enamines,^[50] the term “enamine” was coined in 1927 by Wittig to emphasize the analogy of this class of compounds with enols.^[51] While first examples of enamine chemistry date back to 1884,^[52] the synthetic potential of the reactions of enamines with electrophiles was not realized until 1954 when the pioneering work of Stork^[53] demonstrated their use for α -alkylations and α -acylations of carbonyl compounds.^[54] In these reactions, enamines combine with electrophiles to give iminium ions which are subsequently hydrolyzed to yield α -alkylated carbonyl or 1,3-dicarbonyl compounds, respectively. The chemistry of enamines has extensively been reviewed.^[54] Their strong nucleophilic character is revealed by their reactivity towards Michael acceptors,^[55] acceptor-activated aryl halides,^[56] and electron-deficient dienes which act as π 4-cycloaddition partners.^[57]

Enamines had a unique status as noncharged enolate equivalents until the early 1970s, which they have been sharing with silylated enol ethers since then.^[58] In accord with the lower electronegativity of nitrogen compared to oxygen, enamines are more nucleophilic than enol ethers and, therefore, cannot be replaced by the latter in reactions with weak electrophiles, e. g. allylpalladium complexes.^[59]

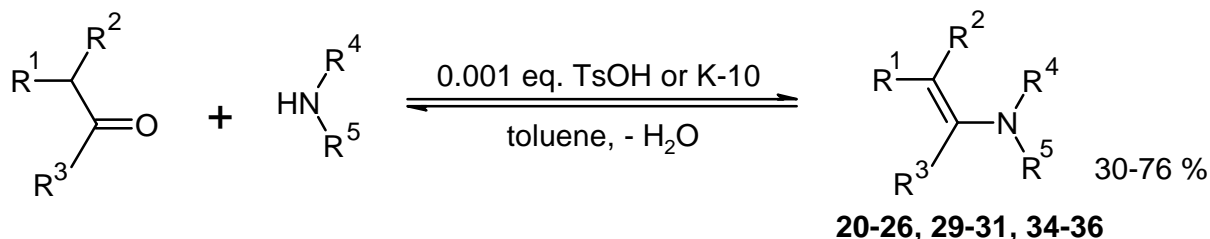
Though structure-reactivity relationships have repeatedly been reported for small groups of enamines,^[60-64] there has not been an attempt to compare reactivities of enamines of widely differing structures. It is the goal now to quantify the nucleophilic reactivities of enamines and to compare them with the reactivities of silyl enol ethers and related electron-rich arenes. This information can then be used to define their potential for a systematic use in synthesis.

4.2 Electrophiles

For characterizing the nucleophilic reactivities of enamines, the following reference electrophiles (Figure 3.4, right side) were employed: $(\text{liI})_2\text{CH}^+$, $(\text{jul})_2\text{CH}^+$, $(\text{ind})_2\text{CH}^+$, $(\text{thq})_2\text{CH}^+$, $(\text{pyr})_2\text{CH}^+$, $(\text{dma})_2\text{CH}^+$, $(\text{mpa})_2\text{CH}^+$, $(\text{dpa})_2\text{CH}^+$, $(\text{mfa})_2\text{CH}^+$, and $(\text{pfa})_2\text{CH}^+$. These benzhydrylium ions cover a wide reactivity range of electrophilicity ($-10.04 < E < -3.14$), and provide the first quantitative comparison of enamines of widely differing reactivity with each other as well as with other types of nucleophiles.

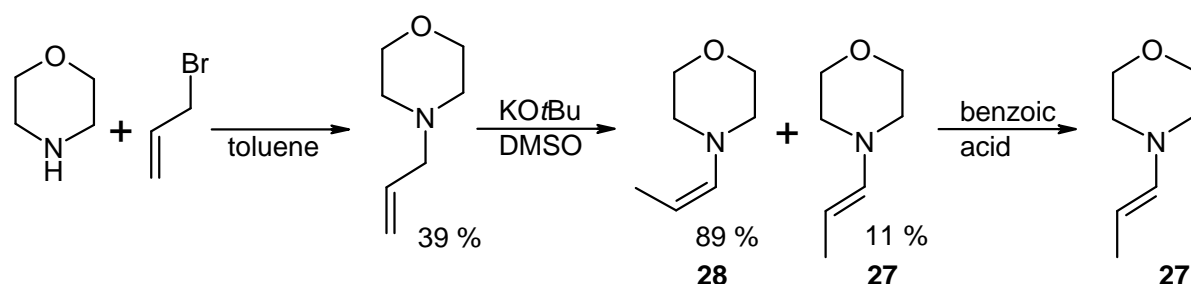
4.3 Nucleophiles

The enamines **20-26**, **29-31**, and **34-36** were prepared by acid catalyzed condensation of ketones or aldehydes with the corresponding secondary amines (Scheme 4.1).^[65]



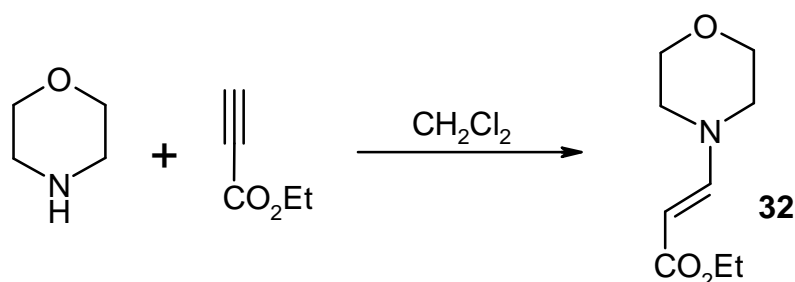
Scheme 4.1: Preparation of the enamines **20-26**, **29-31**, and **34-36** by acid catalyzed condensation.

Reaction of morpholine with 3-bromo-1-propene gave 4-allylmorpholine,^[66] which was converted into enamines **27**, **28** by base-catalyzed (KOtBu/DMSO) isomerization. The 89:11-mixture of **28** and **27** underwent a benzoic acid-catalyzed isomerization to give pure **27** (Scheme 4.2).^[66]



Scheme 4.2: Synthesis of the enamines **27**, **28** by base-catalyzed isomerization of allylamine.

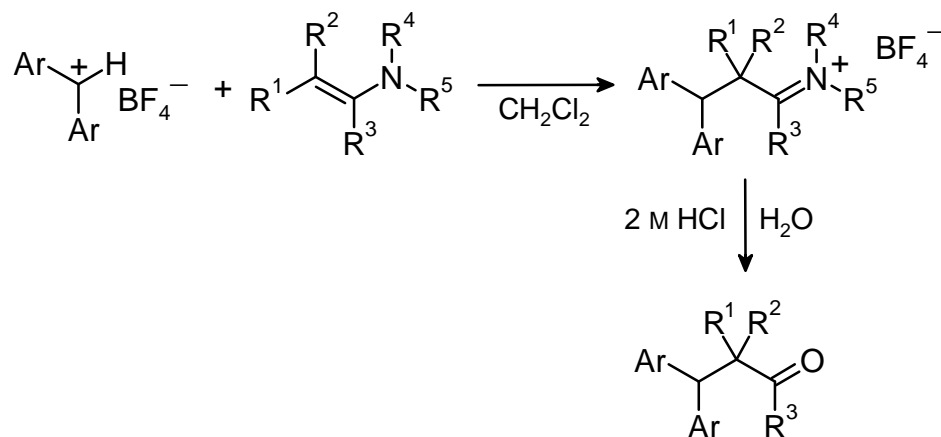
For the preparation of **32**, morpholine was added to ethyl propiolate^[67] (Scheme 4.3). In this reaction only the *E*-isomer was formed.



Scheme 4.3: Synthesis of **32** by addition of morpholine to ethyl propiolate.

4.4 Reaction products

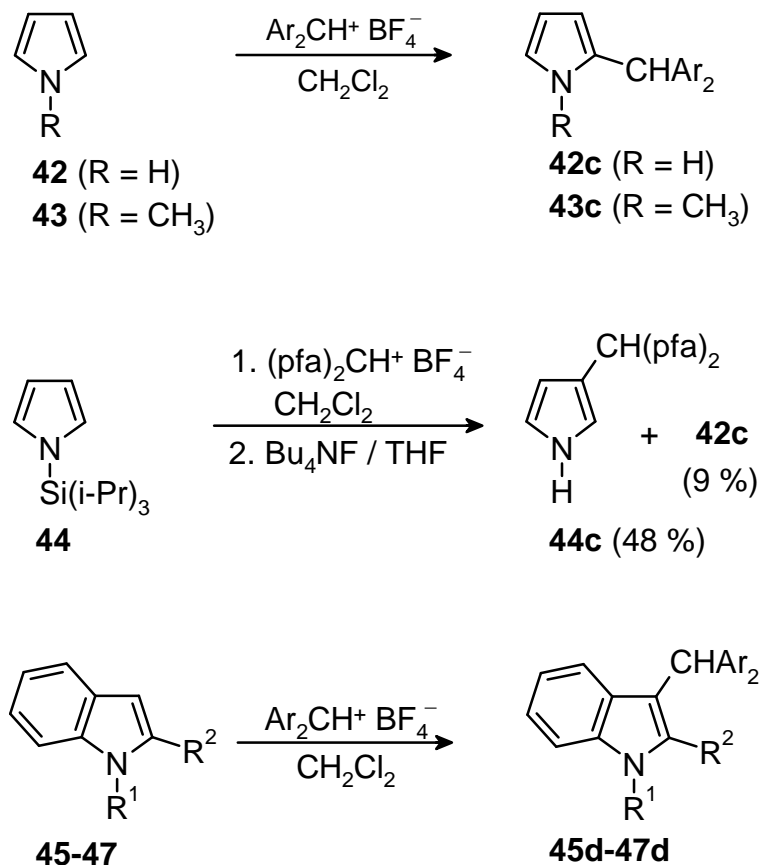
The reactions of the enamines **20-41** with the benzhydrylium salts $\text{Ar}_2\text{CH}^+ \text{BF}_4^-$ produce the iminium tetrafluoroborates **20a-41a**, usually in high yield. These were either isolated and characterized or hydrolyzed to the corresponding ketones or aldehydes **20b-41b** by treatment with dilute hydrochloric acid (Scheme 4.4). Some combinations of enamines with benzhydryl cations are reversible which impedes the isolation of iminium salts (see Table 4.1).



Scheme 4.4: Reactions of enamines with benzhydryl cations.

The NMR analysis of the products **42c** and **43c**^[21] showed that pyrrole **42** (R = H) and its *N*-methylated analogue **43** (R = CH₃) are alkylated by benzhydrylium salts $\text{Ar}_2\text{CH}^+ \text{BF}_4^-$ at position 2 (Scheme 4.5, for yields see Table 4.1), as generally found for electrophilic substitutions of pyrroles.^[68] In accord with the reports by Muchowski and co-workers,^[69] the *N*-triisopropylsilylated pyrrole **44** (R = Si*i*Pr₃) is mainly attacked at the 3-position (Scheme 4.5).

Since the substituted products **42c-44c** are more nucleophilic than **42-44**, they were found only as the predominant products when the pyrroles were used in large excess (10 equiv.) over the benzhydrylium salts.^[21] Alkylation of the indoles **45-47** occurs at position 3 with formation of compounds **45d-47d**, in analogy to previously reported electrophilic substitutions of indoles (Scheme 4.5).^[70,71]



Scheme 4.5: Reactions of substituted pyrroles and indoles with benzhydryl cations.

4.5 Kinetic measurements

The rates of the reactions of the benzhydryl cations with the enamines **20-41**, pyrroles **42-44**, and indoles **45-47** were followed by UV-Vis spectroscopy. The procedure of performing kinetic measurements and calculating rate constants is described in chapter 2 in detail. All rate constants (20 °C) for the reactions of enamines and related compounds with benzhydrylium ions determined are collected in Table 4.1 and are supplemented by some rate constants determined previously.

The last column of Table 4.1 contains those products of the reactions of benzhydryl cations with nucleophiles which were characterized as iminium salts **20a-41a**, carbonyl compounds **20b-41b**, or as the results of electrophilic aromatic substitutions (**42c-44c** or **45d-47d**).

Table 4.1: Second-order rate constants for the reactions of enamines, pyrroles and indoles with benzhydryl cations in CH₂Cl₂ at 20 °C.

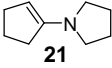
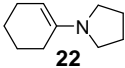
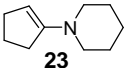
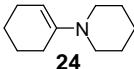
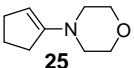
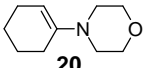
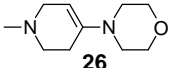
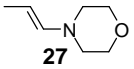
Enamine	<i>N</i>	<i>s</i> ^[a]	Ar ₂ CH ⁺	<i>k</i> ₂ / M ⁻¹ s ⁻¹	Products	
 21	15.91	0.86	(lil) ₂ CH ⁺	1.26 × 10 ⁵	21a (62 %)	
			(jul) ₂ CH ⁺	3.32 × 10 ⁵		
			(thq) ₂ CH ⁺	4.48 × 10 ⁶		21b (39 %)
 22	14.91	0.86	(lil) ₂ CH ⁺	1.48 × 10 ^{4[b]}	22b (65 %)	
			(jul) ₂ CH ⁺	4.59 × 10 ⁴		
			(thq) ₂ CH ⁺	7.30 × 10 ⁵		
			(dma) ₂ CH ⁺	5.33 × 10 ⁶		
 23	15.06	0.82	(lil) ₂ CH ⁺	1.15 × 10 ^{4[b]}	23a (89 %)	
			(jul) ₂ CH ⁺	4.57 × 10 ^{4[b]}		
			(thq) ₂ CH ⁺	4.44 × 10 ⁵		
			(dma) ₂ CH ⁺	3.68 × 10 ⁶		23b (49 %)
 24	13.36 ^[c]	0.81 ^[c]	(lil) ₂ CH ⁺	5.06 × 10 ^{2[c]}	see ref. [26]	
			(jul) ₂ CH ⁺	1.41 × 10 ^{3[c]}	see ref. [26]	
			(pyr) ₂ CH ⁺	3.95 × 10 ^{4[b,c]}		
 25	13.41	0.82	(lil) ₂ CH ⁺	4.70 × 10 ^{2[b]}	25b	
			(jul) ₂ CH ⁺	1.76 × 10 ^{3[b]}		
			(thq) ₂ CH ⁺	1.71 × 10 ^{4[b]}		
			(dma) ₂ CH ⁺	2.44 × 10 ⁵		25a (90%)
			(mpa) ₂ CH ⁺	9.71 × 10 ⁵		
 20	11.40 ^[c]	0.83 ^[c]	(lil) ₂ CH ⁺	1.58 × 10 ^{1[c]}	see ref. [26]	
			(jul) ₂ CH ⁺	3.35 × 10 ^{1[c]}	see ref. [26]	
			(ind) ₂ CH ⁺	1.51 × 10 ^{2[b,c]}	see ref. [26]	
			(thq) ₂ CH ⁺	3.97 × 10 ^{2[b,c]}	see ref. [26]	
			(pyr) ₂ CH ⁺	1.36 × 10 ^{3[b,c]}	see ref. [26]	
			(dma) ₂ CH ⁺	4.69 × 10 ^{3[b,c]}	see ref. [26]	
			(dpa) ₂ CH ⁺	3.38 × 10 ^{5[c]}		
 26	12.03	(0.80)	(dma) ₂ CH ⁺	1.01 × 10 ^{4[b]}	26b (76 %)	
 27	12.06	(0.80)	(dpa) ₂ CH ⁺	7.44 × 10 ⁵		

Table 4.1: Continued

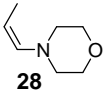
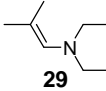
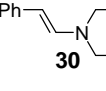
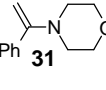
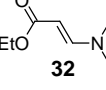
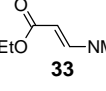
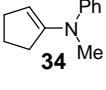
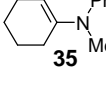
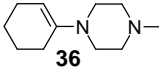
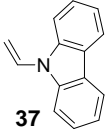
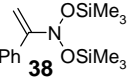
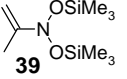
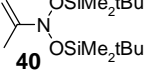
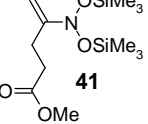
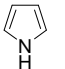
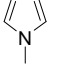
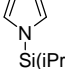
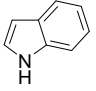
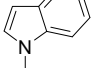
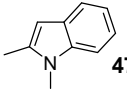
Enamine	<i>N</i>	<i>s</i> ^[a]	Ar ₂ CH ⁺	<i>k</i> ₂ / M ⁻¹ s ⁻¹	Products	
 28	12.26	(0.80)	(dpa) ₂ CH ⁺	1.07 × 10 ⁶ [d]		
 29	10.04	0.82	(dma) ₂ CH ⁺	2.53 × 10 ² [b,e]	29b (52 %)	
			(mpa) ₂ CH ⁺	3.33 × 10 ³ [e]		
			(dpa) ₂ CH ⁺	2.41 × 10 ⁴		
			(mfa) ₂ CH ⁺	1.28 × 10 ⁵		
			(pfa) ₂ CH ⁺	4.24 × 10 ⁵		29a
 30	10.76	0.87	(mpa) ₂ CH ⁺	1.49 × 10 ⁴	30b (70 %)	
			(dpa) ₂ CH ⁺	2.21 × 10 ⁵		
			(mfa) ₂ CH ⁺	1.07 × 10 ⁶		
			(pfa) ₂ CH ⁺	3.72 × 10 ⁶		
 31	9.96	0.79	(thq) ₂ CH ⁺	2.34 × 10 ¹	31b (46 %)	
			(dma) ₂ CH ⁺	2.11 × 10 ² [b]		
			(mpa) ₂ CH ⁺	1.68 × 10 ³		
			(dpa) ₂ CH ⁺	1.36 × 10 ⁴		
			(mfa) ₂ CH ⁺	6.68 × 10 ⁴		
			(pfa) ₂ CH ⁺	2.49 × 10 ⁵		31a (83 %)
 32	8.52	(0.80)	(pfa) ₂ CH ⁺	2.02 × 10 ⁴ [e]		
 33	9.43	(0.80)	(pfa) ₂ CH ⁺	1.07 × 10 ⁵		
 34	12.90	0.79	(lil) ₂ CH ⁺	2.02 × 10 ² [b]	34a (92 %)	
			(jul) ₂ CH ⁺	4.31 × 10 ²		
			(thq) ₂ CH ⁺	5.01 × 10 ³		
			(dma) ₂ CH ⁺	4.96 × 10 ⁴		
			(mpa) ₂ CH ⁺	3.21 × 10 ⁵		
			(dpa) ₂ CH ⁺	2.76 × 10 ⁶		
 35	10.73	0.81	(thq) ₂ CH ⁺	1.04 × 10 ²	35b (35 %)	
			(dma) ₂ CH ⁺	1.05 × 10 ³ [e]		
			(mpa) ₂ CH ⁺	8.43 × 10 ³		
			(dpa) ₂ CH ⁺	8.64 × 10 ⁴		

Table 4.1: Continued

Enamine	<i>N</i>	<i>s</i> ^[a]	Ar ₂ CH ⁺	<i>k</i> ₂ / M ⁻¹ s ⁻¹	Products
 36	12.51	(0.80)	(dma) ₂ CH ⁺	2.45 × 10 ⁴ [b]	36a (93 %), 36b (59 %)
 37	5.02 ^[f]	0.94 ^[f]	(dma) ₂ CH ⁺ (dpa) ₂ CH ⁺	1.35 × 10 ⁻² [f] 1.93 ^[f]	see ref. [72]
 38	4.80 ^[g]	(0.86) ^[g]	various	see ref. [73]	
 39	4.76 ^[g]	0.86 ^[g]	various	see ref. [73]	
 40	4.23 ^[g]	0.93 ^[g]	various	see ref. [73]	
 41	3.84 ^[g]	0.87 ^[g]	various	see ref. [73]	
 42	4.63	(1.00)	(pfa) ₂ CH ⁺	3.12 × 10 ¹	42c (32 %)
 43	5.85 ^[c]	1.03 ^[c]	various	see ref. [21]	
 44	3.12	0.93	(dpa) ₂ CH ⁺ (mfa) ₂ CH ⁺ (pfa) ₂ CH ⁺	4.26 × 10 ⁻² 1.19 × 10 ⁻¹ 1.33	44c (48 %) ^[h]
 45	5.80	(0.80)	(pfa) ₂ CH ⁺	1.34 × 10 ²	45d (70 %)
 46	6.93	(0.80)	(pfa) ₂ CH ⁺	1.09 × 10 ³	46d (22 %)
 47	7.81	(0.80)	(pfa) ₂ CH ⁺	5.47 × 10 ³	47d (34 %)

^[a] Values in parentheses are estimates. ^[b] Eyring activation parameters are given in Table 4.2.

^[c] From ref. [26]. ^[d] Mixture **28/27** = 89/11. ^[e] Reversible reaction, for equilibrium constant see Table 4.3. ^[f] From ref. [72]. ^[g] From ref. [73]. ^[h] The crude product contains also isomer **42c** (9 %) as revealed by NMR spectroscopy.

In cases where the temperature dependence of the rate constants has been determined, the k_2 values given in Table 4.1 are those derived from the Eyring parameters listed in Table 4.2. The temperature variations show that the observed differences in reactivity are predominantly due to enthalpic effects, since ΔS^\ddagger is always around $-100 \text{ J mol}^{-1} \text{ K}^{-1}$, as in previously studied reactions of carbocations with π -nucleophiles.^[26,72-74]

Table 4.2: Eyring activation parameters^[a] for the reactions of benzhydryl cations with enamines in CH_2Cl_2 .

Enamine	Ar_2CH^+	$\Delta H^\ddagger / \text{kJ mol}^{-1}$	$\Delta S^\ddagger / \text{J mol}^{-1} \text{K}^{-1}$
22	(lil) ₂ CH ⁺	16.43 ± 0.70	-108.90 ± 3.34
23	(lil) ₂ CH ⁺	17.13 ± 0.40	-108.65 ± 1.86
23	(jul) ₂ CH ⁺	17.97 ± 0.56	-94.28 ± 2.71
24	(pyr) ₂ CH ⁺	14.33 ± 0.84 ^[b]	-107.88 ± 4.05 ^[b]
25	(lil) ₂ CH ⁺	24.10 ± 0.15	-111.41 ± 0.66
25	(jul) ₂ CH ⁺	22.29 ± 0.38	-106.62 ± 1.68
25	(thq) ₂ CH ⁺	17.55 ± 0.65	-103.91 ± 2.90
20	(ind) ₂ CH ⁺	26.20 ± 0.43 ^[b]	-113.71 ± 1.75 ^[b]
20	(thq) ₂ CH ⁺	24.28 ± 0.42 ^[b]	-112.21 ± 1.83 ^[b]
20	(pyr) ₂ CH ⁺	23.33 ± 0.58 ^[b]	-105.20 ± 2.51 ^[b]
20	(dma) ₂ CH ⁺	20.46 ± 0.94 ^[b]	-104.71 ± 4.15 ^[b]
26	(dma) ₂ CH ⁺	25.39 ± 1.68	-81.51 ± 7.55
29	(dma) ₂ CH ⁺	22.75 ± 0.28	-121.18 ± 1.28
31	(dma) ₂ CH ⁺	35.20 ± 0.41	-80.20 ± 1.71
34	(lil) ₂ CH ⁺	34.17 ± 0.79	-84.11 ± 3.25
36	(dma) ₂ CH ⁺	17.97 ± 0.50	-99.43 ± 2.34

^[a] As indicated by the error limits in ΔH^\ddagger and ΔS^\ddagger , the large number of decimals is per se meaningless, but is needed for reproducing the rate constants in Table 4.1. ^[b] From ref. [26].

4.6 Enamines as ambident nucleophiles

Enamines are ambident nucleophiles, and the second-order rate constants k_2 in Table 4.1, which are derived from the disappearance of the benzhydryl cation absorptions, may either be due to direct formation of the isolated iminium ions or to the initial formation of eneammonium ions which rearrange to the observed products in a successive reaction.

Electrophilic attack at nitrogen has previously been reported for reactions of enamines with protons^[63,75-77] and with alkyl halides.^[78] It was shown that protonation at nitrogen initially yields eneammonium ions which successively rearrange to the more stable iminium ions^[63,76-77] (Figure 4.1).

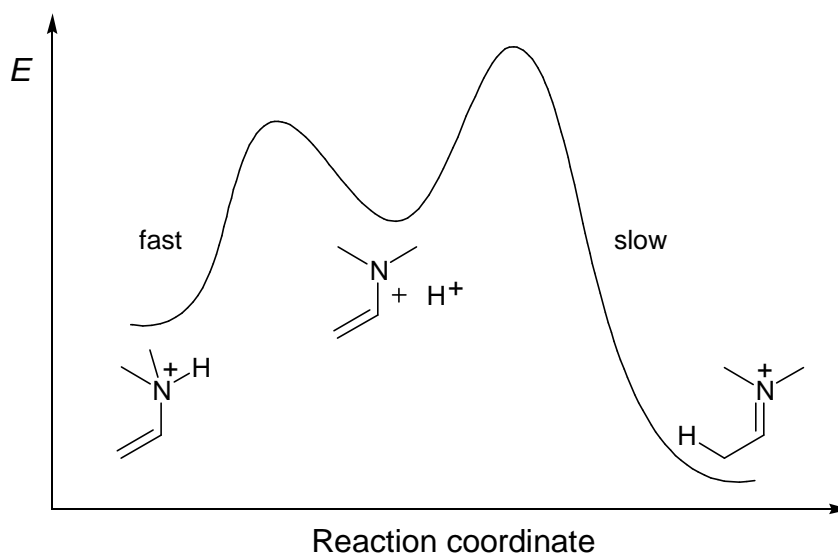
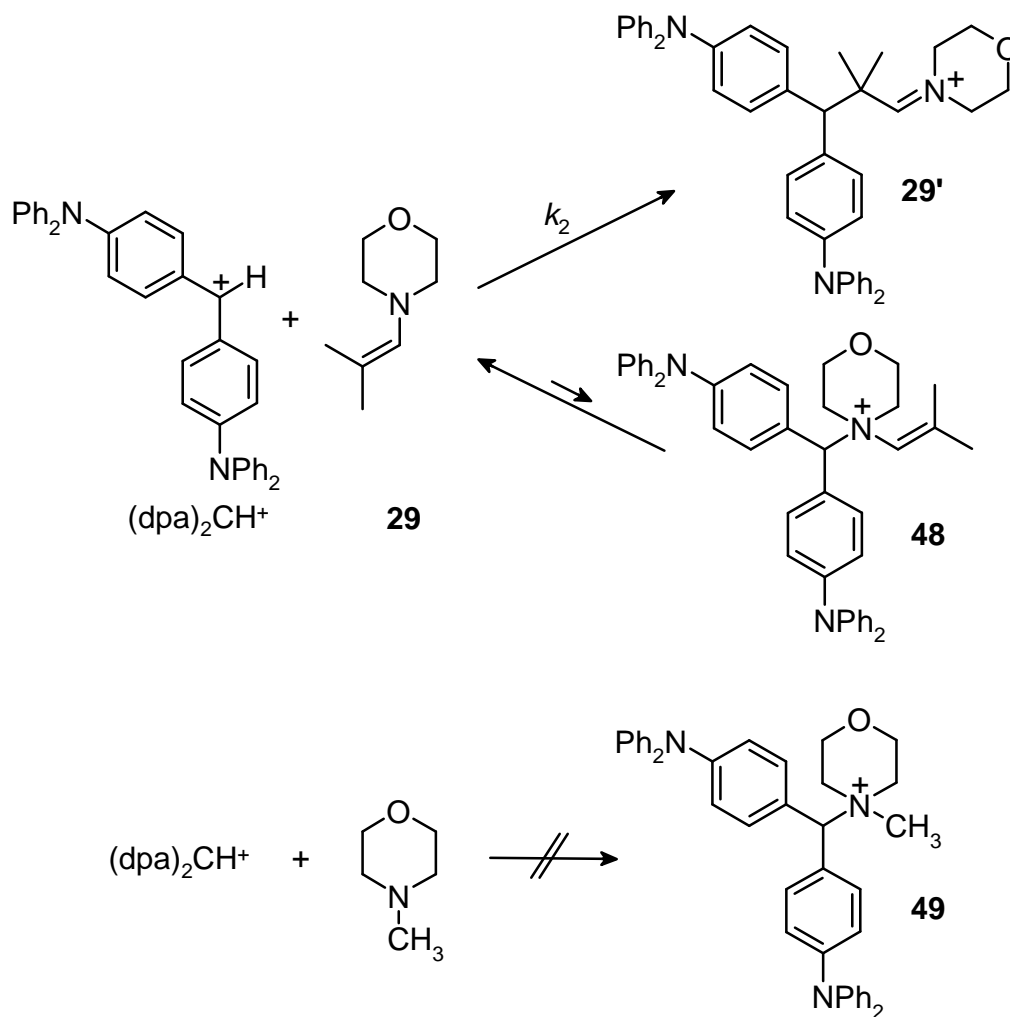


Figure 4.1: Protonation of enamines.

To determine the preferred site of electrophilic attack for the combinations listed in Table 4.1, we have investigated the reactions of benzhydrylium ions with the enamine **29** in detail. Because of the steric shielding of the β -carbon in compound **29** by two methyl groups, in this system the electrophilic attack at nitrogen should be particularly favorable over attack at the β -carbon.

When enamine **29** was treated with $(\text{dpa})_2\text{CH}^+ \text{BF}_4^-$ at 20 °C, the consumption of the benzhydrylium ion was complete within 1 s (UV detection) with a second-order rate constant of $2.41 \times 10^4 \text{ M}^{-1} \text{ s}^{-1}$ (Table 4.1). The ^1H NMR spectrum taken after 30 s indicated the exclusive formation of the iminium ion **29'** (Scheme 4.6).



Scheme 4.6: Reactions of $(\text{dpa})_2\text{CH}^+$ with the enamine **29** and *N*-methylmorpholine.

How can one exclude that the UV-Vis spectroscopically observed reaction (~ 1 s) is due to the formation of **48** while the NMR spectrum shows the structure of the rearranged product **29'**? Under the conditions of the UV-Vis experiment just described, *N*-methylmorpholine does not react with $(\text{dpa})_2\text{CH}^+$ to form the ammonium ion **49** (Scheme 4.6), indicating an equilibrium for *N*-attack which is far on the side of the reactants.^[79]

Since saturated tertiary amines are 10^2 times more basic than the corresponding enamines,^[77b,c] it must be concluded that the equilibrium concentration of **48** must even be smaller than the (nonobservable) equilibrium concentration of the quaternary morpholinium ion **49**. As a consequence, only a negligible concentration of the eneammonium **48** ion can be produced from $(\text{dpa})_2\text{CH}^+$ and **29**. Despite a potentially high rate constant for the formation of **48**, the unfavorable equilibrium constant rules out that the UV-Vis spectroscopically observed reaction is due to *N*-attack.

The ratio *C*- versus *N*-attack should even be higher with the other enamines of Table 4.1, and one can, therefore, generalize that all rate constants in Table 4.1 refer to the attack of the carbocations Ar_2CH^+ at the β -carbon atom of enamines. Since the initial formation of small equilibrium concentrations of eneammonium ions does not have any influence on the rates of consumption of the benzhydrylium ions Ar_2CH^+ by β -carbon attack of the enamines, we will disregard this reversible side reaction in the following discussion.

4.7 Nucleophilicities of enamines

When the rate constants ($\log k$) determined for the reactions of the enamines **20-36** and the pyrrole derivatives **42-44** with Ar_2CH^+ (Table 4.1) are plotted against the *E* parameters of the benzhydryl cations (from Figure 3.4), linear correlations are obtained, from which *s* and *N* according to eq. 1.3 can be determined (Figure 4.2). Since the slopes *s* do not differ widely ($0.79 < s < 1.03$), estimated values of *s* can be used to derive *N* parameters for those compounds which have only been studied with respect to a single benzhydryl cation^[80] (see Table 4.1).

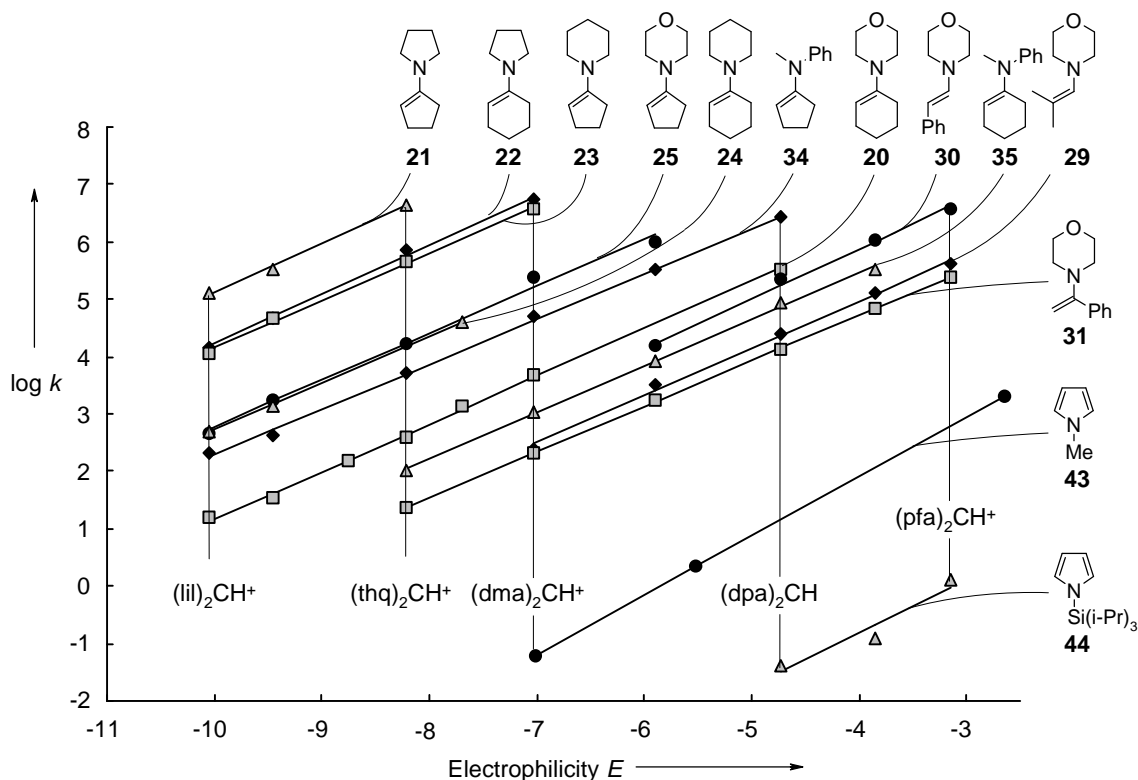


Figure 4.2: Correlations of the rate constants ($\log k$, 20 °C, CH_2Cl_2) for the reactions of enamines **20-35** and pyrroles **43,44** with benzhydryl cations Ar_2CH^+ versus their electrophilic reactivities *E*.

4.8 Intrinsic barriers for the reactions of benzhydrylium ions with enamines

As indicated in the footnotes of Table 4.1, not all reactions of benzhydrylium ions with enamines proceed quantitatively, and in four cases, equilibrium constants have been determined. While **29** reacts quantitatively with $(\text{dpa})_2\text{CH}^+$ and with more electrophilic benzhydrylium ions, equilibrium constants of $3.7 \times 10^4 \text{ M}^{-1}$ and $4.3 \times 10^2 \text{ M}^{-1}$ have been measured for the combinations of **29** with $(\text{mpa})_2\text{CH}^+$ and $(\text{dma})_2\text{CH}^+$, respectively, in dichloromethane at 20 °C.

From the linear correlations between rate and equilibrium constants of the reactions of benzhydrylium ions with nucleophiles,^[47] one can extrapolate that $\log K$ should be 0 for a benzhydrylium ion with $E = -8.55$ (Figure 4.3). Since no far-ranging extrapolation is needed, the calculated intercept on the abscissa of Figure 4.3 is rather reliable though it is based on only two experimental equilibrium constants.

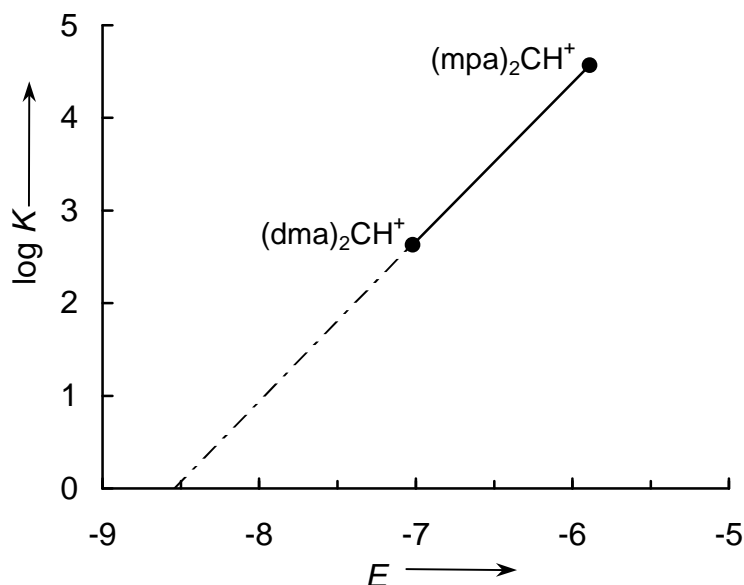


Figure 4.3: Correlation of $\log K$ versus E for the reactions of benzhydryl cations Ar_2CH^+ with **29** in dichloromethane at 20 °C ($\log K = 1.72E + 14.67$, $n = 2$).

In Marcus theory,^[81] the intrinsic rate constant is defined as the rate constant of a reaction that does not have a thermodynamic driving force ($\Delta_r G^\circ = 0$). Thus, the rate constant of the reaction of **29** with the hypothetical benzhydrylium ion of $E = -8.55$ ($\approx (\text{ind})_2\text{CH}^+$) which can be calculated as k_2 (20 °C) = $16.7 \text{ M}^{-1} \text{ s}^{-1}$ by eq. 1.3 equals the intrinsic rate constant. The Eyring equation then allows to derive the intrinsic barrier of this reaction as

$\Delta G_0^\ddagger = 64.9 \text{ kJ mol}^{-1}$ at 20 °C. Intrinsic barriers of 58 to 67 kJ mol^{-1} are calculated by the Marcus equation 4.1.

$$\Delta G^\ddagger = \Delta G_0^\ddagger + 0.5\Delta_r G^\circ + ((\Delta_r G^\circ)^2 / (16\Delta G_0^\ddagger)) \quad (4.1)$$

for the other reactions of benzhydryl cations with enamines for which equilibrium constants have been determined (Table 4.1). As discussed previously,^[47] the work term in the Marcus equation (4.1) can be neglected in ion-molecule reactions.

Table 4.3: Calculation of the intrinsic barriers ΔG_0^\ddagger from the reaction and activation free enthalpies of the reactions of benzhydrylium ions with enamines in CH_2Cl_2 at 20 °C.

Enamine	Ar_2CH^+	K / M^{-1}	$\Delta_r G^\circ / \text{kJ mol}^{-1}$	$\Delta G^\ddagger / \text{kJ mol}^{-1}$	$\Delta G_0^\ddagger / \text{kJ mol}^{-1}$
29	$(\text{dma})_2\text{CH}^+$	4.26×10^2	-14.76	58.27	65.44
29	$(\text{mpa})_2\text{CH}^+$	3.72×10^4	-25.65	51.99	64.17
32	$(\text{pfa})_2\text{CH}^+$	1.08×10^4	-22.63	47.60	58.37
35	$(\text{dma})_2\text{CH}^+$	3.66×10^4	-25.61	54.80	66.99

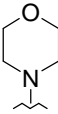
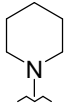
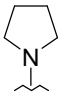
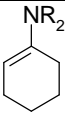
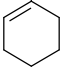
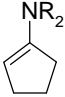
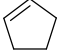
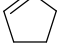
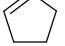
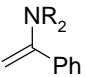
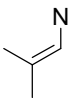
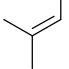
The intrinsic barriers (ΔG_0^\ddagger) in Table 4.3 closely resemble those previously estimated for the reactions of benzhydrylium ions with 2-methyl-1-pentene,^[82] and are larger than those observed for the reactions with phosphanes (see chapter 4) and amines.^[83]

4.9 Structure-reactivity relationships for enamines

The almost parallel lines in Figure 4.2, numerically expressed by the closely similar s -parameters in Table 4.1, imply that the relative reactivities of these enamines are almost independent of the nature of the benzhydrylium ions Ar_2CH^+ (constant selectivity relationship). For that reason, discussions of structure reactivity correlations can be based on the magnitude of N or on relative reactivities towards any specific benzhydrylium ion. We will employ both quantities in the following discussion.

As shown in Table 4.4, the relative reactivities of different types of enamines towards various electrophiles generally decrease in the order pyrrolidine > piperidine > morpholine.

Table 4.4: Comparison of relative rate constants k_{rel} for the reactions of enamines with various electrophiles.

Reactions	Relative Reactivities k_{rel} of Enamines		
			
NR ₂ =			
 + (lil) ₂ CH ⁺ (CH ₂ Cl ₂ , 20 °C)	1	32	937
 + (jul) ₂ CH ⁺ (CH ₂ Cl ₂ , 20 °C)	1	42	1 370
 + (lil) ₂ CH ⁺ (CH ₂ Cl ₂ , 20 °C)	1	24	268
 + (jul) ₂ CH ⁺ (CH ₂ Cl ₂ , 20 °C)	1	26	189
 + (thq) ₂ CH ⁺ (CH ₂ Cl ₂ , 20 °C)	1	26	262
 + PhN ₃ (C ₆ H ₆ , 25 °C) ^[a]	1	—	45
 + PhN ₃ (CHCl ₃ , 44.8 °C) ^[b]	1	5	155
 + Ph ₂ C=C=O (PhCN, 40.3 °C) ^[c]	1	—	1 420
 + H ₃ O ⁺ (H ₂ O, 25 °C) ^[d]	1	452	27 100

^[a] From ref. [60]. ^[b] From ref. [61]. ^[c] From ref. [62]. ^[d] From ref. [63].

The higher reactivity of pyrrolidine compounds compared to piperidine analogues can be explained by the higher *p*-character of the nitrogen lone-pair in a five-membered ring compared with a six-membered ring which is revealed by a lower first vertical ionization potential (IP_1)^[54a,84] of pyrrolidino compared to piperidino compounds (Figure 4.4). Replacement of the 4-CH₂ group in piperidine by the more electronegative oxygen further increases the ionization potential and consequently reduces nucleophilicity. The increasing degree of pyramidalization of nitrogen from pyrrolidino to piperidino and morpholino has also been confirmed by x-ray crystallography of derivatives of these compounds.^[85]

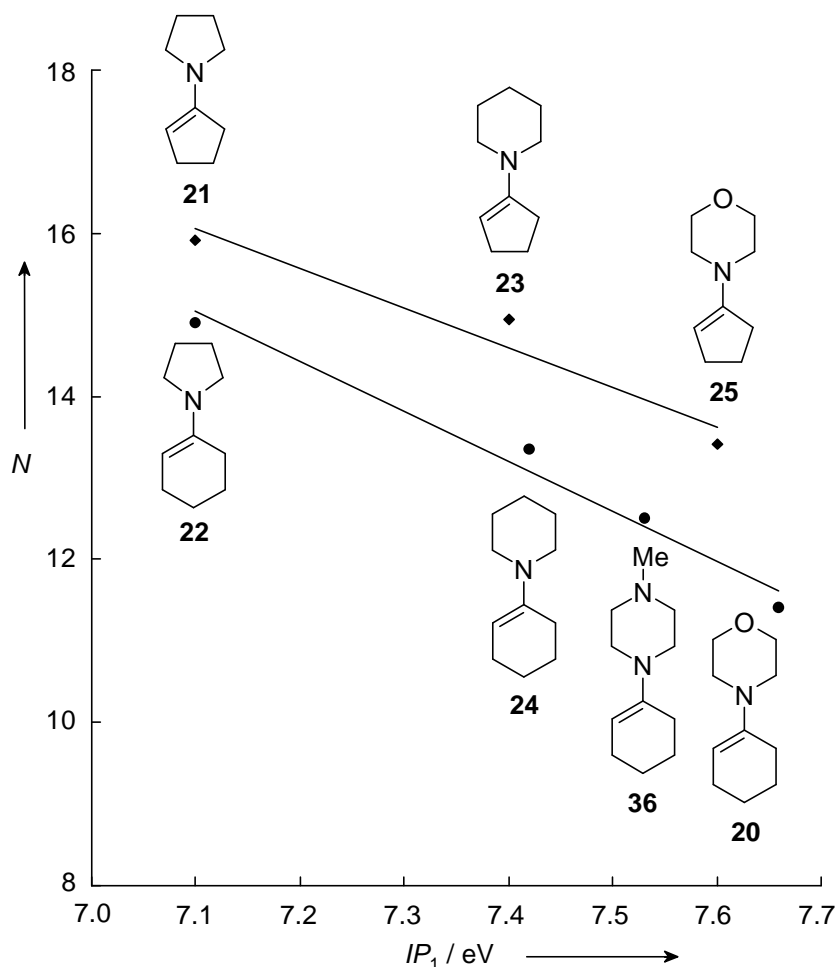
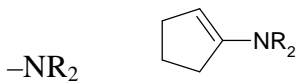
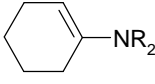
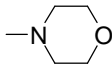
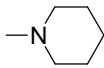
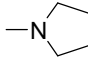


Figure 4.4: Correlation of the nucleophilic reactivities N with the first vertical ionization potentials IP_1 for cyclic enamines^[84] (cyclopentenyls: $N = -4.86IP_1 + 50.54$, $n = 3$, $r^2 = 0.9397$; cyclohexenyls: $N = -6.11IP_1 + 58.44$, $n = 4$, $r^2 = 0.9772$).

Comparison of compounds **25** with **34** or of **20** with **35** (Table 4.1) indicates that enamines with a methylphenylamino group are 3 to 5 times less nucleophilic than analogous structures with morpholino moieties. From the comparison of **32** with **33** (Table 4.1) one can derive that a dimethylamino group activates the double bond five times better than an *N*-morpholino group.

Cyclopentanone-derived enamines in general show higher reactivities than compounds derived from cyclohexanone (Table 4.5), and the ratio decreases in the series morpholino > piperidino > pyrrolidino compounds.

Table 4.5: Comparison of relative rate constants k_{rel} for the reactions of enamines from cyclopentanone and cyclohexanone with electrophiles.

Electrophile (Reaction Conditions)	Relative Reactivities k_{rel} of Enamines	
		
		
(lil) ₂ CH ⁺ (CH ₂ Cl ₂ , 20 °C)	30	1
(jul) ₂ CH ⁺ (CH ₂ Cl ₂ , 20 °C)	53	1
(thq) ₂ CH ⁺ (CH ₂ Cl ₂ , 20 °C)	43	1
(dma) ₂ CH ⁺ (CH ₂ Cl ₂ , 20 °C)	52	1
		
(lil) ₂ CH ⁺ (CH ₂ Cl ₂ , 20 °C)	23	1
(jul) ₂ CH ⁺ (CH ₂ Cl ₂ , 20 °C)	32	1
		
(lil) ₂ CH ⁺ (CH ₂ Cl ₂ , 20 °C)	8.5	1
(jul) ₂ CH ⁺ (CH ₂ Cl ₂ , 20 °C)	7.2	1
(thq) ₂ CH ⁺ (CH ₂ Cl ₂ , 20 °C)	6.1	1
PhN ₃ (C ₆ H ₆ , 25 °C) ^[a]	12	1

^[a] From ref. [60].

As shown in Figure 4.5, analogous dependencies of the nucleophilic reactivities on the ring size are also found for the corresponding 1-(trimethylsiloxy)cycloalkenes^[22,26] and 1-methylcycloalkenes.^[26] The linear correlation between N and S^+ of the substituent R ^[30] corresponds to that previously reported for proton additions to substituted CC-double bonds.^[86]

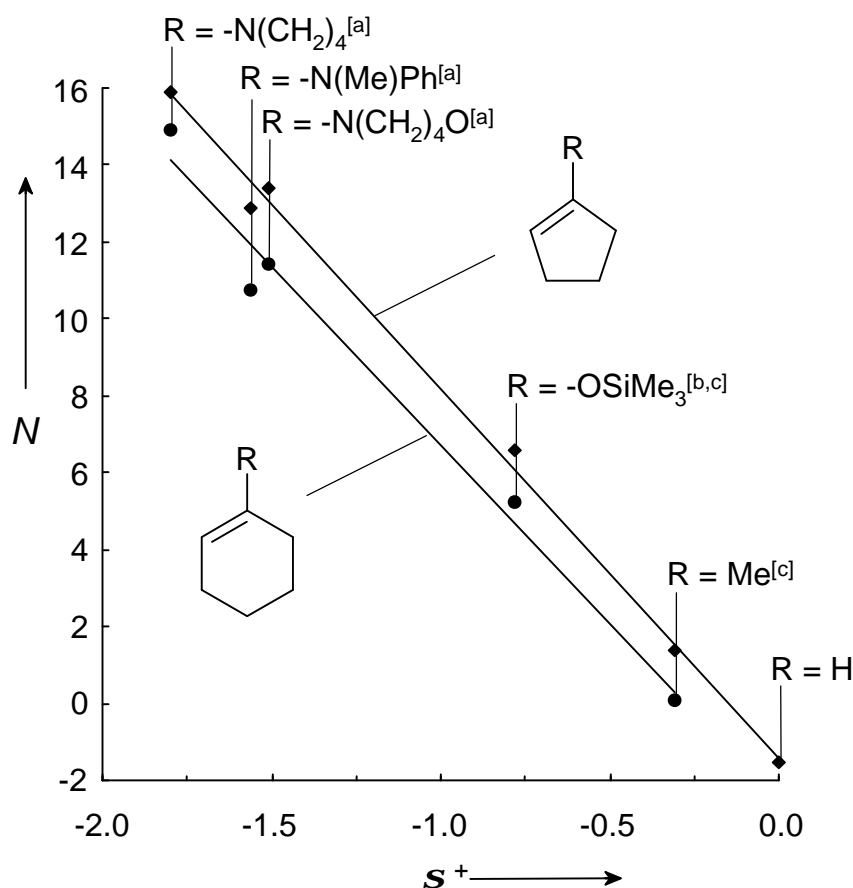


Figure 4.5: Correlation of N with s^+ for cyclic enamines, silyl enol ethers, and alkenes (cyclopentenes: $N = -9.60s^+ - 1.43$, $n = 6$, $r^2 = 0.9967$; cyclohexenes: $N = -9.28s^+ - 2.60$, $n = 5$, $r^2 = 0.9829$). [a] s^+ from ref. [26]. [b] The s^+ value of -OMe was used. [c] s^+ from ref. [30].

Substituents at the **b**-carbon atom (site of electrophilic attack) also have a noticeable influence on the reactivity of enamines. Replacement of substituents with electron donating properties like methyl (compound **27**) by electron withdrawing substituents like ethoxycarbonyl (compound **32**) reduces the reactivity of β C-substituted morpholinoethenes by a factor of about 700 (calculated for $(\text{pfa})_2\text{CH}^+$, CH_2Cl_2 , 20 °C). The corresponding phenyl substituted enamine **30** is in between.

A plot of the N parameters (from Table 4.1) versus the s_p -values^[30] of the **b**-substituents of these enamines shows a linear correlation (Figure 4.6). Since the variable substituent is at a position which does not adopt a formal positive charge in the product, the slope of this correlation is considerably smaller than that in Figure 4.5.

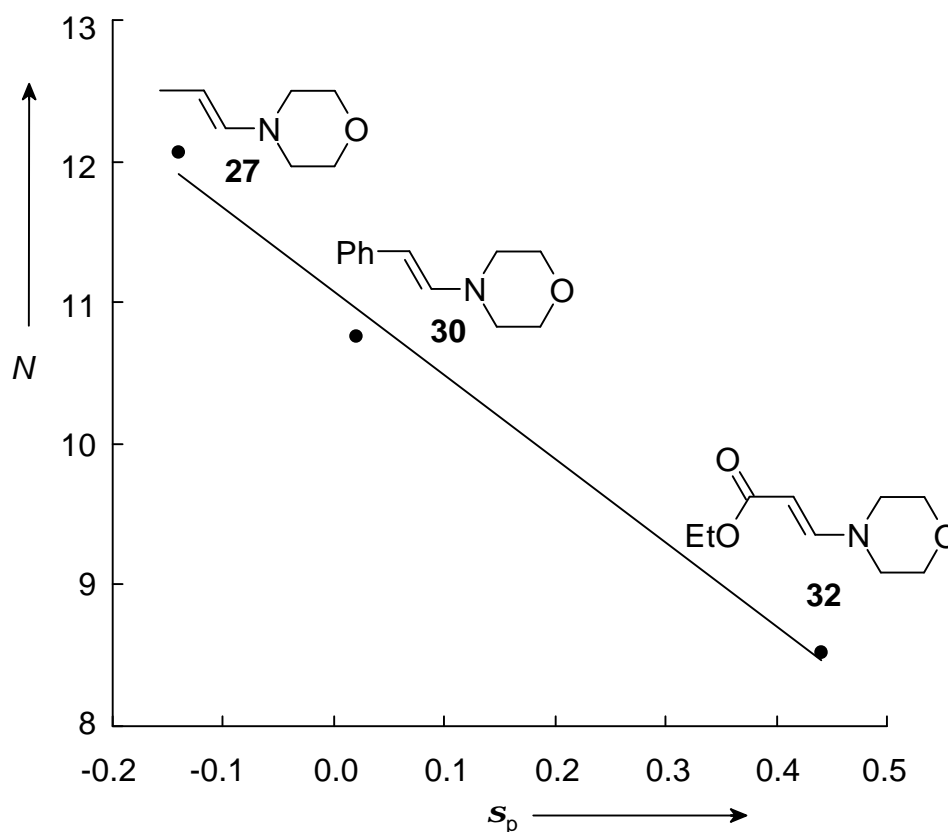
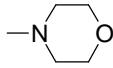
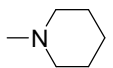
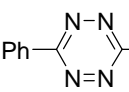


Figure 4.6: Correlation of N with s_p ^[30] for β C-substituted *E*-morpholinoethenes ($N = -5.95s_p + 11.08$, $n = 3$, $r^2 = 0.9898$).

Comparison of compounds **27** and **28** (Table 4.1) shows that *E,Z*-isomeric enamines differ little in reactivity. An additional methyl group at the β -carbon atom (**29**) reduces the reactivity by a factor of 30–40 because of steric shielding.

In contrast to intuition, β -(*N*-morpholino)styrene (**30**) reacts about 15 times faster with benzhydrylium ions than α -(*N*-morpholino)styrene (**31**) (Table 4.6). Obviously, the delocalization of the positive charge by the morpholino group is so efficient that the presence of an additional phenyl group at the new carbocation center is not helpful. In the transition state, the destabilization due to disturbing the amino resonance is more effective than the stabilization by the +M-effect of the phenyl group. Similar reactivity ratios were found for α - and β -aminostyrenes in 1,3-dipolar cycloadditions of phenyl azide^[61] and Diels-Alder reactions with 3,6-diphenyl-1,2,4,5-tetrazine^[64] (Table 4.6).

Table 4.6: Relative rate constants for the reactions of α C- and β C-phenyl-substituted enamines with various electrophiles.

Electrophile (Reaction Conditions)	Relative Reactivities k_{rel} of Enamines		
	$-\text{NR}_2$	$\text{Ph}-\text{C}(\text{NR}_2)=\text{C}$	$\text{Ph}-\text{C}(\text{NR}_2)=\text{C}$
			
$(\text{mpa})_2\text{CH}^+$ (CH_2Cl_2 , 20 °C)	1	8.9	
$(\text{dpa})_2\text{CH}^+$ (CH_2Cl_2 , 20 °C)	1	16	
$(\text{mfa})_2\text{CH}^+$ (CH_2Cl_2 , 20 °C)	1	16	
$(\text{pfa})_2\text{CH}^+$ (CH_2Cl_2 , 20 °C)	1	15	
PhN_3 (CHCl_3 , 30 °C) ^[a]		1	13
 (dioxane, 20 °C) ^[b]	$-\text{NMe}_2$	1	8

^[a] From ref. [61]. ^[b] From ref. [64].

According to Figure 4.7, increasing basicity of the indoles, as expressed by the $\text{p}K_a$ values of their conjugate acids,^[87] is associated with increasing nucleophilicity. The slope of the correlation line (0.50) indicates that roughly 50 % of the changes in $\Delta_r G^\ddagger$ are found in ΔG^\ddagger .

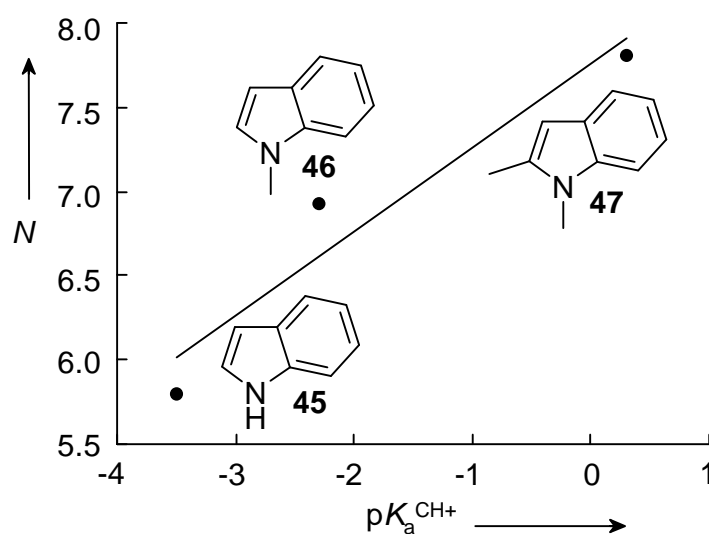


Figure 4.7: Plot of N versus $\text{p}K_a^{\text{CH}^+}$ (H_2O , 25 °C)^[87] for indoles ($N = 0.50 \text{p}K_a^{\text{CH}^+} + 7.76$, $n = 3$, $r^2 = 0.923$).

Comparison of **42-44** indicates that *N*-methylation of pyrrole increases the nucleophilicity by a factor of 20 while *N*-triisopropylsilylation reduces the nucleophilicity by a factor of 23 (calculated for $(\text{pfa})_2\text{CH}^+$, CH_2Cl_2 , 20 °C).

4.10 Conclusion

As outlined in the introduction, enamines have long been known as strong nucleophiles. With the method of using reference electrophiles^[26,80] it has now become possible to compare nucleophilicities of enamines with widely varying reactivity. As shown in Figure 4.8, enamines cover a wide range of nucleophilicity from $N \approx 4$ like typical enol ethers^[26] to $N \approx 16$ like stabilized carbanions in DMSO.^[48] For a typical s value of 0.85, this range corresponds to roughly ten orders of magnitude in rate constants or relative reaction times of 1 minute for **21** versus 20 000 years for **41**. The benefit of this scale for designing syntheses is obvious.

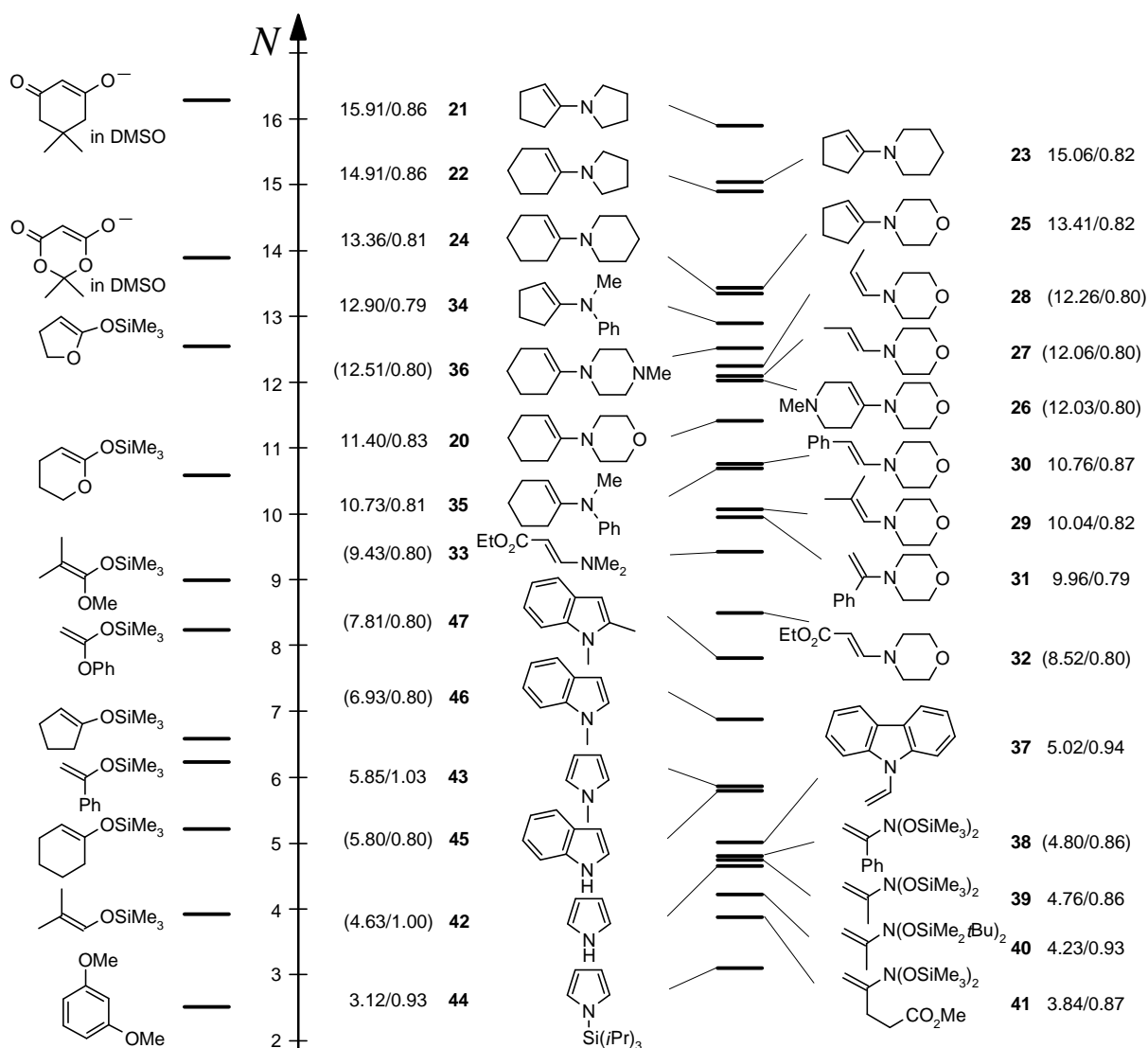


Figure 4.8: Nucleophilicity and slope parameters N/s of enamines, pyrroles and indoles from Table 4.1 compared with other π -systems and carbanions (parentheses indicate estimated values of s). While the N parameters of neutral π -nucleophiles depend little on solvent, nucleophilicity parameters of carbanions refer to the specified solvent.^[48]

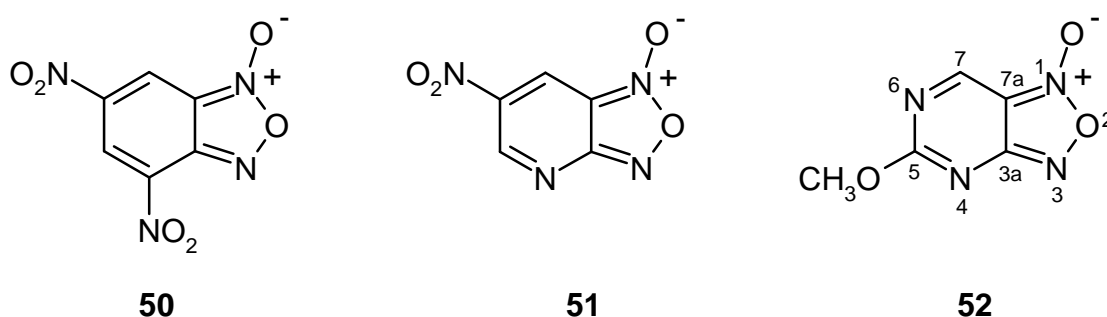
5. 5-Methoxyfuroxano[3,4-*d*]pyrimidine - a highly reactive neutral electrophile

5.1 Introduction

The electron deficiency of aromatic or heteroaromatic rings is significantly increased by annelation of a furoxan ring. There are many examples for the formation of stable anionic σ -complexes in this series.^[90] Nitro substituted benzofuroxanes have been recognized to be strong electrophiles. Since 4,6-dinitrobenzofuroxan (**50**) was found to react with heteroarenes faster than the *p*-nitrobenzenediazonium ion and the proton,^[91] it has been termed a "superelectrophile".^[92] Compound **50** reacts with methanol, ethanethiol, L-cysteine, acetone, cyclopentanone, 1,3-diketones, as well as with aromatic and heteroaromatic compounds even in the absence of a base. The ability of such compounds to react with intracellular amino and thiol functionalities has been considered to be responsible for their antileukemic activity.^[93]

Much attention has been given to aza- and diazabenzofuroxans (Scheme 5.1).^[90a,b,94] Recent investigations have shown that 6-nitro[2,1,3]oxadiazolo[4,5-*b*]pyridine-1-oxide (**51**), an aza-analog of **50**, affords an anionic σ -adduct with OH⁻ which is slightly more stable than the corresponding σ -adduct of **50**.^[95] It was thus indicated that an aza group in the aromatic ring is comparably efficient in promoting σ -adduct formation as a nitro substituent.

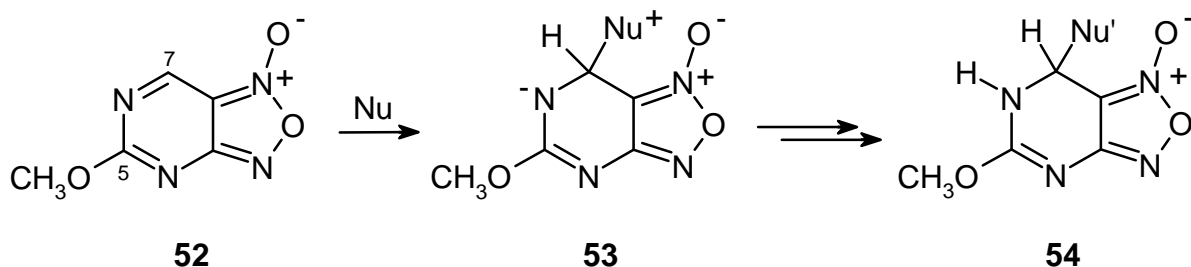
Previously, the formation of σ -adducts was reported, when 5-methoxy[1,2,5]oxadiazolo[3,4-*d*]pyrimidine 1-oxide (5-methoxyfuroxano[3,4-*d*]pyrimidine) (**52**) was dissolved in primary, secondary, or tertiary alcohols as well as in water.^[96] Compound **52** also reacts with carbanions derived from different CH-acids (from $pK_a = 20.0$ (acetone) to 5.21 (dimedone)) to yield the corresponding σ -adducts.^[97]



Scheme 5.1: Structures of 4,6-dinitrobenzofuroxan (**50**), 6-nitro[2,1,3]oxadiazolo[4,5-*b*]pyridine-1-oxide (**51**), and 5-methoxyfuroxano[3,4-*d*]pyrimidine (**52**).

5.2 Synthesis and reaction products

5-Methoxyfuroxano[3,4-*d*]pyrimidine (**52**) was synthesized by Dr. G. Remennikov, and he showed, that it reacts with several electron-rich arenes and ethylene derivatives at C-7 to yield 7-substituted 6,7-dihydro-5-methoxyfuroxano[3,4-*d*]pyrimidines (**54**).^[98] The formation of compounds **54** proceeds through the intermediacy of the zwitterions **53**, which are generated by the attack of nucleophiles at C-7 of **52** (Scheme 5.2).



Scheme 5.2: Reaction of 5-methoxyfuroxano[3,4-*d*]pyrimidine (**52**) with nucleophiles.

Since the change of hybridization of C-7 changes the nature of the conjugated π -system, the reaction described in Scheme 5.2 is associated with a hypsochromic shift in the UV spectrum.

5.3 Kinetic measurements

Kinetic measurements of the reactions of 5-methoxyfuroxano[3,4-*d*]pyrimidine (**52**) with the basis-set nucleophiles (see Figure 3.1) 1-(*N*-morpholino)cyclohexene (**20**), 2-(trimethylsiloxy)-4,5-dihydrofuran (**55**), and 1-(*N*-piperidino)cyclohexene (**24**) by UV-Vis spectroscopy (procedure and evaluation of rate constants is described in detail in Chapter 2) at $\lambda_{\text{max}} = 301$ nm in dichloromethane were performed (Table 5.1). ¹H NMR spectroscopy was used to follow the kinetics of the reaction of **52** with *N*-methylpyrrole (**43**) by Dr. G. Remennikov.

Table 5.1: Second-order rate constants for the reactions of **52** with the nucleophiles **43**, **20**, **55**, and **24**, and determination of the electrophilicity parameter *E* of **52**.

Nucleophile	Solvent	k_2 (20 °C) / M ⁻¹ s ⁻¹	$N^{[a]}$	$s^{[a]}$	<i>E</i>
43	d ₆ -DMSO	$(2.628 \pm 0.128) \times 10^{-3}$ ^[b]	5.85	1.03	-8.36
20	CH ₂ Cl ₂	$(2.634 \pm 0.045) \times 10^2$	11.40	0.83	-8.48
55	CH ₂ Cl ₂	$(5.907 \pm 0.044) \times 10^2$	12.56	0.70	-8.60
24	CH ₂ Cl ₂	$(1.801 \pm 0.037) \times 10^4$	13.36	0.81	-8.10
					$E(\mathbf{52}) = -8.37$ ^[c]

^[a] Data from ref. [26]. ^[b] NMR-kinetic measurement. ^[c] By minimization of $\Delta^2 = \sum(\log k_i - s_i(N_i + E))^2$ as described in ref. [89]. The calculations were actually performed with more decimals of log *k*, *N*, and *s* than indicated in the table. The use of log *k*, *N*, and *s* given in the table leads to slightly deviating results.

Equation 1.3 can now be used to calculate $E(\mathbf{52})$ from the rate constants given in Table 5.1 and the *N*- and *s*-parameters of the basis-set nucleophiles **20**, **24**, **43**, and **55**. Table 5.1 shows that closely similar values of *E* are derived from the reactions of **52** with different nucleophiles, indicating that eq. 1.3 is suitable for describing the reactions under consideration. The good agreement of the *E*-values derived from reactions in dichloromethane (entries 2-4, Table 5.1) with the *E*-value derived from a reaction in DMSO solution (entry 1) cannot a priori be expected since the rates of reactions of neutral nucleophiles with neutral electrophiles yielding zwitterionic intermediates may show considerable solvent dependence.^[99,100] Possibly because of the high polarity of the reactant **52** the solvent dependence of the rate constant is small in these reactions.

5.4 Discussion

With an electrophilicity parameter of $E = -8.37$, 5-methoxyfuroxano[3,4-*d*]pyrimidine (**52**) ranks among the strongest noncharged electrophiles, comparable in its reactivity to stabilized carbocations and cationic metal- π -complexes as shown in Figure 5.1.

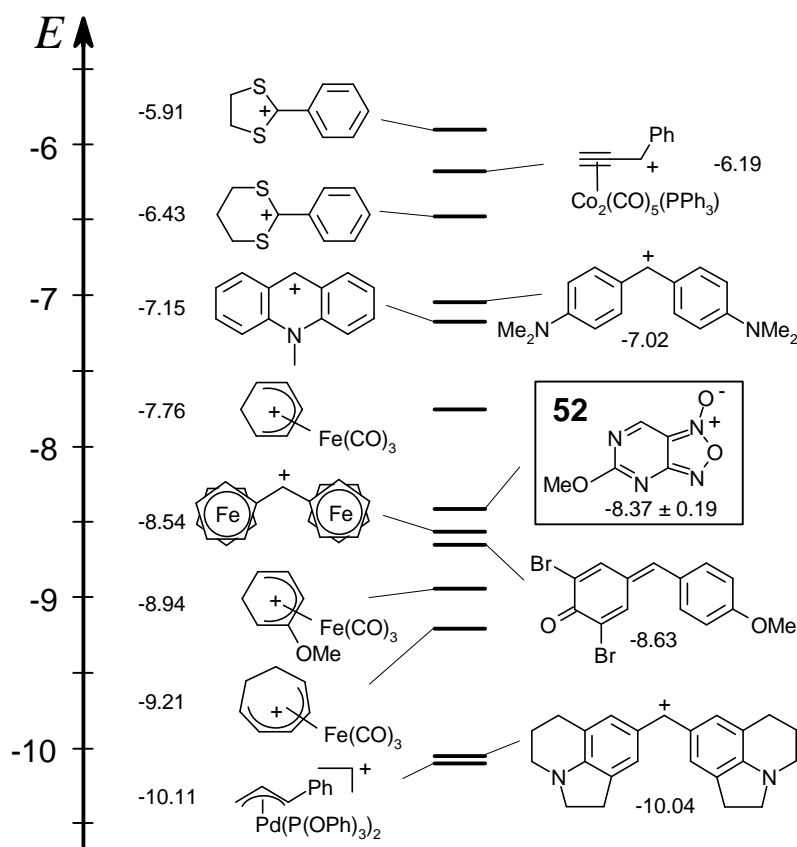
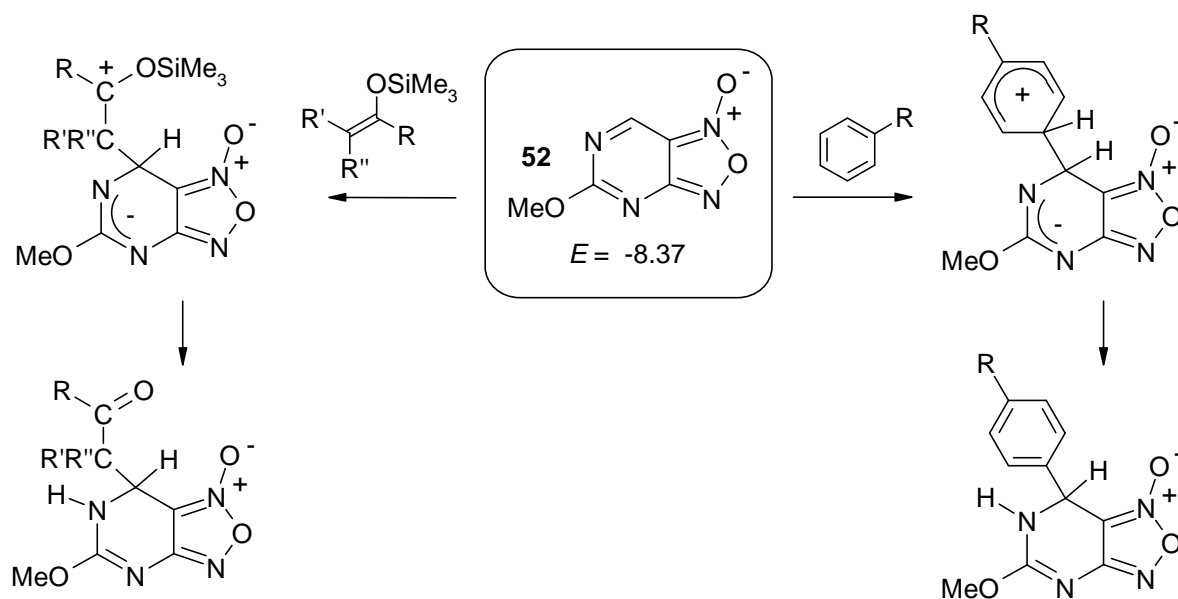


Figure 5.1: Comparison of the electrophilicity E of **52** with that of related charged and noncharged electrophiles.

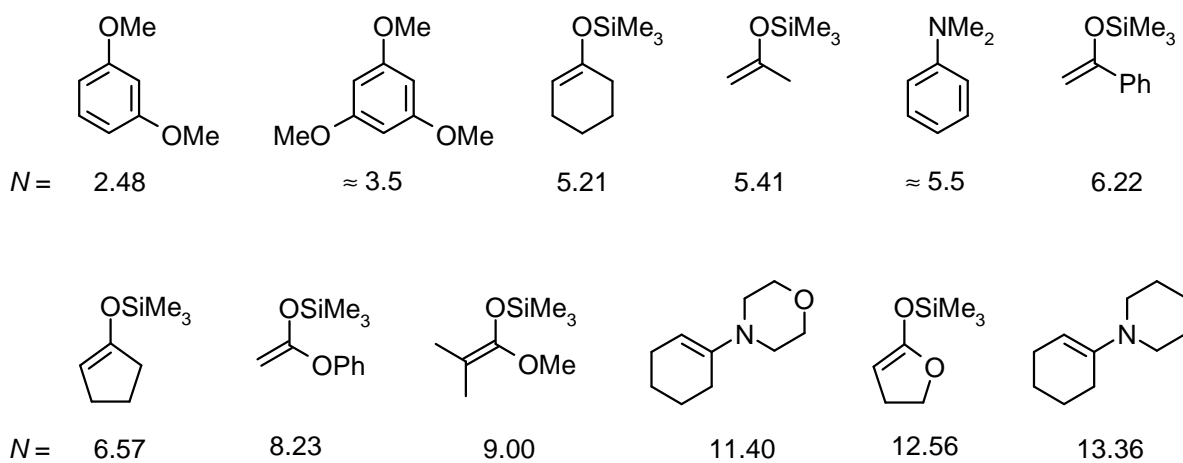
At typical concentrations (1 M), second-order reactions with $k_2 = 1 \times 10^{-4} \text{ M}^{-1} \text{ s}^{-1}$ proceed slowly with a half-life of 3 h. As a consequence of the electrophilicity parameter $E(\mathbf{52}) = -8.37$ derived above, the furoxanopyrimidine **52** can be expected to react with nucleophiles of $N > 3$ to 4 (see Chapter 3.9). This prediction was experimentally verified by Dr. G. Remennikov, who identified several reaction products (Scheme 5.3).

5.5 Conclusion

Anellation of a furoxan ring significantly increases the electron deficiency of the pyrimidine ring with the consequence that noncatalyzed reactions of 5-methoxyfuroxano[3,4-*k*]pyrimidine (**52**) with electron-rich arenes and alkenes become possible. Additions of π -nucleophiles to **52** follow eq. 1.3 and, therefore, allow one to characterize **52** by an electrophilicity parameter. Since the rate-determining step of the reaction sequence shown in Scheme 5.2 resembles that of nucleophilic aromatic substitutions, it is likely that this important class of reactions can also be described by eq. 1.3. Unpublished results by Phan Thanh Binh corroborate this conclusion.



Products isolated from reactions with:



Scheme 5.3: Products from the reactions of **52** with reference nucleophiles.

6. Rates and equilibria for the reactions of tertiary phosphanes and phosphites with carbocations

6.1 Introduction

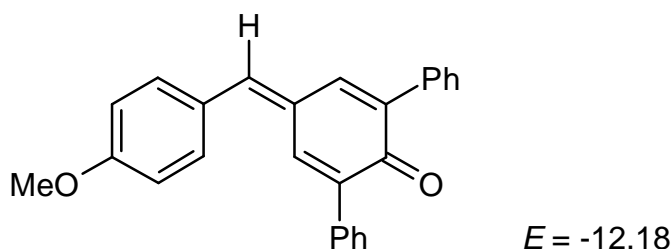
In homogeneous organometallic catalysis aromatic tertiary phosphanes, such as triphenylphosphane, are important ligands that find widespread use.^[101] These compounds stabilize the low oxidation states of the metal centers and can be used to modify both the electronic and steric properties of the catalysts. Substituents at the ortho-, meta-, or para-positions of the aromatic rings offer a means of tailoring the properties of the ligands and affect both the metal-phosphorous bond lengths and associated angles.^[102]

Ways of quantifying the electronic and steric properties of phosphanes have extensively been studied since 1970. Tolman's electronic and steric parameters have been the basis for these studies over the past 30 years.^[102-104] The improvement in NMR techniques and molecular modelling have introduced new possibilities for elucidating the properties of phosphanes.^[105]

In organocatalyses, phosphorous compounds also play an important role. Michael reactions can be catalyzed by phosphanes.^[106] Phosphoramidites and phosphites proved to be efficient catalysts for the Michael reactions of alkenones and alkynones with malonates, α -cyano esters, β -keto esters, and nitro compounds.^[107] In the Baylis-Hillman reaction, phosphanes can be used as effective nucleophilic catalysts.^[108-110]

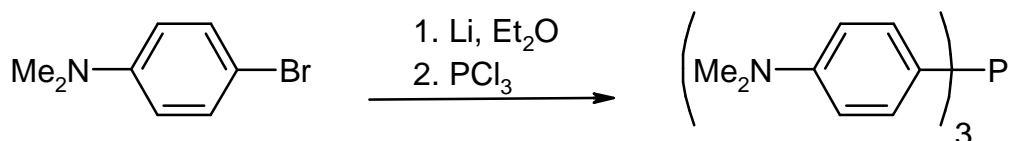
In these reactions, phosphorous compounds are added to Michael systems in the first step of the catalytic cycles. Therefore, phosphorous compounds must act as strong nucleophiles. It was the goal of this investigation to quantify the reactivities of tertiary phosphanes and phosphites. This information can then be used to elucidate their potential in organocatalysis.

We have recommended 22 differently substituted benzhydrylium ions as reference electrophiles for quantifying the reactivities of various types of nucleophiles.^[26,89] (see Chapter 3). For quantifying the nucleophilicities of various phosphanes and phosphites, kinetic measurements with several benzhydrylium ions (Figure 3.4) as well with the quinone methide $\text{ani}(\text{Ph})_2\text{QM}^{[48]}$ (Scheme 6.1) were performed.

**Scheme 6.1:** Structure and electrophilicity of the quinone methide anion(Ph)₂QM.

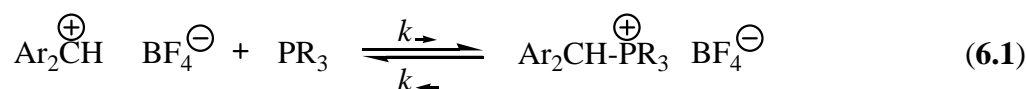
6.2 Nucleophiles

The following tertiary phosphanes and phosphites were purchased: (p-ClC₆H₄)₃P, Ph₃P, (p-MeC₆H₄)₃P, (p-MeOC₆H₄)₃P, (nBu)₃P, (PhO)₃P, (iPr)₃P, (cHex)₃P. Tris(4-dimethylaminophenyl)phosphine (p-Me₂NC₆H₄)₃P was synthesized by the lithium induced coupling of 3 equivalents of 4-bromo-N,N-dimethylaniline to phosphorous trichloride (Scheme 6.2).^[111,112]

**Scheme 6.2:** Synthesis of (p-Me₂NC₆H₄)₃P.

6.3 Reaction products

Since the benzhydrylium ions shown in Figure 3.4 differ considerably in their electrophilicities and Lewis acidities,^[47] not all combinations with the phosphanes and phosphites defined by eq. 6.1 give stable adducts.



56-68

Stable phosphonium salts **56-68** from benzhydrylium ions and phosphanes or phosphites, which have fully been characterized by MS, ¹H NMR, and ¹³C NMR spectroscopy, are listed in Table 6.1.

Table 6.1: ¹H, ¹³C, and ³¹P chemical shifts (CDCl₃) of phosphonium salts from benzhydrylium tetrafluoroborates and phosphorous nucleophiles.

No.	R ₃ P	Ar ₂ CH ⁺	Products	δ (¹ H NMR)	δ (¹³ C NMR)	δ (³¹ P NMR)
				Ar ₂ CH ⁺ PR ₃	Ar ₂ CH ⁺ PR ₃	Ar ₂ CH ⁺ PR ₃
1	(p-ClC ₆ H ₄) ₃ P	(mpa) ₂ CH ⁺	56 (78 %)	6.45	46.7	20.33
2	(p-ClC ₆ H ₄) ₃ P	(pfa) ₂ CH ⁺	57 (81 %)	6.53	46.2	21.14
3	Ph ₃ P	(dma) ₂ CH ⁺	58 (82 %)	6.10	47.7	20.36
4	Ph ₃ P	(mfa) ₂ CH ⁺	59 (65 %)	6.25	46.9	21.10
5	(p-MeC ₆ H ₄) ₃ P	(thq) ₂ CH ⁺	60 (77 %)	5.64	48.8	19.38
6	(p-MeC ₆ H ₄) ₃ P	(dpa) ₂ CH ⁺	61 (79 %)	6.30	47.4	21.33
7	(p-MeOC ₆ H ₄) ₃ P	(jul) ₂ CH ⁺	62 (76 %)	5.32	-----	18.18
8	(p-MeOC ₆ H ₄) ₃ P	(dma) ₂ CH ⁺	63 (98 %)	5.76	48.7	19.32
9	(nBu) ₃ P	(lil) ₂ CH ⁺	64 (83 %)	4.71	46.6	33.49
10	(nBu) ₃ P	(thq) ₂ CH ⁺	65 (83 %)	4.74	45.4	33.53
11	(nBu) ₃ P	(dma) ₂ CH ⁺	66 (93 %)	5.00	45.2	34.07
12	(PhO) ₃ P	(mfa) ₂ CH ⁺	67 (76 %)	4.66	48.4	19.86
13	(nBuO) ₃ P	(dpa) ₂ CH ⁺	68 (50 %)	5.50	45.5	37.05

An analysis of the chemical shifts of the benzhydryl H and C and of the P-nucleus (Ar₂CH⁺PR₃) shows that in the adducts Ar₂CH⁺PR₃ the replacement of weakly electrophilic benzhydryl cations by more reactive ones causes an increase of δ (¹H) and δ (³¹P) while δ (¹³C) decreases (Table 6.1, entries 1/2, 3/4, 5/6, 7/8, 9/10/11). Comparison of entries 3 and 8 in Table 6.1 shows that for the same benzhydryl fragment δ (¹H) and δ (³¹P) decrease while δ (¹³C) increases, when introducing electron donating groups in para-position at triaryl phosphanes.

6.4 Equilibrium constants

While all reactions of trialkylphosphanes and phosphites with benzhydrylium ions, investigated in this work, proceeded with quantitative formation of phosphonium ions, reversible adduct formation was observed for some combinations of triarylphosphanes. Since benzhydrylium ions are colored, in contrast to the triarylphosphanes and the corresponding adducts (phosphonium salts), the equilibrium constants given in Table 6.2 can be derived

from the UV-Vis absorbances of the benzhydrylium ions in the presence of variable concentrations of phosphanes.

Table 6.2: Equilibrium constants K , ΔG° -, ΔH° -, and ΔS° -values^[a] for the reactions of triarylphosphanes with benzhydrylium tetrafluoroborates in CH₂Cl₂ (eq. 6.1).

R ₃ P	Ar ₂ CH ⁺	K (20 °C) / L mol ⁻¹	ΔG° (20 °C) / kJ mol ⁻¹	ΔH° / kJ mol ⁻¹	ΔS° / J K ⁻¹ mol ⁻¹
(p-ClC ₆ H ₄) ₃ P	(thq) ₂ CH ⁺	6.26	-4.47	-34.08	-101.0
	(mpa) ₂ CH ⁺	8.52×10^3	-22.06		
	(dpa) ₂ CH ⁺	7.58×10^5	-33.00		
Ph ₃ P	(lil) ₂ CH ⁺	1.91×10^1	-7.19	-41.25	-116.2
	(jul) ₂ CH ⁺	5.57×10^1	-9.80	-34.57	-84.51
	(thq) ₂ CH ⁺	2.16×10^3	-18.72	-48.38	-101.2
	(dma) ₂ CH ⁺	1.26×10^5	-28.63		
(p-MeC ₆ H ₄) ₃ P	(lil) ₂ CH ⁺	1.38×10^3	-17.61		
	(jul) ₂ CH ⁺	2.41×10^3	-18.98		
	(thq) ₂ CH ⁺	1.69×10^5	-29.34		
(p-MeOC ₆ H ₄) ₃ P	(lil) ₂ CH ⁺	1.79×10^4	-23.86		
	(jul) ₂ CH ⁺	3.38×10^4	-25.41		
	(ind) ₂ CH ⁺	5.45×10^5	-32.19		
	(thq) ₂ CH ⁺	1.03×10^6	-33.75		

Table 6.2 shows that the equilibrium constants increase with increasing electrophilicities of the benzhydrylium ions as well as with increasing electron releasing ability of the p-substituents in the triarylphosphanes.

Combinations of weakly electrophilic benzhydrylium ions with (p-ClC₆H₄)₃P and Ph₃P gave only small product-concentrations at 20 °C. Lowering the temperature shifts the equilibrium to the side of adduct and enabled us to determine the equilibrium constants in these cases. Extrapolation of the plots of ln K versus $1/T$ (van't Hoff equation) yielded K for 20 °C. In all

cases, where the temperature-dependence of the equilibrium constants was investigated, reaction entropies ΔS° and enthalpies ΔH° were calculated by the Gibbs-equation (see Table 6.2).

As shown in Figure 6.1, the free enthalpies ΔG° (20 °C) of the reactions of triarylphosphanes with benzhydrylium ions correlate linearly with σ_p of the corresponding para-substituents.

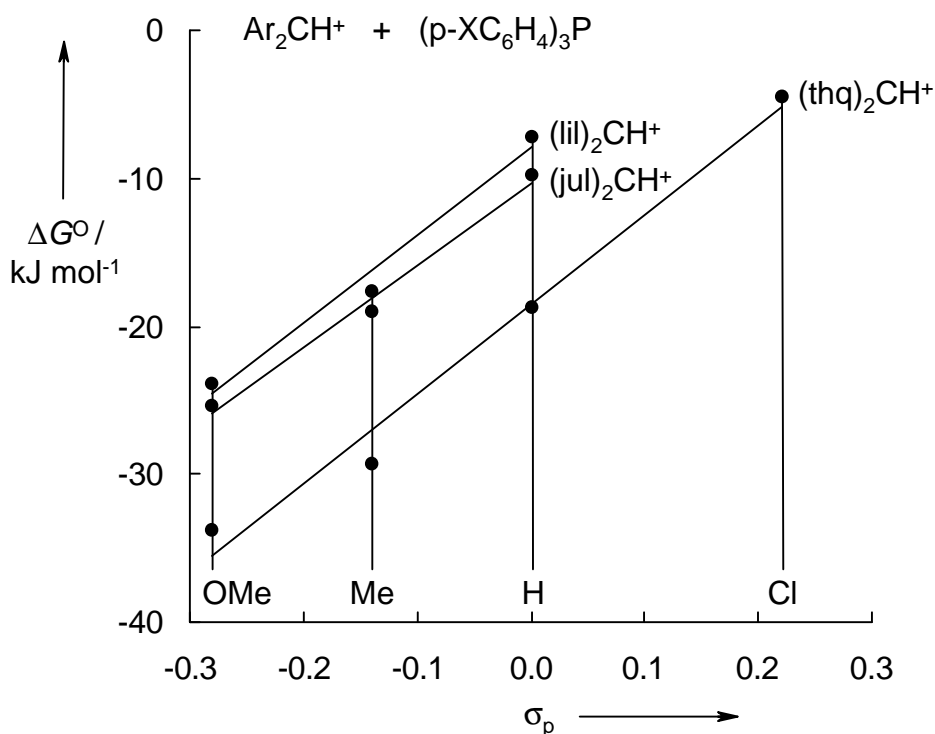


Figure 6.1: Correlation of ΔG° (20 °C) versus σ_p ^[30] for the reactions of $(p\text{-XC}_6\text{H}_4)_3\text{P}$ with Ar_2CH^+ in CH_2Cl_2 at 20 °C.

The linear correlations of $\log K$ for the combinations of triarylphosphanes with various benzhydrylium ions with pK_a of the corresponding phosphanes in nitromethane show slopes of 1.5-1.6 (Figure 6.2). It is presently not understood why substituent variation in the triaryl phosphanes affects carbon basicity to a greater extent than proton basicity.

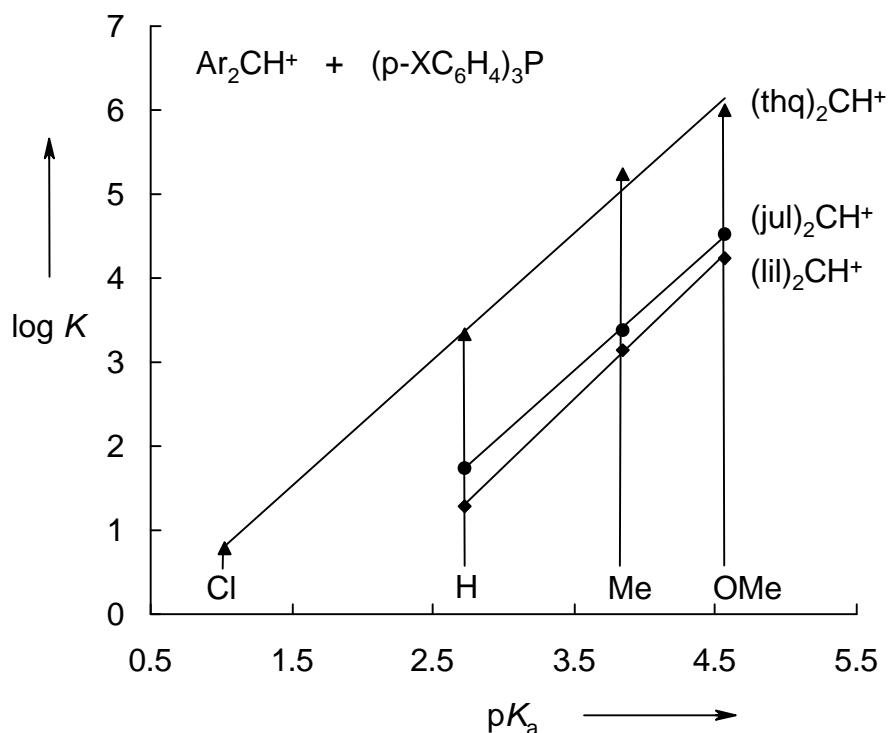


Figure 6.2: Correlations of $\log K$ versus pK_a (CH_3NO_2 ^[113]) for the reactions of $(p\text{-XC}_6\text{H}_4)_3\text{P}$ with Ar_2CH^+ in CH_2Cl_2 at $20\text{ }^\circ\text{C}$.

Kane-Maguire determined the kinetics of the reversible additions of a wide range of tertiary phosphanes to the tropylium ring of the cation $[\text{Cr}(\text{CO})_3(\eta^7\text{-C}_7\text{H}_7)]^+$ in acetone at $20\text{ }^\circ\text{C}$.^[114] From the rate law $k_{\text{obs}} = k_1[\text{R}_3\text{P}] + k_{-1}$ and the equation $K = k_1/k_{-1}$ the equilibrium constants K were calculated. These correlate well with the equilibrium constants K found for the reactions of several benzhydryl cations with the same tertiary phosphanes in methylene chloride (Figure 6.3). Again, substituent variation in the triarylphosphanes affects basicity towards benzhydrylium ions to a greater extent than basicity towards the tropylium complex (slopes: 1.4-1.6).

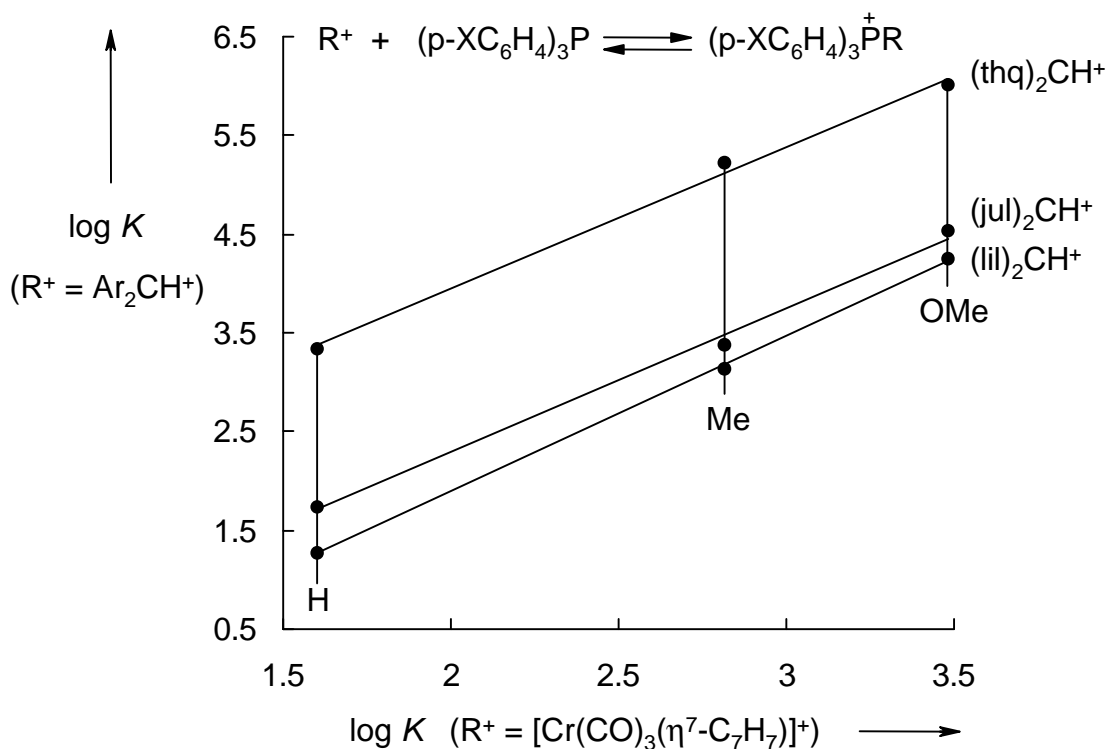


Figure 6.3: Correlation of $\log K$ [Ar_2CH^+] versus $\log K$ [$[\text{Cr}(\text{CO})_3(\eta^7\text{-C}_7\text{H}_7)]^+$] for the additions of para-substituted triaryl phosphanes (slope for $(\text{thq})_2\text{CH}^+ = 1.44$, slope for $(\text{jul})_2\text{CH}^+ = 1.46$, slope for $(\text{lil})_2\text{CH}^+ = 1.58$) to electrophiles.

6.5 Kinetics

The kinetics of the reactions of phosphanes and phosphites with benzhydryl cations and quinone methides were generally investigated under pseudo-first-order conditions by monitoring the decay of the benzhydrylium absorbances at $\lambda_{\text{max}} = 590\text{-}680$ nm after combining the benzhydrylium tetrafluoroborate solutions with 10 to 100 equivalents of PR_3 in dichloromethane. Details of performing kinetic measurements and evaluation of rate constants are given in Chapter 2.

In the case of incomplete consumption of the benzhydrylium ions, the rate constants were determined in analogy to the procedure described in Chapter 2.3. In Figure 6.4, the plots of the absorbances at $\lambda = 622$ nm versus t are shown for different initial concentrations of $(p\text{-ClC}_6\text{H}_4)_3\text{P}$. Higher concentrations of $(p\text{-ClC}_6\text{H}_4)_3\text{P}$ increase the reaction rates and the degree of conversion as determined by consumption of the benzhydrylium ion $(\text{mpa})_2\text{CH}^+$.

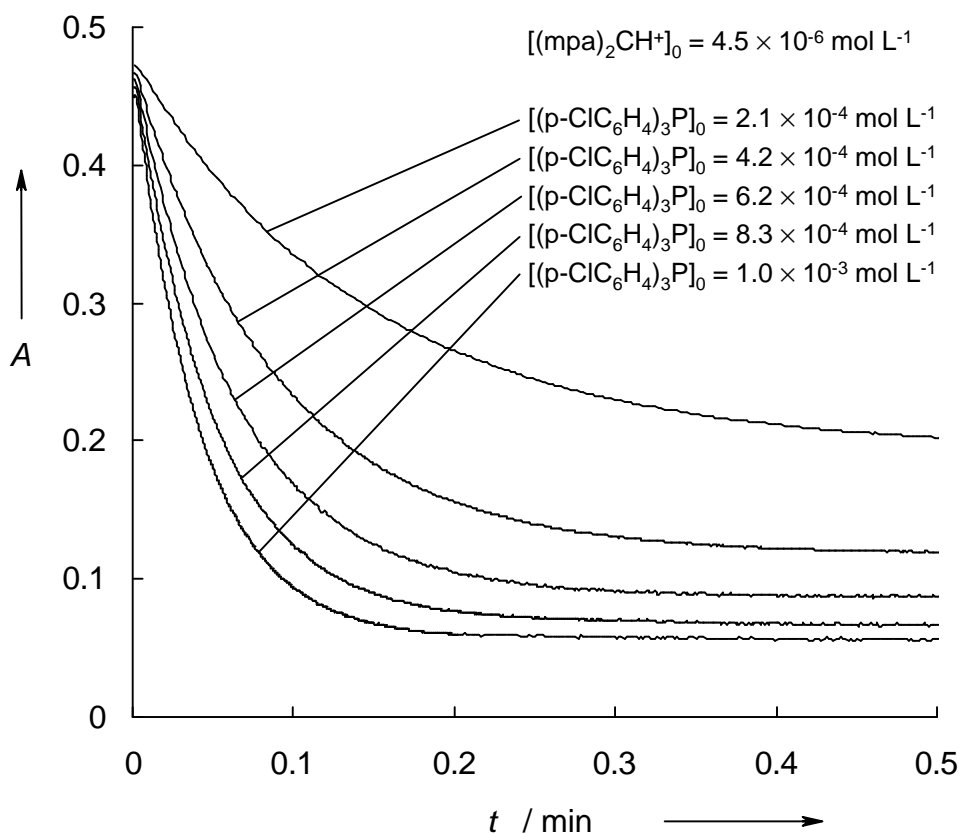


Figure 6.4: Plot of the absorbance at $\lambda = 622$ nm vs t for the reactions of (p-ClC₆H₄)₃P with (mpa)₂CH⁺ with different concentrations of R₃P in CH₂Cl₂ at 20 °C.

As shown in Table 6.3, the kinetics of all combinations of benzhydrylium ions with phosphanes and phosphites could be evaluated by one of these ways, and the equilibrium constants K calculated as the ratio $k_{\rightarrow}/k_{\leftarrow}$ closely resemble those derived from the concentrations of reactants and products (Table 6.2).

Table 6.3: Rate constants (20 °C) for the reactions of benzhydrylium tetrafluoroborates with phosphanes and phosphites in dichloromethane.

R ₃ P	Ar ₂ CH ⁺	<i>E</i>	<i>k</i> ₂ / L mol ⁻¹ s ⁻¹	<i>N</i>	<i>s</i>
(p-ClC ₆ H ₄) ₃ P	(thq) ₂ CH ⁺	-8.22	7.29 × 10 ² [a]		
	(dma) ₂ CH ⁺	-7.02	3.34 × 10 ³ [a]		
	(mpa) ₂ CH ⁺	-5.89	2.09 × 10 ⁴		
	(dpa) ₂ CH ⁺	-4.72	1.20 × 10 ⁵		
	(mfa) ₂ CH ⁺	-3.85	4.97 × 10 ⁵		
	(pfa) ₂ CH ⁺	-3.14	1.17 × 10 ⁶	12.58	0.65
Ph ₃ P	(lil) ₂ CH ⁺	-10.04	4.85 × 10 ² [a]		
	(jul) ₂ CH ⁺	-9.45	2.57 × 10 ³ [a]		
	(pyr) ₂ CH ⁺	-7.69	1.58 × 10 ⁴ [a]		
	(dma) ₂ CH ⁺	-7.02	5.21 × 10 ⁴		
	(mpa) ₂ CH ⁺	-5.89	2.93 × 10 ⁵		
	(mor) ₂ CH ⁺	-5.53	4.27 × 10 ⁵		
	(dpa) ₂ CH ⁺	-4.72	1.79 × 10 ⁶		
	(mfa) ₂ CH ⁺	-3.85	8.27 × 10 ⁶	14.33	0.65
(p-MeC ₆ H ₄) ₃ P	(lil) ₂ CH ⁺	-10.04	2.71 × 10 ³ [a]		
	(jul) ₂ CH ⁺	-9.45	7.15 × 10 ³ [a]		
	(thq) ₂ CH ⁺	-8.22	5.66 × 10 ⁴		
	(dma) ₂ CH ⁺	-7.02	2.43 × 10 ⁵		
	(mpa) ₂ CH ⁺	-5.89	1.27 × 10 ⁶		
	(dpa) ₂ CH ⁺	-4.72	8.30 × 10 ⁶	15.44	0.64
(p-MeOC ₆ H ₄) ₃ P	(lil) ₂ CH ⁺	-10.04	5.07 × 10 ³ [a]		
	(jul) ₂ CH ⁺	-9.45	1.93 × 10 ⁴		
	(thq) ₂ CH ⁺	-8.22	1.03 × 10 ⁵		
	(dma) ₂ CH ⁺	-7.02	4.87 × 10 ⁵		
	(mpa) ₂ CH ⁺	-5.89	2.38 × 10 ⁶	16.17	0.62
(p-Me ₂ NC ₆ H ₄) ₃ P	ani(Ph) ₂ QM	-12.18	6.11 × 10 ³		
	(lil) ₂ CH ⁺	-10.04	2.43 × 10 ⁵		
	(jul) ₂ CH ⁺	-9.45	7.01 × 10 ⁵		

Table 6.3: Continued

R ₃ P	Ar ₂ CH ⁺	<i>E</i>	<i>k</i> ₂ / L mol ⁻¹ s ⁻¹	<i>N</i>	<i>s</i>
(p-Me ₂ NC ₆ H ₄) ₃ P	(ind) ₂ CH ⁺	-8.76	1.41 × 10 ⁶		
	(thq) ₂ CH ⁺	-8.22	3.29 × 10 ⁶		
	(dma) ₂ CH ⁺	-7.02	1.06 × 10 ⁷	18.39	0.64
(iPr) ₃ P	(dma) ₂ CH ⁺	-7.02	2.77 × 10 ⁴	13.37	(0.70) ^[b]
Cy ₃ P	(jul) ₂ CH ⁺	-9.45	2.90 × 10 ³		
	(thq) ₂ CH ⁺	-8.22	2.83 × 10 ⁴		
	(dma) ₂ CH ⁺	-7.02	1.28 × 10 ⁵	14.64	0.68
(nBu) ₃ P	(lil) ₂ CH ⁺	-10.04	6.07 × 10 ³ ^[a]		
	(jul) ₂ CH ⁺	-9.45	1.61 × 10 ⁴ ^[a]		
	(thq) ₂ CH ⁺	-8.22	1.08 × 10 ⁵		
	(dma) ₂ CH ⁺	-7.02	7.68 × 10 ⁵		
	(mpa) ₂ CH ⁺	-5.89	4.68 × 10 ⁶	15.49	0.69
(PhO) ₃ P	(dpa) ₂ CH ⁺	-4.72	3.55		
	(mfa) ₂ CH ⁺	-3.85	2.06 × 10 ¹		
	(pfa) ₂ CH ⁺	-3.14	5.85 × 10 ¹		
	(fur) ₂ CH ⁺ ^[c]	-1.36	2.37 × 10 ³ ^[a]		
	(an) ₂ CH ⁺	0	1.22 × 10 ⁴	5.51	0.76
(nBuO) ₃ P	(lil) ₂ CH ⁺	-10.04	1.62		
	(jul) ₂ CH ⁺	-9.45	4.55		
	(ind) ₂ CH ⁺	-8.76	1.33 × 10 ¹		
	(thq) ₂ CH ⁺	-8.22	3.64 × 10 ¹		
	(pyr) ₂ CH ⁺	-7.69	5.79 × 10 ¹		
	(dma) ₂ CH ⁺	-7.02	2.23 × 10 ²		
	(mpa) ₂ CH ⁺	-5.89	1.34 × 10 ³		
	(mor) ₂ CH ⁺	-5.53	1.87 × 10 ³		
	(dpa) ₂ CH ⁺	-4.72	8.25 × 10 ³		
	(mfa) ₂ CH ⁺	-3.85	3.71 × 10 ⁴		
	(pfa) ₂ CH ⁺	-3.14	1.09 × 10 ⁵	10.36	0.70

^[a] Eyring activation parameters are given in Table 6.4. ^[b] Value of *s* is estimated. ^[c]

Counterion: OTf⁻.

Table 6.4: Eyring activation parameters^[a] for the reactions of benzhydryl cations with R₃P in CH₂Cl₂.

R ₃ P	Ar ₂ CH ⁺	ΔH^\ddagger / kJ mol ⁻¹	ΔS^\ddagger / J mol ⁻¹ K ⁻¹
(p-ClC ₆ H ₄) ₃ P	(thq) ₂ CH ⁺	31.18 ± 1.00	-83.61 ± 4.87
(p-ClC ₆ H ₄) ₃ P	(dma) ₂ CH ⁺	24.67 ± 0.60	-93.19 ± 2.90
Ph ₃ P	(lil) ₂ CH ⁺	35.87 ± 0.75	-71.00 ± 3.62
Ph ₃ P	(jul) ₂ CH ⁺	34.74 ± 1.13	-60.10 ± 5.26
Ph ₃ P	(pyr) ₂ CH ⁺	26.25 ± 0.49	-74.86 ± 2.20
(p-MeC ₆ H ₄) ₃ P	(lil) ₂ CH ⁺	36.18 ± 0.44	-55.65 ± 2.09
(p-MeC ₆ H ₄) ₃ P	(jul) ₂ CH ⁺	31.37 ± 0.47	-63.99 ± 2.22
(p-MeOC ₆ H ₄) ₃ P	(lil) ₂ CH ⁺	34.84 ± 0.36	-55.01 ± 1.71
(nBu) ₃ P	(lil) ₂ CH ⁺	22.44 ± 0.37	-95.81 ± 1.58
(nBu) ₃ P	(jul) ₂ CH ⁺	20.22 ± 1.32	-95.29 ± 5.95
(PhO) ₃ P	(fur) ₂ CH ⁺	30.02 ± 0.25	-77.77 ± 1.48

^[a] As indicated by the error limits in ΔH^\ddagger and ΔS^\ddagger , the large number of decimals is per se meaningless, but are needed for the reproduction of the rate constants in Table 6.3.

6.6 Solvent dependence of the rate constants

In previous work, we have found that the rates of the reactions of carbocations with uncharged nucleophiles are only slightly affected by solvent polarity.^[37,38,115] Figure 6.5 illustrates that the same is true for the reactions of the bis(p-dimethylaminophenyl)carbenium ion (dma)₂CH⁺ with triphenylphosphane. While there are poor correlations between these rate constants and the $E_T(30)$ -values^[100] or dielectricity constants ϵ ,^[100] Figure 6.5 shows that the rate constants decrease slightly with increasing Gutmann's donor numbers DN ^[100] of the solvents.

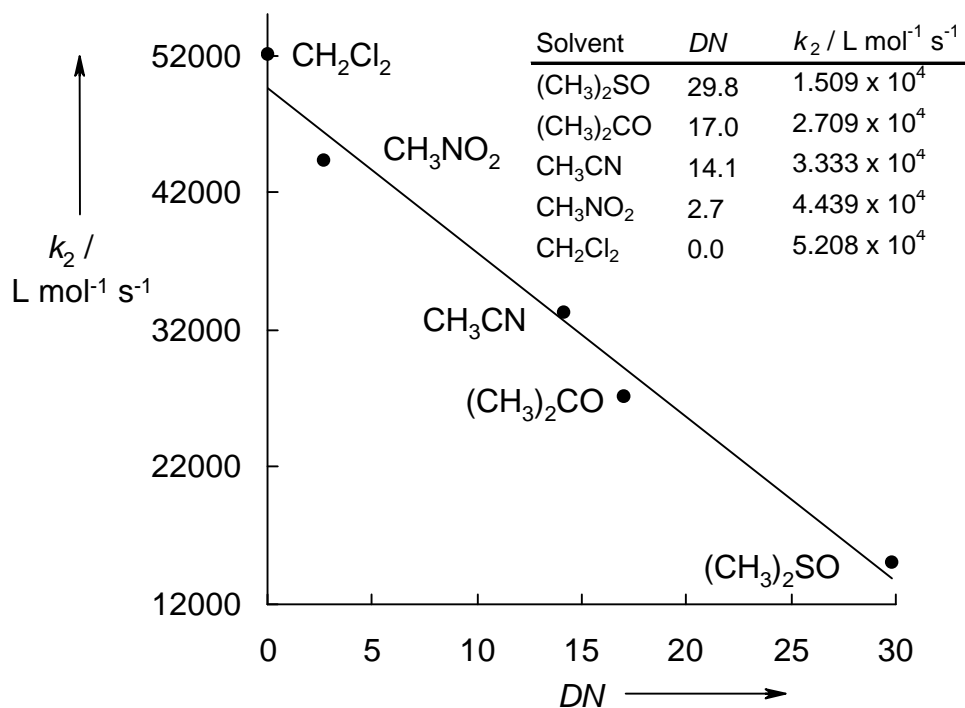


Figure 6.5: Correlation of the rate constants (20 °C) k_2 of the reactions of $(\text{dma})_2\text{CH}^+ \text{BF}_4^-$ with Ph_3P versus $DN^{[100]}$ of the corresponding solvents ($n = 5$, $k_2 = (-1.198 \times 10^3) \times DN + (4.963 \times 10^4)$, $r^2 = 0.9804$).

In contrast, the rate constants of the reactions of $(p\text{-H}_3\text{CO-C}_6\text{H}_4)_2\text{CH}^+ \text{OTf}^-$ with 2-methyl-1-pentene^[37] and of $(p\text{-H}_3\text{CO-C}_6\text{H}_4)\text{PhCH}^+ \text{OTf}^-$ with dimethylphenylsilane^[15] correlate poorly with the donor numbers of the solvents and increase slightly with the corresponding $E_T(30)$ -values. In spite of the existence of these correlations with solvent polarity parameters it should be kept in mind that the solvent effects are minute for all these reactions since charges are neither created nor destroyed in reactions of ions with neutral molecules. Very small solvent effects (nitromethane, acetonitrile, acetone, etc.) have also been reported for the reactions of phosphanes and phosphites with metal-complexes,^[116] metal- π -complexes^[12,117] and tropylium ions.^[13]

6.7 Determination of the nucleophilicities of phosphorous compounds

Figure 6.6 shows that the reactions of benzhydrylium ions with tertiary phosphanes and phosphites also follow eq. 1.3. The nucleophilicity parameters N as well as the slope parameters s derived from these correlations are listed in Table 6.3.

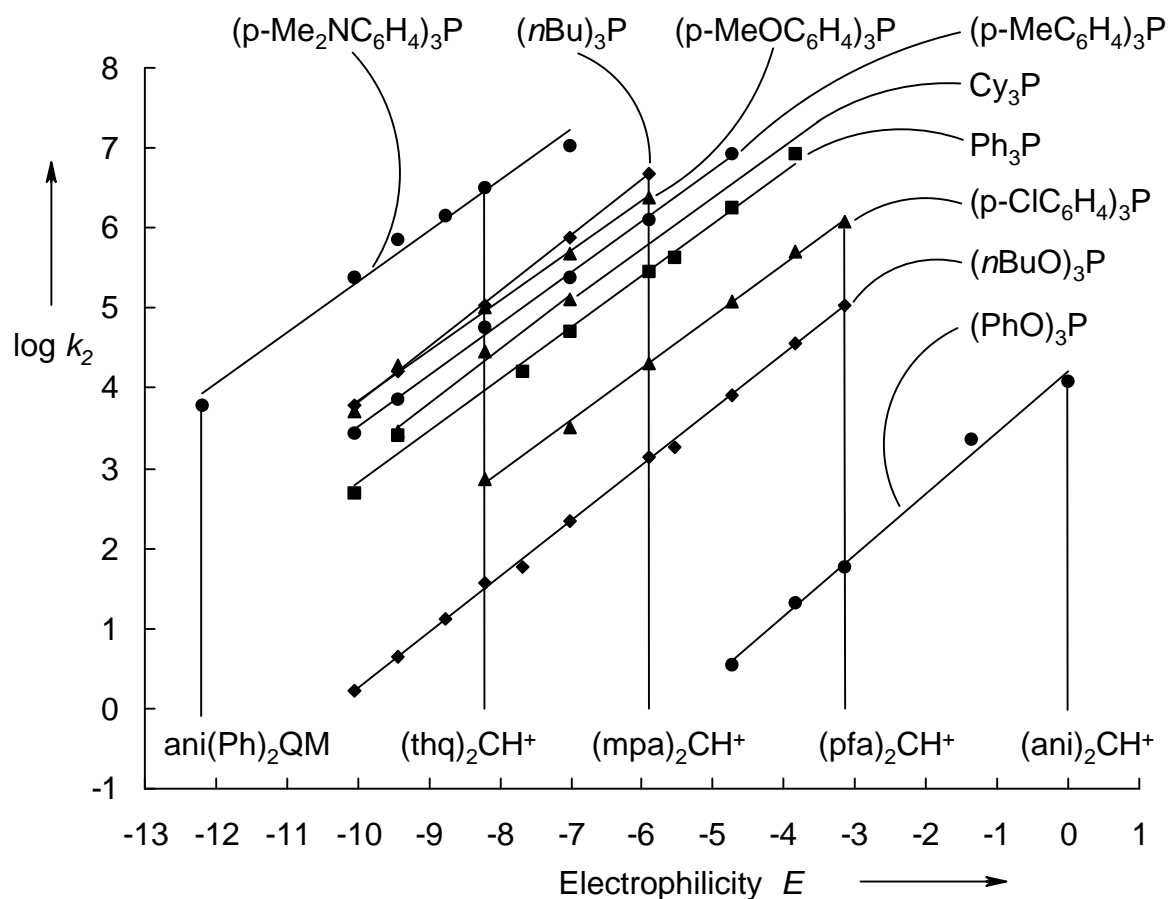


Figure 6.6: Correlations of the rate constants ($\log k$, 20 °C, CH_2Cl_2) for the reactions of R_3P with the benzhydryl cations Ar_2CH^+ versus their E parameters.

It should be noted that even the rate constant for the reaction of tris(*p*-dimethylaminophenyl)phosphane with the quinone methide $\text{ani}(\text{Ph})_2\text{QM}$ ($E = -12.18$) nicely matches the correlation lines demonstrating that the previously determined E parameters for quinone methides^[48,118] are also applicable to reactions with this class of nucleophiles, and that charged and uncharged electrophiles may be used side by side for these analyses.

The close similarity of the slopes which are comparable to those of amines and alkoxides indicates that these reactions may also be described by Ritchie's constant selectivity relationship^[8a,10] as previously noticed by Sweigart and Alavosus.^[13] With the N and s parameters derived from Figure 6.6, we can now compare the reactivities of P-nucleophiles with those of carbanions, amines, enamines, silyl ketene acetals, silyl enol ethers, and allyl stannanes (Figure 6.7).

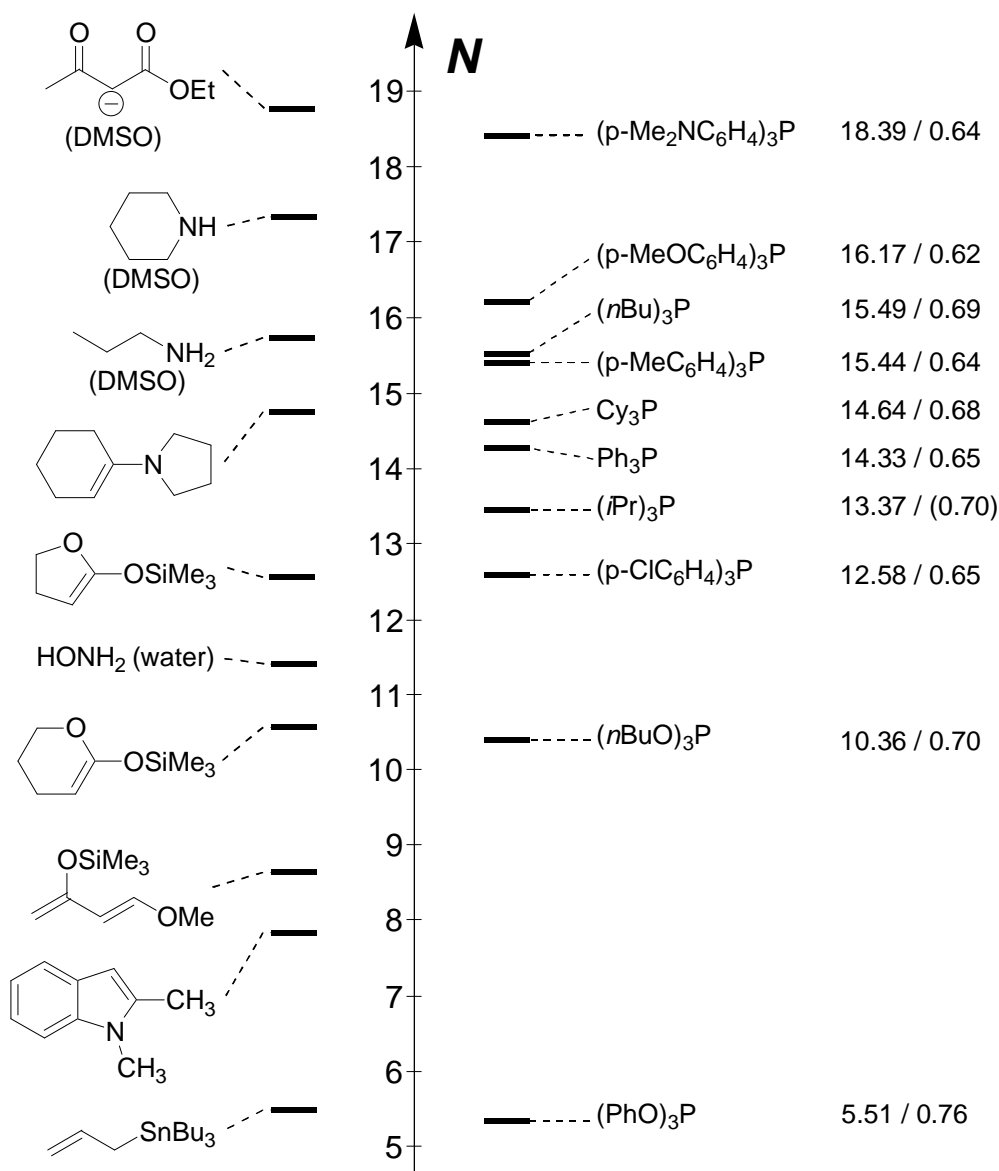


Figure 6.7: Comparison of the nucleophilic reactivities of phosphanes and phosphites with other types of nucleophiles^[48,88] (solvent dichloromethane, if not mentioned otherwise).

Since the quaternary phosphonium ions derived from triaryl- and trialkylphosphanes cannot undergo consecutive reactions, fast backward reactions are responsible for the failure to observe reaction products with certain electrophiles even when the rate constants of the phosphane carbocation combinations are predicted to be fast by equation 1.3.

6.8 Intrinsic barriers

Rate equilibrium relationships provide important informations about the factors that control organic reactivity.^[119,120] However, not many reaction types are known, for which the dependence of rates and equilibria has been determined.^[121] Kane-Maguire and Sweigart reported that numerous reactions of tertiary phosphanes and phosphites with metal-coordinated carbocations, for which rate constants have been determined, proceed with incomplete formation of the adducts.^[12] This observation prompted me to investigate rate equilibrium relationships for the reactions of phosphorous nucleophiles with benzhydrylium ions, which play a key-role in our systematic approach to polar organic reactivity.^[15,17,25]

For only one electrophile, (thq)₂CH⁺, as well as for a single nucleophile, Ph₃P, there are four reaction partners for which rate and equilibrium constants are available. The slopes of the corresponding $\Delta G^\ddagger/\Delta G^0$ correlations in Figures 6.8 and 6.9 (0.42 and 0.48) indicate that variation of the electrophile as well as variation of the nucleophile affects the activation free enthalpies about half as much as the reaction free enthalpies.

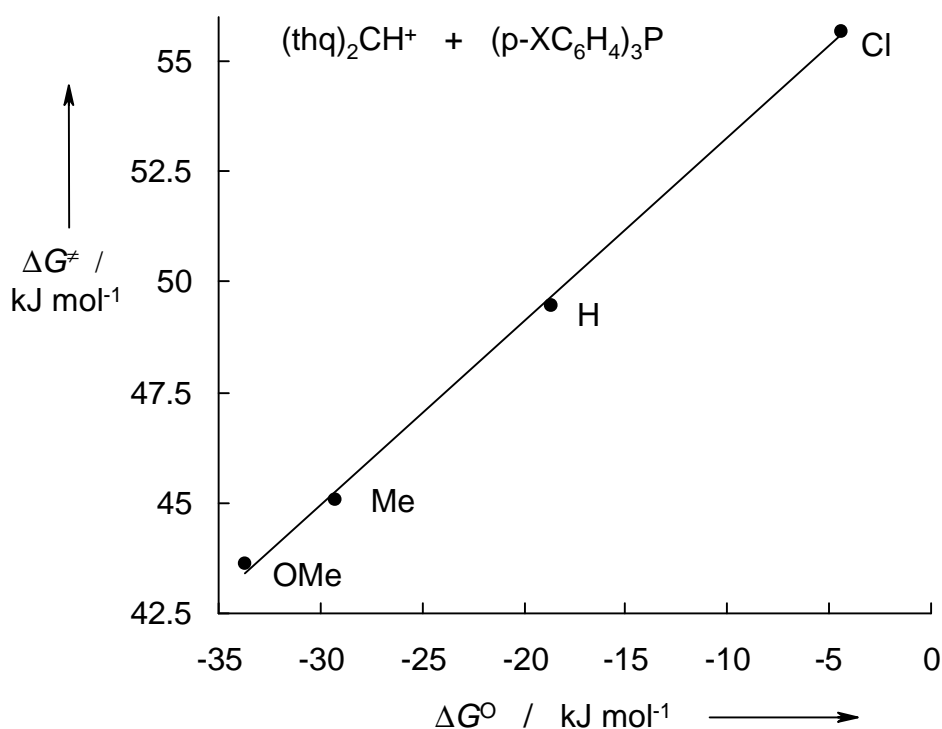


Figure 6.8: Correlation of ΔG^\ddagger with ΔG^0 for the reactions of para substituted triarylphosphanes with (thq)₂CH⁺ in CH₂Cl₂ at 20 °C (n = 4, $\Delta G^\ddagger = 0.416 \times \Delta G^0 + 57.4$, $r^2 = 0.9986$).

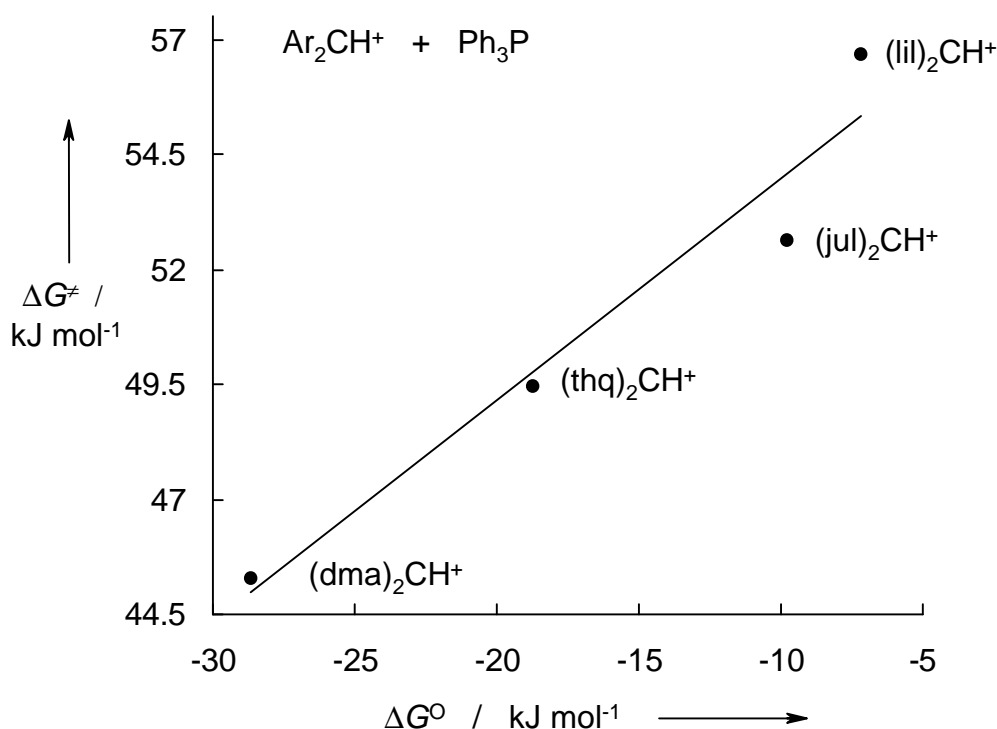


Figure 6.9: Correlation of ΔG^\ddagger with ΔG° for the reactions of Ph_3P with Ar_2CH^+ in CH_2Cl_2 at 20°C ($n = 4$, $\Delta G^\ddagger = 0.482 \times \Delta G^\circ + 58.8$, $r^2 = 0.9413$).

The intercepts of the correlations in Figure 6.8 and 6.9 are similar ($57\text{--}59 \text{ kJ mol}^{-1}$) and correspond to the activation free enthalpy at $\Delta G^\circ = 0$, which has been termed the intrinsic barrier ΔG_0^\ddagger by Marcus.^[81] While the intrinsic barrier has initially been assumed to adopt a characteristic (constant) value for a reaction series,^[81] it has later been recognized that intrinsic barriers may vary also within reaction series.^[122]

Since the last term in the Marcus equation (eq. 4.1) is usually negligible, linear $\Delta G^\ddagger/\Delta G^\circ$ correlations with slopes of $\alpha \approx 0.5$, as shown by Figures 6.8 and 6.9 imply that the intrinsic barriers for the reactions of benzydrylium ions with phosphanes are almost constant. This conclusion is in accord with a recent theoretical analysis of the reactions of benzydrylium ions with nucleophiles, which related the variability of intrinsic barriers with the magnitude of the slope parameters s in eq. 1.3.^[47] It was shown that linear $\log k$ vs E correlations with $s > 0.67$ imply a decrease of the intrinsic barriers with increasing exothermicity, while $s < 0.67$ indicates an increase of the intrinsic barriers with increasing exothermicity.^[47] Consequently,

the *s*-parameters close to 0.67, as listed in Table 6.3 are in accord with constant intrinsic barriers.

These findings are in clear contrast to the situation in reactions of benzhydrylium ions with CH hydride donors (*s* ≈ 1), where the intrinsic barriers decrease when exothermicity is increased by variation of the hydride acceptors, while the intrinsic barriers increase when the exothermicity is increased by variation of the hydride donors.^[123]

With almost constant intrinsic barriers ($\Delta G_0^\ddagger \approx 58 \text{ kJ mol}^{-1}$) for the reactions of phosphanes and phosphites with benzhydrylium ions, one can now use Marcus' theory to calculate ΔG^\ddagger for the reactions of phosphanes with benzhydrylium ions from the reaction free enthalpies reported in Table 6.2 and the intrinsic barrier of $\Delta G_0^\ddagger \approx 58 \text{ kJ mol}^{-1}$ derived from Figures 6.8 and 6.9. Table 6.5 shows that the observed activation free enthalpies (from Table 6.4) generally agree within 2 kJ mol^{-1} with those calculated from eq. 4.1.

Table 6.5: Comparison of experimental activation free enthalpies with those calculated from the Marcus equation (4.1) for $\Delta G_0^\ddagger \approx 58 \text{ kJ mol}^{-1}$ for the reactions of para substituted triarylphosphanes with (Ar)₂CH⁺ in CH₂Cl₂ at 20 °C.

R ₃ P	Ar ₂ CH ⁺	$\Delta G^0 / \text{kJ mol}^{-1}$	$\Delta G_{\text{exp}}^\ddagger / \text{kJ mol}^{-1}$	$\Delta G_{\text{calc}}^\ddagger / \text{kJ mol}^{-1}$
(p-ClC ₆ H ₄) ₃ P	(thq) ₂ CH ⁺	-4.5	55.7	55.8
Ph ₃ P	(lil) ₂ CH ⁺	-7.2	56.7	54.5
Ph ₃ P	(jul) ₂ CH ⁺	-9.8	52.6	53.2
Ph ₃ P	(thq) ₂ CH ⁺	-18.7	49.5	49.0
Ph ₃ P	(dma) ₂ CH ⁺	-28.6	45.3	44.6
(p-MeC ₆ H ₄) ₃ P	(thq) ₂ CH ⁺	-29.3	45.1	44.3
(p-MeOC ₆ H ₄) ₃ P	(thq) ₂ CH ⁺	-33.8	43.6	42.4

6.9 Quantitative analysis of ligand effects

Figure 6.10 shows a good linear correlation between N and Hammett's σ_p constants. It is, therefore, possible to employ Hammett's substituent constants for a reliable prediction of N values of further triarylphosphanes. Electronic effects of the para-substituents in triaryl phosphanes directly affect their nucleophilicities.

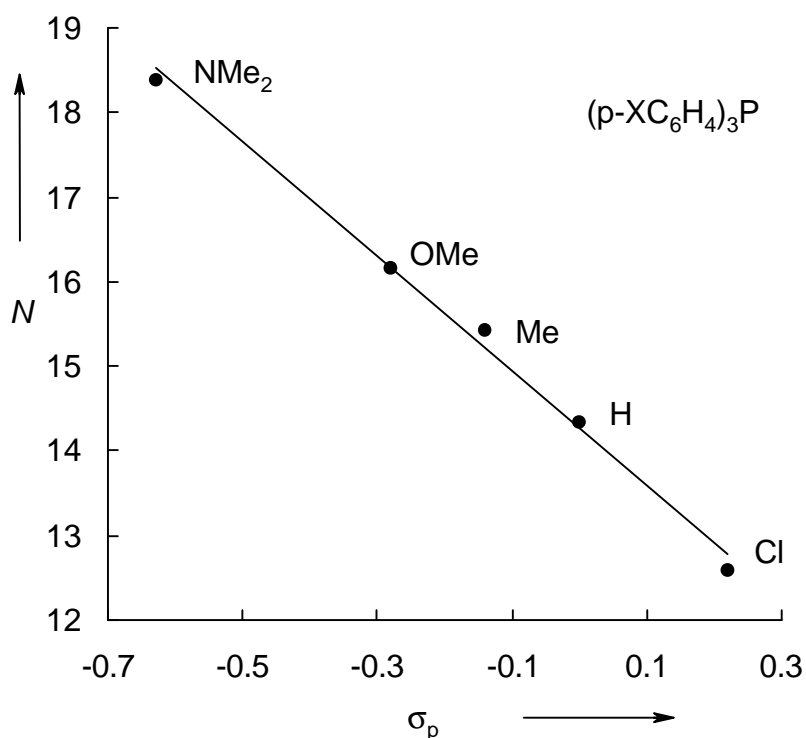


Figure 6.10: Correlation of N with σ_p ^[30] for para substituted triarylphosphanes ($n = 5$, $N = -6.757 \times \sigma_p + (1.426 \times 10^1)$, $r^2 = 0.9939$).

In analogy to the correlation between nucleophilicity and σ_p shown in Figure 6.10, there is also a linear correlation between the nucleophilicity parameters N of triarylphosphanes and their pK_a values in nitromethane (Figure 6.11).

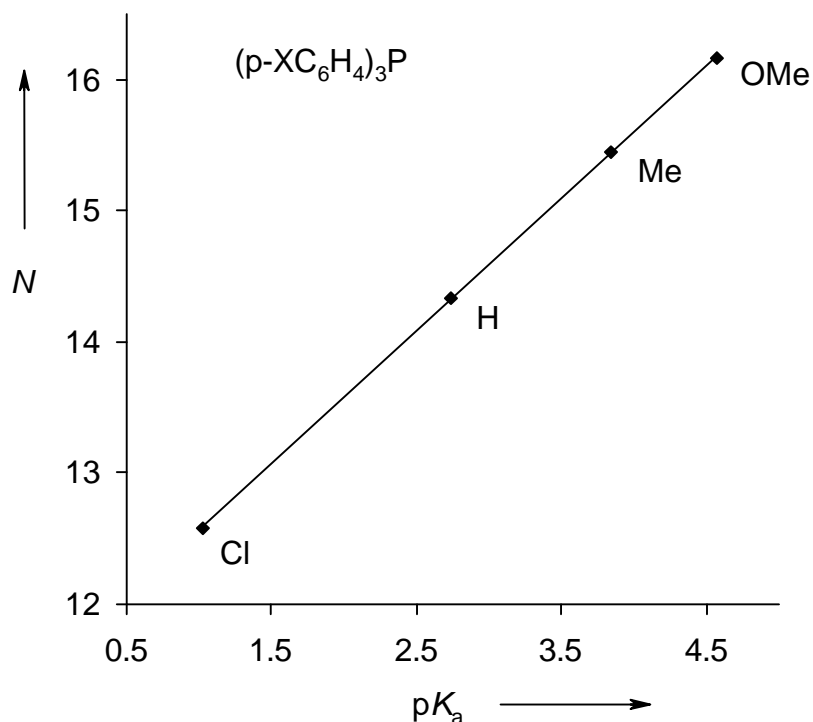


Figure 6.11: Correlation of N with pK_a (CH_3NO_2 ^[113]) for para-substituted triarylphosphanes ($n = 4$, $N = 1.014 \times pK_a + (1.154 \times 10^1)$, $r^2 = 0.9999$).

The half-wave oxidation potentials $E_{1/2}$ of tertiary phosphorous compounds were measured by electrochemical oxidation of these compounds.^[124] Tertiary phosphorous compounds are oxidized irreversibly and consume less than one electron per molecule.^[125] Removing one electron by anodic oxidation results in formation of the cation radicals $\text{R}_3\text{P}^{+\bullet}$ which then enter into fast chemical reactions with nucleophilic components of the solution.

Figure 6.12 shows a good correlation of the nucleophilicities N of six tertiary phosphanes and phosphites with their half-wave oxidation potentials $E_{1/2}$ ($N = -6.411 \times E_{1/2} + 20.205$, $r^2 = 0.9815$) towards the reference electrode Ag/AgNO_3 ($c = 0.1 \text{ M}$) in acetonitrile.

Multiplication of the observed slope with an averaged value of $s \approx 0.65$, for the employed phosphorous compounds results in slope of -4.17 for the correlation of $\log k$ versus $E_{1/2}$. This value is much smaller than the slope, which was found for the correlation between the E parameters of benzhydrylium ions and their reduction potentials in acetonitrile ($E = 14.091 \times E_{\text{red}}^{\text{O}} - 0.279$).^[126]

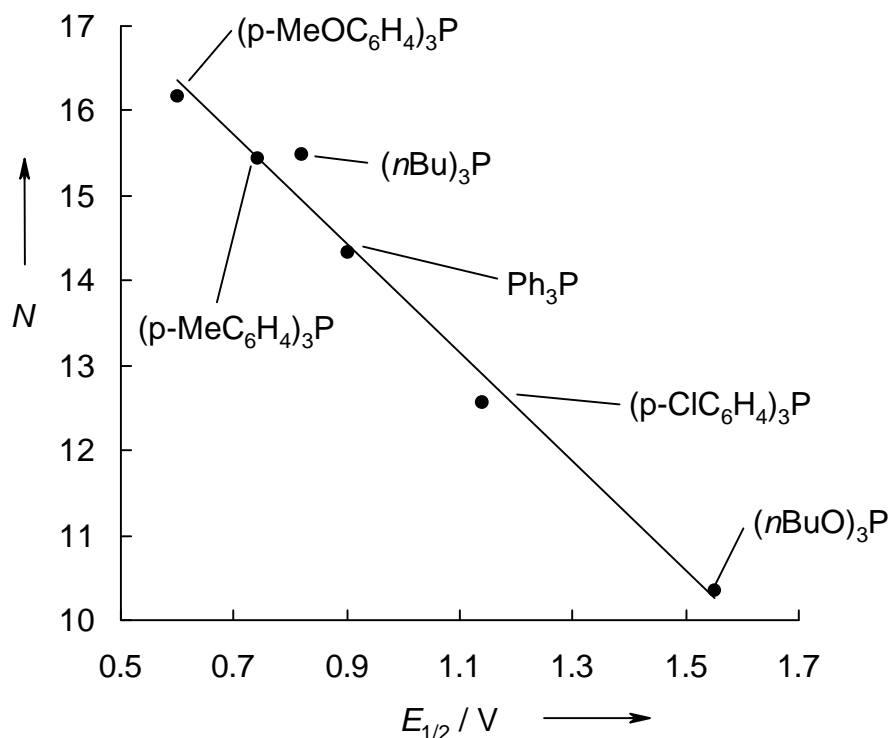


Figure 6.12: Correlation of N with $E_{1/2}^{[127]}$ for tertiary phosphanes and phosphites ($n = 6$, $N = -6.411 \times E_{1/2} + (2.021 \times 10^1)$, $r^2 = 0.9815$).

The correlation in Figure 6.12 shows that the nucleophilicity N increases when oxidation potentials of tertiary phosphanes and phosphites decrease. It is remarkable, that $(\text{PhO})_3\text{P}$ ($E_{1/2} = 1.64$) does not fit into the correlation, shown in Figure 6.12.

Giering suggested the QALE procedure to describe ligand effects in phosphorous(III) compounds by three electronic and one steric parameter (QALE = quantitative analysis of ligand effects).^[128] The electronic parameters are the σ donor capacity (described by the parameter χ_d), the E_{ar} effect (secondary electronic effect), and the π electron acceptor capacity (π_p). The relevant steric parameter is Tolman's cone angle θ .

QALE analysis of the nucleophilicity parameters N , listed in Table 6.3, gave equation 6.2, which expresses N by the four parameters χ_d , θ , E_{ar} , and π_p .

$$N = -0.48588\chi_d - 0.06565\theta + 1.5293E_{\text{ar}} - 0.7921\pi_p + 26.291 \quad (6.2)$$

The four stereoelectronic parameters in eq. 6.2 contribute differently to the magnitude of the N -value of the phosphorous(III) compounds. The largest contribution comes from χ_d which describes the σ electron capacity. The small χ_d values of the trialkylphosphanes imply a high σ electron donor releasing ability which increases nucleophilicity. A large cone angle θ is associated with a decrease in the N value of the phosphorous(III) compound. One can derive that the steric effect of the compound with the the largest cone angle [Cy₃P] compared with the smallest cone angle [(*n*BuO)₃P] accounts for a difference of 3.9 in N . The secondary electronic effect E_{ar} increases the nucleophilicity of triarylphosphanes by 4.1 units in N . The large values for the π electron capacity (π acidity) of the two phosphites account for the lowering of their N values by 2-3 units.

Table 6.6: Stereoelectronic parameters^[128] of tertiary phosphanes and phosphites, comparison of N_{exp} with N_{calc} calculated by eq. 6.2.

R ₃ P	χ_d	θ	E_{ar}	π_p	N_{exp}	N_{calc}
(p-ClC ₆ H ₄) ₃ P	16.8	145	2.7	0	12.58	12.74
Ph ₃ P	13.25	145	2.7	0	14.33	14.46
(p-MeC ₆ H ₄) ₃ P	11.5	145	2.7	0	15.44	15.31
(p-MeOC ₆ H ₄) ₃ P	10.5	145	2.7	0	16.17	15.80
(p-Me ₂ NC ₆ H ₄) ₃ P	5.25	145	2.7	0	18.39	18.35
(<i>n</i> Bu) ₃ P	5.25	136	0	0	15.49	14.81
(<i>i</i> Pr) ₃ P	3.45	160	0	0	13.37	14.11
Cy ₃ P	1.4	170	0	0	14.64	14.45
(PhO) ₃ P	23.6	128	1.3	4.1	5.51	5.16
(<i>n</i> BuO) ₃ P	15.9	110	1.3	2.7	10.36	11.19

Though the available data set is insufficient for rigorously testing the applicability of the QALE model for these purposes, Table 6.6 shows that the QALE analysis (eq. 6.2) reproduces the N parameters with an uncertainty of ± 0.5 units. For that reason one may assume that Giering's parameters can be employed to estimate N parameters of further phosphanes and phosphites.

6.10 Reactions of phosphanes and phosphites with other electrophiles

It has been demonstrated that eq. 1.3 can be used for predicting rate constants for the reactions of nucleophiles with various types of carbocations and metal- π -complexes, though the quality of these correlations is not of equal quality as that of the reactions with the benzhydrylium references. In order to examine the applicability of the nucleophilicity parameters N determined in this work for predicting reactivities toward other types of electrophiles, we have calculated the rate constants for the reactions of phosphanes with electrophiles of known E parameters and compared them with all available data reported in the literature (Table 6.7). Kinetic data from literature, which were not determined at 20 °C have been adjusted to this temperature by reported Eyring activation parameters or estimated entropies of activation.

Table 6.7: Comparison of calculated (eq. 1.3) and experimental rate constants for the reactions of phosphanes and phosphites with electrophiles at 20 °C.

Electrophile	R ₃ P	E	$k_{\text{exp}} / \text{M}^{-1} \text{s}^{-1}$ ($T / \text{°C}$) from lit.	$k_{\text{exp}} (20 \text{ °C})$ $/ \text{M}^{-1} \text{s}^{-1}$	$k_{\text{calc}} (20 \text{ °C})$ $/ \text{M}^{-1} \text{s}^{-1}$
Fe(CO) ₃ C ₇ H ₉ ⁺	Ph ₃ P	-9.19 ^[a]	$2.15 \times 10^2 (20)^{\text{[b]}}$	2.22×10^2	2.19×10^3
Fe(CO) ₃ C ₇ H ₉ ⁺	(p-MeC ₆ H ₄) ₃ P	-9.19 ^[a]	$4.20 \times 10^2 (20)^{\text{[c]}}$	4.20×10^2	1.00×10^4
Fe(CO) ₃ (2-MeO-C ₆ H ₆) ⁺	(PhO) ₃ P	-8.94 ^[a]	$3.60 \times 10^{-3} (20)^{\text{[d]}}$	3.60×10^{-3}	2.47×10^{-3}
Fe(CO) ₃ (2-MeO-C ₆ H ₆) ⁺	(<i>n</i> BuO) ₃ P	-8.94 ^[a]	$1.35 \times 10^1 (20)^{\text{[e]}}$	1.35×10^1	9.86
Fe(CO) ₃ (2-MeO-C ₆ H ₆) ⁺	Ph ₃ P	-8.94 ^[a]	$1.90 \times 10^3 (20)^{\text{[f]}}$	2.51×10^3	3.19×10^3
Fe(CO) ₃ (2-MeO-C ₆ H ₆) ⁺	(p-MeC ₆ H ₄) ₃ P	-8.94 ^[a]	$8.00 \times 10^3 (20)^{\text{[g]}}$	7.26×10^3	1.45×10^4
3,6-(Me ₂ N)-xanthylium ⁺	(<i>n</i> BuO) ₃ P	-8.25 ^[h]	6.8 (25) ^[i]	5.13	3.00×10^1
3,6-(Me ₂ N)-xanthylium ⁺	(<i>n</i> Bu) ₃ P	-8.25 ^[h]	$7.00 \times 10^4 (25)^{\text{[j]}}$	6.18×10^4	9.90×10^4
(4-Me ₂ N-C ₆ H ₄)Ph ₂ C ⁺	(<i>n</i> BuO) ₃ P	-7.93 ^[h]	4.2 (25) ^[k]	3.14	5.02×10^1
(4-Me ₂ N-C ₆ H ₄)Ph ₂ C ⁺	(<i>n</i> Bu) ₃ P	-7.93 ^[h]	$5.60 \times 10^3 (25)^{\text{[l]}}$	4.74×10^3	1.65×10^5
Fe(CO) ₃ (C ₆ H ₇) ⁺	(PhO) ₃ P	-7.78 ^[a]	$3.50 \times 10^{-2} (20)^{\text{[m]}}$	3.50×10^{-2}	1.88×10^{-2}
Fe(CO) ₃ (C ₆ H ₇) ⁺	(<i>n</i> BuO) ₃ P	-7.78 ^[a]	$1.35 \times 10^2 (20)^{\text{[n]}}$	1.42×10^2	6.40×10^1
Fe(CO) ₃ (C ₆ H ₇) ⁺	Ph ₃ P	-7.78 ^[a]	$1.60 \times 10^4 (20)^{\text{[o]}}$	1.31×10^4	1.81×10^4
Fe(CO) ₃ (C ₆ H ₇) ⁺	(<i>n</i> Bu) ₃ P	-7.78 ^[a]	$3.40 \times 10^5 (20)^{\text{[p]}}$	3.40×10^5	2.09×10^5
Fe(CO) ₃ (C ₆ H ₇) ⁺	(p-MeC ₆ H ₄) ₃ P	-7.78 ^[a]	$4.10 \times 10^4 (20)^{\text{[q]}}$	4.54×10^4	7.99×10^4
(4-Me ₂ N-C ₆ H ₄)(C ₇ H ₆) ⁺	(<i>n</i> BuO) ₃ P	-6.24 ^[h]	$6.30 \times 10^1 (25)^{\text{[r]}}$	4.94×10^1	7.66×10^2
(4-Me ₂ N-C ₆ H ₄)(C ₇ H ₆) ⁺	Ph ₃ P	-6.24 ^[h]	$6.00 \times 10^3 (25)^{\text{[s]}}$	5.08×10^3	1.81×10^5

^[a] From ref. [26]. ^[b] Calculated from ref. [12] with $\Delta H^\ddagger = 41 \text{ kJ mol}^{-1}$ and $\Delta S^\ddagger = -60 \text{ J mol}^{-1} \text{ K}^{-1}$ for the reaction in CH₃CN. ^[c] From ref. [12] for the reaction in acetone. ^[d] From ref. [12]

for the reaction in CH₃NO₂.^[e] From ref. [12] for the reaction in acetone.^[f] Calculated from ref. [12] with $\Delta H^\ddagger = 26 \text{ kJ mol}^{-1}$ and $\Delta S^\ddagger = -91 \text{ J mol}^{-1} \text{ K}^{-1}$ for the reaction in CH₃NO₂.^[g] Calculated from ref. [12] with $\Delta H^\ddagger = 24 \text{ kJ mol}^{-1}$ and $\Delta S^\ddagger = -89 \text{ J mol}^{-1} \text{ K}^{-1}$ for the reaction in CH₃NO₂.^[h] From ref. [88].^[i] Calculated from ref. [13] with estimated $\Delta S^\ddagger = -100 \text{ J mol}^{-1} \text{ K}^{-1}$ for the reaction in acetone.^[j] Calculated from ref. [13] with estimated $\Delta S^\ddagger = -100 \text{ J mol}^{-1} \text{ K}^{-1}$ for the reaction in acetone.^[k] Calculated from ref. [13] with estimated $\Delta S^\ddagger = -100 \text{ J mol}^{-1} \text{ K}^{-1}$ for the reaction in acetone.^[l] Calculated from ref. [13] with estimated $\Delta S^\ddagger = -100 \text{ J mol}^{-1} \text{ K}^{-1}$ for the reaction in acetone.^[m] From ref. [12] for the reaction in CH₃NO₂.^[n] Calculated from ref. [12] with $\Delta H^\ddagger = 50 \text{ kJ mol}^{-1}$ and $\Delta S^\ddagger = -33 \text{ J mol}^{-1} \text{ K}^{-1}$ for the reaction in CH₃NO₂.^[o] Calculated from ref. [12] with $\Delta H^\ddagger = 34 \text{ kJ mol}^{-1}$ and $\Delta S^\ddagger = -50 \text{ J mol}^{-1} \text{ K}^{-1}$ for the reaction in CH₃NO₂.^[p] From ref. [12] for the reaction in acetone.^[q] Calculated from ref. [12] with $\Delta H^\ddagger = 21 \text{ kJ mol}^{-1}$ and $\Delta S^\ddagger = -84 \text{ J mol}^{-1} \text{ K}^{-1}$ for the reaction in CH₃NO₂.^[r] Calculated from ref. [13] with estimated $\Delta S^\ddagger = -100 \text{ J mol}^{-1} \text{ K}^{-1}$ for the reaction in acetone.^[s] Calculated from ref. [13] with estimated $\Delta S^\ddagger = -100 \text{ J mol}^{-1} \text{ K}^{-1}$ for the reaction in acetone.

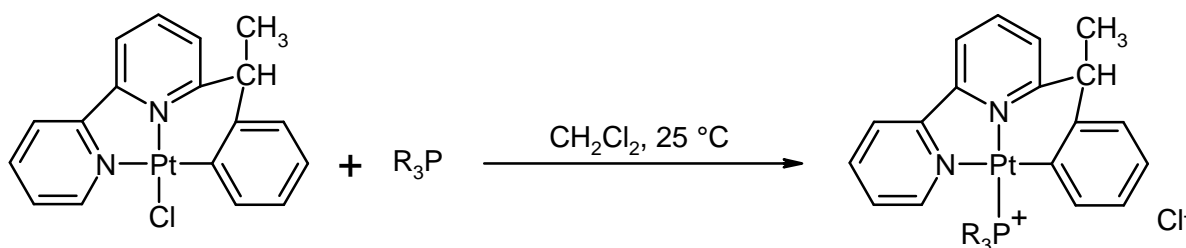
As shown in Table 6.7, the rate constants for the additions of phosphanes and phosphites to metal- π -complexes, xanthylum-, tritylium-, and tropylium ions reported in the literature agree with a standard deviation of factor 6.7 with those calculated by eq. 1.3 from the *N*-, *s*- (this work), and *E*-values (determined previously).

In the Staudinger reaction covalent azides react with trivalent phosphorous compounds to give nitrogen and iminophosphoranes (eq. 6.3) which are widely used in the synthesis of amides,^[129,130] amines,^[131] and a variety of compounds containing carbon-to-nitrogen double bonds.^[132]



The rate constants of the reactions of para-substituted phenyl azides with substituted triphenylphosphanes were determined by J. E. Leffler in benzene at 25 °C.^[133] Figure 6.13 shows that the rates of the reactions of phenyl azide with triaryl phosphanes correlate linearly with the *N* parameters of (p-XC₆H₄)₃P.

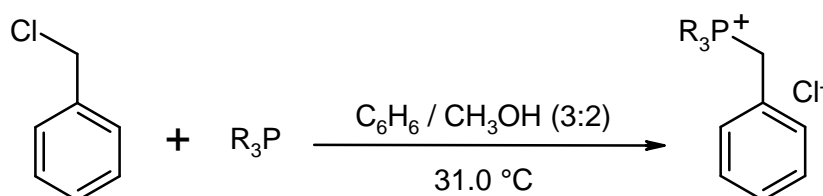
R. Romeo and coworkers studied the kinetics of chloride substitution in the Pt-complex shown in Scheme 6.3, by a series of phosphanes in CH_2Cl_2 at 25 °C.^[134] These substitutions take place in a single step, according to the reaction in Scheme 6.3.



Scheme 6.3: Chloride substitution in the cyclometallated Pt-complex.

The second-order rate constants, observed for these substitution reactions of chloride by para-substituted triaryl phosphanes, correlate well with the N parameters of the triaryl phosphanes (Figure 6.13).

W. E. McEwen^[135] investigated the rates of the S_N2 reactions of benzyl chloride with a variety of tertiary phosphanes in benzene-methanol (3:2) at 31.0 °C (Scheme 6.4).



Scheme 6.4: Reaction of tertiary phosphanes with benzyl chloride.

The rate constants ($\log k$) again correlate linearly with N , a necessary consequence of the linear correlations of ($\log k$) for these three reactions as well as of N with Hammett's parameters σ_p . It would be of interest whether the rates of the reactions of trialkyl phosphanes or of phosphites with these electrophiles also follow the correlations depicted in Figure 6.13.

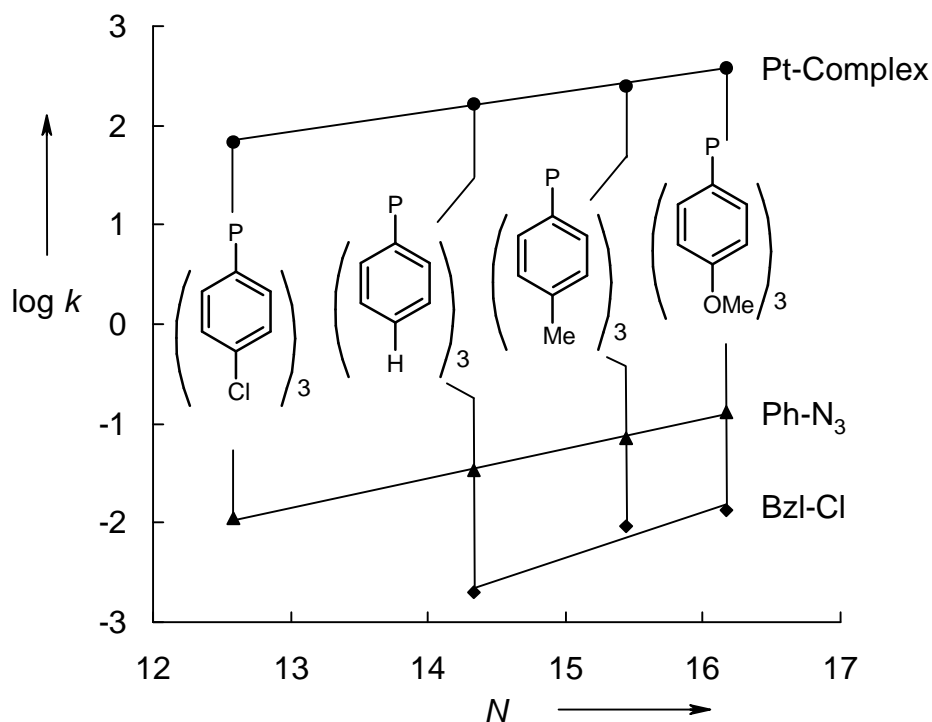


Figure 6.13: Plots of $\log k$ versus N for the reactions of triaryl phosphanes with various electrophiles.

6.11 Conclusion

Phosphanes and phosphites are another class of compounds, the nucleophilicity of which can quantitatively be described by eq. 1.3. By our method of using benzhydrylium ions as electrophiles, it has become possible to directly compare the nucleophilicities of compounds as different as tris(4-dimethylamino)phosphane ($N = 18.39$) and triphenylphosphite ($N = 5.51$), which corresponds to a rate ratio of $1:10^9$ (for $s = 0.70$) or 1 min : 2000 years at 20 °C.

Since comparison with literature data shows that the N/s parameters reported in this work can also be employed for calculating rate constants with other types of electrophiles, one can assume that the N and s parameters reported in this work will reliably predict the rates of combination with all other electrophiles of reported E parameters. Since the intrinsic barrier has been found to be constant ($\Delta G_0^\ddagger \approx 58 \text{ kJ mol}^{-1}$) for the reactions with benzhydrylium ions, combinations of eq. 1.3 and 4.1 may even be employed for a rough estimate of the reaction free enthalpy for the reactions of R₃P with electrophiles.

7. Electrophilicity parameters for metal-p-complexes

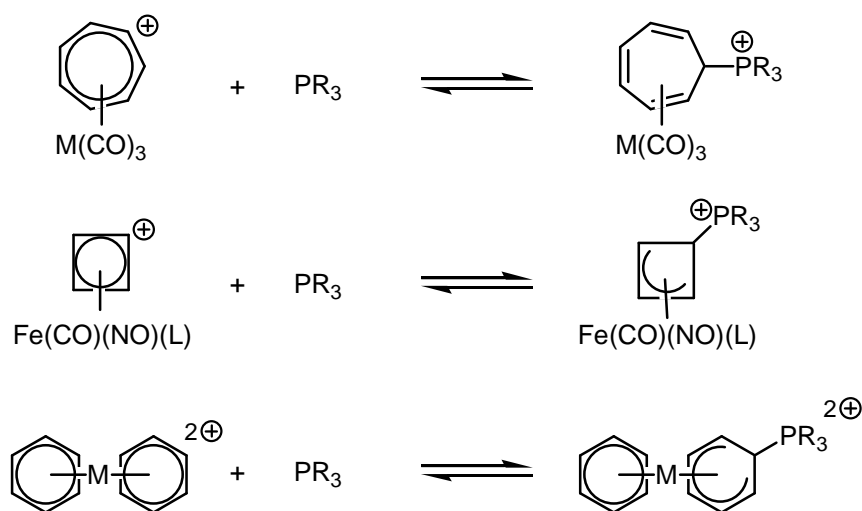
7.1 Introduction

By far most of our knowledge of the electrophilic reactivities of metal- π -complexes comes from the excellent pioneering work of Kane-Maguire and Sweigart, most of which has been published from the mid 1970s to the mid 1980s.^[136] Though different types of nucleophiles have been investigated by these authors, phosphanes and phosphites were the most extensively studied class of nucleophiles, and Kane-Maguire and Sweigart have derived a scale of relative electrophilic reactivities of metal- π -complexes on the basis of their reactivities towards phosphorous nucleophiles.^[12]

Consequent continuation of the development of our reactivity scales as described in refs. [48,89] requires the measurement of rate constants for the reactions of these electrophiles with the reference-nucleophiles, defined in Chapter 3 for determining the *E* parameters of metal- π -complexes. This process would be time-consuming and would not make use of the excellent data set provided by Kane-Maguire, Sweigart, and coworkers. Since recent investigations of the reactions of benzhydrylium ions with phosphanes and phosphites (see Chapter 6) revealed these compounds to be particularly well-behaved nucleophiles, we have decided to deviate from our general procedure and to employ the *N* and *s* parameters of phosphanes and phosphites as well as the extensive literature data for deriving the electrophilicity parameters of metal- π -complexes.

Kane-Maguire, Sweigart, and coworkers studied the nucleophilic additions of various phosphanes, amines, anionic nucleophiles, and aromatic nucleophiles to various metal complexes.^[12] These synthetically useful complexes^[137-139] contain the transition-metal-center (Fe, Mn, Co, Re, Ru, Os, Cr, Mo, W), some ligands (CO, PPh₃, I, NO), and π -hydrocarbons as ligands (C₂H₄, C₄H₄, C₆H₆, C₆H₇, C₇H₇, C₇H₈, C₇H₉, C₈H₁₁). The complexes are either positively charged or neutral.

There exists a large number of rate constants for the additions of tertiary phosphanes and phosphites to the π -hydrocarbon ligands of these metal- π -complexes^[12] (Scheme 7.1).



Scheme 7.1: Typical reactions of tertiary phosphorous nucleophiles with the π -hydrocarbon ligands of transition metal complexes.

7.2 Adaption of rate constants to standard conditions

The rate constants for the additions of phosphanes and phosphites to metal- π -complexes, found in literature,^[12] are listed in Table 7.1. These kinetic investigations were often performed in different solvents (acetone, nitromethane, acetonitrile) and at different temperatures (0, 20, 25 °C).

For linking the kinetic data, provided by Kane-Maguire, Sweigart and coworkers with our kinetic data, some rate constants have been recalculated, using the following procedure:

- Solvent effects are minute for the reactions of metal- π -complexes with phosphanes and phosphites (see Table 7.1), and are therefore neglected. This is in accord with our observation that the rates of the reactions of benzhydrylium ions with phosphanes (Chapter 6), π -nucleophiles (Chapter 4), and hydride donors are not strongly affected by solvents.
- Rate constants which were not measured at 20 °C must be adjusted to this temperature. When possible, the rate constants are recalculated by using activation parameters. If activation parameters are not available, estimated values of activation entropies ΔS^\ddagger (Table 7.1, column 7, values in parentheses are estimated) are employed for adjustment of the rate constants to 20 °C. Because of the small values of ΔH^\ddagger for these reactions, the temperature dependence of the rate constants is relatively small, and the errors introduced by the temperature corrections are negligible.

In Table 7.1 the originally published rate constants, specified by temperature and solvent, for the additions of metal- π -complexes to phosphanes and phosphites are given in column 4, with Eyring activation parameters in columns 5 and 6. The method, which was used for recalculation of the rate constants to 20 °C is shown in column 7. The finally obtained second-order rate constants for reactions at 20 °C are listed in column 8 of Table 7.1.

Table 7.1: Rate constants and Eyring activation parameters for the additions of phosphanes and phosphites to metal- π -complexes, and calculated E -Parameters for the metal- π -complexes.

Metal- π -complex	Phosphane or phosphite	Solvent	$k_2 / \text{M}^{-1} \text{s}^{-1}$ ($T / ^\circ\text{C}$) ^[a]	$\Delta H^\ddagger /$ kJ mol^{-1}	$\Delta S^\ddagger /$ $\text{J mol}^{-1} \text{K}^{-1}$	Method for recalc. ^[b]	$k_2 (20^\circ\text{C}) /$ $\text{M}^{-1} \text{s}^{-1}$ ^[c]	$E^{[d]}$ (calc.)	$E^{[e]}$ (aver.)
$\text{Fe}(\text{CO})_3(\text{C}_6\text{H}_7)^+$	$(n\text{Bu})_3\text{P}$	$(\text{CH}_3)_2\text{CO}$	$3.40 \times 10^5 (20)^{[f]}$				3.40×10^5	-7.47	
	$(p\text{-MeC}_6\text{H}_4)_3\text{P}$	CH_3NO_2	$4.10 \times 10^4 (20)^{[g]}$	21	-84	$\Delta H^\ddagger, \Delta S^\ddagger$	4.54×10^4	-8.16	
	Ph_3P	CH_3NO_2	$1.60 \times 10^4 (20)^{[g]}$	34	-50	$\Delta H^\ddagger, \Delta S^\ddagger$	1.31×10^4	-8.00	
	$(n\text{BuO})_3\text{P}$	CH_3NO_2	$1.35 \times 10^2 (20)^{[g]}$	50	-33	$\Delta H^\ddagger, \Delta S^\ddagger$	1.42×10^2	-7.28	
	$(\text{PhO})_3\text{P}$	CH_3NO_2	$3.50 \times 10^{-2} (20)^{[g]}$				3.50×10^{-2}	-7.43	-7.63 -7.78 ^[r]
$\text{Fe}(\text{CO})_2(\text{PPh}_3)(\text{C}_6\text{H}_7)^+$	Ph_3P	CH_3CN	$1.20 \times 10^2 (20)^{[h]}$	40	-68	$\Delta H^\ddagger, \Delta S^\ddagger$	1.28×10^2	-11.09	-11.09
$\text{Fe}(\text{CO})_3(2\text{-MeOC}_6\text{H}_6)^+$	$(p\text{-MeC}_6\text{H}_4)_3\text{P}$	CH_3NO_2	$8.00 \times 10^3 (20)^{[g]}$	24	-89	$\Delta H^\ddagger, \Delta S^\ddagger$	7.26×10^3	-9.41	
	Ph_3P	CH_3NO_2	$1.90 \times 10^3 (20)^{[g]}$	26	-91	$\Delta H^\ddagger, \Delta S^\ddagger$	2.51×10^3	-9.10	
	$(n\text{BuO})_3\text{P}$	$(\text{CH}_3)_2\text{CO}$	$1.35 \times 10^1 (20)$				1.35×10^1	-8.75	
	$(\text{PhO})_3\text{P}$	CH_3NO_2	$3.60 \times 10^{-3} (20)^{[g]}$				3.60×10^{-3}	-8.73	
	$(n\text{BuO})_3\text{P}$	$(\text{CH}_3)_2\text{CO}$	$1.54 \times 10^4 (20)$				1.54×10^4	-9.42	-9.05 -8.94 ^[r]
$\text{Fe}(\text{CO})_2\text{I}(\text{C}_6\text{H}_7)$	$(n\text{Bu})_3\text{P}$	$(\text{CH}_3)_2\text{CO}$	$1.80 (20)^{[i]}$	32	-130	$\Delta H^\ddagger, \Delta S^\ddagger$	1.97	-15.06	-15.06
$\text{Co}(\text{Cp})(\text{C}_6\text{H}_7)^+$	$(n\text{Bu})_3\text{P}$	$(\text{CH}_3)_2\text{CO}$	$3.10 \times 10^2 (20)^{[h]}$	20			3.10×10^2	-11.88	-11.88
$\text{Mn}(\text{CO})_2(\text{NO})(6\text{-PhC}_6\text{H}_6)^+$	$(n\text{Bu})_3\text{P}$	CH_3NO_2	$1.00 \times 10^3 (25)^{[h]}$			$\Delta S^\ddagger = (-90)$	8.05×10^2	-11.28	
	$(n\text{BuO})_3\text{P}$	CH_3NO_2	$3.00 \times 10^{-1} (25)^{[h]}$			$\Delta S^\ddagger = (-90)$	2.10×10^{-1}	-11.33	-11.30

Table 7.1: Continued

Metal- π -complex	Phosphane or phosphite	Solvent	$k_2 / \text{M}^{-1} \text{s}^{-1}$ ($T / ^\circ\text{C}$) ^[a]	$\Delta H^\ddagger /$ kJ mol^{-1}	$\Delta S^\ddagger /$ $\text{J mol}^{-1} \text{K}^{-1}$	Method for recalc. ^[b]	k_2 (20 $^\circ\text{C}$) / $\text{M}^{-1} \text{s}^{-1}$ ^[c]	E ^[d] (calc.)	E ^[e] (aver.)
$\text{Mn}(\text{CO})_2(\text{NO})(6\text{-CNC}_6\text{H}_6)^+$	Ph_3P	CH_3CN	3.30×10^2 (25) ^[h]			$\Delta S^\ddagger = (-90)$	2.61×10^2	-10.61	-10.61
$\text{Mn}(\text{CO})_2(\text{NO})(6\text{-MeC}_6\text{H}_6)^+$	$(p\text{-MeOC}_6\text{H}_4)_3\text{P}$	CH_3CN	1.30×10^1 (25) ^[h]			$\Delta S^\ddagger = (-90)$	9.72	-14.58	
	$(p\text{-MeC}_6\text{H}_4)_3\text{P}$	CH_3CN	6.90 (25) ^[h]			$\Delta S^\ddagger = (-90)$	5.10	-14.33	
	Ph_3P	CH_3CN	2.00 (25) ^[h]			$\Delta S^\ddagger = (-90)$	1.45	-14.08	-14.32
$\text{Mn}(\text{CO})(\text{NO})(\text{PPh}_3)(6\text{-MeC}_6\text{H}_6)^+$	$(n\text{Bu})_3\text{P}$	CH_3CN	2.10 (25) ^[h]			$\Delta S^\ddagger = (-90)$	1.52	-15.23	-15.23
$\text{Mn}(\text{CO})(\text{NO})(\text{PPh}_3)(\text{C}_6\text{H}_7)^+$	$(n\text{Bu})_3\text{P}$	CH_3CN	4.50×10^3 (25) ^[h]			$\Delta S^\ddagger = (-90)$	3.72×10^3	-10.32	
	Ph_3P	CH_3CN	8.80×10^1 (25) ^[h]			$\Delta S^\ddagger = (-90)$	6.80×10^1	-11.51	
	$(n\text{BuO})_3\text{P}$	CH_3CN	8.50×10^{-1} (25) ^[h]			$\Delta S^\ddagger = (-90)$	6.07×10^{-1}	-10.67	-10.80
$\text{Fe}(\text{CO})_3(\text{C}_7\text{H}_9)^+$	Ph_3P	CH_3CN	2.15×10^2 (20) ^[g]	41	-60	$\Delta H^\ddagger, \Delta S^\ddagger$	2.22×10^2	-10.72	
	$(p\text{-MeC}_6\text{H}_4)_3\text{P}$	$(\text{CH}_3)_2\text{CO}$	4.20×10^2 (20) ^[h]				4.20×10^2	-11.34	-11.03 -9.19 ^[i]
$\text{Fe}(\text{CO})_2\text{I}(\text{C}_7\text{H}_9)$	$(n\text{Bu})_3\text{P}$	$(\text{CH}_3)_2\text{CO}$	2.00×10^{-2} (20) ^[i]				2.00×10^{-2}	-17.95	-17.95
$\text{Co}(\text{Cp})(\text{C}_7\text{H}_9)^+$	$(n\text{Bu})_3\text{P}$	$(\text{CH}_3)_2\text{CO}$	1.50 (20) ^[h]				1.50	-15.23	-15.23
$\text{Mn}(\text{CO})_2(\text{NO})(\text{C}_7\text{H}_9)^+$	$(p\text{-MeOC}_6\text{H}_4)_3\text{P}$	CH_3NO_2	1.10×10^3 (25) ^[h]			$\Delta S^\ddagger = (-90)$	8.87×10^2	-11.42	
	$(p\text{-MeC}_6\text{H}_4)_3\text{P}$	CH_3NO_2	5.90×10^2 (25) ^[h]			$\Delta S^\ddagger = (-90)$	4.71×10^2	-11.26	
	Ph_3P	CH_3NO_2	2.10×10^2 (25) ^[h]			$\Delta S^\ddagger = (-90)$	1.65×10^2	-10.92	
	$(n\text{BuO})_3\text{P}$	CH_3NO_2	3.50 (25) ^[h]			$\Delta S^\ddagger = (-90)$	2.56	-9.78	-10.79

Table 7.1: Continued

Metal- π -complex	Phosphane or phosphite	Solvent	$k_2 / \text{M}^{-1} \text{s}^{-1}$ ($T / ^\circ\text{C}$) ^[a]	$\Delta H^\ddagger /$ kJ mol^{-1}	$\Delta S^\ddagger /$ $\text{J mol}^{-1} \text{K}^{-1}$	Method for recalc. ^[b]	k_2 (20 $^\circ\text{C}$) / $\text{M}^{-1} \text{s}^{-1}$ ^[c]	E ^[d] (calc.)	E ^[e] (aver.)
$\text{Mn}(\text{CO})_3(\text{C}_6\text{H}_6)^+$	$(n\text{Bu})_3\text{P}$	$(\text{CH}_3)_2\text{CO}$	7.70×10^2 (20) ^[j]	31	-84	$\Delta H^\ddagger, \Delta S^\ddagger$	7.50×10^2	-11.32	
	$(n\text{Bu})_3\text{P}$	CH_3NO_2	2.00×10^3 (25) ^[k]			$\Delta S^\ddagger = (-90)$	1.63×10^3	-10.84	-11.08
$\text{Mn}(\text{CO})_3(\text{MeC}_6\text{H}_5)^+$	$(n\text{Bu})_3\text{P}$	CH_3NO_2	1.50×10^3 (25) ^[k]			$\Delta S^\ddagger = (-90)$	1.22×10^3	-11.02	-11.02
$\text{Re}(\text{CO})_3(\text{C}_6\text{H}_6)^+$	$(n\text{Bu})_3\text{P}$	CH_3NO_2	1.80×10^3 (25) ^[k]			$\Delta S^\ddagger = (-90)$	1.46×10^3	-10.90	-10.90
$\text{Re}(\text{CO})_3(\text{MeC}_6\text{H}_5)^+$	$(n\text{Bu})_3\text{P}$	CH_3NO_2	7.50×10^2 (25) ^[k]			$\Delta S^\ddagger = (-90)$	6.01×10^2	-11.46	-11.46
$\text{Fe}(\text{C}_6\text{H}_6)_2^{2+}$	Ph_3P	CD_3CN	3.20×10^5 (20) ^[l]	18	-80	$\Delta H^\ddagger, \Delta S^\ddagger$	2.51×10^5	-6.02	
	$(n\text{BuO})_3\text{P}$	CH_3CN	1.55×10^3 (25) ^[k]			$\Delta S^\ddagger = (-80)$	1.23×10^3	-5.94	-5.98
$\text{Ru}(\text{C}_6\text{H}_6)_2^{2+}$	Ph_3P	CD_3CN	8.40×10^3 (20) ^[l]	30	-67	$\Delta H^\ddagger, \Delta S^\ddagger$	8.73×10^3	-8.27	
	$(n\text{BuO})_3\text{P}$	CH_3CN	7.00×10^1 (25) ^[k]			$\Delta S^\ddagger = (-80)$	5.28×10^1	-7.90	-8.07
$\text{Os}(\text{C}_6\text{H}_6)_2^{2+}$	Ph_3P	CD_3CN	1.50×10^3 (20) ^[l]	37	-59	$\Delta H^\ddagger, \Delta S^\ddagger$	1.29×10^3	-9.54	
	$(n\text{BuO})_3\text{P}$	CH_3CN	2.40×10^1 (25) ^[k]			$\Delta S^\ddagger = (-60)$	1.71×10^1	-8.60	-9.04
$\text{Mn}(\text{CO})_3(\text{C}_7\text{H}_8)^+$	$(p\text{-ClC}_6\text{H}_4)_3\text{P}$	CH_3NO_2	5.30×10^4 (20) ^[l]	21	-84	$\Delta H^\ddagger, \Delta S^\ddagger$	5.54×10^4	-5.28	
	$(n\text{BuO})_3\text{P}$	CH_3NO_2	7.00×10^3 (25) ^[h]			$\Delta S^\ddagger = (-80)$	5.71×10^3	-4.99	
	$(\text{PhO})_3\text{P}$	CH_3NO_2	3.1 (25) ^[m]			$\Delta S^\ddagger = (-80)$	2.22	-5.06	-5.10
$\text{Mn}(\text{CO})_2(\text{PPh}_3)(\text{C}_7\text{H}_8)^+$	Ph_3P	CH_3NO_2	2.10×10^4 (25) ^[h]			$\Delta S^\ddagger = (-80)$	1.78×10^4	-7.79	
	$(n\text{BuO})_3\text{P}$	CH_3NO_2	1.20×10^2 (25) ^[h]			$\Delta S^\ddagger = (-90)$	9.32×10^1	-7.55	-7.66

Table 7.1: Continued

Metal- π -complex	Phosphane or phosphite	Solvent	$k_2 / \text{M}^{-1} \text{s}^{-1}$ ($T / ^\circ\text{C}$) ^[a]	$\Delta H^\ddagger /$ kJ mol^{-1}	$\Delta S^\ddagger /$ $\text{J mol}^{-1} \text{K}^{-1}$	Method for recalc. ^[b]	$k_2 (20^\circ\text{C}) /$ $\text{M}^{-1} \text{s}^{-1}$ ^[c]	$E^{[d]}$ (calc.)	$E^{[e]}$ (aver.)
Fe(Cp)(C ₇ H ₈) ⁺	(<i>n</i> Bu) ₃ P	(CH ₃) ₂ CO	2.20×10^3 (25) ^[h]			$\Delta S^\ddagger = (-80)$	1.76×10^3	-10.79	
	(<i>n</i> BuO) ₃ P	(CH ₃) ₂ CO	5.00×10^{-1} (25) ^[h]			$\Delta S^\ddagger = (-80)$	3.46×10^{-1}	-11.02	-10.90
Cr(CO) ₃ (C ₇ H ₇) ⁺	(<i>n</i> Bu) ₃ P	(CH ₃) ₂ CO	4.10×10^4 (20) ^[n]	25	-71	$\Delta H^\ddagger, \Delta S^\ddagger$	4.20×10^4	-8.79	
	(<i>p</i> -MeC ₆ H ₄) ₃ P	(CH ₃) ₂ CO	8.60×10^3 (20) ^[h]	29	-71	$\Delta H^\ddagger, \Delta S^\ddagger$	8.13×10^3	-9.33	
	Ph ₃ P	(CH ₃) ₂ CO	8.90×10^2 (20) ^[h]				8.90×10^2	-9.79	
	(<i>n</i> BuO) ₃ P	(CH ₃) ₂ CO	8.5 (20) ^[h]	41	-88	$\Delta H^\ddagger, \Delta S^\ddagger$	7.66	-9.10	-9.23
Mo(CO) ₃ (C ₇ H ₇) ⁺	(<i>n</i> Bu) ₃ P	(CH ₃) ₂ CO	7.50×10^3 (0) ^[n]	19	-100	$\Delta H^\ddagger, \Delta S^\ddagger$	1.50×10^4	-9.44	-9.44
W(CO) ₃ (C ₇ H ₇) ⁺	(<i>n</i> Bu) ₃ P	(CH ₃) ₂ CO	3.90×10^3 (0) ^[o]	40	-31	$\Delta H^\ddagger, \Delta S^\ddagger$	1.10×10^4	-9.64	-9.64
Fe(CO) ₂ (NO)(C ₄ H ₄) ⁺	Ph ₃ P	(CH ₃) ₂ CO	4.40×10^4 (20) ^[m]	24	-73	$\Delta H^\ddagger, \Delta S^\ddagger$	4.97×10^4	-7.10	
	(<i>p</i> -ClC ₆ H ₄) ₃ P	(CH ₃) ₂ CO	4.00×10^3 (20) ^[m]	25	-92	$\Delta H^\ddagger, \Delta S^\ddagger$	3.36×10^3	-7.16	
	(<i>n</i> BuO) ₃ P	CH ₃ NO ₂	5.10×10^2 (25) ^[o]			$\Delta S^\ddagger = (-80)$	3.98×10^2	-6.65	-6.95
Fe(CO)(NO)(PPh ₃)(C ₄ H ₄) ⁺	(<i>n</i> Bu) ₃ P	CH ₃ NO ₂	1.20×10^5 (25) ^[o]			$\Delta S^\ddagger = (-80)$	1.03×10^5	-8.23	
	Ph ₃ P	CH ₃ NO ₂	1.70×10^3 (25) ^[o]			$\Delta S^\ddagger = (-80)$	1.35×10^3	-9.51	
	(<i>n</i> BuO) ₃ P	CH ₃ NO ₂	9.80 (25) ^[o]			$\Delta S^\ddagger = (-80)$	7.14	-9.14	-8.94
Fe(Cp)(CO) ₂ (C ₂ H ₄) ⁺	Ph ₃ P	(CH ₃) ₂ CO	1.20×10^2 (20) ^[p]	42	-63	$\Delta H^\ddagger, \Delta S^\ddagger$	1.03×10^2	-11.24	
	(PhO) ₃ P	(CH ₃) ₂ CO	6.00×10^{-4} (20) ^[p]				6.00×10^{-4}	-9.75	-10.38

Table 7.1: Continued

Metal- π -complex	Phosphane or phosphite	Solvent	$k_2 / \text{M}^{-1} \text{s}^{-1}$ ($T / ^\circ\text{C}$) ^[a]	$\Delta H^\ddagger /$ kJ mol^{-1}	$\Delta S^\ddagger /$ $\text{J mol}^{-1} \text{K}^{-1}$	Method for recalc. ^[b]	$k_2 (20^\circ\text{C}) /$ $\text{M}^{-1} \text{s}^{-1}$ ^[c]	$E^{[d]}$ (calc.)	$E^{[e]}$ (aver.)
$\text{Fe}(\text{Cp})(\text{CO})_2(\text{CH}_2\text{CHMe})^+$	$(n\text{Bu})_3\text{P}$	$(\text{CH}_3)_2\text{CO}$	$1.40 \times 10^2 (20)^{[p]}$				1.40×10^2	-12.38	
	Ph_3P	$(\text{CH}_3)_2\text{CO}$	$3.80 (20)^{[p]}$				3.80	-13.44	-12.88
$\text{Co}(\text{Cp})(\text{C}_8\text{H}_{11})^+$	$(n\text{Bu})_3\text{P}$	$(\text{CH}_3)_2\text{CO}$	$4.80 \times 10^4 (20)^{[q]}$	14			4.80×10^4	-8.71	
	Ph_3P	$(\text{CH}_3)_2\text{CO}$	$1.20 \times 10^3 (20)^{[q]}$	21	-110	$\Delta H^\ddagger, \Delta S^\ddagger$	1.99×10^3	-9.26	-8.96

^[a] Actually published rate constants. ^[b] Method for recalculation. ^[c] Published rate constants adjusted to 20 °C from published activation parameters or estimated entropies of activation. ^[d] Calculated by eq. 1.3 using the $k_2 (20^\circ\text{C})$ values from column 8, and the N , and s values of the phosphanes and phosphites from Chapter 6. ^[e] E parameters were calculated by minimization of Δ^2 . ^[f] From ref. [140]. ^[g] From ref. [141]. ^[h] From ref. [142]. ^[i] From ref. [143]. ^[j] From ref. [144]. ^[k] From ref. [145]. ^[l] From ref. [146]. ^[m] From ref. [147]. ^[n] From ref. [148]. ^[o] From ref. [149]. ^[p] From ref. [150]. ^[q] From ref. [151]. ^[r] From ref. [26].

7.3 Determination of the E parameters of metal- π -complexes

From the rate constants for the additions of phosphanes and phosphites to metal- π -complexes adjusted to 20 °C (Table 7.1), and the N and s parameters of the phosphorous nucleophiles (see Chapter 6), the individual E parameters of the metal- π -complexes were calculated by minimizing Δ^2 (eq. 3.1) in accord with the methods for extending the basis set, described in Chapter 3. Table 7.1 lists the E parameters of 32 metal- π -complexes, derived by the procedure described above. In cases where E parameters can be derived from reactions with reference nucleophiles, these data are also given in Table 7.1

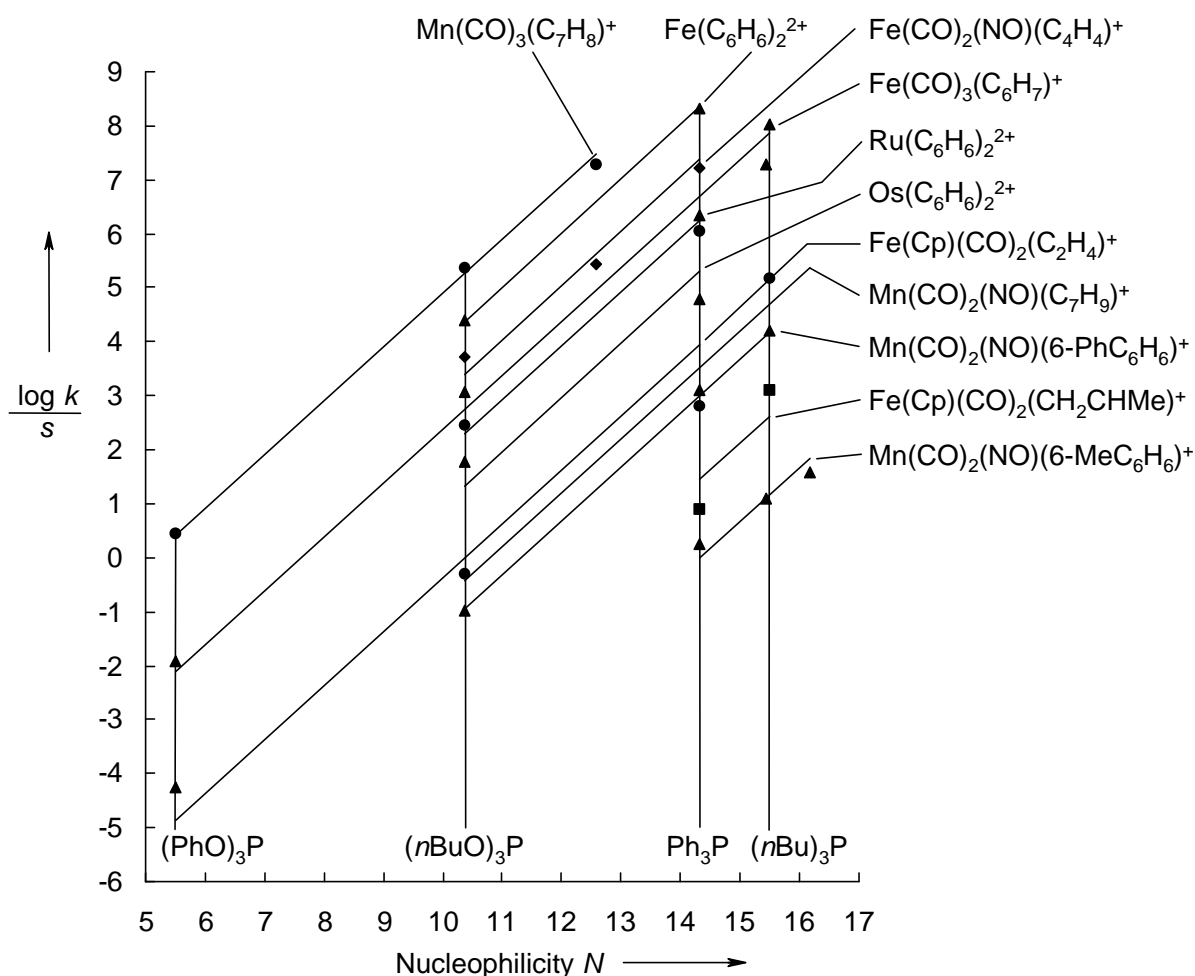


Figure 7.1: Plot of $(\log k) / s$ versus N for the reactions of metal- π -complexes with phosphanes and phosphites.

Figure 7.1 shows that the correlations for the reactions of phosphanes and phosphites with metal- π -complexes are of lower quality than the corresponding correlations for the reactions of P-nucleophiles with benzydrylium ions. We do not think that this is due to the use of

different solvents or to the errors introduced by correcting for the different reaction temperatures. Since both influences are relatively small, it is assumed that the deviations are due to the different environments of the centers of electrophilicity in benzhydrylium ions and some of the metal- π -complexes.

The electrophilicities of the metal- π -complexes are in the range of $-18 < E < -5$ as indicated by Figure 7.2 and are comparable with the electrophilicities of donor-substituted benzhydryl cations and stabilized quinone methides.

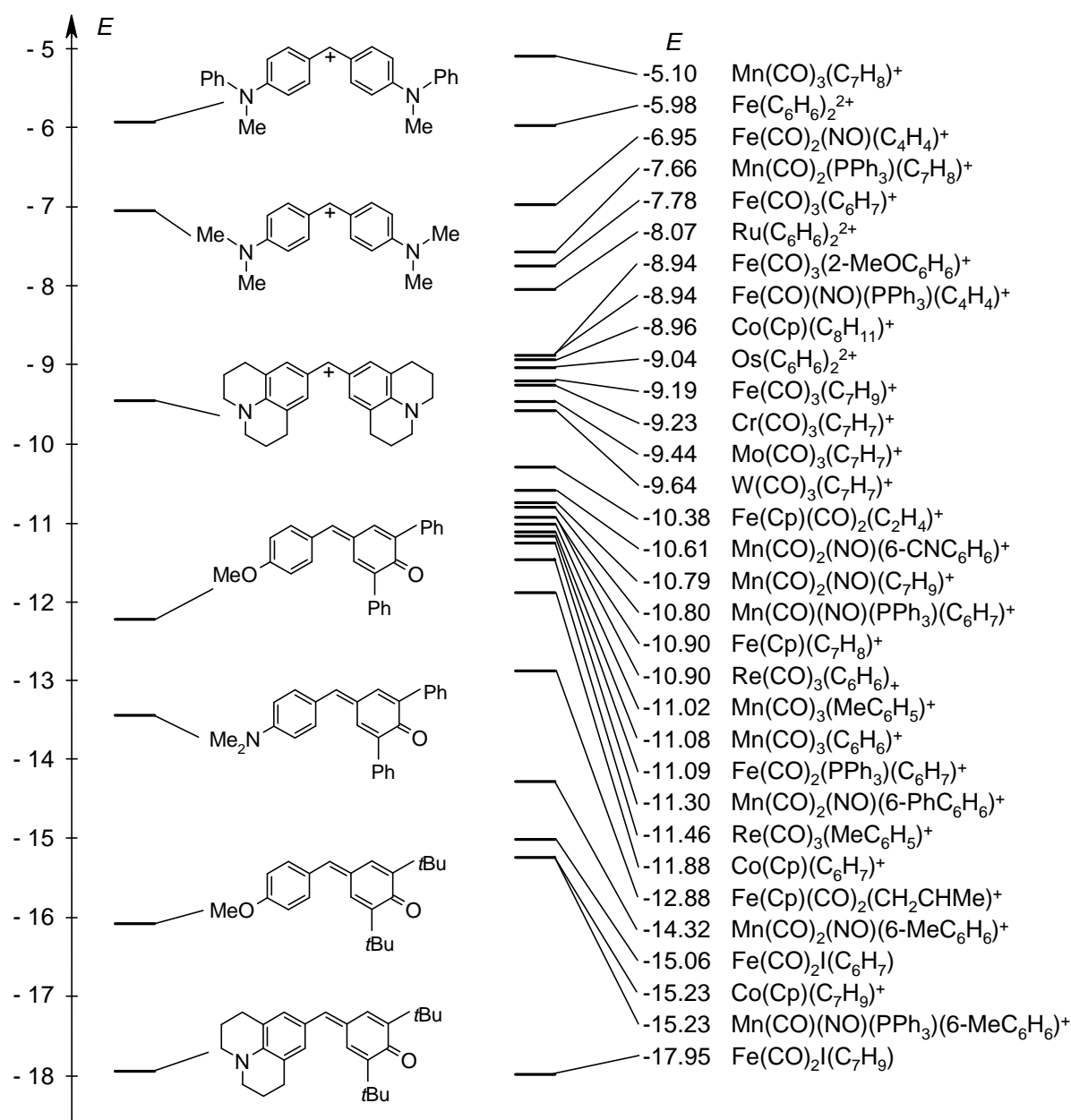


Figure 7.2: Comparison of the electrophilicities E of metal- π -complexes, quinone methides and benzhydryl cations.

Since the tertiary phosphanes and phosphites used for the derivation of the E parameters have closely similar s values (according to eq. 1.3), it is not surprising that the reactivity order expressed by E in Figure 7.2 is almost the same as that derived by Kane-Maguire, Sweigart, and coworkers using Ritchie's constant selectivity approach. The main advantage of defining the reactivity parameter E for these compounds is the fact that it can be combined with the nucleophilicity parameters N and s for predicting their potential for combinations with nucleophiles.

7.4 Checking the reliability of the metal- π -complexes E parameters

As shown in Table 7.1, the electrophilicities of the three metal- π -complexes $\text{Fe}(\text{CO})_3(\text{C}_7\text{H}_9)^+$, $\text{Fe}(\text{CO})_3(2\text{-MeOC}_6\text{H}_6)^+$, and $\text{Fe}(\text{CO})_3(\text{C}_6\text{H}_7)^+$ have previously been characterized by kinetic measurements with reference nucleophiles (electron-rich π -systems).^[26]

The comparison in Table 7.2 shows that both approaches give almost identical E parameters for the cyclohexadienylum complexes (the first two entries). In the third case the deviation is much bigger. Possibly steric effects in the cycloheptadienylum complexes are responsible for the finding that it appears to be less electrophilic toward phosphanes than toward the less bulky π -nucleophiles.

Table 7.2: Comparison of the E parameters of metal- π -complexes, calculated from the rates of the reactions with tertiary phosphorous compounds and reference nucleophiles.

Metal-complex	E from ref. [26]	E calc. from Table 7.1
$\text{Fe}(\text{CO})_3(\text{C}_6\text{H}_7)^+$	-7.78	-7.63 ± 0.35
$\text{Fe}(\text{CO})_3(2\text{-MeOC}_6\text{H}_6)^+$	-8.94	-9.05 ± 0.30
$\text{Fe}(\text{CO})_3(\text{C}_7\text{H}_9)^+$	-9.19	-11.03 ± 0.31

Table 7.3 compares the rates for the reactions of metal- π -complexes with different nucleophiles. The observed rate constants were either measured previously in this group, or taken from literature (see footnotes in Table 7.3).

Table 7.3: Comparison of observed k_2 (obs.) and calculated k_2 (calc.) rate constants for the reactions of metal- π -complexes with other types of nucleophiles in CH_2Cl_2 at 20 °C.

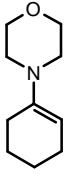
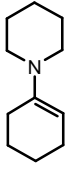
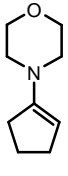
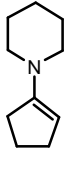
Nucleophile	N	s	metal- π -complex	E	k_2 (obs.) / $\text{L mol}^{-1} \text{s}^{-1}$	k_2 (calc.) / $\text{L mol}^{-1} \text{s}^{-1}$	$k_{\text{obs}} / k_{\text{calc}}$
 20	11.40 ^[b]	0.83 ^[b]	$\text{Fe}(\text{CO})_3(\text{C}_6\text{H}_7)^+$	-7.78	7.24×10^1 ^[a]	1.01×10^3	0.072
			$\text{Fe}(\text{CO})_3(2\text{-MeOC}_6\text{H}_6)^+$	-8.94	9.42 ^[a]	1.10×10^2	0.086
 24	13.36 ^[b]	0.81 ^[b]	$\text{Fe}(\text{CO})_3(\text{C}_6\text{H}_7)^+$	-7.78	9.72×10^2 ^[a]	3.31×10^4	0.029
			$\text{Fe}(\text{CO})_3(2\text{-MeOC}_6\text{H}_6)^+$	-8.94	9.09×10^1 ^[a]	3.80×10^3	0.024
			$\text{Fe}(\text{Cp})(\text{CO})_2(\text{CH}_2\text{CHMe})^+$	-12.88	4.86 ^[c]	2.45	1.98
 25	13.41 ^[d]	0.82 ^[d]	$\text{Fe}(\text{CO})_3(\text{C}_6\text{H}_7)^+$	-7.78	2.27×10^3 ^[a]	4.14×10^4	0.055
			$\text{Fe}(\text{CO})_3(2\text{-MeOC}_6\text{H}_6)^+$	-8.94	2.88×10^2 ^[a]	4.63×10^3	0.062
 23	15.06 ^[d]	0.82 ^[d]	$\text{Fe}(\text{CO})_3(\text{C}_6\text{H}_7)^+$	-7.78	7.41×10^3 ^[a]	9.32×10^5	0.008
			$\text{Fe}(\text{CO})_3(2\text{-MeOC}_6\text{H}_6)^+$	-8.94	2.04×10^3 ^[a]	7.24×10^5	0.003

Table 7.3: Continued

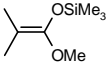
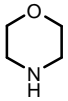
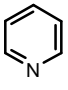
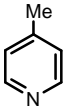
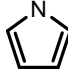
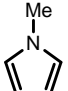
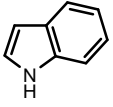
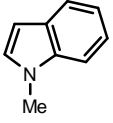
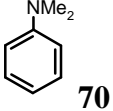
Nucleophile	N	s	metal- π -complex	E	k_2 (obs.) / L mol ⁻¹ s ⁻¹	k_2 (calc.) / L mol ⁻¹ s ⁻¹	$k_{\text{obs}} / k_{\text{calc}}$
 19	9.00 ^[b]	0.98 ^[b]	Fe(Cp)(CO) ₂ (CH ₂ CHMe) ⁺	-12.88	5.20×10^{-2} ^[c]	1.58×10^{-4}	329
 69	16.96 ^[e]	0.67 ^[e]	Fe(CO) ₃ (C ₆ H ₇) ⁺	-7.78	3.96×10^5 ^[f]	1.41×10^6	0.28
			Fe(CO) ₃ (2-MeOC ₆ H ₆) ⁺	-8.94	9.15×10^4 ^[g]	2.36×10^5	0.39
 pHP	13.28 ^[h]	(0.64) ^[h]	Fe(CO) ₃ (C ₆ H ₇) ⁺	-7.78	6.96×10^3 ^[i]	3.31×10^3	2.1
			Fe(CO) ₃ (C ₇ H ₉) ⁺	-9.19	2.56×10^2 ^[j]	4.15×10^2	0.62
 pMeP	14.01 ^[h]	(0.64) ^[h]	Mn(CO) ₂ (NO)(6-MeC ₆ H ₆) ⁺	-14.32	2.56×10^1 ^[k]	1.98×10^{-1}	129
			Mn(CO) ₂ (NO)(6-PhC ₆ H ₆) ⁺	-11.30	1.93×10^1 ^[l]	5.43×10^1	0.36
 42	4.63 ^[d]	(1.00) ^[d]	Fe(CO) ₃ (C ₆ H ₇) ⁺	-7.78	2.50×10^{-1} ^[m]	7.08×10^{-4}	353
			Mn(CO) ₃ (C ₇ H ₈) ⁺	-5.10	4.93×10^{-1} ^[n]	3.39×10^{-1}	1.5
 43	5.85 ^[b]	1.03 ^[b]	Mn(CO) ₃ (C ₇ H ₈) ⁺	-5.10	9.14 ^[o]	5.92	1.5

Table 7.3: Continued

Nucleophile	N	s	metal- π -complex	E	k_2 (obs.) / L mol ⁻¹ s ⁻¹	k_2 (calc.) / L mol ⁻¹ s ⁻¹	$k_{\text{obs}} / k_{\text{calc}}$
 45	5.80 ^[d]	(0.80) ^[d]	Fe(CO) ₃ (C ₆ H ₇) ⁺	-7.78	1.95 × 10 ⁻¹ ^[p]	2.61 × 10 ⁻²	7.5
			Fe(CO) ₃ (2-MeOC ₆ H ₆) ⁺	-8.94	2.10 × 10 ⁻² ^[q]	3.08 × 10 ⁻³	6.8
 46	6.93 ^[d]	(0.80) ^[d]	Fe(CO) ₃ (2-MeOC ₆ H ₆) ⁺	-8.94	6.81 × 10 ⁻² ^[r]	2.47 × 10 ⁻²	2.76
 70	≈ 5.5	1.00	Fe(CO) ₃ (C ₆ H ₇) ⁺	-7.78	4.33 × 10 ⁻³ ^[s]	5.24 × 10 ⁻³	0.83
			Fe(CO) ₂ (NO)(C ₄ H ₄) ⁺	-6.95	9.51 × 10 ⁻³ ^[t]	3.55 × 10 ⁻²	0.27
OH ⁻ (water)	10.47 ^[e]	0.61 ^[e]	Mn(CO) ₃ (C ₆ H ₆) ⁺	-11.08	2.90 × 10 ² ^[u]	4.25 × 10 ⁻¹	682

^[a] Solvent: acetone, from ref. [152]. ^[b] From ref. [26]. ^[c] From ref. [153]. ^[d] See Chapter 4. ^[e] From ref. [88]. ^[f] Calc. from ref. [12] with estimated $\Delta S^\ddagger = -100 \text{ J mol}^{-1} \text{ K}^{-1}$. ^[g] Calc. from ref. [12] with estimated $\Delta S^\ddagger = -100 \text{ J mol}^{-1} \text{ K}^{-1}$. ^[h] From Chapter 8. ^[i] Calc. from ref. [12] with $\Delta H^\ddagger = 37 \text{ kJ mol}^{-1}$ and $\Delta S^\ddagger = -45 \text{ J mol}^{-1} \text{ K}^{-1}$. ^[j] From ref. [12] with $\Delta H^\ddagger = 26 \text{ kJ mol}^{-1}$ and $\Delta S^\ddagger = -110 \text{ J mol}^{-1} \text{ K}^{-1}$. ^[k] From ref. [12] with estimated $\Delta S^\ddagger = -100 \text{ J mol}^{-1} \text{ K}^{-1}$. ^[l] From ref. [12] with estimated $\Delta S^\ddagger = -100 \text{ J mol}^{-1} \text{ K}^{-1}$. ^[m] From ref. [12] with estimated $\Delta S^\ddagger = -100 \text{ J mol}^{-1} \text{ K}^{-1}$. ^[n] From ref. [12] with $\Delta H^\ddagger = 47 \text{ kJ mol}^{-1}$ and $\Delta S^\ddagger = -96 \text{ J mol}^{-1} \text{ K}^{-1}$. ^[o] From ref. [12] with estimated $\Delta S^\ddagger = -100 \text{ J mol}^{-1} \text{ K}^{-1}$. ^[p] From ref. [12] with $\Delta H^\ddagger = 43.5 \text{ kJ mol}^{-1}$ and $\Delta S^\ddagger = -110 \text{ J mol}^{-1} \text{ K}^{-1}$. ^[q] From ref. [12] with $\Delta H^\ddagger = 46 \text{ kJ mol}^{-1}$ and $\Delta S^\ddagger = -120 \text{ J mol}^{-1} \text{ K}^{-1}$. ^[r] From ref. [12] with estimated $\Delta S^\ddagger = -100 \text{ J mol}^{-1} \text{ K}^{-1}$. ^[s] From ref. [12] with $\Delta H^\ddagger = 56 \text{ kJ mol}^{-1}$ and $\Delta S^\ddagger = -99 \text{ J mol}^{-1} \text{ K}^{-1}$. ^[t] From ref. [12] with estimated $\Delta S^\ddagger = -100 \text{ J mol}^{-1} \text{ K}^{-1}$. ^[u] From ref. [12].

Table 7.3 shows a standard deviation of factor 25.7 between observed rate constants and those calculated by the three-parameter equation 1.3. This is quite remarkable in view of the fact that electrophiles of this compilation have been calibrated with respect to phosphanes while the different nucleophiles in this compilation have been calibrated with respect to benzhydrylium ions.

Though it is found that enamines always react more slowly with metal- π -complexes than predicted by eq. 1.3, the deviations between calculated and observed rate constants are in both directions. Since they never exceed 10^3 in a theoretical reactivity range of more than 10^{30} , one can conclude that the E parameters derived in this work are useful for predicting the synthetic potential of metal- π -complexes.

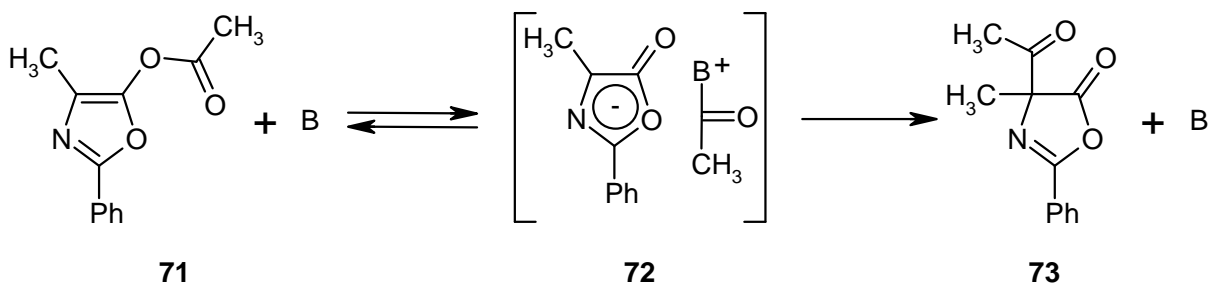
8. Nucleophilic reactivities of pyridine and its derivatives

8.1 Introduction

The preparation of esters and amides by the reaction of acid chlorides, and -anhydrides with amines and alcohols has been known since the beginning of the 19th century. Einhorn described the advantages of the presence of pyridine in reactions of acid chlorides with hydroxy-compounds.^[154] The acetylation of hydroxylic compounds under mild conditions is often achieved with a mixture of acetic anhydride and pyridine. In 1901 Verley and Bölsing^[155] developed a procedure for the quantitative analysis of terpene alcohols in etheric oils, which was later used with success in the chemistry of carbohydrates by Emil Fischer and Bergmann.^[156] This method often failed in the acetylation of sterically hindered alcohols. Therefore new catalysts, based on the pyridine system, were searched. In 1967, Litvinenko and Kirichenko^[157] discovered that the benzylation of *m*-chloroaniline occurs 10^4 times faster when using (4-dimethylamino)pyridine (DMAP) instead of pyridine. In 1969 Steglich and Höfle^[158] reported on the high catalytic efficiency of (4-dimethylamino)pyridine (DMAP) and (4-pyrrolidino)pyridine (pPyrP) as acylation catalysts.

Today, (4-dimethylamino)pyridine (DMAP) is frequently used as a catalyst in many chemical reactions^[159] and is commonly called "Steglich-catalyst".^[160]

The base catalyzed intramolecular acyl shift in 5-acyloxyoxazoles (**71**) has been studied to compare the catalytic activities of bases (Scheme 8.1).^[161] This rearrangement occurs via the formation of the ion pair **72**.



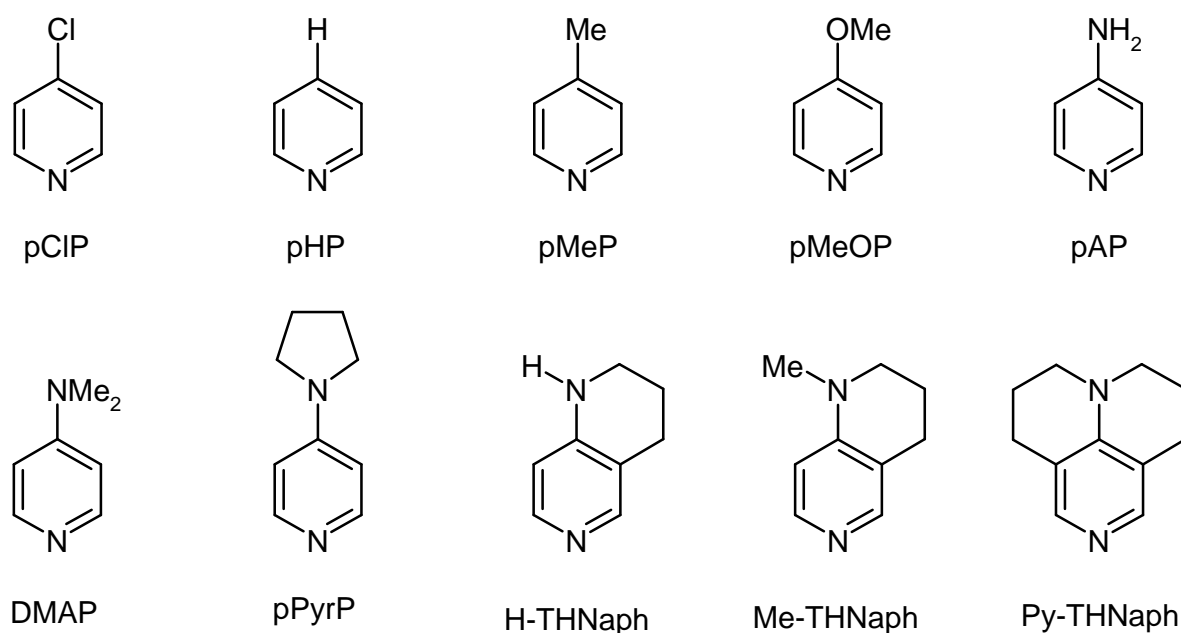
Scheme 8.1: Base catalyzed intramolecular acyl shift from 5-acyloxyoxazole (**71**) to oxazolone (**73**).

A linear correlation between the logarithmic rate constants of these base catalyzed acyl shifts and pK_a of the bases was reported for para-substituted pyridine derivatives.^[162] This relationship indicates that the catalytic activity increases with the basicity of the catalyst. As described in Chapter 4 and 6 linear correlations of the nucleophilicities N with the basicities are found for π -nucleophiles (e. g. enamines) as well for n -nucleophiles (e. g. tertiary phosphanes and phosphites). We, therefore, expect that the nucleophilicities of substituted pyridines also correlate with their basicities.

For a long time (4-pyrrolidino)pyridine (pPyrP) was the catalyst with highest activity in acylation reactions. The lower electrophilicities of $(\text{liI})_2\text{CH}^+$ ($E = -10.04$) and $(\text{jul})_2\text{CH}^+$ ($E = -9.45$), compared with the pyrrolidino substituted benzhydrylium ion $(\text{pyr})_2\text{CH}^+$ ($E = -7.69$) suggested, however, that pyridines annelated by analogous nitrogen heterocycles might be even more basic and nucleophilic than (4-pyrrolidino)pyridine (pPyrP).

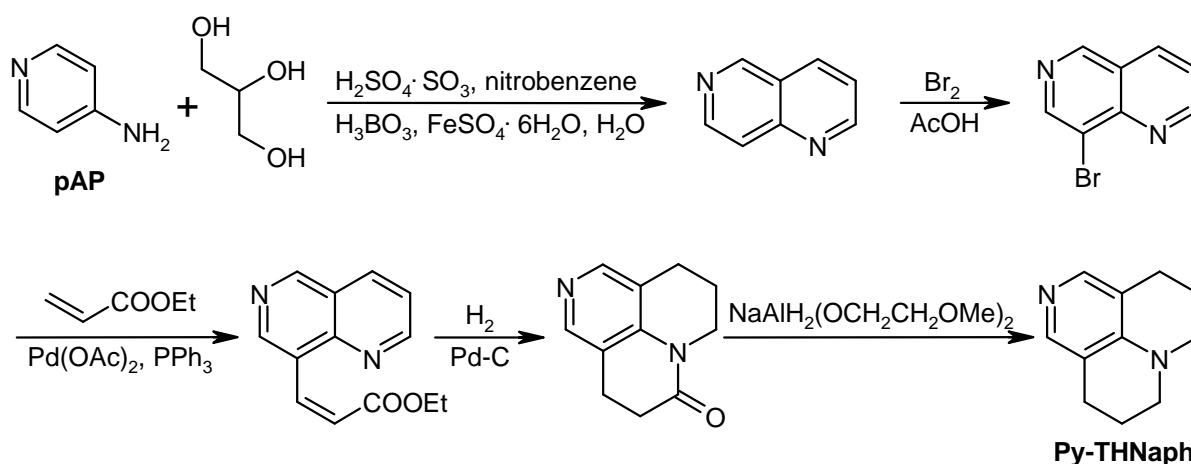
8.2 New pyridine derivatives

The nucleophilic reactivities of the 10 pyridine derivatives, shown in Scheme 8.2, most of which are commercially available, have been investigated.



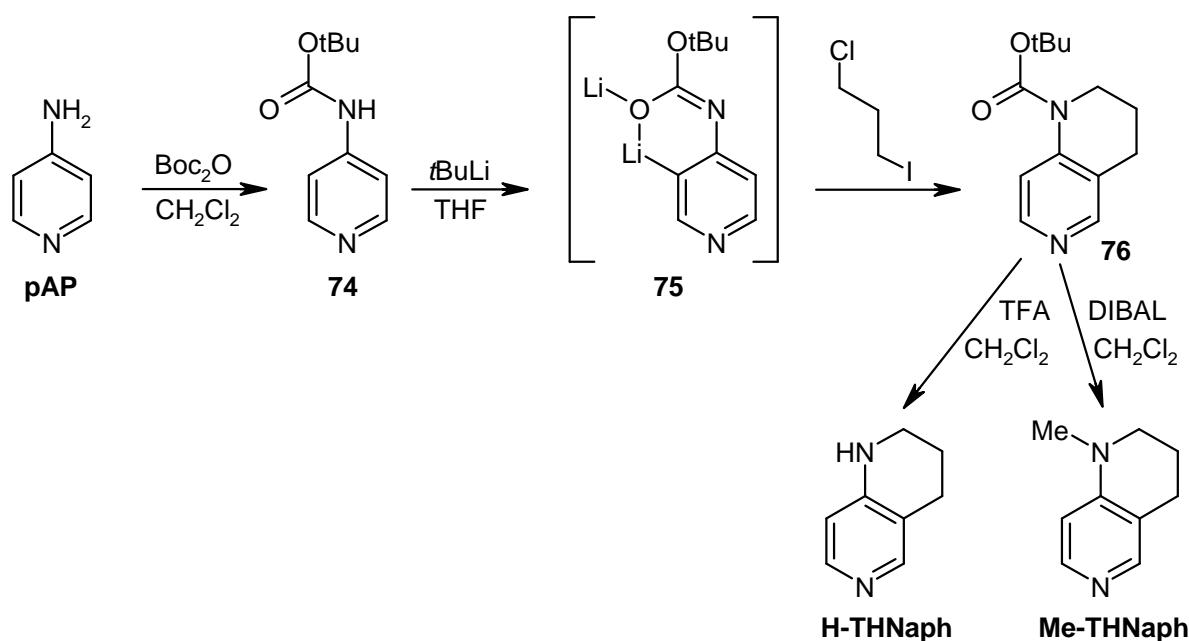
Scheme 8.2: Structures and abbreviations of para-substituted pyridine derivatives.

M. Heinrich^[163] obtained 5,6,9,10-tetrahydro-4H,8H-pyrido[3,2,1-ij]naphthyridine (Py-THNaph) from 4-aminopyridine (pAP), by a modified literature procedure^[164] (Scheme 8.3).



Scheme 8.3: Synthesis of Py-THNaph.

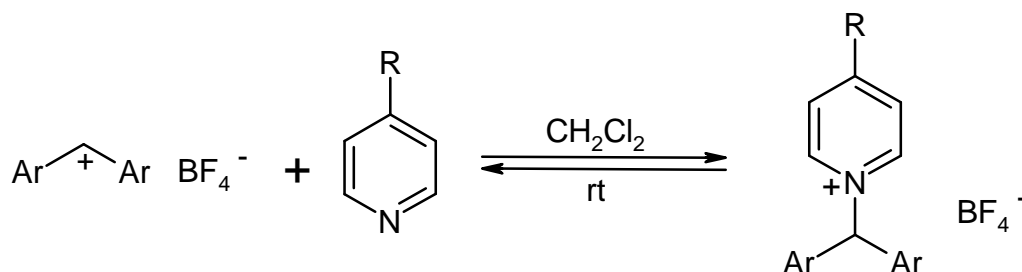
H. Klisa synthesized the pyridine derivatives H-THNaph and Me-THNaph^[165] (Scheme 8.4). Starting with *Boc*-protected 4-aminopyridine (**74**), the 6-membered ring was built up by ortho-lithiation (**75**) and reaction with 1-chloro-3-iodopropane. Removal of the protecting group in **76** by TFA led to compound H-THNaph. Reduction of **76** yielded Me-THNaph (Scheme 8.4).



Scheme 8.4: Synthesis of the pyridine derivatives H-THNaph and Me-THNaph.

8.3 Determination of the nucleophilicities of pyridine derivatives

For determining the nucleophilicities of pyridine derivatives, the rates of their additions to benzhydryl cations (reference electrophiles, see Chapter 3) were measured. The reactions of pyridine derivatives with benzhydryl tetrafluoroborates $\text{Ar}_2\text{CH}^+ \text{BF}_4^-$ produce pyridinium tetrafluoroborates (Scheme 8.5).



Scheme 8.5: Addition of benzhydryl salts to para-substituted pyridine derivatives.

Products **77-79** of the reactions of $(\text{lil})_2\text{CH}^+$, $(\text{jul})_2\text{CH}^+$, and $(\text{dma})_2\text{CH}^+$ with (4-dimethylamino)pyridine (DMAP) were characterized by ^1H NMR and ^{13}C NMR spectroscopy (see Table 8.1). Combinations of highly stabilized benzhydryl cations with pyridine derivatives of low basicity were reversible, which prevented the isolation of the reaction products.

Table 8.1: Yields and chemical shifts (CD_3CN) of pyridinium tetrafluoroborates **77-79** obtained from DMAP and Ar_2CH^+ (see Scheme 8.5).

Ar_2CH^+	Product	$(4-(\text{CH}_3)_2\text{N}-\text{C}_5\text{H}_4\text{N}-\underline{\text{CH}}\text{Ar}_2)^+$		$(4-(\underline{\text{CH}_3})_2\text{N}-\text{C}_5\text{H}_4\text{N}-\text{CHAr}_2)^+$	
		δ (^1H -NMR)	δ (^{13}C -NMR)	δ (^1H -NMR)	δ (^{13}C -NMR)
$(\text{lil})_2\text{CH}^+$	77 (58 %)	6.46	74.3	3.15	39.3
$(\text{jul})_2\text{CH}^+$	78 (68 %)	6.29	73.7	2.96-3.16 ^[a]	39.3
$(\text{dma})_2\text{CH}^+$	79 (72 %)	6.57 ^[b]	73.9 ^[b]	3.18 ^[b]	40.0 ^[b]

^[a] Signal is covered by signals of the benzhydryl substituents. ^[b] Solvent: CDCl_3 .

The ^1H NMR and ^{13}C NMR shifts in Table 8.1 do not correlate with the electrophilicities of the benzhydrylium ions.

The rates of the reactions of benzhydryl cations Ar_2CH^+ with the pyridines were followed by UV-Vis spectroscopy in CH_2Cl_2 . Details for the procedures are explained in Chapter 2. The second-order rate constants are listed in Table 8.2. In the case of reversible reactions,

equilibrium constants were calculated directly from the benzhydrylium absorptions before and after addition of the pyridines (see Chapter 2).

Because of reversible reactions with small degrees of conversion, it was impossible to derive rate constants for the combinations of weak benzhydryl cations, e. g. (lil)₂CH⁺ or (jul)₂CH⁺, with pyridine derivatives containing no or weak donor groups (e. g. Cl, H, Me, MeO). More electrophilic benzhydryl cations reacted to a higher degree of conversion, but at the same time, the reactions became too fast for kinetic observations. A compromise between a high degree of conversion and sufficiently low reaction rates was needed.

Table 8.2: Second order rate constants k_2 , equilibrium constants K , and intrinsic barriers ΔG_0^\ddagger for the additions of pyridine derivatives to benzhydryl cations in CH₂Cl₂ at 20 °C.

No.	Pyridine derivative	Ar ₂ CH ⁺	$E^{[a]}$	k_2 (20 °C) / L mol ⁻¹ s ⁻¹	K (20 °C) / L mol ⁻¹	ΔG_0^\ddagger [b] / kJ mol ⁻¹	N (s = 0.64) ^[c]
1	pCIP	(pfa) ₂ CH ⁺	-3.14	5.15×10^5			12.06
2	pHP	(dpa) ₂ CH ⁺	-4.72	3.03×10^5	2.23×10^4	52.49	13.28
3	pMeP	(dpa) ₂ CH ⁺	-4.72	8.81×10^5	5.07×10^5	53.19	14.01
4	pMeOP	(dpa) ₂ CH ⁺	-4.72	8.98×10^5			14.02
5	pAP	(dma) ₂ CH ⁺	-7.02	3.02×10^5			15.58
6	DMAP	(lil) ₂ CH ⁺	-10.04	6.45×10^3 [d]	5.70×10^3	60.47	
7		(jul) ₂ CH ⁺	-9.45		5.85×10^3	57.80	
8		(ind) ₂ CH ⁺	-8.76	4.89×10^4	1.71×10^5	59.23	
9		(thq) ₂ CH ⁺	-8.22	1.41×10^5	2.81×10^5	57.14	
10		(dma) ₂ CH ⁺	-7.02	6.56×10^5	4.31×10^7	58.55	
11		(mpa) ₂ CH ⁺	-5.89	2.83×10^6			16.14
12	pPyrP	(dma) ₂ CH ⁺	-7.02	9.27×10^5			16.34
13	H-THNaph	(lil) ₂ CH ⁺	-10.04	4.97×10^3			15.82
14	Me-THNaph	(lil) ₂ CH ⁺	-10.04	4.63×10^3			15.77
15	Py-THNaph	(thq) ₂ CH ⁺	-8.22	2.45×10^5			16.64

[a] See Chapter 3. [b] Calculated by the Marcus equation 4.1. [c] For determination see text. [d]

Eyring activation parameters: $\Delta H^\ddagger = 37.11$ kJ mol⁻¹, $\Delta S^\ddagger = -45.26$ J mol⁻¹ K⁻¹.

In the case of DMAP, the rates for the reactions with several benzhydrylium ions have been determined. When the rate constants ($\log k$) are plotted against the E parameters of the benzhydrylium ions, a linear correlation is obtained, from which s and N according to eq. 1.3 can be determined (Figure 8.1).

Estimated values of s are used to derive N parameters for the other pyridine derivatives, which have only been studied with respect to a single benzhydryl cation (see Table 8.2).

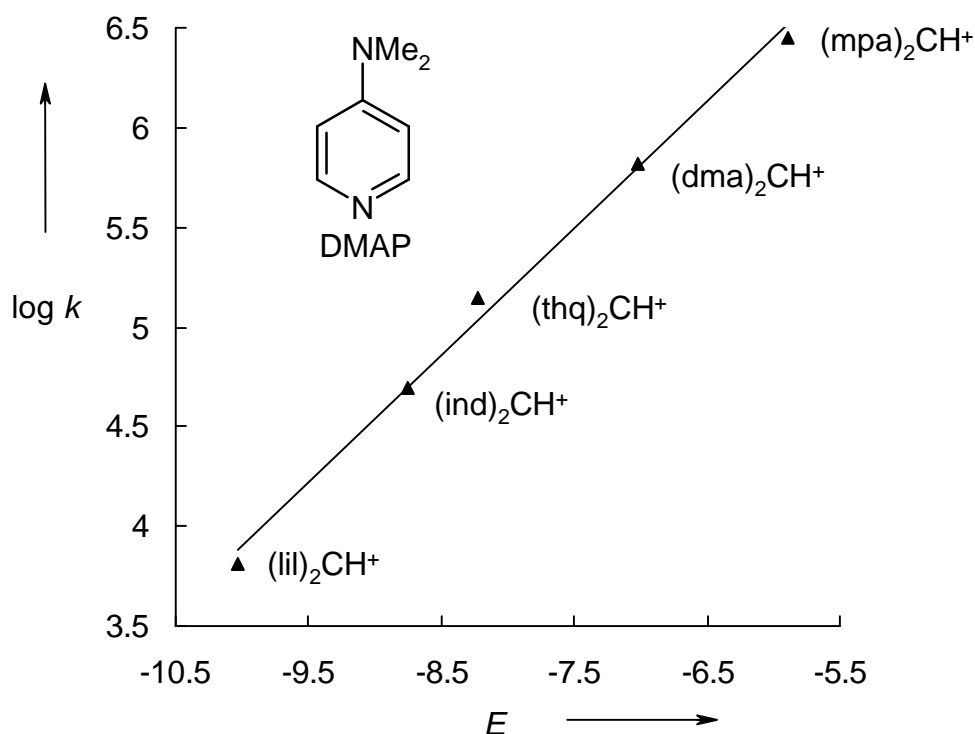


Figure 8.1: Correlation of the rate constants $\log k$ for the reactions of (4-dimethylamino)pyridine (DMAP) with benzhydryl cations in CH_2Cl_2 at 20°C .

Figure 8.2 shows that the nucleophilicities of the pyridine derivatives cover a range from $N \approx 12$ for the chloro-substituted compound pCIP to $N \approx 17$ for Py-THNaph. Pyridines, which contain donor groups as para-substituents, show higher reactivity than the other compounds. pPyrP is 1.4 times more reactive than DMAP, while the bicyclic pyridine derivatives H-THNaph and Me-THNaph are about 0.8 times as reactive than DMAP. The tricyclic compound Py-THNaph is the strongest nucleophile in the pyridine series (1.7 times more reactive than DMAP).

The relative electron donating effect of the substituents which reduces the electrophilicity of benzhydrylium ions in the series $(\text{dma})_2\text{CH}^+ > (\text{pyr})_2\text{CH}^+ > (\text{jul})_2\text{CH}^+$ is also found in the pyridine series. In contrast, annelation of a tetrahydroquinoline ring, which has a strong effect in the benzhydrylium series, increases the nucleophilicity of pyridine less than a *p*-dimethylamino group.

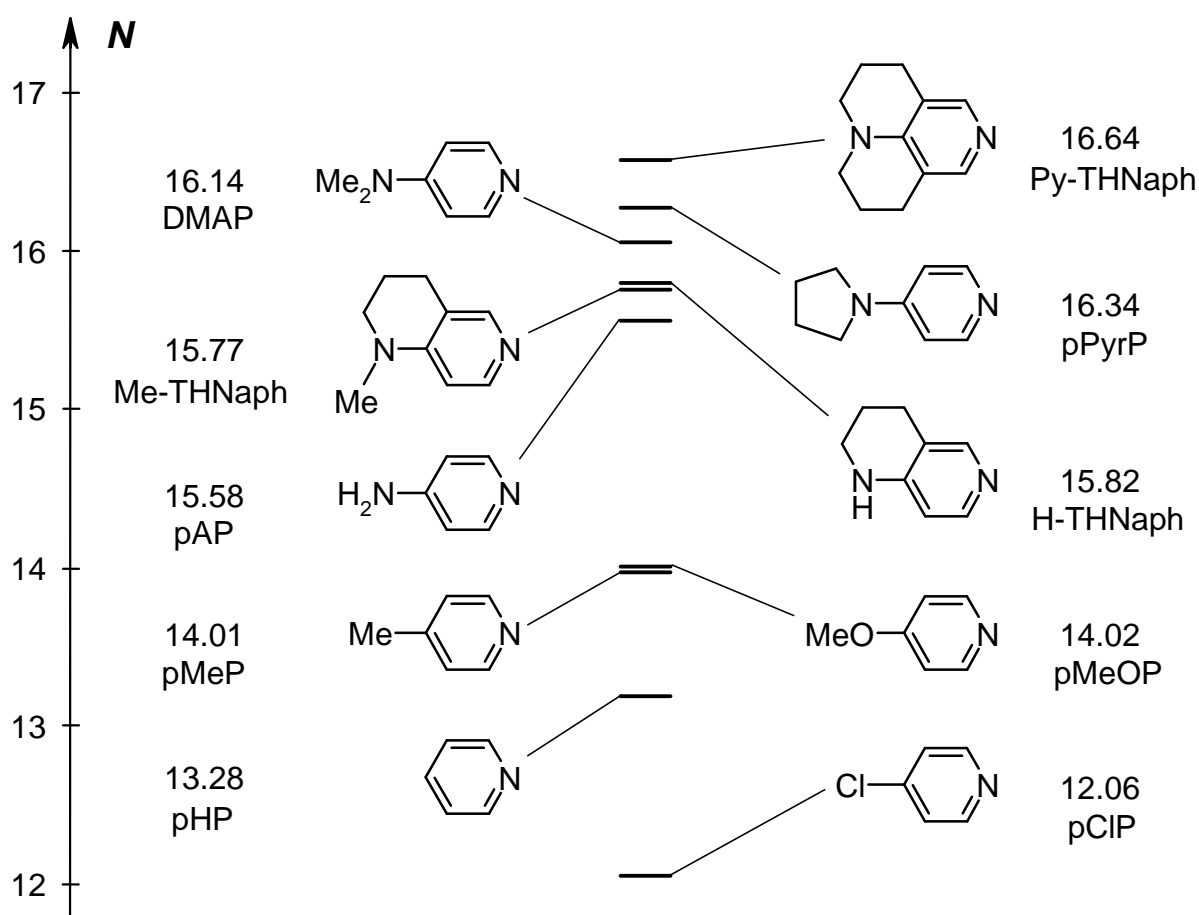
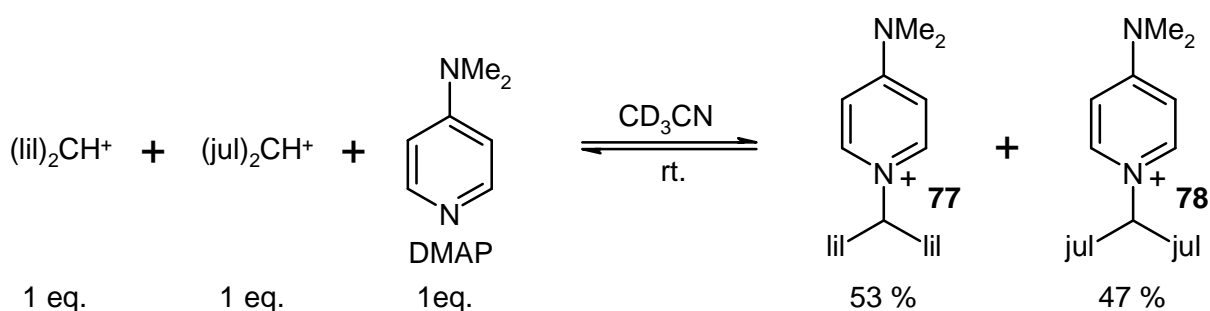


Figure 8.2: Nucleophilicity scale of *para*-substituted pyridine derivatives ($s = 0.64$).

Remarkably, the methoxy group does not increase nucleophilicity much more than the methyl group (Table 8.2, entries 3 and 4).

8.4 Rate-equilibrium relationships

Combinations of highly stabilized benzhydryl cations and non or weakly donor-substituted pyridine derivatives do not give adducts quantitatively. This situation allowed the determination of equilibrium constants for some of these combinations (see Table 8.2). Entries 6 and 7, or 8 and 9 in Table 8.2 indicate, that the equilibrium constants K for the additions of $(\text{lil})_2\text{CH}^+$ and $(\text{jul})_2\text{CH}^+$, or $(\text{ind})_2\text{CH}^+$ and $(\text{thq})_2\text{CH}^+$ to DMAP are nearly the same, despite different reactivities of the employed benzhydryl cations. In order to verify this observation and to exclude that errors are made during the determination of the equilibrium constants, another spectroscopic method was employed. Equal amounts of $(\text{lil})_2\text{CH}^+$, $(\text{jul})_2\text{CH}^+$, and (4-dimethylamino)pyridine (DMAP) were mixed in a nmr tube (CD_3CN). Comparing the integral heights of the methine-protons (chemical shifts are listed in Table 8.1) of both adducts **77** and **78** proved a product ratio of 53:47 % for the employed benzhydrylium ions $(\text{lil})_2\text{CH}^+$ and $(\text{jul})_2\text{CH}^+$ (Scheme 8.6).



Scheme 8.6: NMR-experiment to determine the relative DMAP affinity of $(\text{lil})_2\text{CH}^+$ and $(\text{jul})_2\text{CH}^+$ in CD_3CN .

Figure 8.3 illustrates a plot of $\log k$ versus $\log K$ for combinations of benzhydrylium ions with substituted pyridines in methylene chloride at 20 °C. The quality of the correlation is poor.

Figure 8.3 shows that pyridine (pHP) and the weakly donor substituted 4-methylpyridine (pMeP) react faster than expected from their equilibrium constants. DMAP reacts more slowly than expected from the observed equilibrium constants.

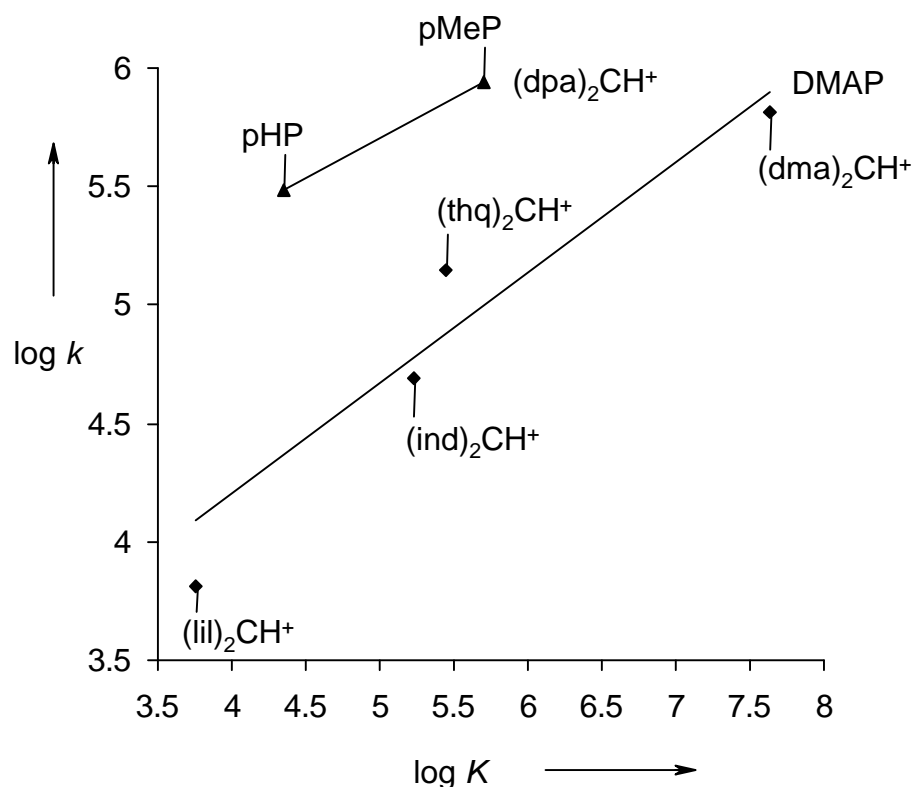


Figure 8.3: Plot of $\log k$ versus $\log K$ for the reactions of $(\text{dpa})_2\text{CH}^+$ with pyridines ($n = 2$, $\log k = 0.314 \times \log K + 3.996$), and DMAP with Ar_2CH^+ ($n = 4$, $\log k = 0.467 \times \log K + 2.337$, $r^2 = 0.9166$) in CH_2Cl_2 at $20\text{ }^\circ\text{C}$.

Two correlation lines are drawn in Figure 8.3. For the upper line, the pyridine derivative is altered, while for the lower line the benzhydrylium ion is altered. Both correlation lines have different slopes, indicating that the intrinsic barrier changes when altering the nucleophile or altering the electrophile. From the intercept on ordinate ($\Delta G^0 = 0\text{ kJ mol}^{-1}$) the intrinsic barrier can be calculated. For the reactions of $(\text{dpa})_2\text{CH}^+$ with pyridines $\Delta G_0^\ddagger \approx 49\text{ kJ mol}^{-1}$ and for the reactions of DMAP with benzhydryl cations $\Delta G_0^\ddagger \approx 59\text{ kJ mol}^{-1}$ is found. Both values are in good accordance with the intrinsic barriers, calculated for the individual electrophile-nucleophile combinations by the Marcus equation 4.1 in Table 8.2 (column 7). For less donor-substituted pyridine derivatives the intrinsic barrier is reduced dramatically ($\approx 9\text{ kJ mol}^{-1}$).

The change of the intrinsic barrier accounts for the observation, that it was difficult to measure rate constants for the reactions of pyridine derivatives of low nucleophilicity. For these compounds the reactions were thermodynamically very unfavorable. When switching to more reactive benzhydryl cations, the reactions became thermodynamically more favorable,

but the reaction rates became too high to be measured with our methods. Because of this behaviour, we did not succeed to determine rate constants for combinations of less donor substituted pyridine derivatives with more than one benzhydrylium ion.

8.5 Comparison of the nucleophilicities of pyridine derivatives with other properties

The moderate quality of the correlation between the N parameters of the pyridines and Hammett's σ_p -parameters (Figure 8.4) can be explained by the fact that the nucleophilic site is the lone pair of the pyridine nitrogen which is perpendicular to the π -system. For that reason, the substituent constant σ_p which describes a combination of mesomeric and inductive effects fails to give a good correlation with N . This is particularly seen in the comparison of methyl and methoxy. Both pyridines, pMeP and pMeOP, are nucleophiles of comparable nucleophilicity, because the +M effect of the p-methoxy group, which is responsible for its more negative σ_p -value cannot operate in the perpendicular lone pair at nitrogen.

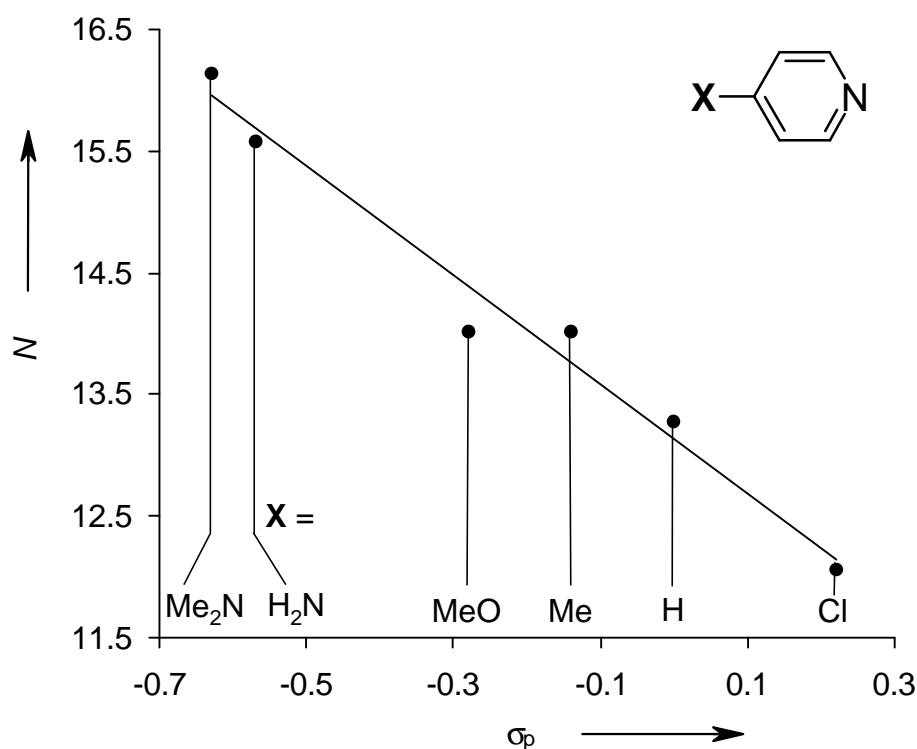


Figure 8.4: Correlation of N with σ_p ^[30] for para-substituted pyridine derivatives ($n = 6$, $N = -4.484 \times \sigma_p + 1.314 \times 10^1$, $r^2 = 0.9756$).

The basicities of *para*-substituted pyridine derivatives correlate linearly with their nucleophilicities (Figure 8.5), similar to the situation found for other classes of *n*-nucleophiles (e. g. phosphanes and phosphites, see Chapter 6). Similar correlations of *N* with pK_a , determined in acetonitrile^[166] and THF^[166] are found, but not added to Figure 8.5 because there exists only few values.

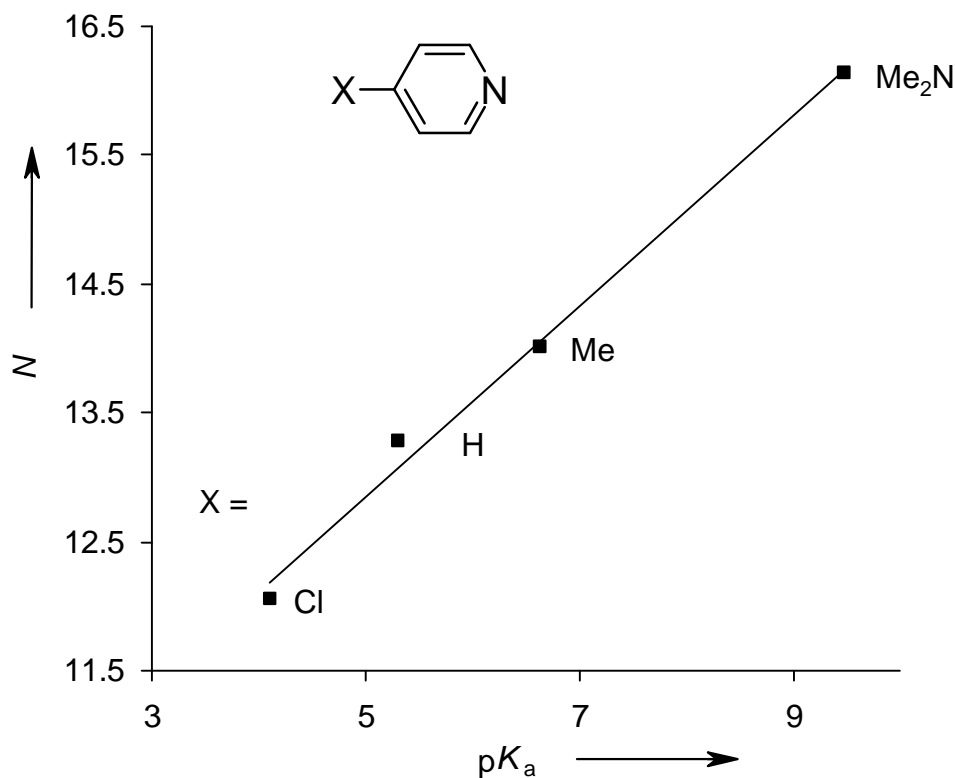
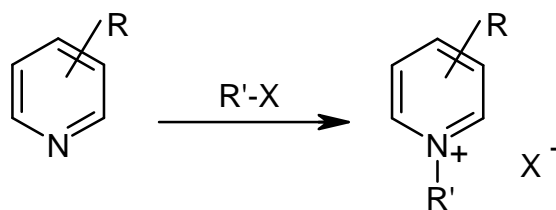


Figure 8.5: Correlation of N with pK_a ^[167] (H_2O) for *para*-substituted pyridine derivatives ($n = 4$, $N = 0.741 \times pK_a + 9.144$, $r^2 = 0.9931$).

8.6 Reactions of pyridines with other electrophiles

It has been demonstrated that eq. 1.3 can be used for predicting rate constants for the reactions of pyridine derivatives with benzhydrylium ions (see Chapter 8.3). In order to examine the applicability of the nucleophilicity parameters N determined in this work for reactions with other electrophiles, we have compared them with kinetic data from the literature.

The quaternization of pyridine and its derivatives was first reported by Menshutkin^[168] in the *N*-methylation of substituted pyridine derivatives^[169] (Scheme 8.7).



Scheme 8.7: Quaternization of pyridine derivatives in the Menshutkin reaction.^[170]

Schaper determined the rates of the methylations of various ortho-, meta-, and para-substituted pyridine derivatives with methyl iodide^[171] and developed quantitative structure-reactivity relationships (multiparameter equations). For para-substituted pyridine derivatives there exists a linear relationship (Figure 8.6) between the logarithmic rate constants for the reactions in nitromethane at 25 °C and their nucleophilicities N , despite different mechanisms (addition to benzhydryl cations but substitution of iodide in methyl iodide).

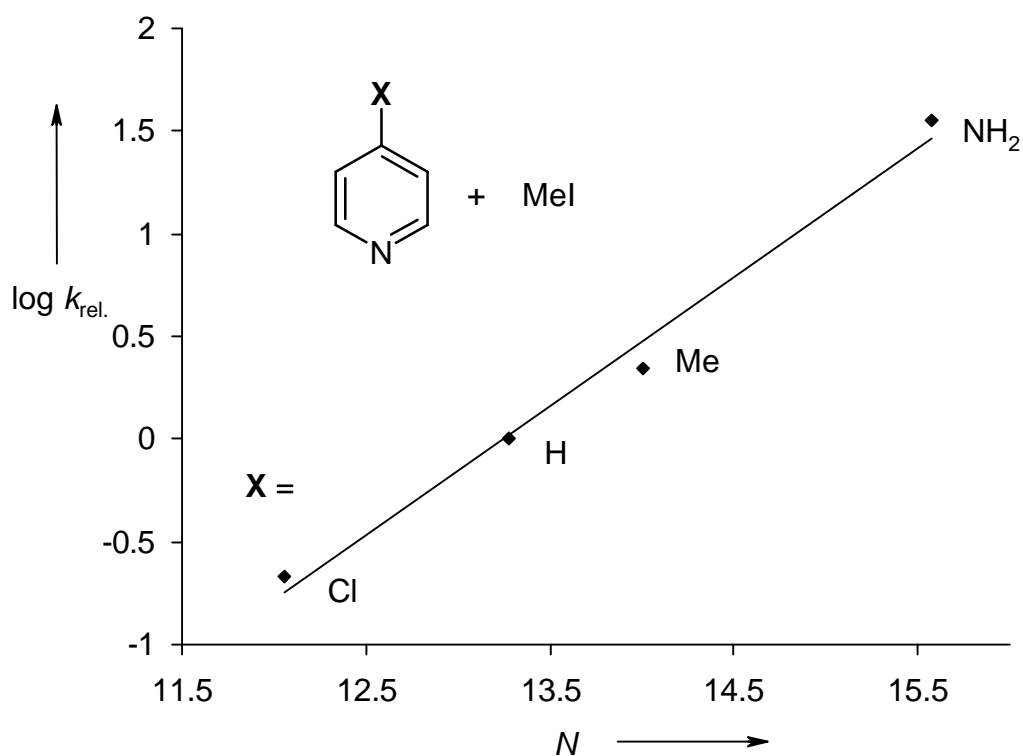


Figure 8.6: Correlation of the logarithmic rate constants of the reactions of methyl iodide with para-substituted pyridines versus their N parameters ($n = 4$, $\log k_{rel} = 0.629 \times N - 8.330$, $r^2 = 0.9881$).

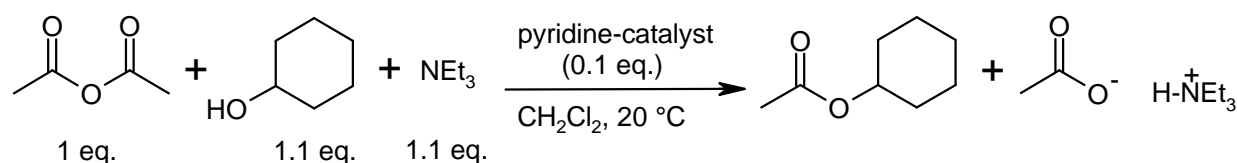
Arnett^[121b] investigated the mechanism of quaternization of a series of pyridines (mostly 3-, and 4-substituted) with several methylating and ethylating reagents in several solvents. The reactions with methyl iodide in acetonitrile were reversible, so that the effect of substituents on free energy, enthalpy, and entropy of activation for the forward and reverse reactions and on the equilibrium constants could be determined. The relationship between thermodynamic and activation parameters was examined, and a gross disparity is found between free energy and enthalpy behaviour compared with that of the entropies. It was concluded that the reactions proceed via a loose transition state, i. e. that the formation of the C-N bond is not far advanced, while the bond rupture between the transferring alkyl group and the leaving group has proceeded to a large extent.

8.7 Catalytic activities of pyridine derivatives in acylation reactions

Pyridine derivatives are good catalysts in base catalyzed reactions, as described at the beginning of this chapter. Litvinenko and Kirichenko^[157] discovered that the benzylation of 3-chloroaniline occurs 10^4 times faster when using (4-dimethylamino)pyridine (DMAP) instead of pyridine (pHP). The high catalytic activity of DMAP is only slightly exceeded by (4-pyrrolidino)pyridine (pPyrP) which is more effective by a factor of 2.3, in the acetylation of 1-ethynylcyclohexanol with acetic anhydride.^[162] M. Heinrich used the same model reaction to determine a 6 times higher catalytic activity of 5,6,9,10-tetrahydro-4H,8H-pyrido[3,2,1-ij]naphthyridine (Py-THNaph) than (4-dimethylamino)pyridine (DMAP) by NMR spectroscopy.^[163]

8.8 Determination of the catalytic activities

The catalytic activities of para-substituted pyridine derivatives in the acetylation of cyclohexanol with acetic anhydride were investigated in methylene chloride at 20 °C (Scheme 8.8). The reactions were carried out with 1 equivalent of acetic anhydride, 1.1 equivalents of cyclohexanol, 1.1 equivalents of triethylamine, and 0.1 equivalents of the pyridine catalyst (for exceptions see Table 8.3). These molar ratios correspond to normal synthetic conditions.



Scheme 8.8: Base catalyzed acetylation of cyclohexanol with acetic anhydride.

The reactions were followed by online IR-spectroscopy (Figure 8.7) using a ReactIR™ 1000 (ASI Applied Systems, Inc., 8223 Cloverleaf Drive, Suite 120, Millersville, MD 21108, U.S.A.). Reactions were monitored using a 5/8" DiComp probe fitted to an HCT detector, which was inserted into the reaction solution. Acquisitions were recorded on a IBM compatible personal computer using ReactIR™ software (V 2.2). Measurements were made in two-necked glass bottles under exclusion of moisture in dry methylene chloride. The temperature was maintained constant within ± 0.2 °C by using a circulating bath cryostat.

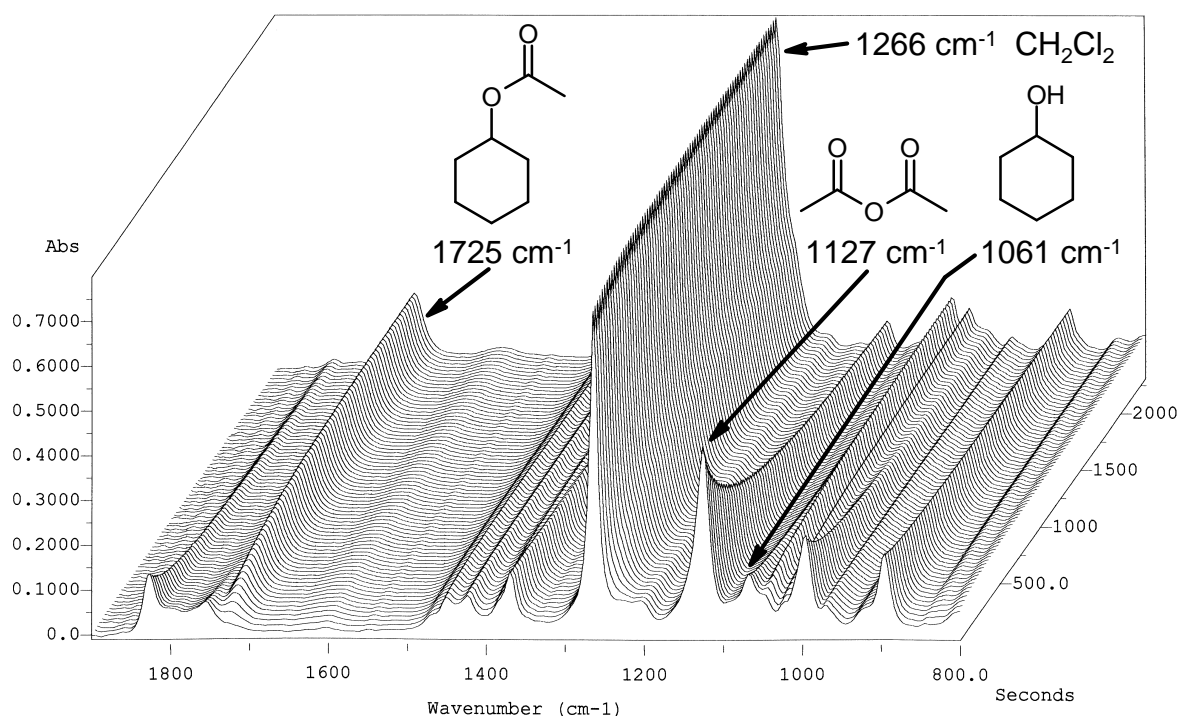


Figure 8.7: IR-spectra of the acetylation of cyclohexanol with acetic anhydride in CH_2Cl_2 at 20 °C.

The second-order rate constants k_2 were obtained from the gradients of the linear plots of the right part of eq. 8.1 versus t (second-order rate law). Equation 8.1 contains the acetic anhydride concentration $[\text{Ac}_2\text{O}]_t$ as the only time-dependent variable.

$$k_2 t = \frac{1}{\Delta} \ln \frac{[\text{Ac}_2\text{O}]_0 ([\text{Ac}_2\text{O}]_t + \Delta)}{([\text{Ac}_2\text{O}]_0 + \Delta) [\text{Ac}_2\text{O}]_t} \quad \text{with: } \Delta = [\text{cHexOH}]_0 - [\text{Ac}_2\text{O}]_0 \quad (8.1)$$

The rates of the acetylations were determined by following the decrease of the absorption band of acetic anhydride at 1127 cm^{-1} . This band was selected because it is very strong and

not covered by other signals (Figure 8.7). The evaluation of other bands produces nearly the same results, as tested in some cases.

In order to study the mechanism, the acetylations of cyclohexanol with acetic anhydride (Scheme 8.8) in the presence of DMAP, were performed with different concentrations of the components (Table 8.3).

Table 8.3: Concentrations and rate constants for the reactions of Ac₂O with cHexOH in presence of DMAP and Et₃N (Scheme 8.8) at 20 °C in CH₂Cl₂ ($\nu = 1127 \text{ cm}^{-1}$, Ac₂O).

No.	[Ac ₂ O] ₀ / mol L ⁻¹	[cHexOH] ₀ / mol L ⁻¹	[Et ₃ N] ₀ / mol L ⁻¹	[DMAP] ₀ / mol L ⁻¹	Conv. / %	k_2 / L mol ⁻¹ s ⁻¹
1	4.772×10^{-1}	5.045×10^{-1}	5.350×10^{-1}	0	[a]	[a]
2	4.772×10^{-1}	5.045×10^{-1}	5.350×10^{-1}	7.447×10^{-3}	83	4.258×10^{-3}
3	4.772×10^{-1}	5.045×10^{-1}	5.350×10^{-1}	1.255×10^{-2}	89	6.921×10^{-3}
4	4.772×10^{-1}	5.045×10^{-1}	5.350×10^{-1}	2.585×10^{-2}	91	1.360×10^{-2}
5	4.772×10^{-1}	5.045×10^{-1}	5.350×10^{-1}	5.293×10^{-2}	92	3.380×10^{-2}
6	4.772×10^{-1}	1.441	5.350×10^{-1}	1.255×10^{-2}	83	6.873×10^{-3} ^[b]
7	4.772×10^{-1}	2.162	5.350×10^{-1}	1.255×10^{-2}	89	6.850×10^{-3} ^[b]
8	4.772×10^{-1}	2.883	5.350×10^{-1}	1.255×10^{-2}	85	6.937×10^{-3} ^[b]
9	4.772×10^{-1}	5.045×10^{-1}	0	5.293×10^{-2}	[c]	[c]

^[a] No reaction observed within 3 h. ^[b] Pseudo-first-order conditions. Rate constant calculated by eq. 2.4 from the initial slope. ^[c] Very slow reaction, not second-order (becomes slower), $\tau_{1/2} \approx 960 \text{ s}$.

No reaction is observed within 3 h, when combining acetic anhydride, triethylamine, and cyclohexanol without DMAP (Table 8.3, entry 1). Varying the concentration of the catalyst in the range of 2 - 11 % (Table 8.3, entries 2-5) indicates that the reaction is first-order in the concentration of the catalyst, as shown by the linear plot of k_2 versus [DMAP] in Figure 8.8.

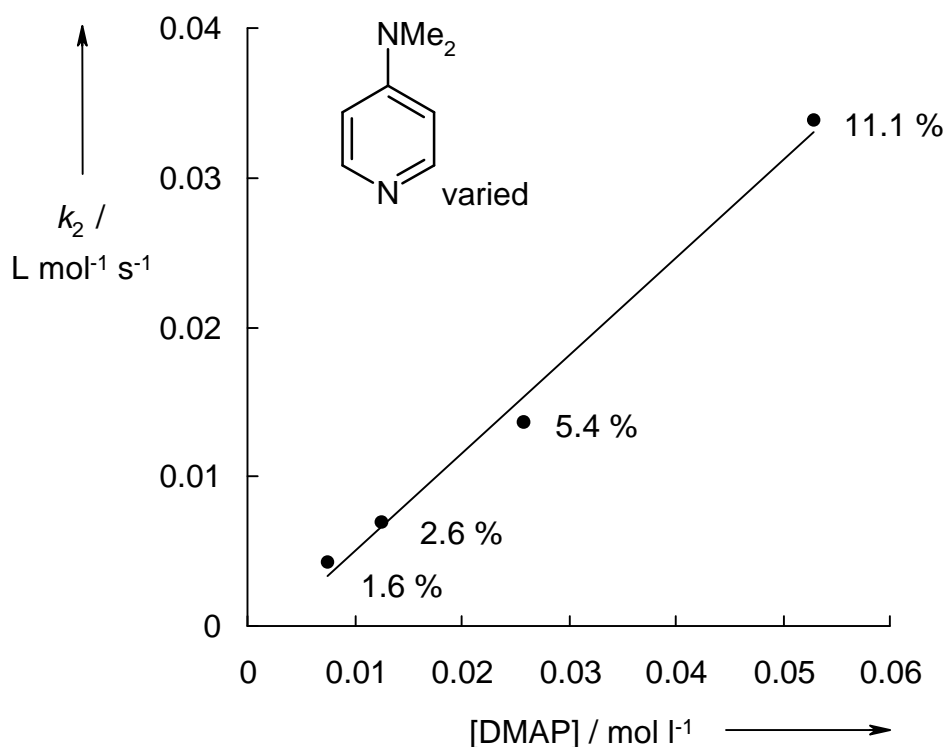


Figure 8.8: Plot of k_2 versus [DMAP] for the reactions of Ac_2O ($c = 4.772 \times 10^{-1} \text{ mol L}^{-1}$) with $c\text{HexOH}$ ($c = 5.045 \times 10^{-1} \text{ mol L}^{-1}$) and NEt_3 ($c = 5.350 \times 10^{-1} \text{ mol L}^{-1}$) in CH_2Cl_2 at 20°C in presence of variable concentrations of DMAP ($n = 4$, $k = (6.350 \times 10^{-1}) \times [\text{DMAP}] - (1.500 \times 10^{-3})$, $r^2 = 0.9915$).

Increasing the concentration of cyclohexanol over the concentration of acetic anhydride (3-6 equivalents), changes the reaction from second-order to pseudo-first-order conditions (Table 8.3, entries 6-8). The plots of $\ln ([\text{Ac}_2\text{O}]_0 - [\text{Ac}_2\text{O}]_{\text{end}} / [\text{Ac}_2\text{O}]_t - [\text{Ac}_2\text{O}]_{\text{end}})$ versus t give straight lines with slopes equal the pseudo-first-order rate constants $k_{1\psi}$. In the case of low concentrations of cyclohexanol (Table 8.3, entry 6) the initial slope (until 20 % conversion) was used for obtaining $k_{1\psi}$.

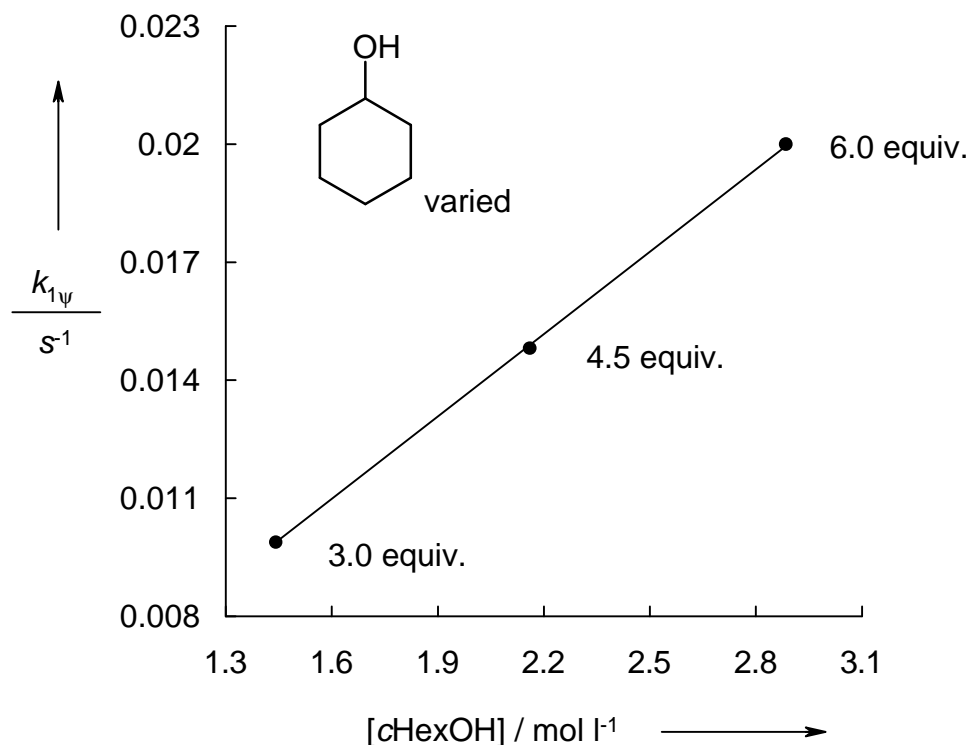


Figure 8.9: Plot of $k_{1\psi}$ versus $[c\text{HexOH}]$ for the reactions of Ac_2O ($c = 4.772 \times 10^{-1} \text{ mol L}^{-1}$) with variable concentrations of $c\text{HexOH}$ in the presence of DMAP ($c = 1.255 \times 10^{-2} \text{ mol L}^{-1}$) and Et_3N ($c = 5.350 \times 10^{-1} \text{ mol L}^{-1}$) in CH_2Cl_2 at 20°C ($n = 3$, $k = (7.006 \times 10^{-3}) \times [c\text{HexOH}] - (2.453 \times 10^{-4})$, $r^2 = 0.9997$).

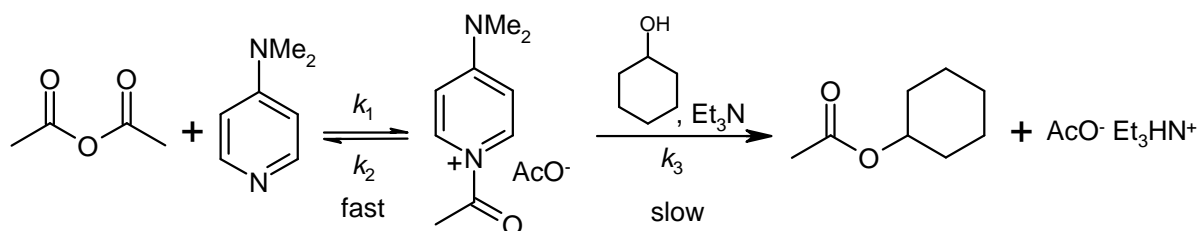
A comparison of the second-order rate constants k_2 , determined under pseudo-first-order conditions (Table 8.3, entries 6-8) with the rate constant k_2 , which was determined under second-order conditions (Table 8.3, entry 3), indicates, that they are similar.

According to the course of the reaction, shown in Scheme 8.8, at least one equivalent of a strong base is necessary, which must be more basic than the catalyst. The use of Et_3N ($\text{p}K_a = 10.65$) prevents protonation DMAP ($\text{p}K_a = 9.70$) by acetic acid, which is formed during the reaction. The acetylation of cyclohexanol without Et_3N is very slow and does not proceed with total conversion of the reactants (Table 8.3, entry 9).

It can be concluded, that the base catalyzed acetylations of cyclohexanol with acetic anhydride, in the presence of DMAP, are first-order in the concentration of the catalyst (Figure 8.8) and first-order in the concentration of the alcohol (Figure 8.9). Figure 8.8 shows a plot of k_2 versus $[\text{DMAP}]$. The slope of this correlation line ($6.350 \times 10^{-1} \text{ L}^2 \text{ mol}^{-2} \text{ s}^{-1}$)

corresponds to the DMAP-concentration independent rate constant, and may be considered as a third-order rate constant.

The linear dependence of the reaction rates on the concentrations of cyclohexanol indicates, that the alcohol must be involved in the rate determining step of the reaction. The following mechanism in Scheme 8.9 is in accord with the proposals in ref. [172].



Scheme 8.9: Proposed mechanism for the base catalyzed acetylation of cyclohexanol.

The reaction starts with a fast attack of the catalyst at acetic anhydride, yielding N-acetylpyridinium acetate. In a subsequent, slower reaction, the acetylpyridinium ion reacts with cyclohexanol and forms cyclohexyl acetate and triethylammonium acetate. Higher concentrations of the catalyst result in the formation of higher concentrations of the reactive intermediate, which increase the rate of the reaction.

8.9 Comparison of the catalytic activities of pyridine derivatives

The base-catalyzed acetylation of cyclohexanol with acetic anhydride (Scheme 8.8) was used to determine the catalytic activities of several pyridines. All reactions were performed according to the procedure, described in Chapter 8.8. Table 8.4 compares the rates, of the acetylations with the rates for the additions to benzhydryl cations.

Table 8.4: Rate constants k_2 for the base-catalyzed acetylations of *c*HexOH with Ac₂O, relative rate constants k_2 (rel.), and relative rate constants for the reactions with (dpa)₂CH⁺.

Catalyst	<i>N</i> (<i>s</i> = 0.64)	$k_2 / \text{L mol}^{-1} \text{s}^{-1}$ acetylation ^[a]	k_2 (rel.) acetylation	k_2 (rel.) ^[b] with (dpa) ₂ CH ⁺
pHP	13.28	8.816×10^{-6}	1	1
pMeP	14.01	1.306×10^{-5}	1.5	2.9
pAP	15.58	1.055×10^{-4}	12.0	29.6
DMAP	16.14	3.380×10^{-2}	3833.9	67.2
pPyrP	16.34	4.554×10^{-2}	5165.6	90.8
Py-THNaph	16.64		(≈ 22000) ^[c]	140.4

^[a] With concentrations: [Ac₂O] = $4.772 \times 10^{-1} \text{ mol L}^{-1}$, [*c*HexOH] = $5.045 \times 10^{-1} \text{ mol L}^{-1}$, [Et₃N] = $5.350 \times 10^{-1} \text{ mol L}^{-1}$, [catalyst] = $5.290 \times 10^{-2} \text{ mol L}^{-1}$ (11 %) in CH₂Cl₂ at 20 °C. ^[b] Rates which were not measured with this cation are calculated from *E*, *N*, and *s* by eq. 1.3. ^[c] Calculated from ref. [163].

The relative rate constants k_2 (rel.) for the base catalyzed acetylations of cyclohexanol with acetic anhydride indicate that DMAP, as catalyst, is 10³ times more reactive than pyridine, while its catalytic activity is only slightly (about 1.3 times) exceeded by pPyrP, according to the results of Steglich.^[162] M. Heinrich showed that the new tricyclic pyridine derivative Py-TNNaph has a 5.8^[163] times higher catalytic activity than DMAP. 4-aminopyridine (pAP) increases the rates of acetylations only slightly, compared with pyridine (pHP), in agreement with observations of Hassner.^[173]

The relative rate constants k_{obs} (rel.) for the additions of pyridine derivatives to (dpa)₂CH⁺ indicate that the reactivity order is the same as found for the base catalyzed acetylations. For weakly donor substituted compounds (pHP, pMeP, pAP), the increase of the rates is higher for the additions to benzhydryl cations than for the catalyzed acetylations. Vice versa, for pyridines with good donors (DMAP, pPyrP, Py-THNaph) the rates of acetylations increase much more than the rates of the additions to benzhydryl cations (Table 8.4).

Table 8.4 shows, that the catalytic activities of pyridines is related to their nucleophilicities, but this relation is not simple and therefore it seems to be problematic to use *N* for predicting the catalytic efficiencies.

9. Conclusion and outlook

The introduction of reference compounds as described in Chapter 3 proved to be very useful for the determination of nucleophilicity and electrophilicity parameters as defined by eq. 1.3

This was shown by adding various new classes of nucleophiles, like enamines (Chapter 4), phosphanes and phosphites (Chapter 6), and pyridines (Chapter 8) as well as by adding new electrophiles (Chapter 5).

Chapter 7 exemplifies that these data can be used for linking kinetic data for electrophile nucleophile combinations from the literature with our reactivity scales. It was shown that the E parameters of 32 metal- π -complexes obtained by correlation can be used for predicting their reactivities with other nucleophiles. One can, therefore expect a rapid growth of our reactivity scales.

Besides further extension of the data set by new compounds, it now becomes essential to search for the physical basis of the reactivity parameters E and N . Quantum chemical calculations as well as correlations with other kinetic and thermodynamic data may contribute to this understanding.

The reversible additions of pyridines (Chapter 8) and of tertiary triarylphosphanes (Chapter 6) to benzhydryl cations allows us to determine intrinsic rate constants for these reactions which are a key to the understanding of organic reactivity. They furthermore provide rate constants for the reverse reactions which can be employed for a systematic evaluation of the nucleofugality of leaving groups.

Since the rates of S_N2 type reactions depend on the nucleophilicity of the entering group as well as on the nucleofugality of the leaving group, it now appears possible also to arrive at a new systematic treatment of bimolecular nucleophilic substitutions.

10. Experimental part

10.1 General conditions

Analytical data: NMR spectra were recorded on a Varian Mercury 200 (200 MHz), Bruker ARX 300 (300 MHz) or Varian VXR 400 S (400 MHz). Chemical shifts are reported as δ -values in ppm relative to tetramethylsilane (δ_{H} : 0.00, δ_{C} : 0.0) or relative to the deuterated solvent peak:^[174] CDCl_3 (δ_{H} : 7.24, δ_{C} : 77.0), CD_2Cl_2 (δ_{H} : 5.32, δ_{C} : 53.5), CD_3CN (δ_{H} : 1.93, δ_{C} : 1.3, 117.7), $(\text{CD}_3)_2\text{SO}$ (δ_{H} : 2.49, δ_{C} : 39.7). Coupling constants are reported in Hz. For the characterization of the observed signal multiplicities the following abbreviations were applied: s (singlet), d (doublet), t (triplet), q (quartet), m (multiplet), as well as br (broad). Signal assignments are based on ^1H - ^1H -COSY, ^1H - ^1H -NOESY, ^1H - ^{13}C -HETCOR, and gHSQC experiments. Infrared spectra were recorded from 4000 - 400 cm^{-1} on a Perkin-Elmer 1420 Infrared Spectrometer or Perkin-Elmer Spectrum 1000. Samples were measured either as a film between sodium chloride plates or as potassium bromide tablets. The absorption bands are reported in wave numbers (cm^{-1}). UV-Vis spectra were recorded on a Beckman DK-2a or Beckman UV 5240. Mass spectra were measured with a Finnigan MAT 95 Q. Elemental analysis were carried out in the "Mikroanalytisches Laboratorium des Departments für Organische Chemie der LMU München". Melting points were determined on a Büchi B540 and are uncorrected. Distillations of small amounts were performed with a "Büchi - Kugelrohrdestillationsapparatur (KGR-50)". In these cases boiling points refer to the oven temperature.

Chromatography: Thin layer chromatography (TLC) was performed using aluminium plates coated with SiO_2 (Merck 60, F-254) or Al_2O_3 (Merck 60, F-254). The chromatograms were viewed under UV light. Column chromatography was performed using SiO_2 60 (Merck) or Al_2O_3 (Fluka, type 507 C neutral or type 5016 A basic).

Solvents: Dichloromethane (Merck, puriss.) was vigorously stirred over concentrated H_2SO_4 to remove traces of olefins (72 h), then washed with water, 5 % aqueous K_2CO_3 solution, and water. After drying over CaCl_2 the solvent was freshly distilled from CaH_2 . Chloroform (Merck, p. A., stabilized with 0.6-1 % ethanol) was stirred twice with concentrated H_2SO_4 for 12 h and washed with water and 5 % aqueous K_2CO_3 solution. The solvent was dried over

CaCl₂, then over P₂O₅, and stored over K₂CO₃. Prior to use, the solvent was filtered over basic alumina (Merck, activity grade 1). Nitromethane (Merck, zur Synthese) was purified by column chromatography through neutral alumina (Merck, activity grade 1). Acetonitrile (Acros, HPLC-grade) was first distilled from CaH₂. It was then refluxed at least 3 days over diphenylketene, from which it was always freshly distilled prior to use. Tetrahydrofuran and diethylether were dried over KOH, stored over sodium, and freshly distilled from sodium prior to use.

Chemicals: The following chemicals were purchased: cyclopentanone (Merck, >99 %), morpholine (Merck, >98 %), p-toluenesulfonic acid (Merck, >98 %), CaH₂ (Acros, 93 %), (4-pyrrolidino)pyridine (Acros, 98 %), 4,4'-difluorobenzophenone (Acros, 99 %), diphenylamine (Acros, 99 %), potassium tert.-butoxide (Merck, >98 %), tetrafluoroboric acid-diethyl ether complex (Fluka, 54 % in diethyl ether), tetrahydro-pyran-2-one (Merck, >99 %), chlorotrimethylsilane (Merck, >99 %), celite (Acros, type 521), tributylphosphine (Fluka, >95 %), tris(4-chlorophenyl)phosphine (Fluka, >98.5 %), triphenylphosphine (Merck, >99 %), tris(4-methylphenyl)phosphine (Lancaster, 97 %), tris(4-methoxyphenyl)phosphine (Lancaster, 98 %), phosphorous acid tributyl ester (Fluka, >95 %), phosphorous acid triphenylester (Acros, 99+ %), tricyclohexylphosphine (Acros, 97 %), triisopropylphosphine (Fluka, 90 %), diisopropylamine (Lancaster 99 %), lithium-granules (Acros), *n*butyllithium (Lancaster, 1.6 M in hexane), cyclohexanone (Fluka, >99.5 %), pyrrolidine (Merck, >99 %), *N*-methylaniline (Lancaster, 98 %), bentonit K-10 (Acros, montmorillonite K-10), acetophenone (Acros, 99 %), isobutyraldehyde (Acros, 99+ %), 3-methyl-2-butanone (Acros, 98 %), titanium tetra chloride (Lancaster, 98+ %), phenylacetaldehyde (Aldrich, 90+ %), propynoic acid ethyl ester (Aldrich, 99 %), indole (Acros, 99+ %), *N*-methylmorpholine (Acros, 99 %), allylbromide (Lancaster, 98+ %), benzoic acid (Lancaster, 99 %), 4-chloropyridine-hydrochloride (Fluka, >99 %), pyridine (Fluka, >99.8 %), 4-methylpyridine (Aldrich, 99 %), 4-methoxypyridine (Aldrich, 97 %), 4-aminopyridine (Merck, >98 %), (4-dimethylamino)pyridine (Merck, >99 %), acetic anhydride (Fluka, >98.0 %), cyclohexanol (Lancaster, 99 %), (*N*-triisopropylsilyl)pyrrole (Aldrich, 95 %), 1-methylindole (Lancaster, 98+ %), 1,2-dimethylindole (Aldrich, 99 %), pyrrole (Lancaster, 98 %), (4-bromophenyl)dimethylamine (Lancaster, 98+ %), phosphorous trichloride (Merck, >99 %), 1-phenyl-1-(trimethylsiloxy)ethene (Fluka, >98.0 %), 1-(trimethylsiloxy)cyclohexene (Fluka, >97 %), 1-(trimethylsiloxy)cyclopentene (Fluka, >98 %), 2,6-di-tert.-butylpyridine (Aldrich, 97 %), 1-methoxy-2-methyl-1-(trimethylsiloxy)propene (Fluka, > 90 %),

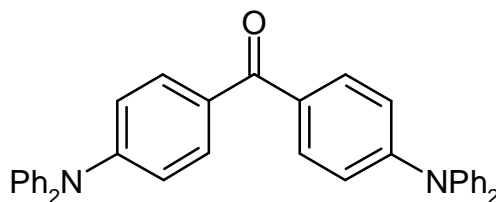
allyltriphenylstannane (Aldrich, 97 %), and allyltributylstannane (Lancaster, 97 %). The following chemicals were taken from the working group supply: 1-phenoxy-1-(trimethylsiloxy)ethene,^[175] tributyl(2-methylallyl)stannane,^[38] allyltriphenylstannane,^[38] and trimethyl(2-methylallyl)silane.^[38]

10.2 Reference scales for the characterization of cationic electrophiles and neutral nucleophiles

10.2.1 Synthesis of benzhydryl cations

Bis(4-diphenylaminophenyl)methanone (2): Potassium tert.-butoxide (8.14 g, 72.5 mmol) was dissolved in dimethyl sulfoxide (80 mL). Successively solutions of diphenylamine (14.7 g, 87.0 mmol) in dimethyl sulfoxide (80 mL) and of 4,4'-difluorobenzophenone (6.33 g, 29.0 mmol) in dimethyl sulfoxide (50 mL) were added. The reaction mixture was stirred for 2 h at ambient temperature and for 3 h at 90 °C before it was allowed to cool to ambient temperature again. The solution was then poured on crushed ice (1 L) and extracted with dichloromethane (3 × 300 mL). The combined organic phases were washed with water (5 × 200 mL), dried and filtered. Evaporation of the solvent in vacuo gave a green and viscous residue which was crystallized from ethanol. Another crystallization delivered bis(4-diphenylaminophenyl)methanone (**9**) (5.49 g, 37 %) as a yellow solid, mp 187–188 °C (from acetone; ref. [176]: 189 °C). ¹H NMR (CDCl₃, 300 MHz): δ = 6.96–7.36 (m, 24 H, ArH), 7.63–7.74 (m, 4 H, ArH) according to ref. [177]; ¹³C NMR (CDCl₃, 75.5 MHz): δ = 119.9, 124.4, 125.8, 129.4 (4 d, Ar), 130.6 (s, Ar), 131.6 (d, Ar), 146.7, 151.4 (2 s, Ar), 193.9 (s, C=O) according to ref. [177]; MS (EI, 70 eV): *m/z* (%): 516 (M⁺, 100), 348 (7) 272 (24), 258 (14), 243 (12), 167 (8).

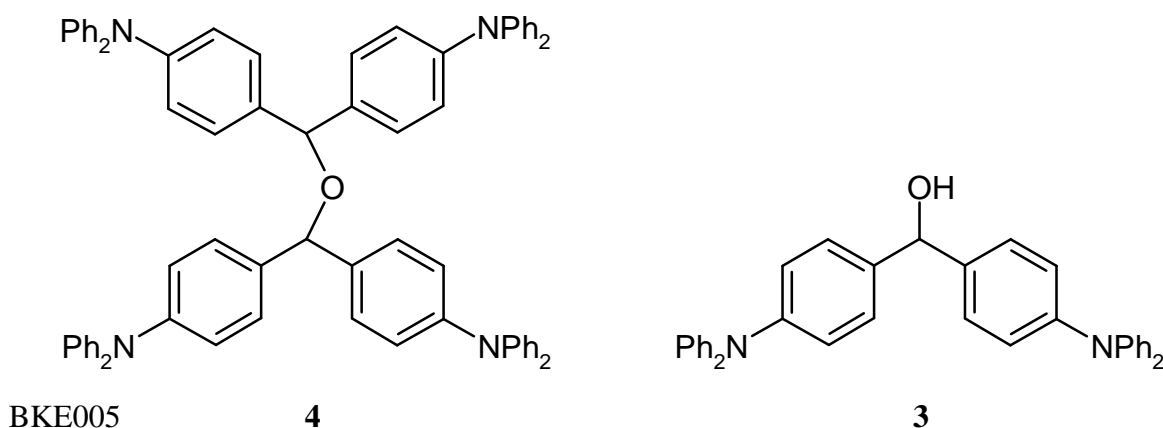
BKE004



2

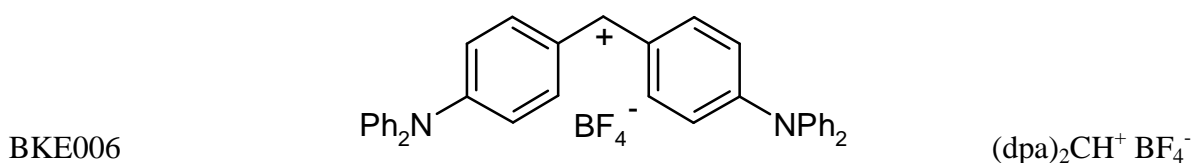
Bis(bis(4-diphenylaminophenyl)methyl)ether (4) and bis(4-diphenylaminophenyl)methanol (3): A suspension of bis(4-diphenylaminophenyl)methanone (**2**) (5.00 g, 9.68 mmol), sodium borohydride (200 mg, 5.29 mmol), and potassium hydroxide (50 mg, 0.89 mmol) in

ethanol (5 mL) was heated at 70 °C. Further portions of sodium borohydride were added after 3 h (200 mg, 5.29 mmol) and 6 h (100 mg, 2.64 mmol), and stirring was continued over night at 70 °C. After cooling, the mixture was hydrolysed with ice-water (250 mL). A yellow solid precipitated which was filtered and washed with water (50 mL). Recrystallization from petrol ether (70–90 °C) gave bis(bis(4-diphenylaminophenyl)methyl)ether (**4**) (3.25g, 66 %) as a colorless solid, mp 133–134 °C. ^1H NMR (CDCl_3 , 300 MHz): δ = 5.36 (s, 2 H, Ar_2CH), 6.99–7.28 (m, 56 H, ArH); ^{13}C NMR (CDCl_3 , 75.5 MHz): δ = 79.6 (d, Ar_2CH), 122.8, 123.3, 124.3, 128.4, 129.2 (5 d, Ar), 136.1, 147.0, 147.7 (3 s, Ar); MS (70 eV), m/z (%): 518 (87), 502 [Ar_2CH] $^+$ (100), 334 (10), 272 (32), 243 (24), 167 (23), 77 (11); and bis(4-diphenylaminophenyl)methanol (**3**) (1.33g, 27 %) as a colorless solid. ^1H NMR (CDCl_3 , 300 MHz): δ = 2.18 (d, J = 3 Hz, 1 H, OH), 5.73 (d, J = 3 Hz, 1 H, Ar_2CH), 6.97–7.25 (m, 28 H, ArH) according to ref. [176]; ^{13}C -NMR (CDCl_3 , 75.5 MHz): δ = 75.7 (d, Ar_2CH), 123.8, 123.6, 127.5, 128.9, 129.2 (5 d, Ar), 137.8, 147.2, 147.7 (3 s, Ar).



Bis(4-diphenylaminophenyl)methylmethyl-tetrafluoroborate $(\text{dpa})_2\text{CH}^+ \text{BF}_4^-$: Dropwise addition of a solution of tetrafluoroboric acid-diethyl ether complex (0.45 ml, 3.29 mmol) in diethyl ether (30 mL) to a solution of bis(bis(4-diphenylaminophenyl)methyl)ether (**4**) (1.78 g, 1.75 mmol) in diethyl ether (50 mL) and stirring for another 30 min gave rise to the formation of a green precipitate. The mixture was filtered, and the solid residue was washed with diethyl ether (50 mL) and dried in vacuo to give bis(4-diphenylaminophenyl)methylmethyl-tetrafluoroborate $(\text{dpa})_2\text{CH}^+ \text{BF}_4^-$ (1.66 g, 81 %) as a dark-green powder. ^1H NMR (CDCl_3 , 300 MHz): δ = 6.94 (d, 4 H, J = 9.0 Hz, ArH), 7.05–7.48 (m, 20 H, ArH), 7.88 (d, 4 H, J = 9.0 Hz, ArH), 8.25 (s, 1 H, Ar_2CH); ^{13}C NMR (CDCl_3 , 75.5 MHz): δ = 118.8, 123.8, 126.7, 128.1, 130.1 (5 d, Ar), 140.5, 142.8, 157.3 (3 s, Ar), 164.8 (d, Ar_2CH); MS (FAB, 70 eV): m/z

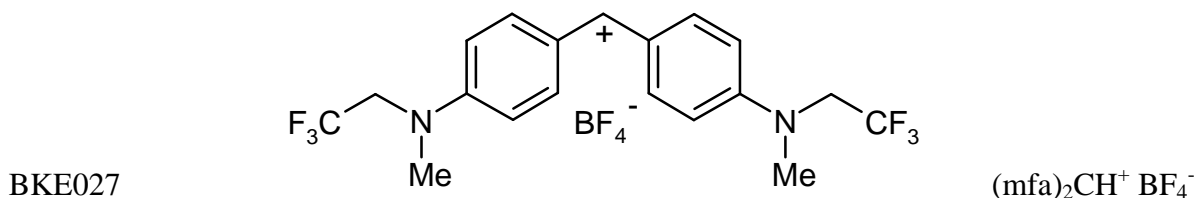
(%): 501 (100) $[M]^+$, 330 (12), 254 (12), 167 (15), 154 (19), 136 (15); IR (KBr): $\nu = 3435$, 3061, 1549, 1468, 1339, 1162, 703, 497 cm^{-1} ; UV/Vis (CH_2Cl_2): $\lambda_{\text{max}} = 674 \text{ nm}$ ($\epsilon_{\text{max}} = 96000 \text{ [cm}^2 / \text{mmol]}$); Anal. Calcd for $\text{C}_{37}\text{H}_{29}\text{BF}_4\text{N}_2$ (588.44): C 75.52, H 4.97, N 4.76. Found: C 75.49, H 4.97, N 4.74.



Using the same procedure, bis(4-diphenylaminophenyl)methanol (**3**) can be converted into $(\text{dpa})_2\text{CH}^+ \text{BF}_4^-$.

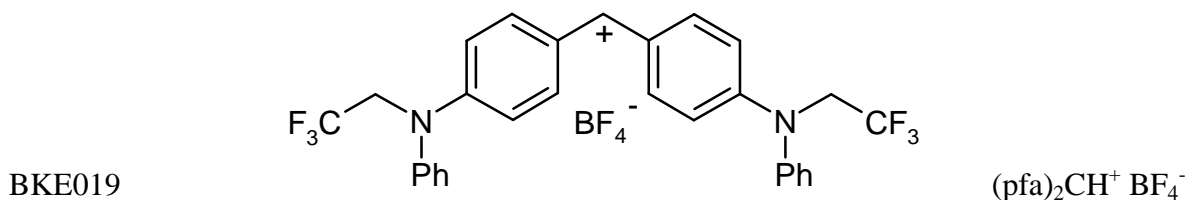
Bis(4-(methyl(2,2,2-trifluoroethyl)amino)phenyl)methylium tetrafluoroborate

(mfa) $_2\text{CH}^+ \text{BF}_4^-$: To a solution of bis(bis(4-(*N*-methyl-*N*-(2,2,2-trifluoroethyl)amino)phenyl)methyl)ether (**8a**) (1.50 g, 1.89 mmol) in diethyl ether (75 mL) was slowly added a solution of $\text{Et}_2\text{O-HBF}_4$ complex (0.26 mL, 1.9 mmol) in diethyl ether (30 mL). After the addition, stirring was continued for 30 min. Then the blue precipitate was collected by filtration under nitrogen, washed with diethyl ether, and dried in vacuo to furnish bis(4-(*N*-methyl-*N*-(2,2,2-trifluoroethyl)amino)phenyl)methylium tetrafluoroborate **(mfa) $_2\text{CH}^+ \text{BF}_4^-$** (1.54 g, 86 %). ^1H NMR (CD_3CN , 300 MHz): $\delta = 3.36$ (s, 6 H, NMe), 4.41 (q, 4 H, $J_{\text{H,F}} = 8.8$ Hz, NCH_2), 7.15, 8.01 ($2 \times \text{AA}'\text{BB}'$ system with $J_{\text{AB}} = 9.3$ Hz, 2×4 H, ArH), 8.18 (s, 1 H, Ar_2CH); ^{13}C NMR (CD_3CN , 75.5 MHz): $\delta = 41.5$ (q, NMe), 53.7 (tq, $J_{\text{C,F}} = 33$ Hz, NCH_2CF_3), 116.3 (d, Ar), 125.8 (sq, $J_{\text{C,F}} = 282$ Hz, NCH_2CF_3), 127.0 (s, Ar), 142.0 (d, Ar), 159.3 (s, Ar), 167.1 (d, Ar_2CH); MS (FAB, 70 eV): m/z (%): 389 (100) $[M]^+$, 289 (7), 154 (18), 137 (36), 109 (19); IR (KBr): $\nu = 3433$, 1564, 1502, 1388, 1151, 1085, 980, 829, 754 cm^{-1} ; UV/Vis (CH_2Cl_2): $\lambda_{\text{max}} = 593 \text{ nm}$ ($\epsilon_{\text{max}} = 138000 \text{ [cm}^2 / \text{mmol]}$); Anal. Calcd for $\text{C}_{19}\text{H}_{19}\text{BF}_{10}\text{N}_2$ (476.17): C 47.93, H 4.02, N 5.88. Found: C 47.97, H 3.96, N 5.85.



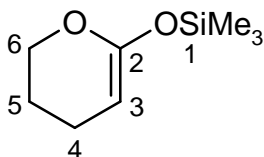
Bis(4-(phenyl(2,2,2-trifluoroethyl)amino)phenyl)methylium tetrafluoroborate (pfa) $_2\text{CH}^+ \text{BF}_4^-$: To a solution of bis(4-(*N*-phenyl-*N*-(2,2,2-trifluoroethyl)amino)phenyl)methanol (**8b**)

(1.50 g, 2.83 mmol) in diethyl ether (100 mL) was slowly added a solution of Et₂O-HBF₄ complex (0.38 mL, 2.8 mmol) in diethyl ether (30 mL). After the addition, stirring was continued for 30 min. Then the blue precipitate was collected by filtration under nitrogen, washed with diethyl ether, and dried in vacuo to furnish bis(4-(*N*-phenyl-*N*-(2,2,2-trifluoroethyl)amino)phenyl)methylmethylm-tetrafluoroborate (pfa)₂CH⁺ BF₄⁻ (1.5 g, 88 %). ¹H NMR (CDCl₃, 300 MHz): δ = 4.62 (q, *J*_{H,F} = 8.3 Hz, 4 H, 2 N-CH₂-CF₃), 6.75-8.00 (m, 18 H, ArH), 8.15 (s, 1 H, 1-H); ¹³C NMR (CD₂Cl₂, 75.5 MHz): δ = 54.8 (tq, *J*_{C,F} = 32.8 Hz, NCH₂CF₃), 127.2, 127.8, 130.0, 130.7, 131.3 (5 d, Ar), 125.3 (sq, *J*_{C,F} = 231 Hz, CF₃), 121.5, 141.8, 159.2 (3 s, Ar), 168.0 (d, Ar₂CH); MS (FAB, 70 eV): *m/z* (%): 513 (100) [M⁺], 430 (8), 264 (18), 165 (10), 109 (12); IR (KBr): ν = 3436, 1555, 1382, 1365, 1133, 1144, 1084, 880, 736 cm⁻¹; UV/Vis (CH₂Cl₂): λ_{max} = 601 nm (ε_{max} = 125000 [cm² / mmol]); Anal. Calcd for C₂₉H₂₃BF₁₀N₂ (600.31): C 58.02, H 3.86, N 4.67. Found: C 58.13, H 3.78, N 4.59.



10.2.2 Synthesis of silyl ketene acetals

2-(Trimethylsiloxy)-5,6-dihydro-4*H*-pyran (9): In a carefully dried, nitrogen-flushed two necked round-bottom flask equipped with a dropping funnel and reflux condensor, a solution of *n*BuLi (1.6 M in hexane) (250 mL, 400 mmol) was added within 1 h at -78 °C to a suspension of diisopropylamine (40.5 g, 400 mmol) in absolute THF (450 mL). After stirring for 0.5 h, a suspension of tetrahydro-pyran-2-one (36.0 g, 360 mmol) in 50 mL THF was added within 1 h at -78 °C. After stirring for 0.25 h chlorotrimethylsilane (73.9 g, 680 mmol) was added rapidly at -78 °C and the reaction-mixture was allowed to warm up to room-temperature within 3 h. The reaction-mixture was concentrated in vacuo up to 100 mL, absolute pentane (100 mL) was added, and the solution was filtered off (using Celite) solid-compounds. The solvent was evaporated in vacuo and the residue is purified by distillation (2 times) to give a colorless oil (49.1 g, 79 %); b.p. 75 °C/11 mbar. ¹H NMR (CDCl₃, 300 MHz): δ = 0.12 (s, 9 H, 1-H), 1.64-1.96 (m, 4 H, 2 × 4-H, 2 × 5-H), 3.72 (t, *J* = 3.7 Hz, 1 H, 3-H), 3.96 (t, *J* = 5.1 Hz, 2 H, 6-H) according to ref. [178]; ¹³C NMR (CDCl₃, 75.5 MHz): δ = -0.2 (q, C-1), 19.7, 22.4 (2 t, C-4, C-5), 66.9 (t, C-6), 73.71 (d, C-3), 154.4 (s, C-2).



BKE007

9

10.2.3 Reactions of nucleophiles with benzhydryl salts

General: All reactions were performed under exclusion of moisture in an atmosphere of dry nitrogen in carefully dried Schlenk glassware using a magnetic stirrer. Dichloromethane was freshly distilled from CaH₂ prior to use, other solvents were dried as described prior in this chapter. The conditions of the reactions were not optimized for high yields.

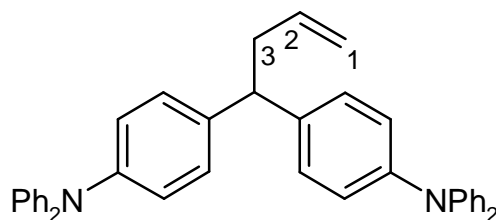
Procedure A: The nucleophile is added to a stirred solution of the carbenium salt Ar₂CH⁺ BF₄⁻ in CH₂Cl₂ at the specified temperature. After fading of the blue color, the reaction mixture is filtered through Al₂O₃ (CH₂Cl₂) on a short column. The solvent is evaporated in vacuo to yield the crude product, which is purified by recrystallization or column chromatography.

Procedure B: The nucleophile is added to a stirred solution of the carbenium salt Ar₂CH⁺ BF₄⁻ in CH₂Cl₂ (60 mL) at the specified temperature under nitrogen. After fading of the color, the reaction mixture is filtered through Al₂O₃ (CH₂Cl₂) on a short column. The solvent is evaporated and the residue is dissolved in hexane. This solution is filtered through Al₂O₃ (hexane) and all stannyl containing substances are washed from the column with a large amount of hexane (300 ml). The product was washed from the column with CH₂Cl₂ and the solvent was evaporated. The products were characterized as described.

4,4-Bis(4-diphenylaminophenyl)-1-butene (12a) was obtained from the tetrafluoroborate salt of (dpa)₂CH⁺ (480 mg, 0.816 mmol) and allyltributylstannane (**12**) (300 μL, 320 mg, 0.966 mmol) at ambient temperature following Procedure B. Recrystallization of residue gave colorless crystals (248 mg, 56 %); mp 138–140 °C (Et₂O/pentane); ¹H NMR (300 MHz, CDCl₃): δ = 2.74 (t, *J* = 7.3 Hz, 2 H, 3-H₂), 3.87 (t, *J* = 7.9 Hz, 1 H, Ar₂CH), 4.88–5.09 (m, 2 H, 1-H₂), 5.60–5.84 (m, 1 H, 2-H), 6.87–7.23 (m, 28 H, ArH); ¹³C NMR (75.5 MHz, CDCl₃): δ = 40.3 (t, C-3), 50.1 (d, Ar₂CH), 116.1 (t, C-1), 122.5, 124.0, 124.0, 128.6, 129.1 (5 d, Ar),

137.0 (d, C-2), 138.9, 145.7, 147.8 (3 s, Ar); MS (EI, 70 eV): m/z (%): 542 (14) [M^+], 502 (100), 251 (15); HRMS calcd for $C_{40}H_{34}N_2$: 542.2722. Found: 542.2723.

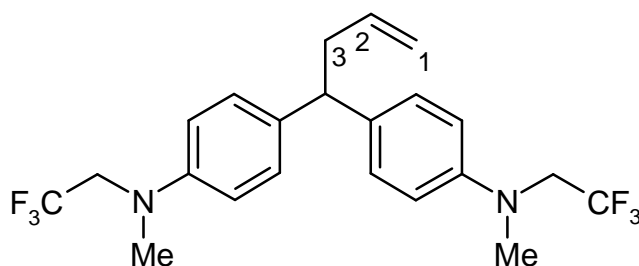
BKE011



12a

4,4-Bis(4-(methyl(2,2,2-trifluoroethyl)amino)phenyl)-1-butene (12b) was obtained from the tetrafluoroborate salt of $(mfa)_2CH^+$ (336 mg, 0.706 mmol) and allyltributylstannane (**12**) (220 μ L, 235 mg, 0.710 mmol) at ambient temperature following Procedure B; colorless powder (242 mg, 80 %). 1H NMR (300 MHz, $CDCl_3$): δ = 2.73 (dd, J = 7.9 Hz, 6.9 Hz, 2 H, 3- H_2), 2.93 (s, 6 H, 2 \times NMe), 3.72 (q, $J_{H,F}$ = 9.1 Hz, 4 H, 2 \times NCH_2CF_3), 3.85 (t, J = 7.9 Hz, 1 H, Ar_2CH), 4.85–5.05 (m, 1- H_2), 5.60–5.80 (m, 1 H, 2- H), 6.60–7.20 (m, 8 H, ArH); ^{13}C NMR (75.5 MHz, $CDCl_3$): δ = 39.0/39.1 (2 q, NMe), 40.2 (t, C-3), 49.2 (d, Ar_2CH), 54.5 (tq, $J_{C,F}$ = 32.6 Hz, NCH_2CF_3), 115.9 (t, C-1), 112.8, 128.5 (2 d, Ar), 125.6 (sq, $J_{C,F}$ = 282.6 Hz, NCH_2CF_3), 137.3 (d, C-2), 134.9, 147.0 (2 s, Ar); MS (EI, 70 eV): m/z (%): 430 (3) [M^+], 389 (100), 305 (10).

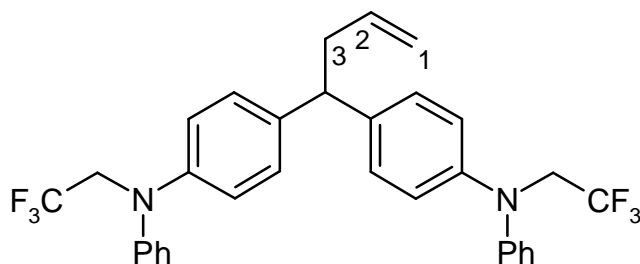
BKE033



12b

4,4-Bis(4-(phenyl(2,2,2-trifluoroethyl)amino)phenyl)-1-butene (12c) was obtained from the tetrafluoroborate salt of $(pfa)_2CH^+$ (0.296 g, 0.493 mmol) and allyltributylstannane (**12**) (160 μ L, 171 mg, 0.516 mmol) at ambient temperature following Procedure B; almost colorless powder (208 mg, 76 %). 1H NMR (300 MHz, $CDCl_3$): δ = 2.76 (dd, J = 8.0 Hz, 6.9 Hz, 2 H, 3- H_2), 3.92 (t, J = 7.9 Hz, 1 H, Ar_2CH), 4.23 (q, $J_{H,F}$ = 8.7 Hz, 4 H, 2 \times NCH_2CF_3), 4.93–5.06 (m, 2 H, 1- H_2), 5.65–5.78 (m, 1 H, 2- H), 6.90–7.27 (m, 18 H, ArH); ^{13}C NMR (75.5 MHz, $CDCl_3$): δ = 40.2 (t, C-3), 49.9 (d, Ar_2CH), 53.9 (tq, $J_{C,F}$ = 33.2 Hz, NCH_2CF_3), 116.3 (t, C-1), 121.0, 121.5, 122.5, 128.9, 129.4 (5 d, Ar), 125.2 (sq, $J_{C,F}$ = 282.9 Hz,

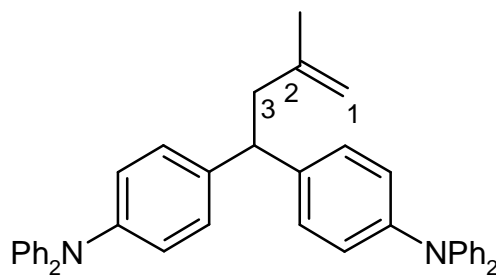
NCH_2CF_3), 136.8 (d, C-2), 139.1, 145.6, 147.5 (3 s, Ar); MS (EI, 70 eV): m/z (%): 554 (3) $[\text{M}]^+$, 513 (100).



BKE025

12c

4,4-Bis(4-diphenylaminophenyl)-2-methyl-1-butene (13a) was obtained from the tetrafluoroborate salt of $(\text{dpa})_2\text{CH}^+$ (482 mg, 0.819 mmol) and trimethyl(2-methylallyl)silane (**13**) (160 μL , 118 mg, 0.920 mmol) at ambient temperature following Procedure A. Recrystallization of the green residue gave almost colorless crystals (343 mg, 75 %); mp 81–83 $^\circ\text{C}$ (Et_2O /pentane). ^1H NMR (300 MHz, CDCl_3): δ = 1.68 (s, 3 H, 2-Me), 2.71 (d, J = 7.7 Hz, 2 H, 3- H_2), 4.05 (t, J = 7.9 Hz, 1 H, Ar_2CH), 4.60, 4.71 (2 s, 2×1 H, 1- H_2), 6.92–7.24 (m, 28 H, ArH); ^{13}C NMR (75.5 MHz, CDCl_3): δ = 22.7 (q, 2-Me), 44.3 (t, C-3), 48.3 (d, Ar_2CH), 112.5 (t, C-1), 122.5, 124.0, 124.0, 128.6, 129.7 (5 d, Ar), 139.3 (s, Ar), 143.5 (s, C-2), 145.7, 147.9 (2 s, Ar); MS (EI, 70 eV): m/z (%): 556 (9) $[\text{M}]^+$, 501 (100), 251 (11); Anal. Calcd for $\text{C}_{41}\text{H}_{36}\text{N}_2$ (556.75): C 88.45, H 6.52, N 5.03. Found: C 88.19, H 6.50, N 4.97.

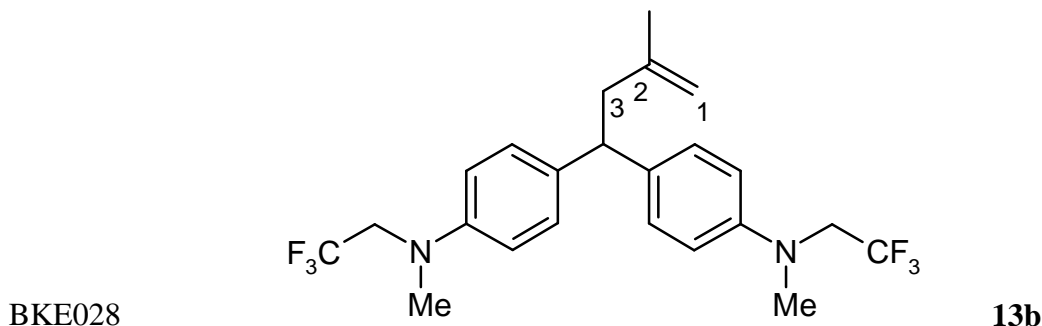


BKE010

13a

4,4-Bis(4-(methyl(2,2,2-trifluoroethyl)amino)phenyl)-2-methyl-1-butene (13b) was obtained from the tetrafluoroborate salt of $(\text{mfa})_2\text{CH}^+$ (295 mg, 0.620 mmol) and trimethyl(2-methylallyl)silane (**13**) (110 μL , 81.0 mg, 0.632 mmol) at ambient temperature following Procedure A. Recrystallization of the brownish residue gave almost colorless crystals (210 mg, 76 %); mp 73–74 $^\circ\text{C}$ (ethanol). ^1H NMR (300 MHz, CDCl_3): δ = 1.67 (s, 3 H, 2-Me), 2.70 (d, J = 8.0 Hz, 2 H, 3- H_2), 2.95 (s, 6 H, $2 \times \text{NMe}$), 3.74 (q, $J_{\text{H,F}}$ = 8.9 Hz, 4 H, $2 \times \text{NCH}_2\text{CF}_3$), 4.03 (t, J = 7.9 Hz, 1 H, Ar_2CH), 4.61, 4.68 (2 s, 2×1 H, 1- H_2), 6.60–7.20 (m, 8 H, ArH); ^{13}C NMR (75.5 MHz, CDCl_3): δ = 22.5 (q, 2-Me), 39.1 (q, NMe), 44.2 (t, C-3), 47.2

(d, Ar₂CH), 54.6 (tq, $J_{C,F} = 32.5$ Hz, NCH₂CF₃), 112.3 (t, C-1), 112.7 (d, Ar), 125.6 (sq, $J_{C,F} = 282.6$ Hz, NCH₂CF₃), 128.5 (d, Ar), 135.1 (s, Ar), 143.8 (s, C-2), 146.9 (s, Ar); MS (EI, 70 eV): m/z (%): 444 (5) [M⁺], 389 (100), 321 (26), 305 (19), 302 (18); Anal. Calcd for C₂₃H₂₆F₆N₂ (444.46): C 62.15, H 5.90, N 6.30. Found: C 61.85, H 5.93, N 6.27.

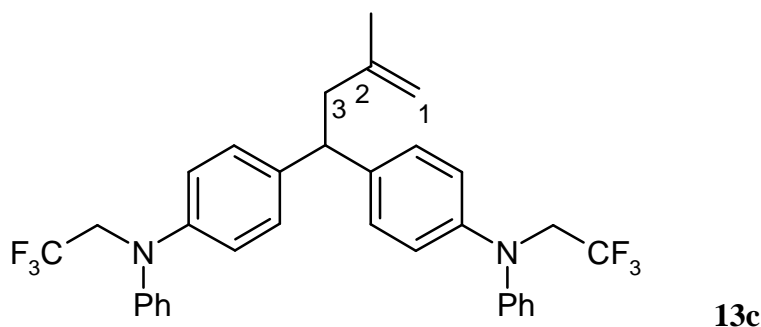


4,4-Bis(4-(phenyl(2,2,2-trifluoroethyl)amino)phenyl)-2-methyl-1-butene (13c) was obtained from the tetrafluoroborate salt of (pfa)₂CH⁺ (375 mg, 0.625 mmol) and trimethyl(2-methylallyl)silane (**13**) (130 μL, 96.0 mg, 0.748 mmol) at ambient temperature following Procedure A; green powder (256 mg, 72 %). ¹H NMR (300 MHz, CDCl₃): δ = 1.67 (s, 3 H, 2-Me), 2.72 (d, $J = 7.8$ Hz, 2 H, 3-H₂), 4.04–4.30 (m, 5 H, Ar₂CH and 2 × NCH₂CF₃), 4.60, 4.70 (2 s, 2 × 1 H, 1-H₂), 6.87–7.27 (m, 18 H, ArH); ¹³C NMR (75.5 MHz, CDCl₃): δ = 22.5 (q, 2-Me), 44.2 (t, C-3), 48.0 (d, Ar₂CH), 53.9 (tq, $J_{C,F} = 33.2$ Hz, NCH₂CF₃), 112.6 (t, C-1), 120.8, 121.5, 122.4 (3 d, Ar), 125.2 (sq, $J_{C,F} = 282.9$ Hz, NCH₂CF₃), 128.9, 129.4 (2 d, Ar), 139.4 (s, Ar), 143.3 (s, C-2), 145.5, 147.5 (2 s, Ar); MS (EI, 70 eV): m/z (%): 568 (3) [M⁺], 513 (100).

The same product **13c** was obtained from the tetrafluoroborate salt of (pfa)₂CH⁺ (369 mg, 0.615 mmol) and tributyl(2-methylallyl)stannane (**14**) (200 μL, 242 mg, 0.701 mmol) at –90 °C following Procedure B. Recrystallization of the pale blue residue gave an almost colorless solid (150 mg, 43 %). The spectral data are identical with those of the same compound obtained from the reaction of (pfa)₂CH⁺ and trimethyl(2-methylallyl)silane (**13**) (see preceding experiment).

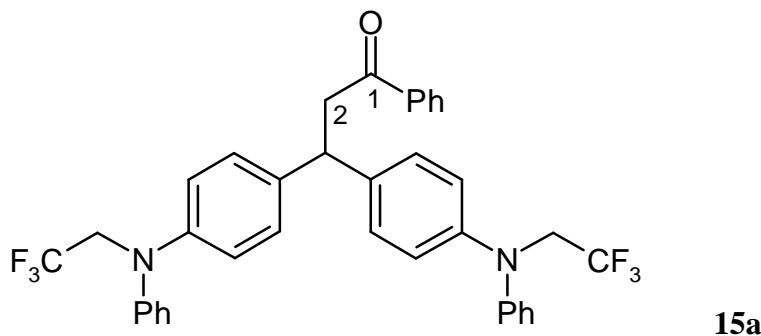
BKE020

BKE024



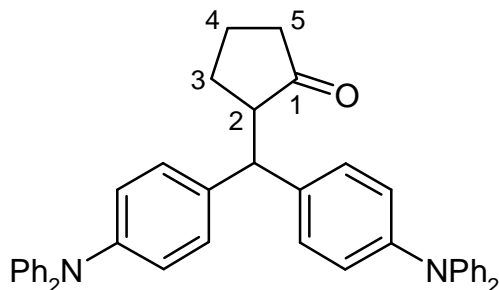
3,3-Bis(4-(phenyl(2,2,2-trifluoroethyl)amino)phenyl)-1-phenyl-1-propanone (15a) was obtained from the tetrafluoroborate salt of $(\text{pfa})_2\text{CH}^+$ (293 mg, 0.488 mmol) and 1-phenyl-1-(trimethylsiloxy)ethene (**15**) (120 μL , 113 mg, 0.585 mmol) at $-90\text{ }^\circ\text{C}$ following Procedure A. Recrystallization of the pale residue gave an almost colorless solid (170 mg, 55 %). ^1H NMR (300 MHz, CDCl_3): $\delta = 3.68$ (d, $J = 7.3$ Hz, 2 H, 2- H_2), 4.24 (q, $J_{\text{H,F}} = 8.7$ Hz, 4 H, $2 \times \text{NCH}_2\text{CF}_3$), 4.74 (t, $J = 7.2$ Hz, 1 H, Ar_2CH), 6.88–7.93 (m, 23 H, ArH and 1-Ph); ^{13}C NMR (75.5 MHz, CDCl_3): $\delta = 44.7$ (d, Ar_2CH), 45.0 (t, C-2), 53.9 (tq, $J_{\text{C,F}} = 33.3$ Hz, NCH_2CF_3), 121.2, 121.3, 122.7 (3 d, Ar and 1-Ph), 125.2 (sq, $J_{\text{C,F}} = 282.9$ Hz, NCH_2CF_3), 128.0, 128.6, 128.8, 129.5, 133.1 (5 d, Ar and 1-Ph), 137.1, 138.5, 145.8, 147.3 (4 s, Ar and 1-Ph), 198.1 (s, C-1); MS (EI, 70 eV), m/z (%): 632 (19) [M^+], 513 (100).

BKE022



2-(Bis(4-diphenylamino)phenyl)methylcyclopentanone (16a) was obtained from the tetrafluoroborate salt of $(\text{dpa})_2\text{CH}^+$ (248 mg, 0.422 mmol) and 1-(trimethylsiloxy)cyclopentene (**16**) (100 μL , 88.0 mg, 0.563 mmol) at $-90\text{ }^\circ\text{C}$ following Procedure A. Recrystallization of the greenish residue gave almost colorless crystals (200 mg, 81 %); mp $91\text{--}92\text{ }^\circ\text{C}$ (Et_2O /Pentane). ^1H NMR (400 MHz, CDCl_3): $\delta = 1.68\text{--}1.88$ (m, 3 H, 3-H, 4- H_2), 1.92–2.02 (m, 1 H, 5-H), 2.14–2.33 (m, 2 H, 3-H, 5-H), 2.83–2.89 (m, 1 H, 2-H), 4.53 (d, $J = 4.9$ Hz, 1 H, Ar_2CH), 6.92–7.30 (m, 28 H, ArH). Signal assignments are based on gHSQC experiments; ^{13}C NMR (75.5 MHz, CDCl_3): $\delta = 20.5$ (t, C-4), 27.3 (t, C-3), 38.4 (t,

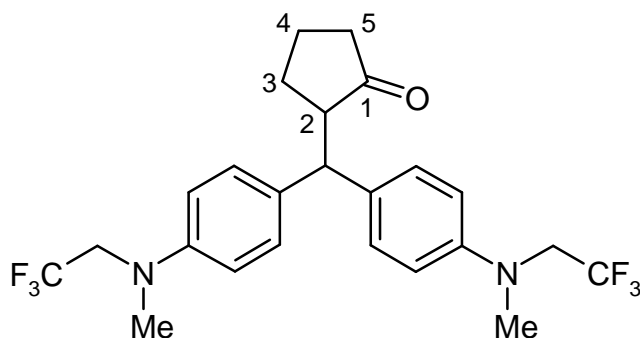
C-5), 48.9 (d, Ar₂CH), 53.4 (d, C-2), 122.6/122.7, 123.4/123.8, 124.1/124.2, 129.1/129.2, 129.1/129.8 (5 × 2 d, Ar), 136.6/137.8, 145.9/146.0, 147.7/147.8 (3 × 2 s, Ar), 219.3 (s, C-1); MS (EI, 70 eV): *m/z* (%): 584 (19) [M⁺], 501 (100), 251 (10), 167 (11), 77 (13); Anal. Calcd for C₄₂H₃₆N₂O (584.76): C 86.27, H 6.21, N 4.79. Found: C 86.08, H 6.20, N 4.81.



BKE009

16a

2-(Bis(4-(methyl(2,2,2-trifluoroethyl)amino)phenyl)methyl)cyclopentanone (16b) was obtained from the tetrafluoroborate salt of (mfa)₂CH⁺ (355 mg, 0.746 mmol) and 1-(trimethylsiloxy)cyclopentene (**16**) (130 μL, 114 mg, 0.730 mmol) at -90 °C following Procedure A. The pale red residue gave after recrystallization (from EtOH) an almost colorless solid (242 mg, 70 %). ¹H NMR (300 MHz, CDCl₃): δ = 1.60–2.35 (m, 6 H, 3-H₂, 4-H₂, 5-H₂), 2.78–2.90 (m, 1 H, 2-H), 2.94/2.97 (2 s, 2 × 3 H, 2 × NMe), 3.69–3.78 (m, 4 H, 2 × NCH₂CF₃), 4.48 (d, *J* = 4.7 Hz, 1 H, Ar₂CH), 6.60–7.20 (m, 8 H, ArH); ¹³C NMR (75.5 MHz, CDCl₃): δ = 20.4 (t, C-4), 27.1 (t, C-3), 38.3 (t, C-5), 38.9/39.0 (2 q, NMe), 48.1 (d, Ar₂CH), 53.2 (d, C-2), 54.3 (tq, *J*_{C,F} = 30.5 Hz, NCH₂CF₃), 112.4/112.5, 128.8/129.4 (2 × 2 d, Ar), 125.5 (sq, *J*_{C,F} = 282.7 Hz, NCH₂CF₃), 132.6/133.5, 146.9/147.0 (2 × 2 s, Ar), 219.5 (s, C-1); MS (EI, 70 eV): *m/z* (%): 472 (19) [M⁺], 389 (100), 321 (13), 305 (14).

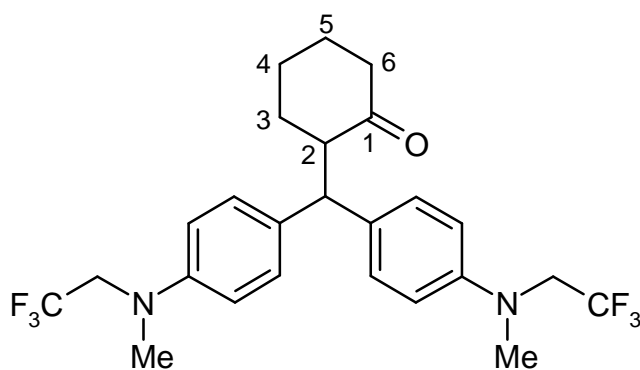


BKE030

16b

2-(Bis(4-(methyl(2,2,2-trifluoroethyl)amino)phenyl)methyl)cyclohexanone (17a) was obtained from the tetrafluoroborate salt of (mfa)₂CH⁺ (315 mg, 0.662 mmol) and 1-(trimethylsiloxy)cyclohexene (**17**) (130 μL, 115 mg, 0.675 mmol) at ambient temperature following Procedure A. Recrystallization of the yellow residue gave colorless crystals (226

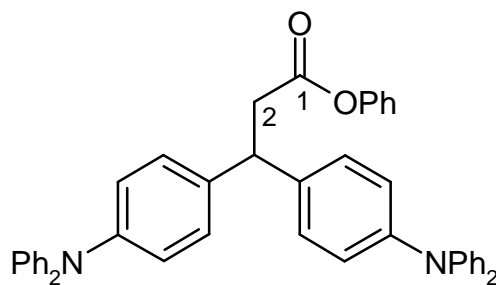
mg, 70 %); mp 113–115 °C (ethanol). ^1H NMR (300 MHz, CDCl_3): δ = 1.23–2.00 (m, 6 H, 4- H_2 , 5- H_2 , 3- H_2), 2.20–2.45 (m, 2 H, 6- H_2), 2.89/2.94 (2 s, 2×3 H, $2 \times \text{NMe}$), 3.15–3.25 (m, 1 H, 2-H), 3.60–3.80 (m, 4 H, $2 \times \text{NCH}_2\text{CF}_3$), 4.17 (d, J = 10.8 Hz, 1 H, Ar_2CH), 6.55–7.20 (m, 8 H, ArH); ^{13}C NMR (75.5 MHz, CDCl_3): δ = 23.9 (t, C-4), 29.0 (t, C-5), 33.02 (t, C-3), 38.8/38.9 (2 q, NMe), 42.0 (t, C-6), 48.9 (d, Ar_2CH), 54.4 (tq, $J_{\text{C,F}}$ = 32.6 Hz, NCH_2CF_3), 55.2 (d, C-2), 112.6/112.7, 128.2/128.8 (2×2 d, Ar), 125.5 (sq, $J_{\text{C,F}}$ = 282.7 Hz, NCH_2CF_3), 133.1/133.9, 146.8/147.0 (2×2 s, Ar), 212.8 (s, C-1); MS (EI, 70 eV): m/z (%): 486 (8) [M^+], 389 (100); Anal. Calcd for $\text{C}_{25}\text{H}_{28}\text{F}_6\text{N}_2\text{O}$ (486.50): C 61.72, H 5.80, N 5.76. Found: C 61.58, H 5.94, N 5.80.



BKE029

17a

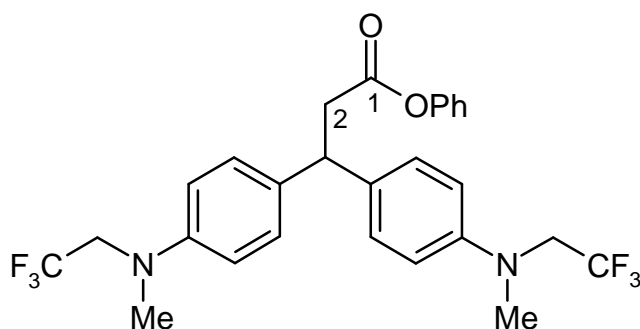
Phenyl 3,3-bis(p-diphenylaminophenyl)propionate (18a) was obtained from the tetrafluoroborate salt of $(\text{dpa})_2\text{CH}^+$ (316 mg, 0.537 mmol) and 1-phenoxy-1-(trimethylsiloxy)ethene (**18**) (200 μL , 197 mg, 0.946 mmol) in CH_2Cl_2 (100 mL) at -90 °C following Procedure A. Recrystallization of the redish residue gave a pale solid (157 mg, 46 %); mp 84–86 °C (Et_2O /pentane). ^1H NMR (300 MHz, CDCl_3): δ = 3.23 (d, J = 8.3 Hz, 2 H, 2- H_2), 4.54 (t, J = 8.2 Hz, 1 H, Ar_2CH), 6.79–7.35 (m, 33 H, ArH and OPh); ^{13}C NMR (75.5 MHz, CDCl_3): δ = 41.3 (t, C-2), 46.4 (d, Ar_2CH), 121.4, 122.7, 124.0, 124.1, 125.8, 128.5, 129.2, 129.3 (8 d, Ar and OPh), 137.2, 146.4, 147.7, 150.6 (4 s, Ar and OPh), 170.5 (s, C-1); MS (EI, 70 eV): m/z (%): 636 (44) [M^+], 501 (100); Anal. Calcd for $\text{C}_{45}\text{H}_{36}\text{N}_2\text{O}_2$ (636.79): C 84.88, H 5.70, N 4.40. Found: C 84.70, H 5.68, N 4.37.



BKE012

18a

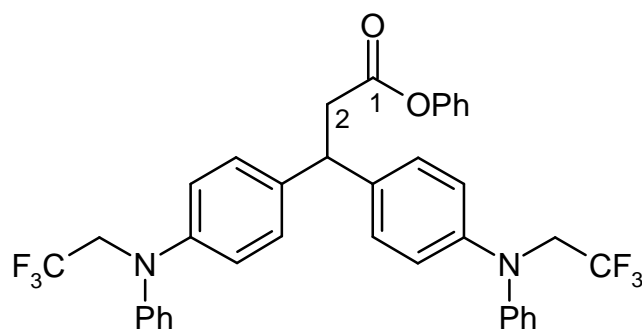
Phenyl 3,3-bis(4-(methyl(2,2,2-trifluoroethyl)amino)phenyl)propionate (18b) was obtained from the tetrafluoroborate salt of $(\text{mfa})_2\text{CH}^+$ (410 mg, 0.861 mmol) and 1-phenoxy-1-(trimethylsiloxy)ethene (**18**) (180 μL , 177 mg, 0.850 mmol) in CH_2Cl_2 (100 mL) at -90°C following Procedure A; yellow powder (285 mg, 64 %). ^1H NMR (300 MHz, CDCl_3): $\delta = 2.94$ (s, 6 H, $2 \times \text{NMe}$), 3.20 (d, $J = 8.4$ Hz, 2 H, 2- H_2), 3.75 (q, $J_{\text{H,F}} = 9.1$ Hz, 4 H, $2 \times \text{NCH}_2\text{CF}_3$), 4.50 (t, $J = 8.2$ Hz, 1 H, Ar_2CH), 6.60–7.20 (m, 13 H, ArH and OPh); ^{13}C NMR (75.5 MHz, CDCl_3): $\delta = 39.0/39.1$ (2 q, NMe), 41.2 (t, C-2), 45.5 (d, Ar_2CH), 54.2 (tq, $J_{\text{C,F}} = 32.6$ Hz, NCH_2CF_3), 112.8, 121.5 (2 d, Ar and OPh), 125.6 (sq, $J_{\text{C,F}} = 283.2$ Hz, NCH_2CF_3), 125.6, 128.3, 129.2 (3 d, Ar and OPh), 133.2, 147.2, 150.6 (3 s, Ar), 170.5 (s, C-1); MS (EI, 70 eV): m/z (%): 524 (26) $[\text{M}^+]$, 389 (100); Anal. Calcd for $\text{C}_{27}\text{H}_{26}\text{F}_6\text{N}_2\text{O}_2$ (524.51): C 61.83, H 5.00, N 5.34. Found: C 61.59, H 5.00, N 5.36.



BKE032

18b

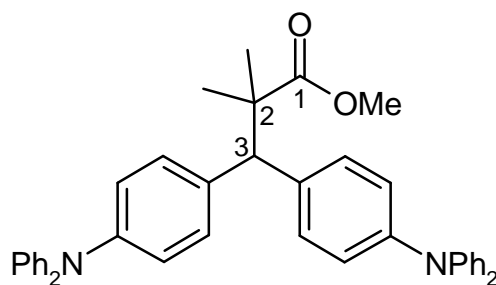
Phenyl 3,3-bis(4-(phenyl(2,2,2-trifluoroethyl)amino)phenyl)propionate (18c) was obtained from the tetrafluoroborate salt of $(\text{pfa})_2\text{CH}^+$ (0.395 g, 0.658 mmol) and 1-phenoxy-1-(trimethylsiloxy)ethene (**18**) (160 μL , 158 mg, 0.758 mmol) in CH_2Cl_2 (100 mL) at -90°C following Procedure A; yellow powder (282 mg, 66 %); ^1H NMR (300 MHz, CDCl_3): $\delta = 3.22$ (d, $J = 8.3$ Hz, 2 H, 2- H_2), 4.23 (q, $J_{\text{H,F}} = 8.7$ Hz, 4 H, $2 \times \text{NCH}_2\text{CF}_3$), 4.57 (t, $J = 8.2$ Hz, 1 H, Ar_2CH), 6.77–7.28 (m, 23 H, ArH and OPh); ^{13}C NMR (75.5 MHz, CDCl_3): $\delta = 41.1$ (t, C-2), 46.1 (d, Ar_2CH), 53.8 (tq, $J_{\text{C,F}} = 33.1$ Hz, NCH_2CF_3), 121.1, 121.4, 121.5, 122.8 (4 d, Ar and OPh), 125.2 (sq, $J_{\text{C,F}} = 282.9$ Hz, NCH_2CF_3), 125.8, 128.7, 129.3, 129.5 (4 d, Ar and OPh), 137.2, 146.1, 147.3, 150.5 (4 s, Ar), 170.3 (s, C-1); MS (EI, 70 eV): m/z (%): 648 (31) $[\text{M}^+]$, 513 (100).



BKE021

18c

Methyl 3,3-bis(4-diphenylaminophenyl)-2,2-dimethylpropionate (19a) was obtained from the tetrafluoroborate salt of $(\text{dpa})_2\text{CH}^+$ (421 mg, 0.716 mmol) and 1-methoxy-2-methyl-1-(trimethylsiloxy)propene (**19**) (170 μL , 146 mg, 0.838 mmol) in CH_2Cl_2 (100 mL) at ambient temperature following Procedure A. Recrystallization of the light yellow residue gave a solid (308 mg, 71 %); mp 177 °C (Et₂O/pentane). ¹H NMR (300 MHz, CDCl₃): δ = 1.28 (s, 6 H, 2-Me₂), 3.52 (s, 3 H, OMe), 4.27 (s, 1 H, Ar₂CH), 6.93–7.21 (m, 28 H, ArH); ¹³C NMR (75.5 MHz, CDCl₃): δ = 24.2 (q, 2-Me₂), 47.0 (s, C-2), 51.6 (q, OMe), 58.3 (d, Ar₂CH), 122.6, 123.1, 124.1, 129.1, 130.4 (5 d, Ar), 135.4, 146.0, 147.7 (3 s, Ar), 177.9 (s, C-1); MS (EI, 70 eV): *m/z* (%): 602 (4) [M⁺], 501 (100), 251 (12), 167 (2); Anal. Calcd for C₄₂H₃₈N₂O₂ (602.78): C 83.69, H 6.35, N 4.65. Found: C 83.56, H 6.12, N 4.64.

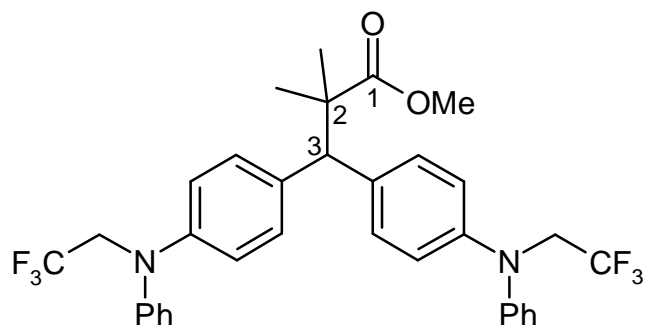


BKE013

19a

Methyl 3,3-bis(4-(phenyl(2,2,2-trifluoroethyl)amino)phenyl)-2,2-dimethylpropionate (19b) was obtained from the tetrafluoroborate salt of $(\text{pfa})_2\text{CH}^+$ (427 mg, 0.711 mmol) and 1-methoxy-2-methyl-1-(trimethylsiloxy)propene (**19**) (160 μL , 138 mg, 0.789 mmol) in CH_2Cl_2 (100 mL) at –90 °C following Procedure A; colorless powder (310 mg, 71 %). ¹H NMR (300 MHz, CDCl₃): δ = 1.28 (s, 6 H, 2-Me₂), 3.50 (s, 3 H, OMe), 4.25 (q, $J_{\text{H,F}}$ = 8.4 Hz, 4 H, 2 × NCH₂CF₃), 4.30 (s, 1 H, Ar₂CH), 6.85–7.29 (m, 18 H, ArH); ¹³C NMR (75.5 MHz, CDCl₃): δ = 24.2 (q, 2-Me₂), 46.8 (s, C-2), 51.6 (q, OMe), 53.8 (tq, $J_{\text{C,F}}$ = 33.2 Hz, NCH₂CF₃), 58.0 (d, Ar₂CH), 120.1, 121.8, 122.9, 129.5, 130.7 (5 d, Ar), 125.2 (sq, $J_{\text{C,F}}$ = 282.9 Hz, NCH₂CF₃),

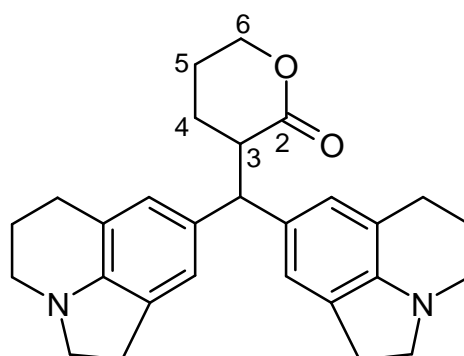
135.4, 145.9, 147.2 (3 s, Ar), 177.9 (s, C-1); MS (EI, 70 eV): m/z (%): 614 (1) [M^+], 513 (100).



BKE023

19b

3-(Bis(lilolidin-8-yl)methyl)tetrahydropyran-2-one (9a) was obtained from the tetrafluoroborate salt of $(\text{lil})_2\text{CH}^+$ (1.02 g, 2.46 mmol) and 2-(trimethylsiloxy)-5,6-dihydro-4*H*-pyran (**9**) (500 μL , 469 mg, 2.72 mmol) in CH_2Cl_2 (100 mL) at ambient temperature following Procedure A. Recrystallization of the yellow residue gave colorless crystals (790 mg, 75 %); mp 95–98 °C (ethanol). ^1H NMR (300 MHz, CDCl_3): δ = 1.48–2.12 (m, 8 H, 4- H_2 , 5- H_2 , 2 \times CH_2), 2.54–2.70 (m, 4 H, 2 \times CH_2), 2.78–2.98 (m, 8 H, 4 \times CH_2), 3.10–3.32 (m, 5 H, 3- H , 2 \times CH_2), 4.14–4.40 (m, 3 H, 6- H_2 , Ar_2CH), 6.62, 6.70, 6.73, 6.83 (4 s, 4 \times 1 H, ArH); ^{13}C NMR (75.5 MHz, CDCl_3): δ = 21.8 (t, C-4), 23.0 (t, C-5), 23.1/23.2 (2 t, CH_2), 23.7/23.8 (2 t, CH_2), 28.6/28.7 (2 t, CH_2), 43.8 (d, C-3), 47.3/47.4 (2 t, CH_2), 50.9 (d, Ar_2CH), 55.1/55.2 (2 t, CH_2), 67.4 (t, C-6), 118.8/118.9 (2 s, Ar), 121.2/121.9, 125.2/126.3 (2 \times 2 d, Ar), 128.5/128.6 (2 s, Ar), 132.9/134.4 (2 s, Ar), 148.1, 148.2 (2 s, Ar), 174.0 (s, C-2); MS (EI, 70 eV): m/z (%): 428 (11) [M^+], 329 (100).

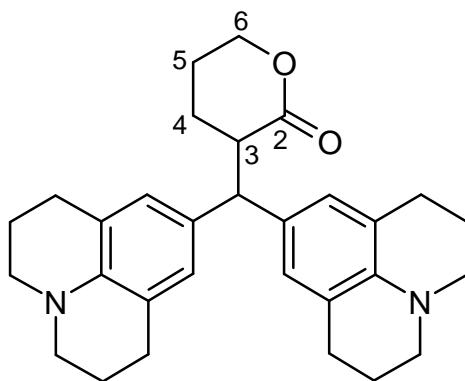


BKE017

9a

3-(Bis(julolidin-9-yl)methyl)tetrahydropyran-2-one (9b) was obtained from the tetrafluoroborate salt of $(\text{jul})_2\text{CH}^+$ (469 mg, 1.06 mmol) and 2-(trimethylsiloxy)-5,6-dihydro-4*H*-pyran (**9**) (200 μL , 188 mg, 1.09 mmol) in CH_2Cl_2 (100 mL) at ambient temperature following Procedure A; colorless powder (415 mg, 86 %). ^1H NMR (300 MHz, CDCl_3): δ =

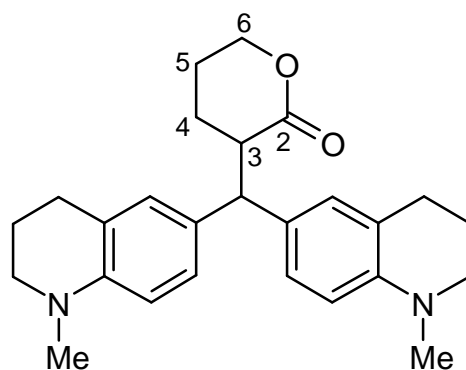
1.45–2.10 (m, 12 H, 4-H₂, 5-H₂, 4 × CH₂), 2.66–2.72 (m, 8 H, 4 × CH₂), 3.04–3.35 (m, 9 H, 3-H, 4 × CH₂), 4.15–4.45 (m, 3 H, 6-H₂, Ar₂CH), 6.65, 6.57 (2 s, 2 × 2 H, ArH); ¹³C NMR (75.5 MHz, CDCl₃): δ = 22.2/22.3 (2 t, CH₂), 23.0 (t, C-4), 27.6/27.7 (2 t, CH₂), 29.6 (t, C-5), 43.9 (d, C-3), 49.8 (d, Ar₂CH), 50.0 (t, CH₂), 67.7 (t, C-6), 121.2/121.3 (2 s, Ar), 126.2/127.1 (2 d, Ar), 129.6/131.2, 141.2/141.2 (2 × 2 s, Ar), 174.1 (s, C-2); MS (EI, 70 eV): *m/z* (%): 456 (15) [M⁺], 357 (100).



BKE016

9b

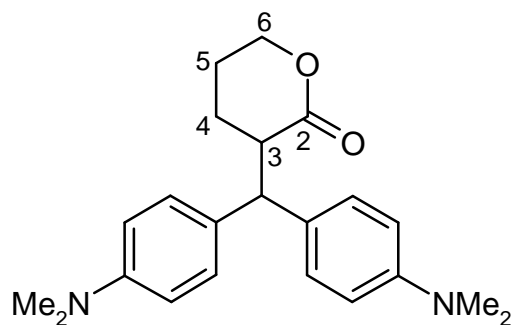
3-(Bis(N-methyl-1,2,3,4-tetrahydroquinolin-6-yl)methyl)tetrahydropyran-2-one (9c) was obtained from the tetrafluoroborate salt of (thq)₂CH⁺ (588 mg, 1.50 mmol) and 2-(trimethylsiloxy)-5,6-dihydro-4*H*-pyran (**9**) (280 μL, 263 mg, 1.53 mmol) in CH₂Cl₂ (100 mL) at –90 °C following Procedure A. Recrystallization of the orange residue gave colorless crystals (394 mg, 65 %); mp 84–86 °C (Et₂O/Pentane). ¹H NMR (300 MHz, CDCl₃): δ = 1.54–2.04 (m, 8 H, 4-H₂, 5-H₂, 2 × CH₂), 2.62–2.76 (m, 4 H, 2 × CH₂), 2.82 (s, 6 H, 2 × NMe), 3.08–3.32 (m, 5 H, 3-H, 2 × CH₂), 4.14–4.40 (m, 3 H, 6-H₂, Ar₂CH), 6.42–7.00 (m, 6 H, ArH); ¹³C NMR (75.5 MHz, CDCl₃): δ = 22.0 (t, C-4), 22.4/22.5 (2 t, CH₂), 22.9 (t, C-5), 27.8/27.9 (2 t, CH₂), 39.0/39.1 (2 q, NMe), 43.9 (d, C-3), 49.6 (d, Ar₂CH), 51.2/51.2 (2 t, CH₂), 67.7 (t, C-6), 110.7/110.8 (2 d, Ar), 122.5/122.6 (2 s, Ar), 125.9/127.1, 128.6/129.2 (2 × 2 d, Ar), 129.9/131.4, 145.0/145.1 (2 × 2 s, Ar), 173.9 (s, C-2); MS (EI, 70 eV): *m/z* (%): 404 (8) [M⁺], 305 (100); Anal. Calcd for C₂₆H₃₂N₂O₂ (404.55): C 77.19, H 7.97, N 6.92. Found: C 76.90, H 8.05, N 6.88.



BKE026

9c

3-(Bis(4-dimethylaminophenyl)methyl)tetrahydropyran-2-one (9d) was obtained from the tetrafluoroborate salt of $(dma)_2CH^+$ (924 mg, 2.72 mmol) and 2-(trimethylsiloxy)-5,6-dihydro-4*H*-pyran (**9**) (500 μ L, 469 mg, 2.72 mmol) in CH_2Cl_2 (100 mL) at -90 °C following Procedure A. Recrystallization of the yellow residue gave almost colorless crystals (680 mg, 71 %); mp 95 – 98 °C (ethanol). 1H NMR (300 MHz, $CDCl_3$): δ = 1.60–2.00 (m, 4 H, 4- H_2 , 5- H_2), 2.84 (s, 12 H, $2 \times NMe_2$), 3.20–3.35 (m, 1 H, 3- H), 4.03–4.28 (m, 2 H, 6- H_2), 4.47 (d, J = 7.1 Hz, 1 H, Ar_2CH), 6.55–7.20 (m, 8 H, ArH); ^{13}C NMR (75.5 MHz, $CDCl_3$): δ = 21.7 (t, C-4), 22.6 (t, C-5), 40.2 (q, NMe_2), 43.6 (d, C-3), 49.3 (d, Ar_2CH), 67.5 (t, C-6), 112.2/112.3, 128.1/129.1 (2×2 d, Ar), 129.9/131.4, 148.6/148.7 (2×2 s, Ar), 173.5 (s, C-2); MS (EI, 70 eV), m/z (%): 352 (9) [M^+], 253 (100), 237 (12).



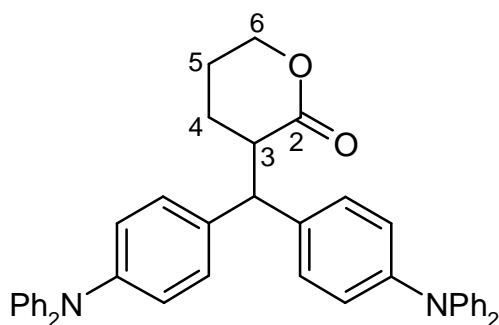
BKE018

9d

3-(Bis(4-diphenylaminophenyl)methyl)tetrahydropyran-2-one (9e) was obtained from the tetrafluoroborate salt of $(dpa)_2CH^+$ (310 mg, 0.527 mmol) and 2-(trimethylsiloxy)-5,6-dihydro-4*H*-pyran (**9**) (120 μ L, 113 mg, 0.655 mmol) in CH_2Cl_2 (100 mL) at -90 °C following Procedure A. Recrystallization of the pale blue residue gave almost colorless crystals (151 mg, 48 %); mp 111 – 112 °C (ethanol). 1H NMR (300 MHz, $CDCl_3$): δ = 1.45–2.05 (m, 4 H, 4- H_2 , 5- H_2), 3.18–3.40 (m, 1 H, 3- H), 4.16–4.45 (m, 2 H, 6- H_2), 4.50 (d, J = 7.8 Hz, 1 H, Ar_2CH), 6.96–7.23 (m, 28 H, ArH); ^{13}C NMR (75.5 MHz, $CDCl_3$): δ = 22.0 (t, C-4), 23.0 (t, C-5), 43.6 (d, C-3), 50.3 (d, Ar_2CH), 67.6 (t, C-6), 122.6/122.7, 123.5/123.7,

124.1/124.2, 129.1/129.2, 128.6, 129.4 (5×2 d, Ar), 135.7/137.3, 145.9/146.2, 147.6/147.7 (3×2 s, Ar), 173.4 (s, C-2); MS (EI, 70 eV): m/z (%): 600 (10) [M^+], 501 (100); Anal. Calcd for $C_{42}H_{36}N_2O_2$ (600.76): C 83.97, H 6.04, N 4.66. Found: C 83.83, H 6.03, N 4.63.

BKE014

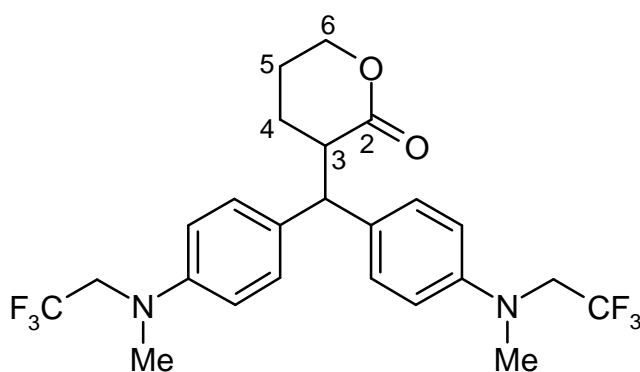


9e

3-(Bis(4-(methyl(2,2,2-trifluoroethyl)amino)phenyl)methyl)tetrahydropyran-2-one (9f)

was obtained from the tetrafluoroborate salt of $(mfa)_2CH^+$ (398 mg, 0.836 mmol) and 2-(trimethylsiloxy)-5,6-dihydro-4*H*-pyran (**9**) (150 μ L, 141 mg, 0.818 mmol) in CH_2Cl_2 (100 mL) at -90 °C following Procedure A; almost colorless solid (203 mg, 51 %). 1H NMR (300 MHz, $CDCl_3$): δ = 1.46–1.96 (m, 4 H, 4- H_2 , 5- H_2), 2.95 (s, 6 H, $2 \times NMe$), 3.22–3.36 (m, 1 H, 3-H), 3.66–3.84 (m, 4 H, $2 \times NCH_2CF_3$), 4.12–4.34 (m, 2 H, 6- H_2), 4.45 (d, J = 7.5 Hz, 1 H, Ar_2CH), 6.62–7.22 (m, 8 H, ArH); ^{13}C NMR (75.5 MHz, $CDCl_3$): δ = 21.8 (t, C-4), 22.9 (t, C-5), 38.9/39.0 (2 q, NMe), 43.5 (d, C-3), 49.5 (d, Ar_2CH), 54.3 (tq, $J_{C,F}$ = 32.3 Hz, NCH_2CF_3), 67.6 (t, C-6), 112.6 (d, Ar), 125.5 (sq, $J_{C,F}$ = 282.9 Hz, NCH_2CF_3), 128.4/129.4 (2 d, Ar), 131.7/133.1, 146.9/147.1 (2×2 s, Ar), 173.6 (s, C-2); MS (EI, 70 eV), m/z (%): 488 (8) [M^+], 389 (100).

BKE031



9f

10.2.4 Concentrations and rate constants of the individual kinetic runs

Table 10.1: Bis(4-bis(2,2,2-trifluoroethyl)aminophenyl)methylm tetrafluoroborate ($(\text{bfa})_2\text{CH}^+ \text{BF}_4^-$) and allyltrimethylsilane (**10**) in CH_2Cl_2 at $\lambda = 600 \text{ nm}$ (Schölly).

No.	$[\text{El}]_0 /$ mol L^{-1}	$[\text{Nuc}]_0 /$ mol L^{-1}	$[\text{Nuc}]_0/[\text{El}]_0$	Conv. / %	$T /$ $^\circ\text{C}$	$k_2 /$ $\text{L mol}^{-1} \text{ s}^{-1}$
160820.PA0	4.745×10^{-5}	3.625×10^{-3}	76	79	20.0	1.727
160820.PA2	4.294×10^{-5}	1.969×10^{-3}	46	70	20.0	1.816

$$\bar{k}_2 (20 \text{ }^\circ\text{C}) = 1.772 \pm 0.045 \text{ L mol}^{-1} \text{ s}^{-1}$$

Table 10.2: Bis(4-(methyl(2,2,2-trifluoroethyl)amino)phenyl)methylm tetrafluoroborate ($(\text{mfa})_2\text{CH}^+ \text{BF}_4^-$) and allyltriphenylstannane (**11**) in CH_2Cl_2 at $\lambda = 593 \text{ nm}$ (J&M).

No.	$[\text{El}]_0 /$ mol L^{-1}	$[\text{Nuc}]_0 /$ mol L^{-1}	$[\text{Nuc}]_0/[\text{El}]_0$	Conv. / %	$T /$ $^\circ\text{C}$	$k_2 /$ $\text{L mol}^{-1} \text{ s}^{-1}$
040720-04	1.571×10^{-5}	8.442×10^{-4}	54	---	20.0	2.221×10^{-1}
040720-01	1.375×10^{-5}	1.320×10^{-3}	96	---	20.0	2.226×10^{-1}
040720-03	1.466×10^{-5}	2.814×10^{-3}	192	---	20.0	2.309×10^{-1}
040720-02	2.101×10^{-5}	4.839×10^{-3}	230	---	20.0	2.215×10^{-1}

$$\bar{k}_2 (20 \text{ }^\circ\text{C}) = (2.243 \pm 0.039) \times 10^{-1} \text{ L mol}^{-1} \text{ s}^{-1}$$

Table 10.3: Bis(4-(phenyl(2,2,2-trifluoroethyl)amino)phenyl)methylm tetrafluoroborate ($(\text{pfa})_2\text{CH}^+ \text{BF}_4^-$) and allyltriphenylstannane (**11**) in CH_2Cl_2 at $\lambda = 601 \text{ nm}$ (J&M).

No.	$[\text{El}]_0 /$ mol L^{-1}	$[\text{Nuc}]_0 /$ mol L^{-1}	$[\text{Nuc}]_0/[\text{El}]_0$	Conv. / %	$T /$ $^\circ\text{C}$	$k_2 /$ $\text{L mol}^{-1} \text{ s}^{-1}$
120720-01	2.105×10^{-5}	1.168×10^{-3}	55	97	20.0	1.074
120720-05	2.337×10^{-5}	1.946×10^{-3}	83	98	20.0	1.102
120720-04	1.979×10^{-5}	2.196×10^{-3}	111	99	20.0	1.087
120720-03	1.196×10^{-5}	1.659×10^{-3}	139	96	20.0	1.056
120720-02	1.349×10^{-5}	2.495×10^{-3}	185	96	20.0	1.030

$$\bar{k}_2 (20\text{ }^\circ\text{C}) = 1.070 \pm 0.025\text{ L mol}^{-1}\text{ s}^{-1}$$

Table 10.4: Bis(4-diphenylaminophenyl)methylium tetrafluoroborate (dpa)₂CH⁺ BF₄⁻ and allyltributylstannane (**12**) in CH₂Cl₂ at λ = 672 nm (J&M).

No.	[<i>El</i>] ₀ / mol L ⁻¹	[<i>Nuc</i>] ₀ / mol L ⁻¹	[<i>Nuc</i>] ₀ /[<i>El</i>] ₀	Conv. / %	<i>T</i> / °C	<i>k</i> ₂ / L mol ⁻¹ s ⁻¹
100720-09	2.668 × 10 ⁻⁵	8.574 × 10 ⁻⁴	32	95	20.0	6.393
100720-10	2.549 × 10 ⁻⁵	1.024 × 10 ⁻³	40	99	20.0	6.374
100720-07	2.668 × 10 ⁻⁵	1.715 × 10 ⁻³	64	97	20.0	6.351
100720-08	2.388 × 10 ⁻⁵	1.919 × 10 ⁻³	80	97	20.0	6.419
100720-11	2.339 × 10 ⁻⁵	3.008 × 10 ⁻³	129	100	20.0	6.474

$$\bar{k}_2 (20\text{ }^\circ\text{C}) = 6.402 \pm 0.042\text{ L mol}^{-1}\text{ s}^{-1}$$

Table 10.5: Bis(4-(methyl(2,2,2-trifluoroethyl)amino)phenyl)methylium tetrafluoroborate (mfa)₂CH⁺ BF₄⁻ and allyltributylstannane (**12**) in CH₂Cl₂ at λ = 593 nm (J&M).

No.	[<i>El</i>] ₀ / mol L ⁻¹	[<i>Nuc</i>] ₀ / mol L ⁻¹	[<i>Nuc</i>] ₀ /[<i>El</i>] ₀	Conv. / %	<i>T</i> / °C	<i>k</i> ₂ / L mol ⁻¹ s ⁻¹
100720-05	1.608 × 10 ⁻⁵	3.740 × 10 ⁻⁴	23	---	20.0	2.749 × 10 ¹
100720-06	1.104 × 10 ⁻⁵	4.812 × 10 ⁻⁴	44	---	20.0	2.881 × 10 ¹
100720-02	1.427 × 10 ⁻⁵	8.295 × 10 ⁻⁴	58	---	20.0	2.892 × 10 ¹
100720-03	1.623 × 10 ⁻⁵	1.321 × 10 ⁻³	81	---	20.0	2.845 × 10 ¹
100720-01	1.708 × 10 ⁻⁵	1.986 × 10 ⁻³	116	---	20.0	2.821 × 10 ¹

$$\bar{k}_2 (20\text{ }^\circ\text{C}) = (2.838 \pm 0.051) \times 10^1\text{ L mol}^{-1}\text{ s}^{-1}$$

Table 10.6: Bis(4-(phenyl(2,2,2-trifluoroethyl)amino)phenyl)methylium tetrafluoroborate (pfa)₂CH⁺ BF₄⁻ and allyltributylstannane (**12**) in CH₂Cl₂ at λ = 600 nm (Schölly).

No.	[<i>El</i>] ₀ / mol L ⁻¹	[<i>Nuc</i>] ₀ / mol L ⁻¹	[<i>Nuc</i>] ₀ /[<i>El</i>] ₀	Conv. / %	<i>T</i> / °C	<i>k</i> ₂ / L mol ⁻¹ s ⁻¹
010820.PA3	2.417 × 10 ⁻⁵	3.613 × 10 ⁻⁴	15	78	20.0	1.088 × 10 ²
010820.PA1	2.263 × 10 ⁻⁵	6.766 × 10 ⁻⁴	30	83	20.0	1.184 × 10 ²
010820.PA2	2.405 × 10 ⁻⁵	1.079 × 10 ⁻³	45	73	20.0	1.125 × 10 ²
010820.PA0	2.899 × 10 ⁻⁵	2.167 × 10 ⁻³	75	46	20.0	1.135 × 10 ²

$$\bar{k}_2(20\text{ °C}) = (1.133 \pm 0.034) \times 10^2 \text{ L mol}^{-1} \text{ s}^{-1}$$

Table 10.7: Bis(4-diphenylaminophenyl)methylium tetrafluoroborate (dpa)₂CH⁺ BF₄⁻ and (2-methylallyl)trimethylsilane (**13**) in CH₂Cl₂ at λ = 640 nm (Schölly).

No.	[<i>El</i>] ₀ / mol L ⁻¹	[<i>Nuc</i>] ₀ / mol L ⁻¹	[<i>Nuc</i>] ₀ /[<i>El</i>] ₀	Conv. / %	<i>T</i> / °C	<i>k</i> ₂ / L mol ⁻¹ s ⁻¹
050620.PA2	7.039 × 10 ⁻⁵	2.432 × 10 ⁻³	35	88	20.0	6.315 × 10 ⁻¹
050620.PA4	8.444 × 10 ⁻⁵	4.376 × 10 ⁻³	52	57	20.0	5.931 × 10 ⁻¹
050620.PA0	7.502 × 10 ⁻⁵	5.184 × 10 ⁻³	70	78	20.0	6.163 × 10 ⁻¹
050620.PA3	6.760 × 10 ⁻⁵	7.007 × 10 ⁻³	104	79	20.0	5.959 × 10 ⁻¹
050620.PA1	6.834 × 10 ⁻⁵	9.444 × 10 ⁻³	140	82	20.0	6.263 × 10 ⁻¹

$$\bar{k}_2(20\text{ °C}) = (6.126 \pm 0.156) \times 10^{-1} \text{ L mol}^{-1} \text{ s}^{-1}$$

Table 10.8: Bis(4-(methyl(2,2,2-trifluoroethyl)amino)phenyl)methylium tetrafluoroborate ($(\text{mfa})_2\text{CH}^+ \text{BF}_4^-$) and (2-methylallyl)trimethylsilane (**13**) in CH_2Cl_2 at $\lambda = 593 \text{ nm}$ (J&M).

No.	$[\text{El}]_0 /$ mol L^{-1}	$[\text{Nuc}]_0 /$ mol L^{-1}	$[\text{Nuc}]_0/[\text{El}]_0$	Conv. / %	$T /$ $^\circ\text{C}$	$k_2 /$ $\text{L mol}^{-1} \text{ s}^{-1}$
030720-13	2.187×10^{-5}	6.138×10^{-4}	28	---	20.0	2.879
030720-12	2.672×10^{-5}	1.500×10^{-3}	56	---	20.0	2.851
030720-15	2.905×10^{-5}	2.283×10^{-3}	79	---	20.0	2.881
030720-11	1.964×10^{-5}	2.205×10^{-3}	112	---	20.0	2.956
030720-16	1.514×10^{-5}	1.785×10^{-3}	118	---	20.0	3.104
030720-14	1.380×10^{-5}	2.323×10^{-3}	168	---	20.0	3.147

$$\bar{k}_2 (20 \text{ }^\circ\text{C}) = 2.970 \pm 0.115 \text{ L mol}^{-1} \text{ s}^{-1}$$

Table 10.9: Bis(4-(phenyl(2,2,2-trifluoroethyl)amino)phenyl)methylium tetrafluoroborate ($(\text{pfa})_2\text{CH}^+ \text{BF}_4^-$) and (2-methylallyl)trimethylsilane (**13**) in CH_2Cl_2 at $\lambda = 601 \text{ nm}$ (J&M).

No.	$[\text{El}]_0 /$ mol L^{-1}	$[\text{Nuc}]_0 /$ mol L^{-1}	$[\text{Nuc}]_0/[\text{El}]_0$	Conv. / %	$T /$ $^\circ\text{C}$	$k_2 /$ $\text{L mol}^{-1} \text{ s}^{-1}$
170720-03	1.990×10^{-5}	6.991×10^{-4}	35	98	20.0	1.328×10^1
170720-04	1.396×10^{-5}	7.358×10^{-4}	53	97	20.0	1.353×10^1
170720-02	2.092×10^{-5}	1.470×10^{-3}	70	98	20.0	1.342×10^1
170720-05	1.269×10^{-5}	1.114×10^{-3}	88	97	20.0	1.365×10^1
170720-01	1.106×10^{-5}	1.296×10^{-3}	117	98	20.0	1.348×10^1

$$\bar{k}_2 (20 \text{ }^\circ\text{C}) = (1.347 \pm 0.012) \times 10^1 \text{ L mol}^{-1} \text{ s}^{-1}$$

Table 8.10: Bis(4-(methyl(2,2,2-trifluoroethyl)amino)phenyl)methylium tetrafluoroborate (mfa)₂CH⁺ BF₄⁻ and tributyl(2-methylallyl)stannane (**14**) in CH₂Cl₂ at λ = 593 nm (Stopped flow).

No.	[<i>El</i>] ₀ / mol L ⁻¹	[<i>Nuc</i>] ₀ / mol L ⁻¹	[<i>Nuc</i>] ₀ /[<i>El</i>] ₀	<i>T</i> / °C	<i>k</i> ₂ / L mol ⁻¹ s ⁻¹
110720-F	5.494 × 10 ⁻⁶	1.230 × 10 ⁻⁴	22	20.0	1.794 × 10 ³
110720-B	5.494 × 10 ⁻⁶	2.459 × 10 ⁻⁴	45	20.0	1.792 × 10 ³
110720-C	5.494 × 10 ⁻⁶	3.689 × 10 ⁻⁴	67	20.0	1.797 × 10 ³
110720-D	5.494 × 10 ⁻⁶	4.919 × 10 ⁻⁴	90	20.0	1.810 × 10 ³
110720-E	5.494 × 10 ⁻⁶	6.148 × 10 ⁻⁴	112	20.0	1.818 × 10 ³

$$\bar{k}_2(20\text{ }^\circ\text{C}) = (1.802 \pm 0.010) \times 10^3 \text{ L mol}^{-1} \text{ s}^{-1}$$

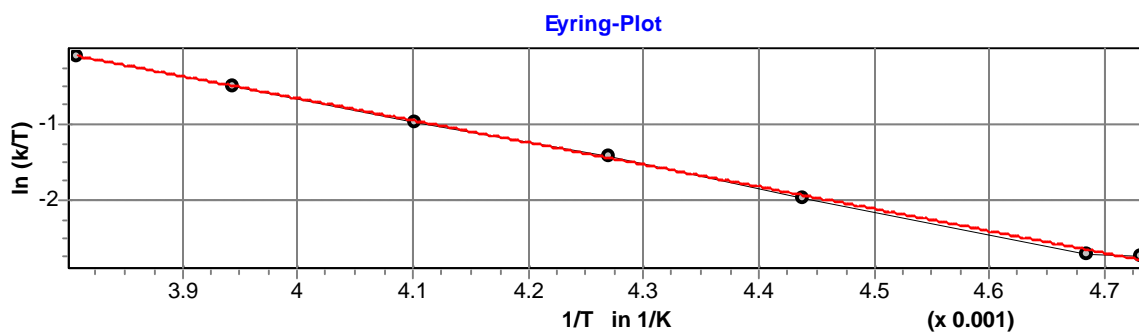
Table 8.11: Bis(4-(phenyl(2,2,2-trifluoroethyl)amino)phenyl)methylium tetrafluoroborate (pfa)₂CH⁺ BF₄⁻ and tributyl(2-methylallyl)stannane (**14**) in CH₂Cl₂ at λ = 601 nm (Stopped flow).

No.	[<i>El</i>] ₀ / mol L ⁻¹	[<i>Nuc</i>] ₀ / mol L ⁻¹	[<i>Nuc</i>] ₀ /[<i>El</i>] ₀	<i>T</i> / °C	<i>k</i> ₂ / L mol ⁻¹ s ⁻¹
130720-A	1.339 × 10 ⁻⁵	1.643 × 10 ⁻⁴	12	20.0	6.827 × 10 ³
130720-B	1.339 × 10 ⁻⁵	3.287 × 10 ⁻⁴	25	20.0	6.865 × 10 ³
130720-C	1.339 × 10 ⁻⁵	4.930 × 10 ⁻⁴	37	20.0	6.968 × 10 ³
130720-D	1.339 × 10 ⁻⁵	6.574 × 10 ⁻⁴	49	20.0	6.990 × 10 ³
130720-E	1.339 × 10 ⁻⁵	8.217 × 10 ⁻⁴	61	20.0	7.007 × 10 ³

$$\bar{k}_2(20\text{ }^\circ\text{C}) = (6.931 \pm 0.072) \times 10^3 \text{ L mol}^{-1} \text{ s}^{-1}$$

Table 10.12: Bis(4-(phenyl(2,2,2-trifluoroethyl)amino)phenyl)methylm tetrafluoroborate (pfa)₂CH⁺ BF₄⁻ and 1-phenyl-1-(trimethylsiloxy)ethene (**15**) in CH₂Cl₂ at λ = 601 nm (J&M).

No.	[<i>EL</i>] ₀ / mol L ⁻¹	[<i>Nuc</i>] ₀ / mol L ⁻¹	[<i>Nuc</i>] ₀ /[<i>EL</i>] ₀	Conv. / %	<i>T</i> / °C	<i>k</i> ₂ / L mol ⁻¹ s ⁻¹
240720-01	1.721 × 10 ⁻⁵	2.157 × 10 ⁻³	125	98	-61.8	1.351 × 10 ¹
240720-02	1.519 × 10 ⁻⁵	2.379 × 10 ⁻³	157	98	-59.7	1.420 × 10 ¹
240720-03	1.322 × 10 ⁻⁵	1.657 × 10 ⁻³	125	98	-47.8	3.124 × 10 ¹
240720-04	1.656 × 10 ⁻⁵	1.453 × 10 ⁻³	88	99	-39.0	5.651 × 10 ¹
240720-05	1.881 × 10 ⁻⁵	1.179 × 10 ⁻³	63	98	-29.4	9.211 × 10 ¹
240720-06	1.437 × 10 ⁻⁵	5.402 × 10 ⁻⁴	38	99	-19.6	1.542 × 10 ²
240720-07	1.521 × 10 ⁻⁵	3.813 × 10 ⁻⁴	25	98	-10.6	2.358 × 10 ²



Eyring parameters:

$$\Delta H^\ddagger = 24.283 \pm 0.357 \text{ kJ mol}^{-1}$$

$$\Delta S^\ddagger = -105.949 \pm 1.533 \text{ J mol}^{-1} \text{ K}^{-1}$$

$$r^2 = 0.9989$$

Arrhenius parameters:

$$E_a = 26.228 \pm 0.360 \text{ kJ mol}^{-1}$$

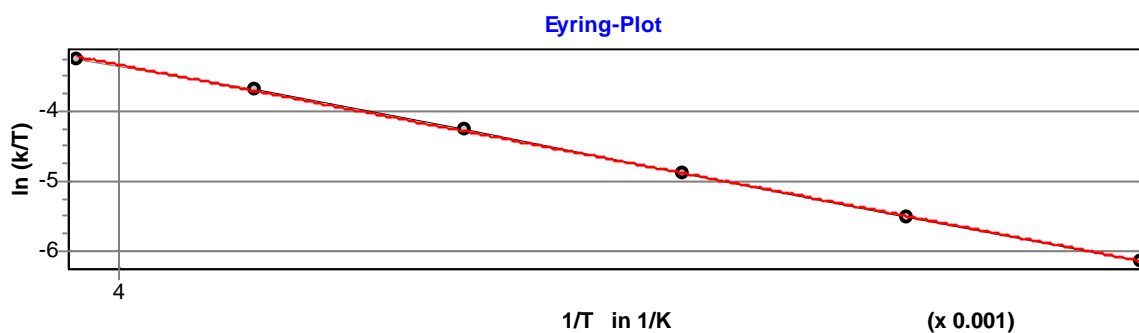
$$\ln A = 17.475 \pm 0.186$$

$$r^2 = 0.9991$$

$$k_2 (20 \text{ }^\circ\text{C}) = (8.418 \pm 0.032) \times 10^2 \text{ L mol}^{-1} \text{ s}^{-1}$$

Table 10.13: Bis(4-diphenylaminophenyl)methylm tetrafluoroborate (dpa)₂CH⁺ BF₄⁻ and 1-(trimethylsiloxy)cyclopentene (**16**) in CH₂Cl₂ at λ = 640 nm (Schölly).

No.	[<i>El</i>] ₀ / mol L ⁻¹	[<i>Nuc</i>] ₀ / mol L ⁻¹	[<i>Nuc</i>] ₀ /[<i>El</i>] ₀	Conv. / %	<i>T</i> / °C	<i>k</i> ₂ / L mol ⁻¹ s ⁻¹
060620.PA0	4.562 × 10 ⁻⁵	5.606 × 10 ⁻³	123	88	-71.4	4.361 × 10 ⁻¹
060620.PA1	4.985 × 10 ⁻⁵	4.900 × 10 ⁻³	98	88	-62.1	8.391 × 10 ⁻¹
060620.PA2	4.176 × 10 ⁻⁵	2.565 × 10 ⁻³	64	87	-52.3	1.661
060620.PA3	4.495 × 10 ⁻⁵	5.524 × 10 ⁻³	123	81	-41.9	3.244
060620.PA4	4.240 × 10 ⁻⁵	3.647 × 10 ⁻³	82	87	-30.9	5.963
060620.PA5	4.662 × 10 ⁻⁵	2.864 × 10 ⁻³	61	80	-20.7	9.764



Eyring parameters:

$$\Delta H^\ddagger = 24.337 \pm 0.220 \text{ kJ mol}^{-1}$$

$$\Delta S^\ddagger = -128.004 \pm 0.979 \text{ J mol}^{-1} \text{ K}^{-1}$$

$$r^2 = 0.9997$$

Arrhenius parameters:

$$E_a = 26.209 \pm 0.210 \text{ kJ mol}^{-1}$$

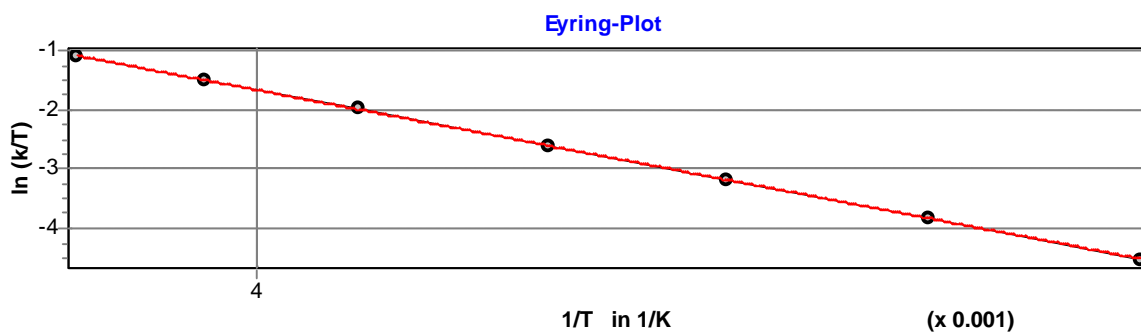
$$\ln A = 14.784 \pm 0.113$$

$$r^2 = 0.9997$$

$$k_2 (20 \text{ }^\circ\text{C}) = (5.800 \pm 0.158) \times 10^1 \text{ L mol}^{-1} \text{ s}^{-1}$$

Table 10.14: Bis(4-(methyl(2,2,2-trifluoroethyl)amino)phenyl)methylmethyl tetrafluoroborate ($(\text{mfa})_2\text{CH}^+ \text{BF}_4^-$) and 1-(trimethylsiloxy)cyclopentene (**16**) in CH_2Cl_2 at $\lambda = 593 \text{ nm}$ (J&M).

No.	$[\text{EI}]_0 /$ mol L^{-1}	$[\text{Nuc}]_0 /$ mol L^{-1}	$[\text{Nuc}]_0/[\text{EI}]_0$	Conv. / %	$T /$ $^\circ\text{C}$	$k_2 /$ $\text{L mol}^{-1} \text{ s}^{-1}$
050720-01	1.996×10^{-5}	2.181×10^{-3}	109	---	-70.9	2.179
050720-02	1.447×10^{-5}	1.976×10^{-3}	137	---	-61.2	4.661
050720-03	1.743×10^{-5}	1.904×10^{-3}	109	---	-51.0	9.260
050720-04	1.799×10^{-5}	1.572×10^{-3}	87	---	-41.2	1.720×10^1
050720-05	1.791×10^{-5}	1.370×10^{-3}	77	---	-29.8	3.311×10^1
050720-06	1.939×10^{-5}	1.059×10^{-3}	55	---	-19.6	5.525×10^1
050720-07	1.667×10^{-5}	5.465×10^{-4}	33	---	-10.5	8.654×10^1

Eyring parameters:

$$\Delta H^\ddagger = 24.922 \pm 0.124 \text{ kJ mol}^{-1}$$

$$\Delta S^\ddagger = -111.825 \pm 0.540 \text{ J mol}^{-1} \text{ K}^{-1}$$

$$r^2 = 0.9999$$

Arrhenius parameters:

$$E_a = 26.834 \pm 0.100 \text{ kJ mol}^{-1}$$

$$\ln A = 16.752 \pm 0.053$$

$$r^2 = 0.9999$$

$$k_2 (20 \text{ }^\circ\text{C}) = (3.194 \pm 0.044) \times 10^2 \text{ L mol}^{-1} \text{ s}^{-1}$$

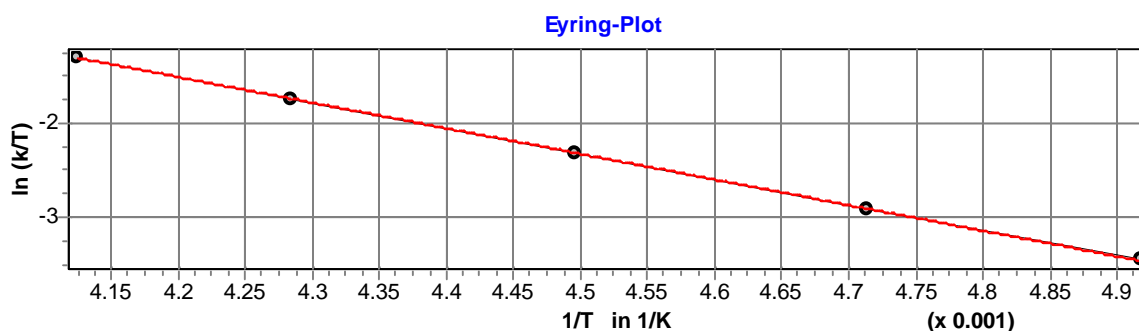
Table 10.15: Bis(4-(methyl(2,2,2-trifluoroethyl)amino)phenyl)methylm tetrafluoroborate ($\text{mfa})_2\text{CH}^+ \text{BF}_4^-$ and 1-(trimethylsiloxy)cyclohexene (**17**) in CH_2Cl_2 at $\lambda = 593 \text{ nm}$ (J&M).

No.	$[\text{El}]_0 /$ mol L^{-1}	$[\text{Nuc}]_0 /$ mol L^{-1}	$[\text{Nuc}]_0/[\text{El}]_0$	Conv. / %	$T /$ $^\circ\text{C}$	$k_2 /$ $\text{L mol}^{-1} \text{ s}^{-1}$
070720-05	1.378×10^{-5}	5.159×10^{-4}	37	---	20.0	2.181×10^1
070720-04	2.001×10^{-5}	1.049×10^{-3}	52	---	20.0	2.085×10^1
070720-02	1.566×10^{-5}	1.173×10^{-3}	75	---	20.0	2.149×10^1
070720-03	1.219×10^{-5}	9.133×10^{-4}	75	---	20.0	2.227×10^1
070720-01	1.198×10^{-5}	1.122×10^{-3}	94	---	20.0	2.199×10^1

$$\bar{k}_2(20 \text{ }^\circ\text{C}) = (2.168 \pm 0.049) \times 10^1 \text{ L mol}^{-1} \text{ s}^{-1}$$

Table 10.16: Bis(4-diphenylaminophenyl)methylm tetrafluoroborate ($\text{dpa})_2\text{CH}^+ \text{BF}_4^-$ and 1-phenoxy-1-(trimethylsiloxy)ethene (**18**) in CH_2Cl_2 at $\lambda = 640 \text{ nm}$ (Schölly).

No.	$[\text{El}]_0 /$ mol L^{-1}	$[\text{Nuc}]_0 /$ mol L^{-1}	$[\text{Nuc}]_0/[\text{El}]_0$	Conv. / %	$T /$ $^\circ\text{C}$	$k_2 /$ $\text{L mol}^{-1} \text{ s}^{-1}$
310520.PA4	5.844×10^{-5}	9.411×10^{-2}	161	82	-69.8	6.437
310520.PA5	5.880×10^{-5}	1.515×10^{-2}	257	70	-61.0	1.139×10^1
310520.PA9	8.365×10^{-5}	1.617×10^{-2}	193	62	-50.7	2.172×10^1
310520.PA7	7.686×10^{-5}	9.520×10^{-3}	124	38	-39.7	4.059×10^1
310520.PA8	8.090×10^{-5}	6.514×10^{-3}	81	49	-30.7	6.544×10^1



Eyring parameters:

$$\Delta H^\ddagger = 22.517 \pm 0.146 \text{ kJ mol}^{-1}$$

$$\Delta S^\ddagger = -115.632 \pm 0.658 \text{ J mol}^{-1} \text{ K}^{-1}$$

$$r^2 = 0.9999$$

Arrhenius parameters:

$$E_a = 24.360 \pm 0.169 \text{ kJ mol}^{-1}$$

$$\ln A = 16.256 \pm 0.092$$

$$r^2 = 0.9999$$

$$k_2 (20 \text{ }^\circ\text{C}) = (5.421 \pm 0.104) \times 10^2 \text{ L mol}^{-1} \text{ s}^{-1}$$

Table 10.17: Bis(4-(methyl(2,2,2-trifluoroethyl)amino)phenyl)methylium tetrafluoroborate (mfa)₂CH⁺ BF₄⁻ and 1-phenoxy-1-(trimethylsiloxy)ethene (**18**) in CH₂Cl₂ at λ = 593 nm (Stopped flow).

No.	[EL] ₀ / mol L ⁻¹	[Nuc] ₀ / mol L ⁻¹	[Nuc] ₀ /[EL] ₀	T / °C	k ₂ / L mol ⁻¹ s ⁻¹
060720-F	7.997 × 10 ⁻⁶	2.388 × 10 ⁻⁴	30	20.0	4.097 × 10 ³
060720-B	7.997 × 10 ⁻⁶	4.775 × 10 ⁻⁴	60	20.0	4.139 × 10 ³
060720-C	7.997 × 10 ⁻⁶	7.163 × 10 ⁻⁴	90	20.0	4.155 × 10 ³
060720-D	7.997 × 10 ⁻⁶	9.550 × 10 ⁻⁴	120	20.0	4.198 × 10 ³
060720-E	7.997 × 10 ⁻⁶	1.194 × 10 ⁻³	150	20.0	4.203 × 10 ³

$$\bar{k}_2 (20 \text{ }^\circ\text{C}) = (4.158 \pm 0.039) \times 10^3 \text{ L mol}^{-1} \text{ s}^{-1}$$

Table 10.18: Bis(4-(phenyl(2,2,2-trifluoroethyl)amino)phenyl)methylium tetrafluoroborate (pfa)₂CH⁺ BF₄⁻ and 1-phenoxy-1-(trimethylsiloxy)ethene (**18**) in CH₂Cl₂ at λ = 601 nm (Stopped flow).

No.	[EL] ₀ / mol L ⁻¹	[Nuc] ₀ / mol L ⁻¹	[Nuc] ₀ /[EL] ₀	T / °C	k ₂ / L mol ⁻¹ s ⁻¹
130720-A	1.339 × 10 ⁻⁵	2.742 × 10 ⁻⁴	21	20.0	1.626 × 10 ⁴
130720-B	1.339 × 10 ⁻⁵	5.484 × 10 ⁻⁴	41	20.0	1.709 × 10 ⁴
130720-C	1.339 × 10 ⁻⁵	8.225 × 10 ⁻⁴	61	20.0	1.733 × 10 ⁴
130720-D	1.339 × 10 ⁻⁵	1.097 × 10 ⁻³	82	20.0	1.770 × 10 ⁴
130720-E	1.339 × 10 ⁻⁵	1.371 × 10 ⁻³	102	20.0	1.778 × 10 ⁴

$$\bar{k}_2 (20 \text{ }^\circ\text{C}) = (1.723 \pm 0.055) \times 10^4 \text{ L mol}^{-1} \text{ s}^{-1}$$

Table 10.19: Bis(4-diphenylaminophenyl)methylium tetrafluoroborate (dpa)₂CH⁺ BF₄⁻ and 1-methoxy-2-methyl-1-(trimethylsiloxy)propene (**19**) in CH₂Cl₂ at λ = 672 nm (Stopped flow).

No.	[<i>El</i>] ₀ / mol L ⁻¹	[<i>Nuc</i>] ₀ / mol L ⁻¹	[<i>Nuc</i>] ₀ /[<i>El</i>] ₀	<i>T</i> / °C	<i>k</i> ₂ / L mol ⁻¹ s ⁻¹
100820-F	7.783 × 10 ⁻⁶	1.728 × 10 ⁻⁴	22	20.0	1.607 × 10 ⁴
100820-B	7.783 × 10 ⁻⁶	3.456 × 10 ⁻⁴	44	20.0	1.638 × 10 ⁴
100820-C	7.783 × 10 ⁻⁶	5.184 × 10 ⁻⁴	67	20.0	1.671 × 10 ⁴
100820-D	7.783 × 10 ⁻⁶	6.911 × 10 ⁻⁴	89	20.0	1.695 × 10 ⁴
100820-E	7.783 × 10 ⁻⁶	8.639 × 10 ⁻⁴	111	20.0	1.701 × 10 ⁴

$$\bar{k}_2 (20 \text{ }^\circ\text{C}) = (1.662 \pm 0.036) \times 10^4 \text{ L mol}^{-1} \text{ s}^{-1}$$

Table 10.20: Bis(4-(phenyl(2,2,2-trifluoroethyl)amino)phenyl)methylium tetrafluoroborate (pfa)₂CH⁺ BF₄⁻ and 1-methoxy-2-methyl-1-(trimethylsiloxy)propene (**19**) in CH₂Cl₂ at λ = 601 nm (Stopped flow).

No.	[<i>El</i>] ₀ / mol L ⁻¹	[<i>Nuc</i>] ₀ / mol L ⁻¹	[<i>Nuc</i>] ₀ /[<i>El</i>] ₀	<i>T</i> / °C	<i>k</i> ₂ / L mol ⁻¹ s ⁻¹
090820-F	6.663 × 10 ⁻⁶	1.479 × 10 ⁻⁴	22	20.0	4.722 × 10 ⁵
090820-B	6.663 × 10 ⁻⁶	2.958 × 10 ⁻⁴	44	20.0	4.771 × 10 ⁵
090820-C	6.663 × 10 ⁻⁶	4.437 × 10 ⁻⁴	67	20.0	4.814 × 10 ⁵
090820-D	6.663 × 10 ⁻⁶	5.916 × 10 ⁻⁴	89	20.0	4.808 × 10 ⁵
090820-E	6.663 × 10 ⁻⁶	7.394 × 10 ⁻⁴	111	20.0	4.871 × 10 ⁵

$$\bar{k}_2 (20 \text{ }^\circ\text{C}) = (4.797 \pm 0.049) \times 10^5 \text{ L mol}^{-1} \text{ s}^{-1}$$

Table 10.21: Bis(lilolidin-8-yl)methylium tetrafluoroborate $(\text{lil})_2\text{CH}^+ \text{BF}_4^-$ and 2-(trimethylsiloxy)-5,6-dihydro-4*H*-pyran (**9**) in CH_2Cl_2 at $\lambda = 640 \text{ nm}$ (Schölly).

No.	$[\text{El}]_0 /$ mol L^{-1}	$[\text{Nuc}]_0 /$ mol L^{-1}	$[\text{Nuc}]_0/[\text{El}]_0$	Conv. / %	$T /$ $^\circ\text{C}$	$k_2 /$ $\text{L mol}^{-1} \text{ s}^{-1}$
270620.PA2	5.821×10^{-5}	3.394×10^{-3}	58	83	20.0	2.795
270620.PA1	5.422×10^{-5}	6.323×10^{-3}	117	80	20.0	2.851
270620.PA0	7.276×10^{-5}	6.788×10^{-3}	93	84	20.0	2.887

$$\bar{k}_2 (20 \text{ }^\circ\text{C}) = 2.844 \pm 0.038$$

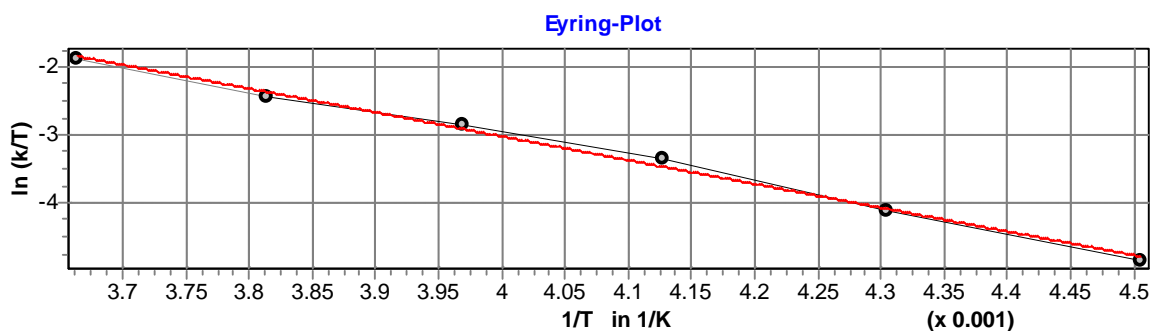
Table 10.22: Bis(julolidin-9-yl)methylium tetrafluoroborate $(\text{jul})_2\text{CH}^+ \text{BF}_4^-$ and 2-(trimethylsiloxy)-5,6-dihydro-4*H*-pyran (**9**) in CH_2Cl_2 at $\lambda = 640 \text{ nm}$ (Schölly).

No.	$[\text{El}]_0 /$ mol L^{-1}	$[\text{Nuc}]_0 /$ mol L^{-1}	$[\text{Nuc}]_0/[\text{El}]_0$	Conv. / %	$T /$ $^\circ\text{C}$	$k_2 /$ $\text{L mol}^{-1} \text{ s}^{-1}$
220620.PA4	4.233×10^{-5}	6.536×10^{-4}	15	81	20.0	1.012×10^1
220620.PA3	5.132×10^{-5}	1.321×10^{-3}	26	74	20.0	1.119×10^1
220620.PA1	5.580×10^{-5}	2.872×10^{-3}	51	80	20.0	1.112×10^1
220620.PA2	4.809×10^{-5}	3.713×10^{-3}	77	50	20.0	1.099×10^1
220620.PA0	5.387×10^{-5}	5.546×10^{-3}	103	63	20.0	1.204×10^1

$$\bar{k}_2 (20 \text{ }^\circ\text{C}) = (1.109 \pm 0.061) \times 10^1 \text{ L mol}^{-1} \text{ s}^{-1}$$

Table 10.23: Bis(*N*-methyl-1,2,3,4-tetrahydroquinolin-6-yl)methylm tetrafluoroborate ($(\text{thq})_2\text{CH}^+ \text{BF}_4^-$) and 2-(trimethylsiloxy)-5,6-dihydro-4*H*-pyran (**9**) in CH_2Cl_2 at $\lambda = 640 \text{ nm}$ (Schölly).

No.	$[\text{El}]_0 /$ mol L^{-1}	$[\text{Nuc}]_0 /$ mol L^{-1}	$[\text{Nuc}]_0/[\text{El}]_0$	Conv. / %	$T /$ $^\circ\text{C}$	$k_2 /$ $\text{L mol}^{-1} \text{ s}^{-1}$
260620.PA0	3.805×10^{-5}	2.951×10^{-3}	78	75	-51.2	1.741
260620.PA1	4.042×10^{-5}	1.567×10^{-3}	39	82	-40.8	3.841
260620.PA2	3.783×10^{-5}	2.934×10^{-3}	78	83	-30.9	8.495
260620.PA3	4.243×10^{-5}	2.632×10^{-3}	62	84	-21.2	1.454×10^1
260620.PA4	3.846×10^{-5}	2.088×10^{-3}	54	70	-11.0	2.277×10^1
260620.PA6	3.569×10^{-5}	1.661×10^{-3}	47	80	-0.2	4.256×10^1



Eyring parameters:

$$\Delta H^\ddagger = 29.175 \pm 0.969 \text{ kJ mol}^{-1}$$

$$\Delta S^\ddagger = -105.943 \pm 3.948 \text{ J mol}^{-1} \text{ K}^{-1}$$

$$r^2 = 0.9956$$

Arrhenius parameters:

$$E_a = 31.217 \pm 0.949 \text{ kJ mol}^{-1}$$

$$\ln A = 17.524 \pm 0.465$$

$$r^2 = 0.9963$$

$$k_2 (20^\circ\text{C}) = (1.132 \pm 0.086) \times 10^2 \text{ L mol}^{-1} \text{ s}^{-1}$$

Table 10.24: Bis(4-dimethylaminophenyl)methylium tetrafluoroborate (dma)₂CH⁺ BF₄⁻ and 2-(trimethylsiloxy)-5,6-dihydro-4*H*-pyran (**9**) in CH₂Cl₂ at λ = 612 nm (Stopped flow).

No.	[<i>El</i>] ₀ / mol L ⁻¹	[<i>Nuc</i>] ₀ / mol L ⁻¹	[<i>Nuc</i>] ₀ /[<i>El</i>] ₀	<i>T</i> / °C	<i>k</i> ₂ / L mol ⁻¹ s ⁻¹
190620-F	5.362 × 10 ⁻⁶	1.268 × 10 ⁻⁴	24	20.0	1.274 × 10 ³
190620-G	5.362 × 10 ⁻⁶	2.535 × 10 ⁻⁴	47	20.0	1.298 × 10 ³
190620-C	5.362 × 10 ⁻⁶	3.803 × 10 ⁻⁴	71	20.0	1.319 × 10 ³
190620-D	5.362 × 10 ⁻⁶	5.070 × 10 ⁻⁴	95	20.0	1.335 × 10 ³
190620-E	5.362 × 10 ⁻⁶	6.338 × 10 ⁻⁴	118	20.0	1.335 × 10 ³

$$\bar{k}_2(20\text{ }^\circ\text{C}) = (1.312 \pm 0.023) \times 10^3 \text{ L mol}^{-1} \text{ s}^{-1}$$

Table 10.25: Bis(4-diphenylaminophenyl)methylium tetrafluoroborate (dpa)₂CH⁺ BF₄⁻ and 2-(trimethylsiloxy)-5,6-dihydro-4*H*-pyran (**9**) in CH₂Cl₂ at λ = 672 nm (Stopped flow).

No.	[<i>El</i>] ₀ / mol L ⁻¹	[<i>Nuc</i>] ₀ / mol L ⁻¹	[<i>Nuc</i>] ₀ /[<i>El</i>] ₀	<i>T</i> / °C	<i>k</i> ₂ / L mol ⁻¹ s ⁻¹
200620-F	5.411 × 10 ⁻⁶	1.127 × 10 ⁻⁴	21	20.0	1.071 × 10 ⁵
200620-B	5.411 × 10 ⁻⁶	2.254 × 10 ⁻⁴	42	20.0	1.115 × 10 ⁵
200620-C	5.411 × 10 ⁻⁶	3.381 × 10 ⁻⁴	63	20.0	1.134 × 10 ⁵
200620-D	5.411 × 10 ⁻⁶	4.508 × 10 ⁻⁴	83	20.0	1.129 × 10 ⁵
200620-E	5.411 × 10 ⁻⁶	5.636 × 10 ⁻⁴	104	20.0	1.137 × 10 ⁵

$$\bar{k}_2(20\text{ }^\circ\text{C}) = (1.117 \pm 0.024) \times 10^5 \text{ L mol}^{-1} \text{ s}^{-1}$$

Table 10.26: Bis(4-(methyl(2,2,2-trifluoroethyl)amino)phenyl)methylmethyl tetrafluoroborate ($(\text{mfa})_2\text{CH}^+ \text{BF}_4^-$) and 2-(trimethylsiloxy)-5,6-dihydro-4*H*-pyran (**9**) in CH_2Cl_2 at $\lambda = 593 \text{ nm}$ (Stopped flow).

No.	$[\text{El}]_0 /$ mol L^{-1}	$[\text{Nuc}]_0 /$ mol L^{-1}	$[\text{Nuc}]_0/[\text{El}]_0$	$T /$ $^\circ\text{C}$	$k_2 /$ $\text{L mol}^{-1} \text{ s}^{-1}$
290620-A	7.997×10^{-6}	1.913×10^{-4}	24	20.0	6.237×10^5
290620-B	7.997×10^{-6}	2.869×10^{-4}	36	20.0	6.392×10^5
290620-C	7.997×10^{-6}	3.826×10^{-4}	48	20.0	6.583×10^5
290620-D	7.997×10^{-6}	4.782×10^{-4}	60	20.0	6.328×10^5
290620-E	7.997×10^{-6}	5.739×10^{-4}	72	20.0	6.461×10^5

$$\bar{k}_2 (20 \text{ }^\circ\text{C}) = (6.400 \pm 0.118) \times 10^5 \text{ L mol}^{-1} \text{ s}^{-1}$$

Table 10.27: Bis(4-diphenylaminophenyl)methylmethyl tetrafluoroborate ($(\text{dpa})_2\text{CH}^+ \text{BF}_4^-$) and 1-(*N*-morpholino)cyclohexene (**20**) in CH_2Cl_2 at $\lambda = 672 \text{ nm}$ (Stopped flow).

No.	$[\text{El}]_0 /$ mol L^{-1}	$[\text{Nuc}]_0 /$ mol L^{-1}	$[\text{Nuc}]_0/[\text{El}]_0$	$T /$ $^\circ\text{C}$	$k_2 /$ $\text{L mol}^{-1} \text{ s}^{-1}$
210620-G	5.819×10^{-6}	1.268×10^{-4}	22	20.0	3.576×10^5
210620-D	5.819×10^{-6}	2.535×10^{-4}	44	20.0	3.193×10^5
210620-C	5.819×10^{-6}	3.803×10^{-4}	65	20.0	3.210×10^5
210620-E	5.819×10^{-6}	5.070×10^{-4}	87	20.0	3.453×10^5
210620-F	5.819×10^{-6}	6.338×10^{-4}	109	20.0	3.473×10^5

$$\bar{k}_2 (20 \text{ }^\circ\text{C}) = (3.381 \pm 0.153) \times 10^5 \text{ L mol}^{-1} \text{ s}^{-1}$$

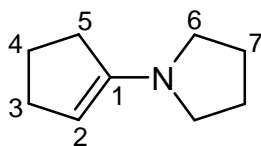
10.3 Structure-nucleophilicity relationships for enamines

10.3.1 Enamine synthesis by condensation of ketones or aldehydes with amines

General procedure: In a round-bottom flask equipped with a Dean-Stark water separator and reflux condenser a mixture of the ketone or aldehyde, amine, catalyst and dry toluene was refluxed until formation of the water had ceased. After filtration, toluene was removed from

the filtrate under vacuum. In order to remove traces of secondary amines, the crude products were distilled over LiAlH_4 under high vacuum to give the corresponding enamine. The products were identified by ^1H and ^{13}C NMR spectroscopy.

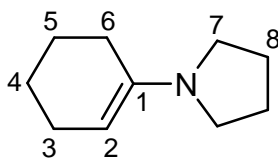
1-(*N*-Pyrrolidino)cyclopentene^[65] (21): A mixture of cyclopentanone (42.1 g, 0.500 mol), pyrrolidine (42.7 g, 0.600 mol), and toluene-*p*-sulfonic acid (100 mg, 0.581 mmol) was refluxed in toluene (100 mL) for 5 h at 140 °C (bath) to give a colorless oil (28.8 g, 42 %); b.p. 73 °C/1.6 mbar. ^1H NMR (300 MHz, CDCl_3): δ = 1.83-2.46 (m, 10 H, 2 × 3-H, 2 × 4-H, 2 × 5-H, 4 × 7-H), 3.05-3.09 (m, 4 H, 6-H), 4.05 (s, 1 H, 2-H); ^{13}C NMR (75.5 MHz, CDCl_3): δ = 23.1, 25.1, 30.7, 32.9 (4 t, C-3, C-4, C-5, C-7), 48.8 (t, C-6), 92.1 (d, C-2), 149.4 (s, C-1) in agreement with data published in ref. [179].



BKE037

21

1-(*N*-Pyrrolidino)cyclohexene^[65] (22): A mixture of cyclohexanone (49.1 g, 0.500 mol), pyrrolidine (42.7 g, 0.600 mol), and toluene-*p*-sulfonic acid (100 mg, 0.581 mmol) was refluxed in toluene (100 mL) for 5 h at 140 °C (bath) to give a colorless oil (36.3 g, 48 %); b.p. 79-80 °C/1.6 mbar. ^1H NMR (300 MHz, CDCl_3): δ = 1.53-2.19 (m, 12 H, 2 × 3-H, 2 × 4-H, 2 × 5-H, 2 × 6-H, 4 × 8-H), 2.98-3.02 (m, 4 H, 7-H), 4.28 (s, 1 H, 2-H); ^{13}C NMR (75.5 MHz, CDCl_3): δ = 22.9, 23.3, 24.4, 24.5, 27.5 (5 t, C-3, C-4, C-5, C-6, C-8), 47.3 (t, C-7), 93.5 (d, C-2), 143.3 (s, C-1) in agreement with data published in ref. [180].

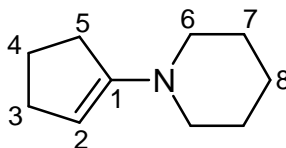


BKE036

22

1-(*N*-Piperidino)cyclopentene^[65] (23): A mixture of cyclopentanone (42.1 g, 0.500 mol), piperidine (51.1 g, 0.600 mol), and toluene-*p*-sulfonic acid (200 mg, 1.16 mmol) was refluxed in toluene (100 mL) for 5 h at 140 °C (bath) to give a colorless oil (49.8 g, 66 %); b.p. 83 °C/1.6 mbar. ^1H NMR (300 MHz, CDCl_3): δ = 1.49-2.39 (m, 12 H, 2 × 3-H, 2 × 4-H, 2 × 5-H, 4 × 7-H, 2 × 8-H), 2.84-2.88 (m, 4 H, 6-H), 4.40 (s, 1 H, 2-H); ^{13}C NMR (75.5 MHz, CDCl_3):

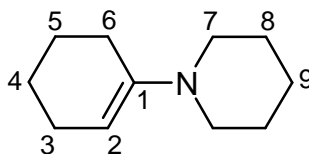
$\delta = 22.6, 24.4, 25.4, 30.3, 31.8$ (5 t, C-3, C-4, C-5, C-7, C-8), 49.4 (t, C-6), 97.1 (d, C-2), 152.1 (s, C-1) in agreement with data published in ref. [181].



BKE003

23

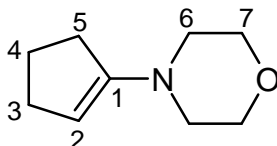
1-(N-Piperidino)cyclohexene^[65] (**24**): A mixture of cyclohexanone (49.1 g, 0.500 mol), piperidine (51.1 g, 0.600 mol), and toluene-*p*-sulfonic acid (150 mg, 0.872 mmol) was refluxed in toluene (100 mL) for 4 h at 140 °C (bath) to give a colorless oil (48.3 g, 58 %); b.p. 88 °C/1.2 mbar. ¹H NMR (300 MHz, CDCl₃): $\delta = 1.48$ -2.09 (m, 14 H, 2 × 3-H, 2 × 4-H, 2 × 5-H, 2 × 6-H, 4 × 8-H, 2 × 9-H), 2.73-2.76 (m, 4 H, 7-H), 4.66 (dd, ³*J* = 3.0 Hz, ³*J* = 3.9 Hz, 1 H, 2-H) in agreement with data published in ref. [182]; ¹³C NMR (75.5 MHz, CDCl₃): $\delta = 22.8, 23.4, 24.5, 24.6, 25.9, 27.6$ (6 t, C-3, C-4, C-5, C-6, C-8, C-9), 48.9 (t, C-7), 99.9 (d, C-2), 146.1 (s, C-1) in agreement with data published in ref. [183].



BKEDip

24

1-(N-Morpholino)cyclopentene^[65] (**25**): A mixture of cyclopentanone (42.1 g, 0.500 mol), morpholine (52.3 g, 0.600 mol), and toluene-*p*-sulfonic acid (200 mg, 1.16 mmol) was refluxed in toluene (100 mL) for 4 h at 140 °C (bath) to give a colorless oil (47.5 g, 62 %); b.p. 82 °C/1.5 mbar. ¹H NMR (300 MHz, CDCl₃): $\delta = 1.85$ -2.38 (m, 6 H, 2 × 3-H, 2 × 4-H, 2 × 5-H), 2.85-2.89 (m, 4 H, 6-H), 3.70-3.73 (m, 4 H, 7-H), 4.44 (s, 1 H, 2-H) in agreement with data published in ref. [184]; ¹³C NMR (75.5 MHz, CDCl₃): $\delta = 22.2, 30.0, 31.1$ (3 t, C-3, C-4, C-5), 48.8 (t, C-6), 66.4 (t, C-7), 97.9 (d, C-2), 151.4 (s, C-1) in agreement with data published in ref. [185].

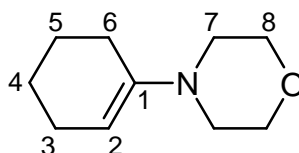


BKE001

25

1-(N-Morpholino)cyclohexene^[65] (**20**): A mixture of cyclohexanone (49.1 g, 0.500 mol), morpholine (52.3 g, 0.600 mol), and toluene-*p*-sulfonic acid (150 mg, 0.872 mmol) was

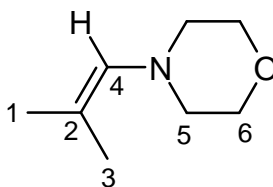
refluxed in toluene (100 mL) for 4 h at 140 °C (bath) to give a colorless oil (53.5 g, 64 %); b.p. 94-95 °C/1.2 mbar. ^1H NMR (300 MHz, CDCl_3): δ = 1.53-2.10 (m, 8 H, $2 \times 3\text{-H}$, $2 \times 4\text{-H}$, $2 \times 5\text{-H}$, $2 \times 6\text{-H}$), 2.75-2.79 (m, 4 H, 7-H), 3.70-3.73 (m, 4 H, 8-H), 4.66 (t, $^3J = 3.8$ Hz, 1 H, 2-H) in agreement with data published in ref. [186]; ^{13}C NMR (75.5 MHz, CDCl_3): δ = 22.6, 23.1, 24.2, 26.7 (4 t, C-3, C-4, C-5, C-6), 48.3 (t, C-7), 66.8 (t, C-8), 100.1 (d, C-2), 145.2 (s, C-1) in agreement with data published in ref. [187].



BKEDip

20

4-(2-Methyl-1-propenyl)morpholine^[188] (**29**): 2-Methylpropanal (71.1 g, 1.00 mol) and morpholine (87.1 g, 1.00 mol) were slowly mixed and refluxed for 4 h at 110 °C (bath). Distillation under reduced pressure yields a colorless oil (107.3 g, 76 %); b.p. 61-62 °C/10 mbar. ^1H NMR (300 MHz, CDCl_3): δ = 1.62/1.68 (2 s, 2×3 H, $3 \times 1\text{-H}$, $3 \times 3\text{-H}$), 2.58-2.61 (m, 4 H, 5-H), 3.71-3.74 (m, 4 H, 6-H), 5.32-5.33 (m, 1 H, 4-H) in agreement with data published in ref. [189]; ^{13}C NMR (75.5 MHz, CDCl_3): δ = 15.4/17.3 (2 q, C-1, C-3), 53.0 (t, C-5), 66.9 (t, C-6), 123.3 (s, C-2), 135.1 (d, C-4) in agreement with data published in ref. [189].

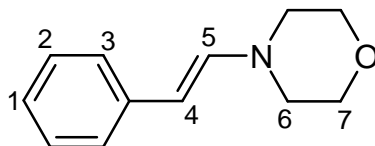


BKE043

29

4-[(trans)-2-Phenylvinyl]morpholine^[190] (**30**): Phenylacetaldehyde (80.0 g, 0.666 mol) and morpholine (116.0 g, 1.331 mol) were slowly (within 0.5 h) mixed and refluxed for 5 h at 120 °C (bath). Distillation under reduced pressure yields a colorless oil (b.p. 145 °C/ 3.3×10^{-2} mbar) which solidifies after several hours. Recrystallization (Et_2O) gives a pale yellow solid (57.1 g, 45 %); m.p. 76-77 °C. ^1H NMR (300 MHz, CDCl_3): δ = 2.92-2.96 (m, 4 H, 7-H), 3.67-3.70 (m, 4 H, 8-H), 5.39 (d, $^3J = 14.2$ Hz, 1 H, 5-H), 6.56 (d, $^3J = 14.2$ Hz, 1 H, 6-H), 6.99-7.23 (m, 5 H, $1 \times 1\text{-H}$, $2 \times 2\text{-H}$, $2 \times 3\text{-H}$) in agreement with data published in ref. [191]; ^{13}C NMR (75.5 MHz, CDCl_3): δ = 48.9 (t, C-7), 66.3 (t, C-8), 101.3 (d, C-5), 124.2 (d, C-3), 124.3 (d, C-1), 128.5 (d, C-2), 138.7 (s, C-4), 139.6 (d, C-6) in agreement with data published

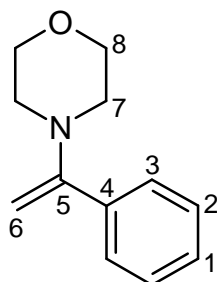
in ref. [191]. The (*trans*)-configuration is derived from the large coupling constant of the vinylic protons (14.2 Hz).



BKE045

30

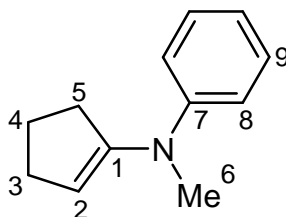
4-(1-Phenylvinyl)morpholine^[192] (**31**): A mixture of acetophenone (60.1 g, 0.500 mol), morpholine (52.3 g, 0.600 mol), and toluene-*p*-sulfonic acid (200 mg, 1.16 mmol) was refluxed in toluene (100 mL) for 10 h at 150 °C (bath) to give a colorless oil (52.1 g, 55 %); b.p. 84-85 °C/1.3 × 10⁻¹ mbar. ¹H NMR (300 MHz, CDCl₃): δ = 2.81-2.84 (m, 4 H, 7-H), 3.74-3.77 (m, 4 H, 8-H), 4.19/4.32 (2 s, 2 × 1 H, 6-H), 7.23-7.47 (m, 5 H, 1 × 1-H, 2 × 2-H, 2 × 3-H) in agreement with data published in ref. [193]; ¹³C NMR (75.5 MHz, CDCl₃): δ = 49.8 (t, C-7), 66.9 (t, C-8), 91.0 (t, C-6), 127.8, 128.0, 128.2 (3 d, Ar), 139.1 (s, Ar), 157.1 (s, C-1) in agreement with data published in ref. [194].



BKE040

31

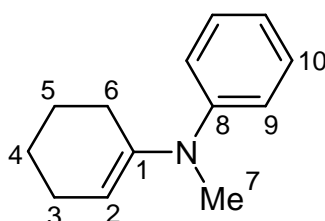
(1-Cyclopentenyl)methylphenylamine^[195] (**34**): A mixture of cyclopentanone (84.1 g, 1.00 mol), *N*-methylaniline (112.5 g, 1.050 mol), and K-10 montmorillonite clay (8.0 g) was refluxed in toluene (200 mL) for 36 h at 160 °C (bath) to give a colorless oil (52.0 g, 30 %); b.p. 98-99 °C/1.2 mbar. ¹H NMR (300 MHz, CDCl₃): δ = 1.45-2.43 (m, 6 H, 2 × 3-H, 2 × 4-H, 2 × 5-H), 3.10 (s, 3 H, 6-H), 4.71 (m_c, 1 H, 2-H) 6.95-7.30 (m, 5 H, 2 × 8-H, 2 × 9-H, 1 × 10-H).



BKE041

34

(1-Cyclohexenyl)methylphenylamine^[196] (**35**): A mixture of cyclohexanone (50.0 g, 0.509 mol), *N*-methylaniline (57.9 g, 0.540 mol), and K-10 montmorillonite clay (4.0 g) was refluxed in toluene (100 mL) for 36 h at 160 °C (bath) to give a colorless oil (42.0 g, 44 %); b.p. 113-114 °C/1.4 mbar. ¹H NMR (300 MHz, CDCl₃): δ = 1.57-2.33 (m, 8 H, 2 × 3-H, 2 × 4-H, 2 × 5-H, 2 × 6-H), 3.01 (s, 3 H, 7-H), 5.38 (m_c, 1 H, 2-H), 6.78-7.24 (m, 5 H, 2 × 9-H, 2 × 10-H, 1 × 11-H) in agreement with data published in ref. [197]; ¹³C NMR (75.5 MHz, CDCl₃): δ = 22.4, 23.2, 24.8, 26.3 (4 t, C-3, C-4, C-5, C-6), 39.3 (q, C-7), 116.3 (d, C-2), 117.5, 118.9, 128.8 (3 d, Ar), 144.0 (s, Ar), 149.0 (s, C-1) in agreement with data published in ref. [198].

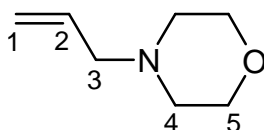


BKE039

35

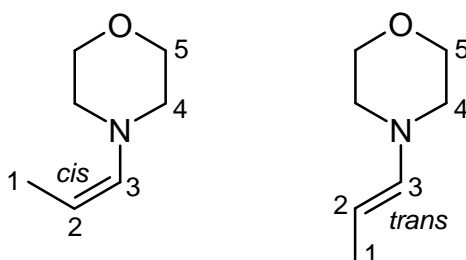
10.3.2 Enamine synthesis by base-catalyzed isomerization of allylamines

4-Allylmorpholine:^[66] In a carefully dried and with nitrogen flushed two-necked round-bottom flask equipped with a dropping funnel and reflux condenser, 3-bromo-1-propene (139.8 g, 1.156 mol) was added dropwise to a mixture of morpholine (201.0 g, 2.307 mol) and dry toluene (250 mL) within 1 h using a water bath for cooling. The reaction mixture was then refluxed for 2 h (bath: 130 °C). After cooling, the reaction mixture was added to a solution of 150 mL of conc. HCl in 100 mL water and extracted with dil. HCl (3 × 50 mL). After addition of NaOH (200 g) in 500 mL of water the separated amine-phase was extracted with toluene (3 × 50 mL), drying with KOH, evaporation of the solvent in vacuo and distillation in high vacuo gave a colorless oil (57.8 g, 39 %); b.p. 156-158 °C. ¹H NMR (300 MHz, CDCl₃): δ = 2.43-2.46 (m, 4 H, 4-H), 2.99 (dt, ³J = 6.4 Hz, ⁴J = 1.3 Hz, 2 H, 3-H), 3.70-3.73 (m, 4 H, 5-H), 5.14-5.24 (m, 2 H, 1-H), 5.78-5.90 (m, 1 H, 2-H); ¹³C NMR (75.5 MHz, CDCl₃): δ = 53.6 (t, C-4), 62.2 (t, C-3), 67.0 (t, C-5), 118.2 (t, C-1), 134.6 (d, C-2).



BKE050

4-[(*cis,trans*)-1-propenyl]morpholine^[66] (**28, 27**): In a round-bottom flask, 4-allylmorpholine (40.0 g, 0.315 mol) was added to a solution of potassium-*t*-butoxide (6.7 g, 0.06 mol) and absolute dimethyl sulfoxide (60 mL). After stirring at room temperature for 36 h, the reaction mixture was distilled to yield **28/27** = 89/11 (from ¹H NMR integrals of 3-H) together with small amounts of DMSO (12.3 g, 31 %). (*cis*)-**28**: ¹H NMR (300 MHz, CDCl₃): δ = 1.68 (dd, ³J = 7.1 Hz, ⁴J = 1.7 Hz, 3 H, 1-H), 2.74-2.77 (m, 4 H, 4-H), 3.70-3.72 (m, 4 H, 5-H), 4.45-4.55 (m, 1 H, 2-H), 5.53 (dd, ³J = 8.7 Hz, ⁴J = 1.7 Hz, 1 H, 3-H) in agreement with data published in ref. [66]; (*trans*)-**27**: ¹H NMR (300 MHz, CDCl₃): δ = 1.76 (dd, ³J = 8.0 Hz, ⁴J = 1.3 Hz, 3 H, 1-H), 2.74-2.77 (m, 4 H, 4-H), 3.72-3.74 (m, 4 H, 5-H), 5.42-5.58 (m, 1 H, 2-H), 6.00 (bd, ³J = 14.8 Hz, 1 H, 3-H) in agreement with data published in ref. [66].



BKE051

89 %

(cis)-**28**

BKE052

11 %

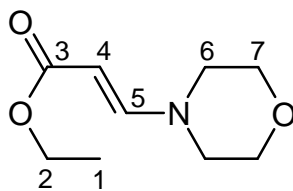
(trans)-**27**

The isomer mixture (12.3 g, 0.097 mol) was combined with benzoic acid (90.0 mg, 0.001 mol). After stirring at room temperature for 5 d, CaH₂ (500 mg) was added. Distillation gave a colorless oil (3.6 g, 29 %), b.p. 72 °C/10 mbar containing only (*trans*)-**27** (¹H NMR).

10.3.3 Enamine synthesis by addition of amine to alkyne

Ethyl-(*trans*)-3-morpholine-4-ylacrylate^[199] (**32**): In a carefully dried, nitrogen-flushed two-necked round-bottom flask equipped with a dropping funnel and reflux condenser, morpholine (8.6 g, 0.10 mol) was added within 30 min to a solution of ethyl propiolate (9.7 g, 0.10 mol) in dry CH₂Cl₂ (25 mL). After 30 min stirring at ambient temperature the reaction mixture was refluxed for 1 h at 50 °C (bath). After removing the solvent under reduced pressure, the residue was distilled under high vacuum to give a colorless oil (16.3 g, 88 %; b.p. 130 °C/4.0 × 10⁻¹ mbar) which solidifies after several hours. ¹H NMR (300 MHz, CDCl₃): δ = 1.26 (t, ³J = 7.2 Hz, 3 H, 1-H), 3.19-3.22 (m, 4 H, 6-H), 3.69-3.72 (m, 4 H, 7-H), 4.14 (q, ³J = 7.2 Hz, 2 H, 2-H), 4.70 (d, ³J = 13.3 Hz, 1 H, 4-H), 7.36 (d, ³J = 13.3 Hz, 1 H, 5-H); ¹³C NMR (75.5 MHz, CDCl₃): δ = 14.7 (q, C-1), 48.7 (t, C-6), 59.2 (t, C-2), 66.3 (t, C-7),

86.2 (d, C-4), 151.8 (d, C-5), 169.5 (s, C-3). The large coupling constant of the vinyl protons (13.3 Hz) indicate (*trans*)-configuration.



BKE047

32

10.3.4 Reactions of enamines, pyrroles, or indoles with benzhydrylium salts

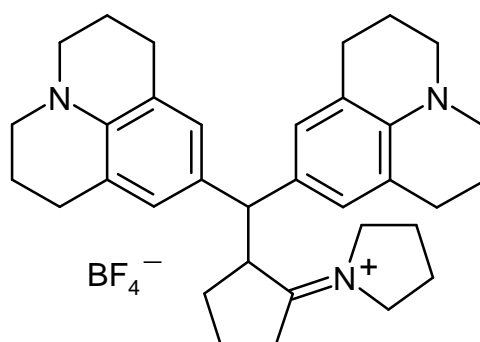
General: The reactions of enamines with benzhydrylium salts $\text{Ar}_2\text{CH}^+ \text{BF}_4^-$ were performed under exclusion of moisture in an atmosphere of dry nitrogen in carefully dried Schlenk glassware. Dichloromethane was freshly distilled from CaH_2 before use, as described prior.

Procedure A: A solution of the freshly distilled or recrystallized enamine was added dropwise to a stirred solution of the benzhydrylium salt in CH_2Cl_2 at room temperature. After fading of the color (in cases of reversible reactions after 2 h at the latest) the solvent was evaporated in vacuo to yield the crude product, which was washed with dry Et_2O and dried several hours in vacuo (10^{-2} mbar).

Procedure B: The crude product obtained by Procedure A was dissolved in dilute HCl and stirred for 30 min. The solution was then neutralized by treatment with dilute NaOH. Extraction with CH_2Cl_2 (3×30 mL), drying of the combined organic layers with MgSO_4 , filtration, and evaporation of the solvent in vacuo gave a product which was purified by recrystallization.

Procedure C: A solution of the benzhydryl salt in dichloromethane (25 mL) was added dropwise to a stirred solution of 10 equiv. of the freshly distilled or recrystallized pyrrole or indole in dichloromethane (25 mL) (An excess of the nucleophile is necessary for trapping the protons which are released during the electrophilic substitution. Reactions with equimolar amounts of the reactants usually do not proceed quantitatively and lead to the formation of side products, e.g., disubstituted arenes). After fading of the color, the solvent was evaporated in vacuo to yield the crude product, which was purified by column chromatography.

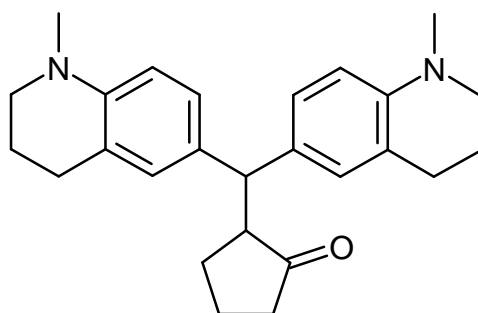
***N*-(2-(Bis(julolidin-9-yl)methyl)cyclopentylidene)pyrrolidinium tetrafluoroborate (21a)** was obtained from 1-(*N*-pyrrolidino)cyclopentene (**21**) (55 mg, 0.40 mmol) and (jul)₂CH⁺ BF₄⁻ (0.18 g, 0.40 mmol) as an orange solid (144 mg, 62 %) following Procedure A. ¹H NMR (300 MHz, CDCl₃): **d** = 1.50–2.25 (m, 16 H), 2.52–3.00 (m, 10 H), 3.01–3.15 (m, 8 H), 3.48–4.05 (m, 6 H), 6.42, 6.64 (2 s, 2 × 2 H, ArH); ¹³C NMR (75.5 MHz, CDCl₃): **d** = 20.2 (t, C-4), 22.0 (t, CH₂), 24.6/24.8 (2 t, CH₂), 27.7 (t, CH₂), 30.0, 34.4 (2 t, C-3 and C-5), 50.5 (t, CH₂), 50.9, 53.7 (2 d, Ar₂CH and C-2), 55.0/55.2 (2 t, CH₂), 121.7 (s, Ar), 126.6/126.9 (2 d, Ar), 128.7 (s, Ar), 141.9/142.1 (2 s, Ar), 197.0 (s, C-1).



NHB18

21a

2-(Bis(*N*-methyl-1,2,3,4-tetrahydroquinolin-6-yl)methyl)cyclopentanone (21b) was obtained from 1-(*N*-pyrrolidino)cyclopentene (**21**) (137 mg, 1.00 mmol) and (thq)₂CH⁺ BF₄⁻ (392 mg, 1.00 mmol) following Procedure B. Crystallization (EtOH) of the crude product gave a brown solid (207 mg, 39 %). ¹H NMR (300 MHz, CDCl₃): **d** = 1.65–2.29 (m, 10 H, 5 × CH₂), 2.59–2.86 (m, 11 H, 2 × CH₂, 2 × NMe, 2-H), 3.13–3.18 (m, 4 H, 2 × CH₂), 4.40 (d, ³J = 4.4 Hz, 1 H, Ar₂CH), 6.42–7.00 (m, 6 H, ArH); ¹³C NMR (75.5 MHz, CDCl₃): **d** = 20.6 (t, C-4), 22.5/22.6 (2 t, CH₂), 27.1 (t, C-3), 27.8/27.9 (2 t, CH₂), 38.6 (t, C-5), 39.1/39.2 (2 q, NMe), 48.2 (d, Ar₂CH), 51.30/51.35 (2 t, CH₂), 53.7 (d, C-2), 110.6/110.8 (2 d, Ar), 122.4/122.7 (2 s, Ar), 126.5/127.7, 129.1/129.6 (2 × 2 d, Ar), 130.9/132.0 (2 s, Ar), 145.0 (s, Ar), 220.4 (s, C-1); MS (70 eV, EI): *m/z* (%): 388 (4) [M⁺], 305 (100) [Ar₂CH⁺], 269 (52), 207 (12).



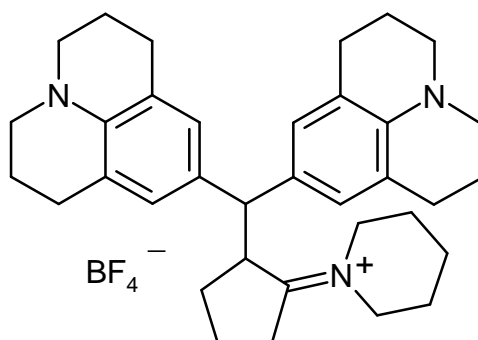
NHB19U

21b

2-(Bis(4-dimethylaminophenyl)methyl)cyclohexanone^[26] (**22b**) was obtained from 1-(*N*-pyrrolidino)cyclohexene (**22**) (151 mg, 0.998 mmol) and $(\text{dma})_2\text{CH}^+ \text{BF}_4^-$ (340 mg, 1.00 mmol) in CH_2Cl_2 (50 mL) following Procedure B. Recrystallization (EtOH) furnished **22b** as a light-brown solid (229 mg, 65 %) which showed identical ^1H and ^{13}C NMR spectra as the corresponding sample that was obtained from 1-(morpholino)cyclohexene and $(\text{dma})_2\text{CH}^+ \text{BF}_4^-$ in ref. [26].

NHB23U

***N*-(2-(Bis(julolidin-9-yl)methyl)cyclopentylidene)piperidinium tetrafluoroborate** (**23a**) was obtained from 1-(*N*-piperidino)cyclopentene (**23**) (54 mg, 0.36 mmol) and $(\text{jul})_2\text{CH}^+ \text{BF}_4^-$ (160 mg, 0.360 mmol) as a dark orange solid (190 mg, 89 %) following Procedure A. ^1H NMR (300 MHz, CDCl_3): δ = 1.30–2.22 (m, 18 H), 2.45–2.87 (m, 8 H), 2.90–3.11 (m, 10 H), 3.27–3.90 (m, 3 H), 4.22 (d, $^3J = 4.4$ Hz, 1 H, Ar_2CH), 6.41, 6.55 (2 s, 2×2 H, ArH); MS (FAB): m/z (%): 504 (1), 464 (2), 442 (12), 438 (10), 373 (4), 357 (100) [Ar_2CH^+].



NHB24

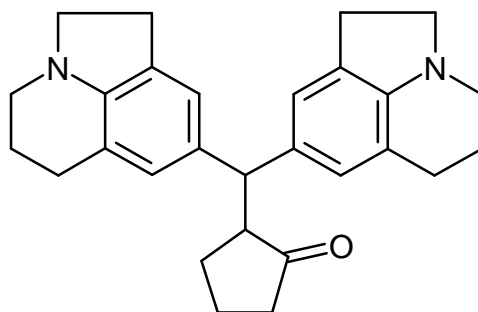
23a

2-(Bis(4-dimethylaminophenyl)methyl)cyclopentanone^[22] (**23b**) was obtained from 1-(*N*-piperidino)cyclopentene (**23**) (153 mg, 1.01 mmol) and $(\text{dma})_2\text{CH}^+ \text{BF}_4^-$ (340 mg, 1.00 mmol) following Procedure B. Crystallization (EtOH) of the crude product gave a light brown solid (166 mg, 49 %) which showed identical ^1H and ^{13}C NMR spectra as the corresponding

sample that was obtained from 1-(trimethylsiloxy)cyclopentene and $(\text{dma})_2\text{CH}^+ \text{BF}_4^-$ in ref. [22].

NHB27U

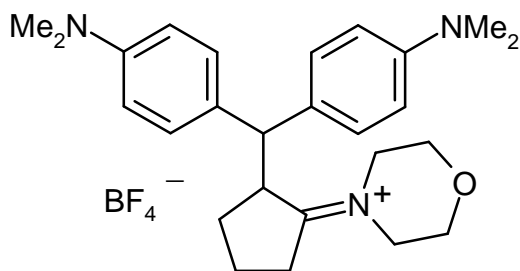
2-(Bis(lilolidin-8-yl)methyl)cyclopentanone (25b) was obtained from 1-(*N*-morpholino)cyclopentene (**25**) (0.216 mL, 1.35 mmol) and $(\text{lil})_2\text{CH}^+ \text{BF}_4^-$ (510 mg, 1.23 mmol) at -90°C as described in Procedure B. ^1H NMR (300 MHz, CDCl_3): δ = 1.66–1.79 (m, 3 H, 3-H and 4- H_2), 1.99–2.10 (m, 4 H, $2 \times \text{CH}_2$), 2.15–2.27 (m, 3 H, 3-H and 5- H_2), 2.56–2.67 (m, 4 H, $2 \times \text{CH}_2$), 2.72–2.95 (m, 9 H, 2-H and $4 \times \text{CH}_2$), 3.12–3.23 (m, 4 H, $2 \times \text{CH}_2$), 4.42 (d, $^3J = 4.3$ Hz, 1 H, Ar_2CH), 6.51, 6.62, 6.73, 6.85 (4 s, 4×1 H, ArH); ^{13}C NMR (75.5 MHz, CDCl_3): δ = 20.43 (t, C-4), 23.19/23.25, 23.82, 23.87 (2×2 t, CH_2), 27.22 (t, C-3), 28.67/28.76 (2 t, CH_2), 38.37 (t, C-5), 47.48/47.56 (2 t, CH_2), 49.49 (d, Ar_2CH), 53.81 (d, C-2), 55.20/55.29 (2 t, CH_2), 118.65/118.78 (2 s, Ar), 121.96/122.58, 125.82/126.75 (2×2 d, Ar), 128.28/128.55, 133.76/134.90 (2×2 s, Ar), 148.05 (s, Ar), 220.08 (s, C-1), signal assignments are based on ^1H , ^{13}C -COSY experiments; MS (EI, 70 eV): m/z (%): 412 (14) [M^+], 329 (100), 165 (12).



BKE002

25b

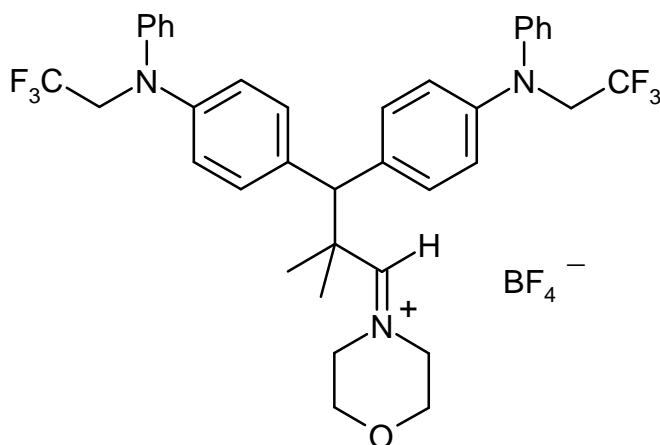
2-(Bis(4-dimethylaminophenyl)methyl)cyclopentenylidene)morpholinium tetrafluoroborate (25a) was obtained from 1-(*N*-morpholino)cyclopentene (**25**) (0.168 mL, 1.12 mmol) and $(\text{dma})_2\text{CH}^+ \text{BF}_4^-$ (380 mg, 1.12 mmol) following Procedure A: pale green powder (498 mg, 90 %). ^1H NMR (300 MHz, CDCl_3): δ = 1.89–2.35 (m, 4 H, 3-H and 4-H), 2.70–2.79 (m, 1 H, $\frac{1}{2} \times \text{CH}_2$), 2.86–2.95 (m, partially superimposed, 1 H, $\frac{1}{2} \times \text{CH}_2$), 2.86, 2.90 (2 s, 2×6 H, NMe_2), 3.00–3.29 (m, 2 H, 5- H_2), 3.60–4.04 (m, 8 H, 2-H, Ar_2CH , $3 \times \text{CH}_2$), 6.59–6.69 (m, 4 H, ArH), 7.02–7.05, 7.15–7.18 (2 m, 2×2 H, ArH); ^{13}C NMR (75.5 MHz, CDCl_3): δ = 19.85 (t, C-4), 29.57 (t, C-3), 33.13 (t, C-5), 40.34/40.39 (2 q, NMe_2), 50.74, 51.09 (2 d, Ar_2CH and C-2), 54.23/54.89, 64.69/65.10 (2×2 t, CH_2), 112.68/112.77 (2 d, Ar), 127.74/128.69 (2 s, Ar), 128.91/129.40 (2 d, Ar), 149.52/149.88 (2 s, Ar), 200.32 (s, C-1), signal assignments are based on ^1H , ^1H - and ^1H , ^{13}C -COSY experiments.



NHB25U

25a

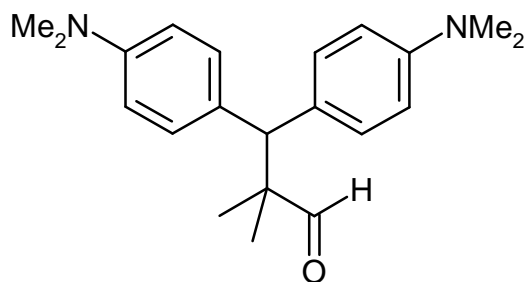
***N*-(3,3-Bis(4-(phenyl(2,2,2-trifluoroethyl)amino)phenyl)-2,2-dimethylpropylidene)morpholinium tetrafluoroborate (29a)** was generated by mixing (*N*-morpholino)isobutene (**29**) (22 mg, 0.16 mmol) and (pfa)₂CH⁺ BF₄⁻ (92 mg, 0.15 mmol) in CDCl₃ (1 mL). The reaction mixture was transferred into an NMR tube and analyzed without isolation. ¹H NMR (200 MHz, CDCl₃): *d* = 1.50 (s, 6 H, CH₃), 3.35, 3.67, 3.90, 4.00 (4 m, 4 × 2 H, morpholino-CH₂), 4.25 (q, *J*(H,F) = 8.7 Hz, 4 H, NCH₂CF₃), 4.40 (s, 1 H, Ar₂CH), 6.82–7.35 (m, 18 H, ArH), 8.52 (s, 1 H, N⁺=CH).



BKE055

29a

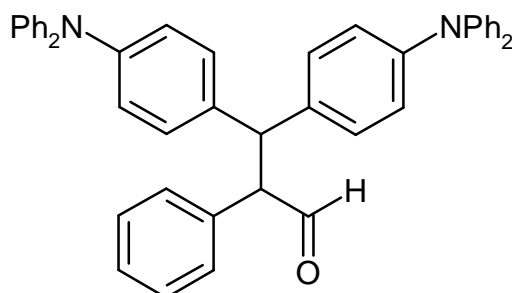
3,3-Bis(4-dimethylaminophenyl)-2,2-dimethylpropanal (29b) was obtained from (*N*-morpholino)isobutene (**29**) (270 mg, 1.91 mmol) and (dma)₂CH⁺ CF₃SO₃⁻ (379 mg, 0.942 mmol) following Procedure B. Crystallization from ethanol gave **29b** as beige needles (170 mg, 52 %). M.p. 102 °C (ethanol); ¹H NMR (300 MHz, CDCl₃): *d* = 1.12 (s, 6 H, 2-CH₃), 2.89 (s, 12 H, NMe₂), 3.99 (s, 1 H, Ar₂CH), 6.60–6.66, 7.08–7.13 (2 m, 2 × 4 H, ArH), 9.69 (s, 1 H, 1-H); ¹³C NMR (75.5 MHz, CDCl₃): *d* = 21.5 (q, 2-CH₃), 40.5 (q, NMe₂), 49.8 (s, C-2), 56.9 (d, Ar₂CH), 112.3 (d, Ar), 129.3 (s, Ar), 130.2 (d, Ar), 149.0 (s, Ar), 207.0 (d, C-1); MS (EI, 70 eV): *m/z* (%): 324 (2) [M⁺], 254 (34), 253 (100), 237 (14), 126 (20); elemental analysis calcd (%) for C₂₁H₂₈N₂O (324.47): C 77.74, H 8.70, N 8.63; found: C 77.74, H 8.87, N 8.73.



NHB33U2

29b

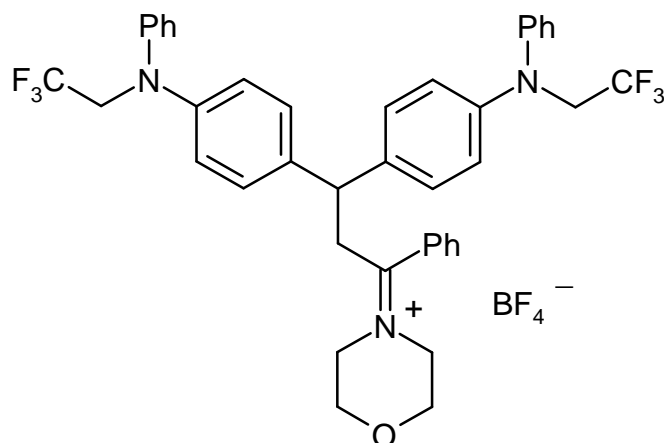
3,3-Bis(4-diphenylaminophenyl)-2-phenylpropanal (27b) was obtained from (*trans*)-**b**-(*N*-morpholino)styrene (**27**) (189 mg, 1.00 mmol) and (dpa)₂CH⁺ BF₄⁻ (589 mg, 1.00 mmol) following Procedure B. Crystallization of the crude product gave a pale green solid (432 mg, 70 %). M.p. 130–131 °C (CH₂Cl₂/*n*-pentane); ¹H NMR (300 MHz, CDCl₃): *d* = 4.30 (dd, ³*J* = 11.7 Hz, ³*J* = 3.3 Hz, 1 H, 2-H), 4.56 (d, ³*J* = 11.7 Hz, 1 H, Ar₂CH), 6.74–7.16 (m, 33 H, ArH), 9.66 (d, ³*J* = 3.3 Hz, 1 H, 1-H); ¹³C NMR (75.5 MHz, CDCl₃): *d* = 51.3 (d, Ar₂CH), 63.9 (d, C-2), 122.6, 122.9, 123.9, 124.0, 124.1, 127.6, 128.9, 129.0, 129.2, 129.2, 129.4, 129.6 (12 d, Ar), 134.9, 136.0, 136.1, 146.0, 146.6, 147.8 (6 s, Ar), 199.3 (d, C-1).



NHB21U

27b

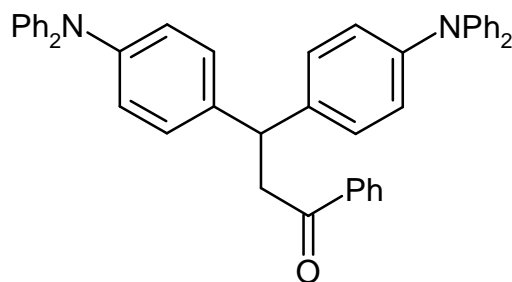
***N*-(3,3-Bis(4-(phenyl(2,2,2-trifluoroethyl)amino)phenyl)-1-phenylpropylidene)morpholinium tetrafluoroborate (31a)** was obtained from *a*-(*N*-morpholino)styrene (**31**) (51 mg, 0.27 mmol) and (pfa)₂CH⁺ BF₄⁻ (163 mg, 0.272 mmol) as a pale violet solid (179 mg, 83 %) following Procedure A. ¹H NMR (300 MHz, CDCl₃): *d* = 3.55–4.05 (m, 11 H, morpholino-CH₂, 2-H₂, Ar₂CH), 4.17 (q, *J*(H,F) = 8.7 Hz, 4 H, NCH₂CF₃), 6.73–7.50 (m, 23 H, ArH); ¹³C NMR (75.5 MHz, CDCl₃): *d* = 44.1 (t, C-2), 47.0 (d, Ar₂CH), 54.1 (tq, *J*(C,F) = 30.2 Hz, NCH₂CF₃), 53.5, 56.1, 65.9, 66.4 (4 t, morpholino-CH₂), 119.7, 123.1, 124.0 (3 d, Ar), 127.0 (s, Ar), 127.4, 128.5, 129.6, 129.7, 132.7 (5 d, Ar), 131.8, 134.6, 146.8 (3 s, Ar), 188.1 (s, C-1), the signal for CF₃ could not be identified.



NHB32

31a

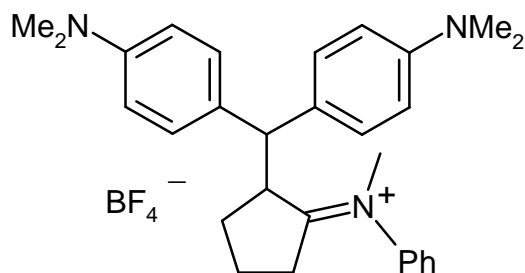
3,3-Bis(4-diphenylaminophenyl)-1-phenylpropan-1-one (31b) was obtained from *a*-(*N*-morpholino)styrene (**31**) (189 mg, 1.00 mmol) and $(\text{dpa})_2\text{CH}^+ \text{BF}_4^-$ (589 mg, 1.00 mmol) following Procedure B. Crystallization of the crude product gave a pale green solid (284 mg, 46 %). M.p. 96–97 °C ($\text{CH}_2\text{Cl}_2/n$ -pentane); ^1H NMR (300 MHz, CDCl_3): \mathbf{d} = 3.67 (d, $^3J = 7.2$ Hz, 2 H, 2-H), 4.71 (t, $^3J = 7.3$ Hz, 1 H, Ar_2CH), 6.95–7.93 (m, 33 H, ArH); ^{13}C NMR (75.5 MHz, CDCl_3): \mathbf{d} = 45.07 (t, C-2), 45.09 (d, Ar_2CH), 122.6, 124.0, 124.1, 128.1, 128.6, 129.1, 133.0 (7 d, Ar), 137.2, 138.5, 146.0, 147.8 (4 s, Ar), 198.5 (s, C-1); MS (70 eV, EI): m/z (%): 620 (22) [M^+], 501 (100) [Ar_2CH^+], 251 (10); elemental analysis calcd (%) for $\text{C}_{45}\text{H}_{36}\text{N}_2\text{O}$ (620.8): C 87.07, H 5.84, N 4.51; found C 87.26, H 6.00, N 4.42.



NHB35U

31b

***N*-(2-(Bis(4-dimethylaminophenyl)methyl)cyclopentylidene)methylphenylammonium tetrafluoroborate (34a)** was obtained from 1-(methylphenylamino)cyclopentene (**34**) (72 mg, 0.42 mmol) and $(\text{dma})_2\text{CH}^+ \text{BF}_4^-$ (142 mg, 0.417 mmol) as a green solid (197 mg, 92 %) following Procedure A. ^{13}C NMR (75.5 MHz, CDCl_3): \mathbf{d} = 20.4 (t), 29.8 (t), 36.0 (t), 40.4 (q, NMe_2), 40.6 (q, NMe_2), 48.8, 51.3, 52.1 (2 d and 1 q, C-2, Ar_2CH , and N^+CH_3), 112.6, 112.9 (2 d, Ar), 117.4 (s, Ar), 122.9, 123.4, 129.1, 129.4, 130.7 (5 d, Ar), 143.4, 149.6, 150.0 (3 s, Ar), 205.5 (s, C-1); MS (FAB): m/z (%): 426 (2) [M^+], 253 (100) [Ar_2CH^+], 237 (11), 174 (13).



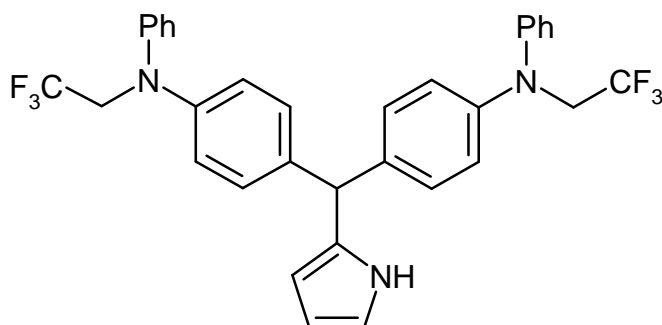
NHB28

34a

2-(Bis(4-diphenylaminophenyl)methyl)cyclohexanone (35b)^[26] was obtained from 1-(methylphenylamino)cyclohexene (**35**) (187 mg, 1.00 mmol) and (dpa)₂CH⁺ BF₄⁻ (589 mg, 1.00 mmol) following Procedure B. Crystallization (CH₂Cl₂/*n*-pentane) of the crude product gave **35b** as a pale brown solid (207 mg, 35 %) which showed identical ¹H and ¹³C NMR spectra as the corresponding sample that was obtained from 1-(trimethylsiloxy)cyclohexene **17** and (dpa)₂CH⁺ BF₄⁻ in ref. [26].

NHB31U

2-(Bis(4-(phenyl(2,2,2-trifluoroethyl)amino)phenyl)methyl)pyrrole (42c) was obtained from pyrrole (**42**) (179 mg, 2.67 mmol) and (pfa)₂CH⁺ BF₄⁻ (160 mg, 0.267 mmol) following Procedure C. Column chromatography (silica gel/CHCl₃) gave a colorless solid (50 mg, 32 %). ¹H NMR (600 MHz, CDCl₃): **d** = 4.19 (q, ³J(H,F) = 8.7 Hz, 4 H, NCH₂CF₃), 5.29 (s, 1 H, Ar₂CH), 5.71–5.75 (m, 1 H, 3-H), 6.07 (dd, *J* = 6.0 Hz, *J* = 2.7 Hz, 1 H, 4-H), 6.60–6.64 (m, 1 H, 5-H), 6.80–7.27 (m, 18 H, ArH), 7.73 (br s, 1 H, NH); ¹³C NMR (75.5 MHz, CDCl₃): **d** = 49.1 (d, Ar₂CH), 54.0 (tq, *J*(C,F) = 33 Hz, NCH₂CF₃) 107.8, 108.3, 117.1, 120.8, 121.7, 123.0 (6 d, Ar), 125.2 (sq, *J*(C,F) = 287 Hz, NCH₂CF₃), 129.5, 129.8 (2 d, Ar), 133.8, 137.2, 146.1, 147.3 (4 s, Ar), signal assignments are based on ¹H, ¹H-COSY experiments.

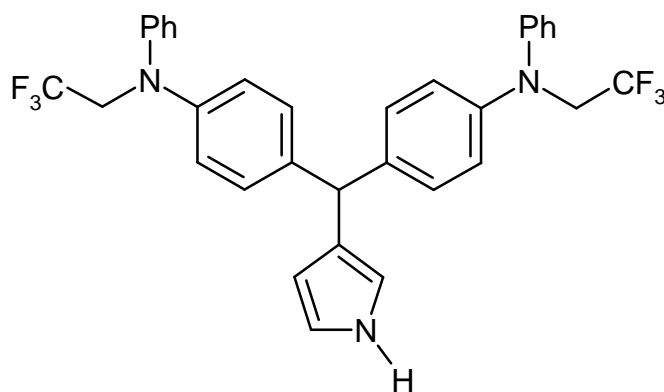


BKE067

42c

3-(Bis(4-(phenyl(2,2,2-trifluoroethyl)amino)phenyl)methyl)pyrrole (44c): A solution of (pfa)₂CH⁺ BF₄⁻ (190 mg, 0.317 mmol) in CH₂Cl₂ (10 mL) was added dropwise to a stirred solution of *N*-(triisopropylsilyl)pyrrole (**44**) (181 mg, 0.814 mmol) in CH₂Cl₂ (30 mL). After

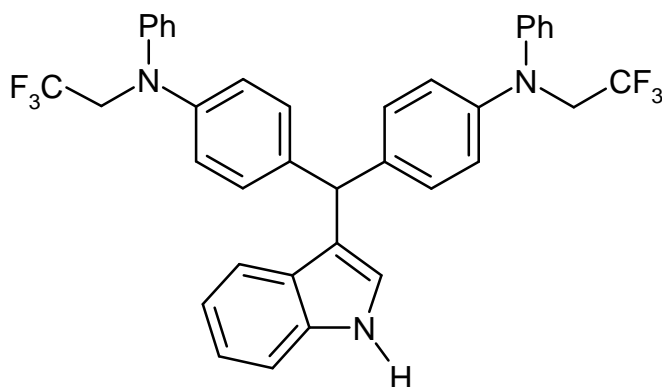
5 min a solution of tetrabutylammonium fluoride in THF ($c = 1 \text{ M}$, 1 mL, 1 mmol) was added. The reaction mixture was subsequently washed with 0.2 M hydrochloric acid (50 mL) and water (50 mL). Separation of the organic layer, drying over CaCl_2 , and evaporation of the solvent in vacuo gave a brownish oil (134 mg, 73 %). Purification by column chromatography (silica gel/ CHCl_3) gave **44c** (88 mg, 48 %) and **42c** (17 mg, 9 %). Characterization of **44c**: ^1H NMR (300 MHz, CDCl_3): $\delta = 4.27$ (q, $J(\text{H},\text{F}) = 8.8 \text{ Hz}$, 4 H, NCH_2CF_3), 5.31 (s, 1 H, Ar_2CH), 6.05 (br s, 1 H, 5-H), 6.36 (br s, 1 H, 2-H), 6.75 (br s, 1 H, 4-H), 6.91–7.33 (m, 18 H, ArH), 8.02 (br s, 1 H, NH); ^{13}C NMR (75.5 MHz, CDCl_3): $\delta = 48.6$ (d, Ar_2CH), 54.1 (tq, $J(\text{C},\text{F}) = 32.7 \text{ Hz}$, NCH_2CF_3), 109.2 (d, C-5), 116.9 (d, C-2), 118.1 (d, C-4), 120.5, 121.7, 122.2, 129.4, 129.5 (5 d, Ar), 125.3 (sq, $J = 279.4 \text{ Hz}$, NCH_2CF_3), 127.1, 140.2, 145.4, 147.6 (4 s Ar), signal assignments are based on ^1H , ^1H - and ^1H , ^{13}C -COSY, gHMBC and NOESY experiments.



BKE073

44c

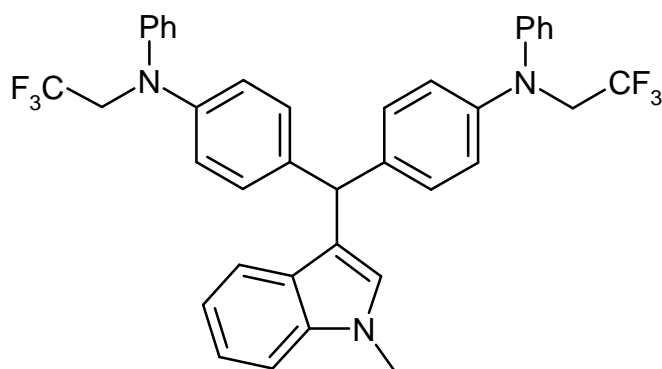
3-(Bis(4-(phenyl(2,2,2-trifluoroethyl)amino)phenyl)methyl)indole (45d) was obtained from indole (**45**) (150 mg, 1.28 mmol) and $(\text{pfa})_2\text{CH}^+ \text{BF}_4^-$ (75 mg, 0.13 mmol) following Procedure C. Column chromatography (silica gel/ CHCl_3) gave a colorless solid (55 mg, 70 %). ^1H NMR (300 MHz, CDCl_3): $\delta = 4.20$ (q, $J(\text{H},\text{F}) = 8.7 \text{ Hz}$, 4 H, NCH_2CF_3), 5.52 (br s, 1 H, Ar_2CH), 6.55 (br s, 1 H, 2-H), 6.83–7.23 (m, 22 H, ArH), 7.86 (br s, 1 H, NH); ^{13}C NMR (75.5 MHz, CDCl_3): $\delta = 47.4$ (d, Ar_2CH), 54.0 (tq, $J(\text{C},\text{F}) = 30.2 \text{ Hz}$, NCH_2CF_3), 111.0, 119.4, 119.9 (3d, Ar), 120.1 (s, Ar), 120.9, 121.4, 122.1, 122.4 (4 d, Ar), 123.8 (d, C-2), 125.2 (sq, $J(\text{C},\text{F}) = 283 \text{ Hz}$, NCH_2CF_3), 126.9 (s, Ar), 129.4, 129.9 (2 d, Ar), 136.7, 138.5, 145.6, 147.5 (4 s, Ar), signal assignments are based on ^1H , ^1H and ^1H , ^{13}C -COSY experiments; MS (70 eV, EI): m/z (%): 628 (35) $[\text{M}]^+$, 513 (100) $[\text{Ar}_2\text{CH}]^+$, 379 (18), 264 (75).



BKE064

45d

1-Methyl-3-(bis(4-(phenyl(2,2,2-trifluoroethyl)amino)phenyl)methyl)indole (46d) was obtained from *N*-methylindole (**46**) (360 mg, 2.74 mmol) and (pfa)₂CH⁺ BF₄⁻ (165 mg, 0.275 mmol) following Procedure C. Column chromatography (silica gel/CHCl₃) gave a colorless solid (38 mg, 22 %). ¹H NMR (300 MHz, CDCl₃): *d* = 3.65 (s, 3 H, NCH₃), 4.21 (q, *J*(H,F) = 8.7 Hz, 4 H, NCH₂CF₃), 5.52 (s, 1 H, Ar₂CH), 6.41 (s, 1 H, 2-H), 6.84–7.24 (m, 22 H, ArH), the presence of additional resonances indicate a contamination of the sample with ca. 15 % of **46**; ¹³C NMR (75.5 MHz, CDCl₃): *d* = 32.7 (q, NCH₃), 47.4 (d, Ar₂CH), 54.1 (tq, *J*(C,F) = 38 Hz, NCH₂CF₃), 109.1, 118.8, 119.9, 120.9, 121.4, 121.6, 122.4 (7 d, Ar), 128.5 (d, C-2), 129.4, 129.9 (2 d, Ar), 138.7, 145.6, 147.5 (3 s, Ar), because of the low signal-to-noise ratio CF₃ and three aromatic carbons could not be identified in the spectra, signal assignments are based on ¹H, ¹³C-COSY experiments; MS (70 eV, EI): *m/z* (%): 642 (32) [M]⁺, 513 (57) [Ar₂CH]⁺, 393 (44), 264 (42).

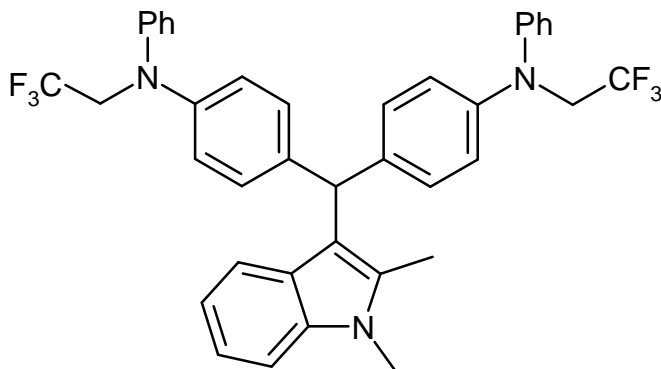


BKE065

46d

1,2-Dimethyl-3-(bis(4-(phenyl(2,2,2-trifluoroethyl)amino)phenyl)methyl)indole (47d) was obtained from 1,2-dimethylindole (**47**) (469 mg, 3.23 mmol) and (pfa)₂CH⁺ BF₄⁻ (194 mg, 0.323 mmol) following Procedure C. Column chromatography (silica gel/CHCl₃) gave a colorless solid (72 mg, 34 %). ¹H NMR (300 MHz, CDCl₃): *d* = 2.19 (s, 3 H, 2-CH₃), 3.57 (s,

3 H, NCH₃), 4.18 (q, $J(\text{H,F}) = 8.7$ Hz, 4 H, NCH₂CF₃), 5.61 (s, 1 H, Ar₂CH), 6.83–7.19 (m, 22 H, ArH), the presence of additional resonances indicate a contamination of the sample with ca. 15 % of **6c**; ¹³C NMR (75.5 MHz, CDCl₃): $\delta = 10.7$ (q, 2-CH₃), 29.5 (q, NCH₃), 46.7 (d, Ar₂CH), 54.0 (tq, $J(\text{C,F}) = 30.2$ Hz, NCH₂CF₃), 108.6 (d, Ar), 113.5 (s, Ar), 118.7, 119.5, 120.2, 120.3, 122.0 (5 d, Ar), 125.2 (sq, $J(\text{C,F}) = 287$ Hz, NCH₂CF₃), 127.3 (s, Ar), 129.3, 130.2 (2 d, Ar), 133.7, 136.7, 139.1, 145.3, 147.7 (5 s, Ar); MS (70 eV, EI): m/z (%): 657 (38) [M⁺], 513 (100) [Ar₂CH⁺], 407 (61), 264 (14).



BKE066

47d

10.3.5 Concentrations and rate constants of the individual kinetic runs

Table 10.28: 1-(*N*-Pyrrolidino)cyclopentene (**21**) and (lil)₂CH⁺ BF₄⁻ in CH₂Cl₂ at $\lambda = 640$ nm (Stopped flow).

No.	[<i>El</i>] ₀ / M	[<i>Nuc</i>] ₀ / M	[<i>Nuc</i>] ₀ /[<i>El</i>] ₀	<i>T</i> / °C	$k_2 / \text{M}^{-1} \text{s}^{-1}$
011200-F	8.456×10^{-6}	1.436×10^{-4}	17	20.0	1.251×10^5
011200-B	8.456×10^{-6}	2.871×10^{-4}	34	20.0	1.245×10^5
011200-C	8.456×10^{-6}	4.307×10^{-4}	51	20.0	1.307×10^5
011200-D	8.456×10^{-6}	5.743×10^{-4}	68	20.0	1.203×10^5
011200-E	8.456×10^{-6}	7.178×10^{-4}	85	20.0	1.290×10^5

$$\bar{k}_2 (20 \text{ }^\circ\text{C}) = (1.259 \pm 0.037) \times 10^5 \text{ M}^{-1} \text{ s}^{-1}$$

Table 10.29: 1-(*N*-Pyrrolidino)cyclopentene (**21**) and (jul)₂CH⁺ BF₄⁻ in CH₂Cl₂ at λ = 640 nm (Stopped flow).

No.	[<i>EL</i>] ₀ / M	[<i>Nuc</i>] ₀ / M	[<i>Nuc</i>] ₀ /[<i>EL</i>] ₀	<i>T</i> / °C	<i>k</i> ₂ / M ⁻¹ s ⁻¹
011200-M	7.130 × 10 ⁻⁶	1.425 × 10 ⁻⁴	20	20.0	3.387 × 10 ⁵
011200-O	7.130 × 10 ⁻⁶	2.851 × 10 ⁻⁴	40	20.0	3.171 × 10 ⁵
011200-I	7.130 × 10 ⁻⁶	4.276 × 10 ⁻⁴	60	20.0	3.182 × 10 ⁵
011200-J	7.130 × 10 ⁻⁶	5.702 × 10 ⁻⁴	80	20.0	3.459 × 10 ⁵
011200-K	7.130 × 10 ⁻⁶	7.127 × 10 ⁻⁴	100	20.0	3.419 × 10 ⁵

$$\bar{k}_2 (20\text{ °C}) = (3.324 \pm 0.122) \times 10^5 \text{ M}^{-1} \text{ s}^{-1}$$

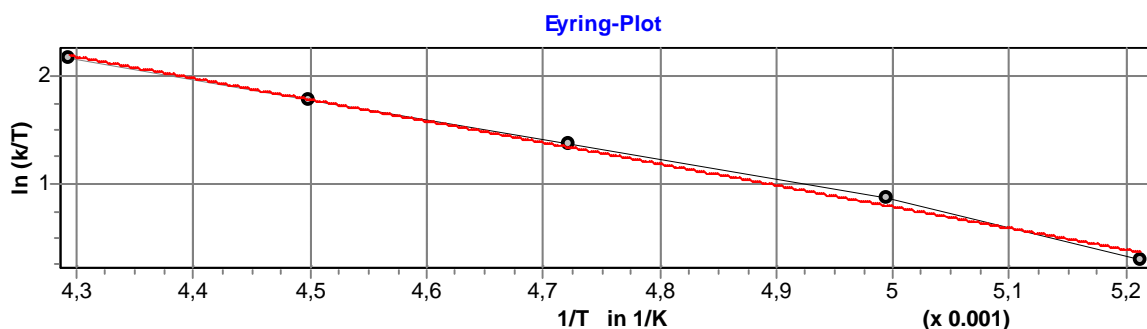
Table 10.30: 1-(*N*-Pyrrolidino)cyclopentene (**21**) and (thq)₂CH⁺ BF₄⁻ in CH₂Cl₂ at λ = 628 nm (Stopped flow).

No.	[<i>EL</i>] ₀ / M	[<i>Nuc</i>] ₀ / M	[<i>Nuc</i>] ₀ /[<i>EL</i>] ₀	<i>T</i> / °C	<i>k</i> ₂ / M ⁻¹ s ⁻¹
100501-D	5.099 × 10 ⁻⁶	1.482 × 10 ⁻⁵	3.4	20.0	4.707 × 10 ⁶
100501-B	5.099 × 10 ⁻⁶	2.351 × 10 ⁻⁵	5.1	20.0	4.112 × 10 ⁶
100501-E	5.099 × 10 ⁻⁶	3.220 × 10 ⁻⁵	6.8	20.0	4.698 × 10 ⁶
100501-A	5.099 × 10 ⁻⁶	4.088 × 10 ⁻⁵	8.5	20.0	4.176 × 10 ⁶
100501-C	5.099 × 10 ⁻⁶	4.957 × 10 ⁻⁵	10	20.0	4.693 × 10 ⁶

$$\bar{k}_2 (20\text{ °C}) = (4.477 \pm 0.273) \times 10^6 \text{ M}^{-1} \text{ s}^{-1}$$

Table 10.31: 1-(*N*-Pyrrolidino)cyclohexene (**22**) and (lil)₂CH⁺ BF₄⁻ in CH₂Cl₂ at λ = 640 nm (Schölly).

No.	[<i>EL</i>] ₀ / M	[<i>Nuc</i>] ₀ / M	[<i>Nuc</i>] ₀ /[<i>EL</i>] ₀	Conv. / %	<i>T</i> / °C	<i>k</i> ₂ / M ⁻¹ s ⁻¹
241100.PA1	2.407 × 10 ⁻⁵	1.500 × 10 ⁻³	62	53	-81.3	2.581 × 10 ²
241100.PA2	2.110 × 10 ⁻⁵	5.258 × 10 ⁻⁴	25	62	-72.9	4.786 × 10 ²
241100.PA3	3.194 × 10 ⁻⁵	6.124 × 10 ⁻⁴	19	55	-61.4	8.234 × 10 ²
241100.PA4	3.355 × 10 ⁻⁵	3.859 × 10 ⁻⁴	12	69	-50.9	1.304 × 10 ³
241100.PA5	3.137 × 10 ⁻⁵	1.804 × 10 ⁻⁴	6	71	-40.2	2.006 × 10 ³



Eyring parameters:

$$\Delta H^\ddagger = 16.426 \pm 0.702 \text{ kJ mol}^{-1}$$

$$\Delta S^\ddagger = -108.901 \pm 3.341 \text{ J mol}^{-1} \text{ K}^{-1}$$

$$r^2 = 0.9945$$

Arrhenius parameters:

$$E_a = 18.180 \pm 0.681 \text{ kJ mol}^{-1}$$

$$\ln A = 17.016 \pm 0.390$$

$$r^2 = 0.9958$$

$$k_2 (20^\circ\text{C}) = (1.482 \pm 0.167) \times 10^4 \text{ M}^{-1} \text{ s}^{-1}$$

Table 10.32: 1-(*N*-Pyrrolidino)cyclohexene (**22**) and (jul)₂CH⁺ BF₄⁻ in CH₂Cl₂ at λ = 640 nm (Stopped flow).

No.	[<i>EL</i>] ₀ / M	[<i>Nuc</i>] ₀ / M	[<i>Nuc</i>] ₀ /[<i>EL</i>] ₀	<i>T</i> / °C	<i>k</i> ₂ / M ⁻¹ s ⁻¹
021200-F	6.698 × 10 ⁻⁶	1.386 × 10 ⁻⁴	21	20.0	4.183 × 10 ⁴
021200-I	6.698 × 10 ⁻⁶	2.079 × 10 ⁻⁴	31	20.0	4.722 × 10 ⁴
021200-B	6.698 × 10 ⁻⁶	2.772 × 10 ⁻⁴	41	20.0	4.451 × 10 ⁴
021200-J	6.698 × 10 ⁻⁶	3.464 × 10 ⁻⁴	52	20.0	4.841 × 10 ⁴
021200-C	6.698 × 10 ⁻⁶	4.157 × 10 ⁻⁴	62	20.0	4.732 × 10 ⁴

$$\bar{k}_2 (20^\circ\text{C}) = (4.586 \pm 0.239) \times 10^4 \text{ M}^{-1} \text{ s}^{-1}$$

Table 10.33: 1-(*N*-Pyrrolidino)cyclohexene (**22**) and (thq)₂CH⁺ BF₄⁻ in CH₂Cl₂ at λ = 628 nm (Stopped flow).

No.	[<i>EL</i>] ₀ / M	[<i>Nuc</i>] ₀ / M	[<i>Nuc</i>] ₀ /[<i>EL</i>] ₀	<i>T</i> / °C	<i>k</i> ₂ / M ⁻¹ s ⁻¹
030501-C	6.119 × 10 ⁻⁶	6.565 × 10 ⁻⁵	11	20.0	7.508 × 10 ⁵
030501-B	6.119 × 10 ⁻⁶	1.313 × 10 ⁻⁴	22	20.0	7.000 × 10 ⁵
030501-A	6.119 × 10 ⁻⁶	2.626 × 10 ⁻⁴	43	20.0	7.377 × 10 ⁵

$$\bar{k}_2 (20^\circ\text{C}) = (7.295 \pm 0.215) \times 10^5 \text{ M}^{-1} \text{ s}^{-1}$$

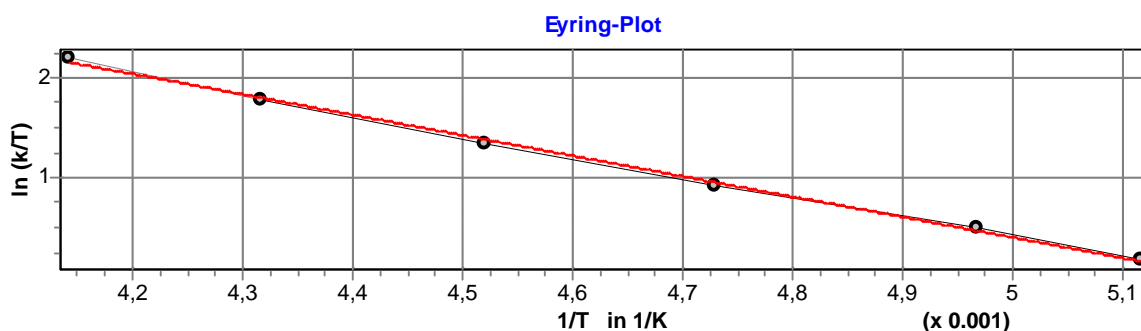
Table 10.34: 1-(*N*-Pyrrolidino)cyclohexene (**22**) and (dma)₂CH⁺ BF₄⁻ in CH₂Cl₂ at λ = 613 nm (Stopped flow).

No.	[<i>EL</i>] ₀ / M	[<i>Nuc</i>] ₀ / M	[<i>Nuc</i>] ₀ /[<i>EL</i>] ₀	<i>T</i> / °C	<i>k</i> ₂ / M ⁻¹ s ⁻¹
160501-D	5.033 × 10 ⁻⁶	1.244 × 10 ⁻⁵	3.0	20.0	4.972 × 10 ⁶
160501-B	5.033 × 10 ⁻⁶	2.241 × 10 ⁻⁵	5.0	20.0	5.438 × 10 ⁶
160501-C	5.033 × 10 ⁻⁶	3.238 × 10 ⁻⁵	6.9	20.0	5.755 × 10 ⁶
160501-A	5.033 × 10 ⁻⁶	4.733 × 10 ⁻⁵	9.9	20.0	5.172 × 10 ⁶

$$\bar{k}_2 (20\text{ °C}) = (5.334 \pm 0.294) \times 10^6 \text{ M}^{-1} \text{ s}^{-1}$$

Table 10.35: 1-(*N*-Piperidino)cyclopentene (**23**) and (lil)₂CH⁺ BF₄⁻ in CH₂Cl₂ at λ = 640 nm (Schölly).

No.	[<i>EL</i>] ₀ / M	[<i>Nuc</i>] ₀ / M	[<i>Nuc</i>] ₀ /[<i>EL</i>] ₀	Conv. / %	<i>T</i> / °C	<i>k</i> ₂ / M ⁻¹ s ⁻¹
100500.PA1	4.658 × 10 ⁻⁵	6.218 × 10 ⁻⁴	13	74	-77.7	2.301 × 10 ²
100500.PA2	5.053 × 10 ⁻⁵	6.745 × 10 ⁻⁴	13	60	-71.8	3.297 × 10 ²
100500.PA3	4.417 × 10 ⁻⁵	5.527 × 10 ⁻⁴	13	46	-61.7	5.338 × 10 ²
100500.PA5	4.738 × 10 ⁻⁵	4.744 × 10 ⁻⁴	10	74	-51.9	8.379 × 10 ²
100500.PA7	5.150 × 10 ⁻⁵	2.644 × 10 ⁻⁴	5	61	-41.5	1.383 × 10 ³
100500.PA8	4.031 × 10 ⁻⁵	2.690 × 10 ⁻⁴	7	35	-31.7	2.196 × 10 ³



Eyring parameters:

$$\Delta H^\ddagger = 17.128 \pm 0.401 \text{ kJ mol}^{-1}$$

$$\Delta S^\ddagger = -108.645 \pm 1.862 \text{ J mol}^{-1} \text{ K}^{-1}$$

$$r^2 = 0.9978$$

Arrhenius parameters:

$$E_a = 18.928 \pm 0.423 \text{ kJ mol}^{-1}$$

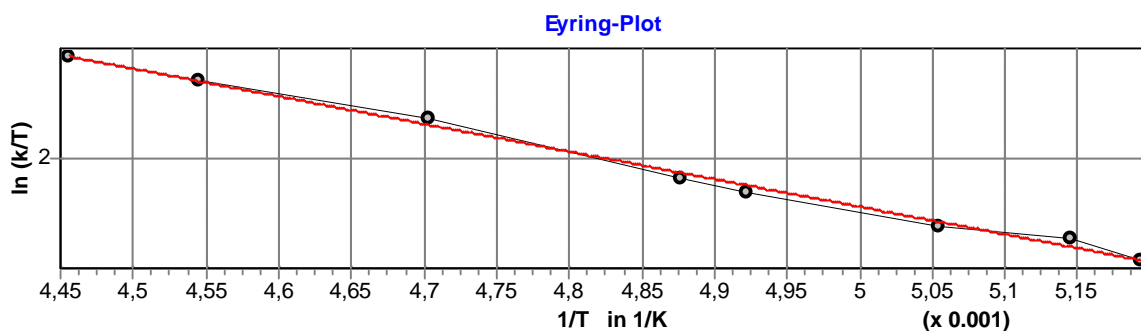
$$\ln A = 17.073 \pm 0.236$$

$$r^2 = 0.9980$$

$$k_2 (20\text{ °C}) = (1.146 \pm 0.067) \times 10^4 \text{ M}^{-1} \text{ s}^{-1}$$

Table 10.36: 1-(*N*-Piperidino)cyclopentene (**23**) and (jul)₂CH⁺ BF₄⁻ in CH₂Cl₂ at λ = 640 nm (Schölly).

No.	[<i>El</i>] ₀ / M	[<i>Nuc</i>] ₀ / M	[<i>Nuc</i>] ₀ /[<i>El</i>] ₀	Conv. / %	<i>T</i> / °C	<i>k</i> ₂ / M ⁻¹ s ⁻¹
161100.PA0	2.200 × 10 ⁻⁵	1.172 × 10 ⁻³	53	65	-80.6	6.366 × 10 ²
161100.PA1	1.975 × 10 ⁻⁵	4.209 × 10 ⁻⁴	21	60	-78.8	7.672 × 10 ²
161100.PA2	2.636 × 10 ⁻⁵	5.617 × 10 ⁻⁴	21	41	-75.3	8.529 × 10 ²
161100.PA3	2.260 × 10 ⁻⁵	3.854 × 10 ⁻⁴	17	33	-70.0	1.141 × 10 ³
161100.PA4	4.256 × 10 ⁻⁵	4.883 × 10 ⁻⁴	11	73	-68.1	1.296 × 10 ³
161100.PA5	2.835 × 10 ⁻⁵	3.253 × 10 ⁻⁴	11	55	-60.5	2.145 × 10 ³
161100.PA6	3.815 × 10 ⁻⁵	3.127 × 10 ⁻⁴	8	48	-53.1	2.964 × 10 ³
161100.PA7	3.427 × 10 ⁻⁵	1.685 × 10 ⁻⁴	5	53	-48.7	3.665 × 10 ³



Eyring parameters:

$$\Delta H^\ddagger = 17.969 \pm 0.556 \text{ kJ mol}^{-1}$$

$$\Delta S^\ddagger = -94.280 \pm 2.707 \text{ J mol}^{-1} \text{ K}^{-1}$$

$$r^2 = 0.9943$$

Arrhenius parameters:

$$E_a = 19.695 \pm 0.561 \text{ kJ mol}^{-1}$$

$$\ln A = 18.757 \pm 0.329$$

$$r^2 = 0.9952$$

$$k_2 (20 \text{ °C}) = (4.565 \pm 0.444) \times 10^4 \text{ M}^{-1} \text{ s}^{-1}$$

Table 10.37: 1-(*N*-Piperidino)cyclopentene (**23**) and (thq)₂CH⁺ BF₄⁻ in CH₂Cl₂ at λ = 624 nm (Stopped flow).

No.	[<i>EL</i>] ₀ / M	[<i>Nuc</i>] ₀ / M	[<i>Nuc</i>] ₀ /[<i>EL</i>] ₀	<i>T</i> / °C	<i>k</i> ₂ / M ⁻¹ s ⁻¹
171100-A	1.963 × 10 ⁻⁵	2.034 × 10 ⁻⁴	10	20.0	4.333 × 10 ⁵
171100-B	1.963 × 10 ⁻⁵	4.067 × 10 ⁻⁴	21	20.0	4.429 × 10 ⁵
171100-C	1.963 × 10 ⁻⁵	6.101 × 10 ⁻⁴	31	20.0	4.455 × 10 ⁵
171100-D	1.963 × 10 ⁻⁵	8.135 × 10 ⁻⁴	41	20.0	4.451 × 10 ⁵
171100-E	1.963 × 10 ⁻⁵	1.017 × 10 ⁻⁴	52	20.0	4.538 × 10 ⁵

$$\bar{k}_2(20\text{ °C}) = (4.441 \pm 0.066) \times 10^5 \text{ M}^{-1} \text{ s}^{-1}$$

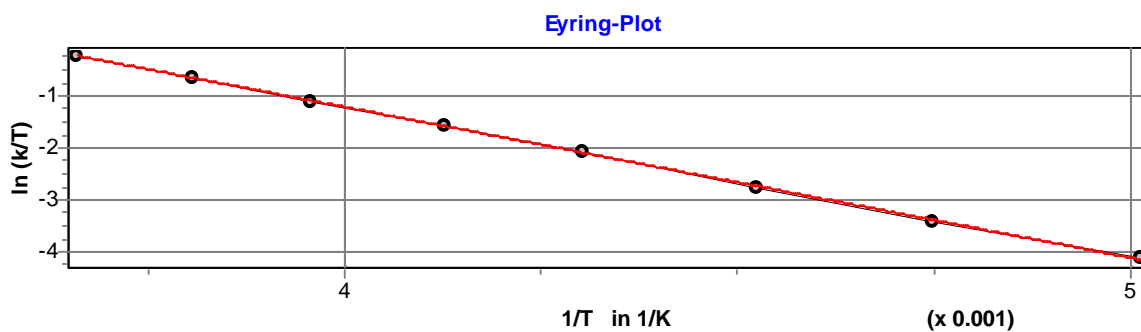
Table 10.38: 1-(*N*-Piperidino)cyclopentene (**23**) and (dma)₂CH⁺ BF₄⁻ in CH₂Cl₂ at λ = 613 nm (Stopped flow).

No.	[<i>EL</i>] ₀ / M	[<i>Nuc</i>] ₀ / M	[<i>Nuc</i>] ₀ /[<i>EL</i>] ₀	<i>T</i> / °C	<i>k</i> ₂ / M ⁻¹ s ⁻¹
220301-C	3.351 × 10 ⁻⁶	1.845 × 10 ⁻⁵	6	20.0	3.766 × 10 ⁶
220301-B	3.351 × 10 ⁻⁶	3.074 × 10 ⁻⁵	9	20.0	3.605 × 10 ⁶
220301-D	3.351 × 10 ⁻⁶	4.304 × 10 ⁻⁵	13	20.0	3.703 × 10 ⁶
220301-A	3.351 × 10 ⁻⁶	6.149 × 10 ⁻⁵	18	20.0	3.656 × 10 ⁶

$$\bar{k}_2(20\text{ °C}) = (3.683 \pm 0.059) \times 10^6 \text{ M}^{-1} \text{ s}^{-1}$$

Table 10.39: 1-(*N*-Morpholino)cyclopentene (**25**) and (lil)₂CH⁺ BF₄⁻ in CH₂Cl₂ at λ = 640 nm (Schölly).

No.	[<i>EL</i>] ₀ / M	[<i>Nuc</i>] ₀ / M	[<i>Nuc</i>] ₀ /[<i>EL</i>] ₀	Conv. / %	<i>T</i> / °C	<i>k</i> ₂ / M ⁻¹ s ⁻¹
040500.PA0	3.707 × 10 ⁻⁵	1.173 × 10 ⁻³	32	84	-73.7	3.151
040500.PA1	3.123 × 10 ⁻⁵	7.904 × 10 ⁻⁴	25	84	-62.6	6.784
040500.PA2	2.802 × 10 ⁻⁵	4.433 × 10 ⁻⁴	16	86	-52.1	1.385 × 10 ¹
040500.PA3	2.455 × 10 ⁻⁵	7.768 × 10 ⁻⁴	32	93	-40.8	2.848 × 10 ¹
040500.PA5	2.623 × 10 ⁻⁵	6.639 × 10 ⁻⁴	25	84	-30.8	4.988 × 10 ¹
040500.PA6	2.382 × 10 ⁻⁵	4.522 × 10 ⁻⁴	19	90	-20.4	8.150 × 10 ¹
040500.PA7	2.468 × 10 ⁻⁵	3.904 × 10 ⁻⁴	16	66	-10.5	1.358 × 10 ²
040500.PA8	2.743 × 10 ⁻⁵	6.941 × 10 ⁻⁴	25	71	0.2	2.135 × 10 ²



Eyring parameters:

$$\Delta H^\ddagger = 24.099 \pm 0.154 \text{ kJ mol}^{-1}$$

$$\Delta S^\ddagger = -111.413 \pm 0.661 \text{ J mol}^{-1} \text{ K}^{-1}$$

$$r^2 = 0.9998$$

Arrhenius parameters:

$$E_a = 26.033 \pm 0.164 \text{ kJ mol}^{-1}$$

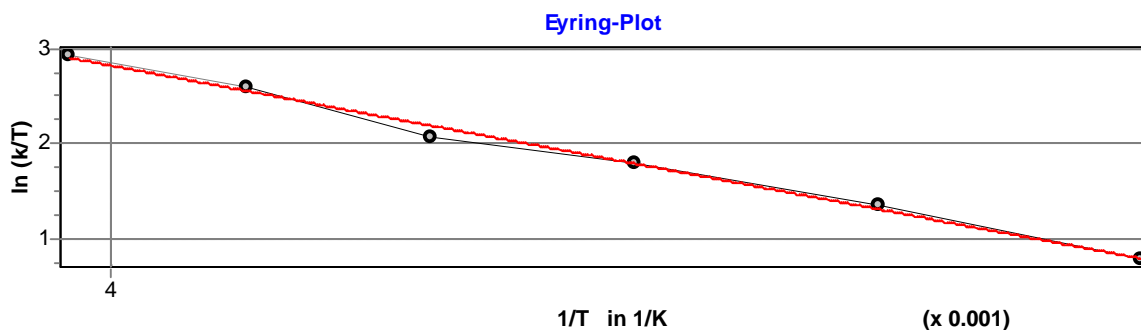
$$\ln A = 16.814 \pm 0.085$$

$$r^2 = 0.9998$$

$$k_2 (20 \text{ }^\circ\text{C}) = (4.703 \pm 0.075) \times 10^2 \text{ M}^{-1} \text{ s}^{-1}$$

Table 10.40: 1-(*N*-Morpholino)cyclopentene (**25**) and $(\text{thq})_2\text{CH}^+ \text{BF}_4^-$ in CH_2Cl_2 at $\lambda = 640$ nm (Schölly).

No.	$[\text{El}]_0 / \text{M}$	$[\text{Nuc}]_0 / \text{M}$	$[\text{Nuc}]_0/[\text{El}]_0$	Conv. / %	$T / \text{ }^\circ\text{C}$	$k_2 / \text{M}^{-1} \text{s}^{-1}$
080520.PA1	2.363×10^{-5}	2.122×10^{-4}	9	85	-71.7	4.398×10^2
080520.PA2	3.623×10^{-5}	4.163×10^{-4}	12	66	-61.2	8.128×10^2
080520.PA4	2.476×10^{-5}	1.779×10^{-4}	7	66	-50.5	1.345×10^3
080520.PA5	4.099×10^{-5}	2.265×10^{-4}	6	56	-40.6	1.846×10^3
080520.PA6	2.423×10^{-5}	1.045×10^{-4}	4	51	-30.9	3.215×10^3
080520.PA7	3.374×10^{-5}	1.118×10^{-4}	3	47	-20.7	4.738×10^3



Eyring parameters:

$$\Delta H^\ddagger = 17.550 \pm 0.652 \text{ kJ mol}^{-1}$$

$$\Delta S^\ddagger = -103.905 \pm 2.896 \text{ J mol}^{-1} \text{ K}^{-1}$$

$$r^2 = 0.9945$$

Arrhenius parameters:

$$E_a = 19.419 \pm 0.663 \text{ kJ mol}^{-1}$$

$$\ln A = 17.682 \pm 0.354$$

$$r^2 = 0.9954$$

$$k_2 (20 \text{ }^\circ\text{C}) = (1.705 \pm 0.136) \times 10^4 \text{ M}^{-1} \text{ s}^{-1}$$

Table 10.41: 1-(*N*-Morpholino)cyclopentene (**25**) and (dma)₂CH⁺ BF₄⁻ in CH₂Cl₂ at λ = 613 nm (Stopped flow).

No.	[<i>EL</i>] ₀ / M	[<i>Nuc</i>] ₀ / M	[<i>Nuc</i>] ₀ /[<i>EL</i>] ₀	<i>T</i> / °C	<i>k</i> ₂ / M ⁻¹ s ⁻¹
190401-B	5.080 × 10 ⁻⁶	8.628 × 10 ⁻⁵	17	20.0	2.323 × 10 ⁵
190401-A	5.080 × 10 ⁻⁶	1.726 × 10 ⁻⁴	34	20.0	2.557 × 10 ⁵
190401-C	5.080 × 10 ⁻⁶	2.588 × 10 ⁻⁴	51	20.0	2.421 × 10 ⁵
190401-D	5.080 × 10 ⁻⁶	3.451 × 10 ⁻⁴	68	20.0	2.446 × 10 ⁵

$$\bar{k}_2 (20 \text{ }^\circ\text{C}) = (2.437 \pm 0.083) \times 10^5 \text{ M}^{-1} \text{ s}^{-1}$$

Table 10.42: 1-(*N*-Morpholino)cyclopentene (**25**) and (mpa)₂CH⁺ BF₄⁻ in CH₂Cl₂ at λ = 622 nm (Stopped flow).

No.	[<i>EL</i>] ₀ / M	[<i>Nuc</i>] ₀ / M	[<i>Nuc</i>] ₀ /[<i>EL</i>] ₀	<i>T</i> / °C	<i>k</i> ₂ / M ⁻¹ s ⁻¹
150501-C	4.911 × 10 ⁻⁶	3.733 × 10 ⁻⁵	8	20.0	9.585 × 10 ⁵
150501-B	4.911 × 10 ⁻⁶	7.466 × 10 ⁻⁵	15	20.0	9.952 × 10 ⁵
150501-E	4.911 × 10 ⁻⁶	1.120 × 10 ⁻⁴	23	20.0	9.585 × 10 ⁵
150501-F	4.911 × 10 ⁻⁶	1.493 × 10 ⁻⁴	30	20.0	9.669 × 10 ⁵
150501-D	4.911 × 10 ⁻⁶	1.867 × 10 ⁻⁴	38	20.0	9.742 × 10 ⁵

$$\bar{k}_2 (20 \text{ }^\circ\text{C}) = (9.707 \pm 0.136) \times 10^5 \text{ M}^{-1} \text{ s}^{-1}$$

Table 10.43: (*trans*)-1-(*N*-Morpholino)propene (**27**) and (dpa)₂CH⁺ BF₄⁻ in CH₂Cl₂ at λ = 672 nm (Stopped flow).

No.	[<i>El</i>] ₀ / M	[<i>Nuc</i>] ₀ / M	[<i>Nuc</i>] ₀ /[<i>El</i>] ₀	<i>T</i> / °C	<i>k</i> ₂ / M ⁻¹ s ⁻¹
270801-E	4.962 × 10 ⁻⁶	5.488 × 10 ⁻⁵	11	20.0	7.722 × 10 ⁵
270801-D	4.962 × 10 ⁻⁶	1.098 × 10 ⁻⁴	22	20.0	7.909 × 10 ⁵
270801-A	4.962 × 10 ⁻⁶	1.646 × 10 ⁻⁴	33	20.0	7.380 × 10 ⁵
270801-B	4.962 × 10 ⁻⁶	2.195 × 10 ⁻⁴	44	20.0	7.250 × 10 ⁵
270801-C	4.962 × 10 ⁻⁶	2.744 × 10 ⁻⁴	55	20.0	6.960 × 10 ⁵

$$\bar{k}_2(20\text{ °C}) = (7.444 \pm 0.338) \times 10^5 \text{ M}^{-1} \text{ s}^{-1}$$

Table 10.44: (*cis*)-1-(*N*-Morpholino)propene^[a] (**28**) and (dpa)₂CH⁺ BF₄⁻ in CH₂Cl₂ at λ = 672 nm (Stopped flow).

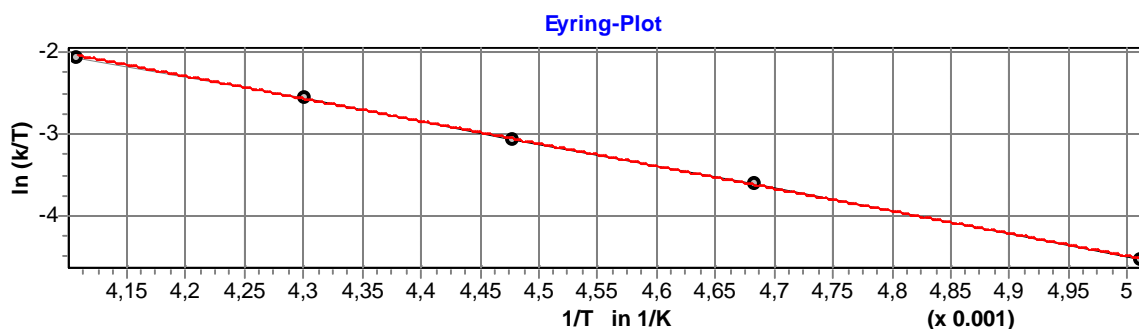
No.	[<i>El</i>] ₀ / M	[<i>Nuc</i>] ₀ / M	[<i>Nuc</i>] ₀ /[<i>El</i>] ₀	<i>T</i> / °C	<i>k</i> ₂ / M ⁻¹ s ⁻¹
170801-B	4.650 × 10 ⁻⁶	5.394 × 10 ⁻⁵	12	20.0	1.148 × 10 ⁶
170801-C	4.650 × 10 ⁻⁶	1.079 × 10 ⁻⁴	23	20.0	1.036 × 10 ⁶
170801-A	4.650 × 10 ⁻⁶	1.618 × 10 ⁻⁴	35	20.0	9.775 × 10 ⁵
170801-D	4.650 × 10 ⁻⁶	2.157 × 10 ⁻⁴	46	20.0	1.141 × 10 ⁶
170801-E	4.650 × 10 ⁻⁶	2.697 × 10 ⁻⁴	58	20.0	1.046 × 10 ⁶

^[a] contaminated by 11 % of (*trans*)-1-(*N*-morpholino)propene (**27**) (¹H NMR)

$$\bar{k}_2(20\text{ °C}) = (1.070 \pm 0.065) \times 10^6 \text{ M}^{-1} \text{ s}^{-1}$$

Table 10.45: (*N*-Morpholino)isobutylene (**29**) and (dma)₂CH⁺ BF₄⁻ in CH₂Cl₂ at λ = 600 nm (Schölly).

No.	[<i>El</i>] ₀ / M	[<i>Nuc</i>] ₀ / M	[<i>Nuc</i>] ₀ /[<i>El</i>] ₀	Conv. / %	<i>T</i> / °C	<i>k</i> ₂ / M ⁻¹ s ⁻¹
050701.PA1	6.349 × 10 ⁻⁵	2.314 × 10 ⁻³	37	81	-73.6	2.133
050701.PA2	6.314 × 10 ⁻⁵	2.301 × 10 ⁻³	37	77	-59.6	5.751
050701.PA3	5.656 × 10 ⁻⁵	3.298 × 10 ⁻³	58	57	-49.8	1.039 × 10 ¹
050701.PA4	5.801 × 10 ⁻⁵	2.537 × 10 ⁻³	44	61	-40.7	1.801 × 10 ¹
050701.PA5	6.162 × 10 ⁻⁵	1.797 × 10 ⁻³	29	51	-29.7	3.048 × 10 ¹



Eyring parameters:

$$\Delta H^\ddagger = 22.749 \pm 0.282 \text{ kJ mol}^{-1}$$

$$\Delta S^\ddagger = -121.183 \pm 1.276 \text{ J mol}^{-1} \text{ K}^{-1}$$

$$r^2 = 0.9995$$

Arrhenius parameters:

$$E_a = 24.575 \pm 0.260 \text{ kJ mol}^{-1}$$

$$\ln A = 15.580 \pm 0.142$$

$$r^2 = 0.9997$$

$$k_2 (20 \text{ }^\circ\text{C}) = (2.528 \pm 0.095) \times 10^2 \text{ M}^{-1} \text{ s}^{-1}$$

Table 10.46: (*N*-Morpholino)isobutylene (**29**) and $(\text{mpa})_2\text{CH}^+ \text{BF}_4^-$ in CH_2Cl_2 at $\lambda = 622 \text{ nm}$ (Stopped flow).

No.	$[\text{El}]_0 / \text{M}$	$[\text{Nuc}]_0 / \text{M}$	$[\text{Nuc}]_0/[\text{El}]_0$	$T / \text{ }^\circ\text{C}$	$k_{\text{eff}} / \text{s}^{-1}$
090701-E	9.735×10^{-6}	3.255×10^{-4}	33	20.0	1.250
090701-D	9.735×10^{-6}	6.509×10^{-4}	67	20.0	2.223
090701-A	9.735×10^{-6}	9.764×10^{-4}	100	20.0	3.274
090701-B	9.735×10^{-6}	1.302×10^{-3}	134	20.0	4.322
090701-C	9.735×10^{-6}	1.627×10^{-3}	167	20.0	5.611

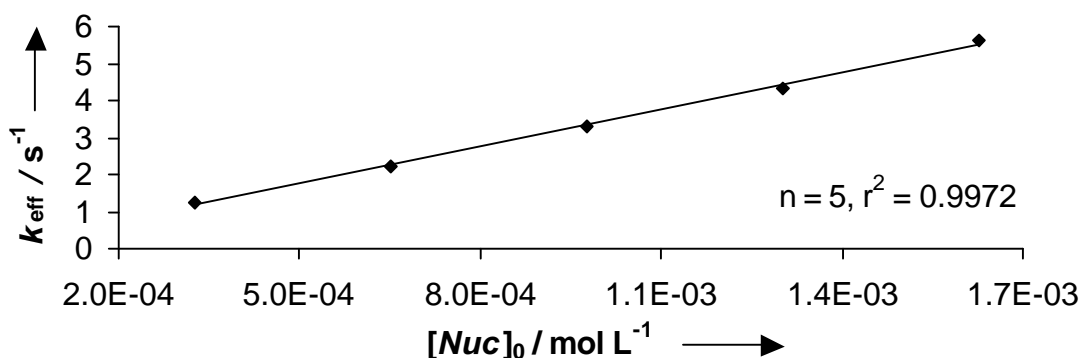


Figure 10.1: Plot of k_{eff} versus $[\text{Nuc}]_0$ ($n = 5$, $k_{\text{eff}} = (3.325 \times 10^3) \times [\text{Nuc}]_0 + 8.931 \times 10^{-2}$, $r^2 = 0.9972$).

$$k_2 (20\text{ }^\circ\text{C}) = 3.325 \times 10^3 \text{ L mol}^{-1} \text{ s}^{-1}$$

$$k_{-2} (20\text{ }^\circ\text{C}) = 8.931 \times 10^{-2} \text{ s}^{-1}$$

$$K (20\text{ }^\circ\text{C}) = 3.723 \times 10^4 \text{ L mol}^{-1}$$

Table 10.47: (*N*-Morpholino)isobutylene (**29**) and (dpa)₂CH⁺ BF₄⁻ in CH₂Cl₂ at λ = 672 nm (Stopped flow).

No.	[<i>El</i>] ₀ / M	[<i>Nuc</i>] ₀ / M	[<i>Nuc</i>] ₀ /[<i>El</i>] ₀	<i>T</i> / °C	<i>k</i> ₂ / M ⁻¹ s ⁻¹
030701-E	1.041 × 10 ⁻⁵	7.322 × 10 ⁻⁵	7	20.0	2.312 × 10 ⁴
030701-D	1.041 × 10 ⁻⁵	1.464 × 10 ⁻⁴	14	20.0	2.368 × 10 ⁴
030701-A	1.041 × 10 ⁻⁵	2.197 × 10 ⁻⁴	21	20.0	2.383 × 10 ⁴
030701-B	1.041 × 10 ⁻⁵	2.929 × 10 ⁻⁴	28	20.0	2.434 × 10 ⁴
030701-C	1.041 × 10 ⁻⁵	3.661 × 10 ⁻⁴	35	20.0	2.557 × 10 ⁴

$$\bar{k}_2 (20\text{ }^\circ\text{C}) = (2.411 \pm 0.083) \times 10^4 \text{ M}^{-1} \text{ s}^{-1}$$

Table 10.48: (*N*-Morpholino)isobutylene (**29**) and (mfa)₂CH⁺ BF₄⁻ in CH₂Cl₂ at λ = 593 nm (Stopped flow).

No.	[<i>El</i>] ₀ / M	[<i>Nuc</i>] ₀ / M	[<i>Nuc</i>] ₀ /[<i>El</i>] ₀	<i>T</i> / °C	<i>k</i> ₂ / M ⁻¹ s ⁻¹
030701-J	1.033 × 10 ⁻⁵	7.365 × 10 ⁻⁵	7	20.0	1.251 × 10 ⁵
030701-I	1.033 × 10 ⁻⁵	1.473 × 10 ⁻⁴	14	20.0	1.273 × 10 ⁵
030701-F	1.033 × 10 ⁻⁵	2.209 × 10 ⁻⁴	21	20.0	1.283 × 10 ⁵
030701-G	1.033 × 10 ⁻⁵	2.946 × 10 ⁻⁴	29	20.0	1.298 × 10 ⁵
030701-H	1.033 × 10 ⁻⁵	3.682 × 10 ⁻⁴	36	20.0	1.311 × 10 ⁵

$$\bar{k}_2 (20\text{ }^\circ\text{C}) = (1.283 \pm 0.021) \times 10^5 \text{ M}^{-1} \text{ s}^{-1}$$

Table 10.49: (*N*-Morpholino)isobutylene (**29**) and (pfa)₂CH⁺ BF₄⁻ in CH₂Cl₂ at λ = 601 nm (Stopped flow).

No.	[<i>EL</i>] ₀ / M	[<i>Nuc</i>] ₀ / M	[<i>Nuc</i>] ₀ /[<i>EL</i>] ₀	<i>T</i> / °C	<i>k</i> ₂ / M ⁻¹ s ⁻¹
030701-O	6.030 × 10 ⁻⁶	6.246 × 10 ⁻⁵	10	20.0	4.087 × 10 ⁵
030701-N	6.030 × 10 ⁻⁶	1.249 × 10 ⁻⁴	21	20.0	4.260 × 10 ⁵
030701-K	6.030 × 10 ⁻⁶	1.874 × 10 ⁻⁴	31	20.0	4.195 × 10 ⁵
030701-L	6.030 × 10 ⁻⁶	2.498 × 10 ⁻⁴	41	20.0	4.420 × 10 ⁵

$$\bar{k}_2 (20\text{ }^\circ\text{C}) = (4.240 \pm 0.121) \times 10^5 \text{ M}^{-1} \text{ s}^{-1}$$

Table 10.50: (*trans*)-*b*-(*N*-Morpholino)styrene (**30**) and (mpa)₂CH⁺ BF₄⁻ in CH₂Cl₂ at λ = 622 nm (Stopped flow).

No.	[<i>EL</i>] ₀ / M	[<i>Nuc</i>] ₀ / M	[<i>Nuc</i>] ₀ /[<i>EL</i>] ₀	<i>T</i> / °C	<i>k</i> ₂ / M ⁻¹ s ⁻¹
120701-I	6.099 × 10 ⁻⁶	5.041 × 10 ⁻⁴	83	20.0	1.626 × 10 ⁴
120701-K	6.099 × 10 ⁻⁶	7.561 × 10 ⁻⁴	124	20.0	1.476 × 10 ⁴
120701-J	6.099 × 10 ⁻⁶	1.008 × 10 ⁻³	165	20.0	1.371 × 10 ⁴

$$\bar{k}_2 (20\text{ }^\circ\text{C}) = (1.491 \pm 0.105) \times 10^4 \text{ M}^{-1} \text{ s}^{-1}$$

Table 10.51: (*trans*)-*b*-(*N*-Morpholino)styrene (**30**) and (dpa)₂CH⁺ BF₄⁻ in CH₂Cl₂ at λ = 672 nm (Stopped flow).

No.	[<i>EL</i>] ₀ / M	[<i>Nuc</i>] ₀ / M	[<i>Nuc</i>] ₀ /[<i>EL</i>] ₀	<i>T</i> / °C	<i>k</i> ₂ / M ⁻¹ s ⁻¹
120701-E	6.580 × 10 ⁻⁶	1.008 × 10 ⁻⁴	15	20.0	2.118 × 10 ⁵
120701-D	6.580 × 10 ⁻⁶	2.016 × 10 ⁻⁴	31	20.0	2.247 × 10 ⁵
120701-A	6.580 × 10 ⁻⁶	3.024 × 10 ⁻⁴	46	20.0	2.218 × 10 ⁵
120701-B	6.580 × 10 ⁻⁶	4.033 × 10 ⁻⁴	61	20.0	2.258 × 10 ⁵
120701-C	6.580 × 10 ⁻⁶	5.041 × 10 ⁻⁴	77	20.0	2.212 × 10 ⁵

$$\bar{k}_2 (20\text{ }^\circ\text{C}) = (2.210 \pm 0.050) \times 10^5 \text{ M}^{-1} \text{ s}^{-1}$$

Table 10.52: (*trans*)-**b**-(*N*-Morpholino)styrene (**30**) and (mfa)₂CH⁺ BF₄⁻ in CH₂Cl₂ at λ = 593 nm (Stopped flow).

No.	[<i>EL</i>] ₀ / M	[<i>Nuc</i>] ₀ / M	[<i>Nuc</i>] ₀ /[<i>EL</i>] ₀	<i>T</i> / °C	<i>k</i> ₂ / M ⁻¹ s ⁻¹
120701-G	9.005 × 10 ⁻⁶	5.041 × 10 ⁻⁵	6	20.0	1.128 × 10 ⁶
120701-F	9.005 × 10 ⁻⁶	1.008 × 10 ⁻⁴	11	20.0	1.075 × 10 ⁶
120701-H	9.005 × 10 ⁻⁶	2.016 × 10 ⁻⁴	22	20.0	9.943 × 10 ⁵

$$\bar{k}_2 (20\text{ °C}) = (1.066 \pm 0.055) \times 10^6 \text{ M}^{-1} \text{ s}^{-1}$$

Table 10.53: (*trans*)-**b**-(*N*-Morpholino)styrene (**30**) and (pfa)₂CH⁺ BF₄⁻ in CH₂Cl₂ at λ = 601 nm (Stopped flow).

No.	[<i>EL</i>] ₀ / M	[<i>Nuc</i>] ₀ / M	[<i>Nuc</i>] ₀ /[<i>EL</i>] ₀	<i>T</i> / °C	<i>k</i> ₂ / M ⁻¹ s ⁻¹
120701-M	6.823 × 10 ⁻⁶	5.041 × 10 ⁻⁵	7	20.0	3.995 × 10 ⁶
120701-N	6.823 × 10 ⁻⁶	7.057 × 10 ⁻⁵	10	20.0	3.675 × 10 ⁶
120701-L	6.823 × 10 ⁻⁶	1.008 × 10 ⁻⁴	15	20.0	3.481 × 10 ⁶

$$\bar{k}_2 (20\text{ °C}) = (3.717 \pm 0.212) \times 10^6 \text{ M}^{-1} \text{ s}^{-1}$$

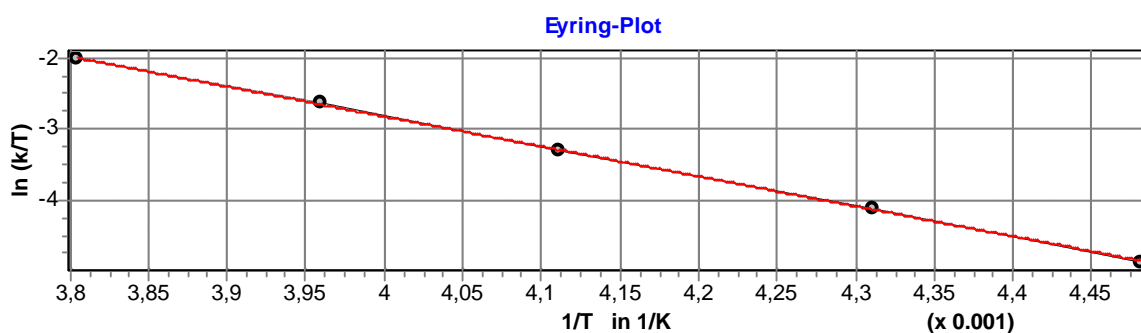
Table 10.54: **a**-(*N*-Morpholino)styrene (**31**) and (thq)₂CH⁺ BF₄⁻ in CH₂Cl₂ at λ = 640 nm (Schölly).

No.	[<i>EL</i>] ₀ / M	[<i>Nuc</i>] ₀ / M	[<i>Nuc</i>] ₀ /[<i>EL</i>] ₀	Conv. / %	<i>T</i> / °C	<i>k</i> ₂ / M ⁻¹ s ⁻¹
010601.PA2	2.987 × 10 ⁻⁵	4.332 × 10 ⁻⁴	15	78	20.0	2.347 × 10 ¹
010601.PA0	3.442 × 10 ⁻⁵	9.982 × 10 ⁻⁴	29	79	20.0	2.330 × 10 ¹
010601.PA1	2.929 × 10 ⁻⁵	2.124 × 10 ⁻³	73	70	20.0	2.356 × 10 ¹

$$\bar{k}_2 (20\text{ °C}) = (2.344 \pm 0.011) \times 10^1 \text{ M}^{-1} \text{ s}^{-1}$$

Table 10.55: *a*-(*N*-Morpholino)styrene (**31**) and (dma)₂CH⁺ BF₄⁻ in CH₂Cl₂ at λ = 600 nm (Schölly).

No.	[<i>El</i>] ₀ / M	[<i>Nuc</i>] ₀ / M	[<i>Nuc</i>] ₀ /[<i>El</i>] ₀	Conv. / %	<i>T</i> / °C	<i>k</i> ₂ / M ⁻¹ s ⁻¹
310501.PA1	3.767 × 10 ⁻⁵	1.023 × 10 ⁻³	27	68	-50.0	1.692
310501.PA2	4.421 × 10 ⁻⁵	1.200 × 10 ⁻³	27	79	-41.2	3.809
310501.PA3	3.919 × 10 ⁻⁵	8.513 × 10 ⁻⁴	22	80	-29.9	8.979
310501.PA4	3.160 × 10 ⁻⁵	5.148 × 10 ⁻⁴	16	76	-20.6	1.818 × 10 ¹
310501.PA5	3.088 × 10 ⁻⁵	3.354 × 10 ⁻⁴	11	81	-10.3	3.519 × 10 ¹



Eyring parameters:

$$\Delta H^\ddagger = 35.203 \pm 0.413 \text{ kJ mol}^{-1}$$

$$\Delta S^\ddagger = -80.197 \pm 1.709 \text{ J mol}^{-1} \text{ K}^{-1}$$

$$r^2 = 0.9996$$

Arrhenius parameters:

$$E_a = 37.213 \pm 0.396 \text{ kJ mol}^{-1}$$

$$\ln A = 20.604 \pm 0.197$$

$$r^2 = 0.9997$$

$$k_2 (20 \text{ °C}) = (2.111 \pm 0.076) \times 10^2 \text{ M}^{-1} \text{ s}^{-1}$$

Table 10.56: *a*-(*N*-Morpholino)styrene (**31**) and (mpa)₂CH⁺ BF₄⁻ in CH₂Cl₂ at λ = 622 nm (Stopped flow).

No.	[<i>El</i>] ₀ / M	[<i>Nuc</i>] ₀ / M	[<i>Nuc</i>] ₀ /[<i>El</i>] ₀	<i>T</i> / °C	<i>k</i> ₂ / M ⁻¹ s ⁻¹
300501-E	1.347 × 10 ⁻⁵	2.220 × 10 ⁻⁴	17	20.0	1.540 × 10 ³
300501-D	1.347 × 10 ⁻⁵	4.440 × 10 ⁻⁴	33	20.0	1.552 × 10 ³
300501-F	1.347 × 10 ⁻⁵	6.661 × 10 ⁻⁴	49	20.0	1.793 × 10 ³
300501-C	1.347 × 10 ⁻⁵	8.881 × 10 ⁻⁴	66	20.0	1.731 × 10 ³
300501-B	1.347 × 10 ⁻⁵	1.110 × 10 ⁻³	82	20.0	1.776 × 10 ³

$$\bar{k}_2 (20 \text{ °C}) = (1.678 \pm 0.110) \times 10^3 \text{ M}^{-1} \text{ s}^{-1}$$

Table 10.57: *a*-(*N*-Morpholino)styrene (**31**) and (dpa)₂CH⁺ BF₄⁻ in CH₂Cl₂ at λ = 672 nm (Stopped flow).

No.	[<i>El</i>] ₀ / M	[<i>Nuc</i>] ₀ / M	[<i>Nuc</i>] ₀ /[<i>El</i>] ₀	<i>T</i> / °C	<i>k</i> ₂ / M ⁻¹ s ⁻¹
290501-E	1.380 × 10 ⁻⁵	1.073 × 10 ⁻⁴	8	20.0	1.327 × 10 ⁴
290501-B	1.380 × 10 ⁻⁵	2.145 × 10 ⁻⁴	16	20.0	1.345 × 10 ⁴
290501-C	1.380 × 10 ⁻⁵	3.218 × 10 ⁻⁴	23	20.0	1.353 × 10 ⁴
290501-D	1.380 × 10 ⁻⁵	4.290 × 10 ⁻⁴	31	20.0	1.377 × 10 ⁴
290501-A	1.380 × 10 ⁻⁵	5.363 × 10 ⁻⁴	39	20.0	1.375 × 10 ⁴

$$\bar{k}_2 (20\text{ °C}) = (1.355 \pm 0.019) \times 10^4 \text{ M}^{-1} \text{ s}^{-1}$$

Table 10.58: *a*-(*N*-Morpholino)styrene (**31**) and (mfa)₂CH⁺ BF₄⁻ in CH₂Cl₂ at λ = 593 nm (Stopped flow).

No.	[<i>El</i>] ₀ / M	[<i>Nuc</i>] ₀ / M	[<i>Nuc</i>] ₀ /[<i>El</i>] ₀	<i>T</i> / °C	<i>k</i> ₂ / M ⁻¹ s ⁻¹
290501-J	7.292 × 10 ⁻⁶	1.073 × 10 ⁻⁴	15	20.0	6.428 × 10 ⁴
290501-F	7.292 × 10 ⁻⁶	2.145 × 10 ⁻⁴	29	20.0	6.512 × 10 ⁴
290501-I	7.292 × 10 ⁻⁶	3.218 × 10 ⁻⁴	44	20.0	6.737 × 10 ⁴
290501-H	7.292 × 10 ⁻⁶	4.290 × 10 ⁻⁴	59	20.0	6.763 × 10 ⁴
290501-G	7.292 × 10 ⁻⁶	5.363 × 10 ⁻⁴	74	20.0	6.940 × 10 ⁴

$$\bar{k}_2 (20\text{ °C}) = (6.676 \pm 0.184) \times 10^4 \text{ M}^{-1} \text{ s}^{-1}$$

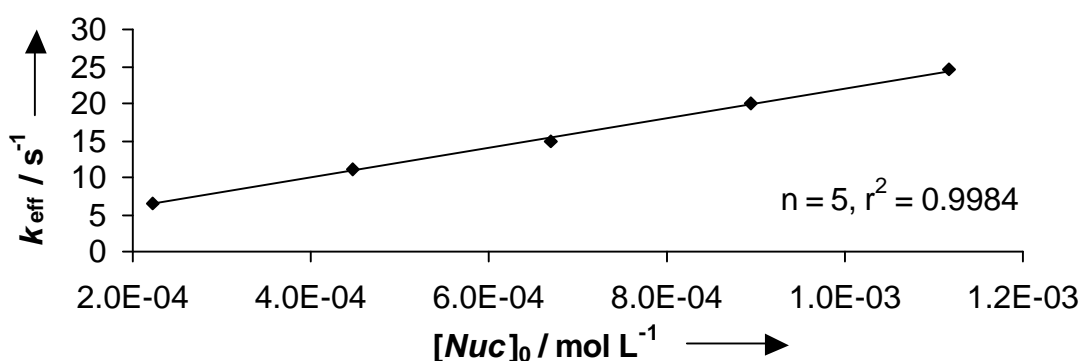
Table 10.59: *a*-(*N*-Morpholino)styrene (**31**) and (pfa)₂CH⁺ BF₄⁻ in CH₂Cl₂ at λ = 601 nm (Stopped flow).

No.	[<i>El</i>] ₀ / M	[<i>Nuc</i>] ₀ / M	[<i>Nuc</i>] ₀ /[<i>El</i>] ₀	<i>T</i> / °C	<i>k</i> ₂ / M ⁻¹ s ⁻¹
290501-O	5.251 × 10 ⁻⁶	1.073 × 10 ⁻⁴	20	20.0	2.403 × 10 ⁵
290501-K	5.251 × 10 ⁻⁶	2.145 × 10 ⁻⁴	41	20.0	2.352 × 10 ⁵
290501-N	5.251 × 10 ⁻⁶	3.218 × 10 ⁻⁴	61	20.0	2.515 × 10 ⁵
290501-M	5.251 × 10 ⁻⁶	4.290 × 10 ⁻⁴	82	20.0	2.573 × 10 ⁵
290501-L	5.251 × 10 ⁻⁶	5.363 × 10 ⁻⁴	102	20.0	2.611 × 10 ⁵

$$\bar{k}_2 (20\text{ °C}) = (2.491 \pm 0.099) \times 10^5 \text{ M}^{-1} \text{ s}^{-1}$$

Table 10.60: Ethyl (*trans*)-3-(*N*-morpholino)acrylate (**32**) and (pfa)₂CH⁺ BF₄⁻ in CH₂Cl₂ at λ = 601 nm (Stopped flow).

No.	[<i>EL</i>] ₀ / M	[<i>Nuc</i>] ₀ / M	[<i>Nuc</i>] ₀ /[<i>EL</i>] ₀	<i>T</i> / °C	<i>k</i> _{eff} / s ⁻¹
240701-E	6.397 × 10 ⁻⁶	2.234 × 10 ⁻⁴	35	20.0	6.459
240701-D	6.397 × 10 ⁻⁶	4.468 × 10 ⁻⁴	70	20.0	1.109 × 10 ¹
240701-A	6.397 × 10 ⁻⁶	6.702 × 10 ⁻⁴	105	20.0	1.490 × 10 ¹
240701-B	6.397 × 10 ⁻⁶	8.936 × 10 ⁻⁴	140	20.0	2.008 × 10 ¹
240701-C	6.397 × 10 ⁻⁶	1.117 × 10 ⁻³	175	20.0	2.452 × 10 ¹

**Figure 10.2:** Plot of *k*_{eff} versus [*Nuc*]₀ (n = 5, *k*_{eff} = (2.019 × 10⁴) × [*Nuc*]₀ + 1.874, r² = 0.9984).

$$k_2 (20\text{ }^\circ\text{C}) = 2.019 \times 10^4 \text{ M}^{-1} \text{ s}^{-1}$$

$$k_{-2} (20\text{ }^\circ\text{C}) = 1.874 \text{ s}^{-1}$$

$$K (20\text{ }^\circ\text{C}) = 1.077 \times 10^4 \text{ M}^{-1}$$

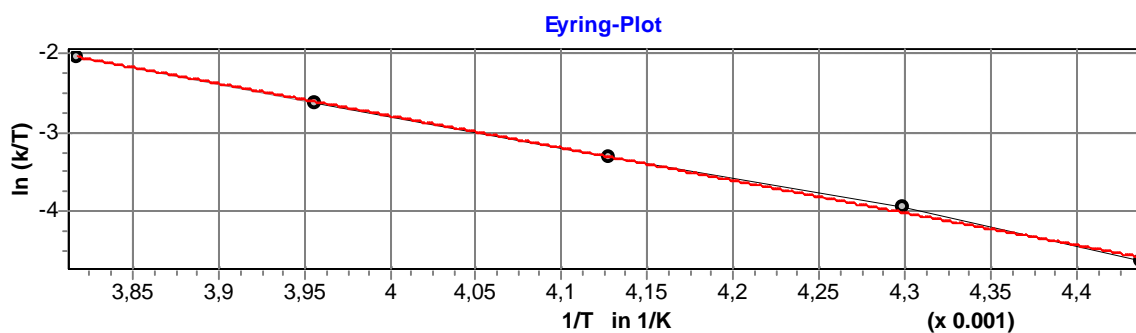
Table 10.61: Ethyl (*trans*)-3-(dimethylamino)acrylate (**33**) and (pfa)₂CH⁺ BF₄⁻ in CH₂Cl₂ at λ = 601 nm (Stopped flow).

No.	[<i>EL</i>] ₀ / M	[<i>Nuc</i>] ₀ / M	[<i>Nuc</i>] ₀ /[<i>EL</i>] ₀	<i>T</i> / °C	<i>k</i> ₂ / M ⁻¹ s ⁻¹
240801-B	5.397 × 10 ⁻⁶	1.589 × 10 ⁻⁴	30	20.0	1.128 × 10 ⁵
240801-C	5.397 × 10 ⁻⁶	2.384 × 10 ⁻⁴	44	20.0	1.027 × 10 ⁵
240801-D	5.397 × 10 ⁻⁶	3.179 × 10 ⁻⁴	59	20.0	1.039 × 10 ⁵
240801-E	5.397 × 10 ⁻⁶	3.974 × 10 ⁻⁴	74	20.0	1.064 × 10 ⁵
240801-G	5.397 × 10 ⁻⁶	5.563 × 10 ⁻⁴	103	20.0	1.112 × 10 ⁵

$$\bar{k}_2(20\text{ °C}) = (1.074 \pm 0.040) \times 10^5 \text{ M}^{-1} \text{ s}^{-1}$$

Table 10.62: 1-(Methylphenylamino)cyclopentene (**34**) and (lil)₂CH⁺ BF₄⁻ in CH₂Cl₂ at λ = 640 nm (Schölly).

No.	[EL] ₀ / M	[Nuc] ₀ / M	[Nuc] ₀ /[EL] ₀	Conv. / %	T / °C	k ₂ / M ⁻¹ s ⁻¹
210601.PA0	3.690 × 10 ⁻⁵	1.106 × 10 ⁻³	30	76	-47.8	2.182
210601.PA1	3.383 × 10 ⁻⁵	1.268 × 10 ⁻³	38	74	-40.5	4.464
210601.PA2	2.473 × 10 ⁻⁵	8.473 × 10 ⁻⁴	34	70	-30.9	8.740
210601.PA3	3.068 × 10 ⁻⁵	6.898 × 10 ⁻⁴	23	65	-20.4	1.820 × 10 ¹
210601.PA4	2.584 × 10 ⁻⁵	6.640 × 10 ⁻⁴	26	59	-11.2	3.392 × 10 ¹



Eyring parameters:

$$\Delta H^\ddagger = 34.168 \pm 0.786 \text{ kJ mol}^{-1}$$

$$\Delta S^\ddagger = -84.105 \pm 3.248 \text{ J mol}^{-1} \text{ K}^{-1}$$

$$r^2 = 0.9984$$

Arrhenius parameters:

$$E_a = 36.186 \pm 0.776 \text{ kJ mol}^{-1}$$

$$\ln A = 20.138 \pm 0.386$$

$$r^2 = 0.9986$$

$$k_2(20\text{ °C}) = (2.017 \pm 0.137) \times 10^2 \text{ M}^{-1} \text{ s}^{-1}$$

Table 10.63: 1-(Methylphenylamino)cyclopentene (**34**) and (jul)₂CH⁺ BF₄⁻ in CH₂Cl₂ at λ = 642 nm (Stopped flow).

No.	[EL] ₀ / M	[Nuc] ₀ / M	[Nuc] ₀ /[EL] ₀	T / °C	k ₂ / M ⁻¹ s ⁻¹
180601-L	5.131 × 10 ⁻⁶	2.036 × 10 ⁻⁴	40	20.0	4.175 × 10 ²
180601-K	5.131 × 10 ⁻⁶	3.394 × 10 ⁻⁴	66	20.0	4.330 × 10 ²
180601-M	5.131 × 10 ⁻⁶	6.787 × 10 ⁻⁴	132	20.0	4.435 × 10 ²

$$\bar{k}_2(20\text{ °C}) = (4.313 \pm 0.107) \times 10^2 \text{ M}^{-1} \text{ s}^{-1}$$

Table 10.64: 1-(Methylphenylamino)cyclopentene (**34**) and (thq)₂CH⁺ BF₄⁻ in CH₂Cl₂ at λ = 628 nm (Stopped flow).

No.	[EL] ₀ / M	[Nuc] ₀ / M	[Nuc] ₀ /[EL] ₀	T / °C	k ₂ / M ⁻¹ s ⁻¹
180601-J	6.037 × 10 ⁻⁶	1.357 × 10 ⁻⁴	23	20.0	4.835 × 10 ³
180601-G	6.037 × 10 ⁻⁶	2.036 × 10 ⁻⁴	34	20.0	5.101 × 10 ³
180601-H	6.037 × 10 ⁻⁶	2.715 × 10 ⁻⁴	45	20.0	5.065 × 10 ³
180601-I	6.037 × 10 ⁻⁶	3.394 × 10 ⁻⁴	56	20.0	5.044 × 10 ³

$$\bar{k}_2(20\text{ °C}) = (5.011 \pm 0.104) \times 10^3 \text{ M}^{-1} \text{ s}^{-1}$$

Table 10.65: 1-(Methylphenylamino)cyclopentene (**34**) and (dma)₂CH⁺ BF₄⁻ in CH₂Cl₂ at λ = 613 nm (Stopped flow).

No.	[EL] ₀ / M	[Nuc] ₀ / M	[Nuc] ₀ /[EL] ₀	T / °C	k ₂ / M ⁻¹ s ⁻¹
180601-F	7.149 × 10 ⁻⁶	6.014 × 10 ⁻⁵	8	20.0	4.664 × 10 ⁴
180601-D	7.149 × 10 ⁻⁶	1.203 × 10 ⁻⁴	17	20.0	4.808 × 10 ⁴
180601-A	7.149 × 10 ⁻⁶	1.804 × 10 ⁻⁴	25	20.0	5.082 × 10 ⁴
180601-B	7.149 × 10 ⁻⁶	2.406 × 10 ⁻⁴	34	20.0	5.152 × 10 ⁴
180601-C	7.149 × 10 ⁻⁶	3.007 × 10 ⁻⁴	42	20.0	5.097 × 10 ⁴

$$\bar{k}_2(20\text{ °C}) = (4.961 \pm 0.190) \times 10^4 \text{ M}^{-1} \text{ s}^{-1}$$

Table 10.66: 1-(Methylphenylamino)cyclopentene (**34**) and (mpa)₂CH⁺ BF₄⁻ in CH₂Cl₂ at λ = 622 nm (Stopped flow).

No.	[EL] ₀ / M	[Nuc] ₀ / M	[Nuc] ₀ /[EL] ₀	T / °C	k ₂ / M ⁻¹ s ⁻¹
130601-K	4.997 × 10 ⁻⁶	6.464 × 10 ⁻⁵	13	20.0	3.334 × 10 ⁵
130601-G	4.997 × 10 ⁻⁶	1.293 × 10 ⁻⁴	26	20.0	3.265 × 10 ⁵
130601-H	4.997 × 10 ⁻⁶	1.939 × 10 ⁻⁴	39	20.0	3.179 × 10 ⁵
130601-I	4.997 × 10 ⁻⁶	2.586 × 10 ⁻⁴	52	20.0	3.141 × 10 ⁵
130601-J	4.997 × 10 ⁻⁶	3.232 × 10 ⁻⁴	65	20.0	3.125 × 10 ⁵

$$\bar{k}_2(20\text{ °C}) = (3.209 \pm 0.079) \times 10^5 \text{ M}^{-1} \text{ s}^{-1}$$

Table 10.67: 1-(Methylphenylamino)cyclopentene (**34**) and (dpa)₂CH⁺ BF₄⁻ in CH₂Cl₂ at λ = 672 nm (Stopped flow).

No.	[<i>El</i>] ₀ / M	[<i>Nuc</i>] ₀ / M	[<i>Nuc</i>] ₀ /[<i>El</i>] ₀	<i>T</i> / °C	<i>k</i> ₂ / M ⁻¹ s ⁻¹
130601-C	5.791 × 10 ⁻⁶	3.232 × 10 ⁻⁵	6	20.0	2.815 × 10 ⁶
130601-F	5.791 × 10 ⁻⁶	5.818 × 10 ⁻⁵	10	20.0	2.738 × 10 ⁶
130601-B	5.791 × 10 ⁻⁶	6.464 × 10 ⁻⁵	11	20.0	2.853 × 10 ⁶
130601-E	5.791 × 10 ⁻⁶	1.293 × 10 ⁻⁴	22	20.0	2.646 × 10 ⁶

$$\bar{k}_2 (20\text{ °C}) = (2.763 \pm 0.079) \times 10^6 \text{ M}^{-1} \text{ s}^{-1}$$

Table 10.68: 1-(Methylphenylamino)cyclohexene (**35**) and (thq)₂CH⁺ BF₄⁻ in CH₂Cl₂ at λ = 628 nm (J&M).

No.	[<i>El</i>] ₀ / M	[<i>Nuc</i>] ₀ / M	[<i>Nuc</i>] ₀ /[<i>El</i>] ₀	Conv. / %	<i>T</i> / °C	<i>k</i> ₂ / M ⁻¹ s ⁻¹
070501-02	1.351 × 10 ⁻⁵	3.104 × 10 ⁻⁴	23	86	20.0	1.136 × 10 ²
070501-03	1.907 × 10 ⁻⁵	8.214 × 10 ⁻⁴	43	95	20.0	1.031 × 10 ²
070501-01	1.736 × 10 ⁻⁵	7.974 × 10 ⁻⁴	46	95	20.0	1.034 × 10 ²
070501-04	2.750 × 10 ⁻⁵	1.579 × 10 ⁻³	57	93	20.0	9.521 × 10 ¹

$$\bar{k}_2 (20\text{ °C}) = (1.038 \pm 0.065) \times 10^2 \text{ M}^{-1} \text{ s}^{-1}$$

Table 10.69: 1-(Methylphenylamino)cyclohexene (**35**) and (dma)₂CH⁺ BF₄⁻ in CH₂Cl₂ at λ = 613 nm (Stopped flow).

No.	[<i>El</i>] ₀ / M	[<i>Nuc</i>] ₀ / M	[<i>Nuc</i>] ₀ /[<i>El</i>] ₀	<i>T</i> / °C	<i>k</i> _{eff} / s ⁻¹
020501-E	8.890 × 10 ⁻⁶	2.141 × 10 ⁻⁴	24	20.0	2.023 × 10 ⁻¹
020501-B	8.890 × 10 ⁻⁶	4.282 × 10 ⁻⁴	48	20.0	4.127 × 10 ⁻¹
020501-C	8.890 × 10 ⁻⁶	6.424 × 10 ⁻⁴	72	20.0	6.359 × 10 ⁻¹
020501-D	8.890 × 10 ⁻⁶	8.565 × 10 ⁻⁴	96	20.0	8.813 × 10 ⁻¹
020501-A	8.890 × 10 ⁻⁶	1.071 × 10 ⁻³	120	20.0	1.090

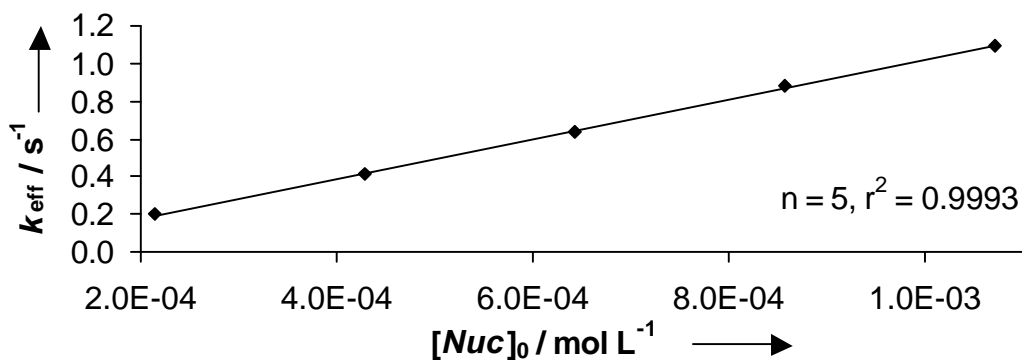


Figure 10.3: Plot of k_{eff} versus $[Nuc]_0$ ($n = 5$, $k_{\text{eff}} = (1.048 \times 10^3) \times [Nuc]_0 + 2.860 \times 10^{-2}$, $r^2 = 0.9993$).

$$k_2 (20 \text{ }^\circ\text{C}) = 1.048 \times 10^3 \text{ M}^{-1} \text{ s}^{-1}$$

$$k_{-2} (20 \text{ }^\circ\text{C}) = 2.860 \times 10^{-2} \text{ s}^{-1}$$

$$K (20 \text{ }^\circ\text{C}) = 3.664 \times 10^4 \text{ M}^{-1}$$

Table 10.70: 1-(Methylphenylamino)cyclohexene (**35**) and $(\text{mpa})_2\text{CH}^+ \text{BF}_4^-$ in CH_2Cl_2 at $\lambda = 622 \text{ nm}$ (Stopped flow).

No.	$[EL]_0 / \text{M}$	$[Nuc]_0 / \text{M}$	$[Nuc]_0/[EL]_0$	$T / \text{ }^\circ\text{C}$	$k_2 / \text{M}^{-1} \text{s}^{-1}$
300401-L	4.256×10^{-6}	2.976×10^{-4}	70	20.0	8.368×10^3
300401-O	4.256×10^{-6}	3.968×10^{-4}	93	20.0	8.503×10^3
300401-K	4.256×10^{-6}	4.960×10^{-4}	117	20.0	8.367×10^3
300401-N	4.256×10^{-6}	6.945×10^{-4}	163	20.0	8.407×10^3
300401-M	4.256×10^{-6}	9.921×10^{-4}	233	20.0	8.492×10^3

$$\bar{k}_2 (20 \text{ }^\circ\text{C}) = (8.427 \pm 0.059) \times 10^3 \text{ M}^{-1} \text{ s}^{-1}$$

Table 10.71: 1-(Methylphenylamino)cyclohexene (**35**) and (dpa)₂CH⁺ BF₄⁻ in CH₂Cl₂ at λ = 672 nm (Stopped flow).

No.	[<i>El</i>] ₀ / M	[<i>Nuc</i>] ₀ / M	[<i>Nuc</i>] ₀ /[<i>El</i>] ₀	<i>T</i> / °C	<i>k</i> ₂ / M ⁻¹ s ⁻¹
300401-J	5.975 × 10 ⁻⁶	9.921 × 10 ⁻⁵	17	20.0	8.602 × 10 ⁴
300401-I	5.975 × 10 ⁻⁶	1.984 × 10 ⁻⁴	33	20.0	8.720 × 10 ⁴
300401-H	5.975 × 10 ⁻⁶	2.976 × 10 ⁻⁴	50	20.0	8.705 × 10 ⁴
300401-G	5.975 × 10 ⁻⁶	3.968 × 10 ⁻⁴	66	20.0	8.633 × 10 ⁴
300401-F	5.975 × 10 ⁻⁶	4.960 × 10 ⁻⁴	83	20.0	8.519 × 10 ⁴

$$\bar{k}_2 (20\text{ }^\circ\text{C}) = (8.636 \pm 0.073) \times 10^4 \text{ M}^{-1} \text{ s}^{-1}$$

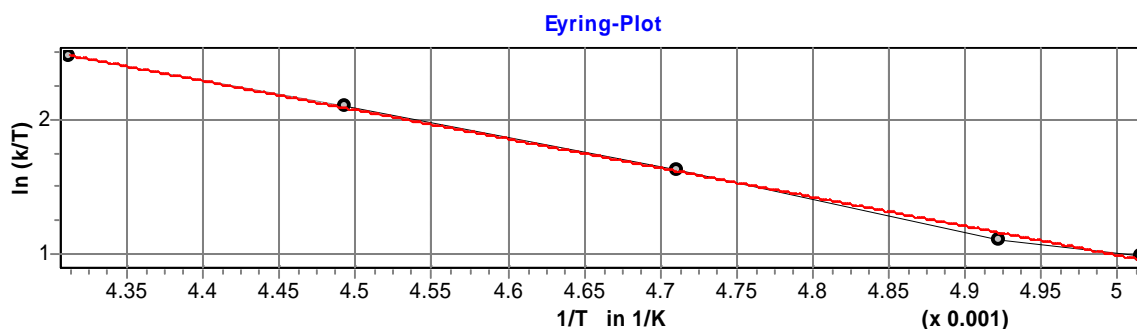
Table 10.72: 1-(Methylphenylamino)cyclohexene (**35**) and (mfa)₂CH⁺ BF₄⁻ in CH₂Cl₂ at λ = 593 nm (Stopped flow).

No.	[<i>El</i>] ₀ / M	[<i>Nuc</i>] ₀ / M	[<i>Nuc</i>] ₀ /[<i>El</i>] ₀	<i>T</i> / °C	<i>k</i> ₂ / M ⁻¹ s ⁻¹
300401-B	5.410 × 10 ⁻⁶	9.921 × 10 ⁻⁵	18	20.0	3.382 × 10 ⁵
300401-A	5.410 × 10 ⁻⁶	1.984 × 10 ⁻⁴	37	20.0	3.357 × 10 ⁵
300401-C	5.410 × 10 ⁻⁶	2.976 × 10 ⁻⁴	55	20.0	3.376 × 10 ⁵
300401-D	5.410 × 10 ⁻⁶	3.968 × 10 ⁻⁴	73	20.0	3.404 × 10 ⁵
300401-E	5.410 × 10 ⁻⁶	4.960 × 10 ⁻⁴	92	20.0	3.497 × 10 ⁵

$$\bar{k}_2 (20\text{ }^\circ\text{C}) = (3.403 \pm 0.049) \times 10^5 \text{ M}^{-1} \text{ s}^{-1}$$

Table 10.73: 1-(1-Cyclohexenyl)-4-methylpiperazine (**36**) and (dma)₂CH⁺ BF₄⁻ in CH₂Cl₂ at λ = 640 nm (Schölly).

No.	[<i>El</i>] ₀ / M	[<i>Nuc</i>] ₀ / M	[<i>Nuc</i>] ₀ /[<i>El</i>] ₀	Conv. / %	<i>T</i> / °C	<i>k</i> ₂ / M ⁻¹ s ⁻¹
AO-142.1	3.94 × 10 ⁻⁵	3.76 × 10 ⁻⁴	9.5	73	-73.8	5.366 × 10 ²
AO-139.1	7.90 × 10 ⁻⁵	9.66 × 10 ⁻⁴	12	70	-70.0	6.190 × 10 ²
AO-142.2	3.86 × 10 ⁻⁵	2.77 × 10 ⁻⁴	7.2	58	-60.9	1.075 × 10 ³
AO-142.3	2.33 × 10 ⁻⁵	1.86 × 10 ⁻⁴	8.0	65	-50.6	1.830 × 10 ³
AO-142.4	2.07 × 10 ⁻⁵	8.26 × 10 ⁻⁵	4.0	83	-41.2	2.747 × 10 ³



Eyring parameters:

$$\Delta H^\ddagger = 17.973 \pm 0.498 \text{ kJ mol}^{-1}$$

$$\Delta S^\ddagger = -99.433 \pm 2.339 \text{ J mol}^{-1} \text{ K}^{-1}$$

$$r^2 = 0.9977$$

Arrhenius parameters:

$$E_a = 19.757 \pm 0.499 \text{ kJ mol}^{-1}$$

$$\ln A = 18.171 \pm 0.282$$

$$r^2 = 0.9981$$

$$k_2 (20 \text{ }^\circ\text{C}) = (2.454 \pm 0.188) \times 10^4 \text{ M}^{-1} \text{ s}^{-1} [200]$$

Table 10.74: Pyrrole (**42**) and (pfa)₂CH⁺ BF₄⁻ in CH₂Cl₂ at λ = 600 nm (Schölly).

No.	[EL] ₀ / M	[Nuc] ₀ / M	[Nuc] ₀ /[EL] ₀	Conv. / %	T / °C	k ₂ / M ⁻¹ s ⁻¹
210801.PA1	2.616 × 10 ⁻⁵	9.176 × 10 ⁻⁴	35	55	20.0	3.083 × 10 ¹
210801.PA2	3.242 × 10 ⁻⁵	1.624 × 10 ⁻³	50	40	20.0	3.313 × 10 ¹
210801.PA3	2.839 × 10 ⁻⁵	3.319 × 10 ⁻³	117	36	20.0	2.973 × 10 ¹

$$\bar{k}_2 (20 \text{ }^\circ\text{C}) = (3.123 \pm 0.142) \times 10^1 \text{ M}^{-1} \text{ s}^{-1}$$

Table 10.75: N-(Triisopropylsilyl)pyrrole (**44**) and (dpa)₂CH⁺ BF₄⁻ in CH₂Cl₂ at λ = 674 nm (J&M).

No.	[EL] ₀ / M	[Nuc] ₀ / M	[Nuc] ₀ /[EL] ₀	Conv. / %	T / °C	k ₂ / M ⁻¹ s ⁻¹
290801-01	2.596 × 10 ⁻⁵	1.745 × 10 ⁻³	67	37	20.0	4.367 × 10 ⁻²
290801-02	2.736 × 10 ⁻⁵	3.218 × 10 ⁻³	118	71	20.0	4.186 × 10 ⁻²
290801-03	2.437 × 10 ⁻⁵	6.514 × 10 ⁻³	267	93	20.0	4.221 × 10 ⁻²

$$\bar{k}_2 (20 \text{ }^\circ\text{C}) = (4.258 \pm 0.078) \times 10^{-2} \text{ M}^{-1} \text{ s}^{-1}$$

Table 10.76: *N*-(Triisopropylsilyl)pyrrole (**44**) and (mfa)₂CH⁺ BF₄⁻ in CH₂Cl₂ at λ = 593 nm (J&M).

No.	[<i>EL</i>] ₀ / M	[<i>Nuc</i>] ₀ / M	[<i>Nuc</i>] ₀ /[<i>EL</i>] ₀	Conv. / %	<i>T</i> / °C	<i>k</i> ₂ / M ⁻¹ s ⁻¹
300801-04	1.545 × 10 ⁻⁵	2.022 × 10 ⁻³	131	70	20.0	1.170 × 10 ⁻¹
300801-03	2.035 × 10 ⁻⁵	3.873 × 10 ⁻³	190	90	20.0	1.271 × 10 ⁻¹
300801-05	1.594 × 10 ⁻⁵	4.172 × 10 ⁻³	262	87	20.0	1.126 × 10 ⁻¹

$$\bar{k}_2 (20\text{ °C}) = (1.189 \pm 0.061) \times 10^{-1} \text{ M}^{-1} \text{ s}^{-1}$$

Table 10.77: *N*-(Triisopropylsilyl)pyrrole (**44**) and (pfa)₂CH⁺ BF₄⁻ in CH₂Cl₂ at λ = 601 nm (J&M).

No.	[<i>EL</i>] ₀ / M	[<i>Nuc</i>] ₀ / M	[<i>Nuc</i>] ₀ /[<i>EL</i>] ₀	Conv. / %	<i>T</i> / °C	<i>k</i> ₂ / M ⁻¹ s ⁻¹
300801-02	1.550 × 10 ⁻⁵	7.682 × 10 ⁻⁴	50	39	20.0	1.114
300801-01	1.369 × 10 ⁻⁵	1.695 × 10 ⁻³	124	70	20.0	1.448
300801-03	1.449 × 10 ⁻⁵	2.872 × 10 ⁻³	198	72	20.0	1.416

$$\bar{k}_2 (20\text{ °C}) = 1.326 \pm 0.151 \text{ M}^{-1} \text{ s}^{-1}$$

Table 10.78: Indole (**45**) and (pfa)₂CH⁺ BF₄⁻ in CH₂Cl₂ at λ = 601 nm (Stopped flow).

No.	[<i>EL</i>] ₀ / M	[<i>Nuc</i>] ₀ / M	[<i>Nuc</i>] ₀ /[<i>EL</i>] ₀	<i>T</i> / °C	<i>k</i> ₂ / M ⁻¹ s ⁻¹
230501-D	4.997 × 10 ⁻⁶	5.250 × 10 ⁻⁴	105	20.0	1.298 × 10 ²
230501-B	4.997 × 10 ⁻⁶	1.050 × 10 ⁻³	210	20.0	1.367 × 10 ²
230501-C	4.997 × 10 ⁻⁶	1.575 × 10 ⁻³	315	20.0	1.352 × 10 ²

$$\bar{k}_2 (20\text{ °C}) = (1.339 \pm 0.030) \times 10^2 \text{ M}^{-1} \text{ s}^{-1}$$

Table 10.79: *N*-Methylindole (**46**) and (pfa)₂CH⁺ BF₄⁻ in CH₂Cl₂ at λ = 601 nm (Stopped flow).

No.	[<i>El</i>] ₀ / M	[<i>Nuc</i>] ₀ / M	[<i>Nuc</i>] ₀ /[<i>El</i>] ₀	<i>T</i> / °C	<i>k</i> ₂ / M ⁻¹ s ⁻¹
170501-A	5.297 × 10 ⁻⁶	9.529 × 10 ⁻⁵	18	20.0	1.089 × 10 ³
170501-E	5.297 × 10 ⁻⁶	2.382 × 10 ⁻⁴	45	20.0	1.074 × 10 ³
170501-F	5.297 × 10 ⁻⁶	4.764 × 10 ⁻⁴	90	20.0	1.083 × 10 ³
170501-D	5.297 × 10 ⁻⁶	7.147 × 10 ⁻⁴	135	20.0	1.068 × 10 ³
170501-C	5.297 × 10 ⁻⁶	9.529 × 10 ⁻⁴	180	20.0	1.110 × 10 ³

$$\bar{k}_2 (20\text{ °C}) = (1.085 \pm 0.015) \times 10^3 \text{ M}^{-1} \text{ s}^{-1}$$

Table 10.80: 1,2-Dimethylindole (**47**) and (pfa)₂CH⁺ BF₄⁻ in CH₂Cl₂ at λ = 601 nm (Stopped flow).

No.	[<i>El</i>] ₀ / M	[<i>Nuc</i>] ₀ / M	[<i>Nuc</i>] ₀ /[<i>El</i>] ₀	<i>T</i> / °C	<i>k</i> ₂ / M ⁻¹ s ⁻¹
050601-I	4.731 × 10 ⁻⁶	9.352 × 10 ⁻⁵	20	20.0	5.666 × 10 ³
050601-C	4.731 × 10 ⁻⁶	1.434 × 10 ⁻⁴	30	20.0	5.650 × 10 ³
050601-B	4.731 × 10 ⁻⁶	2.868 × 10 ⁻⁴	61	20.0	5.219 × 10 ³
050601-A	4.731 × 10 ⁻⁶	4.301 × 10 ⁻⁴	91	20.0	5.335 × 10 ³

$$\bar{k}_2 (20\text{ °C}) = (5.468 \pm 0.195) \times 10^3 \text{ M}^{-1} \text{ s}^{-1}$$

10.4 5-Methoxyfuroxano[3,4-*d*]pyrimidine - a highly reactive neutral electrophile

10.4.1 Concentrations and rate constants of the individual kinetic runs

Table 10.81: 5-Methoxyfuroxano[3,4-*d*]pyrimidine (**52**) and 1-(*N*-morpholino)cyclohexene (**20**) in CH₂Cl₂ at λ = 301 nm (J&M).

No.	[<i>El</i>] ₀ / mol L ⁻¹	[<i>Nuc</i>] ₀ / mol L ⁻¹	[<i>Nuc</i>] ₀ /[<i>El</i>] ₀	Conv. / %	<i>T</i> / °C	<i>k</i> ₂ / L mol ⁻¹ s ⁻¹
160701-09	1.240 × 10 ⁻⁴	5.226 × 10 ⁻⁴	4	58	20.0	2.636 × 10 ²
160701-08	9.712 × 10 ⁻⁵	1.023 × 10 ⁻³	11	53	20.0	2.578 × 10 ²
160701-07	6.166 × 10 ⁻⁵	1.299 × 10 ⁻³	21	55	20.0	2.688 × 10 ²

$$\bar{k}_2 (20\text{ }^\circ\text{C}) = (2.634 \pm 0.045) \times 10^2 \text{ L mol}^{-1} \text{ s}^{-1}$$

Table 10.82: 5-Methoxyfuroxano[3,4-*d*]pyrimidine (**52**) and 2-(trimethylsiloxy)-4,5-dihydrofuran (**55**) in CH₂Cl₂ at $\lambda = 301$ nm (J&M).

No.	[<i>El</i>] ₀ / mol L ⁻¹	[<i>Nuc</i>] ₀ / mol L ⁻¹	[<i>Nuc</i>] ₀ /[<i>El</i>] ₀	Conv. / %	<i>T</i> / °C	<i>k</i> ₂ / L mol ⁻¹ s ⁻¹
160701-06	1.130 × 10 ⁻⁴	4.661 × 10 ⁻⁴	4	56	20.0	5.957 × 10 ²
160701-05	7.357 × 10 ⁻⁵	6.067 × 10 ⁻⁴	8	67	20.0	5.850 × 10 ²
160701-04	1.298 × 10 ⁻⁴	1.338 × 10 ⁻³	10	76	20.0	5.914 × 10 ²

$$\bar{k}_2 (20\text{ }^\circ\text{C}) = (5.907 \pm 0.044) \times 10^2 \text{ L mol}^{-1} \text{ s}^{-1}$$

Table 10.83: 5-Methoxyfuroxano[3,4-*d*]pyrimidine (**52**) and 1-(*N*-piperidino)cyclohexene (**24**) in CH₂Cl₂ at $\lambda = 301$ nm (Stopped flow).

No.	[<i>El</i>] ₀ / mol L ⁻¹	[<i>Nuc</i>] ₀ / mol L ⁻¹	[<i>Nuc</i>] ₀ /[<i>El</i>] ₀	<i>T</i> / °C	<i>k</i> ₂ / L mol ⁻¹ s ⁻¹
170701-E	2.724 × 10 ⁻⁵	2.425 × 10 ⁻⁴	9	20.0	1.807 × 10 ⁴
170701-D	2.724 × 10 ⁻⁵	4.850 × 10 ⁻⁴	18	20.0	1.844 × 10 ⁴
170701-F	2.724 × 10 ⁻⁵	7.275 × 10 ⁻⁴	27	20.0	1.753 × 10 ⁴
170701-B	2.724 × 10 ⁻⁵	9.700 × 10 ⁻⁴	36	20.0	1.645 × 10 ⁴
170701-C	2.724 × 10 ⁻⁵	1.212 × 10 ⁻³	45	20.0	1.595 × 10 ⁴

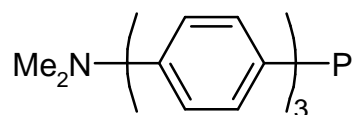
$$\bar{k}_2 (20\text{ }^\circ\text{C}) = (1.801 \pm 0.037) \times 10^4 \text{ L mol}^{-1} \text{ s}^{-1}$$

10.5 Rates and equilibria for the reactions of tertiary phosphanes and phosphites with carbocations

10.5.1 Synthesis of triaryl phosphanes

Tris(4-dimethylaminophenyl)phosphine (p-Me₂NC₆H₄)₃P: In a carefully dried, nitrogen-flushed two necked round-bottom flask equipped with a dropping funnel and reflux condenser, a solution of 4-bromo-N,N-dimethylaniline (24.66 g, 0.123 mol) and 40 mL

absolute Et₂O was added within 30 min to a suspension of lithium-granules (1.88 g, 0.271 mol) and 40 mL absolute Et₂O.^[111] After stirring at room temperature (30 min) the solution was refluxed for 30 min, and diluted with 100 mL absolute Et₂O. At -20 °C a solution of phosphorus trichloride (3.6 mL, 41.2 mmol) and 20 mL absolute Et₂O was added within 30 min.^[112] After stirring at room temperature (1 h), refluxing (1 h), and cooling down, the separated crude product was filtered off, dissolved in 100 mL of 2N HCl and separated by addition of 100 mL of a 10 % NaOH-solution. Filtering off, washing with water, recrystallization (EtOH/CHCl₃ : 10/1), and drying in HV gave pale yellow needles (10.83 g, 68 %); m.p. 280-282 °C (Lit.: 278-282 °C).^[112] ¹H NMR (300 MHz, CDCl₃): δ = 2.92 (s, 18 H, NMe₂), 6.66 (d, ³J = 9.0 Hz, 6 H, Ar), 7.19 (d, ³J = 8.9 Hz, 6 H, Ar) in agreement with data published in ref. [113]; ¹³C NMR (75.5 MHz, CDCl₃): δ = 40.3 (q, NMe₂), 112.2/112.3 (2 d, Ar), 124.4/124.5 (2 s, Ar), 134.4/134.7 (2 d, Ar), 150.4 (s, Ar) in agreement with data published in ref. [201]; ³¹P NMR (81 MHz, CDCl₃): δ = -10.17 (s).



BKE072

(p-Me₂NC₆H₄)₃P

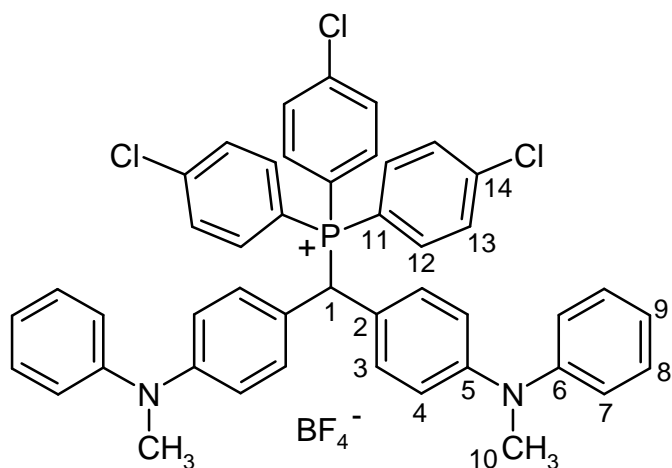
10.5.2 Reactions of phosphanes and phosphites with benzhydryl salts

General procedure: In a carefully dried, nitrogen-flushed Schlenk-flask a solution of the freshly distilled or recrystallized phosphane or phosphite in 2 mL absolute CH₂Cl₂ was added dropwise to a stirred solution of the benzhydryl salt in 50 mL absolute CH₂Cl₂. After stirring at room temperature for 30 min, the solvent was evaporated in vacuo to yield the crude product, which was washed with 10 mL absolute Et₂O and dried several hours in vacuo (10⁻² mbar).

Remarks: Combinations of less reactive benzhydryl salts and less reactive phosphanes or phosphites sometimes are reversible. In such cases, the reaction products were accompanied by small amounts of the reactants. In some cases it was not possible to isolate the products because the degree of conversion was too small.

Bis(4-(methylphenylamino)phenyl)methyl-tris(4-chlorophenyl)-phosphonium tetrafluoroborate (56) was obtained from tris(4-chlorophenyl)phosphine (p-ClC₆H₄)₃P (366 mg, 1

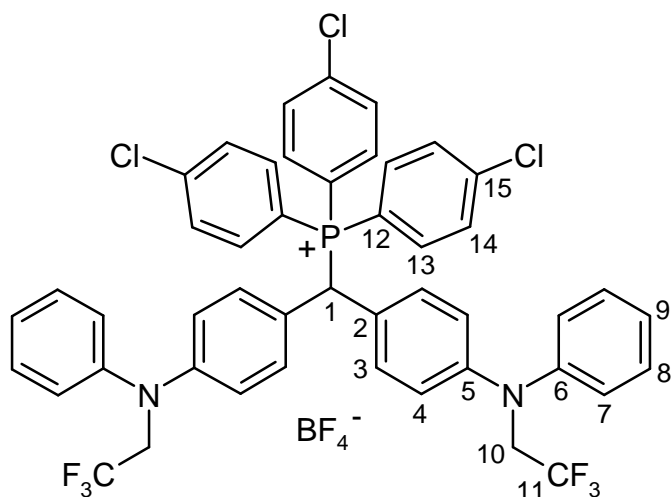
mmol) and bis(4-(methylphenylamino)phenyl)methylm tetrafluoroborate (mpa)₂CH⁺ BF₄⁻ (464 mg, 1 mmol) as a bright-blue solid (647 mg, 78 %). ¹H NMR (300 MHz, CDCl₃): δ = 3.25 (s, 6 H, 10-H), 6.45 (d, *J* = 17.3 Hz, 1 H, 1-H), 6.65-7.60 (m, 30 H, 4 × 3-H, 4 × 4-H, 4 × 7-H, 4 × 8-H, 2 × 9-H, 6 × 12-H, 6 × 13-H); ¹³C NMR (75.5 MHz, CDCl₃): δ = 39.9 (q, C-10), 46.7 (dd, *J* = 37.9 Hz, C-1), 115.9, 124.4, 124.6, 129.5, 130.3, 131.0, 135.8 (7 d, Ar), 115.8/116.9, 121.0, 142.1, 147.5, 149.1 (6 s, Ar); ³¹P NMR (81 MHz, CDCl₃): δ = 20.33 (s); MS (FAB): *m/z* (%): 377 (100) [Ar₂CH]⁺, 272 (4), 254 (2), 196 (4), 165 (4), 154 (11), 136 (13).



NHB13

56

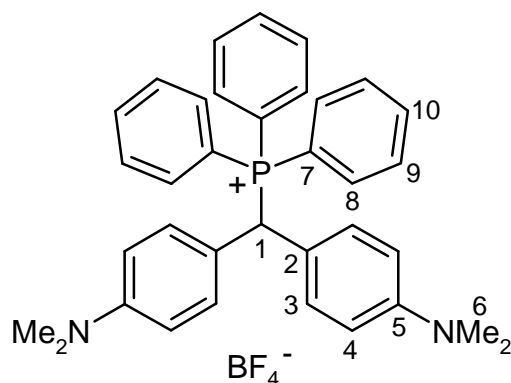
Bis(4-(phenyl(2,2,2-trifluoroethyl)amino)phenyl)methyl-tris(4-chlorophenyl)-phosphonium tetrafluoroborate (57) was obtained from tris(4-chlorophenyl)phosphine (p-ClC₆H₄)₃P (366 mg, 1 mmol) and bis(4-(phenyl(2,2,2-trifluoroethyl)amino)phenyl)methylm tetrafluoroborate (pfa)₂CH⁺ BF₄⁻ (600 mg, 1 mmol) as a dark violet-solid (782 mg, 81 %). ¹H NMR (300 MHz, CDCl₃): δ = 4.25 (q, *J* = 8.6 Hz, 4 H, 10-H), 6.53 (d, *J* = 17.5 Hz, 1 H, 1-H), 6.65-7.58 (m, 30 H, 4 × 3-H, 4 × 4-H, 4 × 7-H, 4 × 8-H, 2 × 9-H, 6 × 13-H, 6 × 14-H); ¹³C NMR (75.5 MHz, CDCl₃): δ = 46.2 (dd, *J* = 41.1 Hz, C-1), 53.5 (tq, *J* = 33.8 Hz, C-10), 124.9 (sq, *J* = 283.2 Hz, C-11), 116.9, 122.7, 123.0, 129.9, 130.4/130.6, 131.2, 135.7/135.9 (9 d, Ar), 115.5/116.6, 121.4, 142.3, 145.7, 148.3 (6 s, Ar); ³¹P NMR (81 MHz, CDCl₃): δ = 21.14 (s); MS (FAB): *m/z* (%): 877 (1) [M]⁺, 513 (100) [Ar₂CH]⁺, 154 (13), 136 (11), 123 (10), 109 (19).



NHB12

57

Bis(4-dimethylaminophenyl)methyl-triphenyl-phosphonium tetrafluoroborate (58) was obtained from triphenylphosphine Ph_3P (262 mg, 1 mmol) and bis(4-dimethylaminophenyl)methylium tetrafluoroborate $(\text{dma})_2\text{CH}^+ \text{BF}_4^-$ (340 mg, 1 mmol) as a bright-blue solid (494 mg, 82 %). ^1H NMR (300 MHz, CDCl_3): $\delta = 2.91$ (s, 12 H, 6-H), 6.10 (d, $J = 16.9$ Hz, 1 H, 1-H), 6.53-7.77 (m, 23 H, 4 \times 3-H, 4 \times 4-H, 6 \times 8-H, 6 \times 9-H, 3 \times 10-H); ^{13}C NMR (75.5 MHz, CDCl_3): $\delta = 40.1$ (q, C-6), 47.7 (dd, $J = 41.1$ Hz, C-1), 112.4, 128.2, 129.7, 134.5, 134.6 (5 d, Ar), 117.8/118.9, 119.5, 149.7 (4 s, Ar); ^{31}P NMR (81 MHz, CDCl_3): $\delta = 20.36$ (s).

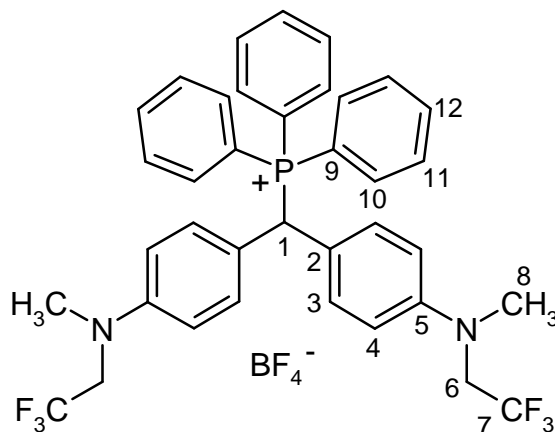


NHB01

58

Bis(4-(methyl(2,2,2-trifluoroethyl)amino)phenyl)methyl-triphenyl-phosphonium tetrafluoroborate (59) was obtained from triphenylphosphine Ph_3P (262 mg, 1 mmol) and bis(4-(methyl(2,2,2-trifluoroethyl)amino)phenyl)methylium tetrafluoroborate $(\text{mfa})_2\text{CH}^+ \text{BF}_4^-$ (476 mg, 1 mmol) as a bright-red solid (476 mg, 65 %). ^1H NMR (300 MHz, CDCl_3): $\delta = 2.98$ (s, 6 H, 8-H), 3.82 (q, $J = 8.8$ Hz, 4 H, 6-H), 6.25 (d, $J = 17.1$ Hz, 1 H, 1-H), 6.58-7.80 (m, 23 H, 4 \times 3-H, 4 \times 4-H, 6 \times 10-H, 6 \times 11-H, 3 \times 12-H); ^{13}C NMR (75.5 MHz, CDCl_3): $\delta = 38.8$ (q, C-

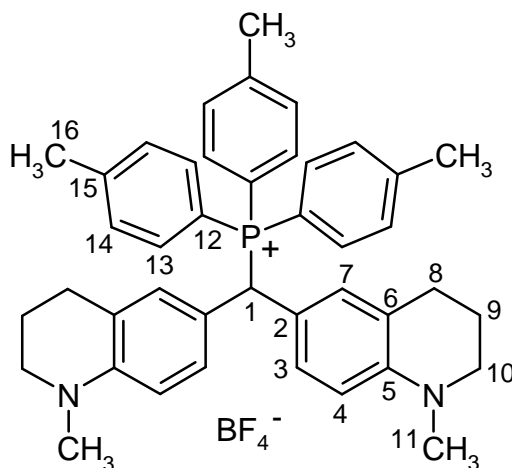
8), 46.9 (dd, $J = 41.7$ Hz, C-1), 53.4 (q, $J = 32.9$ Hz, C-6), 125.2 (sq, $J = 282.9$ Hz, C-7), 112.6, 129.7, 131.1, 134.5, 134.6 (5 d, Ar), 117.6/118.7, 121.0, 148.4 (4 s, Ar); ^{31}P NMR (81 MHz, CDCl_3): $\delta = 21.12$ (s); MS (FAB): m/z (%): 651 (4) $[\text{M}]^+$, 389 (100) $[\text{Ar}_2\text{CH}]^+$, 305 (6), 202 (2), 183 (4), 154 (2), 136 (2).



NHB02

59

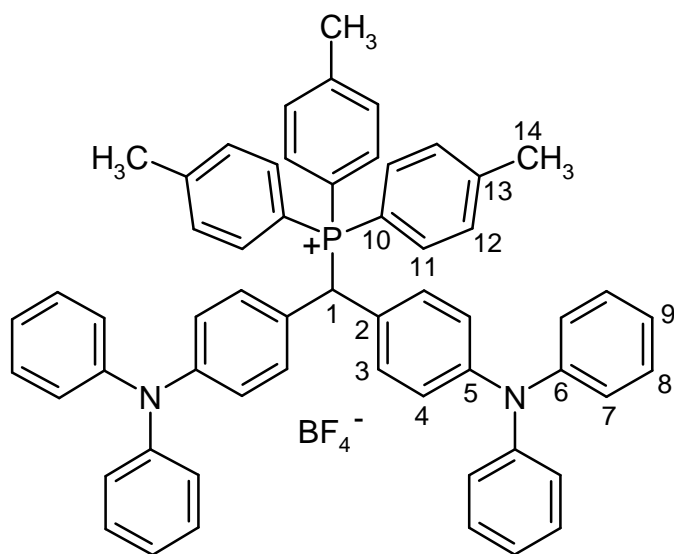
Bis(*N*-methyl-1,2,3,4-tetrahydroquinolin-6-yl)methyl-tris(4-methylphenyl)-phosphonium tetrafluoroborate (60) was obtained from tris(4-methylphenyl)phosphine ($p\text{-MeC}_6\text{H}_4$) $_3\text{P}$ (304 mg, 1 mmol) and bis(*N*-methyl-1,2,3,4-tetrahydroquinolin-6-yl)methylium tetrafluoroborate ($(\text{thq})_2\text{CH}^+ \text{BF}_4^-$) (392 mg, 1 mmol) as a green solid (536 mg, 77 %). ^1H NMR (300 MHz, CDCl_3): $\delta = 1.80\text{-}2.05$ (m, 4 H, 9-H), 2.30-2.60 (m, 4 H, 8-H), 2.48 (s, 9 H, 16-H), 2.84 (s, 6 H, 11-H), 3.15-3.25 (m, 4 H, 10-H), 5.64 (d, $J = 16.7$ Hz, 1 H, 1-H), 6.35-7.58 (m, 18 H, $2 \times 3\text{-H}$, $2 \times 4\text{-H}$, $2 \times 7\text{-H}$, $6 \times 13\text{-H}$, $6 \times 14\text{-H}$); ^{13}C NMR (75.5 MHz, CDCl_3): $\delta = 21.7$ (q, C-16), 21.8 (t, C-9), 27.6 (t, C-8), 38.7 (q, C-11), 48.8 (dd, $J = 42.0$ Hz, C-1), 50.9 (t, C-10), 110.6, 128.8, 130.4, 130.8, 134.7 (5 d, Ar), 115.0, 116.1, 123.1, 145.9, 146.5 (5 s, Ar); ^{31}P NMR (81 MHz, CDCl_3): $\delta = 19.38$ (s); MS (FAB): m/z (%): 609 (2) $[\text{M}]^+$, 367 (32), 305 (100) $[\text{Ar}_2\text{CH}]^+$, 275 (2), 213 (9), 160 (3), 154 (4), 147 (3), 123 (4).



NHB04

60

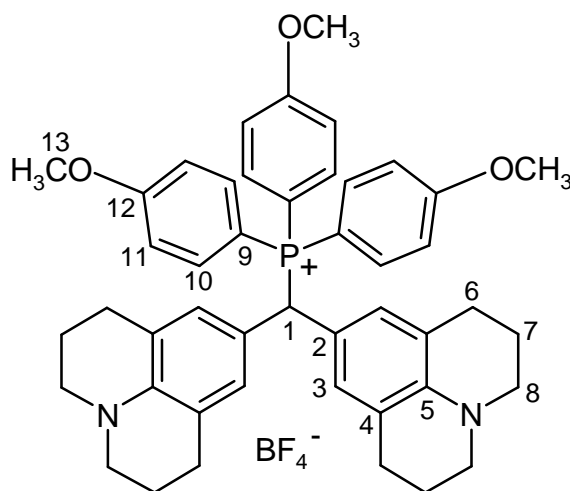
Bis(4-diphenylaminophenyl)methyl-tris(4-methylphenyl)-phosphonium tetrafluoroborate (61) was obtained from tris(4-methylphenyl)phosphine (p-MeC₆H₄)₃P (304 mg, 1 mmol) and bis(4-diphenylaminophenyl)methylium tetrafluoroborate (dpa)₂CH⁺ BF₄⁻ (588 mg, 1 mmol) as a bright-blue solid (703 mg, 79 %). ¹H NMR (300 MHz, CDCl₃): δ = 2.45 (s, 9 H, 14-H), 6.30 (d, *J* = 17.2 Hz, 1 H, 1-H), 6.85-7.40 (m, 40 H, 4 × 3-H, 4 × 4-H, 8 × 7-H, 8 × 8-H, 4 × 9-H, 6 × 11-H, 6 × 12-H); ¹³C NMR (75.5 MHz, CDCl₃): δ = 21.8 (q, C-14), 47.4 (dd, *J* = 45.5 Hz, C-1), 122.2, 123.7, 125.2, 129.4, 130.6/130.8, 131.4/131.5, 134.6/134.8 (10 d, Ar), 114.6, 115.8, 146.1, 147.0, 148.2 (5 s, Ar); ³¹P NMR (81 MHz, CDCl₃): δ = 21.33 (s); MS (FAB): *m/z* (%): 804 (3), [M]⁺, 501 (100) [Ar₂CH]⁺, 367 (3), 254 (3), 211 (3), 167 (3).



NHB03

61

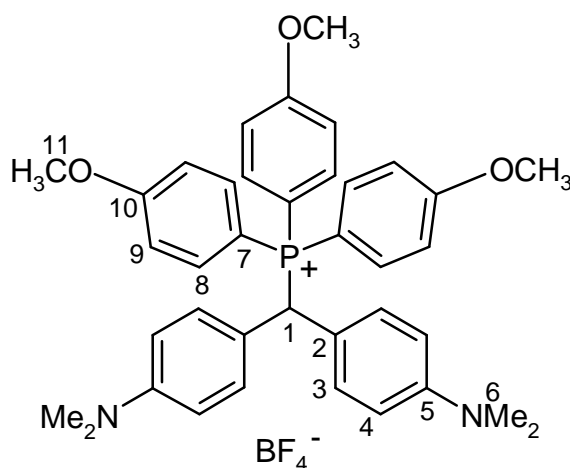
Bis(julolidin-9-yl)methyl-tris(4-methoxyphenyl)-phosphonium tetrafluoroborate (62) was obtained from tris(4-methoxyphenyl)phosphine (p-MeOC₆H₄)₃P (352 mg, 1 mmol) and bis(julolidin-9-yl)methylium tetrafluoroborate (jul)₂CH⁺ BF₄⁻ (444 mg, 1 mmol) as a bright-blue solid (606 mg, 76 %). ¹H NMR (300 MHz, CDCl₃): δ = 1.77-2.00 (m, 8 H, 7-H), 2.40-2.62 (m, 8 H, 6-H), 3.10-3.16 (m, 8 H, 8-H), 3.92 (s, 9 H, 13-H), 5.32 (d, *J* = 16.6 Hz, 1 H, 1-H), 6.80-7.65 (m, 16 H, 4 × 3-H, 6 × 10-H, 6 × 11-H); ³¹P NMR (81 MHz, CDCl₃): δ = 18.18 (s); MS (FAB): *m/z* (%): 709 (3) [M]⁺, 369 (13), 357 (100) [Ar₂CH]⁺, 245 (2), 154 (18), 137 (13).



NHB06

62

Bis(4-dimethylaminophenyl)methyl-tris(4-methoxyphenyl)-phosphonium tetrafluoroborate (63) was obtained from tris(4-methoxyphenyl)phosphine ($p\text{-MeOC}_6\text{H}_4)_3\text{P}$ (352 mg, 1 mmol) and bis(4-dimethylaminophenyl)methylium tetrafluoroborate $(\text{dma})_2\text{CH}^+ \text{BF}_4^-$ (340 mg, 1 mmol) as a blue-green solid (681 mg, 98 %). ^1H NMR (300 MHz, CDCl_3): $\delta = 2.94$ (s, 12 H, 6-H), 3.90 (s, 9 H, 11-H), 5.76 (d, $J = 16.9$ Hz, 1 H, 1-H), 6.60-7.34 (m, 20 H, $4 \times 3\text{-H}$, $4 \times 4\text{-H}$, $6 \times 8\text{-H}$, $6 \times 9\text{-H}$); ^{13}C NMR (75.5 MHz, CDCl_3): $\delta = 40.8$ (q, C-6), 48.7 (dd, $J = 45.5$ Hz, C-1), 55.9 (q, C-11), 113.2, 115.6/115.8, 131.3, 136.5/136.7 (6 d, Ar), 108.5, 109.7, 149.6, 164.4 (4 s, Ar); ^{31}P NMR (81 MHz, CDCl_3): $\delta = 19.32$ (s); MS (FAB): m/z (%): 604 (1) $[\text{M}]^+$, 352 (7), 281 (8), 253 (100) $[\text{Ar}_2\text{CH}]^+$, 221 (9), 207 (11), 147 (28), 136 (15).



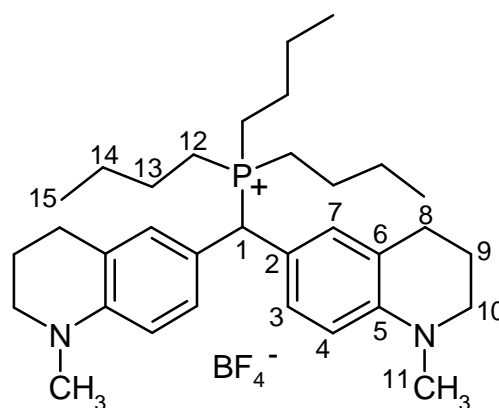
NHB05

63

Bis(*N*-methyl-1,2,3,4-tetrahydroquinolin-6-yl)methyl-(*n*tributyl)-phosphonium tetrafluoroborate (65) was obtained from *n*tributylphosphine ($n\text{Bu}$) $_3\text{P}$ (202 mg, 1 mmol) and bis(*N*-methyl-1,2,3,4-tetrahydroquinolin-6-yl)methylium tetrafluoroborate $(\text{thq})_2\text{CH}^+ \text{BF}_4^-$ (392 mg, 1 mmol) as an orange-red solid (494 mg, 83 %). ^1H NMR (300 MHz, CDCl_3): $\delta =$

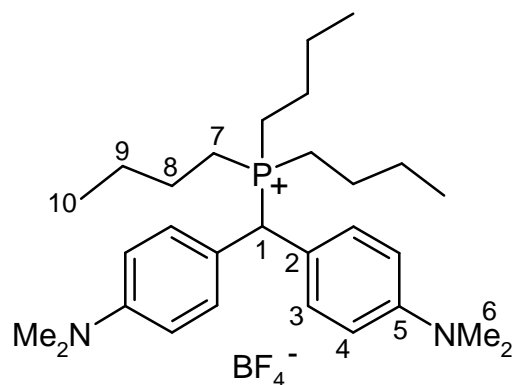
0.87 (t, $J = 6.8$ Hz, 9 H, 15-H), 1.20-1.50 (m, 12 H, 6×13 -H, 6×14 -H), 1.85-2.05 (m, 4 H, 9-H), 2.06-2.23 (m, 6 H, 12-H), 2.63-2.83 (m, 4 H, 8-H), 2.87 (s, 6 H, 11-H), 3.12-3.32 (m, 4 H, 10-H), 4.74 (d, $J = 18.1$ Hz, 1 H, 1-H), 6.54 (d, $J = 8.6$ Hz, 2 H, Ar), 6.99 (s, 2 H, 7-H), 7.12 (d, $J = 8.5$ Hz, 2 H, Ar); ^{13}C NMR (75.5 MHz, CDCl_3): $\delta = 13.3$ (q, C-15), 18.6 (t, C-14), 19.2 (t, C-13), 22.0 (t, C-9), 23.7/23.9/24.1 (3 t, C-12), 27.8 (t, C-8), 39.0 (dd, $J = 41.1$ Hz, C-1), 51.0 (t, C-10), 111.4, 127.6, 129.7 (3 d, Ar), 119.9, 123.9, 146.6 (3 s, Ar); ^{31}P NMR (81 MHz, CDCl_3): $\delta = 33.53$ (s); MS (FAB): m/z (%): 506 (2) $[\text{M}]^+$, 467 (18), 305 (100) $[\text{Ar}_2\text{CH}]^+$, 265 (6), 207 (6), 147 (15), 136 (7).

NHB10



65

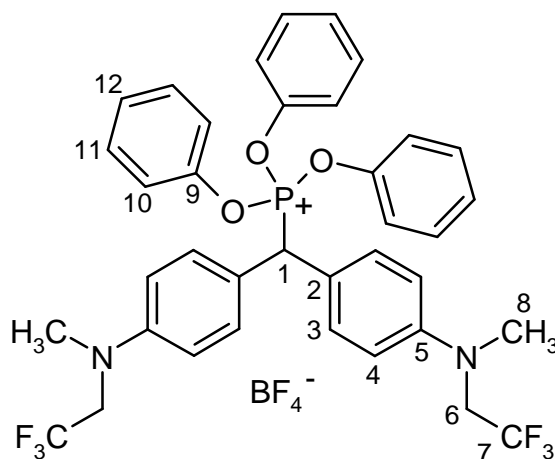
Bis(4-dimethylaminophenyl)methyl-(*n*-tributyl)-phosphonium tetrafluoroborate (66) was obtained from *n*-tributylphosphine ($n\text{Bu}$)₃P (202 mg, 1 mmol) and bis(4-dimethylaminophenyl)methylmethyl tetrafluoroborate (dma)₂CH⁺ BF₄⁻ (340 mg, 1 mmol) as a bright-red solid (505 mg, 93 %). ^1H NMR (300 MHz, CDCl_3): $\delta = 0.86$ (t, $J = 6.7$ Hz, 9 H, 10-H), 1.20-1.45 (m, 12 H, 6×8 -H, 6×9 -H), 2.05-2.30 (m, 6 H, 7-H), 2.95 (s, 12 H, 6-H), 5.00 (d, $J = 18.3$ Hz, 1 H, 1-H), 6.76 (d, $J = 8.8$ Hz, 4 H, Ar), 7.31 (d, $J = 8.8$ Hz, 4 H, Ar); ^{13}C NMR (75.5 MHz, CDCl_3): $\delta = 13.2$ (q, C-10), 18.6 (t, C-9), 19.2 (t, C-8), 23.7/23.9/24.1 (3 t, C-7), 40.7 (q, C-6), 45.2 (dd, $J = 41.4$ Hz, C-1), 113.5, 123.2 (2 d, Ar), 121.1, 149.9 (2 s, Ar); ^{31}P NMR (81 MHz, CDCl_3): $\delta = 34.07$ (s); MS (FAB): m/z (%): 455 (6) $[\text{M}]^+$, 281 (6), 253 (100) $[\text{Ar}_2\text{CH}]^+$, 237 (8), 221 (7), 154 (4), 147 (17), 136 (8).



NHB11

66

Bis(4-(methyl(2,2,2-trifluoroethyl)amino)phenyl)methyl-triphenoxy-phosphonium tetrafluoroborate (67) was obtained from phosphorous acid triphenyl ester ($\text{PhO})_3\text{P}$ (310 mg, 1 mmol) and bis(4-(methyl(2,2,2-trifluoroethyl)amino)phenyl)methylium tetrafluoroborate ($\text{mfa})_2\text{CH}^+ \text{BF}_4^-$ (476 mg, 1 mmol) as a violet-blue solid (600 mg, 76 %). ^1H NMR (300 MHz, CDCl_3): δ = 3.02 (s, 6 H, 8-H), 3.84 (q, J = 8.9 Hz, 4 H, 6-H), 4.66 (d, J = 25.9 Hz, 1 H, 1-H), 6.75-7.48 (m, 23 H, 4 \times 3-H, 4 \times 4-H, 6 \times 10-H, 6 \times 11-H, 3 \times 12-H); ^{13}C NMR (75.5 MHz, CD_3CN): δ = 40.4 (q, C-8), 48.4 (dd, J = 135.9 Hz, C-1), 53.7 (tq, J = 30.2 Hz, C-6), 127.2 (sq, J = 319.3 Hz, C-7), 114.6, 120.2, 125.1, 129.4, 130.2 (5 d, Ar), 145.8, 150.9 (2 s, Ar) (the signal for the third quaternary carbon-atom is missing and probably masked by other intensive signals); ^{31}P NMR (81 MHz, CDCl_3): δ = 19.86 (s); MS (FAB): m/z (%): 651 (7), 622 (10), 389 (100) $[\text{Ar}_2\text{CH}]^+$, 305 (8), 154 (6), 136 (11).

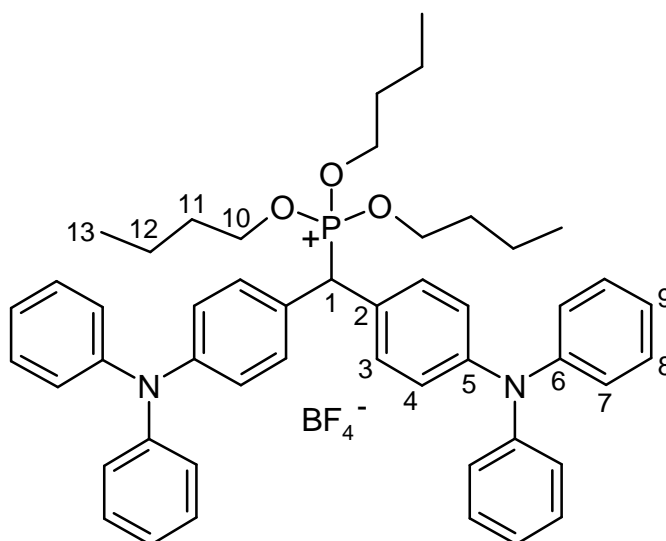


NHB14

67

Bis(4-diphenylaminophenyl)methyl-tris(*n*-butoxy)-phosphonium tetrafluoroborate (68) was obtained from phosphorous acid tributyl ester ($n\text{BuO})_3\text{P}$ (0.250 g, 1 mmol) and bis(4-diphenylaminophenyl)methylium tetrafluoroborate ($\text{dpa})_2\text{CH}^+ \text{BF}_4^-$ (588 mg, 1 mmol) as a blue-green solid (422 mg, 50 %). ^1H NMR (300 MHz, CDCl_3): δ = 0.84-1.02 (m, 9 H, 13-H),

1.24-1.42 (m, 6 H, 12-H), 1.64-1.78 (m, 6 H, 11-H), 4.40-4.54 (m, 6 H, 10-H), 5.50 (d, $J = 25.7$ Hz, 1 H, 1-H), 6.80-7.60 (m, 28 H, 4×3 -H, 4×4 -H, 8×7 -H, 8×8 -H, 4×9 -H); ^{13}C -NMR (75.5 MHz, CDCl_3): $\delta = 13.22$ (q, C-13), 18.13 (t, C-12), 31.54/31.62 (2 t, C-11), 45.52 (dd, $J = 126.5$ Hz, C-1), 73.90/74.02 (2 t, C-10), 122.66, 123.46, 124.68, 129.23, 130.01/130.13 (6 d, Ar), 124.32/124.41, 146.88, 148.05/148.09 (5 s, Ar); ^{31}P NMR (81 MHz, CDCl_3): $\delta = 37.05$ (s); MS (FAB): m/z (%): 694 (28), 501 (100) $[\text{Ar}_2\text{CH}]^+$ 450 (14), 258 (7).



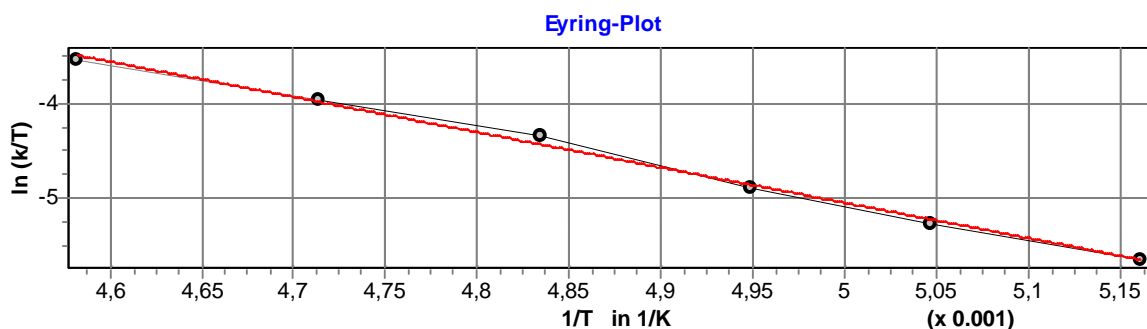
NHB07

68

10.5.3 Concentrations and rate constants of the individual kinetic runs

Table 10.84: Bis(*N*-methyl-1,2,3,4-tetrahydroquinolin-6-yl)methylm tetrafluoroborate $(\text{thq})_2\text{CH}^+ \text{BF}_4^-$ and tris(4-chlorophenyl)phosphine $(\text{p-ClC}_6\text{H}_4)_3\text{P}$ in CH_2Cl_2 at $\lambda = 640$ nm (Schölly).

No.	$[\text{El}]_0 /$ mol L^{-1}	$[\text{Nuc}]_0 /$ mol L^{-1}	$[\text{Nuc}]_0 / [\text{El}]_0$	Conv. / %	$T /$ $^\circ\text{C}$	$k_2 /$ $\text{L mol}^{-1} \text{s}^{-1}$
190201.PA0	1.558×10^{-5}	1.359×10^{-3}	87	52	-79.4	6.867×10^{-1}
190201.PA6	1.469×10^{-5}	2.561×10^{-3}	174	67	-75.0	1.020
190201.PA1	1.443×10^{-5}	1.258×10^{-3}	87	62	-71.1	1.536
190201.PA5	2.006×10^{-5}	2.800×10^{-3}	140	47	-66.3	2.704
190201.PA2	1.579×10^{-5}	2.752×10^{-3}	174	51	-61.0	4.066
190201.PA4	1.451×10^{-5}	2.523×10^{-3}	174	33	-54.9	6.424

Eyring parameters:

$$\Delta H^\ddagger = 31.182 \pm 0.996 \text{ kJ mol}^{-1}$$

$$\Delta S^\ddagger = -83.608 \pm 4.865 \text{ J mol}^{-1} \text{ K}^{-1}$$

$$r^2 = 0.9959$$

Arrhenius parameters:

$$E_a = 32.890 \pm 0.989 \text{ kJ mol}^{-1}$$

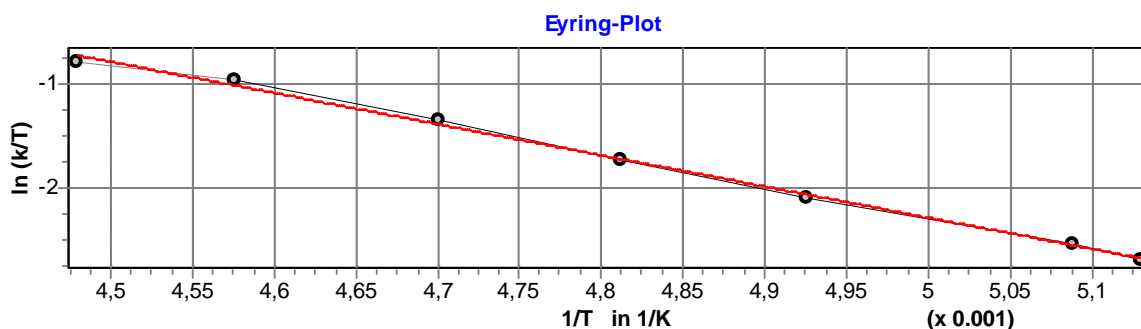
$$\ln A = 20.031 \pm 0.581$$

$$r^2 = 0.9964$$

$$k_2 (20^\circ\text{C}) = (7.293 \pm 1.291) \times 10^2 \text{ L mol}^{-1} \text{ s}^{-1}$$

Table 10.85: Bis(4-dimethylaminophenyl)methylm tetrafluoroborate $(\text{dma})_2\text{CH}^+ \text{BF}_4^-$ and tris(4-chlorophenyl)phosphine $(\text{p-ClC}_6\text{H}_4)_3\text{P}$ in CH_2Cl_2 at $\lambda = 600 \text{ nm}$ (Schölly).

No.	$[\text{EI}]_0 /$ mol L^{-1}	$[\text{Nuc}]_0 /$ mol L^{-1}	$[\text{Nuc}]_0/[\text{EI}]_0$	Conv. / %	$T /$ $^\circ\text{C}$	$k_2 /$ $\text{L mol}^{-1} \text{ s}^{-1}$
230201.PA0	1.400×10^{-5}	1.572×10^{-3}	112	68	-78.2	1.336×10^1
230201.PA6	3.599×10^{-5}	1.616×10^{-3}	45	82	-76.6	1.582×10^1
230201.PA1	3.406×10^{-5}	3.824×10^{-3}	112	66	-70.1	2.518×10^1
230201.PA5	3.935×10^{-5}	1.326×10^{-3}	34	77	-65.3	3.656×10^1
230201.PA2	3.504×10^{-5}	2.754×10^{-3}	79	61	-60.4	5.490×10^1
230201.PA4	3.785×10^{-5}	2.125×10^{-3}	56	57	-54.6	8.311×10^1
230201.PA3	3.748×10^{-5}	1.684×10^{-3}	45	55	-49.9	1.009×10^2



Eyring parameters:

$$\Delta H^\ddagger = 24.667 \pm 0.602 \text{ kJ mol}^{-1}$$

$$\Delta S^\ddagger = -93.188 \pm 2.900 \text{ J mol}^{-1} \text{ K}^{-1}$$

$$r^2 = 0.9970$$

Arrhenius parameters:

$$E_a = 26.397 \pm 0.598 \text{ kJ mol}^{-1}$$

$$\ln A = 18.891 \pm 0.347$$

$$r^2 = 0.9974$$

$$k_2 (20^\circ \text{C}) = (3.336 \pm 0.340) \times 10^3 \text{ L mol}^{-1} \text{ s}^{-1}$$

Table 10.86: Bis(4-(methylphenylamino)phenyl)methylium tetrafluoroborate $(\text{mpa})_2\text{CH}^+$ BF_4^- and tris(4-chlorophenyl)phosphine $(\text{p-ClC}_6\text{H}_4)_3\text{P}$ in CH_2Cl_2 at $\lambda = 622 \text{ nm}$ (Stopped flow).

No.	$[\text{El}]_0 /$ mol L^{-1}	$[\text{Nuc}]_0 /$ mol L^{-1}	$[\text{Nuc}]_0/[\text{El}]_0$	$T /$ $^\circ\text{C}$	$k_{\text{eff}} /$ s^{-1}
220201-H	4.480×10^{-6}	2.079×10^{-4}	46	20.0	6.915
220201-I	4.480×10^{-6}	4.158×10^{-4}	93	20.0	1.142×10^1
220201-J	4.480×10^{-6}	6.237×10^{-4}	139	20.0	1.582×10^1
220201-K	4.480×10^{-6}	8.317×10^{-4}	186	20.0	2.013×10^1
220201-L	4.480×10^{-6}	1.040×10^{-3}	232	20.0	2.433×10^1

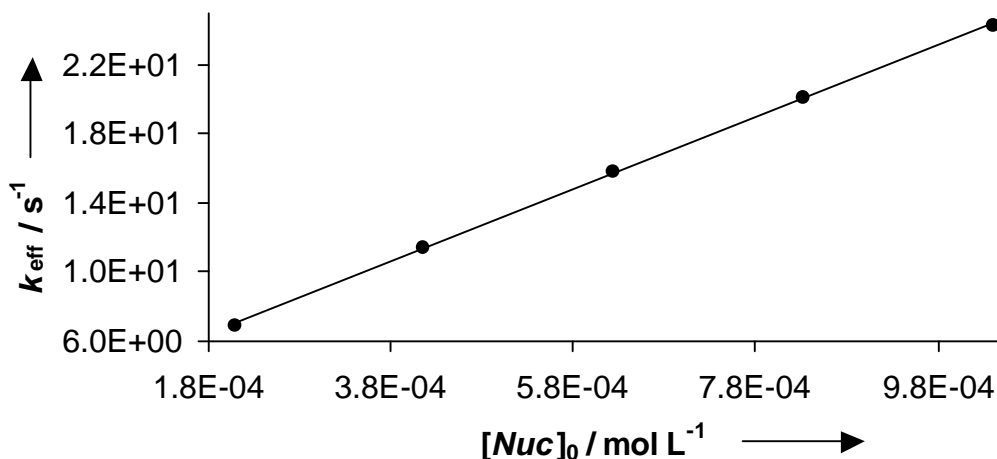


Figure 10.4: Plot of k_{eff} versus $[Nuc]_0$ ($n = 5$, $k_{\text{eff}} = (2.093 \times 10^4) \times [Nuc]_0 + 2.666$, $r^2 = 0.9998$).

$$k_2 (20 \text{ }^\circ\text{C}) = 2.093 \times 10^4 \text{ L mol}^{-1} \text{ s}^{-1}$$

$$k_{-2} (20 \text{ }^\circ\text{C}) = 2.666 \text{ s}^{-1}$$

$$K (20 \text{ }^\circ\text{C}) = 7.852 \times 10^3 \text{ L mol}^{-1}$$

Table 10.87: Bis(4-diphenylaminophenyl)methylium tetrafluoroborate $(\text{dpa})_2\text{CH}^+ \text{BF}_4^-$ and tris(4-chlorophenyl)phosphine $(\text{p-ClC}_6\text{H}_4)_3\text{P}$ in CH_2Cl_2 at $\lambda = 674 \text{ nm}$ (Stopped flow).

No.	$[El]_0 /$ mol L^{-1}	$[Nuc]_0 /$ mol L^{-1}	$[Nuc]_0/[El]_0$	$T /$ $^\circ\text{C}$	$k_2 /$ $\text{L mol}^{-1} \text{ s}^{-1}$
220201-A	5.751×10^{-6}	1.641×10^{-4}	29	20.0	1.193×10^5
220201-B	5.751×10^{-6}	3.282×10^{-4}	57	20.0	1.194×10^5
220201-C	5.751×10^{-6}	4.923×10^{-4}	86	20.0	1.197×10^5
220201-G	5.751×10^{-6}	6.564×10^{-4}	114	20.0	1.205×10^5
220201-F	5.751×10^{-6}	8.205×10^{-4}	143	20.0	1.212×10^5

$$\bar{k}_2 (20 \text{ }^\circ\text{C}) = (1.200 \pm 0.007) \times 10^5 \text{ L mol}^{-1} \text{ s}^{-1}$$

Table 10.88: Bis(4-(methyl(2,2,2-trifluoroethyl)amino)phenyl)methylm tetrafluoroborate ($(\text{mfa})_2\text{CH}^+ \text{BF}_4^-$) and tris(4-chlorophenyl)phosphine ($(\text{p-ClC}_6\text{H}_4)_3\text{P}$) in CH_2Cl_2 at $\lambda = 593 \text{ nm}$ (Stopped flow).

No.	$[\text{El}]_0 /$ mol L^{-1}	$[\text{Nuc}]_0 /$ mol L^{-1}	$[\text{Nuc}]_0/[\text{El}]_0$	$T /$ $^\circ\text{C}$	$k_2 /$ $\text{L mol}^{-1} \text{ s}^{-1}$
200201-A	6.006×10^{-6}	1.112×10^{-4}	19	20.0	5.108×10^5
200201-B	6.006×10^{-6}	2.225×10^{-4}	37	20.0	4.910×10^5
200201-C	6.006×10^{-6}	4.450×10^{-4}	74	20.0	4.902×10^5
200201-D	6.006×10^{-6}	6.675×10^{-4}	111	20.0	4.920×10^5
200201-E	6.006×10^{-6}	3.337×10^{-4}	56	20.0	5.029×10^5

$$\bar{k}_2 (20 \text{ }^\circ\text{C}) = (4.974 \pm 0.082) \times 10^5 \text{ L mol}^{-1} \text{ s}^{-1}$$

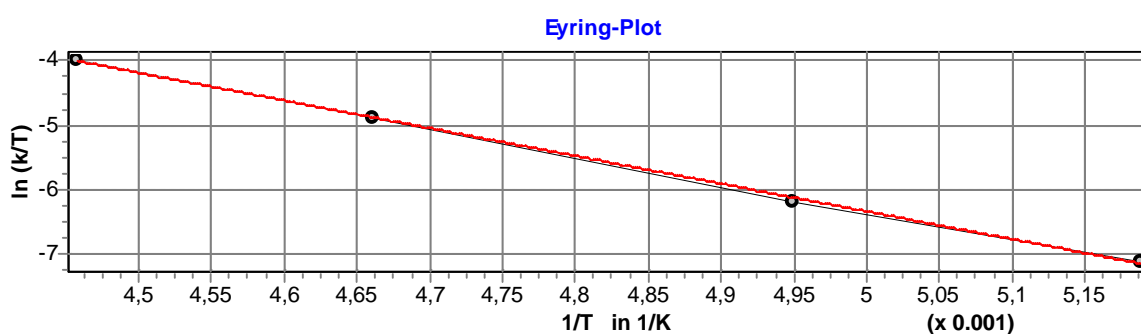
Table 10.89: Bis(4-(phenyl(2,2,2-trifluoroethyl)amino)phenyl)methylm tetrafluoroborate ($(\text{pfa})_2\text{CH}^+ \text{BF}_4^-$) and tris(4-chlorophenyl)phosphine ($(\text{p-ClC}_6\text{H}_4)_3\text{P}$) in CH_2Cl_2 at $\lambda = 601 \text{ nm}$ (Stopped flow).

No.	$[\text{El}]_0 /$ mol L^{-1}	$[\text{Nuc}]_0 /$ mol L^{-1}	$[\text{Nuc}]_0/[\text{El}]_0$	$T /$ $^\circ\text{C}$	$k_2 /$ $\text{L mol}^{-1} \text{ s}^{-1}$
200201-F	5.011×10^{-6}	3.862×10^{-5}	8	20.0	1.213×10^6
200201-I	5.011×10^{-6}	5.793×10^{-5}	12	20.0	1.142×10^6
200201-G	5.011×10^{-6}	7.724×10^{-5}	15	20.0	1.113×10^6
200201-J	5.011×10^{-6}	9.655×10^{-5}	19	20.0	1.202×10^6
200201-H	5.011×10^{-6}	1.159×10^{-4}	23	20.0	1.181×10^6

$$\bar{k}_2 (20 \text{ }^\circ\text{C}) = (1.170 \pm 0.038) \times 10^6 \text{ L mol}^{-1} \text{ s}^{-1}$$

Table 10.90: Bis(lilolidin-8-yl)methylm tetrafluoroborate $(\text{lil})_2\text{CH}^+ \text{BF}_4^-$ and triphenylphosphine Ph_3P in CH_2Cl_2 at $\lambda = 640 \text{ nm}$ (Schölly).

No.	$[\text{El}]_0 /$ mol L^{-1}	$[\text{Nuc}]_0 /$ mol L^{-1}	$[\text{Nuc}]_0/[\text{El}]_0$	Conv. / %	$T /$ $^\circ\text{C}$	$k_2 /$ $\text{L mol}^{-1} \text{ s}^{-1}$
060201.PA0	3.807×10^{-5}	4.301×10^{-3}	113	50	-80.4	1.555×10^{-1}
060201.PA1	4.237×10^{-5}	4.786×10^{-3}	113	58	-71.1	4.153×10^{-1}
060201.PA2	2.353×10^{-5}	4.253×10^{-3}	181	77	-58.6	1.617
060201.PA3	2.657×10^{-5}	3.842×10^{-3}	145	68	-48.8	4.154



Eyring parameters:

$$\Delta H^\ddagger = 35.869 \pm 0.752 \text{ kJ mol}^{-1}$$

$$\Delta S^\ddagger = -71.003 \pm 3.623 \text{ J mol}^{-1} \text{ K}^{-1}$$

$$r^2 = 0.9991$$

Arrhenius parameters:

$$E_a = 37.595 \pm 0.773 \text{ kJ mol}^{-1}$$

$$\ln A = 21.558 \pm 0.448$$

$$r^2 = 0.9992$$

$$k_2 (20 \text{ }^\circ\text{C}) = (4.854 \pm 0.617) \times 10^2 \text{ L mol}^{-1} \text{ s}^{-1}$$

Table 10.91: Bis(julolidin-9-yl)methylm tetrafluoroborate $(\text{jul})_2\text{CH}^+ \text{BF}_4^-$ and triphenylphosphine Ph_3P in CH_2Cl_2 at $\lambda = 642 \text{ nm}$ (J&M).

No.	$[\text{El}]_0 /$ mol L^{-1}	$[\text{Nuc}]_0 /$ mol L^{-1}	$[\text{Nuc}]_0/[\text{El}]_0$	Conv. / %	$T /$ $^\circ\text{C}$	$k_{\text{eff}} /$ s^{-1}
030101-02	9.530×10^{-6}	3.119×10^{-4}	33	87	-78.5	4.195×10^{-4}
030101-03	1.240×10^{-5}	1.044×10^{-3}	84	98	-78.6	1.387×10^{-3}
030101-01	1.292×10^{-5}	1.813×10^{-3}	140	98	-78.4	2.308×10^{-3}
030101-06	1.265×10^{-5}	3.548×10^{-4}	28	87	-68.6	1.432×10^{-3}
030101-04	1.283×10^{-5}	1.080×10^{-3}	84	96	-68.6	4.111×10^{-3}
030101-05	1.191×10^{-5}	1.671×10^{-3}	140	96	-68.5	6.277×10^{-3}
030101-21	1.177×10^{-5}	3.425×10^{-4}	29	83	-63.2	2.436×10^{-3}
030101-20	1.228×10^{-5}	1.072×10^{-3}	87	93	-63.1	7.197×10^{-3}
030101-19	1.415×10^{-5}	1.764×10^{-3}	125	96	-63.3	1.220×10^{-2}
030101-09	1.114×10^{-5}	3.125×10^{-4}	28	73	-58.2	4.098×10^{-3}
030101-08	1.249×10^{-5}	1.051×10^{-3}	84	92	-58.0	1.151×10^{-2}
030101-07	1.211×10^{-5}	1.698×10^{-3}	140	94	-58.2	1.888×10^{-2}
030101-18	1.226×10^{-5}	3.421×10^{-4}	28	67	-53.2	7.938×10^{-3}
030101-17	1.239×10^{-5}	1.037×10^{-3}	84	86	-53.2	1.932×10^{-2}
030101-16	1.289×10^{-5}	1.798×10^{-3}	140	90	-53.2	3.334×10^{-2}
030101-12	1.261×10^{-5}	3.518×10^{-4}	28	57	-47.4	1.566×10^{-2}
030101-11	1.186×10^{-5}	9.927×10^{-4}	84	80	-47.5	3.456×10^{-2}
030101-10	1.236×10^{-5}	1.724×10^{-3}	140	86	-47.3	4.767×10^{-2}
030101-15	1.251×10^{-5}	3.490×10^{-4}	28	35	-37.3	4.901×10^{-2}
030101-14	1.222×10^{-5}	1.022×10^{-3}	84	64	-37.4	9.922×10^{-2}
030101-13	1.232×10^{-5}	1.719×10^{-3}	140	74	-37.3	1.469×10^{-1}

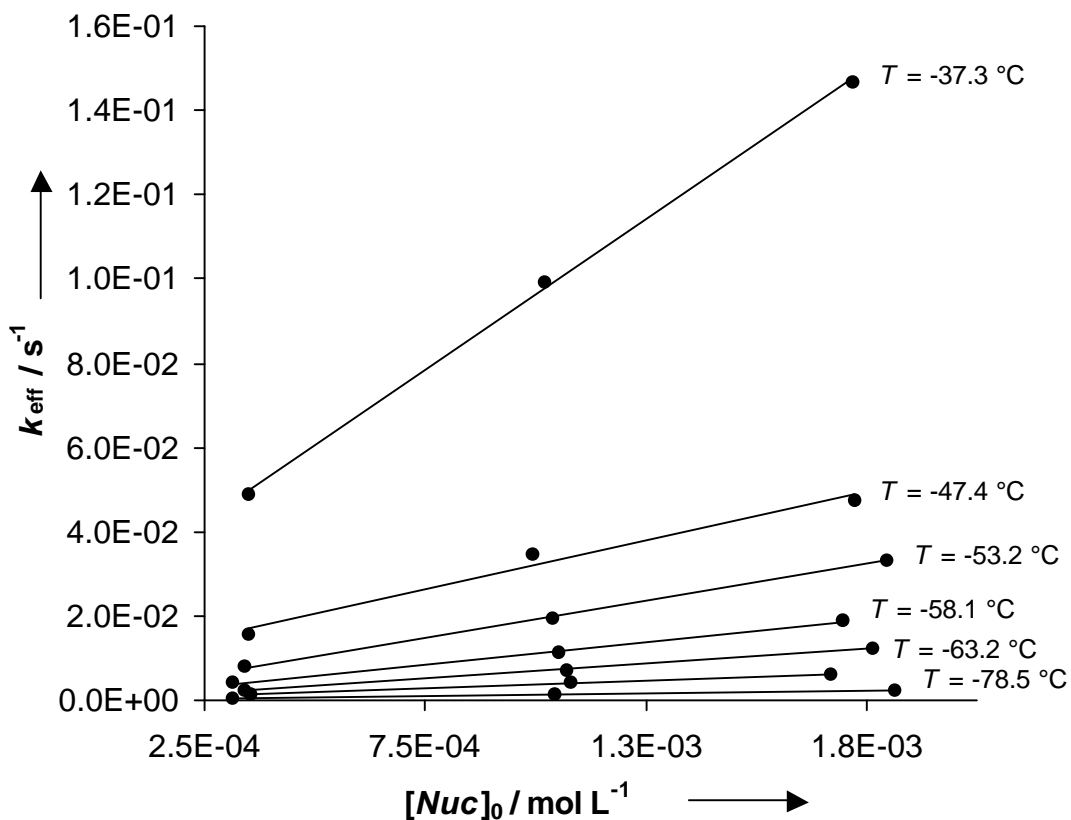
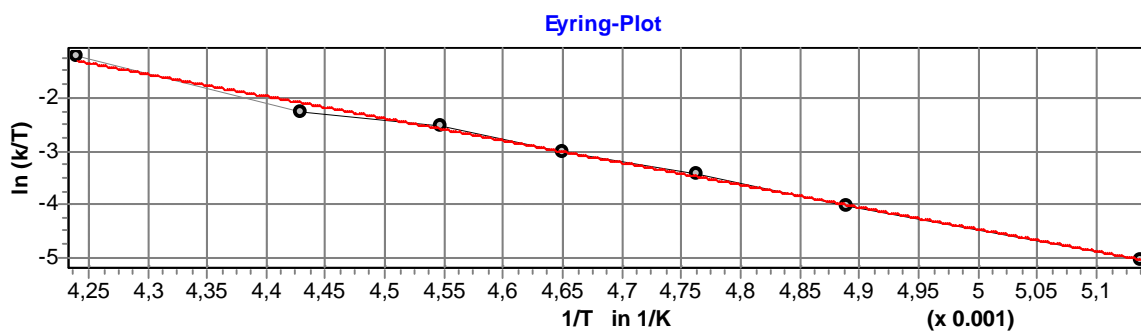


Figure 10.5: Plot of k_{eff} versus $[\text{Nuc}]_0$ for the kinetic experiments from Table 10.91 at different temperatures.

Table 10.92: k_2 , k_{-2} , and K -values for the kinetic experiments from Table 10.91 (for correlations see Figure 10.5).

T (average) / $^{\circ}\text{C}$	k_2 / $\text{L mol}^{-1} \text{s}^{-1}$	k_{-2} / s^{-1}	K / L mol^{-1}	r^2
-78.5	1.258	4.313×10^{-5}	2.916×10^4	0.9992
-68.6	3.682	1.286×10^{-4}	2.862×10^4	1.0000
-63.2	6.866	3.446×10^{-4}	1.992×10^4	0.9991
-58.1	1.065×10^1	6.233×10^{-4}	1.709×10^4	0.9987
-53.2	1.746×10^1	1.705×10^{-3}	1.024×10^4	0.9989
-47.4	2.333×10^1	7.453×10^{-3}	3.130×10^3	0.9800
-37.3	7.143×10^1	2.480×10^{-2}	2.881×10^3	0.9994



Eyring parameters:

$$\Delta H^\ddagger = 34.743 \pm 1.125 \text{ kJ mol}^{-1}$$

$$\Delta S^\ddagger = -60.099 \pm 5.256 \text{ J mol}^{-1} \text{ K}^{-1}$$

$$r^2 = 0.9948$$

Arrhenius parameters:

$$E_a = 36.520 \pm 1.130 \text{ kJ mol}^{-1}$$

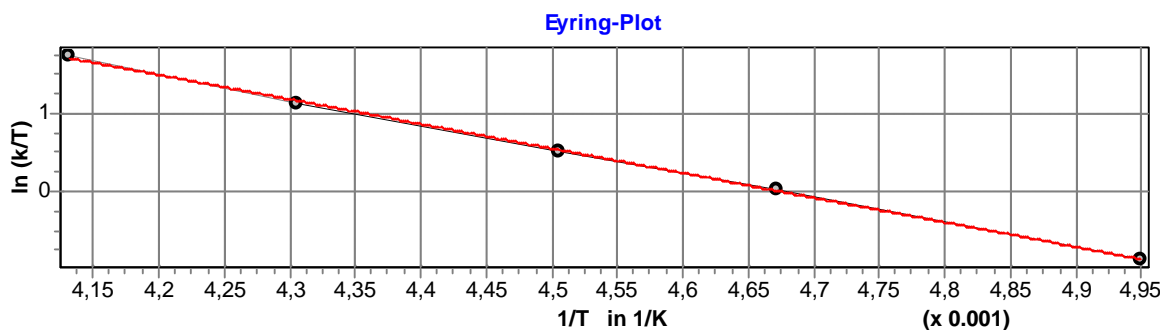
$$\ln A = 22.791 \pm 0.635$$

$$r^2 = 0.9952$$

$$k_2 (20 \text{ }^\circ\text{C}) = (2.568 \pm 0.438) \times 10^3 \text{ L mol}^{-1} \text{ s}^{-1}$$

Table 10.93: Bis(4-(*N*-pyrrolidino)phenyl)methylmethyl tetrafluoroborate $(\text{pyr})_2\text{CH}^+ \text{BF}_4^-$ and triphenylphosphine Ph_3P in CH_2Cl_2 at $\lambda = 640 \text{ nm}$ (Schölly).

No.	$[\text{EL}]_0 /$ mol L^{-1}	$[\text{Nuc}]_0 /$ mol L^{-1}	$[\text{Nuc}]_0/[\text{EL}]_0$	Conv. / %	$T /$ $^\circ\text{C}$	$k_2 /$ $\text{L mol}^{-1} \text{ s}^{-1}$
021120.PA1	2.222×10^{-5}	1.952×10^{-3}	88	86	-71.1	8.476×10^1
021120.PA2	1.926×10^{-5}	1.269×10^{-3}	66	62	-59.1	2.225×10^2
021120.PA7	2.028×10^{-5}	8.911×10^{-4}	44	66	-51.2	3.702×10^2
021120.PA5	1.692×10^{-5}	7.433×10^{-4}	44	51	-40.9	7.145×10^2
021120.PA6	1.463×10^{-5}	3.214×10^{-4}	22	72	-31.1	1.390×10^3



Eyring parameters:

$$\Delta H^\ddagger = 26.247 \pm 0.486 \text{ kJ mol}^{-1}$$

$$\Delta S^\ddagger = -74.863 \pm 2.197 \text{ J mol}^{-1} \text{ K}^{-1}$$

$$r^2 = 0.9990$$

Arrhenius parameters:

$$E_a = 28.082 \pm 0.498 \text{ kJ mol}^{-1}$$

$$\ln A = 21.155 \pm 0.271$$

$$r^2 = 0.9991$$

$$k_2 (20 \text{ }^\circ\text{C}) = (1.581 \pm 0.102) \times 10^4 \text{ L mol}^{-1} \text{ s}^{-1}$$

Table 10.94: Bis(4-dimethylaminophenyl)methylium tetrafluoroborate $(\text{dma})_2\text{CH}^+ \text{BF}_4^-$ and triphenylphosphine Ph_3P in $(\text{CH}_3)_2\text{SO}$ at $\lambda = 616 \text{ nm}$ (Stopped flow).

No.	$[\text{EL}]_0 /$ mol L^{-1}	$[\text{Nuc}]_0 /$ mol L^{-1}	$[\text{Nuc}]_0/[\text{EL}]_0$	$T /$ $^\circ\text{C}$	$k_{\text{eff}} /$ s^{-1}
290301-F	5.503×10^{-6}	2.728×10^{-4}	50	20.0	4.060
290301-G	5.503×10^{-6}	5.455×10^{-4}	99	20.0	8.090
290301-H	5.503×10^{-6}	8.183×10^{-4}	149	20.0	1.237×10^1
290301-I	5.503×10^{-6}	1.091×10^{-3}	198	20.0	1.617×10^1
290301-J	5.503×10^{-6}	1.364×10^{-3}	248	20.0	2.060×10^1

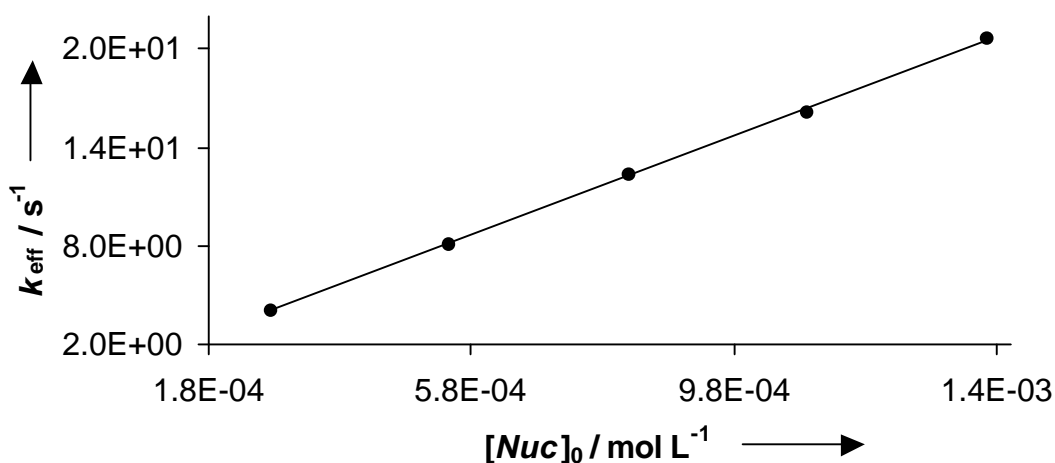


Figure 10.6: Plot of k_{eff} versus $[\text{Nuc}]_0$ ($n = 5$, $k_{\text{eff}} = (1.509 \times 10^4) \times [\text{Nuc}]_0 + 8.970 \times 10^{-2}$, $r^2 = 0.9996$).

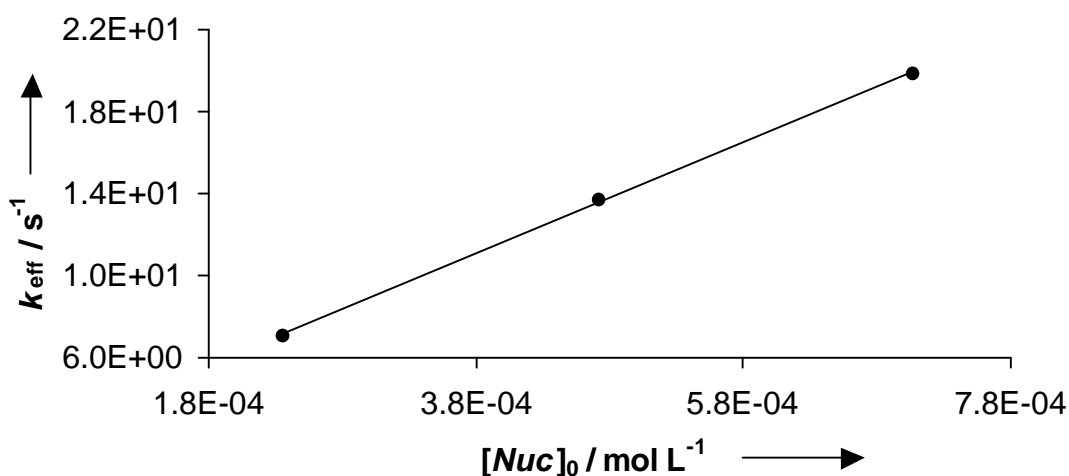
$$k_2 (20 \text{ }^\circ\text{C}) = 1.509 \times 10^4 \text{ L mol}^{-1} \text{ s}^{-1}$$

$$k_2 (20 \text{ }^\circ\text{C}) = 8.970 \times 10^{-2} \text{ s}^{-1}$$

$$K (20 \text{ }^\circ\text{C}) = 1.682 \times 10^5 \text{ L mol}^{-1}$$

Table 10.95: Bis(4-dimethylaminophenyl)methylm tetrafluoroborate $(\text{dma})_2\text{CH}^+ \text{BF}_4^-$ and triphenylphosphine Ph_3P in $(\text{CH}_3)_2\text{CO}$ at $\lambda = 607 \text{ nm}$ (Stopped flow).

No.	$[\text{El}]_0 /$ mol L^{-1}	$[\text{Nuc}]_0 /$ mol L^{-1}	$[\text{Nuc}]_0/[\text{El}]_0$	$T /$ $^\circ\text{C}$	$k_{\text{eff}} /$ s^{-1}
260301-D	6.420×10^{-6}	2.357×10^{-4}	37	20.0	7.098
260301-E	6.420×10^{-6}	4.714×10^{-4}	73	20.0	1.368×10^1
260301-F	6.420×10^{-6}	7.071×10^{-4}	110	20.0	1.987×10^1

**Figure 10.7:** Plot of k_{eff} versus $[\text{Nuc}]_0$ ($n = 3$, $k_{\text{eff}} = (2.709 \times 10^4) \times [\text{Nuc}]_0 + 7.773 \times 10^{-1}$, $r^2 = 0.9997$).

$$k_2 (20 \text{ }^\circ\text{C}) = 2.709 \times 10^4 \text{ L mol}^{-1} \text{ s}^{-1}$$

$$k_{-2} (20 \text{ }^\circ\text{C}) = 7.773 \times 10^{-1} \text{ s}^{-1}$$

$$K (20 \text{ }^\circ\text{C}) = 3.486 \times 10^4 \text{ L mol}^{-1}$$

Table 10.96: Bis(4-dimethylaminophenyl)methylm tetrafluoroborate $(\text{dma})_2\text{CH}^+ \text{BF}_4^-$ and triphenylphosphine Ph_3P in CH_3CN at $\lambda = 613 \text{ nm}$ (Stopped flow).

No.	$[\text{El}]_0 /$ mol L^{-1}	$[\text{Nuc}]_0 /$ mol L^{-1}	$[\text{Nuc}]_0/[\text{El}]_0$	$T /$ $^\circ\text{C}$	$k_{\text{eff}} /$ s^{-1}
260301-A	4.821×10^{-6}	2.428×10^{-4}	50	20.0	8.753
260301-B	4.821×10^{-6}	4.856×10^{-4}	101	20.0	1.719×10^1
260301-C	4.821×10^{-6}	7.284×10^{-4}	151	20.0	2.494×10^1

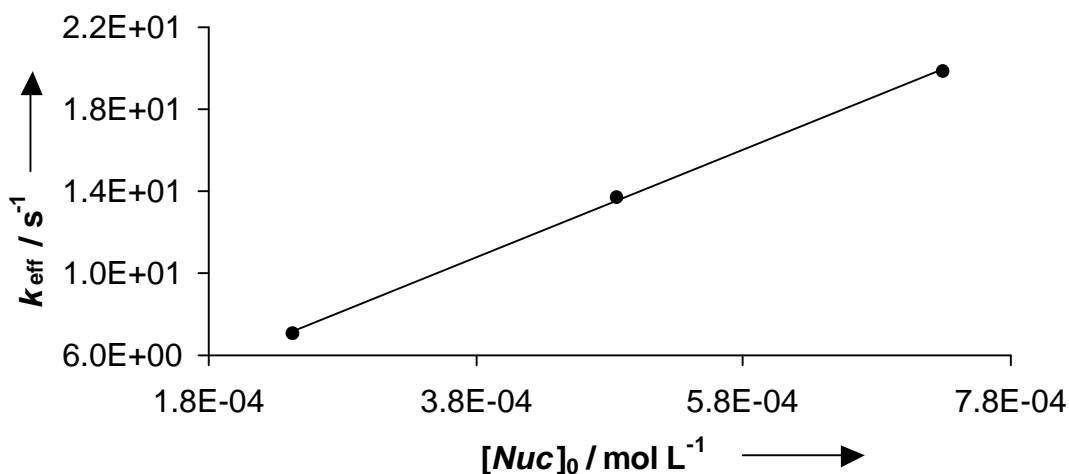


Figure 10.8: Plot of k_{eff} versus $[Nuc]_0$ ($n = 3$, $k_{\text{eff}} = (3.333 \times 10^4) \times [Nuc]_0 + 7.740 \times 10^{-1}$, $r^2 = 0.9997$).

$$k_2 (20 \text{ }^\circ\text{C}) = 3.333 \times 10^4 \text{ L mol}^{-1} \text{ s}^{-1}$$

$$k_{-2} (20 \text{ }^\circ\text{C}) = 7.740 \times 10^{-1} \text{ s}^{-1}$$

$$K (20 \text{ }^\circ\text{C}) = 4.307 \times 10^4 \text{ L mol}^{-1}$$

Table 10.97: Bis(4-dimethylaminophenyl)methylmethyl tetrafluoroborate $(\text{dma})_2\text{CH}^+ \text{BF}_4^-$ and triphenylphosphine Ph_3P in CHCl_3 at $\lambda = 611 \text{ nm}$ (Stopped flow).

No.	$[El]_0 / \text{mol L}^{-1}$	$[Nuc]_0 / \text{mol L}^{-1}$	$[Nuc]_0/[El]_0$	$T / \text{ }^\circ\text{C}$	$k_{\text{eff}} / \text{ s}^{-1}$
260301-G	5.256×10^{-6}	2.654×10^{-4}	51	20.0	1.188×10^1
260301-H	5.256×10^{-6}	5.307×10^{-4}	101	20.0	2.329×10^1
260301-I	5.256×10^{-6}	7.961×10^{-4}	152	20.0	3.442×10^1
260301-J	5.256×10^{-6}	1.061×10^{-3}	202	20.0	4.769×10^1
260301-K	5.256×10^{-6}	1.327×10^{-3}	252	20.0	5.829×10^1

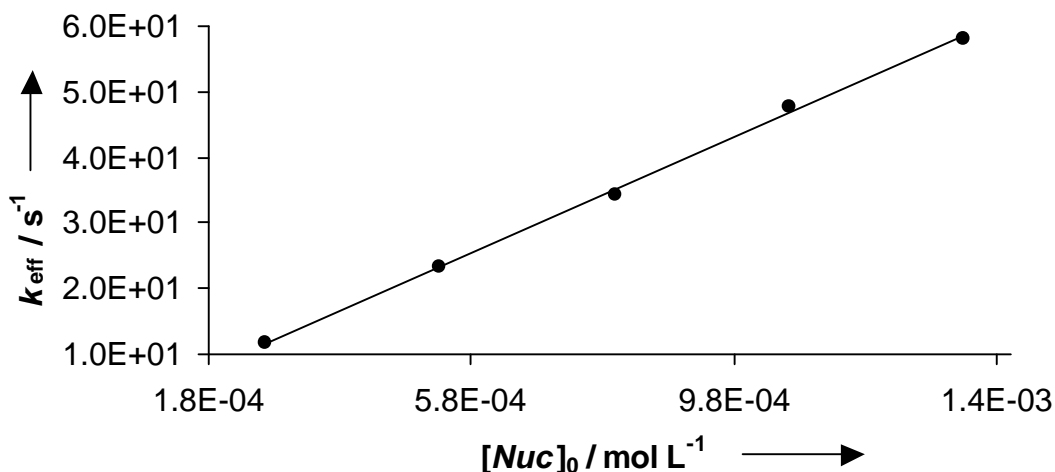


Figure 10.9: Plot of k_{eff} versus $[Nuc]_0$ ($n = 5$, $k_{\text{eff}} = (4.418 \times 10^4) \times [Nuc]_0 + 6.553 \times 10^{-1}$, $r^2 = 0.9990$).

$$k_2 (20 \text{ }^\circ\text{C}) = 4.418 \times 10^4 \text{ L mol}^{-1} \text{ s}^{-1}$$

$$k_{-2} (20 \text{ }^\circ\text{C}) = 6.553 \times 10^{-1} \text{ s}^{-1}$$

$$K (20 \text{ }^\circ\text{C}) = 6.741 \times 10^4 \text{ L mol}^{-1}$$

Table 10.98: Bis(4-dimethylaminophenyl)methylm tetrafluoroborate $(\text{dma})_2\text{CH}^+ \text{BF}_4^-$ and triphenylphosphine Ph_3P in CH_3NO_2 at $\lambda = 609 \text{ nm}$ (Stopped flow).

No.	$[EL]_0 /$ mol L^{-1}	$[Nuc]_0 /$ mol L^{-1}	$[Nuc]_0/[EL]_0$	$T /$ $^\circ\text{C}$	$k_{\text{eff}} /$ s^{-1}
290301-A	4.186×10^{-6}	2.612×10^{-4}	62	20.0	8.753
290301-B	4.186×10^{-6}	5.225×10^{-4}	125	20.0	2.271×10^1
290301-C	4.186×10^{-6}	7.837×10^{-4}	187	20.0	3.108×10^1
290301-D	4.186×10^{-6}	1.045×10^{-3}	250	20.0	4.263×10^1
290301-E	4.186×10^{-6}	1.306×10^{-3}	312	20.0	5.677×10^1

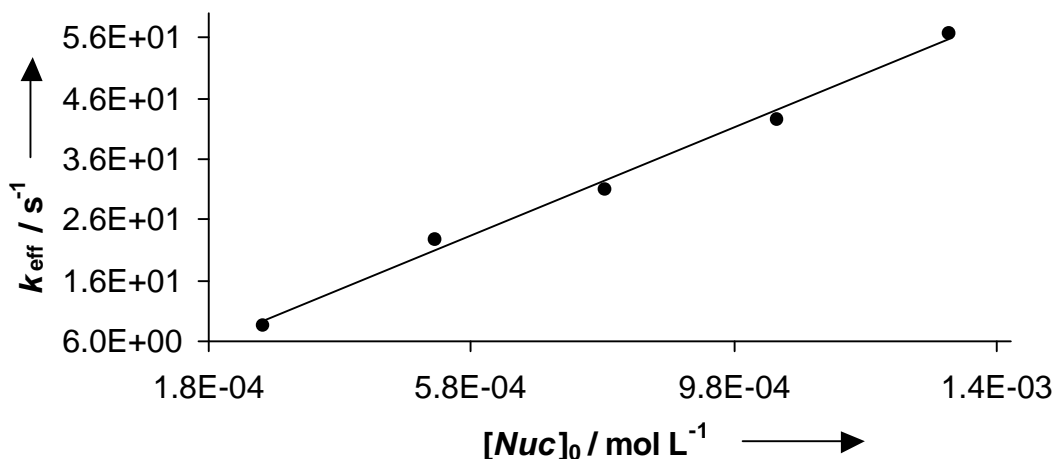


Figure 10.10: Plot of k_{eff} versus $[\text{Nuc}]_0$ ($n = 5$, $k_{\text{eff}} = (4.439 \times 10^4) \times [\text{Nuc}]_0 + 2.260$, $r^2 = 0.9935$).

$$k_2 (20 \text{ }^\circ\text{C}) = 4.439 \times 10^4 \text{ L mol}^{-1} \text{ s}^{-1}$$

$$k_{-2} (20 \text{ }^\circ\text{C}) = 2.260 \text{ s}^{-1}$$

$$K (20 \text{ }^\circ\text{C}) = 1.964 \times 10^4 \text{ L mol}^{-1}$$

Table 10.99: Rate constants k_2 at 20 °C, dielectric constants ϵ_r at 25 °C, $E_T(30)$ -values, and donor numbers (donicities) DN for the reactions of bis(4-dimethylaminophenyl)methylum tetrafluoroborate $(\text{dma})_2\text{CH}^+ \text{BF}_4^-$ and triphenylphosphine Ph_3P in various solvents.

Solvent	$k_2 / \text{L mol}^{-1} \text{ s}^{-1}$	ϵ_r ^[a]	$E_T(30) / \text{kcal mol}^{-1}$ ^[a]	$DN / \text{kcal mol}^{-1}$ ^[a]
$(\text{CH}_3)_2\text{SO}$	1.509×10^4	46.5	45.1	29.8
$(\text{CH}_3)_2\text{CO}$	2.709×10^4	20.6	42.2	17.0
CH_3CN	3.333×10^4	35.9	45.6	14.1
CHCl_3	4.418×10^4	4.8	39.1	
CH_3NO_2	4.439×10^4	35.9	46.3	2.7
CH_2Cl_2	5.208×10^4	8.9	40.7	0.0

^[a] from ref. [100].

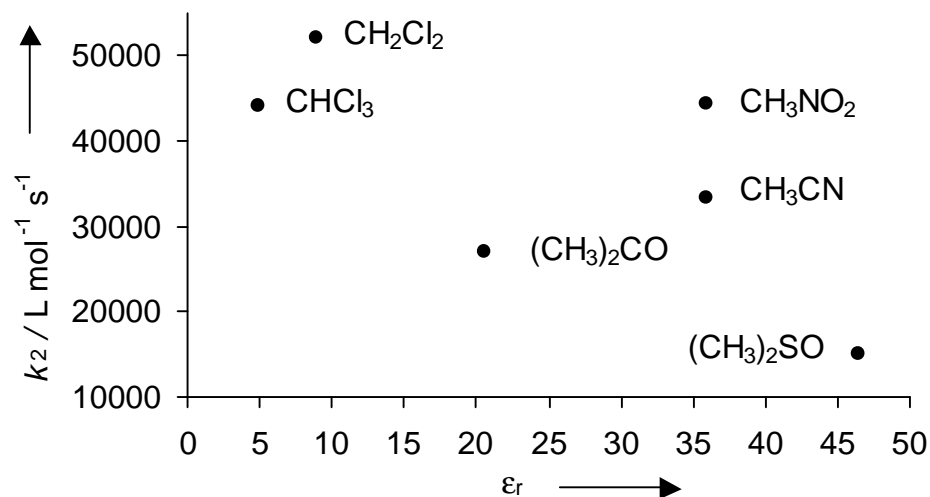


Figure 10.11: Plot of k_2 (20 °C) versus ϵ_r for the reactions of bis(4-dimethylaminophenyl)methylum tetrafluoroborate $(\text{dma})_2\text{CH}^+ \text{BF}_4^-$ and triphenylphosphine Ph_3P in various solvents.

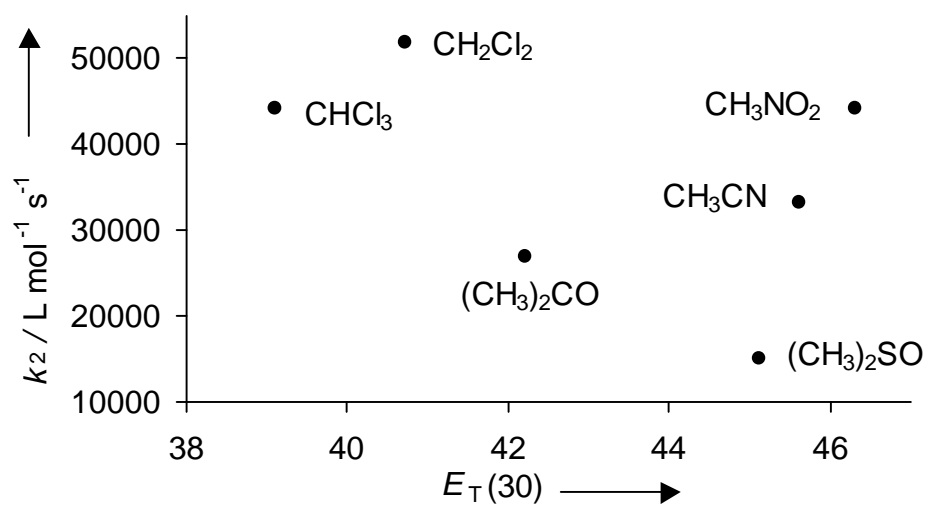


Figure 10.12: Plot of k_2 (20 °C) versus $E_T(30)$ for the reactions of bis(4-dimethylaminophenyl)methylum tetrafluoroborate $(\text{dma})_2\text{CH}^+ \text{BF}_4^-$ and triphenylphosphine Ph_3P in various solvents.

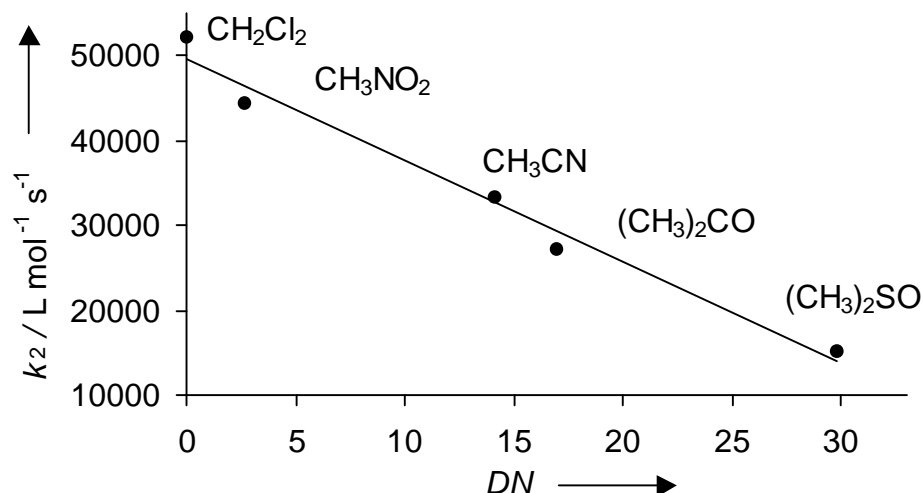


Figure 10.13: Plot of k_2 (20 °C) versus DN for the reactions of bis(4-dimethylaminophenyl)methylum tetrafluoroborate $(\text{dma})_2\text{CH}^+ \text{BF}_4^-$ and triphenylphosphine Ph_3P in various solvents ($n = 5$, $k_2 = (-1.198 \times 10^3) \times DN + (4.963 \times 10^4)$, $r^2 = 0.9804$).

Table 10.100: Bis(4-diphenylaminophenyl)methylum tetrafluoroborate $(\text{dpa})_2\text{CH}^+ \text{BF}_4^-$ and triphenylphosphine Ph_3P in CH_2Cl_2 at $\lambda = 674 \text{ nm}$ (Stopped flow).

No.	$[\text{El}]_0 / \text{mol L}^{-1}$	$[\text{Nuc}]_0 / \text{mol L}^{-1}$	$[\text{Nuc}]_0 / [\text{El}]_0$	$T / \text{°C}$	$k_2 / \text{L mol}^{-1} \text{s}^{-1}$
191200-F	2.542×10^{-6}	3.073×10^{-5}	12	20.0	1.748×10^6
191200-B	2.542×10^{-6}	6.146×10^{-5}	24	20.0	1.808×10^6
191200-C	2.542×10^{-6}	9.219×10^{-5}	36	20.0	1.824×10^6
191200-D	2.542×10^{-6}	1.229×10^{-4}	48	20.0	1.819×10^6
191200-G	2.542×10^{-6}	1.536×10^{-4}	60	20.0	1.753×10^6

$$\bar{k}_2 (20 \text{ °C}) = (1.790 \pm 0.033) \times 10^6 \text{ L mol}^{-1} \text{ s}^{-1}$$

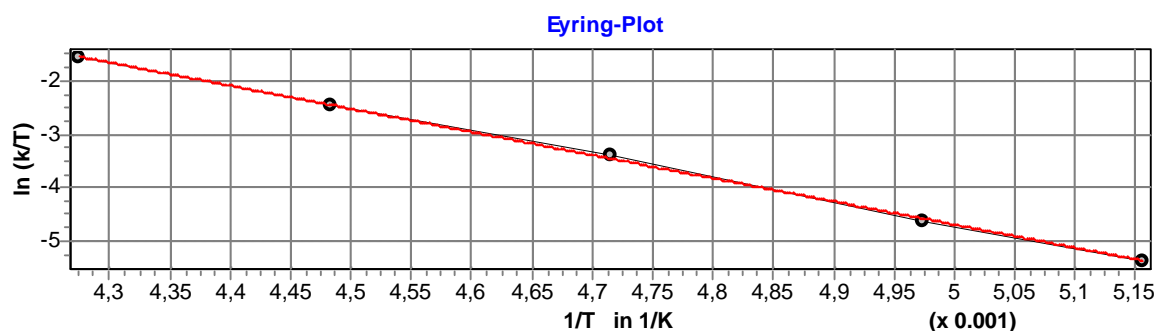
Table 10.101: Bis(4-(methyl(2,2,2-trifluoroethyl)amino)phenyl)methylm tetrafluoroborate $(\text{mfa})_2\text{CH}^+ \text{BF}_4^-$ and triphenylphosphine Ph_3P in CH_2Cl_2 at $\lambda = 593 \text{ nm}$ (Stopped flow).

No.	$[\text{EL}]_0 /$ mol L^{-1}	$[\text{Nuc}]_0 /$ mol L^{-1}	$[\text{Nuc}]_0/[\text{EL}]_0$	$T /$ $^\circ\text{C}$	$k_2 /$ $\text{L mol}^{-1} \text{ s}^{-1}$
240101-C	2.369×10^{-6}	1.079×10^{-5}	5	20.0	8.252×10^6
240101-A	2.369×10^{-6}	2.158×10^{-5}	9	20.0	8.258×10^6
240101-D	2.369×10^{-6}	3.237×10^{-5}	14	20.0	8.042×10^6
240101-E	2.369×10^{-6}	4.316×10^{-5}	18	20.0	8.345×10^6
240101-F	2.369×10^{-6}	5.395×10^{-5}	23	20.0	8.433×10^6

$$\bar{k}_2 (20 \text{ }^\circ\text{C}) = (8.266 \pm 0.130) \times 10^6 \text{ L mol}^{-1} \text{ s}^{-1}$$

Table 10.102: Bis(lilolidin-8-yl)methylm tetrafluoroborate $(\text{lil})_2\text{CH}^+ \text{BF}_4^-$ and tris(4-methylphenyl)phosphine $(\text{p-MeC}_6\text{H}_4)_3\text{P}$ in CH_2Cl_2 at $\lambda = 640 \text{ nm}$ (Schölly).

No.	$[\text{EL}]_0 /$ mol L^{-1}	$[\text{Nuc}]_0 /$ mol L^{-1}	$[\text{Nuc}]_0/[\text{EL}]_0$	Conv. / %	$T /$ $^\circ\text{C}$	$k_2 /$ $\text{L mol}^{-1} \text{ s}^{-1}$
080201.PA0	2.394×10^{-5}	4.156×10^{-3}	174	75	-79.2	9.000×10^{-1}
080201.PA1	2.702×10^{-5}	4.691×10^{-3}	174	80	-72.1	2.013
080201.PA2	2.306×10^{-5}	3.201×10^{-3}	139	81	-61.1	7.096
080201.PA4	2.201×10^{-5}	2.292×10^{-3}	104	-	-50.1	1.931×10^1
080201.PA5	2.228×10^{-5}	1.547×10^{-3}	69	71	-39.2	4.963×10^1



Eyring parameters:

$$\Delta H^\ddagger = 36.179 \pm 0.441 \text{ kJ mol}^{-1}$$

$$\Delta S^\ddagger = -55.651 \pm 2.086 \text{ J mol}^{-1} \text{ K}^{-1}$$

$$r^2 = 0.9996$$

Arrhenius parameters:

$$E_a = 37.946 \pm 0.426 \text{ kJ mol}^{-1}$$

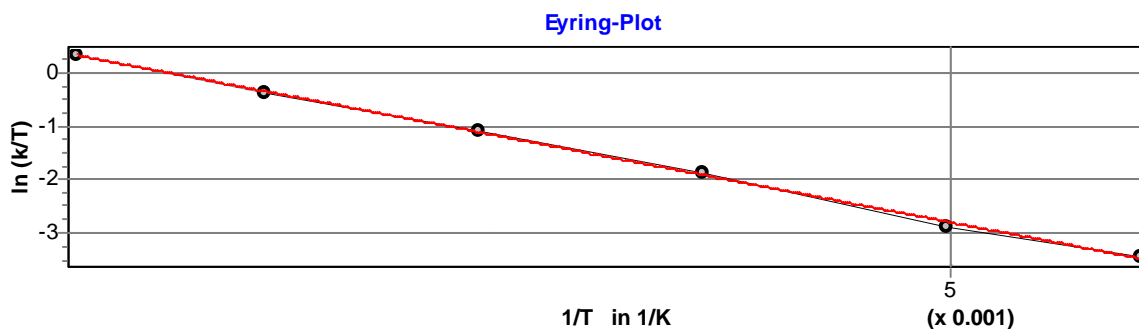
$$\ln A = 23.428 \pm 0.242$$

$$r^2 = 0.9996$$

$$k_2 (20 \text{ }^\circ\text{C}) = (2.709 \pm 0.188) \times 10^3 \text{ L mol}^{-1} \text{ s}^{-1}$$

Table 10.103: Bis(julolidin-9-yl)methylium tetrafluoroborate $(\text{jul})_2\text{CH}^+ \text{BF}_4^-$ and tris(4-methylphenyl)phosphine $(\text{p-MeC}_6\text{H}_4)_3\text{P}$ in CH_2Cl_2 at $\lambda = 640 \text{ nm}$ (Schölly).

No.	$[\text{El}]_0 /$ mol L^{-1}	$[\text{Nuc}]_0 /$ mol L^{-1}	$[\text{Nuc}]_0/[\text{El}]_0$	Conv. / %	$T /$ $^\circ\text{C}$	$k_2 /$ $\text{L mol}^{-1} \text{ s}^{-1}$
190101.PA0	3.980×10^{-5}	2.007×10^{-3}	50	75	-80.1	6.195
190101.PA1	2.999×10^{-5}	2.161×10^{-3}	72	82	-73.0	1.142×10^1
190101.PA2	3.795×10^{-5}	1.914×10^{-3}	50	79	-63.3	3.203×10^1
190101.PA3	3.304×10^{-5}	1.333×10^{-3}	40	59	-53.5	7.309×10^1
190101.PA4	3.921×10^{-5}	1.187×10^{-3}	30	42	-43.2	1.594×10^2
190101.PA5	3.423×10^{-5}	6.905×10^{-4}	20	55	-33.4	3.357×10^2

Eyring parameters:

$$\Delta H^\ddagger = 31.370 \pm 0.474 \text{ kJ mol}^{-1}$$

$$\Delta S^\ddagger = -63.990 \pm 2.219 \text{ J mol}^{-1} \text{ K}^{-1}$$

$$r^2 = 0.9991$$

Arrhenius parameters:

$$E_a = 33.154 \pm 0.478 \text{ kJ mol}^{-1}$$

$$\ln A = 22.435 \pm 0.269$$

$$r^2 = 0.9992$$

$$k_2 (20 \text{ }^\circ\text{C}) = (7.145 \pm 0.513) \times 10^3 \text{ L mol}^{-1} \text{ s}^{-1}$$

Table 10.104: Bis(*N*-methyl-1,2,3,4-tetrahydroquinolin-6-yl)methylm tetrafluoroborate (thq)₂CH⁺ BF₄⁻ and tris(4-methylphenyl)phosphine (p-MeC₆H₄)₃P in CH₂Cl₂ at λ = 628 nm (Stopped flow).

No.	[<i>EL</i>] ₀ / mol L ⁻¹	[<i>Nuc</i>] ₀ / mol L ⁻¹	[<i>Nuc</i>] ₀ /[<i>EL</i>] ₀	<i>T</i> / °C	<i>k</i> ₂ / L mol ⁻¹ s ⁻¹
120101-K	5.409 × 10 ⁻⁶	1.072 × 10 ⁻⁴	20	20.0	5.741 × 10 ⁴
120101-J	5.409 × 10 ⁻⁶	2.143 × 10 ⁻⁴	40	20.0	5.665 × 10 ⁴
120101-I	5.409 × 10 ⁻⁶	3.215 × 10 ⁻⁴	59	20.0	5.672 × 10 ⁴
120101-H	5.409 × 10 ⁻⁶	4.287 × 10 ⁻⁴	79	20.0	5.630 × 10 ⁴
120101-G	5.409 × 10 ⁻⁶	5.359 × 10 ⁻⁴	99	20.0	5.584 × 10 ⁴

$$\bar{k}_2 (20\text{ }^\circ\text{C}) = (5.658 \pm 0.052) \times 10^4 \text{ L mol}^{-1} \text{ s}^{-1}$$

Table 10.105: Bis(4-dimethylaminophenyl)methylm tetrafluoroborate (dma)₂CH⁺ BF₄⁻ and tris(4-methylphenyl)phosphine (p-MeC₆H₄)₃P in CH₂Cl₂ at λ = 612 nm (Stopped flow).

No.	[<i>EL</i>] ₀ / mol L ⁻¹	[<i>Nuc</i>] ₀ / mol L ⁻¹	[<i>Nuc</i>] ₀ /[<i>EL</i>] ₀	<i>T</i> / °C	<i>k</i> ₂ / L mol ⁻¹ s ⁻¹
211200-F	5.197 × 10 ⁻⁶	9.889 × 10 ⁻⁵	19	20.0	2.501 × 10 ⁵
211200-G	5.197 × 10 ⁻⁶	1.978 × 10 ⁻⁴	38	20.0	2.410 × 10 ⁵
211200-H	5.197 × 10 ⁻⁶	2.967 × 10 ⁻⁴	57	20.0	2.430 × 10 ⁵
211200-I	5.197 × 10 ⁻⁶	3.956 × 10 ⁻⁴	76	20.0	2.417 × 10 ⁵
211200-J	5.197 × 10 ⁻⁶	4.945 × 10 ⁻⁴	95	20.0	2.412 × 10 ⁵

$$\bar{k}_2 (20\text{ }^\circ\text{C}) = (2.434 \pm 0.034) \times 10^5 \text{ L mol}^{-1} \text{ s}^{-1}$$

Table 10.106: Bis(4-(methylphenylamino)phenyl)methylm tetrafluoroborate (mpa)₂CH⁺ BF₄⁻ and tris(4-methylphenyl)phosphine (p-MeC₆H₄)₃P in CH₂Cl₂ at λ = 622 nm (Stopped flow).

No.	[<i>El</i>] ₀ / mol L ⁻¹	[<i>Nuc</i>] ₀ / mol L ⁻¹	[<i>Nuc</i>] ₀ /[<i>El</i>] ₀	<i>T</i> / °C	<i>k</i> ₂ / L mol ⁻¹ s ⁻¹
201200-K	2.412 × 10 ⁻⁶	2.780 × 10 ⁻⁵	12	20.0	1.250 × 10 ⁶
201200-G	2.412 × 10 ⁻⁶	5.559 × 10 ⁻⁵	23	20.0	1.265 × 10 ⁶
201200-H	2.412 × 10 ⁻⁶	1.112 × 10 ⁻⁴	46	20.0	1.291 × 10 ⁶
201200-I	2.412 × 10 ⁻⁶	1.668 × 10 ⁻⁴	69	20.0	1.275 × 10 ⁶
201200-J	2.412 × 10 ⁻⁶	2.224 × 10 ⁻⁴	92	20.0	1.259 × 10 ⁶

$$\bar{k}_2 (20\text{ }^\circ\text{C}) = (1.268 \pm 0.014) \times 10^6 \text{ L mol}^{-1} \text{ s}^{-1}$$

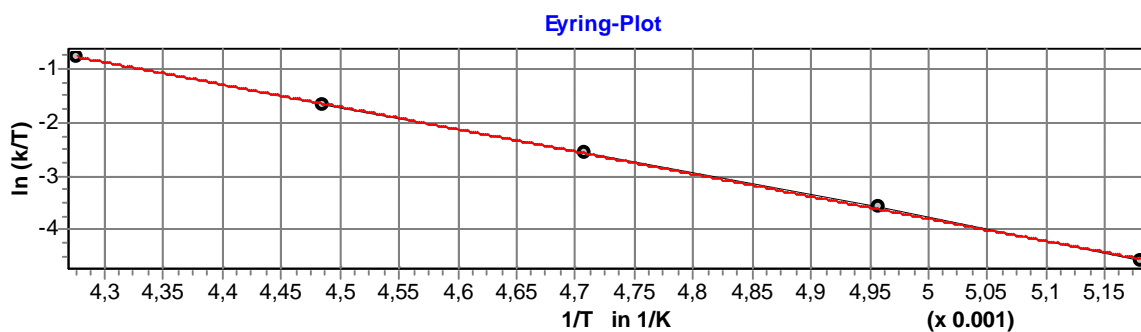
Table 10.107: Bis(4-diphenylaminophenyl)methylm tetrafluoroborate (dpa)₂CH⁺ BF₄⁻ and tris(4-methylphenyl)phosphine (p-MeC₆H₄)₃P in CH₂Cl₂ at λ = 674 nm (Stopped flow).

No.	[<i>El</i>] ₀ / mol L ⁻¹	[<i>Nuc</i>] ₀ / mol L ⁻¹	[<i>Nuc</i>] ₀ /[<i>El</i>] ₀	<i>T</i> / °C	<i>k</i> ₂ / L mol ⁻¹ s ⁻¹
191200-H	2.542 × 10 ⁻⁶	1.656 × 10 ⁻⁵	7	20.0	8.233 × 10 ⁶
191200-K	2.542 × 10 ⁻⁶	2.484 × 10 ⁻⁵	10	20.0	8.347 × 10 ⁶
191200-I	2.542 × 10 ⁻⁶	3.312 × 10 ⁻⁵	13	20.0	8.318 × 10 ⁶
191200-L	2.542 × 10 ⁻⁶	4.140 × 10 ⁻⁵	16	20.0	8.404 × 10 ⁶
191200-J	2.542 × 10 ⁻⁶	4.968 × 10 ⁻⁵	20	20.0	8.220 × 10 ⁶

$$\bar{k}_2 (20\text{ }^\circ\text{C}) = (8.304 \pm 0.070) \times 10^6 \text{ L mol}^{-1} \text{ s}^{-1}$$

Table 10.108: Bis(lilolidin-8-yl)methylmethyl tetrafluoroborate $(\text{lil})_2\text{CH}^+ \text{BF}_4^-$ and tris(4-methoxyphenyl)phosphine $(\text{p-MeOC}_6\text{H}_4)_3\text{P}$ in CH_2Cl_2 at $\lambda = 640 \text{ nm}$ (Schölly).

No.	$[\text{EL}]_0 /$ mol L^{-1}	$[\text{Nuc}]_0 /$ mol L^{-1}	$[\text{Nuc}]_0/[\text{EL}]_0$	Conv. / %	$T /$ $^\circ\text{C}$	$k_2 /$ $\text{L mol}^{-1} \text{s}^{-1}$
090201.PA0	1.789×10^{-5}	3.444×10^{-3}	193	56	-80.1	1.963
090201.PA1	1.732×10^{-5}	3.334×10^{-3}	193	75	-71.4	5.611
090201.PA2	1.712×10^{-5}	2.637×10^{-3}	154	69	-60.7	1.601×10^1
090201.PA3	1.711×10^{-5}	1.976×10^{-3}	116	59	-50.2	4.205×10^1
090201.PA4	1.943×10^{-5}	1.496×10^{-3}	77	48	-39.3	1.083×10^2

Eyring parameters:

$$\Delta H^\ddagger = 34.841 \pm 0.362 \text{ kJ mol}^{-1}$$

$$\Delta S^\ddagger = -55.006 \pm 1.714 \text{ J mol}^{-1} \text{ K}^{-1}$$

$$r^2 = 0.9997$$

Arrhenius parameters:

$$E_a = 36.604 \pm 0.356 \text{ kJ mol}^{-1}$$

$$\ln A = 23.503 \pm 0.202$$

$$r^2 = 0.9997$$

$$k_2 (20 \text{ }^\circ\text{C}) = (5.067 \pm 0.289) \times 10^3 \text{ L mol}^{-1} \text{ s}^{-1}$$

Table 10.109: Bis(julolidin-9-yl)methylium tetrafluoroborate (jul)₂CH⁺ BF₄⁻ and tris(4-methoxyphenyl)phosphine (p-MeOC₆H₄)₃P in CH₂Cl₂ at λ = 642 nm (Stopped flow).

No.	[<i>EL</i>] ₀ / mol L ⁻¹	[<i>Nuc</i>] ₀ / mol L ⁻¹	[<i>Nuc</i>] ₀ /[<i>EL</i>] ₀	<i>T</i> / °C	<i>k</i> ₂ / L mol ⁻¹ s ⁻¹
230101-E	5.329 × 10 ⁻⁶	2.661 × 10 ⁻⁴	50	20.0	2.007 × 10 ⁴
230101-B	5.329 × 10 ⁻⁶	5.321 × 10 ⁻⁴	100	20.0	1.931 × 10 ⁴
230101-D	5.329 × 10 ⁻⁶	7.982 × 10 ⁻⁴	150	20.0	1.885 × 10 ⁴
230101-C	5.329 × 10 ⁻⁶	1.064 × 10 ⁻³	200	20.0	1.929 × 10 ⁴
230101-F	5.329 × 10 ⁻⁶	1.596 × 10 ⁻³	300	20.0	1.906 × 10 ⁴

$$\bar{k}_2 (20\text{ °C}) = (1.932 \pm 0.041) \times 10^4 \text{ L mol}^{-1} \text{ s}^{-1}$$

Table 10.110: Bis(*N*-methyl-1,2,3,4-tetrahydroquinolin-6-yl)methylium tetrafluoroborate (thq)₂CH⁺ BF₄⁻ and tris(4-methoxyphenyl)phosphine (p-MeOC₆H₄)₃P in CH₂Cl₂ at λ = 628 nm (Stopped flow).

No.	[<i>EL</i>] ₀ / mol L ⁻¹	[<i>Nuc</i>] ₀ / mol L ⁻¹	[<i>Nuc</i>] ₀ /[<i>EL</i>] ₀	<i>T</i> / °C	<i>k</i> ₂ / L mol ⁻¹ s ⁻¹
120101-A	5.409 × 10 ⁻⁶	1.137 × 10 ⁻⁴	21	20.0	1.028 × 10 ⁵
120101-B	5.409 × 10 ⁻⁶	2.275 × 10 ⁻⁴	42	20.0	1.036 × 10 ⁵
120101-C	5.409 × 10 ⁻⁶	3.412 × 10 ⁻⁴	63	20.0	1.031 × 10 ⁵
120101-D	5.409 × 10 ⁻⁶	4.550 × 10 ⁻⁴	84	20.0	1.027 × 10 ⁵
120101-E	5.409 × 10 ⁻⁶	5.687 × 10 ⁻⁴	105	20.0	1.024 × 10 ⁵

$$\bar{k}_2 (20\text{ °C}) = (1.029 \pm 0.004) \times 10^5 \text{ L mol}^{-1} \text{ s}^{-1}$$

Table 10.111: Bis(4-dimethylaminophenyl)methylm tetrafluoroborate (dma)₂CH⁺ BF₄⁻ and tris(4-methoxyphenyl)phosphine (p-MeOC₆H₄)₃P in CH₂Cl₂ at λ = 612 nm (Stopped flow).

No.	[<i>EL</i>] ₀ / mol L ⁻¹	[<i>Nuc</i>] ₀ / mol L ⁻¹	[<i>Nuc</i>] ₀ /[<i>EL</i>] ₀	<i>T</i> / °C	<i>k</i> ₂ / L mol ⁻¹ s ⁻¹
211200-A	5.197 × 10 ⁻⁶	1.152 × 10 ⁻⁴	22	20.0	4.912 × 10 ⁵
211200-B	5.197 × 10 ⁻⁶	2.304 × 10 ⁻⁴	44	20.0	4.939 × 10 ⁵
211200-C	5.197 × 10 ⁻⁶	3.457 × 10 ⁻⁴	67	20.0	4.849 × 10 ⁵
211200-D	5.197 × 10 ⁻⁶	4.609 × 10 ⁻⁴	89	20.0	4.825 × 10 ⁵
211200-E	5.197 × 10 ⁻⁶	5.761 × 10 ⁻⁴	111	20.0	4.846 × 10 ⁵

$$\bar{k}_2 (20\text{ °C}) = (4.874 \pm 0.044) \times 10^5 \text{ L mol}^{-1} \text{ s}^{-1}$$

Table 10.112: Bis(4-(methylphenylamino)phenyl)methylm tetrafluoroborate (mpa)₂CH⁺ BF₄⁻ and tris(4-methoxyphenyl)phosphine (p-MeOC₆H₄)₃P in CH₂Cl₂ at λ = 622 nm (Stopped flow).

No.	[<i>EL</i>] ₀ / mol L ⁻¹	[<i>Nuc</i>] ₀ / mol L ⁻¹	[<i>Nuc</i>] ₀ /[<i>EL</i>] ₀	<i>T</i> / °C	<i>k</i> ₂ / L mol ⁻¹ s ⁻¹
201200-F	2.412 × 10 ⁻⁶	1.941 × 10 ⁻⁵	8	20.0	2.337 × 10 ⁶
201200-B	2.412 × 10 ⁻⁶	3.882 × 10 ⁻⁵	16	20.0	2.342 × 10 ⁶
201200-C	2.412 × 10 ⁻⁶	5.823 × 10 ⁻⁵	24	20.0	2.408 × 10 ⁶
201200-D	2.412 × 10 ⁻⁶	7.765 × 10 ⁻⁵	32	20.0	2.395 × 10 ⁶
201200-E	2.412 × 10 ⁻⁶	9.706 × 10 ⁻⁵	40	20.0	2.411 × 10 ⁶

$$\bar{k}_2 (20\text{ °C}) = (2.379 \pm 0.032) \times 10^6 \text{ L mol}^{-1} \text{ s}^{-1}$$

Table 10.113: 4-(4-Methoxybenzylidene)-2,6-di-phenyl-cyclohexa-2,5-dienone ani(Ph)₂QM and tris(4-dimethylaminophenyl)phosphine (p-Me₂NC₆H₄)₃P in CH₂Cl₂ at $\lambda = 413$ nm (Stopped flow).

No.	[<i>El</i>] ₀ / mol L ⁻¹	[<i>Nuc</i>] ₀ / mol L ⁻¹	[<i>Nuc</i>] ₀ /[<i>El</i>] ₀	<i>T</i> / °C	<i>k</i> ₂ / L mol ⁻¹ s ⁻¹
050702-A	3.005×10^{-5}	5.020×10^{-4}	17	20.0	7.153×10^3
050702-B	3.005×10^{-5}	7.605×10^{-4}	26	20.0	6.659×10^3
050702-C	3.005×10^{-5}	1.019×10^{-3}	35	20.0	5.741×10^3
050702-D	3.005×10^{-5}	1.536×10^{-3}	52	20.0	5.720×10^3
050702-E	3.005×10^{-5}	2.053×10^{-3}	69	20.0	5.295×10^3

$$\bar{k}_2 (20 \text{ }^\circ\text{C}) = (6.114 \pm 0.684) \times 10^3 \text{ L mol}^{-1} \text{ s}^{-1}$$

Table 10.114: Bis(lilolidin-8-yl)methylum tetrafluoroborate (lil)₂CH⁺ BF₄⁻ and tris(4-dimethylaminophenyl)phosphine (p-Me₂NC₆H₄)₃P in CH₂Cl₂ at $\lambda = 639$ nm (Stopped flow).

No.	[<i>El</i>] ₀ / mol L ⁻¹	[<i>Nuc</i>] ₀ / mol L ⁻¹	[<i>Nuc</i>] ₀ /[<i>El</i>] ₀	<i>T</i> / °C	<i>k</i> ₂ / L mol ⁻¹ s ⁻¹
020702-C	7.745×10^{-6}	1.078×10^{-4}	14	20.0	2.308×10^5
020702-B	7.745×10^{-6}	2.156×10^{-4}	28	20.0	2.426×10^5
020702-A	7.745×10^{-6}	3.234×10^{-4}	42	20.0	2.421×10^5
020702-D	7.745×10^{-6}	4.312×10^{-4}	56	20.0	2.503×10^5
020702-E	7.745×10^{-6}	5.390×10^{-4}	70	20.0	2.468×10^5

$$\bar{k}_2 (20 \text{ }^\circ\text{C}) = (2.425 \pm 0.066) \times 10^5 \text{ L mol}^{-1} \text{ s}^{-1}$$

Table 10.115: Bis(julolidin-9-yl)methylium tetrafluoroborate (jul)₂CH⁺ BF₄⁻ and tris(4-dimethylaminophenyl)phosphine (p-Me₂NC₆H₄)₃P in CH₂Cl₂ at λ = 642 nm (Stopped flow).

No.	[<i>El</i>] ₀ / mol L ⁻¹	[<i>Nuc</i>] ₀ / mol L ⁻¹	[<i>Nuc</i>] ₀ /[<i>El</i>] ₀	<i>T</i> / °C	<i>k</i> ₂ / L mol ⁻¹ s ⁻¹
010702-H	6.293 × 10 ⁻⁶	1.007 × 10 ⁻⁴	16	20.0	7.026 × 10 ⁵
010702-I	6.293 × 10 ⁻⁶	1.511 × 10 ⁻⁴	24	20.0	7.096 × 10 ⁵
010702-G	6.293 × 10 ⁻⁶	2.015 × 10 ⁻⁴	32	20.0	7.213 × 10 ⁵
010702-J	6.293 × 10 ⁻⁶	2.519 × 10 ⁻⁴	40	20.0	7.007 × 10 ⁵
010702-F	6.293 × 10 ⁻⁶	3.022 × 10 ⁻⁴	48	20.0	6.722 × 10 ⁵

$$\bar{k}_2 (20\text{ °C}) = (7.013 \pm 0.162) \times 10^5 \text{ L mol}^{-1} \text{ s}^{-1}$$

Table 10.116: Bis(*N*-methyl-2,3-dihydro-1H-indol-5-yl)methylium tetrafluoroborate (ind)₂CH⁺ BF₄⁻ and tris(4-dimethylaminophenyl)phosphine (p-Me₂NC₆H₄)₃P in CH₂Cl₂ at λ = 625 nm (Stopped flow).

No.	[<i>El</i>] ₀ / mol L ⁻¹	[<i>Nuc</i>] ₀ / mol L ⁻¹	[<i>Nuc</i>] ₀ /[<i>El</i>] ₀	<i>T</i> / °C	<i>k</i> ₂ / L mol ⁻¹ s ⁻¹
030702-C	6.788 × 10 ⁻⁶	4.690 × 10 ⁻⁵	7	20.0	1.401 × 10 ⁶
030702-D	6.788 × 10 ⁻⁶	7.034 × 10 ⁻⁵	10	20.0	1.327 × 10 ⁶
030702-A	6.788 × 10 ⁻⁶	9.379 × 10 ⁻⁵	14	20.0	1.396 × 10 ⁶
030702-E	6.788 × 10 ⁻⁶	1.172 × 10 ⁻⁴	17	20.0	1.552 × 10 ⁶
030702-B	6.788 × 10 ⁻⁶	1.407 × 10 ⁻⁴	21	20.0	1.379 × 10 ⁶

$$\bar{k}_2 (20\text{ °C}) = (1.411 \pm 0.075) \times 10^6 \text{ L mol}^{-1} \text{ s}^{-1}$$

Table 10.117: Bis(*N*-methyl-1,2,3,4-tetrahydroquinolin-6-yl)methylm tetrafluoroborate (thq)₂CH⁺ BF₄⁻ and tris(4-dimethylaminophenyl)phosphine (p-Me₂NC₆H₄)₃P in CH₂Cl₂ at λ = 628 nm (Stopped flow).

No.	[<i>El</i>] ₀ / mol L ⁻¹	[<i>Nuc</i>] ₀ / mol L ⁻¹	[<i>Nuc</i>] ₀ /[<i>El</i>] ₀	<i>T</i> / °C	<i>k</i> ₂ / L mol ⁻¹ s ⁻¹
010702-C	7.618 × 10 ⁻⁶	6.005 × 10 ⁻⁵	8	20.0	3.442 × 10 ⁶
010702-D	7.618 × 10 ⁻⁶	9.008 × 10 ⁻⁵	12	20.0	3.293 × 10 ⁶
010702-B	7.618 × 10 ⁻⁶	1.201 × 10 ⁻⁴	16	20.0	3.249 × 10 ⁶
010702-E	7.618 × 10 ⁻⁶	1.802 × 10 ⁻⁴	24	20.0	3.154 × 10 ⁶

$$\bar{k}_2 (20\text{ }^\circ\text{C}) = (3.285 \pm 0.104) \times 10^6 \text{ L mol}^{-1} \text{ s}^{-1}$$

Table 10.118: Bis(4-dimethylaminophenyl)methylm tetrafluoroborate (dma)₂CH⁺ BF₄⁻ and tris(4-dimethylaminophenyl)phosphine (p-Me₂NC₆H₄)₃P in CH₂Cl₂ at λ = 613 nm (Stopped flow).

No.	[<i>El</i>] ₀ / mol L ⁻¹	[<i>Nuc</i>] ₀ / mol L ⁻¹	[<i>Nuc</i>] ₀ /[<i>El</i>] ₀	<i>T</i> / °C	<i>k</i> ₂ / L mol ⁻¹ s ⁻¹
030702-A	2.763 × 10 ⁻⁶	1.001 × 10 ⁻⁵	4	20.0	9.179 × 10 ⁶
030702-B	2.763 × 10 ⁻⁶	2.140 × 10 ⁻⁵	8	20.0	1.144 × 10 ⁷
030702-C	2.763 × 10 ⁻⁶	3.279 × 10 ⁻⁵	12	20.0	1.129 × 10 ⁷
030702-D	2.763 × 10 ⁻⁶	5.558 × 10 ⁻⁵	21	20.0	1.047 × 10 ⁷

$$\bar{k}_2 (20\text{ }^\circ\text{C}) = (1.059 \pm 0.090) \times 10^7 \text{ L mol}^{-1} \text{ s}^{-1}$$

Table 10.119: Bis(4-dimethylaminophenyl)methylm tetrafluoroborate (dma)₂CH⁺ BF₄⁻ and triisopropylphosphine (iPr)₂P in CH₂Cl₂ at λ = 612 nm (Stopped flow).

No.	[EL] ₀ / mol L ⁻¹	[Nuc] ₀ / mol L ⁻¹	[Nuc] ₀ /[EL] ₀	T / °C	k ₂ / L mol ⁻¹ s ⁻¹
030102-H	6.679 × 10 ⁻⁶	1.308 × 10 ⁻⁴	20	20.0	2.725 × 10 ⁴
030102-I	6.679 × 10 ⁻⁶	1.962 × 10 ⁻⁴	29	20.0	2.838 × 10 ⁴
030102-J	6.679 × 10 ⁻⁶	2.616 × 10 ⁻⁴	39	20.0	2.926 × 10 ⁴
030102-G	6.679 × 10 ⁻⁶	3.270 × 10 ⁻⁴	49	20.0	2.572 × 10 ⁴

$$\bar{k}_2 (20\text{ °C}) = (2.765 \pm 0.132) \times 10^4 \text{ L mol}^{-1} \text{ s}^{-1}$$

Table 10.120: Bis(julolidin-9-yl)methylm tetrafluoroborate (jul)₂CH⁺ BF₄⁻ and tricyclohexylphosphine Cy₃P in CH₂Cl₂ at λ = 642 nm (Stopped flow).

No.	[EL] ₀ / mol L ⁻¹	[Nuc] ₀ / mol L ⁻¹	[Nuc] ₀ /[EL] ₀	T / °C	k ₂ / L mol ⁻¹ s ⁻¹
030102-A	6.698 × 10 ⁻⁶	3.119 × 10 ⁻⁴	47	20.0	2.752 × 10 ³
030102-B	6.698 × 10 ⁻⁶	4.159 × 10 ⁻⁴	62	20.0	3.076 × 10 ³
030102-C	6.698 × 10 ⁻⁶	5.587 × 10 ⁻⁴	83	20.0	2.866 × 10 ³

$$\bar{k}_2 (20\text{ °C}) = (2.898 \pm 0.134) \times 10^3 \text{ L mol}^{-1} \text{ s}^{-1}$$

Table 10.121: Bis(N-methyl-1,2,3,4-tetrahydroquinolin-6-yl)methylm tetrafluoroborate (thq)₂CH⁺ BF₄⁻ and tricyclohexylphosphine Cy₃P in CH₂Cl₂ at λ = 628 nm (Stopped flow).

No.	[EL] ₀ / mol L ⁻¹	[Nuc] ₀ / mol L ⁻¹	[Nuc] ₀ /[EL] ₀	T / °C	k ₂ / L mol ⁻¹ s ⁻¹
020101-A	6.761 × 10 ⁻⁶	2.873 × 10 ⁻⁴	43	20.0	3.017 × 10 ⁴
020101-B	6.761 × 10 ⁻⁶	3.831 × 10 ⁻⁴	57	20.0	3.076 × 10 ⁴
020101-C	6.761 × 10 ⁻⁶	4.789 × 10 ⁻⁴	71	20.0	2.934 × 10 ⁴
020101-G	6.761 × 10 ⁻⁶	7.184 × 10 ⁻⁴	106	20.0	2.559 × 10 ⁴
020101-F	6.761 × 10 ⁻⁶	9.578 × 10 ⁻⁴	142	20.0	2.541 × 10 ⁴

$$\bar{k}_2 (20\text{ }^\circ\text{C}) = (2.825 \pm 0.229) \times 10^4 \text{ L mol}^{-1} \text{ s}^{-1}$$

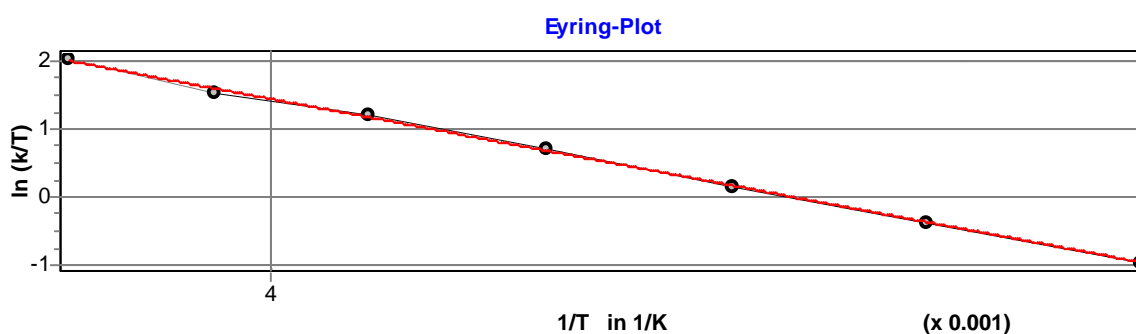
Table 10.122: Bis(4-dimethylaminophenyl)methylmethyl tetrafluoroborate $(\text{dma})_2\text{CH}^+ \text{BF}_4^-$ and tricyclohexylphosphine Cy_3P in CH_2Cl_2 at $\lambda = 612 \text{ nm}$ (Stopped flow).

No.	$[\text{El}]_0 /$ mol L^{-1}	$[\text{Nuc}]_0 /$ mol L^{-1}	$[\text{Nuc}]_0/[\text{El}]_0$	$T /$ $^\circ\text{C}$	$k_2 /$ $\text{L mol}^{-1} \text{ s}^{-1}$
020102-H	7.949×10^{-6}	1.790×10^{-4}	23	20.0	1.235×10^5
020102-K	7.949×10^{-6}	2.685×10^{-4}	34	20.0	1.181×10^5
020102-I	7.949×10^{-6}	3.580×10^{-4}	45	20.0	1.222×10^5
020102-J	7.949×10^{-6}	4.475×10^{-4}	56	20.0	1.476×10^5

$$\bar{k}_2 (20\text{ }^\circ\text{C}) = (1.279 \pm 0.116) \times 10^5 \text{ L mol}^{-1} \text{ s}^{-1}$$

Table 10.123: Bis(lilolidin-8-yl)methylmethyl tetrafluoroborate $(\text{lil})_2\text{CH}^+ \text{BF}_4^-$ and tributylphosphine $(n\text{Bu})_3\text{P}$ in CH_2Cl_2 at $\lambda = 640 \text{ nm}$ (Schölly).

No.	$[\text{El}]_0 /$ mol L^{-1}	$[\text{Nuc}]_0 /$ mol L^{-1}	$[\text{Nuc}]_0/[\text{El}]_0$	Conv. / %	$T /$ $^\circ\text{C}$	$k_2 /$ $\text{L mol}^{-1} \text{ s}^{-1}$
201299.PA1	5.459×10^{-5}	4.114×10^{-4}	8	80	-80.4	7.741×10^1
201299.PA2	7.343×10^{-5}	4.256×10^{-4}	6	81	-71.1	1.479×10^2
201299.PA3	4.186×10^{-5}	3.942×10^{-4}	9	70	-58.6	2.609×10^2
201299.PA4	4.613×10^{-5}	3.259×10^{-4}	7	67	-48.8	4.769×10^2
201299.PA5	3.493×10^{-5}	3.008×10^{-4}	9	75	-48.8	8.058×10^2
201299.PA6	3.239×10^{-5}	2.034×10^{-4}	6	60	-48.8	1.160×10^3
201299.PA7	2.539×10^{-5}	1.530×10^{-4}	6	68	-48.8	2.011×10^3



Eyring parameters:

$$\Delta H^\ddagger = 22.438 \pm 0.366 \text{ kJ mol}^{-1}$$

$$\Delta S^\ddagger = -95.813 \pm 1.584 \text{ J mol}^{-1} \text{ K}^{-1}$$

$$r^2 = 0.9987$$

Arrhenius parameters:

$$E_a = 24.362 \pm 0.364 \text{ kJ mol}^{-1}$$

$$\ln A = 18.685 \pm 0.189$$

$$r^2 = 0.9989$$

$$k_2 (20 \text{ }^\circ\text{C}) = (6.072 \pm 0.240) \times 10^3 \text{ L mol}^{-1} \text{ s}^{-1}$$

Table 10.124: Bis(*N*-methyl-1,2,3,4-tetrahydroquinolin-6-yl)methylium tetrafluoroborate (thq)₂CH⁺ BF₄⁻ and tributylphosphine (*n*Bu)₃P in CH₂Cl₂ at $\lambda = 628 \text{ nm}$ (Stopped flow).

No.	[<i>El</i>] ₀ / mol L ⁻¹	[<i>Nuc</i>] ₀ / mol L ⁻¹	[<i>Nuc</i>] ₀ /[<i>El</i>] ₀	<i>T</i> / °C	<i>k</i> ₂ / L mol ⁻¹ s ⁻¹
100101-F	5.231×10^{-6}	4.982×10^{-5}	10	20.0	1.006×10^5
100101-B	5.231×10^{-6}	9.964×10^{-5}	19	20.0	1.020×10^5
100101-C	5.231×10^{-6}	1.495×10^{-4}	29	20.0	1.107×10^5
100101-D	5.231×10^{-6}	1.993×10^{-4}	38	20.0	1.129×10^5
100101-E	5.231×10^{-6}	2.491×10^{-4}	48	20.0	1.160×10^5

$$\bar{k}_2 (20 \text{ }^\circ\text{C}) = (1.084 \pm 0.061) \times 10^5 \text{ L mol}^{-1} \text{ s}^{-1}$$

Table 10.125: Bis(4-dimethylaminophenyl)methylium tetrafluoroborate (dma)₂CH⁺ BF₄⁻ and tributylphosphine (*n*Bu)₃P in (CH₃)₂CO at $\lambda = 607 \text{ nm}$ (Stopped flow).

No.	[<i>El</i>] ₀ / mol L ⁻¹	[<i>Nuc</i>] ₀ / mol L ⁻¹	[<i>Nuc</i>] ₀ /[<i>El</i>] ₀	<i>T</i> / °C	<i>k</i> ₂ / L mol ⁻¹ s ⁻¹
230301-D	2.987×10^{-6}	8.897×10^{-5}	30	20.0	9.720×10^4
230301-E	2.987×10^{-6}	1.112×10^{-4}	37	20.0	1.187×10^5
230301-F	2.987×10^{-6}	2.224×10^{-4}	75	20.0	1.324×10^5

$$\bar{k}_2 (20 \text{ }^\circ\text{C}) = (1.161 \pm 0.145) \times 10^5 \text{ L mol}^{-1} \text{ s}^{-1}$$

Table 10.126: Bis(4-dimethylaminophenyl)methylm tetrafluoroborate (dma)₂CH⁺ BF₄⁻ and tributylphosphine (nBu)₃P in CH₃CN at λ = 606 nm (Stopped flow).

No.	[<i>El</i>] ₀ / mol L ⁻¹	[<i>Nuc</i>] ₀ / mol L ⁻¹	[<i>Nuc</i>] ₀ /[<i>El</i>] ₀	<i>T</i> / °C	<i>k</i> ₂ / L mol ⁻¹ s ⁻¹
230301-A	2.634 × 10 ⁻⁶	4.458 × 10 ⁻⁵	17	20.0	4.348 × 10 ⁵
230301-B	2.634 × 10 ⁻⁶	6.687 × 10 ⁻⁵	25	20.0	4.548 × 10 ⁵
230301-C	2.634 × 10 ⁻⁶	8.917 × 10 ⁻⁵	34	20.0	4.481 × 10 ⁵

$$\bar{k}_2 (20\text{ °C}) = (4.459 \pm 0.083) \times 10^5 \text{ L mol}^{-1} \text{ s}^{-1}$$

Table 10.127: Bis(4-dimethylaminophenyl)methylm tetrafluoroborate (dma)₂CH⁺ BF₄⁻ and tributylphosphine (nBu)₃P in CH₂Cl₂ at λ = 612 nm (Stopped flow).

No.	[<i>El</i>] ₀ / mol L ⁻¹	[<i>Nuc</i>] ₀ / mol L ⁻¹	[<i>Nuc</i>] ₀ /[<i>El</i>] ₀	<i>T</i> / °C	<i>k</i> ₂ / L mol ⁻¹ s ⁻¹
090101-A	2.822 × 10 ⁻⁶	4.982 × 10 ⁻⁵	18	20.0	7.684 × 10 ⁵
090101-B	2.822 × 10 ⁻⁶	9.964 × 10 ⁻⁵	35	20.0	7.116 × 10 ⁵
090101-C	2.822 × 10 ⁻⁶	1.495 × 10 ⁻⁴	53	20.0	8.046 × 10 ⁵
090101-D	2.822 × 10 ⁻⁶	1.993 × 10 ⁻⁴	71	20.0	7.291 × 10 ⁵
090101-E	2.822 × 10 ⁻⁶	2.491 × 10 ⁻⁴	88	20.0	8.252 × 10 ⁵

$$\bar{k}_2 (20\text{ °C}) = (7.678 \pm 0.431) \times 10^5 \text{ L mol}^{-1} \text{ s}^{-1}$$

Table 10.128: Bis(4-(methylphenylamino)phenyl)methylm tetrafluoroborate (mpa)₂CH⁺ BF₄⁻ and tributylphosphine (nBu)₃P in CH₂Cl₂ at λ = 622 nm (Stopped flow).

No.	[<i>El</i>] ₀ / mol L ⁻¹	[<i>Nuc</i>] ₀ / mol L ⁻¹	[<i>Nuc</i>] ₀ /[<i>El</i>] ₀	<i>T</i> / °C	<i>k</i> ₂ / L mol ⁻¹ s ⁻¹
100101-H	2.395 × 10 ⁻⁶	2.397 × 10 ⁻⁵	10	20.0	4.509 × 10 ⁶
100101-I	2.395 × 10 ⁻⁶	3.596 × 10 ⁻⁵	15	20.0	4.778 × 10 ⁶
100101-L	2.395 × 10 ⁻⁶	4.794 × 10 ⁻⁵	20	20.0	4.602 × 10 ⁶
100101-K	2.395 × 10 ⁻⁶	5.993 × 10 ⁻⁵	25	20.0	4.824 × 10 ⁶

$$\bar{k}_2 (20\text{ }^\circ\text{C}) = (4.678 \pm 0.128) \times 10^6 \text{ L mol}^{-1} \text{ s}^{-1}$$

Table 10.129: Bis(4-diphenylaminophenyl)methylm tetrafluoroborate $(\text{dpa})_2\text{CH}^+ \text{BF}_4^-$ and triphenylphosphite $(\text{PhO})_3\text{P}$ in CH_2Cl_2 at $\lambda = 672 \text{ nm}$ (J&M).

No.	$[\text{El}]_0 /$ mol L^{-1}	$[\text{Nuc}]_0 /$ mol L^{-1}	$[\text{Nuc}]_0 / [\text{El}]_0$	Conv. / %	$T /$ $^\circ\text{C}$	$k_2 /$ $\text{L mol}^{-1} \text{ s}^{-1}$
090301-3	2.341×10^{-5}	4.106×10^{-4}	18	72	20.0	4.198
090301-1	2.474×10^{-5}	8.680×10^{-4}	35	83	20.0	3.611
090301-5	2.255×10^{-5}	1.384×10^{-3}	61	88	20.0	3.387
090301-4	1.767×10^{-5}	2.170×10^{-3}	123	90	20.0	3.308
090301-2	2.590×10^{-5}	2.272×10^{-3}	88	93	20.0	3.229

$$\bar{k}_2 (20\text{ }^\circ\text{C}) = 3.547 \pm 0.350 \text{ L mol}^{-1} \text{ s}^{-1}$$

Table 10.130: Bis(4-(methyl(2,2,2-trifluoroethyl)amino)phenyl)methylm tetrafluoroborate $(\text{mfa})_2\text{CH}^+ \text{BF}_4^-$ and triphenylphosphite $(\text{PhO})_3\text{P}$ in CH_2Cl_2 at $\lambda = 593 \text{ nm}$ (J&M).

No.	$[\text{El}]_0 /$ mol L^{-1}	$[\text{Nuc}]_0 /$ mol L^{-1}	$[\text{Nuc}]_0 / [\text{El}]_0$	Conv. / %	$T /$ $^\circ\text{C}$	$k_2 /$ $\text{L mol}^{-1} \text{ s}^{-1}$
120301-3	1.754×10^{-5}	4.229×10^{-4}	24	89	20.0	2.042×10^1
120301-5	1.230×10^{-5}	4.449×10^{-4}	36	88	20.0	2.183×10^1
120301-1	1.781×10^{-5}	8.586×10^{-4}	48	94	20.0	2.102×10^1
120301-4	1.691×10^{-5}	1.223×10^{-3}	72	94	20.0	1.986×10^1
120301-2	1.841×10^{-5}	2.220×10^{-3}	121	95	20.0	1.992×10^1

$$\bar{k}_2 (20\text{ }^\circ\text{C}) = (2.061 \pm 0.074) \times 10^1 \text{ L mol}^{-1} \text{ s}^{-1}$$

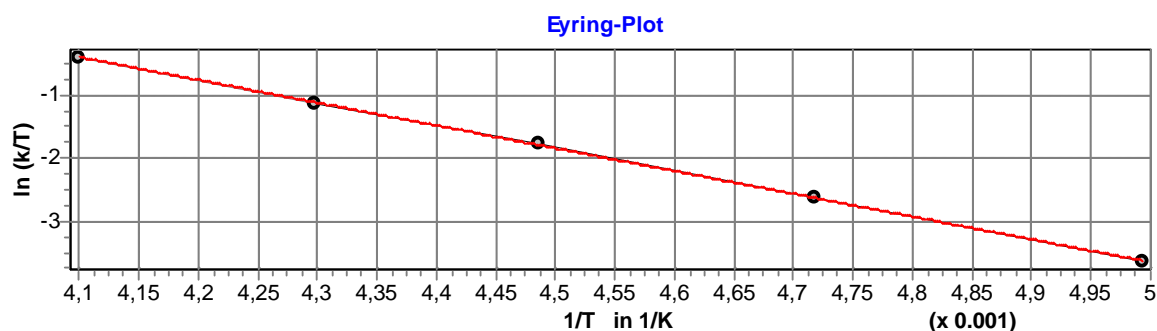
Table 10.131: Bis(4-(phenyl(2,2,2-trifluoroethyl)amino)phenyl)methylium tetrafluoroborate (pfa)₂CH⁺ BF₄⁻ and triphenylphosphite (PhO)₃P in CH₂Cl₂ at λ = 601 nm (J&M).

No.	[<i>El</i>] ₀ / mol L ⁻¹	[<i>Nuc</i>] ₀ / mol L ⁻¹	[<i>Nuc</i>] ₀ / [<i>El</i>] ₀	Conv. / %	<i>T</i> / °C	<i>k</i> ₂ / L mol ⁻¹ s ⁻¹
130301-2	1.509 × 10 ⁻⁵	3.022 × 10 ⁻⁴	20	94	20.0	5.957 × 10 ¹
130301-1	1.382 × 10 ⁻⁵	5.535 × 10 ⁻⁴	40	96	20.0	5.930 × 10 ¹
130301-4	1.705 × 10 ⁻⁵	1.024 × 10 ⁻³	60	97	20.0	5.747 × 10 ¹
130301-5	1.761 × 10 ⁻⁵	1.410 × 10 ⁻³	80	97	20.0	5.780 × 10 ¹
130301-3	1.530 × 10 ⁻⁵	1.532 × 10 ⁻³	100	97	20.0	5.809 × 10 ¹

$$\bar{k}_2(20\text{ °C}) = (5.845 \pm 0.084) \times 10^1 \text{ L mol}^{-1} \text{ s}^{-1}$$

Table 10.132: Bis(2,3-dihydrobenzo[*b*]furan-5-yl)methylium triflate (fur)₂CH⁺ OTf⁻ and triphenylphosphite (PhO)₃P in CH₂Cl₂ at λ = 470 nm (J&M).

No.	[<i>El</i>] ₀ / mol L ⁻¹	[<i>Nuc</i>] ₀ / mol L ⁻¹	[<i>Nuc</i>] ₀ / [<i>El</i>] ₀	Conv. / %	<i>T</i> / °C	<i>k</i> ₂ / L mol ⁻¹ s ⁻¹
160301.PA2	2.382 × 10 ⁻⁵	1.974 × 10 ⁻⁴	83	-72.9	84	5.287
160301.PA3	2.030 × 10 ⁻⁵	3.366 × 10 ⁻³	166	-61.2	80	1.529 × 10 ¹
160301.PA4	2.042 × 10 ⁻⁵	1.693 × 10 ⁻³	83	-50.2	82	3.854 × 10 ¹
160301.PA5	2.234 × 10 ⁻⁵	1.481 × 10 ⁻³	66	-40.5	61	7.580 × 10 ¹
160301.PA6	2.023 × 10 ⁻⁵	1.006 × 10 ⁻³	50	-29.2	57	1.628 × 10 ²



Eyring parameters:

$$\Delta H^\ddagger = 30.019 \pm 0.253 \text{ kJ mol}^{-1}$$

$$\Delta S^\ddagger = -77.772 \pm 1.480 \text{ J mol}^{-1} \text{ K}^{-1}$$

$$r^2 = 0.9998$$

Arrhenius parameters:

$$E_a = 31.851 \pm 0.232 \text{ kJ mol}^{-1}$$

$$\ln A = 20.804 \pm 0.127$$

$$r^2 = 0.9998$$

$$k_2 (20 \text{ }^\circ\text{C}) = (2.371 \pm 0.080) \times 10^3 \text{ L mol}^{-1} \text{ s}^{-1}$$

Table 10.133: Bis(lilolidin-8-yl)methylium tetrafluoroborate $(\text{lil})_2\text{CH}^+ \text{BF}_4^-$ and tributylphosphite $(n\text{BuO})_3\text{P}$ in CH_2Cl_2 at $\lambda = 640 \text{ nm}$ (Schölly).

No.	$[\text{El}]_0 /$ mol L^{-1}	$[\text{Nuc}]_0 /$ mol L^{-1}	$[\text{Nuc}]_0/[\text{El}]_0$	Conv. / %	$T /$ $^\circ\text{C}$	$k_2 /$ $\text{L mol}^{-1} \text{ s}^{-1}$
211299.PA3	3.322×10^{-5}	2.030×10^{-3}	61	92	20.0	1.587
211299.PA1	4.011×10^{-5}	2.586×10^{-3}	65	78	20.0	1.579
211299.PA0	2.595×10^{-5}	2.718×10^{-3}	105	81	20.0	1.655
211299.PA2	2.303×10^{-5}	3.016×10^{-3}	131	88	20.0	1.610
211299.PA4	2.886×10^{-5}	7.559×10^{-3}	262	86	20.0	1.676

$$\bar{k}_2 (20 \text{ }^\circ\text{C}) = 1.621 \pm 0.038 \text{ L mol}^{-1} \text{ s}^{-1}$$

Table 10.134: Bis(4-diphenylaminophenyl)methylium tetrafluoroborate $(\text{dpa})_2\text{CH}^+ \text{BF}_4^-$ and tributylphosphite $(n\text{BuO})_3\text{P}$ in CH_2Cl_2 at $\lambda = 672 \text{ nm}$ (Stopped flow).

No.	$[\text{El}]_0 /$ mol L^{-1}	$[\text{Nuc}]_0 /$ mol L^{-1}	$[\text{Nuc}]_0/[\text{El}]_0$	$T /$ $^\circ\text{C}$	$k_2 /$ $\text{L mol}^{-1} \text{ s}^{-1}$
070620-A	2.529×10^{-6}	5.273×10^{-5}	21	20.0	7.976×10^3
070620-A	2.529×10^{-6}	1.055×10^{-4}	42	20.0	8.162×10^3
070620-A	2.529×10^{-6}	1.582×10^{-4}	63	20.0	8.305×10^3
070620-A	2.529×10^{-6}	2.109×10^{-4}	84	20.0	8.386×10^3
070620-A	2.529×10^{-6}	2.637×10^{-4}	104	20.0	8.403×10^3

$$\bar{k}_2 (20 \text{ }^\circ\text{C}) = (8.246 \pm 0.160) \times 10^3 \text{ L mol}^{-1} \text{ s}^{-1}$$

Table 10.135: Bis(4-(methyl(2,2,2-trifluoroethyl)amino)phenyl)methylm tetrafluoroborate ($\text{mfa})_2\text{CH}^+ \text{BF}_4^-$ and tributylphosphite ($n\text{BuO})_3\text{P}$ in CH_2Cl_2 at $\lambda = 593 \text{ nm}$ (Stopped flow).

No.	$[\text{EL}]_0 /$ mol L^{-1}	$[\text{Nuc}]_0 /$ mol L^{-1}	$[\text{Nuc}]_0/[\text{EL}]_0$	$T /$ $^\circ\text{C}$	$k_2 /$ $\text{L mol}^{-1} \text{ s}^{-1}$
240101-L	1.184×10^{-5}	2.514×10^{-4}	21	20.0	3.661×10^4
240101-H	1.184×10^{-5}	5.029×10^{-4}	43	20.0	3.687×10^4
240101-I	1.184×10^{-5}	7.543×10^{-4}	64	20.0	3.770×10^4
240101-J	1.184×10^{-5}	1.006×10^{-3}	85	20.0	3.701×10^4
240101-K	1.184×10^{-5}	1.257×10^{-3}	106	20.0	3.705×10^4

$$\bar{k}_2(20^\circ\text{C}) = (3.705 \pm 0.036) \times 10^4 \text{ L mol}^{-1} \text{ s}^{-1}$$

Table 10.136: Bis(4-(phenyl(2,2,2-trifluoroethyl)amino)phenyl)methylm tetrafluoroborate ($\text{pfa})_2\text{CH}^+ \text{BF}_4^-$ and tributylphosphite ($n\text{BuO})_3\text{P}$ in CH_2Cl_2 at $\lambda = 601 \text{ nm}$ (Stopped flow).

No.	$[\text{EL}]_0 /$ mol L^{-1}	$[\text{Nuc}]_0 /$ mol L^{-1}	$[\text{Nuc}]_0/[\text{EL}]_0$	$T /$ $^\circ\text{C}$	$k_2 /$ $\text{L mol}^{-1} \text{ s}^{-1}$
250101-F	4.997×10^{-6}	8.693×10^{-5}	17	20.0	1.122×10^5
250101-B	4.997×10^{-6}	1.739×10^{-4}	35	20.0	1.093×10^5
250101-C	4.997×10^{-6}	2.608×10^{-4}	52	20.0	1.085×10^5
250101-D	4.997×10^{-6}	3.477×10^{-4}	70	20.0	1.085×10^5
250101-E	4.997×10^{-6}	4.346×10^{-4}	87	20.0	1.082×10^5

$$\bar{k}_2(20^\circ\text{C}) = (1.093 \pm 0.015) \times 10^5 \text{ L mol}^{-1} \text{ s}^{-1}$$

10.5.4 Concentrations and equilibrium constants

General: The determination of equilibrium constants were performed as described in Chapter 2. K values that have only been measured at one temperature (20°C) are averaged (\bar{K}) and given with standard deviations. When measurements are made at variable temperatures, K (20°C) values have been derived from extrapolations of the linear plots of $\ln K$ versus $1/T_{\text{abs}}$ (van 't Hoff equation).

Table 10.137: Bis(*N*-methyl-1,2,3,4-tetrahydroquinolin-6-yl)methylium tetrafluoroborate (thq)₂CH⁺ BF₄⁻ and tris(4-chlorophenyl)phosphine (p-ClC₆H₄)₃P in CH₂Cl₂ at λ = 628 nm (J&M).

No.	[<i>EL</i>] ₀ / mol L ⁻¹	[<i>Nuc</i>] ₀ / mol L ⁻¹	[<i>EL</i>] / mol L ⁻¹	<i>T</i> / °C	<i>K</i> / L mol ⁻¹
020301-A	2.307 × 10 ⁻⁵	4.400 × 10 ⁻³	3.030 × 10 ⁻⁶	-62.5	1.511 × 10 ³
020301-B	2.294 × 10 ⁻⁵	4.373 × 10 ⁻³	4.347 × 10 ⁻⁶	-57.5	9.820 × 10 ²
020301-C	2.280 × 10 ⁻⁵	4.347 × 10 ⁻³	6.040 × 10 ⁻⁶	-52.9	6.407 × 10 ²
020301-D	2.266 × 10 ⁻⁵	4.320 × 10 ⁻³	7.956 × 10 ⁻⁶	-48.0	4.292 × 10 ²
020301-E	2.252 × 10 ⁻⁵	4.293 × 10 ⁻³	1.008 × 10 ⁻⁵	-43.1	2.883 × 10 ²
020301-F	2.238 × 10 ⁻⁵	4.267 × 10 ⁻³	1.218 × 10 ⁻⁵	-38.3	1.966 × 10 ²
020301-G	2.224 × 10 ⁻⁵	4.240 × 10 ⁻³	1.408 × 10 ⁻⁵	-33.4	1.369 × 10 ²
020301-H	2.210 × 10 ⁻⁵	4.213 × 10 ⁻³	1.569 × 10 ⁻⁵	-28.5	9.710 × 10 ¹
020301-I	2.307 × 10 ⁻⁵	4.186 × 10 ⁻³	1.690 × 10 ⁻⁵	-23.6	7.149 × 10 ¹
020301-J	2.294 × 10 ⁻⁵	4.159 × 10 ⁻³	1.772 × 10 ⁻⁵	-18.6	5.551 × 10 ¹

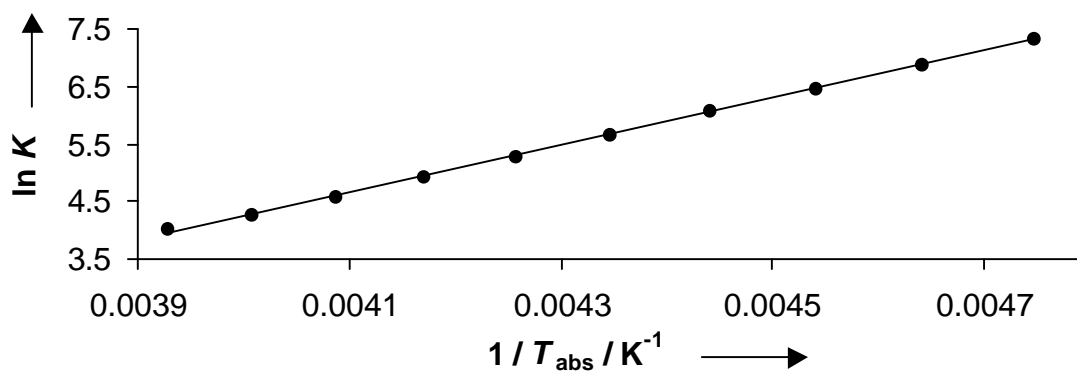


Figure 10.14: Plot of ln *K* versus 1 / *T*_{abs} (n = 10, ln *K* = (4.099 × 10³) × (1 / *T*_{abs}) - (1.215 × 10¹), r² = 0.9994).

$$K (20 \text{ }^\circ\text{C}) = 6.257 \text{ L mol}^{-1}$$

$$\Delta_{\text{R}}H^\circ = -34.079 \text{ kJ mol}^{-1}$$

$$\Delta_{\text{R}}S^\circ = -101.0 \text{ J K}^{-1} \text{ mol}^{-1}$$

Table 10.138: Bis(4-(methylphenylamino)phenyl)methylium tetrafluoroborate (mpa)₂CH⁺ BF₄⁻ and tris(4-chlorophenyl)phosphine (p-ClC₆H₄)₃P in CH₂Cl₂ at λ = 622 nm (J&M).

No.	[<i>El</i>] ₀ / mol L ⁻¹	[<i>Nuc</i>] ₀ / mol L ⁻¹	[<i>El</i>] / mol L ⁻¹	<i>T</i> / °C	<i>K</i> / L mol ⁻¹
260201-A	2.672 × 10 ⁻⁵	1.027 × 10 ⁻⁴	1.501 × 10 ⁻⁵	20.0	8.565 × 10 ³
260201-B	2.736 × 10 ⁻⁵	1.752 × 10 ⁻⁴	1.166 × 10 ⁻⁵	20.0	8.446 × 10 ³
260201-C	2.827 × 10 ⁻⁵	3.614 × 10 ⁻⁴	7.301 × 10 ⁻⁶	20.0	8.437 × 10 ³
260201-D	2.863 × 10 ⁻⁵	7.340 × 10 ⁻⁵	1.853 × 10 ⁻⁵	20.0	8.616 × 10 ³

$$\bar{K} (20\text{ }^\circ\text{C}) = (8.516 \pm 0.077) \times 10^3 \text{ L mol}^{-1}$$

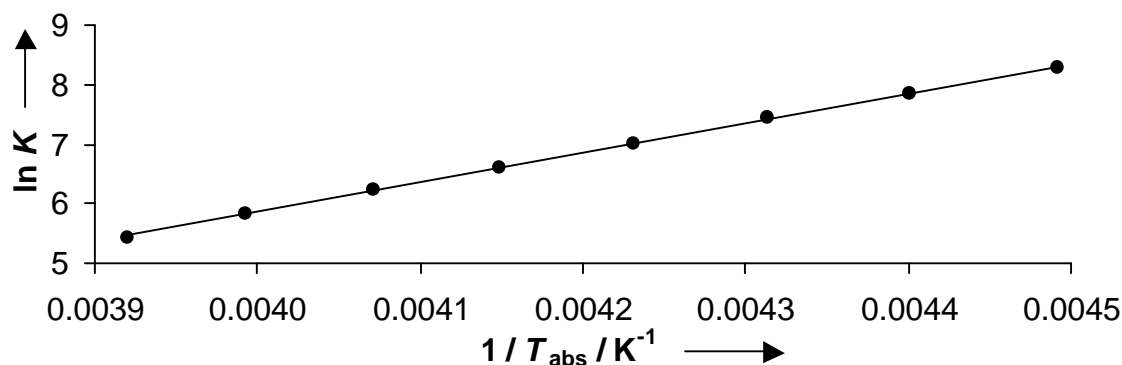
Table 10.139: Bis(4-diphenylaminophenyl)methylium tetrafluoroborate (dpa)₂CH⁺ BF₄⁻ and tris(4-chlorophenyl)phosphine (p-ClC₆H₄)₃P in CH₂Cl₂ at λ = 672 nm (J&M).

No.	[<i>El</i>] ₀ / mol L ⁻¹	[<i>Nuc</i>] ₀ / mol L ⁻¹	[<i>El</i>] / mol L ⁻¹	<i>T</i> / °C	<i>K</i> / L mol ⁻¹
060301-A	1.480 × 10 ⁻⁵	1.431 × 10 ⁻⁵	4.045 × 10 ⁻⁶	20.0	7.466 × 10 ⁵
060301-B	1.587 × 10 ⁻⁵	7.682 × 10 ⁻⁶	9.115 × 10 ⁻⁶	20.0	7.954 × 10 ⁵
060301-C	1.326 × 10 ⁻⁵	3.854 × 10 ⁻⁶	9.873 × 10 ⁻⁶	20.0	7.318 × 10 ⁵

$$\bar{K} (20\text{ }^\circ\text{C}) = (7.579 \pm 0.272) \times 10^5 \text{ L mol}^{-1}$$

Table 10.140: Bis(lilolidin-8-yl)methylium tetrafluoroborate $(\text{lil})_2\text{CH}^+ \text{BF}_4^-$ and triphenylphosphine Ph_3P in CH_2Cl_2 at $\lambda = 639 \text{ nm}$ (J&M).

No.	$[\text{EI}]_0 /$ mol L^{-1}	$[\text{Nuc}]_0 /$ mol L^{-1}	$[\text{EI}] /$ mol L^{-1}	$T /$ $^\circ\text{C}$	$K /$ L mol^{-1}
080301-A	1.738×10^{-5}	1.077×10^{-3}	3.337×10^{-6}	-50.5	3.959×10^3
080301-B	1.728×10^{-5}	1.071×10^{-3}	4.638×10^{-6}	-45.9	2.576×10^3
080301-C	1.718×10^{-5}	1.064×10^{-3}	6.159×10^{-6}	-41.3	1.699×10^3
080301-D	1.708×10^{-5}	1.058×10^{-3}	7.819×10^{-6}	-36.8	1.129×10^3
080301-E	1.698×10^{-5}	1.052×10^{-3}	9.522×10^{-6}	-32.1	7.495×10^2
080301-F	1.688×10^{-5}	1.046×10^{-3}	1.102×10^{-5}	-27.5	5.104×10^2
080301-G	1.677×10^{-5}	1.039×10^{-3}	1.240×10^{-5}	-22.7	3.402×10^2
080301-H	1.667×10^{-5}	1.033×10^{-3}	1.346×10^{-5}	-18.0	2.314×10^2

**Figure 10.15:** Plot of $\ln K$ versus $1 / T_{\text{abs}}$ ($n = 8$, $\ln K = (4.962 \times 10^3) \times (1 / T_{\text{abs}}) - (1.398 \times 10^1)$, $r^2 = 0.9997$).

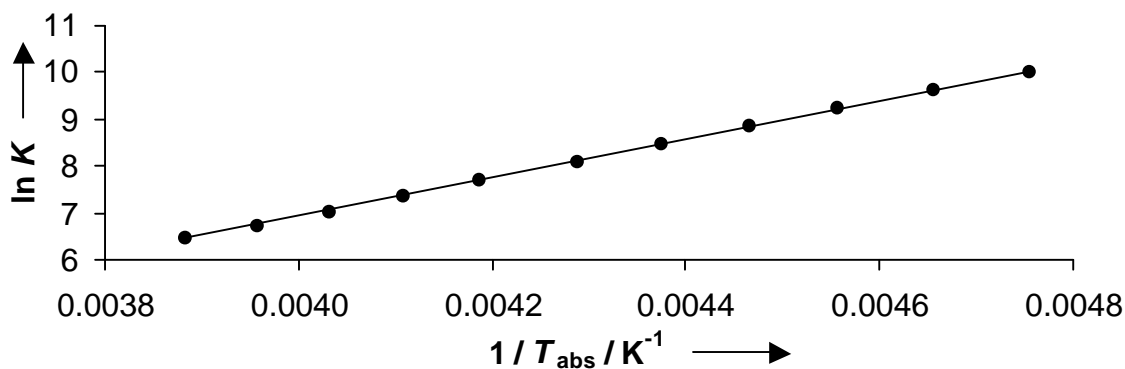
$$K(20 \text{ }^\circ\text{C}) = 1.907 \times 10^1 \text{ L mol}^{-1}$$

$$\Delta_{\text{R}}H^\circ = -41.253 \text{ kJ mol}^{-1}$$

$$\Delta_{\text{R}}S^\circ = -116.2 \text{ J K}^{-1} \text{ mol}^{-1}$$

Table 10.141: Bis(julolidin-9-yl)methylm tetrafluoroborate $(\text{jul})_2\text{CH}^+ \text{BF}_4^-$ and triphenylphosphine Ph_3P in CH_2Cl_2 at $\lambda = 642 \text{ nm}$ (J&M).

No.	$[\text{El}]_0 /$ mol L^{-1}	$[\text{Nuc}]_0 /$ mol L^{-1}	$[\text{El}] /$ mol L^{-1}	$T /$ $^\circ\text{C}$	$K /$ L mol^{-1}
120101-A	1.685×10^{-5}	8.940×10^{-4}	1.325×10^{-6}	-62.8	1.334×10^4
120101-B	1.676×10^{-5}	8.890×10^{-4}	1.858×10^{-6}	-58.3	9.173×10^3
120101-C	1.666×10^{-5}	8.839×10^{-4}	2.597×10^{-6}	-53.7	6.228×10^3
120101-D	1.657×10^{-5}	8.788×10^{-4}	3.505×10^{-6}	-49.2	4.305×10^3
120101-E	1.647×10^{-5}	8.737×10^{-4}	4.660×10^{-6}	-44.6	2.941×10^3
120101-F	1.637×10^{-5}	8.685×10^{-4}	6.008×10^{-6}	-39.9	2.010×10^3
120101-G	1.626×10^{-5}	8.622×10^{-4}	7.506×10^{-6}	-34.3	1.366×10^3
120101-H	1.616×10^{-5}	8.571×10^{-4}	8.915×10^{-6}	-29.7	9.562×10^2
120101-I	1.606×10^{-5}	8.520×10^{-4}	1.018×10^{-5}	-25.1	6.829×10^2
120101-J	1.596×10^{-5}	8.468×10^{-4}	1.116×10^{-5}	-20.4	5.108×10^2
120101-K	1.586×10^{-5}	8.414×10^{-4}	1.188×10^{-5}	-15.6	3.999×10^2

**Figure 10.16:** Plot of $\ln K$ versus $1/T_{\text{abs}}$ ($n = 11$, $\ln K = (4.102 \times 10^3) \times (1/T_{\text{abs}}) - 9.972$, $r^2 = 0.9996$).

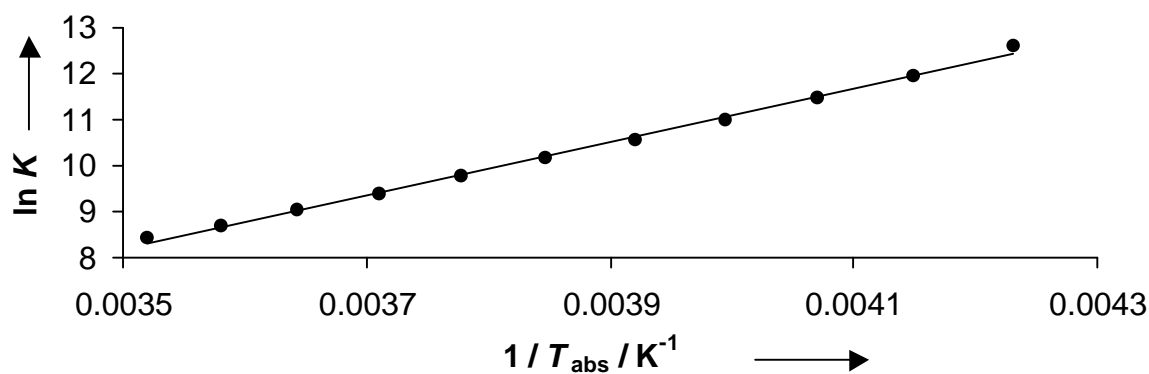
$$K(20^\circ\text{C}) = 5.573 \times 10^1 \text{ L mol}^{-1}$$

$$\Delta_{\text{R}}H^\circ = -34.573 \text{ kJ mol}^{-1}$$

$$\Delta_{\text{R}}S^\circ = -84.51 \text{ J K}^{-1} \text{ mol}^{-1}$$

Table 10.142: Bis(*N*-methyl-1,2,3,4-tetrahydroquinolin-6-yl)methylium tetrafluoroborate (thq)₂CH⁺ BF₄⁻ and triphenylphosphine Ph₃P in CH₂Cl₂ at λ = 628 nm (J&M).

No.	[<i>El</i>] ₀ / mol L ⁻¹	[<i>Nuc</i>] ₀ / mol L ⁻¹	[<i>El</i>] / mol L ⁻¹	<i>T</i> / °C	<i>K</i> / L mol ⁻¹
010301-A	2.338 × 10 ⁻⁵	2.544 × 10 ⁻⁴	3.368 × 10 ⁻⁷	-36.8	2.956 × 10 ⁵
010301-B	2.324 × 10 ⁻⁵	2.529 × 10 ⁻⁴	6.189 × 10 ⁻⁷	-32.1	1.587 × 10 ⁵
010301-C	2.310 × 10 ⁻⁵	2.514 × 10 ⁻⁴	9.892 × 10 ⁻⁷	-27.5	9.748 × 10 ⁴
010301-D	2.296 × 10 ⁻⁵	2.498 × 10 ⁻⁴	1.571 × 10 ⁻⁶	-22.8	5.959 × 10 ⁴
010301-E	2.281 × 10 ⁻⁵	2.483 × 10 ⁻⁴	2.294 × 10 ⁻⁶	-18.1	3.927 × 10 ⁴
010301-F	2.267 × 10 ⁻⁵	2.467 × 10 ⁻⁴	3.299 × 10 ⁻⁶	-13.2	2.583 × 10 ⁴
010301-G	2.252 × 10 ⁻⁵	2.451 × 10 ⁻⁴	4.533 × 10 ⁻⁶	-8.4	1.747 × 10 ⁴
010301-H	2.238 × 10 ⁻⁵	2.435 × 10 ⁻⁴	5.996 × 10 ⁻⁶	-3.6	1.203 × 10 ⁴
010301-I	2.223 × 10 ⁻⁵	2.419 × 10 ⁻⁴	7.671 × 10 ⁻⁶	1.3	8.346 × 10 ³
010301-J	2.209 × 10 ⁻⁵	2.404 × 10 ⁻⁴	9.382 × 10 ⁻⁶	6.1	5.948 × 10 ³
010301-K	2.194 × 10 ⁻⁵	2.387 × 10 ⁻⁴	1.081 × 10 ⁻⁵	11.0	4.523 × 10 ³

**Figure 10.17:** Plot of ln *K* versus 1 / *T*_{abs} (n = 11, ln *K* = (5.818 × 10³) × (1 / *T*_{abs}) - (1.217 × 10¹), r² = 0.9973).

$$K(20\text{ °C}) = 2.162 \times 10^3 \text{ L mol}^{-1}$$

$$\Delta_{\text{R}}H^{\circ} = -48.375 \text{ kJ mol}^{-1}$$

$$\Delta_{\text{R}}S^{\circ} = -101.172 \text{ J K}^{-1} \text{ mol}^{-1}$$

Table 10.143: Bis(4-dimethylaminophenyl)methylmethyl tetrafluoroborate $(\text{dma})_2\text{CH}^+ \text{BF}_4^-$ and triphenylphosphine Ph_3P in CH_2Cl_2 at $\lambda = 613 \text{ nm}$ (J&M).

No.	$[\text{El}]_0 /$ mol L^{-1}	$[\text{Nuc}]_0 /$ mol L^{-1}	$[\text{El}] /$ mol L^{-1}	$T /$ $^\circ\text{C}$	$K /$ L mol^{-1}
270201-A	1.470×10^{-5}	6.766×10^{-6}	1.071×10^{-5}	20.0	1.334×10^5
270201-B	1.762×10^{-5}	2.030×10^{-5}	7.642×10^{-6}	20.0	1.266×10^5
270201-C	1.744×10^{-5}	8.016×10^{-5}	2.009×10^{-6}	20.0	1.186×10^5
270201-D	1.480×10^{-5}	1.023×10^{-5}	9.265×10^{-6}	20.0	1.271×10^5

$$\bar{K} (20^\circ\text{C}) = (1.264 \pm 0.053) \times 10^5 \text{ L mol}^{-1}$$

Table 10.144: Bis(lilolidin-8-yl)methylmethyl tetrafluoroborate $(\text{lil})_2\text{CH}^+ \text{BF}_4^-$ and tris(4-methylphenyl)phosphine $(\text{p-MeC}_6\text{H}_5)_3\text{P}$ in CH_2Cl_2 at $\lambda = 639 \text{ nm}$ (J&M).

No.	$[\text{El}]_0 /$ mol L^{-1}	$[\text{Nuc}]_0 /$ mol L^{-1}	$[\text{El}] /$ mol L^{-1}	$T /$ $^\circ\text{C}$	$K /$ L mol^{-1}
210301-A	1.463×10^{-5}	5.278×10^{-4}	8.509×10^{-6}	20.0	1.378×10^3
210301-B	1.774×10^{-5}	3.204×10^{-4}	1.243×10^{-5}	20.0	1.358×10^3
210301-C	1.723×10^{-5}	1.239×10^{-3}	6.369×10^{-6}	20.0	1.388×10^3

$$\bar{K} (20^\circ\text{C}) = (1.375 \pm 0.013) \times 10^3 \text{ L mol}^{-1}$$

Table 10.145: Bis(julolidin-9-yl)methylium tetrafluoroborate (jul)₂CH⁺ BF₄⁻ and tris(4-methylphenyl)phosphine (p-MeC₆H₅)₃P in CH₂Cl₂ at λ = 642 nm (J&M).

No.	[<i>El</i>] ₀ / mol L ⁻¹	[<i>Nuc</i>] ₀ / mol L ⁻¹	[<i>El</i>] / mol L ⁻¹	<i>T</i> / °C	<i>K</i> / L mol ⁻¹
010201-A	1.776 × 10 ⁻⁵	9.295 × 10 ⁻⁵	1.464 × 10 ⁻⁵	20.0	2.375 × 10 ³
010201-B	1.774 × 10 ⁻⁵	1.857 × 10 ⁻⁴	1.241 × 10 ⁻⁵	20.0	2.383 × 10 ³
010201-C	1.773 × 10 ⁻⁵	2.784 × 10 ⁻⁴	1.082 × 10 ⁻⁵	20.0	2.352 × 10 ³
010201-D	1.771 × 10 ⁻⁵	3.709 × 10 ⁻⁴	9.544 × 10 ⁻⁶	20.0	2.361 × 10 ³
010201-E	1.770 × 10 ⁻⁵	4.632 × 10 ⁻⁴	8.550 × 10 ⁻⁶	20.0	2.357 × 10 ³
010201-F	1.768 × 10 ⁻⁵	5.553 × 10 ⁻⁴	7.714 × 10 ⁻⁶	20.0	2.370 × 10 ³
010201-G	1.767 × 10 ⁻⁵	6.473 × 10 ⁻⁴	7.047 × 10 ⁻⁶	20.0	2.367 × 10 ³
010201-H	1.765 × 10 ⁻⁵	7.392 × 10 ⁻⁴	6.451 × 10 ⁻⁶	20.0	2.385 × 10 ³
010201-I	1.764 × 10 ⁻⁵	8.308 × 10 ⁻⁴	5.941 × 10 ⁻⁶	20.0	2.404 × 10 ³
010201-J	1.762 × 10 ⁻⁵	9.224 × 10 ⁻⁴	5.516 × 10 ⁻⁶	20.0	2.411 × 10 ³
010201-K	1.761 × 10 ⁻⁵	1.014 × 10 ⁻³	5.147 × 10 ⁻⁶	20.0	2.418 × 10 ³
010201-L	1.759 × 10 ⁻⁵	1.105 × 10 ⁻³	4.821 × 10 ⁻⁶	20.0	2.426 × 10 ³
010201-M	1.758 × 10 ⁻⁵	1.196 × 10 ⁻³	4.537 × 10 ⁻⁶	20.0	2.430 × 10 ³
010201-N	1.756 × 10 ⁻⁵	1.287 × 10 ⁻³	4.268 × 10 ⁻⁶	20.0	2.446 × 10 ³
010201-O	1.755 × 10 ⁻⁵	1.378 × 10 ⁻³	4.041 × 10 ⁻⁶	20.0	2.450 × 10 ³
010201-P	1.753 × 10 ⁻⁵	1.468 × 10 ⁻³	3.829 × 10 ⁻⁶	20.0	2.461 × 10 ³
010201-Q	1.752 × 10 ⁻⁵	1.559 × 10 ⁻³	3.644 × 10 ⁻⁶	20.0	2.464 × 10 ³
010201-R	1.750 × 10 ⁻⁵	1.649 × 10 ⁻³	3.488 × 10 ⁻⁶	20.0	2.457 × 10 ³
010201-S	1.749 × 10 ⁻⁵	1.739 × 10 ⁻³	3.319 × 10 ⁻⁶	20.0	2.475 × 10 ³

$$\bar{K} (20 \text{ }^\circ\text{C}) = (2.410 \pm 0.040) \times 10^3 \text{ L mol}^{-1}$$

Table 10.146: Bis(*N*-methyl-1,2,3,4-tetrahydroquinolin-6-yl)methylium tetrafluoroborate (thq)₂CH⁺ BF₄⁻ and tris(4-methylphenyl)phosphine (p-MeC₆H₅)₃P in CH₂Cl₂ at λ = 628 nm (J&M).

No.	[<i>El</i>] ₀ / mol L ⁻¹	[<i>Nuc</i>] ₀ / mol L ⁻¹	[<i>El</i>] / mol L ⁻¹	<i>T</i> / °C	<i>K</i> / L mol ⁻¹
280201-C	1.651 × 10 ⁻⁵	4.929 × 10 ⁻⁶	1.294 × 10 ⁻⁵	20.0	2.030 × 10 ⁵
280201-B	1.474 × 10 ⁻⁵	7.335 × 10 ⁻⁶	1.007 × 10 ⁻⁵	20.0	1.750 × 10 ⁵
280201-A	1.388 × 10 ⁻⁵	1.379 × 10 ⁻⁵	6.746 × 10 ⁻⁶	20.0	1.588 × 10 ⁵
280201-D	1.388 × 10 ⁻⁵	2.753 × 10 ⁻⁵	4.024 × 10 ⁻⁶	20.0	1.386 × 10 ⁵

$$\bar{K} (20\text{ °C}) = (1.688 \pm 0.236) \times 10^5 \text{ L mol}^{-1}$$

Table 10.147: Bis(lilolidin-8-yl)methylium tetrafluoroborate (lil)₂CH⁺ BF₄⁻ and tris(4-methoxyphenyl)phosphine (p-MeOC₆H₅)₃P in CH₂Cl₂ at λ = 639 nm (J&M).

No.	[<i>El</i>] ₀ / mol L ⁻¹	[<i>Nuc</i>] ₀ / mol L ⁻¹	[<i>El</i>] / mol L ⁻¹	<i>T</i> / °C	<i>K</i> / L mol ⁻¹
020201-A	1.640 × 10 ⁻⁵	7.976 × 10 ⁻⁵	7.529 × 10 ⁻⁶	20.0	1.663 × 10 ⁴
020201-B	1.639 × 10 ⁻⁵	9.961 × 10 ⁻⁵	6.502 × 10 ⁻⁶	20.0	1.695 × 10 ⁴
020201-C	1.638 × 10 ⁻⁵	1.194 × 10 ⁻⁴	5.704 × 10 ⁻⁶	20.0	1.720 × 10 ⁴
020201-D	1.636 × 10 ⁻⁵	1.392 × 10 ⁻⁴	5.070 × 10 ⁻⁶	20.0	1.741 × 10 ⁴
020201-E	1.635 × 10 ⁻⁵	1.590 × 10 ⁻⁴	4.551 × 10 ⁻⁶	20.0	1.761 × 10 ⁴
020201-F	1.633 × 10 ⁻⁵	1.787 × 10 ⁻⁴	4.120 × 10 ⁻⁶	20.0	1.780 × 10 ⁴
020201-G	1.632 × 10 ⁻⁵	1.983 × 10 ⁻⁴	3.766 × 10 ⁻⁶	20.0	1.794 × 10 ⁴
020201-H	1.630 × 10 ⁻⁵	2.180 × 10 ⁻⁴	3.462 × 10 ⁻⁶	20.0	1.808 × 10 ⁴
020201-I	1.629 × 10 ⁻⁵	2.376 × 10 ⁻⁴	3.196 × 10 ⁻⁶	20.0	1.825 × 10 ⁴
020201-J	1.627 × 10 ⁻⁵	2.572 × 10 ⁻⁴	2.981 × 10 ⁻⁶	20.0	1.829 × 10 ⁴
020201-K	1.626 × 10 ⁻⁵	2.767 × 10 ⁻⁴	2.766 × 10 ⁻⁶	20.0	1.854 × 10 ⁴
020201-L	1.624 × 10 ⁻⁵	2.962 × 10 ⁻⁴	2.588 × 10 ⁻⁶	20.0	1.867 × 10 ⁴
020201-M	1.623 × 10 ⁻⁵	3.157 × 10 ⁻⁴	2.436 × 10 ⁻⁶	20.0	1.875 × 10 ⁴

$$\bar{K} (20\text{ °C}) = (1.786 \pm 0.064) \times 10^4 \text{ L mol}^{-1}$$

Table 10.148: Bis(julolidin-9-yl)methylium tetrafluoroborate (jul)₂CH⁺ BF₄⁻ and tris(4-methoxyphenyl)phosphine (p-MeOC₆H₅)₃P in CH₂Cl₂ at λ = 642 nm (J&M).

No.	[<i>El</i>] ₀ / mol L ⁻¹	[<i>Nuc</i>] ₀ / mol L ⁻¹	[<i>El</i>] / mol L ⁻¹	<i>T</i> / °C	<i>K</i> / L mol ⁻¹
020201-A	2.117 × 10 ⁻⁵	4.476 × 10 ⁻⁵	9.566 × 10 ⁻⁶	20.0	3.658 × 10 ⁴
020201-B	2.115 × 10 ⁻⁵	6.708 × 10 ⁻⁵	7.345 × 10 ⁻⁶	20.0	3.527 × 10 ⁴
020201-C	2.113 × 10 ⁻⁵	8.935 × 10 ⁻⁵	5.962 × 10 ⁻⁶	20.0	3.428 × 10 ⁴
020201-D	2.110 × 10 ⁻⁵	1.116 × 10 ⁻⁴	4.977 × 10 ⁻⁶	20.0	3.395 × 10 ⁴
020201-E	2.108 × 10 ⁻⁵	1.338 × 10 ⁻⁴	4.271 × 10 ⁻⁶	20.0	3.366 × 10 ⁴
020201-F	2.106 × 10 ⁻⁵	1.559 × 10 ⁻⁴	3.727 × 10 ⁻⁶	20.0	3.357 × 10 ⁴
020201-G	2.104 × 10 ⁻⁵	1.780 × 10 ⁻⁴	3.315 × 10 ⁻⁶	20.0	3.336 × 10 ⁴
020201-H	2.102 × 10 ⁻⁵	2.000 × 10 ⁻⁴	2.977 × 10 ⁻⁶	20.0	3.330 × 10 ⁴
020201-I	2.100 × 10 ⁻⁵	2.220 × 10 ⁻⁴	2.712 × 10 ⁻⁶	20.0	3.309 × 10 ⁴
020201-J	2.098 × 10 ⁻⁵	2.440 × 10 ⁻⁴	2.463 × 10 ⁻⁶	20.0	3.334 × 10 ⁴
020201-K	2.096 × 10 ⁻⁵	2.659 × 10 ⁻⁴	2.272 × 10 ⁻⁶	20.0	3.327 × 10 ⁴
020201-L	2.094 × 10 ⁻⁵	2.878 × 10 ⁻⁴	2.124 × 10 ⁻⁶	20.0	3.292 × 10 ⁴
020201-M	2.092 × 10 ⁻⁵	3.096 × 10 ⁻⁴	1.963 × 10 ⁻⁶	20.0	3.322 × 10 ⁴
020201-N	2.089 × 10 ⁻⁵	3.314 × 10 ⁻⁴	1.831 × 10 ⁻⁶	20.0	3.334 × 10 ⁴
020201-O	2.087 × 10 ⁻⁵	3.531 × 10 ⁻⁴	1.728 × 10 ⁻⁶	20.0	3.318 × 10 ⁴

$$\bar{K} (20\text{ °C}) = (3.376 \pm 0.094) \times 10^4 \text{ L mol}^{-1}$$

Table 10.149: Bis(*N*-methyl-2,3-dihydro-1H-indol-5-yl)methylmethylm tetrafluoroborate (ind)₂CH⁺ BF₄⁻ and tris(4-methoxyphenyl)phosphine (p-MeOC₆H₅)₃P in CH₂Cl₂ at λ = 625 nm (J&M).

No.	[<i>EL</i>] ₀ / mol L ⁻¹	[<i>Nuc</i>] ₀ / mol L ⁻¹	[<i>EL</i>] / mol L ⁻¹	<i>T</i> / °C	<i>K</i> / L mol ⁻¹
160201-A	1.812 × 10 ⁻⁵	6.025 × 10 ⁻⁶	1.300 × 10 ⁻⁵	20.0	4.328 × 10 ⁵
160201-B	1.810 × 10 ⁻⁵	9.032 × 10 ⁻⁶	1.058 × 10 ⁻⁵	20.0	4.735 × 10 ⁵
160201-C	1.809 × 10 ⁻⁵	1.204 × 10 ⁻⁵	8.323 × 10 ⁻⁶	20.0	5.180 × 10 ⁵
160201-D	1.808 × 10 ⁻⁵	1.503 × 10 ⁻⁵	6.398 × 10 ⁻⁶	20.0	5.449 × 10 ⁵
160201-E	1.807 × 10 ⁻⁵	1.803 × 10 ⁻⁵	4.890 × 10 ⁻⁶	20.0	5.556 × 10 ⁵
160201-F	1.806 × 10 ⁻⁵	2.102 × 10 ⁻⁵	3.734 × 10 ⁻⁶	20.0	5.728 × 10 ⁵
160201-G	1.805 × 10 ⁻⁵	2.401 × 10 ⁻⁵	2.890 × 10 ⁻⁶	20.0	5.924 × 10 ⁵
160201-H	1.803 × 10 ⁻⁵	2.699 × 10 ⁻⁵	2.319 × 10 ⁻⁶	20.0	6.010 × 10 ⁵
160201-I	1.802 × 10 ⁻⁵	2.997 × 10 ⁻⁵	1.904 × 10 ⁻⁶	20.0	6.112 × 10 ⁵

$$\bar{K} (20\text{ }^\circ\text{C}) = (5.447 \pm 0.569) \times 10^5 \text{ L mol}^{-1}$$

Table 10.150: Bis(*N*-methyl-1,2,3,4-tetrahydroquinolin-6-yl)methylmethylm tetrafluoroborate (thq)₂CH⁺ BF₄⁻ and tris(4-methoxyphenyl)phosphine (p-MeOC₆H₅)₃P in CH₂Cl₂ at λ = 628 nm (J&M).

No.	[<i>EL</i>] ₀ / mol L ⁻¹	[<i>Nuc</i>] ₀ / mol L ⁻¹	[<i>EL</i>] / mol L ⁻¹	<i>T</i> / °C	<i>K</i> / L mol ⁻¹
150201-A	2.414 × 10 ⁻⁵	7.885 × 10 ⁻⁶	1.662 × 10 ⁻⁵	20.0	1.262 × 10 ⁶
150201-B	2.413 × 10 ⁻⁵	1.051 × 10 ⁻⁵	1.425 × 10 ⁻⁵	20.0	1.096 × 10 ⁶
150201-C	2.412 × 10 ⁻⁵	1.313 × 10 ⁻⁵	1.195 × 10 ⁻⁵	20.0	1.065 × 10 ⁶
150201-D	2.410 × 10 ⁻⁵	1.574 × 10 ⁻⁵	9.777 × 10 ⁻⁶	20.0	1.034 × 10 ⁶
150201-E	2.409 × 10 ⁻⁵	1.836 × 10 ⁻⁵	7.817 × 10 ⁻⁶	20.0	9.990 × 10 ⁵
150201-F	2.408 × 10 ⁻⁵	2.097 × 10 ⁻⁵	6.150 × 10 ⁻⁶	20.0	9.586 × 10 ⁵
150201-G	2.406 × 10 ⁻⁵	2.357 × 10 ⁻⁵	4.793 × 10 ⁻⁶	20.0	9.338 × 10 ⁵
150201-H	2.405 × 10 ⁻⁵	2.618 × 10 ⁻⁵	3.763 × 10 ⁻⁶	20.0	9.147 × 10 ⁵

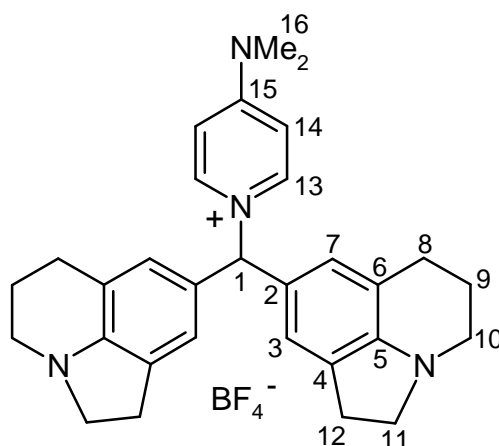
$$\bar{K} (20\text{ }^\circ\text{C}) = (1.033 \pm 0.105) \times 10^6 \text{ L mol}^{-1}$$

10.6 Nucleophilic reactivities of pyridine and its derivatives

10.6.1 Reactions of pyridine derivatives with benzhydryl salts

General procedure: In a carefully dried, nitrogen-flushed Schlenk-flask a solution of the pyridine-derivative in 5 mL absolute CH_2Cl_2 was added dropwise to a solution of the benzhydryl salt in 50 mL absolute CH_2Cl_2 . After stirring at room temperature for 1 h, the solvent was evaporated in vacuo to yield the crude product, which was washed with 20 mL absolute Et_2O and dried several hours in vacuo (10^{-2} mbar).

1-Bis(lilolidin-8-yl)methyl-(4-dimethylamino)pyridinium tetrafluoroborate (77) was obtained from (4-dimethylamino)pyridine (DMAP) (20 mg, 0.164 mmol) and bis(lilolidin-8-yl)methylium tetrafluoroborat $(\text{lil})_2\text{CH}^+ \text{BF}_4^-$ (68 mg, 0.163 mmol) as a bright-blue solid (51 mg, 58 %). ^1H NMR (300 MHz, CD_3CN): $\delta = 1.91\text{-}2.03$ (m, 4 H, 9-H), 2.54-2.60 (m, 4 H, 8-H), 2.78-2.86 (m, 4 H, 12-H), 2.96-2.99 (m, 4 H, 11-H), 3.15 (s, 6 H, 16-H), 3.22-3.30 (m, 4 H, 10-H), 6.46 (s, 1 H, 1-H), 6.56 (s, 2 H, 3-H or 7-H), 6.67 (s, 2 H, 3-H or 7-H), 6.78 (d, $J = 7.9$ Hz, 2 H, 13-H or 14-H), 7.86 (d, $J = 7.9$ Hz, 2 H, 13-H or 14-H); ^{13}C NMR (75.5 MHz, CD_3CN): $\delta = 22.3, 23.3, 27.8, 46.1, 54.3$ (5 t, C-8, C-9, C-10, C-11, C-12), 39.3 (q, C-16), 74.3 (d, C-1), 107.1 (d, C-13 or C-14), 121.8, 126.4 (2 d, C-3, C-7), 140.5 (d, C-13 or C-14), 118.9, 126.3, 129.1, 150.3 (4 s, C-2, C-4, C-5, C-6), 156.3 (s, C-15).

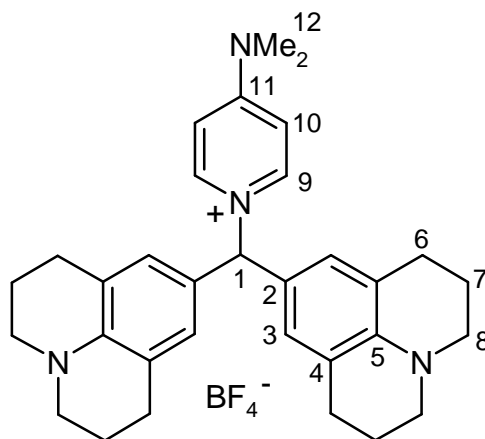


BKE076

77

1-Bis(julolidin-9-yl)methyl-(4-dimethylamino)pyridinium tetrafluoroborate (78) was obtained from (4-dimethylamino)pyridine (DMAP) (20 mg, 0.164 mmol) and bis(julolidin-9-yl)methylium tetrafluoroborat $(\text{jul})_2\text{CH}^+ \text{BF}_4^-$ (73 mg, 0.164 mmol) as a bright-blue solid (63 mg, 68 %). ^1H NMR (300 MHz, CD_3CN): $\delta = 1.81\text{-}2.00$ (m, 8 H, 7-H), 2.59-2.65 (m, 8 H, 6-

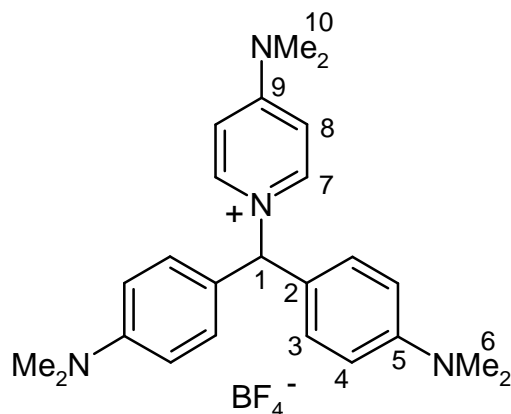
H), 2.96-3.16 (m, 14 H, 8 × 8-H, 6 × 12-H), 6.29 (s, 1 H, 1-H), 6.50 (s, 4 H, 3-H), 6.77 (d, $J = 8.0$ Hz, 2 H, 9-H or 10-H), 7.85 (d, $J = 7.9$ Hz, 2 H, 9-H or 10-H); ^{13}C NMR (75.5 MHz, CD_3CN): $\delta = 21.2$ (t, C-7), 27.1 (t, C-6), 39.3 (q, C-12), 49.1 (t, C-8), 73.7 (d, C-1), 107.1 (d, C-9 or C-10), 121.3 (s, C-4), 122.9 (s, C-2), 126.5 (d, C-3), 140.5 (d, C-9 or C-10), 147.3 (s, C-5), 156.3 (s, C-11).



BKE076

78

1-Bis(4-dimethylaminophenyl)methyl-(4-dimethylamino)pyridinium tetrafluoroborate (79) was obtained from (4-dimethylamino)pyridine (DMAP) (61.8 mg, 0.506 mmol) and bis(4-dimethylaminophenyl)methylium tetrafluoroborate $(\text{dma})_2\text{CH}^+ \text{BF}_4^-$ (172 mg, 0.506 mmol) as a bright-blue solid (169 mg, 72 %). ^1H NMR (300 MHz, CDCl_3): $\delta = 2.93$ (s, 12 H, 6-H), 3.18 (s, 6 H, 10-H), 6.57 (s, 1 H, 1-H), 6.64 (d, $J = 8.7$ Hz, 4 H, 3-H or 4-H), 6.82 (d, $J = 8.0$ Hz, 2 H, 7-H or 8-H), 6.96 (d, $J = 8.7$ Hz, 4 H, 3-H or 4-H), 7.88 (d, $J = 8.0$ Hz, 2 H, 7-H or 8-H); ^{13}C NMR (75.5 MHz, CDCl_3): $\delta = 40.0$ (q, C-6), 53.5 (d, C-1), 73.9 (q, C-10), 107.6 (d, C-7 or C-8), 112.3 (d, C-3 or C-4), 123.5 (s, C-2 or C-5), 129.2 (d, C-3 or C-4), 140.8 (d, C-7 or C-8), 150.5 (s, C-2 or C-5), 156.3 (s, C-9).



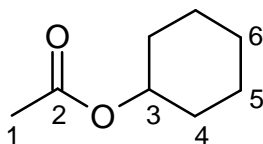
BKE060

79

10.6.2 Synthesis of acetic acid cyclohexyl ester

In a dried, nitrogen-flushed round-bottom flask equipped with a dropping funnel and reflux condenser, acetic anhydride (32.40 g, 0.317 mol) was added within 30 min to a suspension of cyclohexanol (28.20 g, 0.282 mol), triethylamine (36.50 g, 0.361 mol), (4-dimethylamino)pyridine (DMAP) (1.00 g, 0.008 mol), and 100 mL absolute methylene chloride. After 1 h the solvent was removed by vacuo, the residue was solved in 100 mL Et₂O, and washed with 100 mL 2n HCl. The organic layer was washed 2 times with 100 mL saturated NaHCO₃ solution, then dried over MgSO₄. After removing the solvent in vacuo the crude product was purified by distillation to give a colorless oil (21.42 g, 53 %); b.p. 85-86 °C/30 mbar. ¹H NMR (300 MHz, CDCl₃): δ = 1.20-1.28 (m, 1 H, 6-H), 1.31-1.45 (m, 4 H, 2 × 4-H, 2 × 5-H), 1.50-1.58 (m, 1 H, 6-H), 1.69-1.78 (m, 2 H, 5-H), 1.81-1.89 (m, 2 H, 4-H), 1.96 (s, 3 H, 1-H), 4.63-4.71 (m, 1 H, 3-H); ¹³C NMR (75.5 MHz, CDCl₃): δ = 21.4 (q, C-1), 23.8 (t, C-5), 25.3 (t, C-6), 31.6 (t, C-4), 72.6 (d, C-3), 170.5 (s, C-2); Signal assignments are based on ¹H, ¹³C-COSY experiments; in agreement with data published in ref. [202]; elemental analysis calcd (%) for C₈H₁₄O₂ (142.2): C 67.57, H 9.92; found C 67.50, H 10.12.

BKE062



10.6.3 Concentrations and rate constants for the reactions of pyridine derivatives with benzhydryl salts

Table 10.151: Bis(4-(phenyl(2,2,2-trifluoroethyl)amino)phenyl)methylm tetrafluoroborate (pfa)₂CH⁺ BF₄⁻ and 4-chloropyridin (pClIP) in CH₂Cl₂ at λ = 601 nm (J&M).

No.	[<i>EL</i>] ₀ / mol L ⁻¹	[<i>Nuc</i>] ₀ / mol L ⁻¹	[<i>Nuc</i>] ₀ /[<i>EL</i>] ₀	<i>T</i> / °C	<i>k</i> _{eff} / s ⁻¹
241001-A	4.798 × 10 ⁻⁶	3.822 × 10 ⁻⁵	8	20.0	1.282 × 10 ²
241001-B	4.798 × 10 ⁻⁶	7.644 × 10 ⁻⁵	16	20.0	1.424 × 10 ²
241001-C	4.798 × 10 ⁻⁶	1.147 × 10 ⁻⁴	24	20.0	1.694 × 10 ²
241001-D	4.798 × 10 ⁻⁶	1.529 × 10 ⁻⁴	32	20.0	1.848 × 10 ²

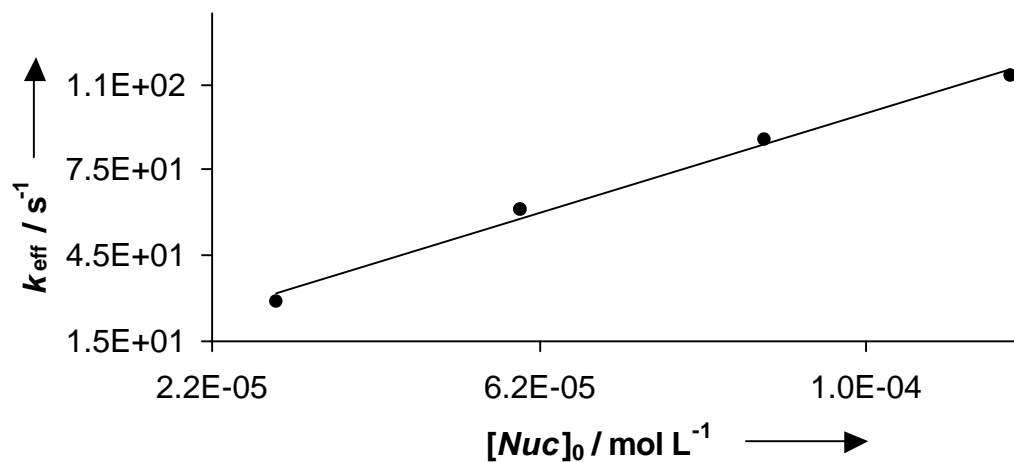


Figure 10.18: Plot of k_{eff} versus $[Nuc]_0$ ($n = 4$, $k_{\text{eff}} = (5.146 \times 10^5) \times [Nuc]_0 + (1.070 \times 10^2)$, $r^2 = 0.9850$).

$$k_2 (20 \text{ }^\circ\text{C}) = 5.146 \times 10^5 \text{ L mol}^{-1} \text{ s}^{-1}$$

$$k_{-2} (20 \text{ }^\circ\text{C}) = 1.070 \times 10^2 \text{ s}^{-1}$$

$$K (20 \text{ }^\circ\text{C}) = 4.809 \times 10^3 \text{ L mol}^{-1}$$

Table 10.152: Bis(4-diphenylaminophenyl)methylmethyl tetrafluoroborate $(\text{dpa})_2\text{CH}^+ \text{BF}_4^-$ and pyridine (pHP) in CH_2Cl_2 at $\lambda = 674 \text{ nm}$ (Stopped flow).

No.	$[EL]_0 /$ mol L^{-1}	$[Nuc]_0 /$ mol L^{-1}	$[Nuc]_0/[EL]_0$	$T /$ $^\circ\text{C}$	$k_{\text{eff}} /$ s^{-1}
091001-D	7.511×10^{-6}	1.545×10^{-4}	21	20.0	9.076×10^1
091001-E	7.511×10^{-6}	3.090×10^{-4}	41	20.0	1.479×10^2
091001-A	7.511×10^{-6}	4.635×10^{-4}	62	20.0	1.843×10^2

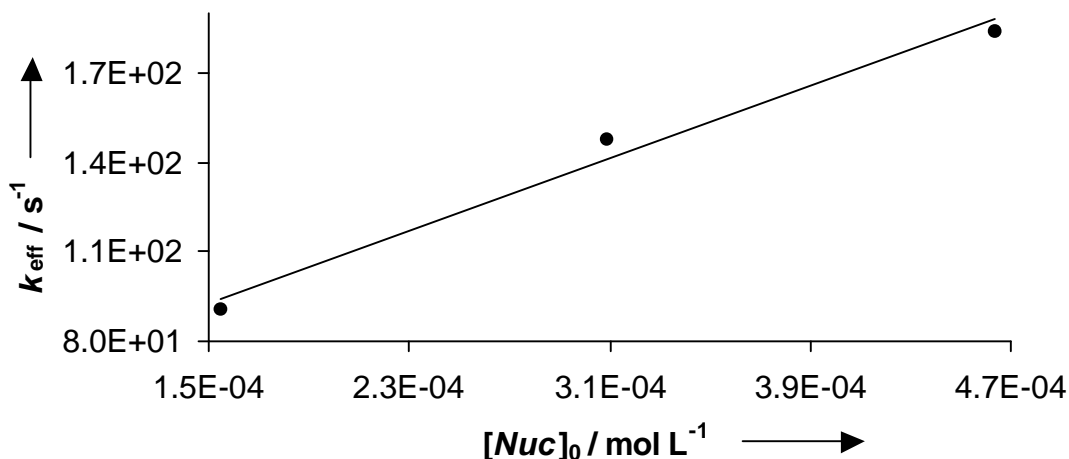


Figure 10.19: Plot of k_{eff} versus $[Nuc]_0$ ($n = 3$, $k_{\text{eff}} = (3.027 \times 10^5) \times [Nuc]_0 + 4.746 \times 10^1$, $r^2 = 0.9838$).

$$k_2 (20 \text{ }^\circ\text{C}) = 3.027 \times 10^5 \text{ L mol}^{-1} \text{ s}^{-1}$$

$$k_{-2} (20 \text{ }^\circ\text{C}) = 4.746 \times 10^1 \text{ s}^{-1}$$

$$K (20 \text{ }^\circ\text{C}) = 6.378 \times 10^3 \text{ L mol}^{-1}$$

Table 10.153: Bis(4-diphenylaminophenyl)methylmethyl tetrafluoroborate $(\text{dpa})_2\text{CH}^+ \text{BF}_4^-$ and 4-methylpyridine (pMeP) in CH_2Cl_2 at $\lambda = 674 \text{ nm}$ (Stopped flow).

No.	$[EL]_0 /$ mol L^{-1}	$[Nuc]_0 /$ mol L^{-1}	$[Nuc]_0/[EL]_0$	$T /$ $^\circ\text{C}$	$k_{\text{eff}} /$ s^{-1}
231001-M	4.303×10^{-6}	2.985×10^{-5}	7	20.0	2.896×10^1
231001-L	4.303×10^{-6}	5.970×10^{-5}	14	20.0	6.133×10^1
231001-I	4.303×10^{-6}	8.955×10^{-5}	21	20.0	8.569×10^1
231001-J	4.303×10^{-6}	1.194×10^{-4}	28	20.0	1.085×10^2

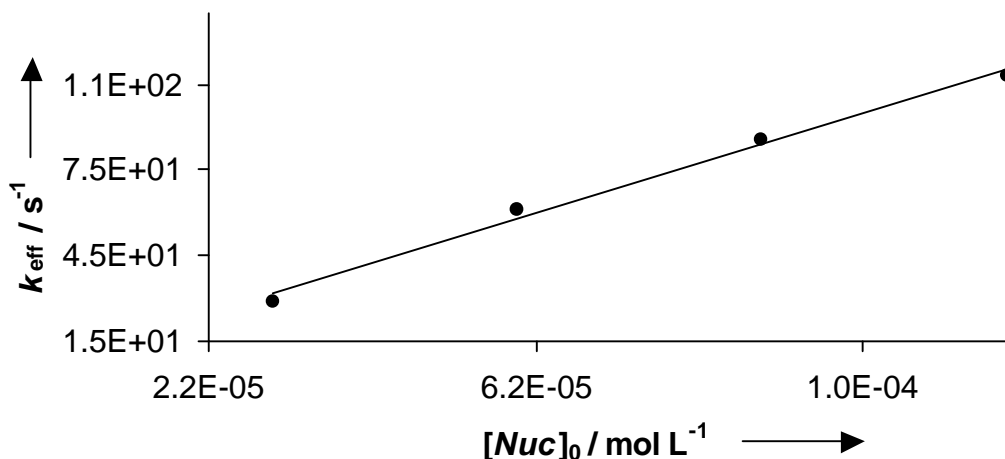


Figure 10.20: Plot of k_{eff} versus $[Nuc]_0$ ($n = 4$, $k_{\text{eff}} = (8.807 \times 10^5) \times [Nuc]_0 + 5.386$, $r^2 = 0.9928$).

$$k_2 (20 \text{ }^\circ\text{C}) = 8.807 \times 10^5 \text{ L mol}^{-1} \text{ s}^{-1}$$

$$k_{-2} (20 \text{ }^\circ\text{C}) = 5.386 \text{ s}^{-1}$$

$$K (20 \text{ }^\circ\text{C}) = 1.635 \times 10^5 \text{ L mol}^{-1}$$

Table 10.154: Bis(4-diphenylaminophenyl)methylmethyl tetrafluoroborate $(\text{dpa})_2\text{CH}^+ \text{BF}_4^-$ and 4-methoxypyridine (pMeOP) in CH_2Cl_2 at $\lambda = 674 \text{ nm}$ (Stopped flow).

No.	$[EI]_0 /$ mol L ⁻¹	$[Nuc]_0 /$ mol L ⁻¹	$[Nuc]_0/[EI]_0$	$T /$ °C	$k_{\text{eff}} /$ s ⁻¹
231001-H	4.303×10^{-6}	2.181×10^{-5}	5	20.0	1.796×10^1
231001-G	4.303×10^{-6}	4.362×10^{-5}	10	20.0	4.345×10^1
231001-D	4.303×10^{-6}	6.543×10^{-5}	15	20.0	6.365×10^1
231001-E	4.303×10^{-6}	8.724×10^{-5}	20	20.0	8.108×10^1
231001-F	4.303×10^{-6}	1.090×10^{-4}	25	20.0	9.701×10^1

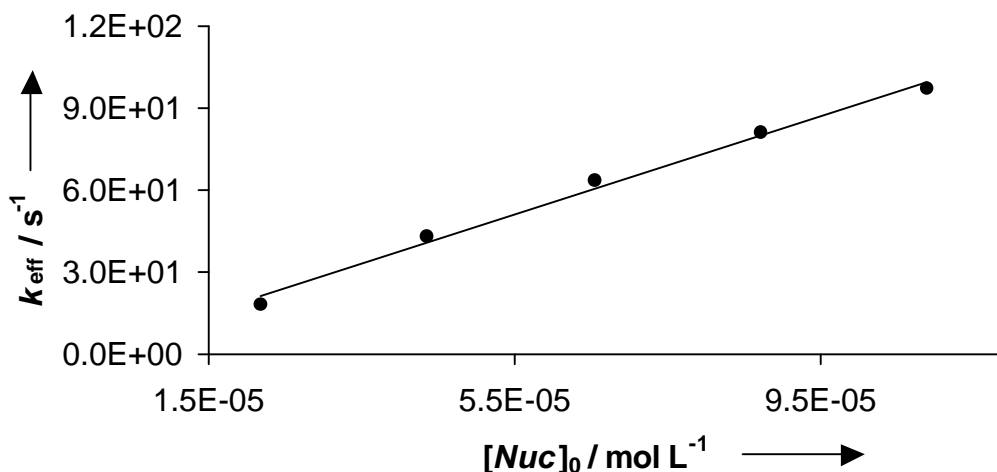


Figure 10.21: Plot of k_{eff} versus $[Nuc]_0$ ($n = 5$, $k_{\text{eff}} = (8.979 \times 10^5) \times [Nuc]_0 + 1.890$, $r^2 = 0.9908$).

$$k_2 (20 \text{ }^\circ\text{C}) = 8.979 \times 10^5 \text{ L mol}^{-1} \text{ s}^{-1}$$

$$k_{-2} (20 \text{ }^\circ\text{C}) = 1.890 \text{ s}^{-1}$$

$$K (20 \text{ }^\circ\text{C}) = 4.751 \times 10^5 \text{ L mol}^{-1}$$

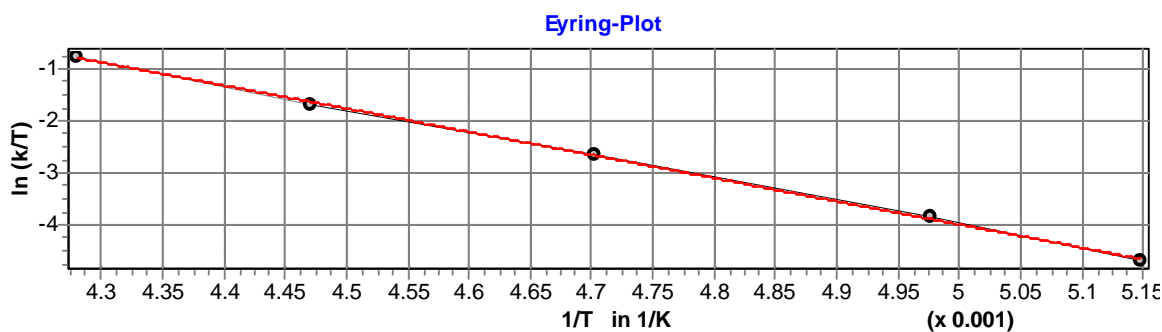
Table 10.155: Bis(4-dimethylaminophenyl)methylmethyl tetrafluoroborate $(\text{dma})_2\text{CH}^+ \text{BF}_4^-$ and 4-aminopyridine (pAP) in CH_2Cl_2 at $\lambda = 612 \text{ nm}$ (Stopped flow).

No.	$[El]_0 /$ mol L^{-1}	$[Nuc]_0 /$ mol L^{-1}	$[Nuc]_0/[El]_0$	$T /$ $^\circ\text{C}$	$k_2 /$ $\text{L mol}^{-1} \text{ s}^{-1}$
111201-E	7.796×10^{-6}	1.120×10^{-4}	14	20.0	3.167×10^5
111201-D	7.796×10^{-6}	2.240×10^{-4}	29	20.0	3.079×10^5
111201-A	7.796×10^{-6}	3.360×10^{-4}	43	20.0	2.978×10^5
111201-B	7.796×10^{-6}	4.479×10^{-4}	58	20.0	2.931×10^5
111201-C	7.796×10^{-6}	5.599×10^{-4}	72	20.0	2.962×10^5

$$\bar{k}_2 (20 \text{ }^\circ\text{C}) = (3.023 \pm 0.087) \times 10^5 \text{ L mol}^{-1} \text{ s}^{-1}$$

Table 10.156: Bis(lilolidin-8-yl)methylm tetrafluoroborate $(\text{lil})_2\text{CH}^+ \text{BF}_4^-$ and (4-dimethylamino)pyridine (DMAP) in CH_2Cl_2 at $\lambda = 640 \text{ nm}$ (Schölly).

No.	$[\text{El}]_0 /$ mol L^{-1}	$[\text{Nuc}]_0 /$ mol L^{-1}	$[\text{Nuc}]_0/[\text{El}]_0$	Conv. / %	$T /$ $^\circ\text{C}$	$k_2 /$ $\text{L mol}^{-1} \text{ s}^{-1}$
151001.PA0	2.995×10^{-5}	3.273×10^{-3}	109	84	-78.9	1.777
151001.PA1	3.613×10^{-5}	3.037×10^{-3}	84	87	-72.2	4.270
151001.PA2	2.692×10^{-5}	2.353×10^{-3}	87	76	-60.5	1.496×10^1
151001.PA3	3.134×10^{-5}	1.712×10^{-3}	55	73	-49.5	4.133×10^1
151001.PA4	2.395×10^{-5}	1.047×10^{-3}	44	90	-39.5	1.085×10^2

Eyring parameters:

$$\Delta H^\ddagger = 37.110 \pm 0.524 \text{ kJ mol}^{-1}$$

$$\Delta S^\ddagger = -45.264 \pm 2.476 \text{ J mol}^{-1} \text{ K}^{-1}$$

$$r^2 = 0.9994$$

Arrhenius parameters:

$$E_a = 38.877 \pm 0.521 \text{ kJ mol}^{-1}$$

$$\ln A = 24.677 \pm 0.296$$

$$r^2 = 0.9995$$

$$k_2 (20 \text{ }^\circ\text{C}) = (6.448 \pm 0.531) \times 10^3 \text{ L mol}^{-1} \text{ s}^{-1}$$

Table 10.157: Bis(*N*-methyl-2,3-dihydro-1H-indol-5-yl)methylm tetrafluoroborate (ind)₂CH⁺ BF₄⁻ and (4-dimethylamino)pyridine (DMAP) in CH₂Cl₂ at λ = 625 nm (Stopped flow).

No.	[<i>El</i>] ₀ / mol L ⁻¹	[<i>Nuc</i>] ₀ / mol L ⁻¹	[<i>Nuc</i>] ₀ /[<i>El</i>] ₀	<i>T</i> / °C	<i>k</i> ₂ / L mol ⁻¹ s ⁻¹
171001-E	7.480 × 10 ⁻⁶	2.493 × 10 ⁻⁴	33	20.0	4.967 × 10 ⁴
171001-D	7.480 × 10 ⁻⁶	4.986 × 10 ⁻⁴	67	20.0	4.703 × 10 ⁴
171001-F	7.480 × 10 ⁻⁶	7.480 × 10 ⁻⁴	100	20.0	4.877 × 10 ⁴
171001-B	7.480 × 10 ⁻⁶	9.973 × 10 ⁻⁴	133	20.0	4.975 × 10 ⁴
171001-C	7.480 × 10 ⁻⁶	1.247 × 10 ⁻³	167	20.0	4.917 × 10 ⁴

$$\bar{k}_2 (20\text{ }^\circ\text{C}) = (4.888 \pm 0.099) \times 10^4 \text{ L mol}^{-1} \text{ s}^{-1}$$

Table 10.158: Bis(*N*-methyl-1,2,3,4-tetrahydroquinolin-6-yl)methylm tetrafluoroborate (thq)₂CH⁺ BF₄⁻ and (4-dimethylamino)pyridine (DMAP) in CH₂Cl₂ at λ = 628 nm (Stopped flow).

No.	[<i>El</i>] ₀ / mol L ⁻¹	[<i>Nuc</i>] ₀ / mol L ⁻¹	[<i>Nuc</i>] ₀ /[<i>El</i>] ₀	<i>T</i> / °C	<i>k</i> ₂ / L mol ⁻¹ s ⁻¹
121001-E	7.587 × 10 ⁻⁶	1.696 × 10 ⁻⁴	22	20.0	1.483 × 10 ⁵
121001-D	7.587 × 10 ⁻⁶	3.392 × 10 ⁻⁴	45	20.0	1.538 × 10 ⁵
121001-A	7.587 × 10 ⁻⁶	5.088 × 10 ⁻⁴	67	20.0	1.270 × 10 ⁵
121001-B	7.587 × 10 ⁻⁶	6.784 × 10 ⁻⁴	89	20.0	1.324 × 10 ⁵
121001-C	7.587 × 10 ⁻⁶	8.480 × 10 ⁻⁴	112	20.0	1.425 × 10 ⁵

$$\bar{k}_2 (20\text{ }^\circ\text{C}) = (1.408 \pm 0.099) \times 10^5 \text{ L mol}^{-1} \text{ s}^{-1}$$

Table 10.159: Bis(4-dimethylaminophenyl)methylium tetrafluoroborate (dma)₂CH⁺ BF₄⁻ and (4-dimethylamino)pyridine (DMAP) in CH₂Cl₂ at λ = 613 nm (Stopped flow).

No.	[El] ₀ / mol L ⁻¹	[Nuc] ₀ / mol L ⁻¹	[Nuc] ₀ /[El] ₀	T / °C	k ₂ / L mol ⁻¹ s ⁻¹
101001-F	7.196 × 10 ⁻⁶	3.798 × 10 ⁻⁵	5	20.0	6.700 × 10 ⁵
101001-G	7.196 × 10 ⁻⁶	5.317 × 10 ⁻⁵	7	20.0	6.547 × 10 ⁵
101001-A	7.196 × 10 ⁻⁶	7.596 × 10 ⁻⁵	11	20.0	6.548 × 10 ⁵
101001-B	7.196 × 10 ⁻⁶	1.519 × 10 ⁻⁴	21	20.0	6.553 × 10 ⁵
101001-C	7.196 × 10 ⁻⁶	2.279 × 10 ⁻⁴	32	20.0	6.432 × 10 ⁵

$$\bar{k}_2 (20\text{ }^\circ\text{C}) = (6.556 \pm 0.085) \times 10^5 \text{ L mol}^{-1} \text{ s}^{-1}$$

Table 10.160: Bis(4-(methylphenylamino)phenyl)methylium tetrafluoroborate (mpa)₂CH⁺ BF₄⁻ and (4-dimethylamino)pyridine (DMAP) in CH₂Cl₂ at λ = 622 nm (Stopped flow).

No.	[El] ₀ / mol L ⁻¹	[Nuc] ₀ / mol L ⁻¹	[Nuc] ₀ /[El] ₀	T / °C	k ₂ / L mol ⁻¹ s ⁻¹
110101-D	2.757 × 10 ⁻⁶	1.973 × 10 ⁻⁵	7	20.0	2.923 × 10 ⁶
110101-E	2.757 × 10 ⁻⁶	2.702 × 10 ⁻⁵	10	20.0	2.961 × 10 ⁶
110101-A	2.757 × 10 ⁻⁶	3.945 × 10 ⁻⁵	14	20.0	2.757 × 10 ⁶
110101-B	2.757 × 10 ⁻⁶	5.918 × 10 ⁻⁵	22	20.0	2.688 × 10 ⁶
110101-F	2.757 × 10 ⁻⁶	7.891 × 10 ⁻⁵	29	20.0	2.819 × 10 ⁶

$$\bar{k}_2 (20\text{ }^\circ\text{C}) = (2.830 \pm 0.101) \times 10^6 \text{ L mol}^{-1} \text{ s}^{-1}$$

Table 10.161: Bis(*N*-methyl-1,2,3,4-tetrahydroquinolin-6-yl)methylmethylium tetrafluoroborate (thq)₂CH⁺ BF₄⁻ and (4-azetidino)pyridine (pAzP) in CH₂Cl₂ at λ = 628 nm (Stopped flow).

No.	[<i>El</i>] ₀ / mol L ⁻¹	[<i>Nuc</i>] ₀ / mol L ⁻¹	[<i>Nuc</i>] ₀ /[<i>El</i>] ₀	<i>T</i> / °C	<i>k</i> ₂ / L mol ⁻¹ s ⁻¹
290502-D	7.995 × 10 ⁻⁶	1.194 × 10 ⁻⁴	15	20.0	2.948 × 10 ⁴
290502-A	7.995 × 10 ⁻⁶	2.389 × 10 ⁻⁴	30	20.0	2.882 × 10 ⁴
290502-C	7.995 × 10 ⁻⁶	3.583 × 10 ⁻⁴	45	20.0	3.191 × 10 ⁴
290502-B	7.995 × 10 ⁻⁶	4.777 × 10 ⁻⁴	60	20.0	3.077 × 10 ⁴

$$\bar{k}_2 (20\text{ }^\circ\text{C}) = (3.025 \pm 0.119) \times 10^4 \text{ L mol}^{-1} \text{ s}^{-1}$$

Table 10.162: Bis(4-dimethylaminophenyl)methylmethylium tetrafluoroborate (dma)₂CH⁺ BF₄⁻ and (4-azetidino)pyridine (pAzP) in CH₂Cl₂ at λ = 612 nm (Stopped flow).

No.	[<i>El</i>] ₀ / mol L ⁻¹	[<i>Nuc</i>] ₀ / mol L ⁻¹	[<i>Nuc</i>] ₀ /[<i>El</i>] ₀	<i>T</i> / °C	<i>k</i> ₂ / L mol ⁻¹ s ⁻¹
290502-B	7.232 × 10 ⁻⁶	1.433 × 10 ⁻⁴	20	20.0	1.630 × 10 ⁵
290502-E	7.232 × 10 ⁻⁶	1.911 × 10 ⁻⁴	26	20.0	1.748 × 10 ⁵
290502-A	7.232 × 10 ⁻⁶	2.389 × 10 ⁻⁴	33	20.0	1.643 × 10 ⁵
290502-D	7.232 × 10 ⁻⁶	3.583 × 10 ⁻⁴	50	20.0	1.894 × 10 ⁵
290502-C	7.232 × 10 ⁻⁶	4.777 × 10 ⁻⁴	66	20.0	1.771 × 10 ⁵

$$\bar{k}_2 (20\text{ }^\circ\text{C}) = (1.737 \pm 0.096) \times 10^5 \text{ L mol}^{-1} \text{ s}^{-1}$$

Table 10.163: Bis(4-diphenylaminophenyl)methylmethylium tetrafluoroborate (dpa)₂CH⁺ BF₄⁻ and (4-azetidino)pyridine (pAzP) in CH₂Cl₂ at λ = 672 nm (Stopped flow).

No.	[<i>El</i>] ₀ / mol L ⁻¹	[<i>Nuc</i>] ₀ / mol L ⁻¹	[<i>Nuc</i>] ₀ /[<i>El</i>] ₀	<i>T</i> / °C	<i>k</i> ₂ / L mol ⁻¹ s ⁻¹
290502-A	7.239 × 10 ⁻⁶	4.777 × 10 ⁻⁵	7	20.0	1.646 × 10 ⁶
290502-D	7.239 × 10 ⁻⁶	7.166 × 10 ⁻⁵	10	20.0	1.851 × 10 ⁶
290502-C	7.239 × 10 ⁻⁶	9.554 × 10 ⁻⁵	13	20.0	1.554 × 10 ⁶

$$\bar{k}_2 (20\text{ }^\circ\text{C}) = (1.684 \pm 0.124) \times 10^6 \text{ L mol}^{-1} \text{ s}^{-1}$$

Table 10.164: Bis(4-dimethylaminophenyl)methylum tetrafluoroborate (dma)₂CH⁺ BF₄⁻ and (4-pyrrolidino)pyridine (pPyrP) in CH₂Cl₂ at λ = 612 nm (Stopped flow).

No.	[<i>El</i>] ₀ / mol L ⁻¹	[<i>Nuc</i>] ₀ / mol L ⁻¹	[<i>Nuc</i>] ₀ /[<i>El</i>] ₀	<i>T</i> / °C	<i>k</i> ₂ / L mol ⁻¹ s ⁻¹
071201-B	8.607 × 10 ⁻⁶	7.557 × 10 ⁻⁵	9	20.0	9.540 × 10 ⁵
071201-D	8.607 × 10 ⁻⁶	1.134 × 10 ⁻⁴	13	20.0	9.367 × 10 ⁵
071201-A	8.607 × 10 ⁻⁶	1.511 × 10 ⁻⁴	18	20.0	9.341 × 10 ⁵
071201-E	8.607 × 10 ⁻⁶	1.889 × 10 ⁻⁴	22	20.0	9.019 × 10 ⁵
071201-C	8.607 × 10 ⁻⁶	2.267 × 10 ⁻⁴	26	20.0	9.076 × 10 ⁵

$$\bar{k}_2 (20\text{ }^\circ\text{C}) = (9.269 \pm 0.194) \times 10^5 \text{ L mol}^{-1} \text{ s}^{-1}$$

Table 10.165: Bis(lilolidin-8-yl)methylum tetrafluoroborate (lil)₂CH⁺ BF₄⁻ and 1,2,3,4-tetrahydro-[1,6]naphthyridine (H-THNaph) in CH₂Cl₂ at λ = 639 nm (Stopped flow).

No.	[<i>El</i>] ₀ / mol L ⁻¹	[<i>Nuc</i>] ₀ / mol L ⁻¹	[<i>Nuc</i>] ₀ /[<i>El</i>] ₀	<i>T</i> / °C	<i>k</i> _{eff} / s ⁻¹
171002-L	5.967 × 10 ⁻⁶	1.006 × 10 ⁻⁴	17	20.0	8.600 × 10 ⁻¹
171002-M	5.967 × 10 ⁻⁶	2.012 × 10 ⁻⁴	34	20.0	1.360
171002-J	5.967 × 10 ⁻⁶	3.018 × 10 ⁻⁴	51	20.0	1.899
171002-K	5.967 × 10 ⁻⁶	5.031 × 10 ⁻⁴	84	20.0	2.855

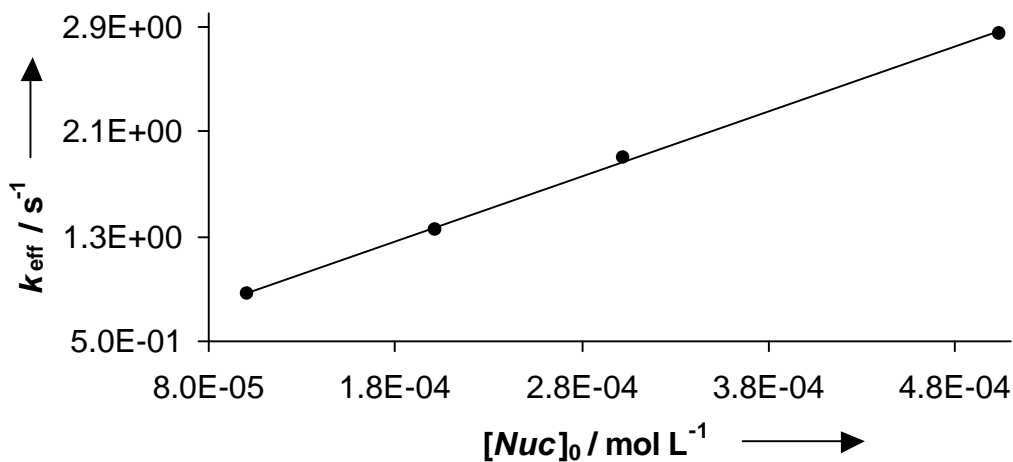


Figure 10.22: Plot of k_{eff} versus $[Nuc]_0$ ($n = 4$, $k_{\text{eff}} = (4.967 \times 10^3) \times [Nuc]_0 + (3.692 \times 10^{-1})$, $r^2 = 0.9994$).

$$k_2 (20 \text{ }^\circ\text{C}) = 4.967 \times 10^3 \text{ L mol}^{-1} \text{ s}^{-1}$$

$$k_{-2} (20 \text{ }^\circ\text{C}) = 3.692 \times 10^{-1} \text{ s}^{-1}$$

$$K (20 \text{ }^\circ\text{C}) = 1.345 \times 10^4 \text{ L mol}^{-1}$$

Table 10.166: Bis(lilolidin-8-yl)methylum tetrafluoroborate $(\text{lil})_2\text{CH}^+ \text{BF}_4^-$ and 1-methyl-1,2,3,4-tetrahydro-[1,6]naphthyridine (Me-THNaph) in CH_2Cl_2 at $\lambda = 639 \text{ nm}$ (Stopped flow).

No.	$[EL]_0 /$ mol L^{-1}	$[Nuc]_0 /$ mol L^{-1}	$[Nuc]_0/[EL]_0$	$T /$ $^\circ\text{C}$	$k_{\text{eff}} /$ s^{-1}
171002-F	5.967×10^{-6}	4.291×10^{-4}	72	20.0	2.808
171002-H	5.967×10^{-6}	5.722×10^{-4}	96	20.0	3.297
171002-G	5.967×10^{-6}	7.152×10^{-4}	120	20.0	4.166
171002-I	5.967×10^{-6}	1.430×10^{-3}	240	20.0	7.387

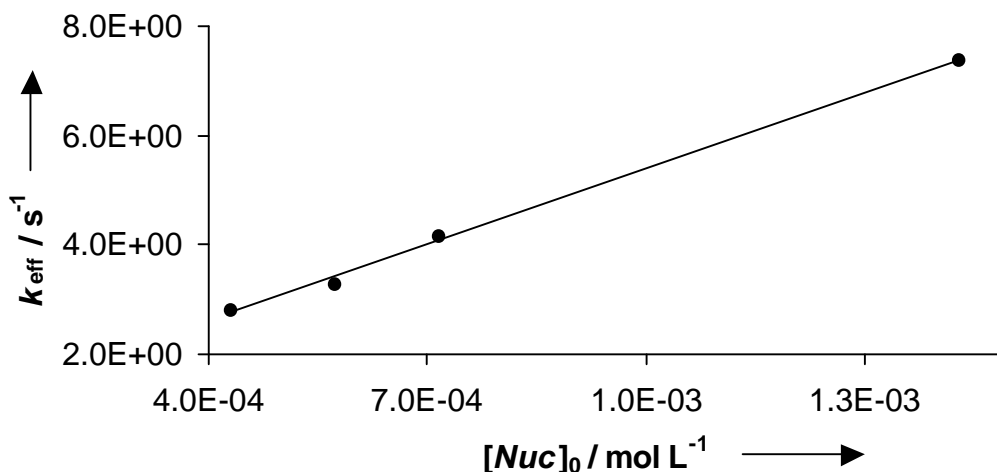


Figure 10.23: Plot of k_{eff} versus $[Nuc]_0$ ($n = 4$, $k_{\text{eff}} = (4.629 \times 10^3) \times [Nuc]_0 + (7.733 \times 10^{-1})$, $r^2 = 0.9981$).

$$k_2 (20 \text{ }^\circ\text{C}) = 4.629 \times 10^3 \text{ L mol}^{-1} \text{ s}^{-1}$$

$$k_{-2} (20 \text{ }^\circ\text{C}) = 7.733 \times 10^{-1} \text{ s}^{-1}$$

$$K (20 \text{ }^\circ\text{C}) = 5.986 \times 10^3 \text{ L mol}^{-1}$$

Table 10.167: Bis(*N*-methyl-1,2,3,4-tetrahydroquinolin-6-yl)methylmethyl tetrafluoroborate ($(\text{thq})_2\text{CH}^+ \text{BF}_4^-$) and 5,6,9,10-tetrahydro-4*H*,8*H*-pyrido[3,2,1-*ij*]naphthyridine (Py-THNaph) in CH_2Cl_2 at $\lambda = 628 \text{ nm}$ (Stopped flow).

No.	$[El]_0 /$ mol L^{-1}	$[Nuc]_0 /$ mol L^{-1}	$[Nuc]_0/[El]_0$	$T /$ $^\circ\text{C}$	$k_2 /$ $\text{L mol}^{-1} \text{ s}^{-1}$
131201-N	5.476×10^{-6}	2.156×10^{-4}	39	20.0	2.499×10^5
131201-L	5.476×10^{-6}	2.515×10^{-4}	46	20.0	2.491×10^5
131201-H	5.476×10^{-6}	2.874×10^{-4}	53	20.0	2.448×10^5
131201-M	5.476×10^{-6}	3.233×10^{-4}	59	20.0	2.419×10^5
131201-I	5.476×10^{-6}	3.593×10^{-4}	66	20.0	2.404×10^5

$$\bar{k}_2 (20 \text{ }^\circ\text{C}) = (2.452 \pm 0.038) \times 10^5 \text{ L mol}^{-1} \text{ s}^{-1}$$

10.6.4 Concentrations and equilibrium constants for the reactions of pyridine derivatives with benzhydryl salts

Table 10.168: Bis(4-diphenylaminophenyl)methylm tetrafluoroborate (dpa)₂CH⁺ BF₄⁻ and pyridine (pHP) in CH₂Cl₂ at λ = 672 nm (J&M).

No.	[<i>El</i>] ₀ / mol L ⁻¹	[<i>Nuc</i>] ₀ / mol L ⁻¹	[<i>El</i>] / mol L ⁻¹	<i>T</i> / °C	<i>K</i> / L mol ⁻¹
131101-A	1.080 × 10 ⁻⁵	1.355 × 10 ⁻⁴	2.959 × 10 ⁻⁶	20.0	2.074 × 10 ⁴
131101-B	1.646 × 10 ⁻⁵	1.034 × 10 ⁻⁴	5.278 × 10 ⁻⁶	20.0	2.298 × 10 ⁴
131101-C	1.184 × 10 ⁻⁵	6.863 × 10 ⁻⁵	9.471 × 10 ⁻⁶	20.0	2.321 × 10 ⁴

$$\bar{K} (20\text{ }^\circ\text{C}) = (2.231 \pm 0.111) \times 10^4 \text{ L mol}^{-1}$$

Table 10.169: Bis(4-diphenylaminophenyl)methylm tetrafluoroborate (dpa)₂CH⁺ BF₄⁻ and 4-methylpyridine (pMeP) in CH₂Cl₂ at λ = 672 nm (J&M).

No.	[<i>El</i>] ₀ / mol L ⁻¹	[<i>Nuc</i>] ₀ / mol L ⁻¹	[<i>El</i>] / mol L ⁻¹	<i>T</i> / °C	<i>K</i> / L mol ⁻¹
141101-A	3.551 × 10 ⁻⁵	6.494 × 10 ⁻⁵	1.996 × 10 ⁻⁶	20.0	5.344 × 10 ⁵
141101-B	3.458 × 10 ⁻⁵	3.165 × 10 ⁻⁵	8.632 × 10 ⁻⁶	20.0	5.278 × 10 ⁵
141101-C	3.293 × 10 ⁻⁵	1.809 × 10 ⁻⁵	1.691 × 10 ⁻⁵	20.0	4.596 × 10 ⁵

$$\bar{K} (20\text{ }^\circ\text{C}) = (5.073 \pm 0.338) \times 10^5 \text{ L mol}^{-1}$$

Table 10.170: Bis(lilolidin-8-yl)methylm tetrafluoroborate (lil)₂CH⁺ BF₄⁻ and (4-dimethylamino)pyridine (DMAP) in CH₂Cl₂ at λ = 639 nm (J&M).

No.	[<i>El</i>] ₀ / mol L ⁻¹	[<i>Nuc</i>] ₀ / mol L ⁻¹	[<i>El</i>] / mol L ⁻¹	<i>T</i> / °C	<i>K</i> / L mol ⁻¹
121201-C	1.693 × 10 ⁻⁵	7.228 × 10 ⁻⁴	3.329 × 10 ⁻⁶	20.0	5.762 × 10 ³
121201-B	1.693 × 10 ⁻⁵	4.829 × 10 ⁻⁴	4.597 × 10 ⁻⁶	20.0	5.703 × 10 ³
121201-A	1.693 × 10 ⁻⁵	2.420 × 10 ⁻⁴	7.335 × 10 ⁻⁶	20.0	5.631 × 10 ³
121201-D	1.848 × 10 ⁻⁵	1.322 × 10 ⁻⁴	1.079 × 10 ⁻⁵	20.0	5.721 × 10 ³

$$\bar{K} (20\text{ }^\circ\text{C}) = (5.704 \pm 0.047) \times 10^3 \text{ L mol}^{-1}$$

Table 10.171: Bis(julolidin-9-yl)methylium tetrafluoroborate $(\text{jul})_2\text{CH}^+ \text{BF}_4^-$ and (4-dimethylamino)pyridin (DMAP) in CH_2Cl_2 at $\lambda = 642 \text{ nm}$ (J&M).

No.	$[\text{El}]_0 /$ mol L^{-1}	$[\text{Nuc}]_0 /$ mol L^{-1}	$[\text{El}] /$ mol L^{-1}	$T /$ $^\circ\text{C}$	$K /$ L mol^{-1}
041201-C	2.161×10^{-5}	4.780×10^{-4}	5.818×10^{-6}	20.0	5.872×10^3
041201-B	2.161×10^{-5}	3.195×10^{-4}	7.753×10^{-6}	20.0	5.848×10^3
041201-A	2.161×10^{-5}	1.601×10^{-4}	1.153×10^{-5}	20.0	5.826×10^3

$$\bar{K} (20\text{ }^\circ\text{C}) = (5.849 \pm 0.019) \times 10^3 \text{ L mol}^{-1}$$

Table 10.172: Bis(*N*-methyl-2,3-dihydro-1H-indol-5-yl)methylium tetrafluoroborate $(\text{ind})_2\text{CH}^+ \text{BF}_4^-$ and (4-dimethylamino)pyridine (DMAP) in CH_2Cl_2 at $\lambda = 625 \text{ nm}$ (J&M).

No.	$[\text{El}]_0 /$ mol L^{-1}	$[\text{Nuc}]_0 /$ mol L^{-1}	$[\text{El}] /$ mol L^{-1}	$T /$ $^\circ\text{C}$	$K /$ L mol^{-1}
061201-B	2.084×10^{-5}	1.547×10^{-4}	7.271×10^{-7}	20.0	2.056×10^5
061201-A	2.084×10^{-5}	7.755×10^{-5}	1.934×10^{-6}	20.0	1.667×10^5
061201-D	2.360×10^{-5}	8.776×10^{-5}	1.972×10^{-6}	20.0	1.658×10^5
061201-C	2.360×10^{-5}	4.395×10^{-5}	5.013×10^{-6}	20.0	1.462×10^5

$$\bar{K} (20\text{ }^\circ\text{C}) = (1.711 \pm 0.216) \times 10^5 \text{ L mol}$$

Table 10.173: Bis(*N*-methyl-1,2,3,4-tetrahydroquinolin-6-yl)methylium tetrafluoroborate $(\text{thq})_2\text{CH}^+ \text{BF}_4^-$ and (4-dimethylamino)pyridine (DMAP) in CH_2Cl_2 at $\lambda = 628 \text{ nm}$ (J&M).

No.	$[\text{El}]_0 /$ mol L^{-1}	$[\text{Nuc}]_0 /$ mol L^{-1}	$[\text{El}] /$ mol L^{-1}	$T /$ $^\circ\text{C}$	$K /$ L mol^{-1}
101201-A	1.690×10^{-5}	7.038×10^{-5}	1.173×10^{-6}	20.0	2.452×10^5
101201-D	2.012×10^{-5}	8.377×10^{-5}	1.682×10^{-6}	20.0	1.678×10^5
101201-C	2.646×10^{-5}	7.348×10^{-5}	1.828×10^{-6}	20.0	2.760×10^5
101201-B	2.646×10^{-5}	3.679×10^{-5}	4.558×10^{-6}	20.0	3.230×10^5

$$\bar{K} (20\text{ }^\circ\text{C}) = (2.814 \pm 0.320) \times 10^5 \text{ L mol}^{-1}$$

Table 10.174: Bis(4-dimethylaminophenyl)methylmethyl tetrafluoroborate $(\text{dma})_2\text{CH}^+ \text{BF}_4^-$ and (4-dimethylamino)pyridine (DMAP) in CH_2Cl_2 at $\lambda = 613 \text{ nm}$ (J&M).

No.	$[\text{EI}]_0 /$ mol L^{-1}	$[\text{Nuc}]_0 /$ mol L^{-1}	$[\text{EI}] /$ mol L^{-1}	$T /$ $^\circ\text{C}$	$K /$ L mol^{-1}
051201-B	2.075×10^{-5}	2.290×10^{-5}	1.444×10^{-5}	20.0	6.225×10^7
051201-C	1.962×10^{-5}	2.165×10^{-5}	2.068×10^{-5}	20.0	4.189×10^7
051201-A	1.886×10^{-5}	2.081×10^{-5}	3.241×10^{-5}	20.0	2.507×10^7

$$\bar{K} (20\text{ }^\circ\text{C}) = (4.307 \pm 1.520) \times 10^7 \text{ L mol}^{-1}$$

10.6.5 Concentrations and rates for the base-catalyzed acetylations of cyclohexanol

General: The IR-kinetics were measured with a ReactIRTM 1000 instrument, controlled by ReactIR Software Version 2 from ASI Applied Systems. All measurements are performed in absolute methylene chloride at 20 °C, educts were purified before use. For the evaluation of the kinetics under second order conditions, the right part of eq. 8.1 was plotted versus t , and the linear part (indicated in the column % conversion) was used to determine k_2 (for detailed information see Chapter 8.8). For the evaluation of the kinetics under pseudo-first-order conditions, $\ln(A_0 - A_{\text{end}} / A_t - A_{\text{end}})$ was plotted versus t , and the linear part (indicated in the column % conversion) was used to determine k .

Table 10.175: Concentrations and rate constants of the reactions $\text{Ac}_2\text{O} / c\text{HexOH} / \text{pyridine}$ (pHP) / NEt_3 at 20 °C in CH_2Cl_2 at $\nu = 1127 \text{ cm}^{-1}$ (Ac_2O).

No.	$[\text{Ac}_2\text{O}]_0 /$ mol L^{-1}	$[c\text{HexOH}]_0 /$ mol L^{-1}	$[\text{NEt}_3]_0 /$ mol L^{-1}	$[\text{pHP}]_0 /$ mol L^{-1}	Conv. / %	$k_2 /$ $\text{L mol}^{-1} \text{ s}^{-1}$
210102-17	4.772×10^{-1}	5.045×10^{-1}	5.350×10^{-1}	5.285×10^{-2}	56	8.816×10^{-6}

Table 10.176: Concentrations and rate constants of the reactions Ac_2O / $c\text{HexOH}$ / 4-methylpyridine (pMeP) / NEt_3 at 20 °C in CH_2Cl_2 at $\nu = 1127 \text{ cm}^{-1}$ (Ac_2O).

No.	$[\text{Ac}_2\text{O}]_0 /$ mol L^{-1}	$[c\text{HexOH}]_0$ $/ \text{mol L}^{-1}$	$[\text{NEt}_3]_0 /$ mol L^{-1}	$[\text{pMeP}]_0 /$ mol L^{-1}	Conv. / %	$k_2 /$ $\text{L mol}^{-1} \text{ s}^{-1}$
210102-16	4.772×10^{-1}	5.045×10^{-1}	5.350×10^{-1}	5.296×10^{-2}	37	1.306×10^{-5}

Table 10.177: Concentrations and rate constants of the reactions Ac_2O / $c\text{HexOH}$ / 4-aminopyridine (pAP) / NEt_3 at 20 °C in CH_2Cl_2 at $\nu = 1127 \text{ cm}^{-1}$ (Ac_2O).

No.	$[\text{Ac}_2\text{O}]_0 /$ mol L^{-1}	$[c\text{HexOH}]_0$ $/ \text{mol L}^{-1}$	$[\text{NEt}_3]_0 /$ mol L^{-1}	$[\text{pAP}]_0 /$ mol L^{-1}	Conv. / %	$k_2 /$ $\text{L mol}^{-1} \text{ s}^{-1}$
170102-12	4.772×10^{-1}	5.045×10^{-1}	5.350×10^{-1}	2.588×10^{-2}	53	5.755×10^{-5}
170102-11	4.772×10^{-1}	5.045×10^{-1}	5.350×10^{-1}	5.288×10^{-2}	37	1.055×10^{-4}

Table 10.178: Concentrations and rate constants of the reactions Ac₂O / cHexOH / (4-dimethylamino)pyridine (DMAP) / NEt₃ at 20 °C in CH₂Cl₂ at $\nu = 1127 \text{ cm}^{-1}$ (Ac₂O).

No.	[Ac ₂ O] ₀ / mol L ⁻¹	[cHexOH] ₀ / mol L ⁻¹	[NEt ₃] ₀ / mol L ⁻¹	[DMAP] ₀ / mol L ⁻¹	Conv. / %	<i>k</i> ₂ / L mol ⁻¹ s ⁻¹
140102-01	4.772×10^{-1}	5.045×10^{-1}	5.350×10^{-1}	5.293×10^{-2}	92	3.380×10^{-2}
140102-02	4.772×10^{-1}	5.045×10^{-1}	5.350×10^{-1}	2.585×10^{-2}	91	1.360×10^{-2}
140102-03	4.772×10^{-1}	5.045×10^{-1}	5.350×10^{-1}	1.255×10^{-2}	89	6.921×10^{-3}
140102-04	4.772×10^{-1}	5.045×10^{-1}	5.350×10^{-1}	7.447×10^{-3}	83	4.258×10^{-3}
280102-22	4.772×10^{-1}	5.045×10^{-1}	0	5.293×10^{-2}	a	a
280102-23	4.772×10^{-1}	5.045×10^{-1}	5.350×10^{-1}	0	b	b
310102-25	4.772×10^{-1}	1.441	5.350×10^{-1}	1.255×10^{-2}	83	6.873×10^{-3} [c]
310102-26	4.772×10^{-1}	2.883	5.350×10^{-1}	1.255×10^{-2}	85	6.937×10^{-3} [c]
310102-27	4.772×10^{-1}	2.162	5.350×10^{-1}	1.255×10^{-2}	89	6.850×10^{-3} [c]

[a] Very slow reaction, not first order (becomes slower), $\tau_{1/2} \approx 960 \text{ s}$. [b] No reaction. [c] Pseudo-first-order conditions.

Table 10.179: Concentrations and rate constants of the reactions Ac₂O / cHexOH / (4-pyrrolidino)pyridine (pPyrP) / NEt₃ at 20 °C in CH₂Cl₂ at $\nu = 1127 \text{ cm}^{-1}$ (Ac₂O).

No.	[Ac ₂ O] ₀ / mol L ⁻¹	[cHexOH] ₀ / mol L ⁻¹	[NEt ₃] ₀ / mol L ⁻¹	[pPyrP] ₀ / mol L ⁻¹	Conv. / %	<i>k</i> ₂ / L mol ⁻¹ s ⁻¹
160102-09	4.772×10^{-1}	5.045×10^{-1}	5.350×10^{-1}	7.447×10^{-3}	87	7.697×10^{-3}
160102-08	4.772×10^{-1}	5.045×10^{-1}	5.350×10^{-1}	1.258×10^{-2}	95	1.337×10^{-2}
160102-07	4.772×10^{-1}	5.045×10^{-1}	5.350×10^{-1}	2.587×10^{-2}	88	2.527×10^{-2}
160102-10	4.772×10^{-1}	5.045×10^{-1}	5.350×10^{-1}	5.296×10^{-2}	90	4.551×10^{-2}

11. References

- [1] A. Lapworth, *Nature* **1925**, *115*, 625.
- [2] (a) C. K. Ingold, *Recl. Trav. Chim. Pays-Bas* **1929**, *42*, 797-812; (b) C. K. Ingold, *J. Chem. Soc.* **1933**, 1120-1127; (c) C. K. Ingold, *Chem. Rev.* **1934**, *15*, 225-274.
- [3] C. G. Swain, C. B. Scott, *J. Am. Chem. Soc.* **1953**, *75*, 141-147.
- [4] (a) J. O. Edwards, *J. Am. Chem. Soc.* **1954**, *76*, 1540-1547; (b) J. O. Edwards, *J. Am. Chem. Soc.* **1956**, *78*, 1819-1820.
- [5] A. J. Parker, *Chem. Rev.* **1969**, *69*, 1-32.
- [6] J. F. Bunnett, *Annu. Rev. Phys. Chem.* **1963**, *14*, 271-290.
- [7] R. G. Pearson, H. Sobel, J. Songstad, *J. Am. Chem. Soc.* **1968**, *90*, 319-326.
- [8] (a) C. D. Ritchie, *Acc. Chem. Res.* **1972**, *5*, 348-354; (b) C. D. Ritchie, J. E. Van Verth, P. O. I. Virtanen, *J. Am. Chem. Soc.* **1982**, *104*, 3491-3497; (c) C. D. Ritchie, *J. Am. Chem. Soc.* **1984**, *106*, 7187-7194.
- [9] C. D. Ritchie, *Can. J. Chem.* **1986**, *64*, 2239-2250.
- [10] C. D. Ritchie, *J. Am. Chem. Soc.* **1975**, *97*, 1170-1179.
- [11] C. D. Ritchie, M. Sawada, *J. Am. Chem. Soc.* **1977**, *99*, 3754-3761.
- [12] L. A. P. Kane-Maguire, E. D. Honig, D. A. Sweigart, *Chem. Rev.* **1984**, *84*, 525-543.
- [13] T. J. Alavosus, D. A. Sweigart, *J. Am. Chem. Soc.* **1985**, *107*, 985-987.
- [14] (a) H. Mayr, R. Schneider, U. Grabis, *Angew. Chem.* **1986**, *98*, 1034-1036; *Angew. Chem., Int. Ed. Engl.* **1986**, *25*, 1017-1019; (b) H. Mayr, R. Schneider, U. Grabis, *J. Am. Chem. Soc.* **1990**, *112*, 4460-4467.
- [15] H. Mayr, M. Patz, *Angew. Chem.* **1994**, *106*, 990-1010; *Angew. Chem., Int. Ed. Engl.* **1994**, *33*, 938-957.
- [16] H. Mayr, O. Kuhn, M. F. Gotta, M. Patz, *J. Phys. Org. Chem.* **1998**, *11*, 642-654.
- [17] H. Mayr, M. Patz, M. F. Gotta, A. R. Ofial, *Pure Appl. Chem.* **1998**, *70*, 1993-2000.
- [18] M. A. Funke, H. Mayr, *Chem. Eur. J.* **1997**, *3*, 1214-1222.
- [19] H. Mayr, K.-H. Müller, *Collect. Czech. Chem. Commun.* **1999**, *64*, 1770-1779.
- [20] H. Mayr, O. Kuhn, C. Schlierf, A. R. Ofial, *Tetrahedron* **2000**, *56*, 4219-4229.
- [21] M. F. Gotta, H. Mayr, *J. Org. Chem.* **1998**, *63*, 9769-9775.
- [22] J. Burfeindt, M. Patz, M. Müller, H. Mayr, *J. Am. Chem. Soc.* **1998**, *120*, 3629-3634.

- [23] B. Kempf, *Diplomarbeit* **2000**, Ludwig-Maximilians-Universität München.
- [24] R. Schmid, V. N. Sapunov, *NON-FORMAL KINETICS*, Verlag Chemie, Weinheim, **1981**.
- [25] H. Mayr, *Angew. Chem.* **1990**, *102*, 1415-1428; *Angew. Chem., Int. Ed. Engl.* **1990**, *29*, 1371-1384.
- [26] H. Mayr, T. Bug, M. F. Gotta, N. Hering, B. Irrgang, B. Janker, B. Kempf, R. Loos, A. R. Ofial, G. Remennikov, H. Schimmel, *J. Am. Chem. Soc.* **2001**, *123*, 9500-9512.
- [27] O. Kuhn, D. Rau, H. Mayr, *J. Am. Chem. Soc.* **1998**, *120*, 900-907.
- [28] (a) N. C. Deno, J. J. Jaruzelski, A. Schriesheim, *J. Am. Chem. Soc.* **1955**, *77*, 3044-3051; (b) N. C. Deno, A. Schriesheim, *J. Am. Chem. Soc.* **1955**, *77*, 3051-3054.
- [29] (a) J. Mindl, M. Vecera, *Collect. Czech. Chem. Commun.* **1971**, *36*, 3621-3632; (b) J. Mindl, M. Vecera, *Collect. Czech. Chem. Commun.* **1972**, *37*, 1143-1149.
- [30] O. Exner, *Correlation Analysis of Chemical Data*, Plenum Press, New York, **1988**.
- [31] J. Shorter in *Supplement F2, The chemistry of amino, nitroso, nitro and related groups* (ed.: S. Patai), Wiley, Chichester, **1996**, Chapter 11, pp. 479-531.
- [32] H. Schimmel, *Dissertation* **2000**, Ludwig-Maximilians-Universität München.
- [33] S. F. Beach, J. D. Hepworth, P. Jones, D. Mason, J. Sawyer, G. Hallas, M. M. Mitchell, *J. Chem. Soc., Perkin Trans. 2* **1989**, 1087-1090.
- [34] C. C. Baker, G. Hallas, *J. Chem. Soc B* **1969**, 1068-1071.
- [35] L. Armstrong, A. M. Jones, *Dyes Pigm.* **1999**, *42*, 65-70.
- [36] G. M. Rubottom, J. M. Gruber, R. Marrero, H. D. Juve, C. W. Kim, *J. Org. Chem.* **1983**, *48*, 4940-4944.
- [37] H. Mayr, R. Schneider, C. Schade, J. Bartl, R. Bederke, *J. Am. Chem. Soc.* **1990**, *112*, 4446-4454.
- [38] G. Hagen, H. Mayr, *J. Am. Chem. Soc.* **1991**, *113*, 4954-4961.
- [39] (a) H. Mayr, R. Pock, *Chem. Ber.* **1986**, *119*, 2473-2496; (b) R. Pock, H. Mayr, *Chem. Ber.* **1986**, *119*, 2497-2509.
- [40] The What'sBest!'s nonlinear solver employs both successive linear programming and generalized reduced gradient algorithms. The minimization procedure for Δ^2 was performed by solving the model several times with different initial values of E , N , and s .

- [41] M. Roth, H. Mayr, *Angew. Chem.* **1995**, *107*, 2428-2430; *Angew. Chem., Int. Ed. Engl.* **1995**, *34*, 2250-2252.
- [42] (a) J. Hine, *Structural Effects on Equilibria in Organic Chemistry*, Robert E. Krieger Publishing Company: Huntington, NY, **1981**; (b) N. B. Chapman in *Advances in Linear Free Energy Relationships* (Ed.: J. Shorter), Plenum Press, London, **1972**.
- [43] Y. Tsuno, M. Fujio, *Adv. Phys. Org. Chem.* **1999**, *32*, 267-385.
- [44] Y. Tsuno, M. Fujio, *Chem. Soc. Rev.* **1996**, 129-139.
- [45] For σ_R^0 constants of amino substituents, see: R. Gawinecki, E. Kolehmainen, R. Kauppinen, *J. Chem. Soc., Perkin Trans. 2* **1998**, 25-29.
- [46] C. Schade, H. Mayr, *Tetrahedron* **1988**, *44*, 5761-5770.
- [47] C. Schindele, K. N. Houk, H. Mayr, *J. Am. Chem. Soc.* **2002**, *124*, 11208-11214.
- [48] R. Lucius, R. Loos, H. Mayr, *Angew. Chem., Int. Ed.* **2002**, *41*, 91-95.
- [49] J. M. Harris in *Nucleophilicity* (Ed.: S. P. McManus), ACS Advances in Chemistry Series 215, American Chemical Society, Washington DC, **1987**.
- [50] C. Mannich, H. Davidsen, *Ber. Dtsch. Chem. Ges.* **1936**, *69*, 2106-2112.
- [51] G. Wittig, H. Blumenthal, *Ber. Dtsch. Chem. Ges.* **1927**, *60*, 1085-1094.
- [52] J. N. Collie, *Liebigs Ann. Chem.* **1884**, *226*, 294-322.
- [53] (a) G. Stork, R. Terrell, J. Szmuszkovicz, *J. Am. Chem. Soc.* **1954**, *76*, 2029-2030; (b) G. Stork, H. K. Landesman, *J. Am. Chem. Soc.* **1956**, *78*, 5128-5129; (c) G. Stork, H. K. Landesman, *J. Am. Chem. Soc.* **1956**, *78*, 5129-5130; (d) G. Stork, A. Brizzolara, H. K. Landesman, J. Szmuszkovicz, R. Terrell, *J. Am. Chem. Soc.* **1963**, *85*, 207-222.
- [54] (a) P. W. Hickmott, *Tetrahedron* **1982**, *38*, 1975-2050; (b) G. Pitacco, E. Valentin in *Supplement F: The chemistry of amino, nitroso and nitro compounds and their derivatives* (Ed.: S. Patai), Wiley, Chichester, **1982**, pp. 623-714; (c) V. G. Granik, *Russ. Chem. Rev.* **1984**, *53*, 383-400; *Usp. Khim.* **1984**, *53*, 651-688; (d) P. W. Hickmott in *The chemistry of enamines* (Ed.: Z. Rappoport), Wiley, Chichester, **1994**, pp. 727-871. (e) S. Hünig, H. Hoch, *Fortschr. Chem. Forsch.* **1970**, *14*, 235-293.
- [55] (a) J. K. Whitesell, M. A. Whitesell, *Synthesis* **1983**, 517-536; (b) G. H. Alt, A. G. Cook in *Enamines: Synthesis, Structure and Reactions* (Ed.: A. G. Cook), 2nd ed., Marcel Dekker, New York, **1988**, chapter 4.

- [56] M. E. Kuehne, *J. Am. Chem. Soc.* **1962**, *84*, 837–847.
- [57] (a) T. Shono, Y. Matsumura, K. Inoue, H. Ohmizu, S. Kashimura, *J. Am. Chem. Soc.* **1982**, *104*, 5753–5757; (b) S.-I. Murahashi, T. Naota, T. Nakato, *Synlett* **1992**, 835–836; (c) R. Chinchilla, J. E. Bäckvall in *The chemistry of enamines* (Ed.: Z. Rappoport), Wiley, Chichester, **1994**, pp. 993–1048.
- [58] (a) P. Brownbridge, *Synthesis* **1983**, 1–28; (b) P. Brownbridge, *Synthesis* **1983**, 85–104; (c) H. U. Reissig, *Chem. Unserer Zeit* **1984**, *18*, 46–53; (d) M. T. Reetz, *Angew. Chem.* **1982**, *94*, 97–109; *Angew. Chem. Int. Ed. Engl.* **1982**, *21*, 96–108; (e) T. Mukaiyama, M. Murakami, *Synthesis* **1987**, 1043–1054; (f) H. U. Reissig, *Top. Curr. Chem.* **1988**, *144*, 73–135; (g) R. Mahrwald, *Chem. Rev.* **1999**, *99*, 1095–1120.
- [59] O. Kuhn, H. Mayr, *Angew. Chem.* **1999**, *111*, 356–358; *Angew. Chem. Int. Ed.* **1999**, *38*, 343–346.
- [60] R. Huisgen, G. Szeimies, L. Möbius, *Chem. Ber.* **1967**, *100*, 2494–2507.
- [61] M. K. Meilahn, B. Cox, M. E. Munk, *J. Org. Chem.* **1975**, *40*, 819–824.
- [62] R. Huisgen, L. A. Feiler, P. Otto, *Chem. Ber.* **1969**, *102*, 3444–3459.
- [63] E. J. Stamhuis, W. Maas, *J. Org. Chem.* **1965**, *30*, 2156–2160.
- [64] J. Sauer in *Comprehensive Heterocyclic Chemistry II*, Vol. 6 (Eds.: A. R. Katritzky, C. W. Rees, E. F. V. Scriven, A. J. Boulton), Pergamon Press, Oxford, **1996**, Chapter 6.21, pp 901–955.
- [65] *Organikum* (19. Aufl.), Edition dt. Verlag der Wissenschaften, Berlin, **1993**.
- [66] J. Sauer, H. Prahl, *Chem. Ber.* **1969**, *102*, 1917–1927.
- [67] C. B. Kanner, U. K. Pandit, *Tetrahedron* **1982**, *38*, 3597–3604.
- [68] T. L. Gilchrist, *Heterocyclic Chemistry*, 3rd ed., Longman, Essex, UK, **1997**.
- [69] (a) B. L. Bray, P. H. Mathies, R. Naef, D. R. Solas, T. T. Tidwell, D. R. Artis, J. M. Muchowski, *J. Org. Chem.* **1990**, *55*, 6317–6328; (b) B. L. Bray, J. M. Muchowski, *J. Org. Chem.* **1988**, *53*, 6115–6118; (c) J. M. Muchowski, D. R. Solas, *Tetrahedron Lett.* **1983**, *24*, 3455–3456.
- [70] H. Hellmann, G. Opitz, *Liebigs Ann. Chem.* **1957**, *604*, 214–221.
- [71] For a review on electrophilic aromatic substitutions at five-membered arenes: A. R. Katritzky, R. Taylor, *Adv. Heterocycl. Chem.* **1990**, *47*, 1–467.
- [72] H. Schimmel, A. R. Ofial, H. Mayr, *Macromolecules* **2002**, *35*, 5454–5458.
- [73] A. D. Dilman, S. L. Ioffe, H. Mayr, *J. Org. Chem.* **2001**, *66*, 3196–3200.

- [74] (a) H. Mayr, C. Fichtner, A. R. Ofial, *J. Chem. Soc., Perkin Trans. 2* **2002**, 1435-1440; (b) C. Fichtner, G. Remennikov, H. Mayr, *Eur. J. Org. Chem.* **2001**, 4451-4456.
- [75] (a) N. J. Leonard, V. W. Gash, *J. Am. Chem. Soc.* **1954**, 76, 2781-2784; (b) G. Opitz, H. Hellmann, H. W. Schubert, *Liebigs Ann. Chem.* **1959**, 623, 117-124.
- [76] G. Opitz, A. Griesinger, *Liebigs Ann. Chem.* **1963**, 665, 101-113.
- [77] (a) E. J. Stamhuis, W. Maas, *Recl. Trav. Chim. Pays-Bas* **1963**, 82, 1155-1158; (b) E. J. Stamhuis, W. Maas, H. Wynberg, *J. Org. Chem.* **1965**, 30, 2160-2163; (c) W. Maas, M. J. Janssen, E. J. Stamhuis, H. Wynberg, *J. Org. Chem.* **1967**, 32, 1111-1115.
- [78] (a) E. Elkik, C. Francesch, *Bull. Soc. Chim. Fr.* **1969**, 903-910; (b) M. E. Kuehne, T. Garbacik, *J. Org. Chem.* **1970**, 35, 1555-1558; (c) U. K. Pandit, W. A. Z. Voorspujij, P. Houdewind, *Tetrahedron Lett.* **1972**, 1997-2000.
- [79] From the high nucleophilicity parameters of amines (see ref. [88]) one can derive that the failure of a reaction with *N*-methylmorpholine cannot be due to a kinetic barrier.
- [80] The method of single-point calibrations is explained in ref. [89].
- [81] R. A. Marcus, *J. Phys. Chem.* **1968**, 72, 891-899.
- [82] H. Mayr, R. Schneider, C. Schade, J. Bartl, R. Bederke, *J. Am. Chem. Soc.* **1990**, 112, 4446-4454.
- [83] H. Mayr, B. Kempf, unpublished results.
- [84] (a) For IP_1 of **21** (7.10 eV), **23** (7.40 eV), and **25** (7.60 eV), see: L. M. Domelsmith, K. N. Houk, *Tetrahedron Lett.* **1977**, 1981-1984; (b) For IP_1 of **22** (7.10 eV), **24** (7.42 eV), and **20** (7.66 eV), see: T. Itoh, K. Kaneda, I. Watanabe, S. Ikeda, S. Teranishi, *Chem. Lett.* **1976**, 227-230; (c) For IP_1 of **36** (7.53 eV), see: W. W. Schoeller, J. Niemann, P. Rademacher, *J. Chem. Soc., Perkin Trans. 2* **1988**, 369-373; (d) See also: F. P. Colonna, G. Distefano, S. Pignataro, G. Pitacco, E. Valentin, *J. Chem. Soc., Faraday Trans. 2* **1975**, 71, 1572-1576.
- [85] K. L. Brown, L. Damm, J. D. Dunitz, A. Eschenmoser, R. Hobi, C. Kratky, *Helv. Chim. Acta* **1978**, 61, 3108-3135.
- [86] (a) K. Oyama, T. T. Tidwell, *J. Am. Chem. Soc.* **1976**, 98, 947-951; (b) V. J. Nowlan, T. T. Tidwell, *Acc. Chem. Res.* **1977**, 10, 252-258.

- [87] For the determination of $pK_a^{CH^+}$ values for **45-H⁺** (-3.5), **46-H⁺** (-2.3), and **47-H⁺** (0.3), see: R. L. Hinman, J. Lang, *J. Am. Chem. Soc.* **1964**, *86*, 3796–3806.
- [88] S. Minegishi, H. Mayr, *J. Am. Chem. Soc.* **2003**, *125*, 286-295.
- [89] H. Mayr, B. Kempf, A. R. Ofial, *Acc. Chem. Res.* **2003**, *36*, 66-77.
- [90] (a) F. Terrier, *Chem. Rev.* **1982**, *82*, 77-152; (b) G. Illuminati, F. Stegel, *Adv. Heterocycl. Chem.* **1983**, *34*, 305-444; (c) E. Buncl, J. M. Dust, F. Terrier, *Chem. Rev.* **1995**, *95*, 2261-2280.
- [91] F. Terrier, E. Kizilian, J. C. Halle, E. Buncl, *J. Am. Chem. Soc.* **1992**, *114*, 1740-1742.
- [92] (a) F. Terrier, R. Goumont, M. J. Pouet, J. C. Halle, *J. Chem. Soc., Perkin Trans.* **1995**, 1629-1637; (b) E. Buncl, R. A. Renfrow, M. J. Strauss, *J. Org. Chem.* **1987**, *52*, 488-495.
- [93] P. B. Ghosh, B. Ternai, M. W. Whitehouse, *Med. Res. Rev.* **1981**, *1*, 159-187.
- [94] (a) A. B. Sheremetev, *Russ. Chem Rev.* **1999**, *68*, 137–148 (*Usp. Khim.* **1999**, *68*, 154-166); (b) M. Sako, S. Oda, S. Ohara, K. Hirota, Y. Maki, *J. Org. Chem.* **1998**, *63*, 6947-6951; (c) G. Ya. Remennikov, *Chem. Heterocycl. Compd.* **1997**, *33*, 1369-1381 (*Khim. Geterotsikl. Soedin.* **1997**, *33*, 1587-1602).
- [95] F. Terrier, M. Sebban, R. Goumont, J. C. Halle, G. Moutiers, I. Cangelosi, E. Buncl, *J. Org. Chem.* **2000**, *65*, 7391-7398.
- [96] G. Ya. Remennikov, V. V. Pirozhenko, I. A. Dyachenko, *Khim. Geterotsikl. Soedin.* **1992**, 101-106.
- [97] G. Ya. Remennikov, V. V. Pirozhenko, S. I. Vdovenko, S. A. Kravchenko, *Chem. Heterocycl. Compd.* **1998**, *34*, 104-110 (*Khim. Geterotsikl. Soedin.* **1998**, *34*, 112-119).
- [98] G. Ya. Remennikov, B. Kempf, A. R. Ofial, K. Polborn, H. Mayr, *J. Phys. Org. Chem.* **2003**, in print.
- [99] G. Steiner, R. Huisgen, *J. Am. Chem. Soc.* **1973**, *95*, 5056-5058.
- [100] C. Reichardt, *Solvents and Solvent Effects in Organic Chemistry*, 2nd ed., VCH, Weinheim, **1988**, p. 147.
- [101] (a) E. Lindner, A. Bader, E. Glaser, P. Wegner, *J. Mol. Cat.* **1989**, *56*, 86-94; (b) E. Lindner, B. Karle, *Chem. Ber.* **1990**, *123*, 1469-1473; (c) E. Lindner, *Chem. Ber.* **1990**, *123*, 459-465; (d) E. Lindner, A. E. Ekkehard, B. Andres, *Chem. Ber.* **1988**, *121*, 829-832.

- [102] C. A. Tolman, *Chem. Rev.* **1977**, 77, 313-348.
- [103] C. A. Tolman, *J. Am. Chem. Soc.* **1970**, 92, 2953-2956.
- [104] C. A. Tolman, *J. Am. Chem. Soc.* **1970**, 92, 2956-2965.
- [105] (a) C. J. Elsevier, B. Kowall, H. Kragten, *Inorg. Chem.* **1995**, 34, 4836-4839; (b) S. Song, E. C. Alyea, *Can. J. Chem.* **1996**, 74, 2304-2320; (c) T. L. Brown, K. J. Lee, *Coord. Chem. Rev.* **1993**, 128, 89-116; (d) J. M. Smith, B. C. Taverner, N. J. Coville, *J. Organomet. Chem.* **1997**, 530, 131-140.
- [106] D. A. White, M. M. Baizer, *Tetrahedron Lett.* **1973**, 3597.
- [107] R. B. Grossman, S. Comesse, R. M. Rasne, K. Hattori, M. N. Delong, *J. Org. Chem.* **2003**, 68, 871-874.
- [108] F. Roth, P. Gygax, G. Frater, *Tetrahedron Lett.* **1992**, 33, 1045.
- [109] F. Dinon, E. Richards, P. J. Murphy, D. E. Hibbs, M. B. Hursthouse, K. M. A. Malik, *Tetrahedron Lett.* **1999**, 40, 3279-3282.
- [110] S. A. Frank, D. J. Mergott, W. R. Roush, *J. Am. Chem. Soc.* **2002**, 124, 2404-2405.
- [111] H. Gilman, E. A. Zoellner, W. M. Selby, *J. Am. Chem. Soc.* **1933**, 55, 1252-1257.
- [112] G. Tomaschewski, *J. Prakt. Chem.* **1966**, 33, 168-177.
- [113] T. Allman, R. G. Goel, *Can. J. Chem.* **1982**, 60, 716-722.
- [114] L. A. P. Kane-Maguire, M. Manthey, J. G. Atton, G. R. John, *Inorg. Chim. Acta* **1995**, 240, 71-79.
- [115] H. Mayr, N. Basso, G. Hagen, *J. Am. Chem. Soc.* **1992**, 114, 3060-3066.
- [116] G. Gardaci, S. M. Murgia, A. Foffani, *J. Organomet. Chem.* **1970**, 23, 265-273.
- [117] L. A. P. Kane-Maguire, *J. Chem. Soc., Dalton Trans.* **1979**, 873-878.
- [118] R. Lucius, H. Mayr, *Angew. Chem.* **2000**, 112, 2086-2089; *Angew. Chem. Int. Ed.* **2000**, 39, 1995-1997.
- [119] (a) J. E. Leffler, E. Grunwald, *Rates and Equilibria of Organic Reactions*, Wiley, New York, **1963**; (b) N. B. Chapman, J. Shorter, *Advances in Linear Free Energy Relationships*, Plenum Press, London, **1972**.
- [120] A. Williams, *Adv. Phys. Org. Chem.*, **1992**, 27, 1-55.
- [121] (a) C. F. Bernasconi, G. D. Leonarduzzi, *J. Am. Chem. Soc.* **1982**, 104, 5133; (b) E. M. Arnett, R. Reich, *J. Am. Chem. Soc.* **1980**, 102, 5892; (c) C. F. Bernasconi, R. B. Killion, *J. Am. Chem. Soc.* **1988**, 110, 7506; (d) J. E. Dixon, T. C. Bruice, *J. Am. Chem. Soc.* **1971**, 93, 3248.

- [122] (a) M. Kreevoy, *J. Am. Chem. Soc.* **1997**, *119*, 2722-2728; (b) M. Kreevoy, I.-S. Han Lee, *J. Am. Chem. Soc.* **1984**, *106*, 2550-2553.
- [123] E.-U. Würthwein, G. Lang, L. H. Schappele, H. Mayr, *J. Am. Chem. Soc.* **2002**, *124*, 4084-4092.
- [124] A. S. Romakhin, E. V. Nikitin, O. V. Parakin, Yu. A. Ignat'ev, B. S. Mironov, Yu. M. Kargin, *Zh. Obshch. Khim. / J. Gen. Chem. USSR* **1986**, *56*, 2597-2601.
- [125] (a) W. B. Gara, B. P. Roberts, *J. Chem. Soc., Perkin Trans. 2* **1978**, *2*, 150; (b) W. B. Gara, B. P. Roberts, *Chem. Commun.* **1975**, *23*, 949; (c) H. Ohmori, K. Sakai, N. Nagai, Y. Mizuki, M. Masui, *Chem. Pharm. Bull.* **1985**, *33*, 373-376; (d) M. Masui, Y. Mizuki, K. Sakai, C. Ueda, H. Ohmori, *Chem. Commun.* **1984**, *13*, 843-844; (e) H. Ohmori, H. Maeda, T. Takanami, M. Masui, *Recent Advances in Electroorganic Synthesis*, Marcel Dekker, New York, **1989**, pp. 29-32; (f) H. Ohmori, H. Maeda, M. Kikuoka, T. Maki, M. Masui, *Tetrahedron* **1991**, *47*, 767-776.
- [126] A. R. Ofial, K. Ohkubo, S. Fukuzumi, R. Lucius, H. Mayr, *J. Am. Chem. Soc.*, submitted.
- [127] Yu. M. Kargin, Yu. G. Budnikova, *Zh. Obshch. Khim.* **2001**, *71*, 1472-1502; *Russ. J. Gen. Chem.* **2001**, *71*, 1393-1421.
- [128] D. Woska, A. Prock, W. P. Giering, *Organometallics* **2000**, *19*, 4629-4638.
- [129] L. Horner, A. Gross, *Liebigs Ann. Chem.* **1955**, *117*, 591.
- [130] (a) S. Eliana, J. I. Armstrong, C. R. Bertozzi, *Org. Lett.* **2000**, *2*, 2141-2143; (b) E. Saxon, C. R. Bertozzi, *Science* **2000**, *287*, 2007-2010; (c) E. Saxon, S. Luchansky, H. C. Hang, C. Yu, C. S. Lee, C. R. Bertozzi, *J. Am. Chem. Soc.* **2002**, *124*, 14893-14902.
- [131] H. Zimmer, G. Singh, *J. Org. Chem.* **1963**, *28*, 483.
- [132] (a) H. Staudinger, J. Meyer, *Chem. Ber.* **1920**, *53*, 72; (b) H. Staudinger, E. Hauser, *Helv. Chim. Acta* **1921**, *4*, 861; (c) H. Ulrich, A. A. Sayigh, *Angew. Chem.* **1962**, *74*, 900; (d) W. S. Wadsworth, W. D. Emmons, *J. Am. Chem. Soc.* **1962**, *84*, 1316; (e) A. Messmer, I. Pinter, F. Szegö, *Angew. Chem.* **1964**, *76*, 227.
- [133] J. E. Leffler, R. D. Temple, *J. Am. Chem. Soc.* **1967**, *89*, 5235-5246.
- [134] R. Romeo, M. R. Plutino, L. M. Scolaro, S. Stoccoro, *Inorg. Chim. Acta* **1997**, *265*, 225-233.
- [135] W. E. McEwan, A. B. Janes, J. W. Knapczyk, V. L. Kyllingstad, W.-I. Shiau, S. Shore, J. H. Smith, *J. Am. Chem. Soc.* **1978**, *100*, 7304-7311.

- [136] (a) G. J. Atton, L. A. P. Kane-Maguire, *J. Organomet. Chem.* **1983**, *246*, C23-C26; (b) D. J. Evans, L. A. P. Kane-Maguire, *J. Organomet. Chem.* **1982**, *232*, C9-C12; (c) J. G. Atton, L. A. P. Kane-Maguire, P. A. Williams, G. R. Stephenson, *J. Organomet. Chem.* **1982**, *232*, C5-C8; (d) L. Cosslett, L. A. P. Kane-Maguire, *J. Organomet. Chem.* **1979**, *178*, C17-C19; (e) D. W. Clack, L. A. P. Kane Maguire, *J. Organomet. Chem.* **1978**, *145*, 201-206; (f) L. A. P. Kane-Maguire, C. A. Mansfield, *J. Chem. Soc., Dalton Trans.* **1976**, 2192-2196; (g) D. A. Sweigart, M. Gower, L. A. P. Kane-Maguire, *J. Organomet. Chem.* **1976**, *108*, C15-C17; (h) C. A. Mansfield, K. M. Al-Kathumi, L. A. P. Kane-Maguire, *J. Organomet. Chem.* **1974**, *71*, C11-C13; (i) L. A. P. Kane-Maguire, *J. Chem. Soc. A* **1971**, 1602-1606.
- [137] (a) D. A. White, *Organomet. Chem. Rev., Sect. A* **1968**, *3*, 497; (b) A. J. Birch, I. D. Jenkins, *Transition Metal Organometallics in Organic Synthesis*, H. Alper, Ed., Academic Press, New York, **1976**, Vol 1, p. 1; (c) S. G. Davies, M. L. H. Green, D. M. P. Mingos, *Tetrahedron* **1978**, *34*, 3047; (d) A. J. Birch, *Ann. N. Y. Acad. Sci.* **1980**, *333*, 107; (e) A. J. Birch, L. F. Kelly, A. S. Narula, *Tetrahedron* **1982**, *38*, 1813; (f) A. J. Pearson in *Comprehensive Organometallic Chemistry* (Eds.: G. Wilkinson, F. G. A. Stone, E. W. Abel), Pergamon Press, New York, **1982**, Vol. 8, Chapter 58; (g) M. F. Semmelhack, J. L. Garcia, D. Cortes, R. Farina, R. Hong, B. K. Carpenter, *Organometallics* **1983**, *2*, 467; (h) B. M. Trost, T. R. Verhoeven in *Comprehensive Organometallic Chemistry* (Eds.: G. Wilkinson, F. G. A. Stone, E. W. Abel), Pergamon Press, New York, **1982**, Vol. 8, Chapter 57; (i) J. P. Collman, L. S. Hegedus, *Principles and Applications of Organotransition Metal Chemistry*, University Science Books, Mill Valey, CA, **1980**, Chapters 12, 15; (j) P. Lennon, A. M. Rosan, M. Rosenblum, *J. Am. Chem. Soc.* **1977**, *99*, 8426; (k) M. R. Baar, B. W. Roberts, *J. Chem. Soc., Chem. Commun.* **1979**, 1129.
- [138] P. L. Pauson, *J. Organomet. Chem.* **1980**, *200*, 207.
- [139] P. Hackett, B. F. G. Johnson, J. Lewis, G. Jaouen, *J. Chem. Soc., Dalton Trans.* **1982**, 1247.
- [140] J. G. Atton, L. A. P. Kane-Maguire, *J. Chem. Soc., Dalton Trans.* **1982**, 1491.
- [141] G. R. John, L. A. P. Kane-Maguire, *J. Chem. Soc., Dalton Trans.* **1979**, 873.
- [142] L. A. P. Kane-Maguire, E. D. Honig, D. A. Sweigart, *Chem. Rev.* **1984**, *84*, 525-543.

- [143] M. Gower, G. R. John, L. A. P. Kane-Maguire, T. I. Salzer, *A. J. Chem. Soc., Dalton Trans.* **1979**, 2003.
- [144] L. A. P. Kane-Maguire, D. A. Sweigart, *Inorg. Chem.* **1979**, *18*, 700.
- [145] Y. K. Chung, E. D. Honig, D. A. Sweigart, *J. Organomet. Chem.* **1983**, 256, 277.
- [146] P. S. Domaille, S. D. Ittel, J. P. Jesson, D. A. Sweigart, *J. Organomet. Chem.* **1980**, *202*, 191.
- [147] D. Birney, A. Crane, D. A. Sweigart, *J. Organomet. Chem.* **1978**, *152*, 187.
- [148] G. R. John, L. A. P. Kane-Maguire, D. A. Sweigart, *J. Organomet. Chem.* **1976**, *120*, C47.
- [149] H. S. Choi, D. A. Sweigart, *Organometallics* **1982**, *1*, 60.
- [150] L. Cosslett, L. A. P. Kane-Maguire, *J. Organomet. Chem.* **1979**, *178*, C17.
- [151] L. A. P. Kane-Maguire, P. D. Moucher, A. Salzer, *A. J. Organomet. Chem.* **1979**, *168*, C42.
- [152] N. Hering, *Diplomarbeit* **1996**, Technische Hochschule Darmstadt.
- [153] K. H. Müller, *Dissertation* **1997**, Technische Hochschule Darmstadt.
- [154] A. Einhorn, F. Hollandt, *Liebigs Ann. Chem.* **1898**, *301*, 95-115.
- [155] A. Verley, F. Bölsing, *Ber. Dtsch. Chem. Ges.* **1901**, *34*, 3354; **1901**, *34*, 3359.
- [156] E. Fischer, M. Bergmann, *Ber. Dtsch. Chem. Ges.* **1917**, *50*, 1047.
- [157] L. M. Litvinenko, A. I. Kirichenko, *Dokl. Akad. Nauk SSSR, Ser. Khim.* **1967**, *176*, 97.
- [158] W. Steglich, G. Höfle, *Angew. Chem.* **1969**, *81*, 1001; *Angew. Chem. Int. Ed. Engl.* **1969**, *8*, 981.
- [159] (a) K. A. Connors, K. S. Albert, *J. Pharm. Sci.* **1973**, *62*, 845; (b) E. L. Rowe, S. M. Machkovech, *J. Pharm. Sci.* **1977**, *66*, 273.
- [160] R. Brückner, *Reaktionsmechanismen*, Spektrum, Akad. Verl., Heidelberg, **1996**.
- [161] (a) W. Steglich, G. Höfle, *Tetrahedron Lett.* **1970**, 4727; (b) W. Steglich, G. Höfle, *Chem. Ber.* **1969**, *102*, 883.
- [162] G. Höfle, W. Steglich, H. Vorbrüggen, *Angew. Chem.* **1978**, *90*, 602-615.
- [163] M. Heinrich, *Dissertation* **2003**, Ludwig-Maximilians-Universität München.
- [164] (a) Y. Hamada, I. Takeuchi, *Chem. Pharm. Bull.* **1971**, *19*, 1857-1862; (b) T. Sakamoto, N. Miura, Y. Kondo, H. Yamanaka, *Chem. Pharm. Bull.* **1986**, *34*, 2018-2023.
- [165] H. Klisa, *Diplomarbeit* **2002**, Ludwig-Maximilians-Universität München.

- [166] T. Rodima, I. Kaljurand, A. Pihl, V. Mäemets, I. Leito, I. A. Koppel, *J. Org. Chem.* **2002**, *67*, 1873-1881.
- [167] E. M. Arnett, G. Scorrano, *Adv. Phys. Org. Chem.* **1976**, *13*, 82-153.
- [168] M. Menshutkin, *Z. Phys. Chem.* **1890**, *5*, 589.
- [169] (a) G. F. Duffin in A. R. Katritzky, *Advances in Heterocyclic Chemistry Vol. 3*, Academic Press, New York, **1964**; (b) H. C. Brown, A. Cahn, *J. Am. Chem. Soc.* **1955**, *77*, 1715; (c) N. Tokura, Y. Kondo, *Bull. Chem. Soc. Jpn.* **1964**, *37*, 133; (d) L. W. Deady, *Aust. J. Chem.* **1973**, *26*, 1949.
- [170] K. J. Schaper, *Arch. Pharm. (Weinheim, Ger.)* **1978**, *311*, 641-649.
- [171] K. J. Schaper, *Arch. Pharm. (Weinheim, Ger.)* **1978**, *311*, 650-663.
- [172] (a) C. F. Braga, C. A. M. Abreu, N. M. Lima Filho, Y. Queneau, G. Descotes, *React. Kinet. Catal. Lett.* **2002**, *77*, 91-102; (b) S.-F. Lin, K. A. Connors, *J. Pharm. Sc.* **1981**, *70*, 235-238; (c) Y. S. Simanenko, V. A. Savelova, L. M. Litvinenko, I. A. Belousova, V. A. Dadali, T. M. Zubareva, *Zh. Org. Khim. / J. Org. Chem. USSR* **1985**, *21*, 135-145; (d) L. I. Bondarenko, A. I. Kirichenko, L. M. Litvinenko, I. N. Dmitrenko, V. D. Kobets, *Zh. Org. Khim. / J. Org. Chem. USSR* **1981**, *17*, 2588-2594; (e) L. P. Drizhd, L. I. Bondarenko, V. A. Savelova, L. M. Litvinenko, A. I. Kirichenko, A. A. Yakovets, *Zh. Org. Khim. / J. Org. Chem. USSR* **1984**, *20*, 2401-2407.
- [173] A. Hassner, L. R. Krepski, V. Alexanian, *Tetrahedron* **1978**, *34*, 2069-2076.
- [174] M. Hesse, H. Meier, B. Zeeh, *Spektroskopische Methoden in der organischen Chemie*, Georg Thieme Verlag, Stuttgart, **1995**.
- [175] E. W. Colvin, *Silicon Reagents in Organic Synthesis*, Academic Press, London, 1990.
- [176] D. Hellwinkel, H. G. Gaa, R. Gottfried, *Z. Naturforsch. B* **1986**, *41*, 1045-1060.
- [177] N. A. Evans, *Aust. J. Chem.* **1983**, *36*, 409-413.
- [178] N. Slougui, G. Rousseau, *Tetrahedron* **1985**, *41*, 2643-2652.
- [179] D. P. Kelly, J. J. Giansiracusa, D. R. Leslie, I. D. McKern, G. C. Sinclair, *J. Org. Chem.* **1988**, *53*, 2497-2504.
- [180] G. A. Lean, B. J. L. Rayles, D. M. Smith, M. J. Bruce, *J. Chem. Res. (M)* **1996**, *10*, 2623-2639.
- [181] R. Westerman, *J. Org. Chem.* **1977**, *42*, 2249-2252.

- [182] D. W. Clack, A. H. Jackson, N. Prasitpan, P. V. R. Shannan, *J. Chem. Soc. Perkin Trans. 2* **1982**, 909-916.
- [183] K. Blau, V. Voerckel, *J. Prakt. Chem.* **1989**, 331, 285-292.
- [184] Y. Yamamoto, C. Matui, *J. Org. Chem.* **1998**, 63, 377-378.
- [185] P. Schwotzer, *Helv. Chim. Acta* **1977**, 60, 1501-1502.
- [186] I. S. Darwish, C. Patel, M. J. Miller, *J. Org. Chem.* **1993**, 58, 6072-6075.
- [187] A. J. Birch, *J. Chem. Soc. C* **1971**, 2409-2411.
- [188] E. Benzing, *Angew. Chem.* **1959**, 71, 521.
- [189] R. Knorr, P. Loew, P. Hassel, *Synthesis* **1983**, 785-786.
- [190] W. Ziegenbein, W. Franke, *Chem. Ber.* **1957**, 90, 2291.
- [191] A. Tillack, H. Trauthwein, C. G. Hartung, M. Eichberger, S. Pitter, A. Jansen, M. Reller, *Monatsh. Chem.* **2000**, 131, 12, 1327-1334.
- [192] (a) G. L. May, J. T. Pinkey, *Aust. J. Chem.* **1982**, 35, 1859-1871; (b) S. Hünig, K. Hübner, E. Benzing, *Chem. Ber.* **1962**, 95, 926-936.
- [193] S. H. Pine, R. J. Pettit, G. D. Geib, S. G. Cruz, C. H. Gallego, *J. Org. Chem.* **1985**, 50, 1212-1216.
- [194] F. Schoen, *Tetrahedron* **1975**, 31, 671-676.
- [195] The synthesis was performed analogously to that described in ref. [196].
- [196] S. K. Dewan, U. V. Malik, D. Malik, *J. Chem. Res. (S)* **1995**, 21.
- [197] B. Capan, Z. Wu, *J. Org. Chem.* **1990**, 55, 2317-2324.
- [198] B. Caubere, *Bull. Soc. Chim. Fr.* **1970**, 2418-2421.
- [199] M. S. South, T. L. Jakuboski, M. D. Westmeyer, D. R. Dukesherer, *J. Org. Chem.* **1996**, 61, 8921-8934.
- [200] B. Kempf, N. Hampel, A. R. Ofial, H. Mayr, *Chem. Eur. J.* **2003**, 9, 2209-2218.
- [201] W. N. Chou, M. Pomerantz, *J. Org. Chem.* **1991**, 56, 2762-2769.
- [202] Z. Jedlinski, A. Misiolek, W. Glowkowski, H. Janeczek, A. Wolinska, *Tetrahedron* **1990**, 46, 3547-3558.

Lebenslauf

Persönliche Daten

Name: Bernhard Kempf
Geburtsdatum: 21.02.1973
Geburtsort: Buchloe
Familienstand: verheirated

Schulbildung

9/80 - 7/84 Grundschole Hirschzell
9/84 - 7/93 Jakob Bruker Gymnasium Kaufbeuren
Abschluss: Allgemeine Hochschulreife

Zivildienst

7/93 - 9/94 Altenheim zum Heiligen Geist, Kaufbeuren

Hochschulausbildung

11/94 - 9/99 Studium Chemie Diplom, Ludwig-Maximilians-Universität München, Abschluss: Dipl.-Chem. Univ.
9/99 - 2/00 Diplomarbeit am Department für Organische Chemie der Ludwig-Maximilians-Universität München unter Anleitung von Prof. Dr. H. Mayr.
5/00 - 6/03 Promotion am Department für Organische Chemie der Ludwig-Maximilians-Universität München unter Anleitung von Prof. Dr. H. Mayr.

Berufstätigkeit

1/98 - 3/98 Studentische Hilfskraft am Department für Anorg. Chemie.
10/99 - 2/00 Studentische Hilfskraft am Department für Org. Chemie.
5/00 - 6/03 Wissenschaftlicher Mitarbeiter am Department für Organische Chemie der Ludwig-Maximilians-Universität München.

